

Report Number: 10361

March 2012

Validation of Assessment Methods for Production Scale Girth Welding of High Strength Steel Pipelines with Multiple Pipe Sources

Not Restricted

Restricted to: US Department of Transportation
& GL Noble Denton

Prepared for:

Max Kieba

US Department of Transportation

Pipeline and Hazardous Materials Safety
Administration
Office of Pipeline Safety
1200 New Jersey Avenue
SE Building, Second Floor
Washington DC 20590
USA

Contract DTPH56-07-T-000006

Customer Reference:

Prepared by:

Troy Swankie

GL Industrial Services UK Ltd trading as GL Noble Denton

Holywell Park
Ashby Road
Loughborough
Leicestershire
LE11 3GR
United Kingdom

Tel: +44 (0)1509 28 2057
Fax: +44 (0)1509 28 3119

E-mail: Troy.Swankie@gl-group.com

Website: www.gl-nobledenton.com

DTPH56-07-T-000006 WP #275



This Report is protected by copyright and may not be reproduced in whole or in part by any means without the approval in writing of GL Noble Denton, Inc. No Person, other than the Customer for whom it has been prepared, may place reliance on its contents and no duty of care is assumed by GL Noble Denton toward any Person other than the Customer.

This Report must be read in its entirety and is subject to any assumptions and qualifications expressed therein. Elements of this Report contain detailed technical data which is intended for analysis only by persons possessing requisite expertise in its subject matter.

GL Noble Denton is the trading name of GL Industrial Services USA, Inc.

GL Industrial Services USA, Inc. is a company incorporated in Delaware and its headquarters at 600 Bent Creek Blvd., Suite 100, Mechanicsburg, PA17050, USA

Report Issue / Amendment Record

Report Title: Validation of Assessment Methods for Production Scale Girth Welding of High Strength Steel Pipelines with Multiple Pipe Sources	
Report Number: 10361	Project Title: Validation of Assessment Methods for Production Scale Girth Welding of High Strength Steel Pipelines with Multiple Pipe Sources
	Project SAP Code: 1/14025

Amendment details

Issue	Description of Amendment	Originator/Author
0.0	Comments: DOT PHMSA Minor editorial recommendations provided electronically in the draft report issued for review. Commented file reference: PHMSA_DTPH56-07-T-000006_Final_Report_DRAFT_Valid_of_Methods_for_HS_Steel_10361_COTR_comments(1)	Max Kieba (Originator) Troy Swankie (Author)

Report approval

Issue	Checked by	Approved by	Date
0.0	Vinod Chauhan (Principal Consultant, GL Noble Denton) Ian Wood (Electricore Inc) Spencer Quong (Quong and Associates, Inc)	Neil Bramley (Manager, GL Noble Denton)	28 November 2011
1.0	Vinod Chauhan (Principal Consultant, GL Noble Denton)	Neil Bramley (Manager, GL Noble Denton)	28 March 2012

Previous issues of this document shall be destroyed or marked SUPERSEDED

Project Code: 1/14025

Distribution

Name	Company
Max Kieba Jim Merritt Robert Smith	US Department of Transportation Pipeline and Hazardous Materials Safety Administration Office of Pipeline Safety 1200 New Jersey Avenue SE Building, Second Floor Washington DC 20590 USA
Ian Wood	Electricore, Inc. 27943 Smyth Drive, Suite 105 Valencia, CA 91355 USA
Richard Espiner	BP Exploration (UK) Sunbury Business Park Chertsey Road Sunbury-on-Thames Middlessex TW16 7LN UK

DISCLAIMER

This report is furnished to the U.S. Department of Transportation (DOT), and Electricore, Inc. (Electricore) under the terms of DOT contract DTPH56-07-T-000006 between DOT and Electricore, and Electricore agreement DTPH56-07-T-000006 between Electricore, GL Industrial Services USA, Inc. (GL) and BP Exploration (BP). This research was funded in part under the Department of Transportation, Pipeline and Hazardous Materials Safety Administration’s Pipeline Safety Research and Development Program. The views and conclusions contained in this document are those of the authors and should not be interpreted as representing the official policies, either expressed or implied, of the Pipeline and Hazardous Materials Safety Administration, or the U.S. Government. The contents of this report are published as received from GL. The opinions, findings and conclusions expressed in this report are those of the authors and not necessarily those of DOT, Electricore or BP. Publication of this report by Electricore should not be considered an endorsement by Electricore, BP or GL, or the accuracy or validity of any opinions, findings or conclusions expressed herein.

In publishing this report, Electricore, BP and GL make no warranty or representation, expressed or implied, with respect to the accuracy, completeness, usefulness, or fitness for purpose of the information contained herein, or that the use of any information, method, process, or apparatus disclosed in this report may not infringe on privately owned rights. Electricore, BP and GL assume no liability with respect to the use of, or for damages resulting from the use of, any information method, process, or apparatus described in this report. The text of this publication, or any part thereof, may not be reproduced or transmitted in any form by any means, electronic or mechanical, including photocopying, recording, storage in an information retrieval system, or otherwise, without written approval of Electricore, BP and GL.

Executive Summary

There is an increasing need to deliver energy from sources in remote areas to demand centers. For example, in North America, the delivery of gas from Alaska to demand centers in the lower 48 states is of major economic and strategic interest. This will require the design and construction of large diameter, long distance pipelines through adverse environments. The economics of these pipelines are dependent on the use of high strength steels to reduce the tonnage of steel required and on high productivity girth welding processes to shorten the construction period.

Robust inspection methods are required to reliably detect and size any defects which may occur during welding, and an equally robust method is required to assess the impact of those defects on the safe operation of the pipeline.

There are a number of methods that are commonly used for the assessment of a girth weld containing a 'fabrication' defect. These range from the more generic workmanship (or weld quality) defect acceptance limits to the more complex pipeline specific engineering critical assessment (ECA) methodologies where defect limits are derived based on the pipe size, material properties and pipeline loading conditions.

The ECA approach is widely used to derive girth weld defect acceptance limits that are specific to a pipeline. They are based on either semi-analytical methods or on the results of large-scale tests on pipeline girth welds. There is no one standardized method.

The guidance produced by the European Pipeline Research Group (EPRG) is an example of an established methodology based on the results of large-scale tests, while commonly used pipeline specific analytical assessment methods include API 1104^a and CSA Z662^a. Other commonly used semi-analytical methods, which are more generic in application, include API 579-1/ASME FFS-1^a and BS 7910^a.

The application of any of these methods has certain limitations. For example, there is no 'upper limit' to line pipe strength specified for use of the ECA methodology presented in API 1104, although there are limitations to some of the equations used within the procedure which limit their range of applicability up to grade X80 line pipe. Similarly, the EPRG guidelines are limited to pipelines constructed from grade X70 line pipe; although much work has been undertaken to demonstrate the applicability of the guidelines to pipelines constructed from grade X80 line pipe, an updated guidance document has yet to be published.

The objective of this project was to investigate the applicability of these 'established' methods for defining girth weld defect acceptance criteria for pipelines constructed from grade X100 line pipe.

BP provided the project with ten girth welds following completion of their full-scale X100 operational trial at GL Noble Denton's Spadeadam test facility located in Cumbria, England. This BP project involved the construction of two sections of 48in diameter pipeline. The construction process replicated full-scale practice, where the pipeline was welded above ground and then lowered into the ditch and backfilled. The pipeline test sections were then pressure cycled at a frequency to simulate 40 years of operation over a two year period. The project team selected the most appropriate girth welds that they considered would enable the effects of material variability between abutting pipes, different heats, and different pipe manufacturers to be investigated.

A materials test program was developed to fully characterize the performance of each girth weld. In total, 217 tensile tests, 108 Charpy impact tests and 54 fracture mechanics tests were undertaken, in addition to weld macro sections and hardness surveys. The test program concluded with 30 curved wide plate (CWP)

^a API – American Petroleum Institute; CSA – Canadian Standards Association; ASME – American Society of Mechanical Engineers; BS – British Standard

'mid-scale' tests, of which 19 specimens contained machined surface breaking defects of specified depth and length dimensions. The remaining CWP specimens contained either natural welding defects (e.g., lack of penetration, lack of side wall fusion or porosity), deliberate defects that were introduced during welding, or combinations of natural and deliberate defects.

Each CWP test was assessed using the procedures given in API 1104 (Option 2), EPRG, CSA Z662, BS 7910 and API 579-1/ASME FFS-1. The results of the small-scale test program for each weld were used as input into each assessment. The results of the assessments were compared with the results from the CWP tests to assess the limitations of each assessment method.

In general, each assessment method performed well, giving a conservative prediction of failure stress. However, the accuracy of the prediction was found to vary significantly.

The conclusions and recommendations from the work undertaken are given below.

Conclusions

A comprehensive test program was undertaken to fully characterize the mechanical properties of the 10 girth welds. The main conclusions from the tests undertaken are presented below;

1. Two hundred and seventeen tensile tests were undertaken to characterize the stress-strain behavior of the girth welds. The following observations were made;
 - The line pipe achieved the specified minimum yield and tensile strength requirements of the line pipe specification, ANSI/API 5L.
 - The stress-strain response of the line pipe in the pipe longitudinal direction was similar, unlike the response of the line pipe in the transverse direction, where the post yield behavior was found to vary considerably.
 - The properties were found to vary significantly depending on the type of test specimen; round bar or flat strip.
 - The properties of the weld metal varied significantly around the pipe circumference, showing a sinusoidal trend; yield strength was lowest at approximately the 6 and 12 o'clock positions and highest at approximately the 3 and 9 o'clock positions. The strength was also observed to vary through the weld thickness; the highest strength measured in the weld root and mid thickness regions, lowest at the weld cap.
 - The properties of the line pipe varied greatly between the different pipe manufacturers and plate sources; although not one consistently achieved the highest average values of yield or tensile strength, yield to tensile strength ratio or elongation.
 - The variation in strength observed between the different pipe manufacturers and plate sources resulted in a wide range of weld metal strength mismatch, ranging from 11% undermatching to 26% overmatching
2. One hundred and eight Charpy impact tests were undertaken. The impact energy measured in each weldment achieved the minimum and average requirements stipulated within API 1104, EPRG and CSA Z662, suggesting that the girth welds would behave in a ductile manner

3. Fifty four fracture mechanics tests were undertaken. The results from the tests suggest the potential for failure to occur in a brittle manner; the lowest CTOD^b measured for the heat affect zone was 0.0016in (0.04mm), and the weld metal was 0.0031in (0.08mm).
4. Thirty curved wide plate (CWP) tests were undertaken.
 - The CWP specimens with machined defects of varying length and height, up to 4in and 0.157in (100x4mm), with a defect area up to 6% of the specimen cross section, failed in a ductile manner, either by gross section or net section yielding.
 - The CWP specimens that contained either natural welding defects, deliberate defects introduced during welding, or combinations of natural and deliberate defects had a defect area up to 25% of the specimen cross section. The two specimens with the larger defect areas failed by local collapse (stress and strain at failure less than the yield strength and 0.5%, respectively). The remaining specimens failed in a ductile manner, either by gross section or net section yielding.
 - The results of the CWP specimens demonstrated that a girth weld is more tolerant to embedded defects when compared with an equivalent size surface breaking defect

The results of the mechanical test program were used towards assessing the limitation of the girth weld defect acceptance procedures, API 1104, CSA Z662 and EPRG, and the more generic fracture mechanics procedures given in BS 7910 and API 579-1/ASME FFS-1. The main conclusions from the analyses undertaken are presented below;

1. Verification of the applicability of API 1104, EPRG, CSA Z662, BS 7910 and API 579-1/ASME FFS-1 assessment methods to grade X100 pipelines was based on the performance of CWP tests undertaken on one pipe size; 48in (1220mm) diameter x 0.78in (19.8mm) wall thickness.
2. The following points are concluded from the assessments undertaken to **API 1104 (Option 2)**;
 - The procedure is based on calculating limiting defect sizes for surface breaking defects. There is no distinction between surface and embedded defects. The calculated limits are considered to be equally applicable to equivalent size embedded defects.
 - The analysis procedure is complex and not all equations within the procedure are valid for grade X100.
 - Despite these limitations the procedure gave conservative predictions of failure stress for all, except one CWP specimen (the predicted failure stress was 3% lower than the actual failure stress). In many cases the ratio of predicted failure stress to actual failure stress was close to 1.0.
 - The least accurate (most conservative) predictions were for the natural/deliberate welding defects, embedded within the pipe wall.
3. The following points are concluded from **EPRG** assessments undertaken;
 - The procedure is based on calculating limiting defect sizes for surface breaking defects. There is no distinction between surface and embedded defects. The calculated limits are considered to be equally applicable to equivalent size embedded defects.
 - The defect size limits are straight forward to calculate and the criteria easy to use.

^b CTOD – crack tip opening displacement; a measure of fracture toughness

- The limits calculated using the net-section collapse model are conservative when compared with the CWP test data.
 - The defect size limits recommended for inclusion in the EPRG guidance document for X80 grade pipelines appear suitable for grade X100 pipelines. However, the length of the defects tested did not extend to the $7t$ (t is the pipe wall thickness) limit proposed.
 - The CWP data for the natural/deliberate welding defects show that the proposed defect size limits are also applicable to equivalent sized embedded defects.
4. The following points are concluded from the assessments undertaken to **CSA Z662**;
- The procedure can be used for calculating defect size limits for either surface breaking defects or embedded defects.
 - The analysis procedure for brittle fracture is complex and not simple to use. For example, the user is required to interpret a log-log plot to construct a table of defect height as a function of length.
 - The procedure gave conservative predictions of failure stress, 2% or more when compared with the actual test data.
5. The following points are concluded from the assessments undertaken to **BS 7910** and **API 579-1/ASME FFS-1**;
- The procedure for calculating defect size limits for either surface breaking or embedded defects is complex and best undertaken using commercially available software.
 - The defect limits calculated are specific to the pipe size, pipeline loading conditions and material properties; calculations can still be performed even if the weldment has poor toughness and/or strength as these are direct inputs into the assessment.
 - The result of each CWP test was correctly predicted as a 'failure' using both methods.
 - Sensitivity studies were undertaken to determine the critical failure stress;
 - i. For the BS 7910 assessments, the ratio of actual to predicted failure stress ranged from 1.15 to 6.5 for all CWP specimen except for three. The failure stress of those specimens was predicted to be very low, resulting in ratios of 11.5, 19.8 and 23.0.
 - ii. For the API 579-1/ASME FFS-1 assessments, the ratio of actual to predicted failure stress ranged from 1.48 to 5.6 for all CWP specimen except for four, which had ratios of 11.3, 11.4, 13.9 and 19.9.
 - Sensitivity studies were undertaken assuming that the behavior of the girth welds was independent of fracture toughness;
 - i. For the **BS 7910** assessment, the ratio of actual to predicted failure stress ranged from 1.07 to 1.45.
 - ii. For the **API 579-1/ASME FFS-1** assessment, the ratio of actual to predicted failure stress ranged from 1.06 to 1.97.
 - The differences between the BS7910 and API 579-1/ASME FFS-1 results are due to the brittle fracture assessment and treatment of welding residual stress. The plastic collapse solutions, although different, give similar results.

Recommendations

The principal recommendations from the work undertaken are:

1. Consideration should be given to undertaking additional testing to investigate the influence of pipe diameter and wall thickness as verification of the applicability of the different assessment methods has been based on one pipe size; 48in (1220mm) diameter x 0.78in (19.8mm) wall thickness.
2. Consideration should be given to providing more detailed guidance given in API 1104 and CSA Z662 on the type, orientation and number of tests, and the sampling position around the pipe circumference to fully characterize the behavior of the weldment.
3. Consideration should be given to including a testing plan in the EPRG guidelines to ensure sufficient testing is undertaken to fully characterize the behavior of the weldment.
4. Some equations in the API 1104 procedure are limited to grade X80 line pipe. The validity of these to grade X100 needs to be assessed or consideration should be given to updating the procedure with more appropriate models, for example those published by the University of Gent as they provide an improved fit to available experimental data and have been validated for grade X100.

Contents

1	Introduction	1
2	Objectives	2
3	Overview of Girth Weld Assessment Methods	2
3.1	API 1104 Appendix A	3
3.2	European Pipeline Research Group	10
3.3	CSA Z662 Annex K	13
3.4	Alternative Methods Based on Fracture Mechanics	17
4	Source of Material for Testing	22
4.1	Pipeline Welding.....	22
4.2	Inspection of Girth Welds	23
5	Identification of Girth Welds for Testing	24
6	Material’s Test Program	25
6.1	Weld Macro-Sections	27
6.2	Hardness Surveys	27
6.3	Tensile Tests.....	28
6.4	Charpy Impact Tests	46
6.5	Fracture Mechanics Tests	51
7	Curved Wide Plate Tests	58
7.1	Specimen Preparation	58
7.2	Instrumentation	59
7.3	Test Method	59
7.4	Post Test Metallographic Examination.....	59
7.5	Analysis.....	60
7.6	Results	60
8	Evaluation of the Performance of Girth Welds in X100 Pipelines	75
8.1	Comparison of CWP Test Results with API 1104 Option 2.....	75
8.2	Comparison of CWP Test Results with EPRG Tier 2.....	77
8.3	Comparison of CWP Test Results with CSA Z662.....	80
8.4	Comparison of the CWP Test Results with BS 7910.....	84
8.5	Comparison of CWP Test Results with API 579-1/ASME FFS-1	90
9	Discussion	93
9.1	Girth Weld Defect Acceptance Criteria Performance.....	95
10	Conclusions	98
11	Recommendations	101

12	References	102
Appendix A	Weld Macro Sections and Vickers Hardness Surveys	A-1
Appendix B	Tensile Test Results: Stress-Strain Curves	B-1
Appendix C	Calculation of Fracture Toughness: CTOD, J and K	C-1
Appendix D	Fracture Mechanics Test Results: Force versus Clip Opening	D-1
Appendix E	Curved Wide Plate Test Results	E-1
Appendix F	API 1104 Appendix A, Option 2 Assessments	F-1
Appendix G	EPRG Assessments	G-1
Appendix H	CSA Z662 Assessments	H-1
Appendix I	BS 7910 Assessments	I-1
Appendix J	API 579-1/ASME FFS-1 Assessments	J-1

1 Introduction

There is an increasing requirement to deliver energy from sources in remote areas to demand centers. In North America, the delivery of gas from Alaska to demand centers in the lower 48 states is of major economic and strategic interest. This will require the design and construction of large diameter, long distance pipelines through adverse environments. The economics of these pipelines are dependent on the use of high strength steels to reduce the tonnage of steel required and on high productivity welding processes to shorten the construction period. The girth welds may be required to withstand high loadings, for example in areas of discontinuous permafrost. Robust inspection and assessment methods are required to detect any defects which may occur. The development of steels and welding techniques is largely carried out in a laboratory environment on a limited range of materials and issues such as variability between pipe suppliers, different material heats and the transfer of technology from the laboratory to the field are not generally addressed.

In 2006 BP commissioned the construction of a full scale operational trial of X100 line pipe at GL Noble Denton's Spadeadam test facility located in Cumbria, England [1][2]. This involved the construction of two sections of 48in diameter pipeline. The construction process replicated full scale practice, with the pipeline welded above ground and then lowered into the ditch and backfilled. The pipeline test sections were designed to ASME B31.8 [3] to a design factor of 0.8, with additional guidance taken from CSA Z662 [4]. The test sections were then pressure cycled for two years with an accelerated load spectrum simulating a little over 40 years of operation.

Completion of the operational trial has provided the project with an opportunity to investigate many of the issues highlighted above, and raised at a workshop held at National Institute of Standards and Technology (NIST) in January 2006. The mainline welds were produced using the high productivity CAPS system, which is a dual tandem gas metal arc welding (GMAW) process developed specifically for mainline girth welding of high strength line pipe such as X100. Pipe was sourced from two world class pipe mills, with the plate supply for one mill coming from two sources. Multiple heats of plate were provided by each mill.

New welding techniques will inevitably be developed, but these are unlikely to be assessed on the same scale as the welds produced for the operational trial. Typically, new techniques/procedures are trialed on a small number of welds made with a restricted amount of parent pipe. This will cause problems with introducing the processes to general use:

- The development welds will have been made under 'laboratory' conditions rather than on an actual construction spread. On a spread there will usually be adverse weather conditions and greater difficulty with alignment and root fit up.
- Typically only a small number of welds will be produced during a development program, often using only a single welding station. Hence the inherent variability of the welding process, equipment and operators may not be fully explored.
- The effects of variability (in dimensions, chemical composition and mechanical properties) of the parent pipe, both joint to joint and heat to heat, can not be explored unless a large amount of pipe is available. On a major project it is inevitable that pipe will be procured from more than one supplier, adding a further source of variability.

If these issues are not understood, problems will arise during the construction of major pipeline projects as the welding techniques developed in the laboratory are transferred into the field. This may result in costly delays to the project and the delivery of energy.

2 Objectives

The objectives of the project are:

- To test a large set of girth welds produced under realistic conditions by a state of the art high productivity GMAW system.
- To demonstrate the effect of material variability between pipes, between heats and between line pipe manufacturers.
- To assess the capabilities of commonly used weld defect assessment methods against the performance of a large set of welds made under field production conditions.

To achieve these objectives BP has provided the project with ten girth welds from the X100 operational trial. Following a review of a range of different methods for assessing the acceptability of a defect in a girth weld, a major test program was developed, which included 30 curved wide plate (CWP) tests. The tests were undertaken by Professor Rudi Denys and his colleagues at Laboratorium Soete, University of Gent, Belgium. The results from the test program were then assessed using different girth weld assessment methods, to determine whether they were suitable for assessing the performance of a girth weld defect in a pipeline constructed from grade X100 line pipe from multiple pipe sources.

This report is structured as follows:

- Section 3 provides an overview of US, European and Canadian girth weld assessment methods, and the US and European fracture mechanics assessment methods that are commonly used to assess the criticality of a girth weld defect.
- Section 4 provides an overview of the BP X100 operational trial, summarizing the construction of the pipeline sections and test conditions.
- Section 5 provides an overview of the criteria used to select the ten girth welds for testing.
- Section 6 provides a comprehensive overview of the small-scale tests undertaken to characterize each weldment.
- Section 7 provides a detailed overview of the CWP tests undertaken.
- Section 8 provides a summary of the results of the assessment undertaken of the CWP specimens using the methods presented in Section 3.
- Section 9 provides a discussion on the experimental work and subsequent analyses undertaken.
- Section 10 and Section 11 provide conclusions and recommendations, respectively.

The nomenclature and units (whether US Customary or SI) used to present the different assessment methods in Section 3 are consistent with the method being discussed.

Thereafter, presentation of the results from the material's test program and subsequent analysis of the data is provided in both US Customary and SI units, as appropriate.

3 Overview of Girth Weld Assessment Methods

There are a number of methods that are commonly used for the assessment of a girth weld containing a fabrication flaw. These range from the more generic *workmanship* (or *weld-quality*) defect acceptance limits to the more complex pipeline specific Engineering Critical Assessment (ECA) methodologies where defect acceptance limits are derived based on the pipe size, material properties and design loading conditions.

The defect acceptance limits specified in workmanship standards reflect the capabilities of radiography as the inspection technique for detecting and quantifying welding defects. These limits can be very conservative and may result in unnecessary and costly repairs. However, a benefit from application of these limits is that welding quality is maintained. API 1104 [5] was the first to adopt workmanship based limits for the evaluation of girth weld quality in 1953. Other, similar approaches have been developed over the years, such as those found in CSA Z662 [6], BS 4515 [7] and EPRG [8].

The ECA approach is widely used to derive girth weld defect acceptance limits unique to a pipeline. The recommended weld defect acceptance criteria are based on either analytical methods or on the analysis of the results of large-scale tests on pipeline girth welds. There is no one standardized method.

The EPRG approach is an example of an established methodology based on the results of large-scale tests, while commonly used pipeline specific analytical assessment methods include API 1104 and CSA Z662. Other commonly used analytical methods, which are more generic in application, include BS 7910 [9] and API 579-1/ASME FFS-1 [10].

The analytical ECA methods allow the maximum tolerable size of weld defects, including surface breaking and embedded circumferential defects, to be determined on a fitness-for-purpose basis using recognized and well-tried fracture mechanics methods. A typical ECA involves assessing the significance of such defects with regard to failure mechanisms that the pipeline may experience during construction, commissioning and service. These failure mechanisms include fracture and plastic collapse, under static loading conditions, and fatigue under cyclic loading conditions. The most commonly used approach to assess the significance of defects with regard to fracture and plastic collapse is the Failure Assessment Diagram (FAD), which was first introduced in the mid 1970's by the British Nuclear Industry [11]. The FAD approach involves the calculation of a fracture parameter, equal to the ratio of the elastic crack driving force to the material's fracture toughness, and a plastic collapse parameter defined as either the ratio of applied load to the limit load or, equivalently, the ratio of the reference stress to the yield strength. The reference stress characterizes the increase in stress in the vicinity of a defect due to the presence of the defect. The fracture and plastic collapse parameters are represented on a vertical axis and a horizontal axis, respectively. The axes are joined by a Failure Assessment Curve (FAC), which incorporates the effect of plasticity on crack driving force. If the assessment point, corresponding to the fracture and plastic collapse parameters, falls within the area bounded by the axes and the FAC, the defect is considered acceptable, otherwise the defect is deemed unacceptable, i.e., it could lead to failure. An example of a FAD is given in Figure 1.

By contrast EPRG is not based on the FAD. Instead, EPRG assumes failure will be by plastic collapse, and application of the method requires Charpy impact energy of the weldment to exceed 22(30)ft-lb (30(40)J) min(avg).

The following methods are described in more detail below; API 1104, EPRG, CSA Z662, BS 7910 and API 579-1/ASME FFS-1. Reference is also made, where appropriate, to proposed enhancements to the *standard* method, to extend the range of applicability of the assessment method to higher strength steels.

3.1 API 1104 Appendix A

API 1104 Appendix A [1] provides three options for the determination of acceptance limits for planar defects; Options 1, 2 and 3, in order of increasing complexity. The procedures are a comprehensive update to the previous edition [12], which comprised only one approach.

Use of the procedures is limited to the following conditions:

- Circumferential welds between pipes of equal nominal wall thickness.

- All welds are inspected.
- Maximum axial design stress (i.e., the maximum total axial stress at any given time during the design life of the pipeline) is not greater than the pipe specified minimum yield strength (SMYS).
- Maximum axial design strain is not greater than 0.5%.
- No gross weld strength undermatch (i.e., the weld tensile strength must not be less than the line pipe specified minimum tensile strength (SMTS), and the cross-weld specimen should not fail in the weld).
- No onerous fatigue crack growth in construction and under service conditions over its design life (provided the fatigue spectrum severity is not greater than 5×10^6 , and referenced fatigue crack growth curves are considered appropriate. The fatigue spectrum should consider, but not be limited to, stresses imposed during hydrotesting, operation, installation, maintenance, and where applicable, thermal, seismic and subsidence/ground movement).
- No sub-critical crack growth (e.g., creep and environmentally assisted crack growth).
- No dynamic loading.
- Welds in pump and compressor stations, repair welds, fittings and valves in the main line are excluded.

3.1.1 Option 1 Method

Option 1 is the simplest method and is given in graphical form. In addition to the general conditions specified above, use of Option 1 is limited to the following additional conditions:

- Minimum fracture toughness, expressed in terms of crack tip opening displacement (CTOD or δ), is not less than 0.004in (0.10mm).
- The min(avg) Charpy impact energy is greater than 22(30)ft-lb (30(40)J).

Two graphs are provided that give defect acceptance levels (defect height against length, normalized by the pipe wall thickness and pipe circumference respectively) at various applied load levels. The choice of which graph to use depends on the toughness of the weldment.

- CTOD greater than 0.004in (0.10mm) but not greater than 0.010in (0.254mm).
- CTOD greater than 0.010in (0.254mm).

Although not specified, it is assumed that the toughness limit applies to the lowest value of CTOD measured from a set of three 'valid' test results (i.e., results from specimens where the fatigue crack has sampled the same type and proportion of microstructure, and the results are within 'scatter' limits, such as those specified in BS 7910).

For the CTOD range 0.004 to 0.010in, critical defect size is dependent on toughness for deep defects, but plastic collapse controlled for shallow defects. The loci of allowable defect size as a function of load level were 'calibrated' to a CTOD of 0.004in. At this toughness level, the safety factor on defect length is approximately 1.5 (the safety factor increases with increasing toughness level).

For a CTOD greater than 0.010in the critical defect size is largely independent of toughness. The loci of allowable defect size as a function of load level were obtained from a plastic collapse solution, and a safety factor of 1.5 was applied to the computed defect length.

Interpolation between adjacent curves is recommended if the particular load level is not defined, alternatively the next higher load level curve is to be used.

The load level is defined as the ratio of the maximum allowable design stress to the material flow stress. The flow stress can be defined as the average of the yield and tensile strength. An alternative recommendation is an estimation procedure developed by Webster and Bannister [13].

For a given load level, the normalized defect height (up to 50% of the pipe wall thickness) can be determined for any normalized defect length up to 0.125 (i.e., 12.5%) of the pipe circumference.

The procedure does not discriminate between surface breaking and buried defects; they are treated the same.

A procedure is also provided for taking into account defect height uncertainty and inspection error for defining defect acceptance tables of allowable defect height and length.

Use of this procedure is demonstrated by a worked example; presented in API 1104, Appendix A, section A.5.1.2.2.

3.1.2 Option 2 Method

The FAD approach presented in API 1104 as Option 2 has been developed specifically for the assessment of defects in pipeline girth welds.

In addition to the limitations of the use of API 1104 Appendix A presented in Section 3.1, use of Option 2 is limited to the following additional conditions, at the minimum design temperature:

- Minimum CTOD is greater than 0.002in (0.05mm).
- The weld metal strength is not less than the strength of the line pipe.
- When defect free welds are tested, failure occurs in the base metal, NOT in the heat affected zone (HAZ) or weld metal.
- The applied longitudinal stress is not greater than SMYS and the applied longitudinal strain is not greater than 0.5%.

The FAC is taken from British Energy's R6 procedure [14] where it is defined as 'Option 1'.

The critical defect size is calculated iteratively using Equations [1] through to [16], given below. A summary of the assessment procedure recommended in API 1104 is as follows:

1. Select an initial defect size (it is suggested that the initial height should be a maximum or 50% of the pipe wall thickness).
2. Calculate the assessment point; K_r , L_r using the equations below.
3. If the assessment point lies within or outside the FAC, increase or decrease the defect length accordingly and repeat step 2 until the assessment point falls on the FAC. *This represents a critical defect height and length combination for the pipe size, material and loading conditions.*
4. Decrease the defect height (suggested increment of 5% of the pipe wall thickness), and repeat steps 2 and 3 until the critical length has been calculated.
5. Repeat for as many 'defect height' increments as required, and produce a table of critical defect height and corresponding length. Include a safety factor of 1.5 on defect length.

The total defect height and length should be no greater than 50% of the pipe wall thickness and 12.5% of the pipe circumference respectively.

As with Option 1, the procedure does not discriminate between surface breaking and buried defects; they are treated the same.

It is recommended in API 1104 that the assumed height uncertainty should be the lesser of 0.06in (1.5mm) and 8% of the pipe wall thickness. No reduction in allowable defect height is considered necessary if the allowance for inspection is better than the assumed height uncertainty.

The key components in the FAD procedure are provided below, taken directly from API 1104, Appendix A, section A.5.1.3.3. Additional information is provided for clarity.

The failure assessment curve is given by:

$$K_r = f(L_r) = (1 - 0.14L_r^2) [0.3 + 0.7 \exp(-0.65L_r^6)] \quad [1]$$

Where: K_r = The ratio of applied stress intensity factor to the material's fracture toughness
 L_r = The ratio of applied net section stress to the material's flow strength

The cut-off of the failure assessment curve on the L_r axis is given by:

$$L_r^{cut-off} = \frac{\sigma_f}{\sigma_y} \quad [2]$$

Where: σ_f = Flow stress (units: ksi)
 σ_y = Material's yield strength (units: ksi)

The flow stress is taken as the average of the specified minimum yield and tensile strength, SMYS and SMTS, or alternatively by:

$$\sigma_f = \sigma_y \left[1 + \left(\frac{21.75}{\sigma_y} \right)^{2.30} \right] \quad [3]$$

However, Equation [3] is applicable to line pipe of strength grade X52 up to X80.

The following procedure is used to determine the assessment point, K_r , where:

$$K_r = \sqrt{\frac{\delta_e}{\delta_{mat}}} \quad [4]$$

Where: δ_{mat} = CTOD – the fracture toughness of the material (units: in)
 δ_e = Elastic component of the CTOD driving force (units: in)

$$\delta_e = d_n \frac{J_e}{\sigma_y} \quad [5]$$

Where: J_e = Elastic component of the J-Integral (units: lb/in)
 d_n = J-Integral to CTOD conversion factor

$$d_n = 3.69 \left(\frac{1}{n} \right)^2 - 3.19 \left(\frac{1}{n} \right) + 0.882 \quad [6]$$

Where: n = Strain hardening exponent determined from the Ramberg-Osgood relationship (see Equation [7])

$$\varepsilon = \frac{\sigma}{E} + \left(0.005 - \frac{\sigma_y}{E} \right) \left(\frac{\sigma}{\sigma_y} \right)^n \quad [7]$$

Where: ε = Strain
 σ = Stress (units: ksi)
 E = Modulus of elasticity (units: ksi)

Equally, the strain hardening exponent may be estimated from the yield to tensile strength ratio, Y/T:

$$n = \frac{\ln\left(\frac{\varepsilon_t}{0.005}\right)}{\ln\left(\frac{1}{Y/T}\right)} \quad [8]$$

Where: ε_t = Uniform strain

API 1104 recommends the use of the following equation to determine the ratio Y/T for line pipe grades X52 up to X80:

$$\frac{Y}{T} = \frac{1}{1 + 2\left(\frac{21.75}{\sigma_y}\right)^{2.30}} \quad [9]$$

The uniform strain (commonly referred to as uEL), is estimated from:

$$\varepsilon_t = -0.00175\sigma_y + 0.22 \quad [10]$$

The elastic component of the J-Integral is given by:

$$J_e = \frac{K_I^2}{E/(1-\nu^2)} \quad [11]$$

Where: ν = Poisson's ratio

K_I is the Mode I stress intensity factor, given by:

$$K_I = \sigma_a \sqrt{\pi a} F_b \quad [12]$$

Where: σ_a = Applied stress (units: ksi)
 a = Defect height (units: in)
 F_b = A function depending on pipe diameter ratio, α , relative defect length, β , and relative defect height, η (see Equation [13])

$$F_b(\alpha, \beta, \eta) = \begin{cases} F_{bo}(\alpha, \beta, \eta) & \eta \geq 0.1, \beta \leq \frac{80\eta}{\pi\alpha} \\ F_{bo}\left(\alpha, \beta = \frac{80\eta}{\pi\alpha}, \eta\right) & \eta \geq 0.1, \beta > \frac{80\eta}{\pi\alpha} \\ F_{bo}\left(\alpha, \beta = \frac{80\eta}{\pi\alpha}, 0.1\right) & \eta < 0.1 \end{cases} \quad [13]$$

Where:

$$F_{bo}(\alpha, \beta, \eta) = \left(1.09 + 2.31\alpha^{0.791} \beta^{0.906} \eta^{0.983} + \frac{m_1}{\alpha\beta} + \alpha^{0.806} \beta m_2 \right) \quad [14]$$

$$m_1 = -0.00985 - 0.163\eta - 0.345\eta^2$$

$$m_2 = -0.00416 - 2.18\eta + 0.155\eta^2$$

The following procedure is used to determine the assessment point, L_r , where:

$$L_r = \frac{\sigma_a}{\sigma_c} \quad [15]$$

Where the reference stress (collapse stress), σ_c is given by:

$$\sigma_c = \begin{cases} \left[\frac{\pi}{4} + 385(0.05 - \eta\beta)^{2.5} \right] \left[\cos\left(\frac{\eta\beta\pi}{2}\right) - \frac{\eta \sin(\beta\pi)}{2} \right] \sigma_y & \eta\beta < 0.05 \\ \frac{\pi}{4} \left[\cos\left(\frac{\eta\beta\pi}{2}\right) - \frac{\eta \sin(\beta\pi)}{2} \right] \sigma_y & \eta\beta \geq 0.05 \end{cases} \quad [16]$$

The development and validation of the procedure is detailed in Reference [15]. The authors state that previous experimental validation of the procedure was limited to data from X70 or lower grade pipes, but that in the current project the procedure was validated against experimental data from X70 and X100 pipes. An example of the procedure is given in Appendix G of the report.

There have been some concerns raised over the application of the procedures, which resulted in several papers at the Pipeline Technology Conference (Ostend, Belgium, 2009). Some of the concerns raised are discussed below.

API 1104 does not explicitly state an upper limit on pipe grade, inferring that the procedure is suitable regardless of strength. However, an upper limit of grade X80 is specified for Equations [3] and [10].

The procedure makes use of the Ramberg-Osgood equation which is commonly used to describe the post-yield behavior of the line pipe material; both small scale and extensive yielding. However, the Ramberg-Osgood model cannot provide a good approximation for grade X100 line pipe since the post-yield behavior is complex, exhibiting what is termed 'double-n' behavior (i.e., two strain hardening exponents are required

to describe the full post-yield stress-strain response; one to describe small scale yielding behavior, and another to describe the extensive yielding behavior). Guidance on how to derive an appropriate strain hardening exponent for line pipe exhibiting this ‘double-n’ behavior is thus required.

Such a model has been developed by the University of Gent [16], which is capable of describing this ‘double-n’ type of behavior. The model is still based on the Ramberg-Osgood equation, but one equation is used to describe the small-scale yielding behavior, and a second equation is used to describe the extensive yielding behavior. A third equation provides a smooth transition between the two power law curves.

The University of Gent model was validated using 146 stress-strain curves of grade X60 up to X100, and the Y/T ratio varied from 0.68 to 0.94. The referenced paper presents a comparison between the conventional Ramberg-Osgood model stress-strain estimation, and the University of Gent model for eight stress strain curves that exhibit increasing double-n behavior to illustrate the increasing deficiencies of the Ramberg-Osgood model and the goodness of fit of the University of Gent model.

An additional area of concern is the use of Equation [10] to estimate uniform strain. Denys et al., [17] advise caution as the equation produces an ‘averaged’ fit to experimental data, and can therefore give an overestimate of uniform strain (i.e., un-conservative). They also propose that uniform strain cannot be estimated from yield strength alone and that consideration also needs to be given to the Y/T ratio. The authors propose the use of a set four equations that provide a lower bound experimental estimate of uniform strain from yield strength for specific Y/T ranges from a yield strength of 60ksi (415N/mm²) up to 108ksi (750N/mm²); grades X60 through to X100+:

$$\begin{aligned}
 uEL_{(for\ Y/T \leq 0.85)} &= 4.55 + \exp\left(\frac{600 - \sigma_y}{80}\right) - \frac{\sigma_y}{440} && \% \\
 uEL_{(for\ 0.85 < Y/T \leq 0.90)} &= 6.30 + \exp\left(\frac{505 - \sigma_y}{40}\right) - \frac{\sigma_y}{210} && \% \\
 uEL_{(for\ 0.90 < Y/T \leq 0.93)} &= 7.00 + \exp\left(\frac{500 - \sigma_y}{40}\right) - \frac{\sigma_y}{160} && \% \\
 uEL_{(for\ Y/T > 0.93)} &= 8.00 + \exp\left(\frac{490 - \sigma_y}{40}\right) - \frac{\sigma_y}{120} && \%
 \end{aligned}
 \tag{17}$$

Where: σ_y = Yield strength (units: N/mm²)

3.1.3 Option 3 Method

Option 3 is recommended when the pipeline is subjected to cyclic loading such that *significant* growth of the defect is expected during construction and under service conditions, over the design life of the pipeline.

API 1104 recommends the use of fracture mechanics assessment procedures such as those in BS 7910 (see Section 3.4).

A fatigue fracture mechanics analysis is also required to determine the ‘starting’ defect acceptance criteria (i.e., table of critical defect height versus length). The fatigue crack growth curve (i.e., Paris Law) used in the assessment must be appropriate for the type of service seen by the pipeline. Static fracture mechanics analyses are also required to ensure that failure of the proposed starting defect size does not occur before the end of the service life. If failure is predicted the starting defect size must be reduced so that the service life can be achieved.

3.2 European Pipeline Research Group

The EPRG guidelines for the assessment of defects in transmission pipeline girth welds were first published in 1996 [8]. The guidelines are structured in three Tiers and specify defect acceptance levels in Tier 1 (defined as *good workmanship*), and defect limits in Tiers 2 and 3 (based on *fitness-for-purpose*). The guidelines were the product of a literature review, and an extensive program of small- and full-scale tests. Use of the guidelines is dependent on the girth weld achieving a minimum toughness requirement; defect limits based on limit load/net section collapse calculations can then be used.

The guidance specifies both defect 'acceptance' levels (in Tier 1) and defect 'limits' (Tiers 2 and 3). The acceptance levels of Tier 1 are those considered by welding workmanship standards such as BS 4515 [18] and API 1104 [19]. Defects considered unacceptable to the workmanship limits of Tier 1 will require some remedial work to maintain good workmanship, but may not affect the fitness-for-purpose of the weld.

The defect limits of Tiers 2 and 3 are unlikely to be considered acceptable to Tier 1, but do not affect the fitness-for-purpose of the girth weld, and hence do not require repair.

Since the defect limits are based on experimental data generated as part of the project, and collected from external sources, the limits are restricted in part by empirical limits. For example, experimental data was available for pipes ranging in thickness from 0.276 to 1.00in (7 to 25mm), and in most cases the yield strength of the weld exceeded the yield strength of the parent pipe.

A brief description of each Tier is given below.

3.2.1 Acceptance Levels Based on Workmanship Limits (Tier 1)

Tier 1 limits can only be applied to pipeline girth welds if certain geometrical, toughness and strength requirements are achieved. Use of the limits is dependent on the Charpy impact energy of the weldment achieving a min(avg) of 22(30)ft-lb (30(40)J) in a full-size specimen, tested at the minimum design temperature of the pipeline. In addition full pipe wall thickness cross weld flat strap tensile specimens are required (note, the weld reinforcement must be removed prior to testing to avoid the influence of geometrical constraint). The tests are acceptable if the specimens fail in the weld metal, or in the weld with a tensile strength greater than the specified minimum tensile strength of the pipe.

The defect acceptance levels of Tier 1 are based on the good workmanship levels given in welding codes such as BS 4515 and API 1104.

It should be noted that use of these guidelines does not consider the effect of pressure cycling on the fatigue performance of the girth weld.

3.2.2 Defect Limits Based on Fitness-for-Purpose (Tiers 2 and 3)

The Tier 2 or 3 limits can be applied to pipeline girth welds provided the Tier 1 requirements (Charpy impact energy and cross weld tensile properties) are achieved, together with additional requirements, as detailed below:

- The pipe diameter must be greater than 30in (762mm).
- The wall thickness must be greater than 0.276in (7mm), but not greater than 1.00in (25mm).
- The yield to tensile strength ratio of the pipe must not be greater than 0.9 (i.e., $Y/T \leq 0.90$) for Tier 2, and 0.85 for Tier 3.
- Line pipe up to and including grade X70 (i.e., SMYS of 70ksi (483N/mm²)).

- The defect height does not exceed 0.118in (3mm) - i.e., the assumed height of a single weld run. Defects greater than 0.118in (3mm) in height, must either be repaired or subject to a more detailed assessment. Furthermore, coplanar defects in the through-thickness direction are required to be assessed for interaction using the procedures in PD 6493 [20].
- The yield strength of the weld metal must not be less than the yield strength of the pipe.
- The girth weld must be between pipes of equal grade and thickness, and be subjected to 100% non-destructive testing (NDT).
- For the application of Tier 2, the total applied axial strain (tension and bending) must not be greater than 0.5%.
- For the application of Tier 3, the total applied axial stress (tension and bending) must not be greater than the pipe yield strength.
- In addition to the Charpy impact energy requirement of 22(30)ft-lb (30(40)J), Tier 3 requires a min(avg) CTOD fracture toughness of 0.004(0.006)in (0.10(0.15)mm), at the minimum design temperature of the pipeline.

The defect limits are based on small-scale, wide plate and full-scale tests, BS 4515, PD 6493 and on a plastic collapse approach proposed by Kastner [21].

Guidance is provided on the shape and profile of the defect(s), cap and root undercut, planar and non-planar defects as well as adjacent defects in relation to interaction and accumulation. The focus of this review is on planar defects, which considers defects such as cap and root undercut, inadequate root penetration, incomplete/lack of fusion in the cap and/or root, cold laps, lack of side wall fusion and lack of inter-run fusion. The reader should refer to the EPRG guidance document for guidance on other types of welding defects.

The Tier 2 limits are expressed as a function of the pipe wall thickness, up to a maximum height of 0.118in (3mm). The length of the defect is limited to a maximum of 7 times the pipe wall thickness (i.e., 7t) per 12in (300mm) length of weld.

The Tier 3 limits are expressed as a percentage of the pipe circumference, and reference is made to Figure 1 of the guidance document which provides loci of defect length (normalized by the pipe circumference) as a function of pipe wall thickness for individual planar defects, total limit for all planar defects, and interacting planar defects. As an alternative to the Tier 3 defect limits, EPRG proposes that other recognized fitness-for-purpose methods can be used.

Since their introduction, EPRG member companies have increasingly used the Tier 2 guidelines as a basis for post construction defect assessment. Furthermore, the guidelines have been incorporated into the European standard for pipeline welding, EN 12732 [22] and the Australian pipeline code, AS 2885 [23]. Since early 2000, additional work has been undertaken to extend the Tier 2 guidance to include:

- Defect limits for girth welds in grade X80 pipelines
- Extension of the upper limit on pipe wall thickness from 1in (25mm) to 1.18in (30mm)
- Defect limits for defect heights up to 0.197in (5mm)
- Criteria to assess adjacent defects for interaction and determination of an effective defect size

These recommended revisions to the EPRG Tier 2 guidelines have recently been presented at two major conferences; Pipeline Technology Conference (Ostend, Belgium, 2009) [24] and the ASME International

Pipeline Conference 2010 (Calgary, Canada, 2010) [25]. A formal update of the original EPRG guidelines is yet to be published.

To summarize the development, the underlying available data for failure of welds has increased significantly since publication of the original guidelines. The revisions proposed were based on the results of a further 485 CWP test results held by University of Gent, of which 132 relate directly to X80 grade material.

A condition that is also recommended for new pipeline constructions is the requirement for the minimum weld metal yield strength to be no less than the line pipe SMYS plus five standard deviations (it is suggested that the standard deviation of yield strength is taken as 2.9ksi (20N/mm²)). The aim of this recommendation is to ensure that none of the welds along the pipeline spread undermatch the actual yield strength of either adjacent pipe length.

An increase in defect height limit from 0.118 to 0.197in (3 to 5mm) was motivated by the increasing use of AUT that, unlike radiography, provide an indication of defect height. When an allowance is made for tool sizing error, typically 0.039in (1mm), this could mean that the corresponding reported defect height is too restrictive. Accordingly, while the maximum allowable height has been increased there is a decrease in allowable length due to the same net-section collapse section being used to define the limits; the maximum allowable defect area of 7% in a 12in (300mm) arc length remaining the same.

The 132 X80 CWP tests undertaken confirmed that the net-section collapse solution used in the development of the original guidelines was still appropriate for matched and overmatched welds that exceeded the min(avg) Charpy requirements.

The following section details the assessment methodology for defining the defect limits, which are pertinent to the assessment undertaken as part of this work to investigate the applicability of the guidelines towards grade X100 pipelines.

3.2.3 Estimation of the Tier 2 Defect Size Limits

Provided that the weldment achieves/exceeds the Charpy impact energy requirement the defect size limits can be calculated using the standard net-section collapse model for a 'flat plate' containing a single defect loaded in tension, where:

$$\sigma_c = \sigma_f \left[1 - \frac{lh}{Wt} \right] \quad [18]$$

Where:

- σ_c = Applied remote tensile stress at collapse (units: N/mm²)
- σ_f = Flow stress (units: N/mm²)
- l = Defect length (units: mm)
- h = Defect height (units: mm)
- W = Plate width or arc length (units: mm)
- t = Pipe wall thickness (units: mm)

The flow stress is taken as the average of the yield and ultimate tensile strength.

When the applied axial stress is set to the pipe metal yield strength (i.e., $\sigma_c = \sigma_y$), Equation [18] can be re-arranged to predict the defect length as a function of pipe wall thickness, plate width (or arc length), and defect height, where:

$$l = \frac{Wt}{h} \left[1 - \frac{2\sigma_y}{\sigma_y + \sigma_t} \right] \quad [19]$$

Alternatively, if the Y/T ratio in the pipe axial direction is known, defect length can be calculated from:

$$l = \frac{Wt}{h} \left[\frac{1 - (Y/T)}{1 + (Y/T)} \right] \quad [20]$$

The defect is assumed to be rectangular in shape. This assumption is conservative for irregularly shaped defects, provided the maximum height is used in the assessment. Comparison of large diameter full-scale pipe bend tests and tension loaded CWP tests has shown that conservative predictions are obtained if the arc length of the CWP specimen is 12in (300mm), which equates to approximately 10% of the circumference of a large diameter pipe.

Regardless of the NDT method used, EPRG Tier 2 specifies that the through-thickness defect height must not be greater than 0.118in (3mm). From Equation [20], for a Y/T ratio of 0.87 and an arc length of 12in (300mm), the maximum allowable length of a defect height of 0.118in (3mm) is:

$$l = 6.95t \quad [21]$$

EPRG rounded this limit to $7t$, which gives a defect area limit of 7% per 12in (300mm) weld length.

By using the maximum allowable defect size, $7t \times 3\text{mm}$ (length \times height), it is assumed that a Charpy impact energy of 22(30)ft-lb (30(40)J) is achieved at the minimum design temperature, and the weld metal is not undermatching.

3.3 CSA Z662 Annex K

CSA Z662 Annex K provides a fracture mechanics based methodology for determining the maximum size of defect that a pipeline girth weld can tolerate.

For a given defect height the allowable defect length is the lesser of the maximum allowable defect length to prevent brittle fracture and the maximum allowable defect length to prevent plastic collapse, $L_1 \text{ max}$ and $L_2 \text{ max}$ respectively (defined below). Separate analyses are required; a brittle fracture assessment and a plastic collapse assessment. Regardless of the value of $L_1 \text{ max}$ and $L_2 \text{ max}$, the maximum allowable length is limited to 10% of the nominal pipe circumference. This limit was imposed because there were no full-scale fracture data to enable validation of the method for longer defects. Furthermore, it was considered that there was little practical need to consider them.

The methodology was developed specifically for pipeline girth welds and is based on the methods described in the 1980 edition of PD 6493 [20], which was replaced in 1999 by BS 7910. The current edition of CSA Z662 now references BS 7910:2005 [9]. The procedure was developed and validated in a major research program involving full-scale fracture tests of girth welds containing defects. The tests were performed using pipe with an outside diameter ranging from 20 to 42in (508 to 1067mm) with a wall thickness ranging from 0.268 to 0.591in (6.8 to 15.0mm), tested at temperatures as low as -121°F (-85°C). Most of the work was performed at the University of Waterloo and the Welding Institute of Canada and was sponsored by Nova Corporation of Alberta and the Pipeline Research Committee of the American Gas Association.

CSA Z662 specifies that a stress analysis must be undertaken to determine the axial and longitudinal stresses to which the weld will be subjected during construction and operation.

Where the axial stress is tensile, the value is to be multiplied by 1.5 and added to the longitudinal contribution of all other stresses (except for welding residual stresses since analysis of full-scale test results

showed that the effect of residual stress on the applied strain to failure was insignificant [26]) in order to determine the maximum effective applied tensile bending stress, which is an essential input in the assessment method.

Where the axial stress is compressive the value is added to the longitudinal contribution of all other stresses (except for welding residual stresses) in order to determine the maximum effective applied tensile bending stress.

The assessment method assumes that the defect is positioned at the location of maximum longitudinal tensile stress in the pipe subject to longitudinal bending. In such a situation the tensile stress decreases in the circumferential direction so that the ends of the defect are located in a region of tensile stress that is less than the maximum stress. This bending situation was also used in the aforementioned full-scale tests that were performed to establish the equations used in the analyses. When an axial stress is present, it is uniform around the circumference and, unlike a bending stress, does not decrease towards the end of a defect. Consequently the axial stress is considered to be equivalent to 1.5 times a bending stress with the same maximum value.

A fatigue analysis is not a requirement of CSA Z662 since the limit imposed on the maximum defect depth ensures that under the most severe fatigue loading caused by pressure fluctuations, the resulting stress intensity factor range at the tip of the defect would be less than the threshold for fatigue crack growth.

CSA Z662 also requires mechanical testing of the weldment:

- Tensile testing is to be undertaken to ensure that the measured yield strength of the weldment is not less than the specified minimum yield strength of the line pipe.
- Charpy impact tests are to be undertaken at the minimum design temperature of the pipeline. The specimens are to be orientated transverse to the weld and notched in the through thickness direction at the weld metal centre line. Section K.5.2 specifies a Charpy impact energy of 30ft-lb (40J), but it is not specified whether this is the minimum or average value.
- Fracture mechanics tests are to be undertaken according to *either* BS 7448:Part 2 [27] or ASTM E1290 [28] to determine values of CTOD at the minimum design temperature of the pipeline. The specimens are to be extracted from the weld 12 o'clock position and be orientated transverse to the weld. Rectangular Bx2B (where B is the specimen thickness) specimens notched in the through thickness direction sampling the weld metal centerline and the HAZ, and square section BxB specimens that are surface notched, sampling the weld metal at the weld root, and the position where the highest hardness was recorded (this usually relates to the lowest toughness region of the weld). There is no minimum CTOD requirement; the minimum measured value is used in the assessment to determine the maximum defect size.

Calculation of the maximum size of defect to prevent brittle fracture

Section K.5.3.3. of CSA Z662 outlines the procedure for determining the maximum size of defect for the avoidance of brittle fracture.

The first step in the analysis is to calculate an effective defect size parameter:

$$\bar{a} = C \frac{\delta}{\epsilon_y} \quad [22]$$

Where: \bar{a} = Effective defect size parameter (units: mm)

The parameter 'C' is given by the following:

$$C = \begin{cases} \frac{1}{2\pi \left(\frac{\sigma_a}{\sigma_y} \right)^2} & \text{for } \frac{\sigma_a}{\sigma_y} \leq 0.5 \\ \frac{1}{2\pi \left(\frac{\epsilon_a}{\epsilon_y} - 0.25 \right)} & \text{for } \frac{\sigma_a}{\sigma_y} > 0.5 \end{cases} \quad [23]$$

- Where:
- σ_a = Maximum effective applied tensile bending stress (units: N/mm²)
 - σ_y = Specified minimum yield strength of pipe (units: N/mm²)
 - ϵ_a = Maximum effective applied tensile bending strain
 - δ = CTOD (units: mm)
 - ϵ_y = Elastic yield strain (= σ_a / E)
 - E = Modulus of elasticity (units: N/mm²)

The next step depends on whether the defect is surface breaking or buried.

For surface breaking defects, the next step is to normalize \bar{a} with respect to the pipe nominal wall thickness, t . Then, using Figure K.4 of CSA Z662, determine the actual defect depth ratio, d/t (where d is defect depth, units: mm) for convenient values of the defect aspect ratio, d/L_1 (where L_1 is the defect length, units: mm). Eight loci are provided in Figure K.4 for d/L_1 ranging from 0.01, (i.e., a long shallow defect) up to 0.5 (i.e., a spherical defect).

This approach reflects the concepts and the approach of PD 6493, although for depth to length ratios less than 0.1, Figure K.4 varies from the equivalent figure in PD 6493. The aforementioned analysis of full-scale test data showed the equivalent curves in PD 6493 produce a minimum strain safety factor of less than 1 for long shallow defects [26]. The curves in Figure K.4 provide a more consistent and higher safety factor (2.0 to 4.3) on the strain to failure.

For buried defects, the next step is to calculate the parameter:

$$\frac{\bar{a}}{2\rho + d} \quad [24]$$

- Where: ρ = Minimum distance between the defect and the surface of the weldment (units: mm)

Then, using Figure K.5 of CSA Z662, determine the actual buried defect dimensions, $d/(2\rho+d)$ for convenient values of the defect aspect ratio, d/L_1 (where L_1 is the defect length). Six loci are provided in Figure K.5 for d/L_1 ranging from 0.0 (it should be noted that this curve is intended to represent a lower bound that is a *very small number*, rather than literally zero) up to 0.99 (i.e., a spherical defect).

Where the minimum ligament dimension between the defect and the surface of the weldment is equal to or greater than the defect height, then the defect is to be treated as a buried defect. However, if the minimum ligament dimension is less than the defect height, the defect is to be treated as a surface breaking defect with an effective height equal to the defect height *plus* the minimum ligament dimension.

Calculation of the maximum size of defect to prevent plastic collapse

Section K.5.3.4. of CSA Z662 outlines the procedure for determining the maximum size of defect for the avoidance of plastic collapse.

In the 2003 edition of CSA Z662 the procedure was replaced in its entirety. The original method used a modified ligament instability model and was considered valid when it was first introduced (failure is assumed to occur once the plastic zone size in the section containing the defect extends past approximately 10% of the pipe circumference). However, it was also recognized that the original approach was highly conservative.

Since the 1999 edition of CSA Z662 a considerable amount of work was undertaken by the pipeline industry and the Pipeline Research Council International, Inc (PRCI) which demonstrated that the Miller solution [29], with modifications, gave an appropriate and improved expression for determining the load for plastic collapse. This approach has been validated by many years of practical application, by detailed numerical analyses, and by comparison to full-scale fracture tests. The method recommended in CSA Z662 incorporates a safety factor of 2 on defect length and also uses a conservative definition of flow stress.

The maximum length of defect ($L_2 \max$) to prevent plastic collapse for each type, location and depth of defect is calculated using the following:

$$\frac{\sigma_a}{\sigma_f} = \begin{cases} \frac{\cos(\eta\beta\pi) - \frac{\eta \sin(2\beta\pi)}{2}}{1 + \left(\frac{4}{\pi} - 1\right) \frac{\eta\beta}{0.025}} & \text{for } \eta\beta \leq 0.025 \\ \frac{\cos(\eta\beta\pi) - \frac{\eta \sin(2\beta\pi)}{2}}{\frac{4}{\pi}} & \text{for } \eta\beta > 0.025 \end{cases} \quad [25]$$

Where: σ_a = Maximum effective applied tensile bending stress (units: N/mm²)
 σ_f = Flow stress (units: N/mm²)

The relative defect depth, η is given by:

$$\eta = \frac{d}{t} \quad [26]$$

Where: d = Defect depth (units: mm)
 t = Nominal pipe wall thickness (units: mm)

The relative defect length, β is given by:

$$\beta = \frac{2c}{\pi D} \quad [27]$$

Where: $2c$ = Defect depth (units: mm)
 D = Pipe outside diameter (units: mm)

Note, in the current edition of API 1104, π is missing from the expression for β .

The maximum defect length $L_2 \max$ is $2c_{max}$, which is determined iteratively by plotting the relationship between η and β for a series of σ_d/σ_f values.

3.4 Alternative Methods Based on Fracture Mechanics

3.4.1 BS 7910

BS 7910 is the British Standard for undertaking a fracture mechanics based engineering critical assessment of the significance of defects in metallic structures. The document was initially published in 1980 as PD 6493 [20].

BS 7910 provides guidance on fracture assessments using the FAD approach and fatigue assessments using the Paris Law. The guidance is thorough and versatile, but can be relatively complex to apply since it requires a high level of proficiency in fracture mechanics and a multi-disciplinary understanding of the parameters required to conduct an assessment. In comparison with pipeline-specific ECA procedures, such as those of API 1104 and EPRG, BS 7910 can offer more versatility and permit a wider range of conditions (including joint and defect geometry, loading type, material properties, and failure mechanisms) to be assessed.

There are three levels of fracture assessment in BS 7910, the choice of level depends on the materials involved, the input data available and the conservatism required:

- Level 1 – is a simplified assessment method applicable where there is limited information available on material properties or applied stresses
- Level 2 – is the normal assessment method and is used where single value measurements of fracture toughness are available
- Level 3 – is appropriate for ductile materials and enables a tearing resistance analysis to be undertaken

3.4.1.1 Level 1

Level 1 contains two methods; Level 1A and 1B. Conservative estimates of applied stresses, residual stress and fracture toughness are used. The Level 1A method is based on a conservative FAD and the FAC is a rectangle. Level 1B is a manual estimation method and does not employ an FAD. It is this method that is used in CSA Z662 to determine the maximum size of defect to prevent brittle fracture

3.4.1.2 Level 2

There are several options for defining the FAC, which joins the fracture axis to the plastic collapse axis of a FAD, depending on the available data and required accuracy. Greater accuracy may be achieved if the FAC is based on the actual stress-strain curve of the material. There are two assessment methods; Level 2A and 2B:

- Level 2A – a generalized FAD, for continuous or discontinuous yielding
- Level 2B – a material specific FAD for continuous or discontinuous yielding

The generalized Level 2A FAD requires knowledge of the yield and tensile strength of the pipe material and whether the stress-strain response of the pipe includes a yield discontinuity. The material-specific Level 2B FAD can be constructed using stress-strain curves, with and without a yield discontinuity.

The material-specific Level 2B FAD provides a less conservative result than the generalized FAD. However, caution should be exercised when constructing a material-specific FAD for the assessment of a pipeline girth weld. Stress-strain curves from the longitudinal direction are required; sufficient tests should be undertaken to ensure that the variations in pipe properties around the circumference and between different heats are taken into account. The curve used to construct the FAD should be defined such that it provides a lower bound to all other curves. The assessment can be further refined if overmatching is taken into account. However, there are no published generalized mismatch limit load solutions (that are required to define a mismatch value of L_r) for circumferential finite length part-thickness flaws in cylinders.

The assessment uses a single-point value of fracture toughness, which is taken as the lowest of δ_c , δ_u or δ_m when expressed in terms of CTOD (or the corresponding value in terms of J). These data are generally determined from standardized single edge notch bend (SENB) specimens tested in accordance with BS 7448:Part 2 or an equivalent standard. However, as a result of a joint industry project conducted by SINTEF, TWI and Det Norske Veritas (DNV) and the publication of its findings as a DNV Recommended Practice, RP-F108 [30], single edge notch tension (SENT) specimens are increasingly used in the offshore pipeline industry to determine fracture toughness for assessing pipelines subjected to significant plastic straining. This is because the SENT specimen can provide a 'less conservative' and 'more realistic' estimate of the toughness of a girth weld as the applied load is similar; an SENT specimen is loaded in tension, a pipe is predominantly loaded in tension, an SENB specimen is loaded in bending.

Consideration also needs to be given to the effect of welding residual stresses, transverse to the girth weld. BS 7910 requires that these are included in a fracture assessment and provides guidance covering welds in the as-welded and post-weld-heat-treated conditions, including models to allow for relaxation of residual stresses due to proof loading and/or interaction with applied (mechanical) stresses. The conservative option is to assume that the welding residual stress is constant through the pipe wall and has a magnitude equal to the yield strength of the weaker of the pipe and weld metals. Alternatively, residual stress profiles recommended in Annex Q of BS 7910 can be used.

3.4.1.3 Level 3

The Level 3 method is appropriate for ductile materials that exhibit stable tearing (or a material that fails in a brittle manner following a period of ductile tearing). There are three assessment methods; Level 3A, 3B and 3C. Each assessment method uses a different assessment curve and applies a ductile tearing analysis. The analysis results in a plot of either a single assessment point or a locus of points. For the ductile tearing analysis, the fracture toughness is required in the form of a δ (or J) tearing resistance curve, which is generally determined from standardized SENB specimens tested in accordance with BS 7448:Part 4 [31] or an equivalent standard. The Level 3 assessment methods are:

Level 3A – employs the generalized FAD of Level 2A (i.e., not requiring stress-strain data).

Level 3B – employs the material specific FAD of Level 2B.

Level 3C – J-Integral. A FAD specific to the material and component geometry is obtained by determining the J-Integral using both elastic and elastic-plastic finite element analysis of the component containing the defect and subjected to specific loads of interest.

3.4.1.4 Fatigue Assessment

Although not explicitly mentioned above when describing the different assessment levels, BS 7910 also provides comprehensive guidance for undertaking a fatigue assessment, which is based on the Paris Law.

Recommendations are available in the form of simple laws and a more precise 2-stage relationship. For the latter, both the mean and mean+two standard deviations curves are given for an R ratio (i.e., the ratio of

minimum to maximum applied stress during fatigue loading) less than 0.5, and R greater than 0.5. However, for conservatism BS 7910 recommends the use of the mean+two standard deviations curve (R greater than 0.5) for the assessment of welded components, which allows for the influence of residual stresses.

Consideration is also given to environmental influences; the guidance covers marine corrosion, with and without cathodic protection, and fatigue crack growth at elevated temperature.

Alternatively, if a fatigue crack growth law applicable to the material and service conditions is available, this may also be used.

3.4.2 API 579-1/ASME FFS-1

API 579-1/ASME FFS-1 is the API/ASME standard for undertaking a fitness-for-service assessment. The document is comprehensive and provides guidance for the assessment of a range of different defect and damage types, under static, fatigue or creep loading conditions. Part 3 of the document is concerned with the assessment of brittle fracture, and Part 9 is concerned with the assessment of crack-like flaws.

Similar to the BS 7910 approach, API 579-1/ASME FFS-1 provides guidance on fracture assessments using the FAD approach, and fatigue assessments using the Paris Law. API 579-1/ASME FFS-1 also has three assessment levels, however, they are different to those specified in BS 7910. The levels in API 579-1/ASME FFS-1 are:

- Level 1 – assessments are limited to crack-like defects in pressurized cylinders, spheres or flat plates.
- Level 2 – can be used for general shell structures including crack-like defects located at structural discontinuities. Detailed information on material properties and loading conditions is required, and stress analysis (based on code equations, closed form solutions, or a numerical analysis) is required to determine the state of stress at the location of the defect.
- Level 3 – can be used to assess those cases that do not meet the requirements for Level 1 or 2 assessments. Level 3 is also used for the assessment of defects that may grow in service due to loading or environmental conditions.

3.4.2.1 Level 1

The applicability of this assessment procedure is subject to a number of limitations, which, in relation to a pipeline, include:

- Dynamic loading effects are not significant (e.g., earthquake, impact, water hammer, etc).
- The loading conditions and/or environment will not result in crack growth.
- The pipe diameter to wall thickness ratio (D/t) is not less than 10.
- The pipe wall thickness, at the defect location, is not greater than 1.5in (38mm).
- Defect length is not greater than 8in (200mm).
- The defect must be perpendicular to a principal stress direction (else defect projection rules must be applied), and at a specified distance from a major structural discontinuity.
- Internal pressure loading only (producing only membrane stresses).
- The membrane stresses are within the limits of the original pipeline design code.

- If the defect is to be subjected to a pressure test, the metal temperature of the component must be above the MAT (i.e., the Minimum Allowable Temperature; the lowest possible metal temperature for a given material and thickness based on its resistance to brittle fracture) during the test, and the defect should be re-examined after the test to ensure that it has not increased in size.
- The weld joint is either a single- or double-V configuration (the residual stresses are based on Annex E of the document).
- The SMYS and SMTS of the base material must be less than 40ksi (276 N/mm²) and 70ksi (483 N/mm²), respectively, and the weld is produced using an electrode compatible with the base metal.
- The fracture toughness of the weldment exceeds K_{IC} (which is a size independent, lower bound value of fracture toughness).

The assessment is based on screening charts; the selection of which depends on the orientation of the defect. The chart provides loci of acceptable defect sizes (height and length), for defects located in the base metal or weld metal (with or without post weld heat treatment). Use of these charts requires a reference temperature to be determined, procedures for which are also provided.

If the actual defect size is less than the acceptable defect size, determined using the screening charts, the defect is considered to be safe, and the pipeline is acceptable for continued service. Otherwise, the input data used in the assessment can be refined and the analysis repeated, the pipeline can be re-rated or the defective weld repaired, or a Level 2 or 3 assessment can be undertaken.

3.4.2.2 Level 2

The applicability of this assessment procedure is subject to the following limitations:

- Dynamic loading effects are not significant (e.g., earthquake, impact, water hammer, etc).
- The loading conditions and/or environment will not result in crack growth.

The Level 2 assessment procedure provides a better estimate of the structural integrity of a component with a crack-like defect, than a Level 1 assessment. This procedure makes use of partial safety factors to account for the uncertainty with some of the inputs in the assessment (e.g., defect size, material properties, and applied loadings).

The following information is required to undertake an assessment:

- Determine the stress distribution(s) at the defect location and classify them into Primary, Secondary and Residual stresses.
- Determine the material properties for the conditions being assessed; tensile properties (this can be measured values or specified minimum values) and material fracture toughness (this can be actual or mean values, or a lower bound estimate).
- Defect dimensions from the inspection data.

The above are then required to be modified by applying an appropriate partial safety factor to each input; API 579-1/ASME FFS-1 provides details of how this is done.

The next stage in the assessment is to calculate the assessment point for the FAD, from the above modified inputs. The abscissa of the FAD is the load ratio which is calculated from the reference stress for primary loads and the material yield strength, where:

$$L_r^p = \frac{\sigma_{ref}^p}{\sigma_{ys}} \quad [28]$$

The ordinate of the FAD is the toughness ratio which is calculated from the stress intensity factor (K_I) and material toughness (K_{mat}). The stress intensity factor comprises two parts; that due to the modified primary stress and modified defect size, denoted K_I^p and that due to the secondary and residual stresses and modified defect size, denoted K_I^{SR} . The toughness ratio is thus calculated from:

$$K_r = \frac{K_I^p + \Phi K_I^{SR}}{K_{mat}} \quad [29]$$

The Φ term is a plasticity correction factor, which takes account of the interaction between fracture and plasticity.

A step by step procedure is provided in API 579-1/ASME FFS-1, section 9.4.3 for deriving all of these quantities, with reference given to Appendices C and D for stress intensity and reference stress solutions, respectively.

The Level 2 FAD is defined using the following equation:

$$K_r = \left(1 - 0.14(L_r^p)^2\right) \left(0.3 + 0.7 \exp\left[-0.65(L_r^p)^6\right]\right) \quad \text{for } L_r^p \leq L_{r(\max)}^p \quad [30]$$

If the assessment gives an 'unacceptable' result, as with the Level 1 procedure the input data used in the assessment can be refined and the analysis repeated, the pipeline can be re-rated or the defective weld repaired, or a Level 3 assessment can be undertaken.

3.4.2.3 Level 3

The Level 3 assessment procedure provides the best estimate of the structural integrity of a component with a crack-like defect. In addition, this method is required for the assessment of crack growth. This procedure should be used when the Level 1 or 2 methods cannot be applied, or produce overly conservative results. A Level 3 assessment is also typically required when; an advanced stress analysis is required to determine the applied stresses; the defect is growing (or anticipated to grow) in service and a remaining life assessment or on-stream monitoring is required; or if high gradients in stress, material fracture toughness, or material and/or tensile strength exist at the location of the defect (e.g., mismatch between the weld and base metal). There are five methods in a Level 3 assessment:

- Method A – Based on the Level 2 assessment procedure, except that the FAD is used for the acceptance criteria with user specified partial safety factors based on a risk assessment. Alternatively a probabilistic analysis can be undertaken.
- Method B – Based on the Level 2 assessment procedure, except that the FAD is constructed based on the actual material properties. The method can only be used for the assessment of crack-like defects in the base or weld metal as it requires a material specific stress-strain curve to define the FAD. This method should not be used for the assessment of defects in the HAZ.
- Method C – Based on the Level 2 assessment procedure, except that the FAD is constructed based on the actual loading conditions, component geometry and material properties. This method requires the use of partial safety factors or undertaking a probabilistic analysis.

- Method D – a ductile tearing analysis where the fracture tearing resistance is defined as a function of the amount of stable ductile tearing. This method requires the use of partial safety factors or undertaking a probabilistic analysis.
- Method E – Recognizes the use of alternative assessment methods such as BS 7910, subject to supplemental requirements that may include the use of partial safety factors or a probabilistic analysis.

4 Source of Material for Testing

The girth welds for testing were provided by BP from a recently completed full-scale operational field trial of a pipeline constructed from grade X100 line pipe. The 'X100 operational trial' involved laying 2,625ft (800m) of 48in (1220mm) diameter, 0.78in (19.8mm) nominal wall thickness pipe in two sections. Section A was approximately 1,970ft (600m) in length and Section B approximately 655ft (200m) in length [2].

The pipeline test sections were designed to ASME B31.8 [3] to a design factor of 0.8, with additional guidance taken from CSA Z662 [4]. BP arranged the manufacture and coating of the line pipe. The pipe was coated externally with a single layer fusion bonded epoxy (FBE) coating and internally with a flow coat. Two pipe mills produced the test pipes from three plate suppliers (A, B and C) and the arrangement of the pipe joints in the test sections took account of the need to ensure that both sources were equally subjected to all the test conditions prescribed.

As far as was practicable, mainline construction methods were used, similar to those which would be expected to be used on future pipeline projects using this material. Section A was constructed to 'good pipeline practice' to simulate a pipeline in normal service and a normal cathodic protection (CP) level was maintained along its length. In contrast, Section B incorporated numerous instances of pipeline defects and damage and the CP level was varied along its length:

- A third of the length of the test section had no cathodic protection applied during the trial and had remained at the pipe's free corrosion potential (-0.676 to -0.798mV with respect to a copper/copper sulphate reference electrode).
- The middle third of the test section had cathodic protection applied at a polarized potential of approximately -850 to -950mV (intermediate potential).
- The polarized potential on the remainder of the test section was adjusted to cover the range -1200 to -1300mV (high potential)

The pipe sections were subjected to a hydrostatic pressure test on commission to the requirements of ASME B31.8. The test pressure was 225 barg, equivalent to 1.25 times the design pressure. Both pipe sections were then subjected to accelerated pressure cycling for a two year period to simulate a 40 year design life plus a 20% life extension (i.e., 48 years total service life).

Details of the construction of the pipeline test sections that is considered pertinent to this project are summarized below.

4.1 Pipeline Welding

One of the objectives of the operational trial was to utilize the latest welding technology which might be used on a real pipeline construction project.

A comprehensive overview of the construction of the pipeline sections is given in a recent publication that was presented at the 8th ASME International Pipeline Conference (IPC2010), Calgary, Canada [2]. A brief summary is provided below.

The project specification was based on API 1104 [32], supplemented with additional requirements for X100 by BP.

Qualification of the mainline welding procedure was carried out in the Serimax workshops at Mitry Mory (near Paris), in 2006. The test welds were produced on short lengths of line pipe from the operational trial. A hydraulic pipe facing machine was used to produce a 5° narrow gap, J-prep weld bevel design (see Figure 2).

The root pass was made using a single wire pulsed GMAW technique and the internal line-up clamp was released after 100% completion of the hot pass. Tandem P-GMAW (Pulsed Gas Metal Arc Welding) was used for the hot pass, fill and cap. The welding parameters are summarized in Table 1.

For the production main line welds an industry standard pipe-facing machine was used to bevel the pipe ends which were then preheated using an oxy-propane flame torch prior to making up the joint, and again just prior to welding, if needed. A pneumatic internal line-up clamp was used to set the joint for welding; resulting in pipe to pipe misalignment of less than 1mm.

In addition, tie-in and fabrication welding procedures were also produced. Only the tie-in procedure specific to a weld tested in this project is summarized below. The reader is directed to the aforementioned IPC2010 publication for details on the other procedures developed.

The pipe ends for the tie-in welds were prepped with a 28° single bevel which was produced by flame-cutting and grinding. This was to simulate the field welding procedure. Line-up was achieved using a combination of an external clamp and '*bullet tacks*' to give a root gap of 0.12 to 0.18in (3.0 to 4.5mm). Preheat was applied using propane flame torches.

The root pass was deposited using semi-automatic STT® (Surface Tension Transfer®) with a vertical-down progression. Lincoln Pipeliner 80SG wire, powered by an Invertec II machine, was used for the root pass. The wire diameter was 0.04in (1.0mm), and the AWS classification is A5.28 ER80S-G.

The hot pass, fill and cap were made using mechanized Flux-Cored Arc Welding (FCAW) with a vertical-up progression. The wire chosen for the mechanized FCAW tie-in welding was Tubrod OK15.09; a 0.05in (1.2mm) diameter, 3% Ni wire with a rutile flux, which was manufactured by ESAB. The EN classification for this wire is T 69 4 Z P M 2 H5. For simplicity, the same shielding gas mixture (82% Ar 18% CO₂) was used for all weld procedures developed. The welding parameters are summarized in Table 2.

Sufficient welds were made to qualify the three pipe sources and each weld was inspected visually and using X-radiography in accordance with the project specification. Mechanical testing comprised all weld metal tensile testing, Charpy impact testing, fracture toughness testing and hardness surveys.

4.2 Inspection of Girth Welds

A total of 58 main line tandem GMAW welds were produced. Inspection was undertaken during construction using X-radiography with a single wall single image '*panoramic*' technique. The welds were sentenced according to workmanship criteria given in GIS-43 331 [33]; no weld repairs were required.

A total of four tie-in welds were produced. Each weld was inspected by double wall single image radiography and found to be acceptable to the aforementioned specification.

AUT (Automated Ultrasonic Testing) was carried out on all of the mainline girth welds using a phased-array system. Calibration was based on a 0.08in (2mm) flat-bottomed hole and the reporting threshold was set at

40% FSH. All indications above the recording threshold of 40% FSH were evaluated with respect to position and characteristics. However, the results were presented for information only, and as such no acceptance criteria were applied.

The most common indication was lack of side-wall fusion (LOSWF); which is typical of low heat input narrow gap welding processes. Several instances of lack of inter-run fusion (LOIRF) were also reported; each of which was found to occur at the sides of the weld (i.e., at the weld 3 and 9 o'clock positions).

5 Identification of Girth Welds for Testing

The two pipeline sections of the X100 Operation Trial comprised 79 girth welds in total; Section A had 58 girth welds (51 off X100-X100 welds and 7 off X100-X80 welds), and Section B had 21 (19 off X100-X100 welds, and 2 off X100-X80 welds). Following approval by BP, this project was to be provided with up to ten of the welds for detailed testing. Selection of those welds considered to be of most benefit to the project was based on the following criteria:

1. Weld type (e.g., mainline, tie-in)
2. The level of weld strength overmatch (i.e., comparison of the all weld metal strength with the strength of the abutting pipes)
3. Identification of the pipe supplier and pipe heat number to ensure that the pipes selected were sufficient to test a 'wide' range of pipeline properties
4. Comparison of the AUT and radiographic inspection records so that consideration could be given to the type and size of defects present

The following information was provided to the project by BP to enable the review and selection process:

1. As-built weld map
2. Line pipe tensile properties from production tests
3. Weld procedure qualification test data
4. AUT close out report which provided a comparison and summary of the results of the radiographic and AUT inspections

The line pipe tensile properties from the production tests were obtained from round bar and flat strap specimens extracted from the pipe longitudinal direction, and round bar specimens extracted from the pipe transverse direction.

The all weld metal tensile properties were obtained from prismatic tensile test specimens; a client requirement for the weld procedure qualification testing undertaken.

A full appraisal of the tensile properties (from the pipe production test records and weld procedure qualification testing) and the radiographic and AUT inspection findings for all welds was thus undertaken and on the basis of that analysis the following welds were selected for detailed testing:

Weld ID	Type	Pipe Source	Same heat?	Comment
A06	Mainline	Source B Source B	Y	Small scale tests and CWP tests
A17	Tie-in	Source C Source C	Y	
A33	Mainline	Source B Source A	N	
A44	Mainline	Source C Source B	N	
A46	Mainline	Source C Source C	N	
A50	Mainline	Source B Source B	N	
B03	Mainline	Source C Source C	N	Small scale tests and CWP tests Contains deliberate welding defects
B06	Mainline	Source A Source B	N	
B08	Mainline	Source C Source C	N	
B10	Mainline	Source A Source C	N	Detailed tensile testing

6 Material’s Test Program

A comprehensive material’s test program was developed, which comprised a series of small-scale tests (tensile, Charpy and fracture mechanics tests) and mid-scale CWP tests to fully characterize the defect tolerance of grade X100 line pipe, and enable an assessment of the validity of existing girth weld acceptance standards for high strength steel pipelines.

The CWP specimen was first developed by Laboratory Soete (University of Gent, Belgium) in 1979 to study the structural relevance of girth welds with low fracture toughness. Since 1979, Laboratory Soete has undertaken in excess of 1,000 tests to study the effects of the following on the strain capacity of girth welds containing a single or multiple defect(s):

- Weld metal strength mismatch
- Toughness
- Flaw type (surface breaking and embedded defects) and size
- Interaction of adjacent defects
- Y/T ratio and strain hardening capacity

In the mid 1990’s the CWP test data were used to develop the EPRG Tier 2 defect acceptance levels for stress-based design and the girth weld toughness requirement; min(avg) Charpy impact energy of 22(30)ft-lb (30(40)J), to ensure failure by plastic collapse at strains not less than 0.5% [34]. However, this is

based on the defect area ratio being not greater than 7% of the specimen cross section area, the Y/T ratio being not greater than 0.9, and the weld strength being not less than the pipe strength. More recently a revision to the EPRG guidelines has been recommended to extend the guidelines to higher strength steels; grade X80 line pipe, based on the results of a significant number of CWP tests [35].

Over the last decade the CWP test specimen has evolved into a widely applied test method for:

- Optimizing material requirements and strain based defect acceptance procedures
- Characterizing the failure behavior of girth welds and determining the maximum (limit) strain capacity
- Quantifying the effect of weld strength mismatch and tearing behavior
- Validation of numerical methods / defect assessment methods

To fully characterize the behavior of a girth weld it is necessary to undertake a series of small scale tests to determine the variability in mechanical properties of the base metal (parent pipe) and weld metal around the circumference of the pipe, and adjacent to the position where the CWP specimen(s) was/were extracted.

The small scale test program comprised the following:

- Weld macro-sections (generally at the weld 12, 3 and 6 o'clock locations)
- Tensile tests – the pipe and weld metal tensile properties and the shape of their post yield stress-strain response are critical variables to enable the level of weld strength mismatch to be determined and to quantify the measured strain capacity. The following tests were undertaken at ambient laboratory temperature:
 - Base metal 'full thickness' strip specimens, extracted from both the longitudinal and transverse directions of each pipe
 - Base metal 'round bar' specimens, extracted from the transverse direction of each pipe
 - All weld metal 'round bar' specimens, extracted from the weld cap and weld root regions
 - Cross-weld 'full thickness' strip specimens
- Charpy impact tests – the Charpy impact energy of the weldment (weld metal and HAZ) is measured at the minimum design temperature of -4°F (-20°C) using full size specimens with a through-thickness notch in the weld direction. The tests will be used to confirm the mode of failure (ductile, brittle, or within the ductile-brittle transition region) and whether the weldment achieves the 22(30)ft-lb (30(40)J) Charpy impact energy requirement of EPRG and API 1104. CSA Z662 specifies a Charpy impact energy of 30ft-lb (40J), although it is not stated whether this is a minimum or average requirement.
- Fracture toughness tests – the fracture toughness of the weldment (weld metal and HAZ) is measured at the minimum design temperature of -4°F (-20°C) using rectangular (Bx2B, where B is thickness) SENB specimens with a through thickness notch in the weld direction. Although not a requirement for an EPRG assessment, it is required for an assessment to API 1104 and CSA Z662. Furthermore, when undertaking a fracture mechanics assessment using procedures such as BS 7910 [9] and API 579-1/ASME FFS-1 [10], a value of fracture toughness is a necessary input in the assessment.

The type, position (around the pipe circumference) and number of tests undertaken was not the same for each weld selected for testing. Depending on the results of some of the initial tensile tests undertaken, either 3 or 4 CWP tests were undertaken per weld. Consequently, this impacted on the number and position

of the remaining small scale test specimens. Furthermore, due to the variation in all weld metal tensile properties that was observed around the circumference of the weld, weld B10 was utilized for detailed tensile testing, using different types of test specimen at different through-wall locations. At equi-spaced increments around the circumference of weld B10, all weld metal round bar specimens were extracted from the weld root (11 specimens), approximate mid thickness (11 specimens) and weld cap regions (11 specimens). In addition, at the same circumferential positions, 11 prismatic (rectangular) specimens were extracted that sampled almost the full weld depth and thickness. To compliment the series of tensile tests undertaken, macro-sections were taken at each location and a through wall thickness hardness survey was undertaken on each section, at the weld centre-line.

Figure 3 shows a typical girth weld cutting plan and approximate location of the different types of test specimen in relation to the CWP test specimen. The exact specimen type, orientation, location and number of each test specimen extracted from each weld is summarized in Table 3.

The position of each specimen is referenced to a mark that was '*hard stamped*' onto the pipe surface as a zero datum and direction indicator for the radiographic inspection. The mark was positioned at the weld top-dead-center (i.e., the weld 12 o'clock position), and increased in the clockwise direction when viewed in the direction of the pipe lay.

The following sections describe the test methods and results obtained from the test program.

6.1 Weld Macro-Sections

In general three longitudinal cross sections (i.e., transverse to the girth weld) were extracted from each weld, adjacent to where each CWP was extracted, for macroscopic examination. Each cross section was ground, polished and etched using a 2% nital solution to reveal the weld, HAZ and surrounding microstructure, and then photographed. The macro section photographs are presented in Appendix A and show the weld pass sequence, macrostructure of the as-deposited and re-heated weld metal regions, the fusion line profile and the extent of the HAZ.

In addition, eleven longitudinal cross sections were extracted from weld B10, at equi-spaced increments around the pipe circumference, for macroscopic examination. The macro-section photographs are presented in Appendix A.

The reinforcement of the weld cap was measured and found not to exceed 3mm, which is the upper limit specified in API 1104. In addition the reinforcement of the weld root was measured and found not to exceed 2mm.

With the exception of the tie in weld (A17), weld bead height was found to be dependent on sampling position; around 3 and 9 o'clock positions the beads were thinner towards the outer diameter with corresponding changes in the amount of grain refined weld metal. The bead height of weld A17 showed little variation around the weld circumference.

6.2 Hardness Surveys

A Vickers hardness survey was undertaken for each weld, on each macrosection (see Section 6.1). A 10kg load was used throughout. Measurements were undertaken according to EN 1043-1:1996 and ISO 6507-2 comprising three traverses parallel to the pipe surface; 0.06in (1.5mm) below the weld cap, at the pipe mid-wall thickness and 0.06in (1.5mm) up from the weld root. Each traverse comprised 11 hardness measurements; Indents 1 (Pipe 1 parent), 2-4 (Pipe 1 HAZ), 5-7 (weld metal), 8-10 (Pipe 2 HAZ) and 11 (Pipe 2 parent). For each weld, the individual hardness measurements are presented in Appendix A,

together with the weld macro-section and a plot of the data to show the variations in hardness through the weldment.

The hardness values, averaged through the pipe wall thickness (i.e., weld cap, root and mid-thickness), are summarized in Appendix A, Table A10. As can be seen;

- The average pipe metal hardness ranged from 295-297 HV10 for Pipe A, 272-300 HV10 for Pipe B and 271-291 HV10 for Pipe C
- The average HAZ hardness ranged from 279-282 HV10 for Pipe A, 263-292 HV10 for Pipe B and 252-272 HV10 for Pipe C (excluding weld A17). The average hardness of the HAZ of the tie in weld A17 was lower, ranging from 248-251 HV10
- The average HAZ hardness was found to be consistently lower than the average pipe metal hardness for each pipe source, inferring HAZ softening in all welds. As can be seen, Pipe C appears to have a higher sensitivity to HAZ softening
- There was very little variation in average weld metal hardness, ranging from 290-296 HV10 (excluding weld A17). As can be seen, the average weld metal hardness is similar, if not greater than the corresponding pipes
- The average weld metal hardness of the tie-in weld (A17) was much lower than the other, main-line welds; 267 HV10. Although the average hardness was greater than the respective average HAZ hardness, it was significantly less than the respective average pipe metal hardness
- A number of the pipes were from the same production heat;
 - Source B – 6 of the 7 pipes were from the same heat. No clear heat-to-heat trend was observed as the averaged pipe and HAZ hardness data from the seventh pipe was within the scatter of the six pipes from the same heat
 - Source C – of the 9 pipes tested there were 3 production heats; one set of 5 pipes, and two sets of 2 pipes. Despite three groups of data from Source C pipe to compare, there were no clear differences observed between heats.

In addition, a through-thickness hardness survey at the weld metal centre line was undertaken on each of the eleven macro-sections extracted from weld B10. Hardness measurements were recorded at 0.06in (1.5mm) increments, starting 0.04in (1mm) up from the weld root (see Figure A20). The individual hardness measurements are presented in Table A11, and the weld macro-section and corresponding hardness profiles are given in Figure A21 to Figure A24 at each circumferential position. Figure A25 is a graph presenting all through-thickness weld hardness data to highlight trends.

The hardness ranged from 266-331 HV10; the lowest hardness values were measured in the weld cap region, the highest individual hardness peaks occurred at the weld root and near weld mid-thickness. It is likely that the reduction in hardness in the near weld cap region is attributed to the lower cooling rate (or the increase in welding cooling time) associated with the welding process.

6.3 Tensile Tests

API 1104, CSA Z662 and EPRG do not explicitly state the tensile test standard to use, although API 1104 and EPRG do specify a test specimen design. For the tests undertaken in this work, the test procedure given in BS EN 10002-1 [36] has been used. It should be noted that BS EN 10002-1 was withdrawn in August 2009, and replaced with BS EN ISO 6892-1 [37]. However, the basic test method has not changed, whether the test is undertaken under stress or strain rate control.

Although the test standard does specify 'preferred' test specimens of specific dimensions, in recognition that it may not always be possible to obtain the specified shape and dimensions, testing of other specimen sizes, and shapes, is permitted.

Both round bar (RB) and rectangular shaped specimens were tested, sampling the pipe material in the longitudinal and transverse directions, and the weld metal in the direction of the weld. In addition, rectangular shaped specimens were used to test the weldment in the pipe longitudinal direction. Information on the shape, orientation and size of each specimen tested is given in the following subsections where the test results are reviewed.

The test specimens were all loaded under strain rate control, at a constant machine cross head displacement rate. All testing was undertaken at ambient laboratory temperature, approximately 68°F (20°C).

An initial study was undertaken to determine the variation in weld metal strength around the pipe circumference, which can vary significantly [38]. Similar results have been reported [39][40] but the position relating to the location of maximum and minimum strength is seen to vary around the pipe circumference. Hence for these tests it was considered important to characterize the circumferential variation in tensile properties specific to the welds being tested.

6.3.1 Variation in weld metal tensile properties through the pipe wall thickness, around the pipe circumference

Weld B10 was subject to detailed testing to determine the through-thickness variation in weld metal tensile properties around the pipe circumference. A total of 44 tests were undertaken; RB specimens were extracted from the weld at three through-wall locations; weld cap region, mid-thickness, and weld root region (see Figure 4), and a rectangular section specimen sampling almost the full-thickness of the weld (see Figure 5). Due to availability of material it was only possible to extract 11 sets of specimens around the pipe circumference.

Due to the narrowness of the weld the diameter of the cap and root tensile specimens was 0.217in (5.5mm). The mid-thickness specimen was slightly larger with a diameter of 0.315in (8.0mm). As shown in Figure 4, the mid-thickness specimen also sampled a small portion of the HAZ on either side of the weld. The rectangular specimen had dimensions 0.591x0.157in (15x4mm), width and thickness respectively.

The test results are presented in Table 4 through to Table 11 and the circumferential variation in yield and tensile strength is shown in Figure 6 through to Figure 9.

6.3.1.1 Weld cap region

Each specimen was extracted from the centre line of the weld; the centre of the specimen being approximately 0.157in (4mm) below the pipe outer surface. From the results presented in Table 4 and shown in Figure 6 it can be seen that there is a significant variation in both yield and tensile strength around the pipe circumference. In addition the Y/T ratio can also be seen to vary circumferentially.

The test results from Table 4 are summarized in Table 5 in terms of minimum and maximum measured values, maximum difference, average value and standard deviation.

There was a 14ksi (95N/mm²) difference between the minimum and maximum measured values of yield strength, and 5ksi (35N/mm²) difference in tensile strength. The minimum measured values of yield and tensile strength occurred at approximately the 6 and 12 o'clock positions, with the maximums at around 3 and 9 o'clock. The variance in Y/T ratio was found to be a maximum at 6 and 12 o'clock, and a minimum at

3 and 9 o'clock. The minimum measured elongation (uEL) of the specimens was 7.8%; the maximum was 9.8%.

The shape of the individual stress-strain curves were also found to differ depending on the circumferential position of the specimen; at the 6 o'clock position 'double n' behavior was observed, while at the 9 o'clock position discontinuous yielding with a Lüders plateau was observed.

6.3.1.2 Weld root region

Each specimen was extracted from the centre line of the weld; the centre of the specimen being approximately 0.276in (7mm) up from the pipe inner surface. From the results presented in Table 6 and shown in Figure 7 it can be seen that there is a large variation in both yield and tensile strength around the pipe circumference but, unlike for the weld cap region, the difference is fairly consistent.

The test results from Table 6 are summarized in Table 7 in terms of minimum and maximum measured values, maximum difference, average value and standard deviation.

There was a 9ksi (61N/mm²) difference between the minimum and maximum measured values of yield strength, and 6ksi (43N/mm²) difference in tensile strength. The minimum measured values of yield and tensile strength occurred at approximately the 6 and 12 o'clock positions, with the maximums at around 3 and 9 o'clock. The Y/T ratio shows very little variation around the pipe circumference. Furthermore, the weld root has a lower strain capacity than the weld cap region; the minimum and maximum uEL measurements being 5.2 and 7.7%.

Again, the shape of the stress strain curves was found to differ too; both 'double n' and discontinuous yielding with a Lüders plateau were observed.

6.3.1.3 Weld mid-thickness region

Each specimen was extracted from the centre line of the weld at approximately mid-thickness. As noted above, this specimen sampled both weld metal and HAZ as the specimen diameter was slightly larger than the width of the weld. However, from the results presented in Table 8 and shown in Figure 8 it can be seen that they are very similar to those measured at the weld root region in terms of circumferential variation, magnitude and scatter of yield and tensile strength; there was a 9ksi (61N/mm²) difference between the minimum and maximum measured values of yield strength, and 7ksi (48N/mm²) difference in tensile strength. The variation in Y/T ratio and uEL was also comparable to the weld root region. Furthermore, the shape of the stress strain curves was found to differ too; both 'double n' and discontinuous yielding with a Lüders plateau were observed.

The test results from Table 8 are summarized in Table 9 in terms of minimum and maximum measured values, maximum difference, average value and standard deviation.

6.3.1.4 Full weld thickness

Each specimen was extracted from the centre line of the weld, sampling almost the full weld thickness. The position and specimen width was such that it enveloped the weld cap and root regions sampled with the RB specimens. From the results presented in Table 10 and shown in Figure 9 it can be seen that the circumferential variation in tensile properties compare more with those measured at the weld root region. Furthermore, the shape of the stress strain curves was found to differ too; both 'double n' and discontinuous yielding with a Lüders plateau were observed.

The test results from Table 10 are summarized in Table 11 in terms of minimum and maximum measured values, maximum difference, average value and standard deviation. As can be seen there was an 11ksi

(75N/mm²) difference between the minimum and maximum measured values of yield strength, and 6ksi (41N/mm²) difference in tensile strength. The Y/T ratio varied from 0.93 up to 0.97 and the minimum measured uEL was 6.3%.

6.3.1.5 Comparison of results

The through-wall variation in yield and tensile strength around the pipe circumference is shown in Figure 10 and Figure 11 respectively. As can be seen, the tensile properties of the weld cap region are lower than those measured in the weld root region, at the same circumferential position. The results from the rectangular specimens are also shown, and compare well with the measured properties in the weld root.

The same trends are apparent when examining the through-thickness Y/T ratio around the pipe circumference (see Figure 12); the rectangular specimen gives similar results to those from the weld root RB specimens. The weld cap region gives similar values, except at the 6 and 12 o'clock locations, where the Y/T ratio is much lower by comparison.

The RB data for the mid-thickness region has been excluded from this comparison as the specimens sampled both weld and HAZ microstructure.

6.3.2 Tensile Properties of each Weld

In contrast to the all weld metal specimen through-wall sampling plan for weld B10, only weld cap and root specimens were extracted from the remaining welds. The through-wall sampling position of the all weld specimens is shown in Figure 13; the centre of the weld cap specimen being approximately 0.236in (6mm) below the pipe outer surface, and the weld root specimen being approximately 0.276in (7mm) up from the pipe inner surface.

The results from the tensile tests undertaken on each weldment are summarized below.

6.3.2.1 Weld A 06

The test results are summarized in Table 12 and presented in Figure 14 through to Figure 21.

Figure 14 compares the yield strength of the pipe in the longitudinal direction with the all weld metal test results. As can be seen the yield strength of Pipe 1 is similar to that for Pipe 2, which is not unexpected as both pipes were from Source B, and from the same production heat. There is little scatter in the data; the difference between the maximum and minimum yield strength for Pipe 1 was 2ksi (14N/mm²), and 5ksi (34N/mm²) for Pipe 2, with an average yield strength of 112ksi (772N/mm²) and 114ksi (786N/mm²) respectively. In contrast the weld metal yield strength exhibits significant scatter; the difference between the maximum and minimum values was 15ksi (103N/mm²), with an average yield strength of 120ksi (828N/mm²).

The data are also presented in Figure 15 as a function of their position around the circumference of the weld. As can be seen, the weld data appears to follow a sinusoidal trend, comparable to the detailed study of weld B10; yield strength is a maximum at near 3 and 9 o'clock, and a minimum at near 12 and 6 o'clock. It can be inferred from this plot that, depending on the circumferential position of the specimen(s), the weld can either be considered to under- or over-match the pipe material.

Figure 16 compares the minimum, maximum and average values of yield strength for the pipes with the weld metal. The presentation illustrates the importance of sampling multiple locations around the pipe/weld circumference when quantifying the level of pipe/weld mismatch.

For Pipe 1, the yield strength mismatch varies from a matched condition to being over-matched:

- comparing the pipe maximum with the weld minimum gives -0.9%
- comparing the pipe minimum with the weld maximum gives +14.8%
- comparing the pipe average with the weld average gives +7.1%

For Pipe 2, the yield strength mismatch varies from an under-matched condition to being over-matched:

- comparing the pipe maximum with the weld minimum gives -4.7%
- comparing the pipe minimum with the weld maximum gives +13.6%
- comparing the pipe average with the weld average gives +5.1%

The Y/T ratios are compared in Figure 17. Pipe 1 and Pipe 2 were quite similar, although Pipe 2 exhibited a higher degree of scatter. In general, Y/T for the weld metal was found to be higher than both pipes. To summarize, the minimum, maximum, average and standard deviation values were:

- Pipe 1 0.91 (min), 0.93 (max), 0.92 (avg), 0.007 (STDV)
- Pipe 2 0.90 (min), 0.94 (max), 0.92 (avg), 0.013 (STDV)
- Weld metal 0.91 (min), 0.97 (max), 0.95 (avg), 0.023 (STDV)

The strain capacity is compared in Figure 18. Pipe 1 was found to have a slightly greater strain capacity than Pipe 2, and the weld metal exceeded both pipes. To summarize, the minimum, maximum, average and standard deviation values were:

- Pipe 1 4.1% (min), 5.3% (max), 4.7% (avg), 0.55% (STDV)
- Pipe 2 2.2% (min), 4.8% (max), 3.8% (avg), 1.02% (STDV)
- Weld metal 5.9% (min), 9.5% (max), 7.6% (avg), 1.54% (STDV)

Two longitudinally orientated full-thickness flat tensile (FT) specimens were extracted from the weldment at the 12 and 6 o'clock locations, sampling Pipe 1, Pipe 2 and the weld metal. At the 12 o'clock position failure occurred in the base metal of Pipe 1 and at the 6 o'clock position failure occurred within the HAZ of Pipe 1, confirming Pipe 1 to be the weaker material in the longitudinal direction.

For completeness, the tensile properties in the pipe transverse direction were also measured. The results are compared with the weld metal properties in a similar manner to the longitudinal test results; yield strength (Figure 19), Y/T ratio (Figure 20) and strain capacity (Figure 21).

Figure 19 includes the transverse yield strength of Pipes 1 and 2 measured using both RB and full-thickness FT specimens. The RB specimens were extracted at the 8 and 10 o'clock positions, and the FT specimens at approximately the 7 o'clock position. As can be seen the yield strength of Pipe 1 is similar to Pipe 2; and the RB results are higher than the FT results. The pipe properties are similar to those measured in the weld metal.

From Figure 20 the Y/T ratios from the RB specimens from Pipe 1 and 2 are similar, and generally higher than the weld metal. In contrast the Y/T ratios from the FT specimens are much lower than those measured from the RB specimens.

The strain capacity of the transverse specimens is presented in Figure 21. As can be seen from the results of the pipe RB specimens, both Pipe 1 and Pipe 2 have very little strain capacity, less than 1%. In contrast the FT specimens exhibited a strain capacity greater than 4%. The strain capacity of the weld metal was much greater.

6.3.2.2 Weld A17

The test results are summarized in Table 13 and presented in Figure 22 through to Figure 29.

Figure 22 compares the yield strength of the pipe in the longitudinal direction with the all weld metal test results. Pipe 1 and Pipe 2 are from Source C and production heat; the yield strength was slightly lower in Pipe 2, with both pipes exhibiting very little scatter and variation in strength around the pipe circumference; the difference between the maximum and minimum yield strength for Pipe 1 was 3ksi (21N/mm²), and 4ksi (28N/mm²) for Pipe 2, with an average yield strength of 114ksi (786N/mm²) and 108ksi (745N/mm²) respectively. The root region of the weld metal exhibited lower strength than the cap region, which was comparable to the pipe strength. For the weld as a whole, the difference between the maximum and minimum values was 12ksi (83N/mm²), with an average yield strength of 108ksi (745N/mm²).

The data are also presented in Figure 23 as a function of their position around the circumference of the weld. The sinusoidal trend observed for welds B10 and A06 is less pronounced, but this is likely due to the positions the specimens were extracted from, and the variation in strength observed between the weld root and cap regions. However, a sinusoidal trend has been superimposed onto Figure 23. As shown, the weld yield strength data envelopes the data from both pipes, hence depending on the circumferential position of the specimen(s), the weld varies from under- to over-matched. The level of mismatch is shown in Figure 24, comparing the minimum, maximum and average values of yield strength with the weld metal.

For Pipe 1, the yield strength mismatch varies from an under-matched condition to being matched:

- Comparing the pipe maximum with the weld minimum gives -11.3%
- Comparing the pipe minimum with the weld maximum gives +1.7%
- Comparing the pipe average with the weld average gives -4.6%

For Pipe 2, the yield strength mismatch varies from an under-matched condition to being over-matched:

- Comparing the pipe maximum with the weld minimum gives -7.5%
- Comparing the pipe minimum with the weld maximum gives +7.5%
- Comparing the pipe average with the weld average gives +0.1%

The Y/T ratios are compared in Figure 25. Pipe 1 and Pipe 2 were similar, but it was found to be much higher in the weld metal. To summarize:

- Pipe 1 0.89 (min), 0.90 (max), 0.90 (avg), 0.004 (STDV)
- Pipe 2 0.89 (min), 0.92 (max), 0.90 (avg), 0.008 (STDV)
- Weld metal 0.93 (min), 0.96 (max), 0.95 (avg), 0.010 (STDV)

The strain capacity is compared in Figure 26. Pipe 1 was found to have a slightly greater strain capacity than Pipe 2, and the weld metal exceeded both pipes. To summarize:

- Pipe 1 3.5% (min), 5.9% (max), 4.6% (avg), 0.92 (STDV)
- Pipe 2 3.9% (min), 5.2% (max), 4.7% (avg), 0.51 (STDV)
- Weld metal 5.7% (min), 9.2% (max), 7.1% (avg), 1.21 (STDV)

Two longitudinally orientated full-thickness FT specimens were extracted from the weldment at the 12 and 6 o'clock locations; at both locations failure occurred in the weld metal.

For completeness, the tensile properties in the pipe transverse direction were also measured. The results are compared with the weld metal properties in a similar manner to the longitudinal test results; yield strength (Figure 27), Y/T ratio (Figure 28) and strain capacity (Figure 29). To summarize:

- The FT specimens gave a lower yield strength than the RB specimens
- The yield strength of Pipe 1 and Pipe 2 is greater than the weld metal strength
- The Y/T ratios (based on RB specimens) for Pipe 1, Pipe 2 and the weld metal are similar. The FT gave much lower Y/T ratios
- The weld metal has a much greater strain capacity than Pipe 1 or Pipe 2. All specimens exhibited a uEL of 4% or more, except one of the specimens from Pipe 2 which exhibited a uEL of only 0.5%

6.3.2.3 Weld A33

The test results are summarized in Table 14 and presented in Figure 30 through to Figure 37.

Figure 30 compares the yield strength of the pipe in the longitudinal direction with the all weld metal test results. Despite Pipe 1 and Pipe 2 being from different sources (Source A and B, respectively), the yield strength was similar, with both pipes exhibiting very little scatter and variation in strength around the pipe circumference; the difference between the maximum and minimum yield strength for Pipe 1 was 5ksi (34N/mm²), and 3ksi (21N/mm²) for Pipe 2, with an average yield strength of 114ksi (786N/mm²) and 113ksi (779N/mm²) respectively. The weld metal yield strength was higher than either pipe, and there was little difference observed between the weld root and cap regions. For the weld as a whole, the difference between the maximum and minimum values was 11ksi (76N/mm²), with an average yield strength of 123ksi (848N/mm²).

The data are also presented in Figure 31 as a function of their position around the circumference of the weld. A sinusoidal trend in weld metal strength was observed. As shown, regardless of circumferential position, the weld metal over-matches the pipe materials. The level of over-match is shown in Figure 32, comparing the minimum, maximum and average values of yield strength with the weld metal.

For Pipe 1, the yield strength mismatch varies from a matched condition to being over-matched:

- Comparing the pipe maximum with the weld minimum gives +0.1%
- Comparing the pipe minimum with the weld maximum gives +14.7%
- Comparing the pipe average with the weld average gives +8.3%

For Pipe 2, the yield strength mismatch also varies from a matched condition to being over-matched:

- Comparing the pipe maximum with the weld minimum gives +2.2%
- Comparing the pipe minimum with the weld maximum gives +15.0%
- Comparing the pipe average with the weld average gives +9.0%

The Y/T ratios are compared in Figure 33. Pipe 2 was consistently higher than Pipe 1, and the weld metal was higher still. To summarize:

- Pipe 1 0.90 (min), 0.93 (max), 0.91 (avg), 0.014 (STDV)
- Pipe 2 0.86 (min), 0.88 (max), 0.87 (avg), 0.006 (STDV)
- Weld metal 0.94 (min), 0.99 (max), 0.96 (avg), 0.016 (STDV)

The strain capacity is compared in Figure 34. Pipe 1 was found to have a slightly greater strain capacity than Pipe 2, and the weld metal exceeded both pipes. To summarize, the minimum, maximum, average and standard deviation values were:

- Pipe 1 3.5% (min), 4.8% (max), 4.3% (avg), 0.51 (STDV)
- Pipe 2 3.1% (min), 4.2% (max), 3.8% (avg), 0.43 (STDV)
- Weld metal 7.0% (min), 8.5% (max), 7.7% (avg), 0.50 (STDV)

Two longitudinally orientated full-thickness FT specimens were extracted from the weldment at the 12 and 6 o'clock locations; at the 12 o'clock location failure occurred in the HAZ of Pipe 1, while at the 6 o'clock location failure occurred in the weld metal.

For completeness, the tensile properties in the pipe transverse direction were also measured. The results are compared with the weld metal properties in a similar manner to the longitudinal test results; yield strength (Figure 35), Y/T ratio (Figure 36) and strain capacity (Figure 37). To summarize:

- The FT and RB specimens from Pipe 1 were similar, but for Pipe 2 the FT gave a lower yield strength than the RB specimens.
- The yield strength of Pipe 1 was within the scatter of the yield strength measured for the weld metal. The yield strength of Pipe 2 was slightly higher.
- The Y/T ratios (based on RB specimens) for Pipe 1 were similar to those measured in the weld metal. Pipe 2 was higher.
- The strain capacity of Pipe 1 and Pipe 2 was similar, although low. In contrast, the weld metal had a much greater strain capacity than either pipe.

6.3.2.4 Weld A44

The test results are summarized in Table 15 and presented in Figure 38 through to Figure 45.

Figure 38 compares the yield strength of the pipe in the longitudinal direction with the all weld metal test results. Despite Pipe 1 and Pipe 2 being from different sources (Source B and C, respectively), the yield strength was similar, with both pipes exhibiting very little scatter and variation in strength around the pipe circumference; the difference between the maximum and minimum yield strength for Pipe 1 was 5ksi (34N/mm²), and 2ksi (14N/mm²) for Pipe 2, and both with an average yield strength of 111ksi (766N/mm²). The weld metal yield strength was slightly higher than either pipe, and there was little difference observed between the weld root and cap regions. For the weld as a whole, the difference between the maximum and minimum values was 3ksi (21N/mm²), with an average yield strength of 117ksi (807N/mm²).

The data are also presented in Figure 39 as a function of their position around the circumference of the weld. Due to the limited number of data points a sinusoidal trend in weld metal strength was not clear. As shown, regardless of circumferential position, the weld metal over-matches the pipe materials. The level of over-match is shown in Figure 40, comparing the minimum, maximum and average values of yield strength with the weld metal.

For Pipe 1, the yield strength mismatch varies from a matched condition to being over-matched:

- Comparing the pipe maximum with the weld minimum gives +1.3%
- Comparing the pipe minimum with the weld maximum gives +8.7%
- Comparing the pipe average with the weld average gives +5.5%

For Pipe 2, the yield strength is over-matched:

- Comparing the pipe maximum with the weld minimum gives +3.5%
- Comparing the pipe minimum with the weld maximum gives +8.2%
- Comparing the pipe average with the weld average gives +5.9%

The Y/T ratios are compared in Figure 41. Pipe 2 was slightly higher than Pipe 1, but the weld metal was generally higher still. To summarize:

- Pipe 1 0.90 (min), 0.91 (max), 0.91 (avg), 0.002 (STDV)
- Pipe 2 0.92 (min), 0.96 (max), 0.93 (avg), 0.023 (STDV)
- Weld metal 0.94 (min), 0.96 (max), 0.95 (avg), 0.013 (STDV)

The strain capacity is compared in Figure 42. Pipe 1 and Pipe 2 were similar. The weld metal exceeded both pipes. To summarize, the minimum, maximum, average and standard deviation values were:

- Pipe 1 4.6% (min), 6.0% (max), 5.3% (avg), 0.72 (STDV)
- Pipe 2 4.6% (min), 4.9% (max), 4.7% (avg), 0.16 (STDV)
- Weld metal 5.8% (min), 8.5% (max), 7.5% (avg), 1.53 (STDV)

Two longitudinally orientated full-thickness FT specimens were extracted from the weldment at the 12 and 6 o'clock locations; at the 12 o'clock location failure occurred in Pipe 2, while at the 6 o'clock location failure occurred in the HAZ of Pipe 2.

For completeness, the tensile properties in the pipe transverse direction were also measured. The results are compared with the weld metal properties in a similar manner to the longitudinal test results; yield strength (Figure 43), Y/T ratio (Figure 44) and strain capacity (Figure 45). To summarize:

- The FT and RB specimens from Pipe 1 were similar, but for Pipe 2 the FT gave a lower yield strength than the RB specimens.
- The yield strength of Pipe 2 was marginally higher than Pipe 1, which was marginally higher than the weld.
- The Y/T ratios (based on RB specimens) for Pipe 2 was significantly higher than Pipe 1 or the weld metal, which were similar.
- The strain capacity of Pipe 1 was slightly lower than Pipe 2. The weld metal strain capacity was greater than either pipe.

6.3.2.5 Weld A46

The test results are summarized in Table 16 and presented in Figure 46 through to Figure 53.

Figure 46 compares the yield strength of the pipe in the longitudinal direction with the all weld metal test results. Pipe 1 and Pipe 2 were from Source C, but a different production heat. Despite this, the yield strength was similar, with both pipes exhibiting very little scatter and variation in strength around the pipe circumference; the difference between the maximum and minimum yield strength for Pipe 1 was 3ksi (21N/mm²), and 2ksi (14N/mm²) for Pipe 2, and both with an average yield strength of 108ksi (745N/mm²). The weld metal yield strength was significantly higher than either pipe, and there was little difference observed between the weld root and cap regions. For the weld as a whole, the difference between the maximum and minimum values was 13ksi (90N/mm²), with an average yield strength of 128ksi (883N/mm²).

The data are also presented in Figure 47 as a function of their position around the circumference of the weld. A sinusoidal trend in weld metal strength was observed. As shown, regardless of circumferential position, the weld metal significantly over-matches the pipe materials. The level of over-match is shown in Figure 48, comparing the minimum, maximum and average values of yield strength with the weld metal.

For Pipe 1, the yield strength is over-matched:

- Comparing the pipe maximum with the weld minimum gives +9.4%
- Comparing the pipe minimum with the weld maximum gives +25.2%
- Comparing the pipe average with the weld average gives +18.4%

For Pipe 2, the yield strength is over-matched:

- Comparing the pipe maximum with the weld minimum gives +11.3%
- Comparing the pipe minimum with the weld maximum gives +25.7%
- Comparing the pipe average with the weld average gives +18.9%

The Y/T ratios are compared in Figure 49. Pipe 2 was slightly higher than Pipe 1. The weld metal was significantly higher than either pipe. To summarize:

- Pipe 1 0.88 (min), 0.91 (max), 0.89 (avg), 0.011 (STDV)
- Pipe 2 0.89 (min), 0.91 (max), 0.90 (avg), 0.006 (STDV)
- Weld metal 0.94 (min), 0.99 (max), 0.97 (avg), 0.017 (STDV)

The strain capacity is compared in Figure 50. There was little difference between the pipe and weld metal. On average the weld metal had a slightly higher strain capacity than Pipe 1, which was slightly higher than Pipe 2. To summarize, the minimum, maximum, average and standard deviation values were:

- Pipe 1 3.8% (min), 5.9% (max), 5.2% (avg), 0.88 (STDV)
- Pipe 2 4.3% (min), 5.8% (max), 4.9% (avg), 0.65 (STDV)
- Weld metal 3.2% (min), 7.4% (max), 6.0% (avg), 1.47 (STDV)

Two longitudinally orientated full-thickness FT specimens were extracted from the weldment at the 12 and 6 o'clock locations; both specimens failed in the parent material of Pipe 2.

For completeness, the tensile properties in the pipe transverse direction were also measured. The results are compared with the weld metal properties in a similar manner to the longitudinal test results; yield strength (Figure 51), Y/T ratio (Figure 52) and strain capacity (Figure 53). To summarize:

- The FT and RB specimens from Pipe 1 and Pipe 2 were similar.
- The weld metal yield strength was slightly higher than the pipe strength.
- The Y/T ratios (based on RB specimens) for Pipes 1 and 2 were similar, and within the scatter of the weld metal results.
- The strain capacity of Pipe 1 and Pipe 2 was similar. The weld metal exhibited the greatest strain capacity, with the exception of one specimen at approximately the 3 o'clock location which was significantly lower than the parent pipe.

6.3.2.6 Weld A50

The test results are summarized in Table 17 and presented in Figure 54 through to Figure 61.

Figure 54 compares the yield strength of the pipe in the longitudinal direction with the all weld metal test results. Pipe 1 and Pipe 2 were from Source B, but a different production heat. Despite this, the yield strength was similar, with both pipes exhibiting very little scatter and variation in strength around the pipe circumference; the difference between the maximum and minimum yield strength for Pipe 1 was 3ksi (21N/mm²), and 6ksi (41N/mm²) for Pipe 2, with an average yield strength of 111ksi (766N/mm²) and 112ksi (772N/mm²) respectively. The weld metal yield strength was significantly higher than either pipe, and there was little difference observed between the weld root and cap regions. For the weld as a whole, the difference between the maximum and minimum values was 11ksi (76N/mm²), with an average yield strength of 123ksi (848N/mm²).

The data are also presented in Figure 55 as a function of their position around the circumference of the weld. A sinusoidal trend in weld metal strength was observed. As shown, regardless of circumferential position, the weld metal significantly over-matches the pipe materials. The level of over-match is shown in Figure 56, comparing the minimum, maximum and average values of yield strength with the weld metal.

For Pipe 1, the yield strength is over-matched:

- Comparing the pipe maximum with the weld minimum gives +6.9%
- Comparing the pipe minimum with the weld maximum gives +19.8%
- Comparing the pipe average with the weld average gives +11.1%

For Pipe 2, the yield strength is over-matched:

- Comparing the pipe maximum with the weld minimum gives +4.3%
- Comparing the pipe minimum with the weld maximum gives +19.9%
- Comparing the pipe average with the weld average gives +9.6%

The Y/T ratios are compared in Figure 57. Pipe 2 was generally lower than Pipe 1, which was slightly lower than the weld metal. To summarize:

- Pipe 1 0.93 (min), 0.97 (max), 0.95 (avg), 0.015 (STDV)
- Pipe 2 0.89 (min), 0.95 (max), 0.91 (avg), 0.025 (STDV)
- Weld metal 0.95 (min), 0.98 (max), 0.96 (avg), 0.010 (STDV)

The strain capacity is compared in Figure 58. The weld metal strain capacity was consistently higher than the pipe materials, and Pipe 2 was slightly greater than Pipe 1. To summarize, the minimum, maximum, average and standard deviation values were:

- Pipe 1 2.4% (min), 3.7% (max), 3.0% (avg), 0.68 (STDV)
- Pipe 2 3.7% (min), 6.0% (max), 4.8% (avg), 0.97 (STDV)
- Weld metal 5.5% (min), 8.5% (max), 7.3% (avg), 1.38 (STDV)

Two longitudinally orientated full-thickness FT specimens were extracted from the weldment at the 12 and 6 o'clock locations; at the 12 o'clock location failure occurred in the base metal of Pipe 1, while at the 6 o'clock location failure occurred in the HAZ of Pipe 1.

For completeness, the tensile properties in the pipe transverse direction were also measured. The results are compared with the weld metal properties in a similar manner to the longitudinal test results; yield strength (Figure 59), Y/T ratio (Figure 60) and strain capacity (Figure 61). To summarize:

- The FT specimens gave a lower yield strength than the RB specimens.
- The yield strength of the weld metal and Pipe 2 was similar. The yield strength of Pipe 1 was slightly lower.
- The Y/T ratios (based on RB specimens) were the highest for Pipe 2, and lowest for Pipe 1. The weld metal values were bounded by Pipe 1 and Pipe 2.
- The strain capacity of Pipe 1 and Pipe 2 was very poor; Pipe 2 was slightly greater than Pipe 1. In contrast the strain capacity of the weld metal was significantly higher.

6.3.2.7 Weld B03

The test results are summarized in Table 18 and presented in Figure 62 through to Figure 69.

Figure 62 compares the yield strength of the pipe in the longitudinal direction with the all weld metal test results. Pipe 1 and Pipe 2 were from Source C, but a different production heat. Despite this, the yield strength was similar, with both pipes exhibiting very little scatter and variation in strength around the pipe circumference; the difference between the maximum and minimum yield strength for Pipe 1 was 4ksi (28N/mm²), and 3ksi (21N/mm²) for Pipe 2, with an average yield strength of 106ksi (731N/mm²) and 107ksi (738N/mm²) respectively. The weld metal yield strength was significantly higher than either pipe, and there was little difference observed between the weld root and cap regions. For the weld as a whole, the difference between the maximum and minimum values was 12ksi (83N/mm²), with an average yield strength of 124ksi (855N/mm²).

The data are also presented in Figure 63 as a function of their position around the circumference of the weld. A sinusoidal trend in weld metal strength was observed. As shown, regardless of circumferential position, the weld metal significantly over-matches the pipe materials. The level of over-match is shown in Figure 64, comparing the minimum, maximum and average values of yield strength with the weld metal.

For Pipe 1, the yield strength is over-matched:

- Comparing the pipe maximum with the weld minimum gives +9.0%
- Comparing the pipe minimum with the weld maximum gives +24.5%
- Comparing the pipe average with the weld average gives +16.8%

For Pipe 2, the yield strength is over-matched:

- Comparing the pipe maximum with the weld minimum gives +9.1%
- Comparing the pipe minimum with the weld maximum gives +22.8%
- Comparing the pipe average with the weld average gives +16.5%

The Y/T ratios are compared in Figure 65. Pipe 1 was slightly lower than Pipe 2. In contrast the weld metal was significantly higher. To summarize:

- Pipe 1 0.87 (min), 0.90 (max), 0.89 (avg), 0.011 (STDV)
- Pipe 2 0.89 (min), 0.91 (max), 0.90 (avg), 0.008 (STDV)
- Weld metal 0.94 (min), 0.98 (max), 0.96 (avg), 0.017 (STDV)

The strain capacity is compared in Figure 66. The weld metal strain capacity was slightly higher than the pipe materials, which were similar. To summarize, the minimum, maximum, average and standard deviation values were:

- Pipe 1 4.9% (min), 5.7% (max), 5.4% (avg), 0.32 (STDV)
- Pipe 2 3.8% (min), 6.2% (max), 5.2% (avg), 0.88 (STDV)
- Weld metal 5.4% (min), 9.1% (max), 6.7% (avg), 1.27 (STDV)

Two longitudinally orientated full-thickness FT specimens were extracted from the weldment at approximately the 11 and 2 o'clock locations; at both locations failure occurred in the HAZ of Pipe 2.

For completeness, the tensile properties in the pipe transverse direction were also measured. The results are compared with the weld metal properties in a similar manner to the longitudinal test results; yield strength (Figure 67), Y/T ratio (Figure 68) and strain capacity (Figure 69). To summarize:

- The FT specimens gave a lower yield strength than the RB specimens.
- The yield strength of Pipe 1 and Pipe 2 was similar, while the weld metal was slightly higher.
- The Y/T ratios (based on RB specimens) of Pipe 1 and Pipe 2 were similar, and within the scatter exhibited by the weld metal data.
- The strain capacity of the weld metal was consistently higher than the pipe metal, and Pipe 1 was slightly greater than Pipe 2.

6.3.2.8 Weld B06

The test results are summarized in Table 19 and presented in Figure 70 through to Figure 77.

Figure 70 compares the yield strength of the pipe in the longitudinal direction with the all weld metal test results. Pipe 1 and Pipe 2 were from Source B and A, respectively. The yield strength of Pipe 1 was generally lower than Pipe 2, although the results for Pipe 1 were fairly scattered; the difference between the maximum and minimum yield strength for Pipe 1 was 10ksi (69N/mm²), and 3ksi (21N/mm²) for Pipe 2, with an average yield strength of 107ksi (738N/mm²) and 114ksi (786N/mm²) respectively. The weld metal yield strength was generally higher than Pipe 2. There appears very little circumferential variation in weld metal yield strength, and the weld root would appear to have a slightly higher strength than the weld root. For the weld as a whole, the difference between the maximum and minimum values was 7ksi (48N/mm²), with an average yield strength of 121ksi (835N/mm²).

The data are also presented in Figure 71 as a function of their position around the circumference of the weld. Although not entirely clear, a sinusoidal trend has been superimposed onto the weld data. As shown, regardless of circumferential position, the weld metal over-matches the pipe materials. The level of over-match is shown in Figure 72, comparing the minimum, maximum and average values of yield strength with the weld metal.

For Pipe 1, the yield strength is over-matched:

- Comparing the pipe maximum with the weld minimum gives +4.8%
- Comparing the pipe minimum with the weld maximum gives +21.6%
- Comparing the pipe average with the weld average gives +13.2%

For Pipe 2, the yield strength is over-matched:

- Comparing the pipe maximum with the weld minimum gives +2.5%

- Comparing the pipe minimum with the weld maximum gives +11.9%
- Comparing the pipe average with the weld average gives +6.7%

The Y/T ratios are compared in Figure 73. Pipe 2 was significantly lower than Pipe 1, which exhibited a high degree of scatter. The weld metal values were higher and exhibited little scatter. To summarize:

- Pipe 1 0.90 (min), 0.95 (max), 0.93 (avg), 0.023 (STDV)
- Pipe 2 0.88 (min), 0.89 (max), 0.89 (avg), 0.006 (STDV)
- Weld metal 0.95 (min), 0.97 (max), 0.96 (avg), 0.009 (STDV)

The strain capacity is compared in Figure 74. The weld metal strain capacity was significantly higher than the pipe materials (with the exception of one specimen sampling the weld root at around the 6 o'clock location, which was comparable to the pipe materials), which were similar. To summarize, the minimum, maximum, average and standard deviation values were:

- Pipe 1 3.4% (min), 4.0% (max), 3.6% (avg), 0.28 (STDV)
- Pipe 2 3.5% (min), 5.3% (max), 4.3% (avg), 0.75 (STDV)
- Weld metal 3.8% (min), 8.0% (max), 7.0% (avg), 1.60 (STDV)

Two longitudinally orientated full-thickness FT specimens were extracted from the weldment at the 12 and 4 o'clock locations; at the 4 o'clock location failure occurred in the HAZ of Pipe 1, while at the 4 o'clock location failure occurred in the base metal of Pipe 1.

For completeness, the tensile properties in the pipe transverse direction were also measured. The results are compared with the weld metal properties in a similar manner to the longitudinal test results; yield strength (Figure 75), Y/T ratio (Figure 76) and strain capacity (Figure 77). To summarize:

- The FT specimens gave a lower yield strength than the RB specimens.
- The yield strength of Pipe 2 was slightly higher than Pipe 1. The weld metal yield strength was bounded by Pipes 1 and 2.
- The Y/T ratios (based on RB specimens) of Pipe 1 and Pipe 2 were similar, and slightly higher than the weld metal.
- The strain capacity of the weld metal was generally higher than Pipe 1 and Pipe 2. Pipe 1 exhibited a very low strain capacity at the 6 o'clock position.

6.3.2.9 Weld B08

The test results are summarized in Table 20 and presented in Figure 78 through to Figure 85.

Figure 78 compares the yield strength of the pipe in the longitudinal direction with the all weld metal test results. Pipe 1 and Pipe 2 were from Source C, but a different production heat. Despite this, the yield strength was similar, with both pipes exhibiting very little scatter and variation in strength around the pipe circumference; the difference between the maximum and minimum yield strength for Pipe 1 was 8ksi (55N/mm²), and 4ksi (28N/mm²) for Pipe 2, with an average yield strength of 109ksi (752N/mm²) and 108ksi (745N/mm²) respectively. The weld metal yield strength was significantly higher than either pipe, and there was little difference observed between the weld root and cap regions. For the weld as a whole, the difference between the maximum and minimum values was 16ksi (110N/mm²), with an average yield strength of 126ksi (869N/mm²).

The data are also presented in Figure 79 as a function of their position around the circumference of the weld. A sinusoidal trend in weld metal strength was observed. As shown, regardless of circumferential position, the weld metal significantly over-matches the pipe materials. The level of over-match is shown in Figure 80, comparing the minimum, maximum and average values of yield strength with the weld metal.

For Pipe 1, the yield strength is over-matched:

- Comparing the pipe maximum with the weld minimum gives +3.1%
- Comparing the pipe minimum with the weld maximum gives +25.7%
- Comparing the pipe average with the weld average gives +15.5%

For Pipe 2, the yield strength is over-matched:

- Comparing the pipe maximum with the weld minimum gives +6.5%
- Comparing the pipe minimum with the weld maximum gives +26.0%
- Comparing the pipe average with the weld average gives +16.8%

The Y/T ratios are compared in Figure 81. The weld metal values were significantly higher than Pipe 1 and Pipe 2, which were similar. To summarize:

- Pipe 1 0.89 (min), 0.92 (max), 0.90 (avg), 0.012 (STDV)
- Pipe 2 0.89 (min), 0.92 (max), 0.90 (avg), 0.009 (STDV)
- Weld metal 0.94 (min), 0.98 (max), 0.96 (avg), 0.019 (STDV)

The strain capacity is compared in Figure 82. The weld metal strain capacity was slightly higher than the pipe materials, which were similar. To summarize, the minimum, maximum, average and standard deviation values were:

- Pipe 1 4.0% (min), 5.8% (max), 4.7% (avg), 0.78 (STDV)
- Pipe 2 3.5% (min), 5.5% (max), 4.9% (avg), 0.85 (STDV)
- Weld metal 5.3% (min), 8.1% (max), 6.6% (avg), 1.10 (STDV)

Two longitudinally orientated full-thickness FT specimens were extracted from the weldment at the 11.5 and 6 o'clock locations; at both locations failure occurred in the HAZ of Pipe 2.

For completeness, the tensile properties in the pipe transverse direction were also measured. The results are compared with the weld metal properties in a similar manner to the longitudinal test results; yield strength (Figure 83), Y/T ratio (Figure 84) and strain capacity (Figure 85). To summarize:

- The FT specimens gave a lower yield strength than the RB specimens.
- The yield strength of Pipe 1 and Pipe 2 was similar. The weld metal was slightly higher, although exhibited a high degree of scatter.
- The Y/T ratios (based on RB specimens) are similar throughout the weldment, although the weld metal results were fairly scattered.
- The strain capacity of the weld metal was consistently higher than the pipe metal, and Pipe 2 was slightly greater than Pipe 1.

6.3.3 Summary of Tensile Properties

The following trends were observed in the line pipe, from FT specimens extracted from the longitudinal orientation:

- Despite significant variations in yield and tensile strength and elongation, each specimen produced a similar shaped stress-strain curve
- The measured yield and tensile strength of each specimen exceeded SMYS and SMTS
- Yield strength observations:
 - The average yield strength of pipe from Source B was slightly higher than that from Sources A and C, which were similar
 - Pipe from Source A recorded the lowest value of yield strength and pipe from Source B the highest.
 - The difference between the maximum and minimum measured values for each pipe source was similar
- Tensile strength observations:
 - The average tensile strength of pipe from Source C (121 ksi (834 N/mm²)) was slightly lower than that from Sources A and B, which were the same (123 ksi (847 N/mm²))
 - Pipe from Source A recorded both the lowest and highest value of tensile strength; 110 ksi (757 N/mm²) and 132 ksi (907 N/mm²)
 - The difference between the maximum and minimum measured values was greatest for pipe from Source A (22 ksi (150 N/mm²)), and least for pipe from Source C (11 ksi (73 N/mm²))
- Y/T ratio observations:
 - The average Y/T ratio of pipe from Source B (0.92) was slightly higher than that from Sources A and C, which were the same (0.90)
 - The minimum Y/T from each pipe Source was similar, 0.86 to 0.88
 - The maximum Y/T was measured in pipe from Source B, 0.97
- Strain capacity, uEL:
 - The average uEL of pipe from Source C (4.98%) was greater than that for pipe from Source B (4.19%), which was greater than that for pipe from Source A (3.72%)
 - Pipe from Source B recorded the lowest value of uEL (2.16%) and pipe from Source C the highest (6.18%)
 - The difference between the maximum and minimum measured uEL was greatest for pipe from Source B (3.84%) and least for pipe from Source A (1.16%)
- Pipe heat to heat comparisons:
 - Source B – five of the pipes from the set of six tested were from the same heat. Analysis of the minimum, maximum, average and maximum difference is the same as that calculated for the complete set of pipes
 - Source C – of the nine pipes tested, five were from one heat (C1), 2 were from another heat (C2) and the remaining two were from another heat (C3). In general;

- The average yield and tensile strengths of C1 were greater than C2 and C3, which were the same
- C1 gave the lowest and highest measure of yield strength, compared with C2 and C3. A similar trend was observed with the measured tensile strength
- The minimum, maximum, average and maximum difference of the Y/T ratio and uEL were similar for C1, C2 and C3

The following trends were observed in the line pipe, from specimens extracted from the transverse orientation:

- Differences were observed in the stress-strain response of the line pipe (see Figure 86), that did not appear to be influenced by position around the pipe circumference. Furthermore, there was also a difference in behavior due to the different type of test specimen; RB compared with a FT specimen;
 - Transverse RB specimens exhibited three distinctly different responses:
 - A 'standard' stress-strain response with a rising stress-strain post yield behavior
 - A maximum stress coincidental with the upper yield point, followed by an instantaneous partial drop off in stress and then a slow rise in stress with increasing strain
 - A maximum stress coincidental with the upper yield point, followed by a reduction in stress with increasing strain
 - Transverse FT specimens exhibited similar behavior; a smooth 'rounded' stress-strain curve
- FT specimens gave a lower value of yield strength compared with the RB specimens extracted from the same location of the individual pipe. The tensile strengths were similar; hence the FT specimens consistently gave a lower Y/T
- The yield and tensile strength measured from each RB and FT specimen exceeded SMYS and SMTS.
- The trends described below are based on the results of the RB tensile tests, due to the limited number of tests undertaken on FT transverse specimens:
 - Yield strength observations:
 - The average yield strength of pipe from Source A was greater than Source B, which was greater than Source C
 - Pipe from Source B recorded the lowest value of yield strength, and pipe from Source A the highest.
 - The difference between the maximum and minimum measured values for each pipe source was greatest for Source A, with pipe from Source B and C exhibiting a similar scatter.
 - Tensile strength observations:
 - The average tensile strength of pipe from Source A (129 ksi (888 N/mm²)) was greater than Source B (126 ksi (872 N/mm²)), which was greater than Source C (125 ksi (860 N/mm²))

- Pipe from Source B recorded the lowest value of tensile strength (120 ksi (825 N/mm²)), and pipe from Source A the highest (135 ksi (931 N/mm²))
- The difference between the maximum and minimum measured values for each pipe source was greatest for Source A, with pipe from Source C exhibiting the lowest scatter
- Y/T ratio observations:
 - The minimum, maximum, average and maximum difference of the Y/T ratio was similar for each pipe source
- Strain capacity, uEL:
 - The average uEL of pipe from Source C (4.60%) was greater than that for Source A and B, which were similar; 2.47% and 2.00% respectively.
 - Each pipe source recorded a very low value of uEL; Source A (0.40%), Source B (0.38%) and Source C (0.39%)
 - Pipe from Source B and C exhibited the greatest strain capacity; maximum values of 5.64% (Source B) and 5.66% (Source C); hence these pipe sources also exhibited the greatest scatter.
- Pipe heat to heat comparisons (the trends are compared in a similar manner to those for the longitudinal FT specimens above; pipe from Source C, designated C1, C2 and C3)
 - The average yield and tensile strengths of C1 were greater than C2, which was greater than C3
 - The minimum yield and tensile strengths were measured in C1 and C2
 - C1 also gave the highest individual value of yield and tensile strength; hence C1 also exhibited the greatest degree of scatter (i.e., difference between the maximum and minimum values)
 - The minimum, maximum, average and maximum difference of the Y/T ratio and uEL were similar for C1, C2 and C3
 - With the exception of the one low value of uEL measured in C1 (0.39 %), the maximum and average values were similar for C1, C2 and C3

In summary the observed trends in the stress-strain response of the line pipe were different in the longitudinal direction, compared with the transverse direction. Furthermore, the post-yield behavior in the transverse direction showed variable behavior, which did not appear to be influenced by the position around the pipe circumference that the specimen was extracted.

In contrast, the heat to heat trends described above for the longitudinal direction (FT specimens) and the transverse direction (RB specimens) were found to be similar, although only pipe from Source C could be compared.

The following trends were observed from the all weld metal tests:

- There is a sinusoidal trend in weld metal yield strength around the pipe circumference; the minimum yield strength is measured around the 12 and 6 o'clock locations, the maximum yield strength is measured around the 3 and 9 o'clock locations
- The Y/T ratios were generally higher than those measured in the line pipe

- The strain capacity of the weld metal was greater than that measured in the line pipe

The following trends were noted from the cross weld metal tests (recall, the reinforcement provided by the weld cap and root was removed prior to testing):

- The failure stress of each specimen exceeded SMTS
- Most specimens failed in the HAZ or pipe metal, generally on the side that exhibited the lower strength in the longitudinal pipe metal tests
- Three specimens failed in the weld metal; A17 (12 and 6 o'clock position) and A33 (6 o'clock position), where the tensile strength of the weld metal under-matched the tensile strength of the pipe metal

6.4 Charpy Impact Tests

The dimensions of the Charpy test specimen specified in the European standard, BS EN 10045-1 [41] are identical to those specified in the US standard, ASTM E23 [42] (specimen Type A). Furthermore, the requirements of the test machine are almost identical; the radius of the support anvils being 0.039in (1mm), the distance between the supports being 1.58in (40mm), and the impact velocity (BS EN 10045 specifies a velocity at impact between 16.5 and 18ft/s (5 and 5.5m/s), while ASTM E23 specifies between 10 and 20ft/s (3 and 6m/s)). The only difference is the size of the radius specified for the striker; BS EN 10045-1 specifies a 0.079in (2mm) radius, while ASTM E23 specifies a 0.315in (8mm) radius. Studies were performed by the Pressure Vessel Research Committee (PVRC) on Charpy V-notch test specimens certified by the NIST from 1in (25.4mm) thick ASTM A516 Gr70 plate; 38 ksi (260 N/mm²) SMYS and 70 ksi (480 N/mm²) SMTS, and from 1in (25.4mm) thick ASTM A517 GrF plate; 100 ksi (690 N/mm²) SMYS and 115 ksi (790 N/mm²) SMTS. The test specimens were oriented in the longitudinal direction of the plates, taken from the ¼ thickness location. The test results showed no significant differences in the results of the Charpy impact energy values obtained with the different sized striker radius.

6.4.1 Method

Twelve full-size; 0.394x0.394in (10x10mm) Charpy 'V' notch specimens were extracted from the root region of each girth weld. With the exception of weld B06, 6 specimens sampled the weld at the 12 o'clock position and the remaining 6 specimens sampled the 6 o'clock position. The Charpy specimens for weld B06 sampled the weld at the 12 and 4 o'clock positions. All specimens were orientated transverse to the girth weld. For each set of 6 specimens; 3 specimens were notched at the weld metal centre-line, and the remaining 3 were notched at the fusion line (FL) sampling 50% HAZ and 50% weld metal.

Each specimen was prepared and tested at a temperature of -4°F (-20°C) according to BS EN 10045-1. The Charpy impact energy was recorded for each test, and each tested specimen was measured and the fracture surface features examined to determine the extent of lateral expansion (i.e., the reduction in specimen thickness) and the percentage shear area.

The same test machine was used throughout, a TINIUS OLSEN, which had a 295 ft-lb (400 J) capacity. Cooling of the test specimens was achieved by immersing them in a refrigerated bath of alcohol. Once at temperature they were left to soak for 15 minutes to enable a uniform temperature distribution through the specimen thickness. The soak temperature was 1.5°F (1°C) lower than the target test temperature to account for the slight increase in specimen temperature once it is removed from the cooling bath and subsequently tested. The actual test is undertaken within 15 seconds on removal of the specimen from the cooling bath.

The results from the tests undertaken are discussed in detail below in relation to the recorded Charpy impact energy and shear area. The measured values of lateral expansion are reported in the results tables for information only. US customary units are used to describe the results; however the referenced Tables and Figures present the results in US customary units and SI units.

6.4.2 Results

Both the EPRG and API 1104 Appendix A acceptance standards require the minimum and average Charpy impact energy of the weld to be greater than 22 and 30 ft-lb (30 and 40 J) for each notch location, respectively. In addition, API 1104 requires that the percentage shear area should be greater than 50%. Although both methods specify the same specimen orientation and notch direction, EPRG specifies that the notch of the Charpy specimen should sample the weld root region, while API 1104 specifies that the notch should sample close to the weld cap.

The individual results for each girth weld are first summarized. A comparison is then made between pipes obtained from the same source, and from the same production heat.

6.4.2.1 Summary of Individual Test Results

Weld A06 achieved the impact energy requirements of both EPRG and API 1104, and the shear area requirement of API 1104. The results are presented in Table 25 and Figure 87. Both pipes were from Source B and from the same production heat.

The HAZ/FL specimens associated with Pipe 1 sampled approximately the 12 o'clock position, and Pipe 2 the 6 o'clock position. The Charpy impact energy recorded at each position was similar, but exhibited significant scatter; Pipe 1 had a min (avg) of 44 (63) ft-lb with a STDV of 23 ft-lb, and Pipe 2 had 51 (112) ft-lb with a STDV of 60 ft-lb. The shear area for Pipe 1 ranged from 50 to 80% and Pipe 2 from 50 to 100%, inferring that at -4°F (-20°C) the HAZ/FL region of the weld is in the ductile-brittle transition region.

The Charpy impact energy recorded for the weld metal which was sampled at approximately the 6 and 12 o'clock positions was much greater than the HAZ/FL regions. At the 6 o'clock position the min (avg) Charpy impact energy was 121 (133) ft-lb with a STDV of 13 ft-lb, and at the 12 o'clock position was 100 (113) ft-lb with a STDV of 11 ft-lb. The shear area of each specimen was not less than 90%, inferring that at -4°F (-20°C) the weld metal is predominantly ductile.

Weld A17 achieved the impact energy requirements of both EPRG and API 1104, and the shear area requirement of API 1104. The results are presented in Table 26 and Figure 88. Both pipes were from Source C and from the same production heat.

The HAZ/FL specimens associated with Pipe 1 sampled approximately the 12 o'clock position, and Pipe 2 the 6 o'clock position. The Charpy impact energy at both positions was good; Pipe 1 had a min (avg) of 95 (103) ft-lb with a STDV of 13 ft-lb, and Pipe 2 had 139 (142) ft-lb with a STDV of 5 ft-lb. The shear area for Pipe 1 ranged from 85 to 95%, and Pipe 2 was 100%, inferring that at -4°F (-20°C) the HAZ/FL region of the weld is predominantly ductile.

The Charpy impact energy recorded for the weld metal which was sampled at approximately the 6 and 12 o'clock positions was similar, but significantly less than that measured at the HAZ/FL. At the 6 o'clock position the min (avg) Charpy impact energy was 58 (60) ft-lb with a STDV of 3 ft-lb, and at the 12 o'clock position was 62 (67) ft-lb with a STDV of 6 ft-lb. The shear area of each specimen was not less than 85%, inferring that at -4°F (-20°C) the weld is predominantly ductile.

Weld A33 achieved the impact energy requirements of both EPRG and API 1104, but one specimen failed the shear area requirement of API 1104. The results are presented in Table 27 and Figure 89. Pipe 1 was from Source B and Pipe 2 from Source A.

The HAZ/FL specimens associated with Pipe 1 sampled approximately the 12 o'clock position, and Pipe 2 the 6 o'clock position. The Charpy impact energy recorded at each position was not too dissimilar, although Pipe 2 did have one surprisingly low result; Pipe 1 had a min (avg) of 72 (111) ft-lb with a STDV of 60 ft-lb, and Pipe 2 had 33 (127) ft-lb with a STDV of 81 ft-lb. As can be seen, both sets of data exhibited significant scatter. The shear area for Pipe 1 ranged from 55 to 100% and Pipe 2 from 40 to 80%, inferring that at -4°F (-20°C) the HAZ/FL region of the weld is in the ductile-brittle transition region. The low Charpy impact energy and shear area for test 65 (Pipe 2) was out of context with the other 2 tests from the set of three specimens, both of which recorded a Charpy impact energy greater than 170 ft-lb and shear area of 100%.

The Charpy impact energy recorded for the weld metal which was sampled at approximately the 6 and 12 o'clock positions was similar, and within the scatter of the HAZ/FL Charpy impact energy results. At the 6 o'clock position the min (avg) Charpy impact energy was 122 (134) ft-lb with a STDV of 14 ft-lb, and at the 12 o'clock position was 107 (123) ft-lb with a STDV of 14 ft-lb. The shear area of each specimen was 100%, inferring that at -4°F (-20°C) the weld metal is ductile.

Weld A44 achieved the impact energy requirements of both EPRG and API 1104, and the shear area requirement of API 1104. The results are presented in Table 28 and Figure 90. Pipe 1 was from Source C and Pipe 2 was from Source B.

The HAZ/FL specimens associated with Pipe 1 sampled approximately the 12 o'clock position, and Pipe 2 the 6 o'clock position. The Charpy impact energy at both positions was good, despite one test result for Pipe 1; Pipe 1 had a min (avg) of 68 (153) ft-lb with a STDV of 74 ft-lb, and Pipe 2 had 185 (187) ft-lb with a STDV of 2 ft-lb. The shear area for Pipe 1 ranged from 60 (test 126) to 100% (tests 124 and 125), and Pipe 2 was 100%. Hence, at -4°F (-20°C) the HAZ/FL region of the weld is predominantly ductile.

The Charpy impact energy recorded for the weld metal which was sampled at approximately the 6 and 12 o'clock positions was good and not too dissimilar to the HAZ/FL results. The results for the 12 o'clock position were slightly lower than those at 6 o'clock; at the 6 o'clock position the min (avg) Charpy impact energy was 142 (160) ft-lb with a STDV of 15 ft-lb, and at the 12 o'clock position was 114 (131) ft-lb with a STDV of 18 ft-lb. The shear area of each specimen was 100%, except for one test results that had a shear area of 95% (test 122). At -4°F (-20°C) the weld metal is ductile.

Weld A46 achieved the impact energy requirements of both EPRG and API 1104, and the shear area requirement of API 1104. The results are presented in Table 29 and Figure 91. Both pipes were from Source C, although from different production heats.

The HAZ/FL specimens associated with Pipe 1 sampled approximately the 12 o'clock position, and Pipe 2 the 6 o'clock position. The Charpy impact energy at both positions was good and exhibited little scatter; Pipe 1 had a min (avg) of 180 (184) ft-lb with a STDV of 4 ft-lb, and Pipe 2 had 163 (168) ft-lb with a STDV of 5 ft-lb. The shear area for each specimen was 100%. At -4°F (-20°C) the HAZ/FL region of the weld is ductile.

The Charpy impact energy recorded for the weld metal which was sampled at approximately the 6 and 12 o'clock positions was good and similar, although slightly lower than the HAZ/FL results. At the 6 o'clock position the min (avg) Charpy impact energy was 107 (132) ft-lb with a STDV of

31 ft-lb, and at the 12 o'clock position was 91 (117) ft-lb with a STDV of 23 ft-lb. The shear area of each specimen was 100%, with the exception of one specimen (test 121) which had a shear area of 85% (this specimen also recorded the lowest weld metal Charpy impact energy). At -4°F (-20°C) the weld is predominantly ductile.

Weld A50 achieved the impact energy requirements of both EPRG and API 1104, and the shear area requirement of API 1104. The results are presented in Table 30 and Figure 92. Both pipes were from Source B, although from different production heats.

The HAZ/FL specimens associated with Pipe 1 sampled approximately the 12 o'clock position, and Pipe 2 the 6 o'clock position. The Charpy impact energy recorded at the 12 o'clock position was better than that recorded at the 6 o'clock position, and exhibited significantly less scatter; Pipe 1 had a min (avg) of 184 (195) ft-lb with a STDV of 11 ft-lb, and Pipe 2 had 56 (124) ft-lb with a STDV of 64 ft-lb. The shear area for Pipe 1 ranged from 55 to 100%, inferring that at -4°F (-20°C) the HAZ/FL region associated with Pipe 1 is in the ductile-brittle transition region. In contrast the shear area for Pipe 2 was 100% (i.e., fully ductile).

The Charpy impact energy recorded for the weld metal which was sampled at approximately the 6 and 12 o'clock positions was not too dissimilar and exhibited little scatter in the test results. At the 6 o'clock position the min (avg) Charpy impact energy was 97 (105) ft-lb with a STDV of 7 ft-lb, and at the 12 o'clock position was 121 (127) ft-lb with a STDV of 7 ft-lb. The shear area of each specimen was not less than 90%, inferring that at -4°F (-20°C) the weld metal is predominantly ductile.

Weld B03 achieved the impact energy requirements of both EPRG and API 1104, and the shear area requirement of API 1104. The results are presented in Table 31 and Figure 93. Both pipes were from Source C, although from different production heats.

The HAZ/FL specimens associated with Pipe 1 sampled approximately the 12 o'clock position, and Pipe 2 the 6 o'clock position. The Charpy impact energy recorded at each position was similar, but exhibited significant scatter; Pipe 1 had a min (avg) of 71 (121) ft-lb with a STDV of 58 ft-lb, and Pipe 2 had 63 (126) ft-lb with a STDV of 59 ft-lb. The shear area for Pipe 1 ranged from 55 to 100% and Pipe 2 from 75 to 100%, inferring that at -4°F (-20°C) the HAZ/FL region of the weld is in the ductile-brittle transition region.

The Charpy impact energy recorded for the weld metal which was sampled at approximately the 6 and 12 o'clock positions was good and exhibited little scatter in the test data. The results for the 6 o'clock position were slightly lower than those at 12 o'clock; at the 6 o'clock position the min (avg) Charpy impact energy was 80 (94) ft-lb with a STDV of 16 ft-lb, and at the 12 o'clock position was 124 (137) ft-lb with a STDV of 12 ft-lb. The shear area of each specimen was not less than 90%, inferring that at -4°F (-20°C) the weld metal is predominantly ductile.

Weld B06 achieved the impact energy requirements of both EPRG and API 1104, but one specimen failure the shear area requirement of API 1104. The results are presented in Table 32 and Figure 94. Pipe 1 was from Source A and Pipe 2 was from Source B.

The HAZ/FL specimens associated with Pipe 1 sampled approximately the 12 o'clock position, and Pipe 2 the 4 o'clock position. The Charpy impact energy at both positions was consistently low; Pipe 1 had a min (avg) of 33 (66) ft-lb with a STDV of 28 ft-lb, and Pipe 2 had 35 (74) ft-lb with a STDV of 60 ft-lb. The shear area for Pipe 1 ranged from 45 (test 125) to 65%, and Pipe 2 ranged from 50 to 85%, inferring that at -4°F (-20°C) the HAZ/FL region of the weld is in the ductile-brittle transition region.

The Charpy impact energy recorded for the weld metal which was sampled at approximately the 4 and 12 o'clock positions were similar, but relatively low. However, the test results were better than for the HAZ/FL region. At the 4 o'clock position the min (avg) Charpy impact energy was 86 (96) ft-lb with a STDV of 12 ft-lb, and at the 12 o'clock position was 63 (97) ft-lb with a STDV of 32 ft-lb. The shear area of each specimen was 100%, inferring that at -4°F (-20°C) the weld metal is ductile. The shear area of each specimen was not less than 75%, inferring that at -4°F (-20°C) the weld metal is predominantly ductile.

Weld B08 achieved the impact energy requirements of both EPRG and API 1104, and the shear area requirement of API 1104. The results are presented in Table 33 and Figure 95. Both pipes were from Source C, although from different production heats.

The HAZ/FL specimens associated with Pipe 1 sampled approximately the 12 o'clock position, and Pipe 2 the 6 o'clock position. The Charpy impact energy recorded at the 6 o'clock position was better than that recorded at the 12 o'clock position; Pipe 1 had a min (avg) of 89 (131) ft-lb with a STDV of 45 ft-lb, and Pipe 2 had 187 (192) ft-lb with a STDV of 7 ft-lb. The shear area for Pipe 1 ranged from 55 to 100%, inferring that at -4°F (-20°C) the HAZ/FL region associated with Pipe 1 is in the ductile-brittle transition region. In contrast the shear area for Pipe 2 was 100% (i.e., fully ductile).

The Charpy impact energy recorded for the weld metal which was sampled at approximately the 6 and 12 o'clock positions were not too dissimilar, although the 12 o'clock position was slightly lower; at the 6 o'clock position the min (avg) Charpy impact energy was 111 (137) ft-lb with a STDV of 36 ft-lb, and at the 12 o'clock position was 93 (108) ft-lb with a STDV of 13 ft-lb. The shear area of each specimen at the 12 o'clock position was 95%, and at the 6 o'clock position was 100%. At -4°F (-20°C) the weld metal is predominantly ductile.

6.4.2.2 Comparison of Test Results

Comparison of HAZ/FL results from welds produced from pipes from the same source and same production heat.

A number of the pipes tested were from the same source, with some pipes from the same production heat. Table 34 summarizes those welds and corresponding pipe sections that can be compared to assess the consistency of the Charpy properties during production welding.

There were five welds that had one or both pipes from Source B that were from the same production heat; welds A06, A33, A44, A50 and B06. The scatter in the test data was large; at the 6 o'clock position the Charpy impact energy ranged from 51 to 189 ft-lb and shear area from 50 to 100%. The spread in test data was similar at the 12 o'clock position; Charpy impact energy ranging from 44 to 206 ft-lb and shear area from 50 to 100%. Although there was only one set of data at the 4 o'clock position, this recorded the lowest Charpy impact energy of 35 ft-lb, but the shear area was not less than 50%.

There were four welds that had one or both pipes from Source C that were from the same production heat (designated #2); welds A17, A44, A46 and B03. Weld A17 was produced using a tie-in weld procedure and the results are discussed in detail in Section 6.4.2.1. The specimens were all extracted from the 12 o'clock position for welds A44, A46 and B03. The scatter in the test data was large; the Charpy impact energy ranged from 68 to 199 ft-lb and shear area from 50 to 100%.

There were two welds that had one pipe from Source C that were from the same production heat (designated #3); welds A46 and B08. The specimens were all extracted from the 6 o'clock position and exhibited very little scatter; the Charpy impact energy ranged from 163 to 200 ft-lb and all specimens exhibited 100% shear area.

There were two welds that had one pipe from Source C that were from the same production heat (designated #4); welds B03 and B08. The specimens sampled the 6 o'clock (weld B03) and 12 o'clock (weld B08) positions, and gave comparable results; the Charpy impact energy ranged from 63 to 178 ft-lb and the shear area ranged from 55 to 100%.

Comparison of all weld metal results

Since the same main line weld procedure was used throughout the project, despite welding pipes from different sources the Charpy properties for the weld metal should be comparable. The results for the specimens notched at the weld metal centerline are presented in Table 35 and Figure 96. The results for weld A17 have been separated out in Figure 96 as this girth weld was produced using a tie-in weld procedure.

As can be seen there is significant scatter in the test data at both the 6 o'clock and 12 o'clock positions. The Charpy impact energy of all test data at the 6 o'clock position ranged from 80 to 178 ft-lb and at the 12 o'clock position the test data ranged from 63 to 150 ft-lb. The Charpy impact energy from the test data at the 4 o'clock position fell with these ranges. The shear area at the different circumferential positions sampled showed that at -4°F (-20°C) the weld metal is essentially ductile; at 4 o'clock the minimum shear area was 75%, and at both the 6 and 12 o'clock positions the minimum shear area was 85%. A large number of the specimens exhibited fully ductile behavior (shear area of 100%).

6.5 Fracture Mechanics Tests

The British and American standards for the measurement of fracture toughness are very similar in principle, differing mainly in small details of the test and in the terminology used. Both have published standards for 'combined' fracture toughness test methods, allowing measurement of critical values of CTOD, J and K.

BS 7448 is the British Standard for fracture mechanics toughness tests and is published in 4 parts; Part 1 is for parent materials, Part 2 is for weldments, Part 3 is for dynamic fracture and Part 4 is for tearing resistance curves and initiation values of fracture toughness. ASTM E1820 [43] is the American publication, and coexists with older test methods for measurement of CTOD (ASTM E1290 [44]) and K (ASTM E399 [45]). It should be noted that, unlike BS 7448, ASTM E1820 does not explicitly address the testing of weldments.

The largest difference between the standards is in the equations used to calculate CTOD; for certain materials there can be a significant difference in the calculated values of CTOD.

Although the EPRG girth weld defect acceptance standard does not require a measure of the fracture toughness of the weldment, it is a requirement of API 1104. API 1104 recommends the use of BS 7448: Part 2 [27]. It should be noted that BS 7448: Part 2 has been superseded by BS EN ISO 15653:2010 [46], however the method of testing and analysis has not changed.

For consistency with the requirements of API 1104 the fracture mechanics tests have been undertaken and resulted to the requirements of BS 7448: Part 2.

6.5.1 Method

Six Bx2B (thickness x width) SENB fracture mechanics specimens were extracted from each girth weld. All specimens were orientated such that their length was normal to the girth weld and width (2B) was in the circumferential direction. The crack tip was orientated in the through thickness direction, parallel to the weld. The specimen thickness (B) was equal to the pipe thickness less the minimum amount of machining considered necessary to produce the Bx2B specimen geometry from a curved pipe segment. Three

specimens were notched at the weld metal centerline, and the remaining three were notched at the fusion line sampling 50% HAZ and 50% weld metal.

Each specimen was prepared and tested in three-point-bend loading at a temperature of -4°F (-20°C) according to BS 7448: Part 2, as recommended in API 1104.

The same test machine was used throughout; an ESH, which had a 33,700 lbf (150kN) capacity.

Prior to notching each specimen, the specimen faces were ground to a fine finish and a 5% nital solution was applied to the weld region to reveal the microstructure. This enable accurate placement of the notch; either at the weld metal centerline or 50/50 about the fusion line (sampling 50% weld metal, 50% HAZ).

After the specimen had been notched the ligament ahead of the machined notch was locally compressed according to the procedures in Appendix D of BS 7448: Part 2 to reduce the welding residual stresses to low and uniform levels and enable the growth of an acceptably straight crack from the machined notch.

Each specimen was then fatigue pre-cracked at ambient laboratory temperature according to the procedure recommended in BS 7448: Part 2 to produce a sharp crack of depth, a_0 , approximately equal to half the specimen width, W ($0.45 \leq a_0/W \leq 0.70$).

A refrigerated alcohol bath was used to cool the specimen and the test was undertaken while the specimen was immersed in the cooling medium. The alcohol was constantly re-circulated and heavily agitated for optimum control of the test temperature to within 0.2°C . A thermocouple was used to monitor the specimen temperature.

A clip gauge was used to monitor and record the opening displacement of the crack faces during the test. The clip gauge was mounted between two knife edges; placed either side of the notch opening.

Each specimen was then loaded in three-point-bending to failure.

On completion of each test, the fracture faces were measured to confirm the initial crack length (i.e., the crack length from the pre-cracking stage) and the final crack length, and hence the extent of any ductile tearing. In addition, the fracture surfaces were photographed to record the appearance of the fracture surface features for future observation.

Single point values of fracture toughness; CTOD, J and K were calculated for each specimen tested (the equations are presented in Appendix C). The fracture toughness parameters are described below:

- K 'Stress Intensity Factor' is considered a stress-based estimate of fracture toughness and is derived from a function that depends on the applied force at fracture and the specimen geometry (specimen thickness, width and crack length)
- CTOD 'Crack tip opening displacement' is considered a strain-based estimate of fracture toughness and can be separated into two components; elastic and plastic. The elastic component is calculated from K. For the plastic component it is assumed that the specimen rotates about a fixed point in the un-cracked ligament and is calculated from the crack mouth opening displacement (measured using a clip gauge) and the relative crack dimensions in relation to the specimen width.
- J 'J-Integral' is an energy based estimate of fracture toughness and can be separated into two components; elastic and plastic. As with CTOD, the elastic component is calculated from K, while the plastic component is calculated from the plastic area beneath the force versus clip opening displacement record.

These three parameters can be related to one another. However, the relationship is not unique and depends on the material tensile properties and specimen geometry. K is an appropriate parameter when the

material behavior is essentially elastic (brittle), but becomes increasingly conservative with increasing plasticity. For elastic-plastic material behavior CTOD and J are the most appropriate parameters to use.

CTOD is calculated to enable a comparison of the fracture toughness of the weldment with the acceptance criteria in API 1104 (note, EPRG does not require fracture toughness testing). J has been calculated as it is used to assess the fracture performance of the curved wide plate tests undertaken which are reported later (Sections 8.5 and 8.4). Although not used in this work, K is reported for completeness.

CTOD was determined from the clip gauge that was used to monitor and record the opening of the faces during the test. The area beneath the force versus clip opening displacement test record was used to calculate J. A corresponding value of K was calculated from the applied force at the point on the force versus clip opening displacement test record at which CTOD and J were calculated. The values of fracture toughness from each test record were calculated using values of yield and tensile strength that were measured adjacent to the position where the specimens were extracted.

As specified in BS 7448: Part 2 the tensile properties used to calculate fracture toughness corresponded to the region in which the crack tip was located. When the crack tip was located completely in the weld metal, all weld metal tensile properties were used. Where the crack tip was located in, or partially in, the HAZ, the higher of the parent material and weld metal strengths were used.

The tensile properties were measured at ambient laboratory temperature, approximately 68°F (20°C), hence the appropriate value of yield strength at the fracture test temperature of -4°F (-20°C) was estimated from the equation given in BS 7448: Part 2, where:

$$R_{p0.2} = R_{p0.2(RT)} + \frac{10^5}{(491 + 1.8T)} - 189 \quad [31]$$

Where: $R_{p0.2}$ = Predicted yield strength (units: N/mm²)
 $R_{p0.2(RT)}$ = Yield strength at room temperature (units: N/mm²)
 T = Test temperature (units: °C)

Equation [31] is only applicable for estimating the yield strength of a ferritic material at temperatures less than room temperature.

No correction was applied to the tensile strength to account for the reduced test temperature.

The results from the tests undertaken are discussed in detail below.

6.5.2 Results

API 1104 Appendix A requires a minimum CTOD of 0.004in (0.10mm) or 0.010in (0.25mm) from a Bx2B specimen, tested at or below the minimum design temperature. This is particularly relevant for the Option 1 assessment method; however, such limits are not required for Option 2, just the measure of CTOD to enable the toughness ratio K_r to be calculated. In contrast, EPRG does not require determination of CTOD.

The individual results for each girth weld are first summarized. Note, the units used are consistent with the requirements of BS 7448: Part 2; CTOD is expressed in mm, J in kJ/m² and K in MPa√m. These units are consistent with those specified in ASTM E 1820 [43].

The failure behavior of each specimen is described by one of three terms, depending on the amount of ductile tearing (i.e., extension of the original crack length) and the force achieved during the test. These are denoted type 'c', type 'u' or type 'm';

- Type 'c' is used to describe the critical value of fracture toughness at the onset of brittle crack extension (or pop-in) when the average stable crack extension is less than 0.008in (0.2mm).
- Type 'u' is used to describe the critical value of fracture toughness at the onset of brittle crack extension (or pop-in) when the average crack extension is equal to or greater than 0.008in (0.2mm).
- Type 'm' is used to describe the value of fracture toughness at the first attainment of a maximum force plateau for fully plastic behavior.

A 'pop-in' event is a discontinuity in the force versus displacement record. The pop-in corresponds to a sudden increase in displacement and, generally, a sudden decrease in force. Subsequently the displacement and force increase relatively slowly to above their respective values at pop-in. A pop-in is considered 'significant' if the force drop and displacement increase is greater than 1% (less than 1% and the pop-in can be ignored).

The individual force versus clip opening displacement records are provided in Appendix D.

A comparison is then made of the entire weld metal test results, and the HAZ test results are compared in relation to the pipe source and production heat.

6.5.2.1 Summary of Individual Test Results

Weld A06 Each specimen was extracted from the weld 7 o'clock position. Both adjoining pipes were from Source B and from the same production heat. The weld was produced using the 'main line' welding procedure. The notch for the HAZ test specimens was placed on the same side of the weld for consistency. The results are presented in Table 36 and Figure 97. The force versus clip opening displacement plots are provided in Figure D1 of Appendix D.

As can be seen from the results the weld metal toughness is marginally higher than the HAZ. The minimum measured values of CTOD, J and K in the weld metal were 0.12mm, 130.5KJ/m² and 125.1MPa√m from specimen A06-7-C2. The minimum measured values in the HAZ were 0.05mm, 64.5KJ/m² and 104.0MPa√m from specimen A06-7-C4.

One of the HAZ specimens (ID, A06-7-C4) failed the CTOD requirement of API 1104.

The weld metal tests comprised two type 'm' failures and one type 'c' (failure was due to a significant pop-in). The HAZ specimens failed prior to achieving a maximum force plateau; two type 'c' test results and one type 'u'.

Weld A17 The weld metal specimens were extracted from the weld 1 o'clock position, the HAZ specimens were extracted from the weld 2 o'clock position. Both adjoining pipes were from Source C and from the same production heat. The girth weld was produced using the 'tie-in' weld procedure. The notch for the HAZ test specimens was placed on the same side of the weld for consistency. The results are presented in Table 37 and Figure 98. The force versus clip opening displacement plots are provided in Figure D2 of Appendix D.

As can be seen from the results the weld metal toughness is marginally lower than the HAZ. The minimum measured values of CTOD, J and K in the weld metal were 0.11mm, 118.3KJ/m² and 114.7MPa√m (specimen A17-1-C3 recorded the lowest CTOD and J, but specimen A17-1-C1 recorded the lowest value of K). The minimum measured values in the HAZ were 0.17mm, 183.4KJ/m² and 1263.4MPa√m from specimen A17-2-C4.

Each specimen achieved the CTOD requirement of API 1104.

The weld metal and HAZ tests all achieved a maximum force plateau prior to failure. The failure type for each specimen was type 'm'.

Weld A33 Each specimen was extracted from the weld 7 o'clock position. The adjoining pipes were from Source A and B; the HAZ notch sampled Source B pipe. The weld was produced using the 'main line' welding procedure. The notch for the HAZ test specimens was placed on the same side of the weld for consistency. The results are presented in Table 38 and Figure 99. The force versus clip opening displacement plots are provided in Figure D3 of Appendix D.

As can be seen from the results the weld metal toughness is similar to the HAZ toughness. The minimum measured values of CTOD, J and K in the weld metal were 0.10mm, 115.0KJ/m² and 124.0MPa√m from specimen A33-7-C2. The minimum measured values in the HAZ were 0.09mm, 101.0KJ/m² and 119.9MPa√m from specimen A33-7-C4.

One of the HAZ specimens (ID, A33-7-C4) failed the CTOD requirement of API 1104.

Despite the fracture toughness of the weld metal and HAZ being similar, the weld metal exhibited greater ductility; two of the specimens exhibited type 'm' failures and one type 'c' (failure was due to a significant pop-in). In contrast the HAZ specimens all failed prior to achieving a maximum force plateau; two type 'u' test results (one specimen, A33-7-C4 failed due to a significant pop-in) and one type 'c'. Note, the specimen that recorded the type 'c' failure did not produce the lowest toughness value of the HAZ specimens.

Weld A44 Each specimen was extracted from the weld 7 o'clock position. The adjoining pipes were from Source B and C; the HAZ notch sampled Source C pipe. The weld was produced using the 'main line' welding procedure. The notch for the HAZ test specimens was placed on the same side of the weld for consistency. The results are presented in Table 39 and Figure 100. The force versus clip opening displacement plots are provided in Figure D4 of Appendix D.

As can be seen from the results there was little scatter in the weld metal toughness; the results are within the minimum and maximum values measured in the HAZ. The minimum measured values of CTOD, J and K in the weld metal were 0.15mm, 162.8KJ/m² and 124.0MPa√m (specimen A44-7-C2 recorded the lowest CTOD and J, but specimen A44-7-C1 recorded the lowest value of K). The minimum measured values in the HAZ were 0.07mm, 74.2KJ/m² and 106.7MPa√m from specimen A44-7-C4.

One of the HAZ specimens (ID, A44-7-C4) failed the CTOD requirement of API 1104.

The weld metal exhibited good ductility; each specimen exhibited type 'm' failures. In contrast only one specimen exhibited a type 'm' failure, the other two failed prior to achieving a maximum force plateau; one type 'c' failure and type 'u'.

Weld A46 Each specimen was extracted from the weld 7 o'clock position. Both adjoining pipes were from Source C, although from different production heats. The weld was produced using the 'main line' welding procedure. The notch for the HAZ test specimens was placed on the same side of the weld for consistency. The results are presented in Table 40 and Figure 101. The force versus clip opening displacement plots are provided in Figure D5 of Appendix D.

As can be seen from the results the weld metal and HAZ exhibited low toughness and were similar in magnitude. The minimum measured values of CTOD, J and K in the weld metal were 0.07mm, 82.3KJ/m² and 109.9MPa√m from specimen A46-7-C2. The minimum measured values in the HAZ were 0.10mm, 115.1KJ/m² and 120.3MPa√m from specimen A46-7-C4.

One of the HAZ specimens (ID, A46-7-C2) failed the CTOD requirement of API 1104.

Despite low toughness two of the weld metal specimens exhibited good ductility, exhibiting type 'm' failures. However, the third specimen exhibited a type 'c' failure; due to a significant pop-in. Two of the HAZ specimens exhibited type 'u' failure, the third achieved a maximum force plateau resulting in a type 'm' failure.

Weld A50 Each specimen was extracted from the weld 7 o'clock position. Both adjoining pipes were from Source B, although from different production heats. The weld was produced using the 'main line' welding procedure. The notch for the HAZ test specimens was placed on the same side of the weld for consistency. The results are presented in Table 41 and Figure 102. The force versus clip opening displacement plots are provided in Figure D6 of Appendix D.

As can be seen from the results the weld metal toughness is higher than the HAZ. The HAZ specimens exhibited significant scatter, unlike the weld metal specimens. The minimum measured values of CTOD, J and K in the weld metal were 0.15mm, 159.2KJ/m² and 125.7MPa√m (specimen A50-7-C1 recorded the lowest CTOD and J, but specimen A50-7-C3 recorded the lowest value of K). The minimum measured values in the HAZ were 0.04mm, 43.4KJ/m² and 89.8MPa√m from specimen A50-7-C4.

Two of the HAZ specimens (ID, A50-7-C4 and A50-7-C5) failed the CTOD requirement of API 1104.

The weld metal exhibited good ductility; each specimen exhibited type 'm' failure. In contrast the HAZ specimens failed prior to achieving a maximum force plateau; two type 'c' failures (one specimen, A50-7-C4 failed due to a significant pop-in) and one type 'u'.

Weld B03 The weld metal specimens were extracted from the weld 6 o'clock position. One of the HAZ specimens was extracted from the weld 6 o'clock position; the other two were extracted from the 5 o'clock position. The notch for the HAZ test specimens was placed on the same side of the weld for consistency. Both adjoining pipes were from Source C, although from different production heats. The weld was produced using the 'main line' welding procedure. The results are presented in Table 42 and Figure 103. The force versus clip opening displacement plots are provided in Figure D7 of Appendix D.

As can be seen from the results the weld metal toughness is marginally higher than the HAZ. The minimum measured values of CTOD, J and K in the weld metal were 0.07mm, 85.4KJ/m² and 119.6MPa√m from specimen B03-6-C1. The minimum measured values in the HAZ were 0.06mm, 77.9KJ/m² and 116.1MPa√m from specimen B03-5-C6.

One of the weld metal specimens (ID, B03-6-C1) and one HAZ specimen (ID, B03-5-C6) failed the CTOD requirement of API 1104.

The weld metal tests comprised two type 'm' failures and one type 'c' (failure was due to a significant pop-in). The HAZ specimens failed prior to achieving a maximum force plateau; two type 'c' test results (one specimen, B03-5-C5 failed due to a significant pop-in) and one type 'u'.

Weld B06 The weld metal specimens were extracted from the weld 3 o'clock position. One of the HAZ specimens was extracted from the weld 3 o'clock position; the other two were extracted from the 11 o'clock position. The adjoining pipes were from Source A and B; the HAZ notch sampled Source A pipe. The weld was produced using the 'main line' welding procedure. The results are presented in Table 43 and Figure 104. The force versus clip opening displacement plots are provided in Figure D8 of Appendix D.

As can be seen from the results the weld metal toughness is higher than the HAZ. The minimum measured values of CTOD, J and K in the weld metal were 0.14mm, 162.6KJ/m² and

138.9MPa \sqrt{m} from specimen B06-3-C2. The minimum measured values in the HAZ were 0.08mm, 96.7KJ/m² and 125.6MPa \sqrt{m} from specimen B06-11-C6.

Two of the HAZ specimens (ID, B06-3-C4 and B06-11-C6) failed the CTOD requirement of API 1104.

The weld metal exhibited good ductility; two specimens exhibited type 'm' failure, the other specimen type 'u'. The HAZ specimens failed prior to achieving a maximum force plateau; one type 'u' failure and two type 'c'.

Weld B08 The weld metal specimens were extracted from the weld 11 o'clock position. The HAZ specimens were extracted from the weld 11, 5 and 6 o'clock positions. Both adjoining pipes were from Source C, although from different production heats. The weld was produced using the 'main line' welding procedure. The notch for the HAZ test specimens was placed on the same side of the weld for consistency. The results are presented in Table 44 and Figure 105. The force versus clip opening displacement plots are provided in Figure D9 of Appendix D.

As can be seen from the results the weld metal and HAZ exhibited low toughness, although the weld metal toughness was slightly higher. The minimum measured values of CTOD, J and K in the weld metal were 0.10mm, 126.4KJ/m² and 132.7MPa \sqrt{m} from specimen B08-11-C2. The minimum measured values in the HAZ were 0.08mm, 96.7KJ/m² and 125.6MPa \sqrt{m} (specimen B08-5-C5 recorded the lowest CTOD and J, but specimen B08-6-C6 recorded the lowest value of K).

Each specimen achieved the CTOD requirement of API 1104.

The weld metal exhibited good ductility; two specimens exhibited type 'm' failure, the other specimen type 'u'. The HAZ specimens failed prior to achieving a maximum force plateau; two type 'u' failures and one type 'c'.

6.5.2.2 Comparison of Test Results

All test data

Weld A17 was produced using a 'tie-in' weld procedure; all other welds tested were produced using the 'main line' weld procedure.

The CTOD results of all weld metal tests are compared in Figure 106-(a). As can be seen four of the twenty-seven specimens tested resulted in a type 'c' failure. Each specimen failed due to a significant pop-in. Two specimens resulted in type 'u' failure. The remaining twenty-one specimens exhibited fully ductile behavior (failure type 'm'). Only two of the specimens failed to achieve the minimum CTOD requirement of API 1104.

The CTOD results of the HAZ tests are compared in Figure 106-(b). Compared with the weld metal tests, the majority of the twenty-seven specimens tested resulted in either type 'c' (eleven specimens) or type 'u' (eleven specimens) failure. Only 5 specimens exhibited fully ductile behavior, with a resulting toughness similar to that exhibited by the weld metal. In general, the toughness of the HAZ region was low; nine specimens failed to achieve the minimum CTOD requirement of API 1104. A point to note is that the HAZ results are from pipes from each of the three sources and are therefore to some extent subject to the variability in pipe mechanical properties and chemistry. The HAZ results are compared in greater detail in the following subsection, considering the consistency in results from pipes from the same source and same production heat.

For completeness the fracture mechanics test data are also compared in terms of J and K in Figure 107 and Figure 108 respectively.

HAZ test data

In this section the HAZ toughness is compared with consideration given to the pipe source and production heat.

Three of the welds tested were from Source B and from the same production heat; welds A06, A33 and A50. The CTOD data are compared in Figure 109-(a). As can be seen the measured toughness is relatively poor, with one of the specimens tested not achieving the minimum CTOD requirement of API 1104. The minimum measured CTOD was 0.04mm, the maximum was 0.19mm and the average was 0.10mm (STDV of 0.05mm). The data set consisted of five type 'c' failures and five type 'u'. Only two of the specimens failed due to a significant pop-in; interestingly they were the two specimens that gave the minimum and maximum measure of CTOD.

For completeness the results are also presented in terms of J (see Figure 110-(a)) and K (see Figure 111-(a)).

Four of the welds tested were from Source C and from the same production heat; welds A17 (produced using a tie-in weld procedure), A44, A46 and B03. The CTOD data are compared in Figure 109-(b). As can be seen there is significant scatter in the results; three specimens exhibiting type 'c' failure, four type 'u' and five type 'm'. Two of the specimens tested did not achieve the minimum CTOD requirement of API 1104. The minimum measured CTOD was 0.06mm (type 'c'), the maximum was 0.36mm (type 'm') and the average was 0.18mm (STDV of 0.09mm). The specimen that recorded the lowest CTOD failed due to a significant pop-in.

For completeness the results are also presented in terms of J (see Figure 110-(b)) and K (see Figure 111-(b)).

A point to note by comparing the fracture toughness data from Source B (Figure 109-(a)) with that from Source C (Figure 109-(b)) is that the HAZ associated with Source C pipe is more ductile and has better fracture toughness properties.

7 Curved Wide Plate Tests

The curved wide plate (CWP) test specimens were manufactured and tested according to in-house procedures that have been developed by Laboratory Soete (University of Gent, Belgium) since 1979. Details of the test specimen preparation, instrumentation and test method are given below, followed by a summary of the test results.

7.1 Specimen Preparation

Each specimen was flame-cut from the pipe section. The longitudinal edges of the specimen were then machined straight and parallel to each other. The weld reinforcement (root and cap) was not removed.

The nominal dimensions of the CWP specimen are shown in Figure 112, expressed in relation to the arc length; 12in (300mm). The overall specimen dimensions are 1.4W (length of attachment weld) by 4W (overall specimen length). The length of the prismatic 'gauge' section is 3W, with the girth weld at mid-length.

The length to width ratio of the prismatic gauge section ensures that a region of uniform straining between the defect and each of the end regions of the specimen through which the load is applied.

A surface breaking defect was introduced at the weld root, sampling either weld metal or the HAZ. A 0.006in (0.15mm) wide chevron cutting wheel was used to produce the defect. Based on the result of the Charpy

impact tests, fatigue pre-cracking was not required since the Charpy impact energy exceeded a min(avg) of 22(30) ft-lb (30(40)J) for all welds.

Each CWP specimen was subjected to detailed metrology to determine the minimum thickness of each pipe, arc length and parallelism of the specimen gauge length.

The CWP specimen was then welded to re-usable loading lugs, which enabled the specimens to be connected to the test machine. To prevent out-of-plane bending of the cross section during loading, the loading lugs were carefully aligned with the centroid of the CWP specimen prior to welding.

7.2 Instrumentation

Linear variable differential transformers (LVDTs) were used to measure elongation of Pipe 1 and Pipe 2, remote from the weld, and the global elongation of the specimen. In addition, a clip gauge was used to measure the crack mouth opening displacement (CMOD) of the defect. The position of the instrumentation is shown in Figure 113, together with the corresponding gauge lengths.

The applied load was output directly from the load cell within the test machine.

7.3 Test Method

Once the CWP was positioned within the test machine and the instrumentation attached and verified, the specimen was cooled to the test temperature of -4°F (-20°C) using curved cooling boxes that were firmly clamped against the inner and outer surfaces of the specimen. Cooling was achieved with refrigerated methanol, in a closed loop system. The specimen temperature was monitored using two thermocouples that were located adjacent to the machined defect and on the pipe surface at a distance of 1.7W from the defect. Prior to undertaking the test, the specimen was held at temperature for a period not less than 1 hour to enable the temperature to stabilize and ensure a uniform temperature distribution through the specimen cross section.

The test was undertaken under displacement control, at a constant rate of 1 mm/min. The test was stopped when either failure occurred or a maximum load was achieved during loading.

On completion of the test the fracture surfaces were sprayed with a protective coating to mitigate degradation of the fracture surface features. For those tests that were stopped without failure of the specimen, the spray was directed into the notch mouth in case there was any tearing from the notch tip.

7.4 Post Test Metallographic Examination

On completion of the test, photographs were taken of the tested specimen and the fracture surfaces were then cut from the specimen. The fracture surface features were then photographed and the dimensions of the defect were measured.

For those specimens that fractured during the test a stereoscope was used to identify the fracture initiation point or the deepest point of the notch, as appropriate. The fracture surface was sectioned at this point about a plane perpendicular to the fracture surface, to reveal the position of the notch in relation to the target location. The cross section was ground, polished and etched using a 2% nital solution to reveal the weld, HAZ and surrounding microstructure, and then photographed. For those specimens targeting the HAZ, the position of the notch tip in relation to the fusion boundary was measured.

7.5 Analysis

The plastic straining capacity and defect tolerance were quantified by means of the remote (pipe metal) failure strains. A pipe metal failure strain of 0.5% was used as a performance requirement, i.e., the Gross Section Yielding or pipe yielding criterion:

Local Collapse	LC	- collapse of the remaining ligament below the surface breaking defect
Net Section Yield	NSY	- collapse of the section containing the defect without significant straining of the parent material
Gross Section Yield	GSY	- collapse by gross straining remote from the defect. A pipe metal strain of 0.5% is required to consider GSY has been achieved

The average gross strain was calculated by dividing the overall elongation of the specimen by the gauge length, $2W$. The corresponding strains in each pipe were calculated by dividing the pipe metal elongations by the gauge length, $0.5W$.

The average value of remote strain in the pipes is calculated from the overall elongation and CMOD measurements, since the overall elongation is composed of the CMOD and the elongation of the adjacent pipes.

The gross section stress was calculated from the load recorded during the test and the minimum gross cross sectional area.

7.6 Results

A summary of the individual test results for each weld is presented below.

7.6.1 Weld A06

Four CWP specimens were extracted from Weld A06. Table 45 shows the position that each specimen was extracted from around the weld circumference, together with details of the specimen and notch dimensions. Each specimen was notched at the weld root; 3 specimens sampled the HAZ (A06-WP1-H1, A06-WP2-H2 and A06-WP3-H3), and 1 specimen sampled the weld metal centerline (A06-WP1-W).

The test results are presented in Table 46 and individual graphs of gross stress versus strain, and CMOD versus strain are presented in Appendix E; Figure E1 through to Figure E20.

The behavior of each CWP specimen is summarized below:

- WP-H1
- The defect was located in the HAZ of Pipe 1
 - The defect dimensions were; 0.118x1.97in (3.0x50mm), which correspond to 2.46% of the specimen cross section area
 - The pipe and global strains at failure exceeded 0.5%; the minimum measured strain was 2.44% in Pipe 2
 - The gross stress at failure exceeded;
 - the *minimum* yield strength between the parent pipe and weld metal measured **at the CWP location**. The weld metal matched the parent pipe
 - the *minimum* yield strength of the parent pipe and weld metal measured around the weld circumference. The weld metal matched the parent pipe

- the *average* yield strength of the parent pipe and weld metal measured around the weld circumference. The weld metal overmatched the parent pipe
 - There was no clear fracture initiation point. The fracture faces were sectioned mid-way along the defect length; the tip of the machined defect was located in the coarse/fine grained HAZ microstructure, +0.024in (+0.60mm) from the fusion line
 - The CWP specimen failed by GSY
- WP-H2
- The defect was located in the HAZ of Pipe 1
 - The defect dimensions were; 0.118x3.94in (3.0x100mm), which correspond to 4.9% of the specimen cross section area
 - The pipe and global strains at failure exceeded 0.5%; the minimum measured strain was 0.69% in Pipe 2
 - The gross stress at failure exceeded;
 - the *minimum* yield strength between the parent pipe and weld metal measured **at the CWP location**. The weld metal overmatched the parent pipe
 - the *minimum* yield strength of the parent pipe and weld metal measured around the weld circumference. The weld metal matched the parent pipe
 - the *average* yield strength of the parent pipe and weld metal measured around the weld circumference. The weld metal overmatched the parent pipe
 - A fracture initiation point was observed. The fracture faces were sectioned at the fracture initiation point; the tip of the machined defect was located in the coarse grained HAZ microstructure, on the fusion line
 - The CWP specimen failed by GSY
- WP-H3
- The defect was located in the HAZ of Pipe 1
 - The defect dimensions were; 0.157x3.94in (4.0x100mm), which correspond to 6.52% of the specimen cross section area
 - The pipe and global strains at failure exceeded 0.5%; the minimum measured strain was 0.53% across the weldment, which was comparable to the pipe strains
 - The gross stress at failure was slightly less than;
 - the *minimum* yield strength between the parent pipe and weld metal measured **at the CWP location** (2ksi (14N/mm²)). The weld metal overmatched the parent pipe
 - the *minimum* yield strength of the parent pipe and weld metal measured around the weld circumference (1.5ksi (10N/mm²)). The weld metal matched the parent pipe
 - the *average* yield strength of the parent pipe and weld metal measured around the weld circumference (2.5ksi (17N/mm²)). The weld metal overmatched the parent pipe
 - A fracture initiation point was observed. The fracture faces were sectioned at the fracture initiation point; the tip of the machined defect was located in the coarse grained HAZ microstructure, on the fusion line
 - The CWP specimen failed by GSY

- WP-W
- The defect was located in the weld metal.
 - The defect dimensions were; 0.118x1.97in (3.0x50mm), which correspond to 2.46% of the specimen cross section area
 - The pipe and global strains at failure exceeded 0.5%; the minimum measured strain was 2.14% in Pipe 2
 - The gross stress at failure exceeded;
 - the *minimum* yield strength between the parent pipe and weld metal measured **at the CWP location**. The weld metal overmatched the parent pipe
 - the *minimum* yield strength of the parent pipe and weld metal measured around the weld circumference. The weld metal matched the parent pipe
 - the *average* yield strength of the parent pipe and weld metal measured around the weld circumference. The weld metal overmatched the parent pipe
 - There was no clear fracture initiation point. The fracture faces were sectioned mid-way along the defect length; the tip of the machined defect was located in the coarse grained (columnar) weld metal, and the crack propagated through the weld
 - The CWP specimen failed by GSY

7.6.2 Weld A17

Four CWP specimens were extracted from Weld A17. Table 47 shows the position that each specimen was extracted from around the weld circumference, together with details of the specimen and notch dimensions. Each specimen was notched at the weld root; 3 specimens sampled the HAZ (A17-WP1-H1, A17-WP2-H2 and A17-WP3-H3), and 1 specimen sampled the weld metal centerline (A17-WP1-W).

The test results are presented in Table 48 and individual graphs of gross stress versus strain, and CMOD versus strain are presented in Appendix E; Figure E21 through to Figure E40.

The behavior of each CWP specimen is summarized below:

- WP-H1
- The defect was located in the HAZ of Pipe 1
 - The defect dimensions were; 0.118x1.97in (3.0x50mm), which correspond to 2.46% of the specimen cross section area
 - The pipe and global strains at failure exceeded 0.5%; the minimum measured strain was 0.83% in Pipe 1
 - The gross stress at failure exceeded;
 - the *minimum* yield strength between the parent pipe and weld metal measured **at the CWP location**. The weld metal under-matched the parent pipe
 - the *minimum* yield strength of the parent pipe and weld metal measured around the weld circumference. The weld metal under-matched the parent pipe
 - the *average* yield strength of the parent pipe and weld metal measured around the weld circumference. The weld metal under-matched the parent pipe
 - There was no clear fracture initiation point. The fracture faces were sectioned mid-way along the defect length; the tip of the machined defect was located in the coarse grained

- HAZ microstructure, +0.006in (+0.16mm) from the fusion line
- The CWP specimen failed by GSY
- WP-H2
- The defect was located in the HAZ of Pipe 2
 - The defect dimensions were; 0.118x3.94in (3.0x100mm), which correspond to 4.94% of the specimen cross section area
 - The pipe and global strains at failure exceeded 0.5%; the minimum measured strain was 0.58% in Pipe 1
 - The gross stress at failure;
 - was slightly less than the *minimum* yield strength between the parent pipe and weld metal measured **at the CWP location**; 1.3ksi (9N/mm²). The weld metal matched the parent pipe
 - exceeded the *minimum* yield strength of the parent pipe and weld metal measured around the weld circumference. The weld metal under-matched the parent pipe
 - exceeded the *average* yield strength of the parent pipe and weld metal measured around the weld circumference. The weld metal matched the parent pipe
 - There was no clear fracture initiation point. The fracture faces were sectioned mid-way along the defect length; the tip of the machined defect was located in the coarse grained (columnar) weld metal, -0.02in (-0.50mm) from the fusion line. There was slow stable crack growth in the weld metal, which propagated towards the fusion line
 - The CWP specimen failed by GSY
- WP-H3
- The defect was located in the HAZ of Pipe 1
 - The defect dimensions were; 0.118x3.94in (3.0x100mm), which correspond to 4.93% of the specimen cross section area
 - The pipe and global strains at failure exceeded 0.5%; the minimum measured strain was 0.52% in Pipe 1
 - The gross stress at failure;
 - was slightly less than the *minimum* yield strength between the parent pipe and weld metal measured **at the CWP location** (1ksi (7N/mm²)). The weld metal overmatched the parent pipe
 - exceeded the *minimum* yield strength of the parent pipe and weld metal measured around the weld circumference. The weld metal under-matched the parent pipe
 - exceeded the *average* yield strength of the parent pipe and weld metal measured around the weld circumference. The weld metal under-matched the parent pipe
 - There was no clear fracture initiation point. The fracture faces were sectioned mid-way along the defect length; the tip of the machined defect was located in the coarse grained (columnar) weld metal, -0.018in (-0.45mm) from the fusion line. There was slow stable crack growth in the weld metal, which propagated towards the fusion line
 - The CWP specimen failed by GSY
- WP-W
- The defect was located in the weld metal.

- The defect dimensions were; 0.118x1.97in (3.0x50mm), which correspond to 2.46% of the specimen cross section area
- The pipe and global strains at failure exceeded 0.5%; the minimum measured strain was 1.58% in Pipe 1
- The gross stress at failure exceeded;
 - the *minimum* yield strength between the parent pipe and weld metal measured **at the CWP location**. The weld metal slightly under-matched the parent pipe
 - the *minimum* yield strength of the parent pipe and weld metal measured around the weld circumference. The weld metal under-matched the parent pipe
 - the *average* yield strength of the parent pipe and weld metal measured around the weld circumference. The weld metal under-matched the parent pipe
- There was no clear fracture initiation point. The fracture faces were sectioned mid-way along the defect length; the tip of the machined defect was located in the coarse grained (columnar) and grain refined weld metal
- The CWP specimen failed by GSY

7.6.3 Weld A33

Four CWP specimens were extracted from Weld A33. Table 49 shows the position that each specimen was extracted from around the weld circumference, together with details of the specimen and notch dimensions. Each specimen was notched at the weld root; 3 specimens sampled the HAZ (A33-WP1-H1, A33-WP2-H2 and A33-WP3-H3), and 1 specimen sampled the weld metal centerline (A33-WP1-W).

The test results are presented in Table 50 and individual graphs of gross stress versus strain, and CMOD versus strain are presented in Appendix E; Figure E41 through to Figure E60.

The behavior of each CWP specimen is summarized below:

- WP-H1
- The defect was located in the HAZ of Pipe 1
 - The defect dimensions were; 0.118x1.97in (3.0x50mm), which correspond to 2.46% of the specimen cross section area
 - The pipe and global strains at failure exceeded 0.5%; the minimum measured strain was 1.11% in Pipe 2
 - The gross stress at failure exceeded;
 - the *minimum* yield strength between the parent pipe and weld metal measured **at the CWP location**. The weld metal overmatched the parent pipe
 - the *minimum* yield strength of the parent pipe and weld metal measured around the weld circumference. The weld metal overmatched the parent pipe
 - the *average* yield strength of the parent pipe and weld metal measured around the weld circumference. The weld metal overmatched the parent pipe
 - A fracture initiation point was observed. The fracture faces were sectioned at the fracture initiation point; the tip of the machined defect was located in the coarse grained HAZ microstructure, +0.005in (+0.13mm) from the fusion line. The crack propagated along the

fusion line.

- The CWP specimen failed by GSY
- WP-H2
- The defect was located in the HAZ of Pipe 1
 - The defect dimensions were; 0.118x3.94in (3.0x100mm), which correspond to 4.96% of the specimen cross section area
 - The pipe and global strains at failure exceeded 0.5%; the minimum measured strain was 0.87% in Pipe 2
 - The gross stress at failure;
 - was slightly less than the *minimum* yield strength between the parent pipe and weld metal measured **at the CWP location**; 3.5ksi (24N/mm²). The weld metal overmatched the parent pipe
 - exceeded the *minimum* yield strength of the parent pipe and weld metal measured around the weld circumference. The weld metal overmatched the parent pipe
 - exceeded the *average* yield strength of the parent pipe and weld metal measured around the weld circumference. The weld metal overmatched the parent pipe
 - A fracture initiation point was observed. The fracture faces were sectioned at the fracture initiation point; the tip of the machined defect was located in the coarse/fine grained HAZ microstructure, +0.018in (+0.45mm) from the fusion line. The crack then propagated towards the coarse grained HAZ microstructure and then along the fusion line.
 - The CWP specimen failed by GSY
- WP-H3
- The defect was located in the HAZ of Pipe 1
 - The defect dimensions were; 0.157x3.94in (4.0x100mm), which correspond to 6.54% of the specimen cross section area
 - The pipe and global strains at failure exceeded 0.5%; the minimum measured strain was 0.57% in Pipe 1
 - The gross stress at failure was slightly less than;
 - the *minimum* yield strength between the parent pipe and weld metal measured **at the CWP location** (3.8ksi (26N/mm²)). The weld metal overmatched the parent pipe
 - the *minimum* yield strength of the parent pipe and weld metal measured around the weld circumference (1.2ksi (8N/mm²)). The weld metal overmatched the parent pipe
 - the *average* yield strength of the parent pipe and weld metal measured around the weld circumference (3.2ksi (22N/mm²)). The weld metal overmatched the parent pipe
 - A fracture initiation point was observed. The fracture faces were sectioned at the fracture initiation point; the tip of the machined defect was located in the coarse grained HAZ microstructure, on the fusion line. The crack propagated along the fusion line.
 - The CWP specimen failed by GSY
- WP-W
- The defect was located in the weld metal.
 - The defect dimensions were; 0.118x1.97in (3.0x50mm), which correspond to 2.46% of the

specimen cross section area

- The pipe and global strains at failure exceeded 0.5%; the minimum measured strain was 1.34% in Pipe 2
- The gross stress at failure exceeded;
 - the *minimum* yield strength between the parent pipe and weld metal measured **at the CWP location**. The weld metal slightly overmatched the parent pipe
 - the *minimum* yield strength of the parent pipe and weld metal measured around the weld circumference. The weld metal overmatched the parent pipe
 - the *average* yield strength of the parent pipe and weld metal measured around the weld circumference. The weld metal overmatched the parent pipe
- A fracture initiation point was observed. The fracture faces were sectioned at the fracture initiation point; the tip of the machined defect was located in the coarse grained (columnar) weld metal. The crack propagated towards and then along the fusion line.
- The CWP specimen failed by GSY

7.6.4 Weld A46

Four CWP specimens were extracted from Weld A46. Table 51 shows the position that each specimen was extracted from around the weld circumference, together with details of the specimen and notch dimensions. Each specimen was notched at the weld root, sampling the HAZ.

The test results are presented in Table 52 and individual graphs of gross stress versus strain, and CMOD versus strain are presented in Appendix E; Figure E61 through to Figure E80.

The behavior of each CWP specimen is summarized below:

- WP-H1
- The defect was located in the HAZ of Pipe 1
 - The defect dimensions were; 0.118x1.97in (3.0x50mm), which correspond to 2.46% of the specimen cross section area
 - The pipe and global strains at failure exceeded 0.5%; the minimum measured strain was 2.04% in Pipe 1
 - The gross stress at failure exceeded;
 - the *minimum* yield strength between the parent pipe and weld metal measured **at the CWP location**. The weld metal overmatched the parent pipe
 - the *minimum* yield strength of the parent pipe and weld metal measured around the weld circumference. The weld metal overmatched the parent pipe
 - the *average* yield strength of the parent pipe and weld metal measured around the weld circumference. The weld metal overmatched the parent pipe
 - There was no clear fracture initiation point. The fracture faces were sectioned mid-way along the defect length; the tip of the machined defect was located in the coarse grained (columnar) weld metal, -0.03in (-0.75mm) from the fusion line. The crack propagated towards and along the fusion line in one half of the specimen, but through the weld metal in the other half

- The CWP specimen failed by GSY
- WP-H2
- The defect was located in the HAZ of Pipe 2
 - The defect dimensions were; 0.118x2.95in (3.0x75mm), which correspond to 3.69% of the specimen cross section area
 - The pipe and global strains at failure exceeded 0.5%; the minimum measured strain was 1.07% in Pipe 1
 - The gross stress at failure exceeded;
 - the *minimum* yield strength between the parent pipe and weld metal measured **at the CWP location**. The weld metal overmatched the parent pipe
 - the *minimum* yield strength of the parent pipe and weld metal measured around the weld circumference. The weld metal overmatched the parent pipe
 - the *average* yield strength of the parent pipe and weld metal measured around the weld circumference. The weld metal overmatched the parent pipe
 - A fracture initiation point was observed. The fracture faces were sectioned at the fracture initiation point; the tip of the machined defect was located in the coarse grained (columnar) weld metal, -0.008in (-0.20mm) from the fusion line. The crack propagated towards and then along the fusion line until failure occurred
- WP-H3
- The CWP specimen failed by GSY
- The defect was located in the HAZ of Pipe 1
 - The defect dimensions were; 0.118x3.94in (3.0x100mm), which correspond to 4.95% of the specimen cross section area
 - The pipe and global strains at failure exceeded 0.5%; the minimum measured strain was 0.81% across the weldment, which was comparable to the pipe strains
 - The gross stress at failure exceeded;
 - the *minimum* yield strength between the parent pipe and weld metal measured **at the CWP location**. The weld metal overmatched the parent pipe
 - the *minimum* yield strength of the parent pipe and weld metal measured around the weld circumference. The weld metal overmatched the parent pipe
 - the *average* yield strength of the parent pipe and weld metal measured around the weld circumference. The weld metal overmatched the parent pipe
 - A fracture initiation point was observed. The fracture faces were sectioned at the fracture initiation point; the tip of the machined defect was located in the coarse grained HAZ microstructure, on the fusion line. The crack propagated along the fusion line until failure occurred
- WP-H4
- The CWP specimen failed by GSY
- The defect was located in the HAZ of Pipe 1
 - The defect dimensions were; 0.157x3.94in (4.0x100mm), which correspond to 6.53% of the specimen cross section area

- The pipe and global strains at failure exceeded 0.5%; the minimum measured strain was 0.48% in Pipe 1, which was similar to the strain measured across the weldment
- The gross stress at failure was less than;
 - the *minimum* yield strength between the parent pipe and weld metal measured **at the CWP location** (3.0ksi (21N/mm²)). The weld metal slightly overmatched the parent pipe
 - the *minimum* yield strength of the parent pipe and weld metal measured around the weld circumference (2.9ksi (20N/mm²)). The weld metal overmatched the parent pipe
 - the *average* yield strength of the parent pipe and weld metal measured around the weld circumference (3.9ksi (27N/mm²)). The weld metal overmatched the parent pipe
- A fracture initiation point was observed. The fracture faces were sectioned at the fracture initiation point; the tip of the machined defect was located in the coarse grained HAZ microstructure, +0.008in (+0.20mm) from the fusion line. The crack propagated towards and then along the fusion line until failure occurred
- The CWP specimen failed by NSY

7.6.5 Weld A50

Three CWP specimens were extracted from Weld A50. Table 53 shows the position that each specimen was extracted from around the weld circumference, together with details of the specimen and notch dimensions. Each specimen was notched at the weld root; 2 specimens sampled the HAZ (A50-WP1-H1 and A50-WP2-H2), and 1 specimen sampled the weld metal centerline (A50-WP1-W).

The test results are presented in Table 54 and individual graphs of gross stress versus strain, and CMOD versus strain are presented in Appendix E; Figure E81 through to Figure E89.

The behavior of each CWP specimen is summarized below:

- WP-H1
- The defect was located in the HAZ of Pipe 1
 - The defect dimensions were; 0.118x1.97in (3.0x50mm), which correspond to 2.47% of the specimen cross section area
 - The pipe and global strains at failure exceeded 0.5%; the minimum measured strain was 2.28% in Pipe 2. However, the test was terminated without failure due to excessive straining of Pipe 1; 5.14% at maximum load
 - The gross stress achieved during the test exceeded;
 - the *minimum* yield strength between the parent pipe and weld metal measured **at the CWP location**. The weld metal overmatched the parent pipe
 - the *minimum* yield strength of the parent pipe and weld metal measured around the weld circumference. The weld metal overmatched the parent pipe
 - the *average* yield strength of the parent pipe and weld metal measured around the weld circumference. The weld metal overmatched the parent pipe
 - The specimen was sectioned mid-way along the defect length; the tip of the machined defect was located in the coarse grained HAZ microstructure, on the fusion line. A small crack had initiated at the tip of the machined defect, which had begun to propagate along

the fusion line

- Although the test was terminated prior to failure, if failure was to occur it would have been by GSY

WP-H2

- The defect was located in the HAZ of Pipe 1
- The defect dimensions were; 0.157x3.94in (4.0x100mm), which correspond to 6.55% of the specimen cross section area
- The pipe and global strains at failure exceeded 0.5%; the minimum measured strain was 1.04% in Pipe 2
- The gross stress at failure exceeded;
 - the *minimum* yield strength between the parent pipe and weld metal measured **at the CWP location**. The weld metal overmatched the parent pipe
 - the *minimum* yield strength of the parent pipe and weld metal measured around the weld circumference. The weld metal overmatched the parent pipe
 - the *average* yield strength of the parent pipe and weld metal measured around the weld circumference. The weld metal overmatched the parent pipe
- A fracture initiation point was observed. The fracture faces were sectioned at the fracture initiation point; the tip of the machined defect was located in the coarse grained (columnar) weld metal, -0.004in (-0.10mm) from the fusion line. The crack propagated towards and then along the fusion line until failure occurred
- The CWP specimen failed by GSY

WP-W

- The defect was located in the weld metal.
- The defect dimensions were; 0.118x1.97in (3.0x50mm), which correspond to 2.46% of the specimen cross section area
- The pipe and global strains during the test exceeded 0.5%; the minimum measured strain was 1.54% in Pipe 2. However, the test was terminated without failure due to excessive straining of Pipe 1; 9.6%
- The gross stress achieved during the test exceeded;
 - the *minimum* yield strength between the parent pipe and weld metal measured **at the CWP location**. The weld metal overmatched the parent pipe
 - the *minimum* yield strength of the parent pipe and weld metal measured around the weld circumference. The weld metal overmatched the parent pipe
 - the *average* yield strength of the parent pipe and weld metal measured around the weld circumference. The weld metal overmatched the parent pipe
- The specimen was sectioned mid-way along the defect length; the tip of the machined defect was located in the coarse grained and grain refined weld metal. A small crack had initiated at the tip of the machined defect
- Although the test was terminated prior to failure, if failure was to occur it would have been by GSY

7.6.6 Weld B03

Four CWP specimens were extracted from Weld B03. Table 55 shows the position that each specimen was extracted from around the weld circumference, together with details of the specimen and defect dimensions.

The test results are presented in Table 56 and individual graphs of gross stress versus strain, and CMOD versus strain are presented in Appendix E; Figure E90 through to Figure E97.

The behavior of each CWP specimen is summarized below:

- WP1
- There were two interacting defects, lack of root penetration and lack of side wall fusion, which combined had dimensions; 0.179x5.94in (4.54x151mm). The defect was surface breaking, at the HAZ of the weld toe
 - The pipe and global strains at failure exceeded 0.5%; the minimum measured strain was 2.27% in Pipe 1
 - The gross stress at failure exceeded;
 - the *minimum* yield strength between the parent pipe and weld metal measured **at the CWP location**. The weld metal overmatched the parent pipe
 - the *minimum* yield strength of the parent pipe and weld metal measured around the weld circumference. The weld metal overmatched the parent pipe
 - the *average* yield strength of the parent pipe and weld metal measured around the weld circumference. The weld metal overmatched the parent pipe
 - The CWP specimen failed by GSY
- WP2
- The defect was a deliberate lack of side wall fusion of dimensions; 0.067x7.95in (1.7x202mm). The defect was embedded, with a minimum ligament dimension of 0.29in (7.3mm) from the outer surface of the pipe. The defect correspond to 5.57% of the specimen cross section area
 - The pipe and global strains at failure exceeded 0.5%; the minimum measured strain was 4.43% across the weldment, which was similar to the strain measured in Pipe 1
 - The gross stress at failure exceeded;
 - the *minimum* yield strength between the parent pipe and weld metal measured **at the CWP location**. The weld metal overmatched the parent pipe
 - the *minimum* yield strength of the parent pipe and weld metal measured around the weld circumference. The weld metal overmatched the parent pipe
 - the *average* yield strength of the parent pipe and weld metal measured around the weld circumference. The weld metal overmatched the parent pipe
 - The CWP specimen failed by GSY
- WP3
- The defect was a deliberate lack of side wall fusion of dimensions; 0.256x4.55in (6.5x116mm), which correspond to 12.30% of the specimen cross section area, with a minimum ligament depth to the inner surface of the pipe of 0.21in (5.4mm).
 - The pipe and global strains at failure exceeded 0.5%; the minimum measured strain was 3.15% in Pipe 1
 - The gross stress at failure exceeded;

- the *minimum* yield strength between the parent pipe and weld metal measured **at the CWP location**. The weld metal overmatched the parent pipe
 - the *minimum* yield strength of the parent pipe and weld metal measured around the weld circumference. The weld metal overmatched the parent pipe
 - the *average* yield strength of the parent pipe and weld metal measured around the weld circumference. The weld metal overmatched the parent pipe
 - The CWP specimen failed by GSY
- WP4
- The defect was a deliberate intermittent lack of side wall fusion of dimensions; 0.173x5.77in (4.4x147mm), which correspond to 10.58% of the specimen cross section area, with a minimum ligament depth to the outer surface of the pipe of 0.30in (7.6mm)
 - The pipe and global strains at failure exceeded 0.5%; the minimum measured strain was 0.59% in Pipe 2, which was similar to the total strain measured across the weldment of 0.75%
 - The gross stress at failure exceeded;
 - the *minimum* yield strength between the parent pipe and weld metal measured **at the CWP location**. The weld metal overmatched the parent pipe
 - the *minimum* yield strength of the parent pipe and weld metal measured around the weld circumference. The weld metal overmatched the parent pipe
 - the *average* yield strength of the parent pipe and weld metal measured around the weld circumference. The weld metal overmatched the parent pipe
 - The CWP specimen failed by GSY

7.6.7 Weld B06

Four CWP specimens were extracted from Weld B06. Table 57 shows the position that each specimen was extracted from around the weld circumference, together with details of the specimen and defect dimensions.

The test results are presented in Table 58 and individual graphs of gross stress versus strain, and CMOD versus strain are presented in Appendix E; Figure E98 through to Figure E106.

The behavior of each CWP specimen is summarized below:

- WP1
- The specimen was originally intended to test a deliberate lack of root penetration defect of dimensions; 0.04x6.5in (1x165mm). However, on completion of the test additional defects were found when examining the fracture surface features. The following defects were found when examining the fracture surface;
 - Lack of root penetration (deliberate surface breaking defect on the fusion line of Pipe 1) of dimensions; 0.079x6.06in (2x154mm)
 - Lack of side wall fusion (hot pass, fusion line of Pipe 1) of dimensions; 0.075x9.53in (1.9x242mm), with a minimum ligament depth to the inner surface of the pipe of 0.094in (2.4mm)
 - Intermittent lack of side wall fusion (hot pass, fusion line of Pipe 2) of dimensions; 0.079x3.03in (2x77mm), with a minimum ligament depth to the inner surface of the pipe of 0.134in (3.4mm)

- The pipe and global strains at failure exceeded 0.5%; the minimum measured strain was 0.83% in Pipe 2
- The gross stress at failure exceeded;
 - the *minimum* yield strength between the parent pipe and weld metal measured **at the CWP location**. The weld metal overmatched the parent pipe
 - the *minimum* yield strength of the parent pipe and weld metal measured around the weld circumference. The weld metal overmatched the parent pipe
 - the *average* yield strength of the parent pipe and weld metal measured around the weld circumference. The weld metal overmatched the parent pipe
- The CWP specimen failed by GSY

WP2

- Deliberate undercutting was expected at the location where the CWP was extracted.
- The test was terminated, without failure of the CWP specimen due to excessive strain in Pipe 1 (5.33%), compared with Pipe 2 (0.47%) The weld metal strength overmatched both pipes
- The gross stress achieved during the test;
 - exceeded the *minimum* yield strength between the parent pipe and weld metal measured **at the CWP location**. The weld metal overmatched the parent pipe
 - exceeded the *minimum* yield strength of the parent pipe and weld metal measured around the weld circumference. The weld metal overmatched the parent pipe
 - was equal to the minimum *average* yield strength of the parent pipe and weld metal measured around the weld circumference. The weld metal overmatched the parent pipe
- Although the test was terminated prior to failure, if failure was to occur it would have been by GSY

WP3

- The defect was a natural welding defect of intermittent lack of side wall fusion plus porosity with dimensions; 0.236x5.71in (6.0x145mm), which corresponds to 14.04% of the specimen cross section area, with a minimum ligament depth to the outer surface of the pipe of 0.23in (5.8mm).
- The test was stopped prior to failure of the CWP specimen as the remote strain in Pipe 1 had exceeded 5.25% at maximum load. The strength of Pipe 1 was significantly higher than Pipe 2, which recorded a remote strain of only 0.75% on termination of the test. The weld metal strength overmatched both pipes
- The gross stress achieved during the test exceeded;
 - the *minimum* yield strength between the parent pipe and weld metal measured **at the CWP location**. The weld metal overmatched the parent pipe
 - the *minimum* yield strength of the parent pipe and weld metal measured around the weld circumference. The weld metal overmatched the parent pipe
 - the minimum *average* yield strength of the parent pipe and weld metal measured around the weld circumference. The weld metal overmatched the parent pipe

- Although the test was terminated prior to failure, if failure was to occur it would have been by GSY
- WP4
- The defect was a deliberate lack of side wall fusion of dimensions; 0.197x5.67in (5.0x144mm), which correspond to 11.57% of the specimen cross section area, with a minimum ligament depth to the outer surface of the pipe of 0.276in (7.0mm)
 - The pipe and global strains at failure exceeded 0.5%; the minimum measured strain was 0.55% in Pipe 2, which was similar to the total strain measured across the weldment of 0.69% as both pipes were reasonably well matched for strength
 - The gross stress at failure;
 - Was less than the *minimum* yield strength between the parent pipe and weld metal measured **at the CWP location** (5.1ksi (35N/mm²)). The weld metal overmatched the parent pipe
 - Exceeded the *minimum* yield strength of the parent pipe and weld metal measured around the weld circumference. The weld metal overmatched the parent pipe
 - Exceeded the *average* yield strength of the parent pipe and weld metal measured around the weld circumference. The weld metal overmatched the parent pipe
 - The CWP specimen failed by NSY

7.6.8 Weld B08

Three CWP specimens were extracted from Weld B08. Table 59 shows the position that each specimen was extracted from around the weld circumference, together with details of the specimen and defect dimensions.

The test results are presented in Table 60 and individual graphs of gross stress versus strain, and CMOD versus strain are presented in Appendix E; Figure E107 through to Figure E112.

The behavior of each CWP specimen is summarized below:

- WP1
- The specimen was originally intended to test a deliberate lack of side wall fusion defect of dimensions; 0.04x6.5in (1x165mm). However, on completion of the test additional defects were found when examining the fracture surface features. The following defects were found;
 - Lack of side wall fusion (deliberate) of dimensions; 0.354x6.81in (9x173mm), with a minimum ligament depth to the inner surface of the pipe of 0.02in (0.5mm)
 - Lack of side wall fusion (hot pass, fusion line of Pipe 1) of dimensions; 0.075x9.53in (1.9x242mm), with a minimum ligament depth to the inner surface of the pipe of 0.094in (2.4mm)
 - Intermittent lack of side wall fusion (hot pass, fusion line of Pipe 2) of dimensions; 0.079x3.03in (2x77mm), with a minimum ligament depth to the inner surface of the pipe of 0.134in (3.4mm)
 - Combined, the defects corresponded to 25.4% of the specimen cross section area
 - The pipe and global strains at failure were less than 0.5%; the minimum and maximum measured strains were 0.29% across the weldment and 0.30% in both Pipe 1 and Pipe 2

- The gross stress at failure was less than;
 - the *minimum* yield strength between the parent pipe and weld metal measured **at the CWP location** (22.3ksi (154N/mm²)). The weld metal overmatched the parent pipe
 - the *minimum* yield strength of the parent pipe and weld metal measured around the weld circumference (20.4ksi (141N/mm²)). The weld metal overmatched the parent pipe
 - the *average* yield strength of the parent pipe and weld metal measured around the weld circumference (22.6ksi (156N/mm²)). The weld metal overmatched the parent pipe
 - The CWP specimen failed by LC.
- WP2
- Based on the post construction radiographic inspection records from the X100 operational trial the CWP specimen was expected to contain intermittent lack of side wall fusion up to 6.3in (160mm) in length. However, on termination of the test, no defect was found.
 - The test was stopped prior to failure of the CWP specimen with uniform strain throughout both pipes and across the weldment of approximately 4.3%. The strength of both pipes was similar. The weld metal strength overmatched both pipes
 - The gross stress achieved during the test exceeded;
 - the *minimum* yield strength between the parent pipe and weld metal measured **at the CWP location**. The weld metal overmatched the parent pipe
 - the *minimum* yield strength of the parent pipe and weld metal measured around the weld circumference. The weld metal overmatched the parent pipe
 - the *minimum average* yield strength of the parent pipe and weld metal measured around the weld circumference. The weld metal overmatched the parent pipe
 - Although the test was terminated prior to failure, if failure was to occur it would have been by GSY
- WP3
- The defect was a deliberate lack of side wall fusion of dimensions; 0.425x5.71in (10.8x145mm), which correspond to 25.49% of the specimen cross section area, with a minimum ligament depth to the outer surface of the pipe of 0.165in (4.2mm)
 - The pipe and global strains at failure were less than 0.5%; each recording a value of approximately 0.34%
 - The gross stress at failure was less than;
 - the *minimum* yield strength between the parent pipe and weld metal measured **at the CWP location** (19.0ksi (131N/mm²)). The weld metal overmatched the parent pipe
 - the *minimum* yield strength of the parent pipe and weld metal measured around the weld circumference (4.5ksi (31N/mm²)). The weld metal overmatched the parent pipe
 - the *average* yield strength of the parent pipe and weld metal measured around the weld circumference (21.2ksi (146N/mm²)). The weld metal overmatched the parent pipe
 - The CWP specimen failed by LC

8 Evaluation of the Performance of Girth Welds in X100 Pipelines

In this section the different methods presented in Section 3 for determining girth weld defect acceptance limits are appraised for use with grade X100 pipelines. The mechanical properties determined for each weldment, reported in Section 6, are essential inputs to each assessment method, and the limits derived are validated by comparison with the results of the curved wide plate test program presented in Section 7.

8.1 Comparison of CWP Test Results with API 1104 Option 2

As discussed in Section 3.1, it is claimed that Option 2 is applicable to pipelines constructed from grade X100 line pipe, despite certain limitations to the equations embedded within the procedure.

Application of the procedure is dependent on the mechanical properties of the pipe and weld, and loading conditions (refer to Section 3.1), the main criteria being;

- The weld metal strength is not less than the strength of the line pipe, which must not be less than SMYS
- The minimum CTOD is greater than 0.002in (0.05mm)
- The applied longitudinal stress is not greater than SMYS and the applied longitudinal strain is not greater than 0.5%

Of the nine welds subjected to detailed tensile testing, only main line weld A06 and tie-in weld A17 exhibited weld metal yield strength undermatching. Yield strength mismatch was assessed by comparing;

1. The maximum pipe strength with the weld minimum
2. The minimum pipe strength with the weld maximum, and
3. The average pipe strength with the weld average.

The results from each comparison varied significantly. For weld A06, undermatching was observed in Pipe 1 and Pipe 2 when comparing the results based on (1); -0.9% and -4.7% respectively. For weld A17, a higher level of undermatching was observed in Pipe 1 and Pipe 2 when comparing the results based on (1); -11.3% and -7.5% respectively, and in Pipe 1 when comparing the results based on (3); -4.6%.

A total of fifty-four fracture mechanics tests were undertaken to characterize the fracture toughness of the weld and HAZ of the nine girth welds tested. All test results exceeded the minimum CTOD requirement of 0.002in (0.05mm), except for one; weld A50 specimen 7-C4 which measured 0.0014in (0.035mm).

The analysis procedure detailed in Section 3.1.2 has been used to undertake the following;

1. Construct loci of critical defect height as a function of defect length specific to each weld and compare this with the defects tested. Each locus was constructed based on the minimum tensile properties and fracture toughness measured in each weldment. The applied longitudinal stress in the analysis was set equal to SMYS of grade X100 line pipe.
2. Construct a material specific FAD for each weldment. Analyze the CWP tests undertaken to determine the assessment point (K_r , L_r), and compare this with the corresponding FAC.
3. Based on (2) above, determine the critical stress for failure of the CWP test specimen. This was done by varying the applied longitudinal stress until the assessment point (K_r , L_r) was coincident with the FAC. The critical stress was then compared with the actual test failure stress to determine a margin of safety.

An assessment of each individual test undertaken is presented in Appendix F. A summary of the results is presented below. The results of the CWP tests from the A-series welds, which had machined defects in the weld root region (either at the weld metal centre or in the HAZ) are discussed first, followed by the B-series welds.

8.1.1 A-Series Welds

The results of the analyses undertaken of Weld A06 are presented below. This is followed by a summary of the results from the remaining A-series welds, with additional detail provided in Appendix F. It should be noted that the analyses undertaken do not consider the potential for defect sizing error.

A locus of critical defect height as a function of defect length is presented in Figure 114 for weld A06. The analysis was undertaken based on the minimum tensile properties measured throughout the weldment, and the minimum measured CTOD. The applied longitudinal stress was set equal to the line pipe SMYS. The inputs to the assessment are given in Table 61.

As can be seen from Figure 114, no specimen would be predicted to fail at an applied longitudinal stress less than SMYS, as the CWP defect sizes are below the allowable defect size locus. This was confirmed by the CWP test results, with each specimen failing at a stress in excess of SMYS.

The CWP test results are presented in Figure 115, compared with the FAD specific to the weldment. The longitudinal stress input in the analysis was the global stress at failure of the CWP specimen. A conservative assessment of the CWP test specimens was undertaken as the tensile properties used to results the specimens were the same as those used to construct the FAD; the minimum tensile properties measured around the pipe circumference. Despite this added conservatism, all assessment points lay outside of the FAC.

The analysis was repeated for each CWP specimen, varying only the longitudinal stress in each assessment to determine the 'minimum' critical stress values for each specimen. The critical stress is the value of longitudinal stress where the corresponding assessment point (K_r , L_r) is coincidental with the FAC. The results of the analysis are shown in Figure 116, and the predicted values of critical stress for each CWP specimen are given in Table 61. Also given in Table 61 is the corresponding margin of safety for each specimen; defined as the ratio of the actual CWP specimen failure stress divided by the critical stress. As shown, the actual failure stress was not less than 5% higher than the predicted critical stress.

The analyses undertaken of welds A17 (Table 62 and Figure F1) and A33 (Table 63 and Figure F2) gave similar results to A06, although the minimum margin of safety on failure stress reduced to 4% and 1% respectively. As noted above though, the CWP specimens were analyzed using the minimum measured tensile properties; the higher the tensile properties used in the analysis the greater then margin of safety would be.

For weld A46 (Table 64 and Figure F3) the results of each CWP specimen lay close to the FAD, with a margin of safety ranging from -3% to +4%, although the critical failure stress predicted for each was at least 12% higher than SMYS. This is why each defect was considered safe when the CWP defect dimensions were plotted against the critical defect locus, as the analysis assumed a maximum allowable longitudinal stress of SMYS.

For weld A50 (Table 65 and Figure F4), CWP specimens H1 and W gave similar results to welds A06, A17 and A33. However, the defect dimensions of CWP specimen H2 were considered to be borderline unacceptable when compared with the critical defect locus. The actual specimen failed at a higher stress, approximately 15% higher than SMYS and 1% higher than the minimum yield strength used to construct the FAD. This is why the defect was considered acceptable when compared with the FAC.

8.1.2 B-Series Welds

The CWP specimens extracted from the B-series welds comprised predominantly embedded defects, that were introduced either deliberately (produced by modifications to the weld procedure, with some disc grinding) or naturally.

The Option 2 assessment procedure considers surface breaking defects only, as a worst case defect. The assumption being that an equivalent size embedded defect will have an increased margin of safety.

The analysis undertaken of the B-series welds is identical to that for the A-series welds. The results of the assessments are discussed below.

For Weld B03 (Table 66 and Figure F5), the locus of critical defect height would suggest that the failure stress of CWP specimens WP1, WP3 and WP4 would be less than SMYS, unlike WP2. A critical stress calculation predicts the maximum longitudinal stress to be up to 23% less than SMYS (CWP specimen WP3). However plotting the actual CWP test results against the FAD (Figure F6(b)) shows there to be a significant margin of safety against failure; actual failure stresses between 12% and 24% higher than SMYS.

Similarly, for Weld B06 (Table 67 and Figure F6), the locus of critical defect height would suggest that the failure stress of each CWP specimen would be less than SMYS. However, the maximum stress at failure (or termination of the test) was up to 12% higher than SMYS, and up to 4% higher than the minimum measured yield strength of the weldment. The margin of safety is shown in Figure F6(b), where the actual CWP test results are plotted against the FAD.

The analysis undertaken of weld B08 (Table 68 and Figure F7) and the corresponding CWP specimens gave similar results to weld B06. As seen in Figure F7(b) the defects in the CWP specimens would be considered unacceptable with failure stresses less than SMYS. This was correct; the actual failure stress of each CWP specimen was approximately 10% less than SMYS. However, when the results of the CWP specimens are plotted with respect to the material specific FAD for the weldment, the assessment points lay outside the FAD showing a positive margin of safety.

8.1.3 Concluding Comments

As discussed, some of the equations used in the assessment procedure are not yet validated for use with grade X100. Despite this, the Option 2 method performed well, giving conservative predictions of failure stress for all, except one CWP test (specimen A46-WP-H4, the actual failure stress being 3% less than that predicted). In many cases, the predicted failure stress was very close to the actual failure stress; ratio of actual to predicted failure stress being 1.0. The accuracy of the predicted failure stresses varied, the least accurate being 60% higher than the actual failure stress. The least accurate predictions generally came from the B-series welds, the CWP specimens mainly had deliberate or natural welding defects embedded within the weldment.

Despite the CWP specimens testing pipe from three different sources, with varying levels of weld strength under- and over-matching, the applicability of API 1104 Option 2 to girth welds in X100 pipelines appears promising. However, only one pipe diameter and wall thickness has been tested. It is recommended that additional pipe sizes are tested before the method can be considered valid for X100 pipelines.

8.2 Comparison of CWP Test Results with EPRG Tier 2

As discussed in Section 3.2, the EPRG guidelines have only recently been extended to include pipelines constructed from grade X80 line pipe; they have not been formally accepted for use with grade X100 line pipe. The philosophy that was used to validate use of the guidelines for grade X80 pipelines is used below to assess the suitability of the approach to grade X100 pipelines.

Application of the EPRG guidelines requires the following;

- The Charpy impact energy (based on a full-size Charpy specimen) of the region containing the defect exceeds the min(avg) requirements of 22(30) ft-lb (30(40)J)
- The pipe's Y/T ratio in the axial direction is not greater than 0.90
- The weld metal yield strength matches or overmatches the pipe
- The total axial strain across the weldment is not greater than 0.5%
- The defect area in a 12in (300mm) arc length is not greater than 7%

For the CWP tests undertaken in this work, each weldment achieved the Charpy impact energy requirements. However, both the pipe and weld metal tensile properties varied significantly; resulting in weld metal yield strength mismatch ranging from -11% (undermatch) up to +26% (overmatch), and Y/T ratios ranging from 0.86 to 0.99.

An assessment of each individual test undertaken is presented in Appendix G. A summary of the results is presented below. The results of the CWP tests from the A-series welds, which had machined defects in the weld root region (either at the weld metal centre or in the HAZ) are discussed first, followed by the B-series welds.

8.2.1 A-Series Welds

The data are presented in Figure 117 in terms of remote strain at failure plotted against the relative cross section area of the defect normalized by the gross cross section area of the CWP specimen (I_h/Wt). The horizontal line represents the EPRG performance criterion of 0.5% remote strain. The data have been grouped in relation to the level of yield strength mismatch of the weld metal in relation to the parent pipe; under-matched, matched and overmatched.

The level of mismatch is defined as a percentage of the parent pipe yield strength. For this illustration;

- Matched (M) – the pipe and weld metal yield strength are within $\pm 2\%$ of each other
- Under-matched (UM) – the weld metal strength is less than the pipe, within the range -2% to -10%
- Overmatched (OM) – the weld metal strength is greater than the pipe. Due to the level of mismatch, this data has been separated into two ranges;
 - OM range from +2% to +10%
 - OM greater than 10%

As can be seen in Figure 117, all defects tested to failure achieve the EPRG performance criterion of 0.5% remote strain.

There appears to be a negligible influence of weld metal yield strength mismatch for small defect areas (up to 2.5%), although there may be an effect for larger defects; for a defect area ratio of 5% the under-matched weld (-3% yield strength mismatch) gave the lowest failure strain (0.57%), compared with the matched and overmatched welds which gave failure strains between 0.81 to 0.93%.

Although the number of data points is limited and they represent only one pipe wall thickness, provided the weld metal yield strength is not less than the pipe yield strength, the EPRG performance criterion of 0.5% strain is achieved when the defect area ratio is not greater than 6.5%. Due to the limited number of tests undertaken, the maximum defect area ratio of 7% per 12in (300mm) length of weld cannot be confirmed for grade X100, although the data would suggest this would be achievable.

The defects tested in this work ranged in both height, 0.118in (3mm) and 0.157in (4mm) and length, from 1.97in to 3.94in (50mm to 100mm). Figure 118 and Figure 119 present the CWP test data in terms of remote strain at failure plotted against defect length ratio, l/t (defect length normalized by the pipe wall thickness) for defects up to 0.118in (3mm) in height (Figure 118) and 0.157in (4mm) in height (Figure 119).

The data are compared against the EPRG Tier 2 recommended limits on defect length as a function of defect height recommended for grade X80 pipelines. It should be noted that for a Y/T ratio of 0.9, the allowable defect lengths, expressed as a function of the pipe wall thickness, are calculated to be 5.3t (defect height up to 0.118in (3mm)), 3.9t (defect height up to 0.157in (4mm)) and 3.2t (defect height up to 0.197in (5mm)). However, when recommending the EPRG limits for grade X80 pipelines the theoretical limits were ‘manually’ increased following a review of the University of Gent CWP database of 485 test results; 132 results being obtained from grade X80 pipe, as the calculated length limits were considered to be too conservative. The following limits were recommended for pipe up to, and including grade X80;

	Maximum allowable defect length as a function of defect height (h)		
	$h \leq 0.118\text{in}$ ($h \leq 3\text{mm}$)	$0.118 < h \leq 0.157\text{in}$ ($3 < h \leq 4\text{mm}$)	$0.157 < h \leq 0.197\text{in}$ ($4 < h \leq 5\text{mm}$)
$Y/T \leq 0.9$	$\leq 7t$	$\leq 5t$	$\leq 3t$

Notes: length limit is ‘per’ 12in (300mm) length of weld (pipe diameters greater than 30in)

As can be seen in Figure 118, although the test results show that each specimen achieved the EPRG 0.5% remote strain performance criterion, the defect length ratio of the CWP specimens tested only extended to 5t; hence the validity of the 7t length limit cannot be confirmed.

In contrast however, Figure 119 shows that the CWP test results support the 5t length limit for defects up to 0.157in (4mm) in height.

8.2.2 B-Series Welds

Of the eleven CWP specimens tested from the B-series welds, eight were tested to failure. The other three tests were terminated without failure due to the amount of strain accumulated in one or both pipes. Post test examination of the three specimens confirmed that two of the CWP specimens (B06-WP2 and B08-WP2) had no defect present; contrary to the results of the inspections undertaken on commission of the BP X100 operational trial. Although the third CWP specimen (B06-WP3) had a significant ‘embedded’ defect, the strength of the weldment was sufficient to shield the defect, with the majority of the measured strain occurring in pipe A, which resulted in the test being terminated.

Of the eight specimens tested to failure, two specimens contained a surface breaking defect. The other 6 specimens contained an embedded defect. The results of the eight specimens tested to failure are presented in Figure 120, together with the result of the CWP specimen that contained an embedded defect, which was not tested to failure. As can be seen, the results show a high degree of scatter, compared with the results from the A-series weld tests presented in Figure 117.

Only one specimen had a defect area ratio less than 7% of the specimen cross section; an EPRG requirement. The defect area ratio in the remaining specimens exceeded the EPRG limit; ranging from 10.6 to 27.0%. As shown in Figure 120, only two specimens failed to achieve the EPRG performance criterion of 0.5% remote strain; two specimens each containing an embedded defect that had a defect area ratio of 25.4% and 25.5%, both of which were extracted from weld B08

As with the A-series welds, the level of weld metal yield strength overmatch was assessed based on the measured tensile properties adjacent to the location from which the individual specimens were extracted. Each CWP was overmatched; ranging from 5 to 24%. The data are compared in Figure 121. There appears to be no clear effect of the level of weld metal yield strength overmatch; the only conclusion to be drawn from Figure 120 and Figure 121 is that for the tests undertaken the EPRG defect area limit of 7% is conservative, provided the weld metal yield strength overmatches the parent pipe.

The data has been separated out further by considering the effect of defect height, in addition to weld metal yield strength mismatch. The data are presented in Figure 122 through to Figure 124, for defect heights up to 0.118in (3mm), from 0.157 to 0.197in (4 to 5mm) and greater than 0.197in (5mm) comparing the remote strain at failure against the defect length ratio. Again, there appears to be no clear effect of the level of weld metal yield strength overmatch. It is possible that comparison of the test results is more difficult due to the different types of natural and deliberate welding defects tested and compared, and the method used to determine the relevant defect size for assessment; i.e., a containment rectangle.

8.2.3 Concluding Comments

The results of the CWP tests undertaken on the A-series welds provided good supporting evidence of the potential extension of the EPRG guidelines to grade X100 pipelines. Unfortunately the defect sizes tested were not sufficient to verify use of the existing EPRG limits for grade X80 pipelines; the defect length ratio only extended to 5t rather than the 7t limit. Nevertheless, as discussed, the X100 data do support use of the theoretical limits calculated for grade X80 pipelines; 5.3t for a defect height up to 0.118in (3mm), 3.9t for a defect height up to 0.157in (4mm) and 3.2t for a defect height up to 0.197in (5mm).

The effect of yield strength mismatch is not clear, except for the larger defects tested where under-matched welds exhibited slightly lower strains to failure than similar sized defects in overmatched welds.

The CWP test data from the B-series welds demonstrate that a girth weld is more tolerant to larger embedded defects than surface breaking defects, upon which the EPRG limits are based.

Although the analyses undertaken would suggest that the EPRG guidelines may be applicable to grade X100 pipelines, the CWP test results are limited in number. Although pipe from different sources and two different weld preparations have been tested, only one thickness of pipe, 0.78in (19.8mm), has been considered. More testing is required to verify the applicability of the EPRG method to grade X100 pipelines.

8.3 Comparison of CWP Test Results with CSA Z662

As discussed in Section 3.3, application of the procedure is dependent on the mechanical properties of the pipe and weld, and loading conditions, the main criteria being;

- The yield strength of the weldment is not less than SMYS of the line pipe
- The Charpy impact energy of the weld metal is to be greater than 30ft-lb (40J), although it is not stated whether this is the minimum or average value
- Although there is a requirement for CTOD testing, no minimum value is specified. The minimum measured value of CTOD is used in the assessment to determine the maximum defect size
- Stress analysis is to be undertaken to determine the axial and longitudinal stresses to which the weld will be subjected to during construction and operation. The analysis method requires input of the maximum applied longitudinal tensile bending stress.

Of the nine welds subjected to detailed mechanical testing, all measured values of yield strength were not less than SMYS and the measured Charpy impact energy was not less than 30ft-lb (40J), be it minimum or average.

The analysis procedure detailed in Section 3.3 has been used to undertake the following;

1. Construct the two loci of critical defect height as a function of defect length for the prevention of brittle fracture and plastic collapse respectively, and compare these loci with the CWP specimen defects. Each locus was constructed based on the minimum measured mechanical properties of the weldment, and the applied longitudinal tensile bending stress used in the analysis was limited to SMYS.
2. For each CWP specimen tested, determine the theoretical maximum longitudinal bending stress for failure. The limiting maximum stress was then compared with the actual test failure stress to determine a factor of safety.

An assessment of each individual test undertaken is presented in Appendix H. A summary of the results is presented below. The results of the CWP tests from the A-series welds, which had machined defects in the weld root region (either at the weld metal centre or in the HAZ) are discussed first, followed by the B-series welds.

8.3.1 A-Series Welds

The results of the analyses undertaken of Weld A06 are presented below. This is followed by a summary of the results from the remaining A-series welds, with additional detail provided in Appendix H. It should be noted that the analyses undertaken do not consider the potential for defect sizing error.

The assessment method presented in CSA Z662 is not the most straightforward to apply, so a brief description is given below of the steps undertaken to determine, in particular, the locus of critical defect size for the prevention of brittle fracture.

The first step in the analysis procedure was to calculate the critical defect size locus for the prevention of brittle fracture. Equations [22] and [23] were used to determine the size parameter, \bar{a} which was then normalized with respect to the nominal pipe wall thickness, t . Using Figure 125 (Figure K.4 from CSA Z662), a vertical line was drawn at \bar{a}/t , and horizontal lines were extended to the ordinate axis from the intersections of the vertical line and the d/L curves. This data was then used to construct a graph of defect length as a function of d/t , and a power law curve was fit to the data.

Then next step was to calculate the critical defect size locus for the prevention of plastic collapse. This was done using equation [25], the solution used was dependent on the quantity $\eta\beta$; η being the ratio of defect depth to nominal pipe wall thickness and β the ratio of defect length to pipe circumference. For a range of d/t ratios (0.1 through to 0.9, in increments of 0.1) a corresponding value of critical length was calculated, assuming the applied tensile bending stress to be equal to SMYS. The data were used to construct a graph of defect length as a function of d/t .

The two loci were combined onto one graph and presented with the defect sizes from the CWP specimens. The curves for weld A06 are presented in Figure 126. As can be seen, critical defect sizes are limited by the brittle fracture curve. The defect sizes of three of the CWP specimens fall below the limiting curve, and are therefore predicted to fail at a tensile bending stress greater than SMYS. In contrast the defect dimensions of CWP specimen H4 lay outside the limiting curve, meaning that the CWP specimen would be predicted to fail at a stress less than SMYS.

The same analysis procedures were used to determine the maximum applied tensile bending stress for failure by brittle fracture and plastic collapse, respectively for the actual CWP specimen defect dimensions.

For the brittle fracture prediction, since d/t and d/L are known values, a value of $\bar{\sigma}/t$ can readily be determined from the graph. Using the equations, the applied tensile bending stress is varied until the calculated value of $\bar{\sigma}/t$ achieves the value read from the graph; this being the critical value of tensile bending stress for failure.

The results of the analyses undertaken of Weld A06 are presented in Table 69. As can be seen;

- The predicted critical stress for CWP specimens H1, H2 and WP1 was not less than SMYS
- The predicted critical stress for CWP specimen H3 was approximately 14% less than SMYS
- The predicted critical stress for CWP specimens H1 and W1 was limited by the plastic collapse equation, and H2 and H3 were limited by the brittle fracture equation, these being the predicted failure modes
- The actual stress at failure of each CWP specimen was between 14 and 25% greater than SMYS, and between 7 and 33% greater than the predicted critical stress for each CWP specimen

For Weld A17, all CWP defects were below the brittle fracture and plastic collapse failure loci (see Figure H1), inferring that the maximum allowable tensile bending stress for failure would be greater than SMYS. As seen in Table 70, the predicted critical stress for each CWP specimen was between 4 and 6% higher than SMYS; the analysis being limited by the plastic collapse equation. The analysis also showed a good margin of safety between the actual stress at failure of each CWP specimen and the predicted critical stress; the actual stress at failure being between 9 and 13% greater than the predicted critical stress.

For Weld A33, all CWP defects were below the brittle fracture and plastic collapse failure loci (see Figure H2), inferring that the maximum allowable tensile bending stress for failure would be greater than SMYS. As seen in Table 71, the predicted critical stress for CWP specimens H1, H2 and WP1 was between 13 and 16% higher than SMYS; the analysis being limited by the plastic collapse equation. The predicted critical stress for CWP specimen H3 was slightly less than SMYS, albeit by only 1%. This is in contradiction to Figure H2, as the defect dimensions lay beneath the limiting curve. The differing results are due to the method for developing the brittle fracture defect locus as the analysis is dependent on estimating values from a log-log graph, and then fitting a power law curve to the 'best guess' data. The analysis also showed a good margin of safety between the actual stress at failure of each CWP specimen and the predicted critical stress; the actual stress at failure being between 4 and 15% greater than the predicted critical stress.

For Weld A46, all CWP defects were below the brittle fracture and plastic collapse failure loci (see Figure H3), inferring that the maximum allowable tensile bending stress for failure would be greater than SMYS. As seen in Table 72, the predicted critical stress for each CWP specimen was between 7 and 12% higher than SMYS; the analysis being limited by the plastic collapse equation. The analysis also showed a reasonable margin of safety between the actual stress at failure of each CWP specimen and the predicted critical stress; the actual stress at failure being between 2 and 7% greater than the predicted critical stress.

For Weld A50, the defect sizes for CWP specimens H1 and W1 lay below the limiting failure loci, inferring that the critical stress at failure would be greater than SMYS (see Figure H4). In contrast the defect dimensions of CWP specimen H2 lay outside the brittle fracture loci inferring that the maximum allowable tensile bending stress for failure to occur would be less than SMYS. This is also shown in the results of the analysis presented in Table 73, where the predicted critical stress for failure of CWP specimen H1 and W1 are 13% higher than SMYS, and H2 is 17% lower. The analysis also showed a good margin of safety between the actual stress at failure of each CWP specimen and the predicted critical stress; the actual stress at failure being between 5 and 38% greater than the predicted critical stress.

8.3.2 B-Series Welds

The CWP specimens extracted from the B-series welds comprised predominantly embedded defects, that were introduced either deliberately (produced by modifications to the weld procedure, with some disc grinding) or naturally.

The results of the analysis of each CWP specimen are presented separately due to the dependency of the failure loci on the minimum ligament distance of the buried defect.

For weld B03, the results of the analysis are presented in Figure H5 through to Figure H8, and given in Table 74. The surface breaking defect of CWP specimen WP1 was predicted to fail at a tensile bending stress less than SMYS; the defect dimensions were above the brittle fracture and plastic collapse critical defect size loci (Figure H5). This was confirmed following a critical stress analysis, which was calculated to be 51.6ksi (356N/mm²); brittle fracture being the predicted failure mode. In contrast, the test failure stress was approximately 19% greater than SMYS, and 2.3 times greater than the predicted critical stress. The analysis of the embedded defects in CWP specimens WP2, WP3 and WP4 suggested that the maximum allowable tensile bending stress would be less than SMYS. However, the predicted critical stresses were within -3% and +5% of SMYS, with the actual stress at failure of each CWP specimen being between 13 and 24% greater than the predicted critical stress.

For weld B06, the results of the analysis are presented in Figure H9 through to Figure H11, and given in Table 75. The defect dimensions of each CWP specimen lay outside the critical defect size loci for both brittle fracture and plastic collapse, inferring that each specimen would fail at a tensile bending stress less than SMYS. The results of a critical stress analysis predict failure would occur by plastic collapse at a stress level within 5% of SMYS. The actual failure stress of each CWP specimen was not less than 12% greater than SMYS. The analysis also showed a good margin of safety between the actual stress at failure of each CWP specimen and the predicted critical stress; the actual stress at failure was not less than 15% greater than the predicted critical stress. CWP specimen WP2 was not assessed as no defect was found on completion of the test.

For weld B08, the results of the analysis are presented in Figure H12 and Figure H13, and given in Table 76. The defect dimensions of each CWP specimen lay outside the critical defect size loci for both brittle fracture and plastic collapse, inferring that each specimen would fail at a tensile bending stress less than SMYS. The results of a critical stress analysis of WP1 predict failure would occur by brittle fracture at a critical stress approximately equal to 78% of SMYS. The actual failure stress of the specimen was less than SMYS, but approximately 14% greater than the predicted critical stress. CWP specimen WP3 was predicted to fail by plastic collapse at a critical stress approximately equal to 86% of SMYS. The actual failure stress was also less than SMYS, but approximately 5% greater than the predicted critical stress. CWP specimen WP2 was not assessed as no defect was found on completion of the test.

8.3.3 Concluding Comments

The CSA Z662 procedure was successfully used to predict a conservative value of failure stress for each CWP test specimen. Each predicted failure stress was less than the actual test failure stress by 2% or more. Calculation of the critical defect size locus for the prevention of failure by plastic collapse was straightforward, unlike the analysis procedure for the prevention of brittle fracture. Whether predicting the critical value of axial bending stress for known defect dimensions or constructing a critical defect size locus, the method is reliant on the User's interpretation of log-log graphs, and a goodness of fit of a power law to the data.

The procedures would suggest that they are applicable to grade X100 pipelines. However, it should be noted that the CWP test results are limited in number. Furthermore, although pipe from different sources

and two different weld preparations have been tested, only one thickness of pipe, 0.78in (19.8mm), has been considered.

8.4 Comparison of the CWP Test Results with BS 7910

The CWP test results were analyzed using the Level 2A fracture mechanics assessment method in BS 7910. A general overview of the procedure was provided in Section 3.4.1.

The results of the tensile tests undertaken for each girth weld tested showed that the level of yield strength mismatch between the parent material and weld metal varied significantly, ranging from an under-matched condition (-11.3%) through to an over-matched condition (+26.0%).

Weld strength mismatch effects should not influence defect assessment procedures using stress-based methods, if these are limited to purely elastic conditions. However, mismatch will influence assessments undertaken for situations where plasticity is developed at the crack tip because of its effect on applied fracture mechanics parameters and the possible effect on material fracture toughness. The effect of weld strength mismatch in service applications depends on the type of weld and on its orientation relative to the applied stresses. It also depends on the dimensions of any crack-like defects present relative to the width of the weld and to the width and thickness of the whole joint.

The general effect of strength mismatch in defect-free girth welds is to concentrate plastic strains into the lower strength material when the loading exceeds that necessary to cause yield. If the loading does not achieve yield, the only effect of strength mismatch is on the level of residual stress.

The presence of defects in the welded joint complicates this situation. The effect of planar defects in a welded joint depends on their overall dimensions relative to the joint geometry. For through-thickness cracks at the centre line of a girth weld and contained wholly within weld metal of different strength from the parent material, the resultant yielding behavior depends on the ratios of crack length to weld width, and crack length to plate width.

Results from experimental and finite element analyses show that, for through-thickness cracks which are short compared to the weld length and shorter than the weld width, over-matching weld metal strength can protect the crack plane against net section yielding. This is because a yielding cross section may be available through the parent pipe, which therefore yields first.

For through-thickness cracks, research has shown that adopting a homogeneous approximation of the lower strength material, all base metal for over-matched welds and all weld metal for under-matched welds, will always produce a conservative result.

With part-thickness cracks in girth welds, the possibility of yielding has to be considered on the remaining ligament of the thickness as well as on the weld width and the pipe net section. In general, shallow part thickness flaws in over-matching weld metal will receive substantial protection against yielding, but they will be vulnerable in under-matching welds and the extent of this vulnerability cannot be accurately defined at present.

Unless specific solutions are available to assess the effect of weld strength mismatch, safe assessments will be made of defects in welded regions (weld metal and HAZ) if the tensile properties used are the lower of the parent metal, weld metal or HAZ. Unless HAZ softening is a concern, BS 7910 does not require the yield strength and tensile strength of the HAZ to be determined.

For a component in the as-welded condition with a defect lying in a plane parallel to the welding direction (i.e. the stresses to be considered are perpendicular to the weld), BS 7910 recommends that the residual stress should be assumed to be equal to the lesser of the room temperature yield strengths of the weld or parent metal.

In addition, where the mismatch is greater than 25%, BS 7910 recommends that special consideration is given to the fracture toughness data being used (reference Section I of BS 7910).

The following analysis was undertaken for each weldment;

1. Prediction of the critical defect size locus for the weldment

The following analyses were undertaken for each CWP test;

1. Assessment based on the global stress at failure during the test to confirm whether the assessment point lies inside or outside the FAC.
2. Criticality study – calculation of the critical failure stress for the assessment point to lay on the FAC, and determination of the margin of safety on predicted failure stress when compared with the actual test result.
3. Combined criticality and sensitivity study – investigation of the significance of material toughness on failure stress when compared with the failure stress from the test.

For the assessment of the critical defect size locus for each weldment, the tensile properties used were the lower of those extracted from the pipe longitudinal direction and all weld metal. The tests were undertaken at ambient laboratory temperature; hence although appropriate for defining the level of welding residual stress, an estimate of the increase in strength at the CWP test temperature of -4°F is required. The increase in yield strength was estimated using an estimation procedure given in BS 7448 Part 2. The tensile strength was assumed to increase in relation to the material Y/T ratio; the yield strength at -4°F was divided by the specimen Y/T ratio at ambient temperature.

For the assessment of the individual CWP specimens, the tensile properties used were the lower of those extracted from the pipe longitudinal direction and all weld metal, at (or nearest to) the circumferential location the CWP specimen was extracted.

Only limited fracture toughness data was obtained from each weld; three specimens sampling all weld metal and a further three sampling the HAZ. The specimens were extracted from nominally the same location around the weld circumference, although the position varied between welds depending on the number of CWP specimens that were extracted. For each assessment the minimum value of toughness from each set of three specimens was used, as recommended in Appendix K of BS 7910. J values of fracture toughness were used; BS 7910 calculates equivalent values of K from either CTOD or J for determination of the fracture ratio K_r , unlike J the conversion from CTOD requires consideration of the work hardening capability of the material and the crack tip and geometric constraint by a factor 'X' which generally varies between 1 and 2 (the appropriate value to input is usually determined from elastic analysis which models structural constraint).

The CWP tests undertaken on the A-series welds contained machined defects at the weld root, and the B-series specimens contained both natural and deliberate welding defects.

To calculate the critical defect size locus for each weldment, the analyses were undertaken using the standard solutions for a surface breaking defect and an embedded defect in a 'curved plate'; the input pipe geometry being the nominal pipe diameter and wall thickness.

To simulate the CWP test conditions, the analyses were undertaken using the standard solutions for a surface breaking defect or an embedded defect in a 'flat plate'; the dimensions of which were obtained from the detailed metrology of each test specimen.

For both the pipe and CWP specimen analyses the girth weld was idealized as a full penetration butt-weld. The magnitude of the corresponding stress concentration associated with the geometric discontinuity is dependent on the width of the weld cap or root, depending on the through wall position of the defect. The

cap and root width was measured from the weld macrographs; values of 0.197in (5mm) and 0.591in (15mm) were used in the assessments.

For the pipe analysis, the input primary membrane stress (P_m) was set equal to SMYS, consistent with the limitation on longitudinal tensile stress in API 1104. To simulate the CWP test the global stress measured from the CWP test specimen was input as a primary membrane stress.

'As-welded' residual stresses were assumed in each analysis, the magnitude of which was set equal to the minimum yield strength from the parent materials and weld metal tensile tests, measured at ambient laboratory temperature; approximately 68°F (20°C). Residual stress relaxation was enabled in each assessment due to the magnitude of the primary stress.

The assessments undertaken on the A-series welds are presented in Section 8.4.1 and the B-series welds are presented in Section 8.4.2.

8.4.1 A-Series Welds

A locus of critical height as a function of length for a surface breaking defect is presented in Figure 127 for weld A06. The analysis is based on the minimum measured tensile and fracture toughness properties of the weldment, and the maximum allowable tensile stress in the pipe longitudinal direction is limited to SMYS. The defect sizes from the CWP specimens extracted from weld A06 are also included. As can be seen, the CWP defect sizes lay above the critical defect size locus inferring that the CWP specimens would fail at a stress less than SMYS. However, each CWP specimen failed at a stress greater than SMYS, the minimum recorded failure stress was from specimen H3; 114.1 ksi (787 N/mm²). Figure 127 shows the conservatism in the BS 7910 assessment method.

A more detailed analysis was undertaken to determine the level of conservatism in the BS 7910 assessment method. Due to the similarity in the assessments undertaken, a detailed overview is provided of the analysis and results of CWP specimen A06-WP-H1. The remaining assessments undertaken of the A-series welds follow the same procedure. The input data and results for each assessment are presented in Appendix I.

Analysis of the test failure conditions of CWP specimen A06-WP-H1 resulted in an assessment point outside the FAC, with K_r and L_r of 0.987 and 1.175 respectively, as shown in Figure 128.

A sensitivity study was undertaken to determine the critical value of primary membrane stress (P_m) for the assessment point to lay on the FAC of Figure 128; the critical value of P_m was predicted to be 29.92 ksi (206.3 N/mm²), which compared with the actual failure stress from the test of 125.46 ksi (865 N/mm²) resulted in a conservative margin of safety of 4.19.

A further sensitivity study was undertaken to investigate the effect of material toughness on the predicted failure stress; toughness was increased in small increments and for each new toughness value a critical value of P_m was determined for the assessment point to lay on the FAC. The assessment was considered toughness independent (i.e., collapse dominated) when subsequent increases in toughness resulted in no increase in the predicted failure stress. The critical value of P_m , assuming the behavior of the weld to be toughness independent is predicted to be 111.93 ksi (771.7 N/mm²), which compared well with the actual test result, giving a conservative margin of safety between the actual and predicted failure stress of 1.12.

The CWP test specimen exhibited good ductility; the strain at failure in Pipe 1 and Pipe 2 was in excess of 2.44%, with the average strain across the weldment being 2.87% at failure. This was also reflected in the fracture mechanics tests with each specimen exhibiting a maximum force plateau prior to failure, although the measured toughness was low. A point to consider is that the 'deeply notched' single edge notch bend specimen geometry is recommended in the fracture test standards as it is designed to give a high degree of constraint at the crack tip, resulting in a conservative 'lower bound' value of fracture toughness. In reality,

the toughness of the material is dependent on the constraint imposed by the structural geometry and the actual defect present, and can be significantly higher than that measured using the highly constrained 'standard' specimen geometry. The failure stress of the CWP exceeded the yield strength of the material; hence failure was by gross scale yielding. Based on the behavior of the CWP test specimen, failure was controlled by the tensile properties across the weldment, with negligible effect of material fracture toughness.

The remaining A-series welds were analyzed in the same way as detailed above to determine a locus of critical defect height versus length of surface breaking defects. The individual CWP test specimens were then analyzed to determine a critical value of tensile failure stress, and hence margin of safety, and a toughness independent value of failure stress. The input data and results of each analysis are presented in detail in Appendix I; Table I1 and Table I2.

As presented in Section 7.6, each CWP specimen from the A-series welds failed at a global stress in excess of SMYS. Hence, as the critical defect size locus is limited to SMYS, all CWP defect sizes tested would in theory fall beneath the critical defect size locus for the particular weldment. It should be noted however that the critical defect size loci are lower bounding curves, based on the minimum measured tensile properties and fracture toughness properties of the weldment. If the actual material properties at the CWP location were used the weld would be more tolerant to larger defects. As can be seen in Figure I2 to Figure I5, for all of the defects tested, the defect size fell above the critical defect size locus thus inferring that the specimens would fail at a stress less than SMYS.

As can be seen from the results presented in Table I2 a conservative prediction of failure stress was determined for each specimen, as the margin between actual and predicted stress was greater than 1; ranging from 1.18 up to 23.0. This large variation between actual and predicted failure stress was found to be due to the input value of fracture toughness for each assessment. The predicted failure stresses assuming toughness independence were found to be in much better agreement with the failure stresses from the CWP specimens; the predictions were conservative, ranging from 1.07 to 1.22. These toughness independent predicted values of failure stress are more representative of the actual tests as each CWP specimen failed by plastic collapse.

8.4.2 B-Series Welds

The CWP test specimens from the B-series welds tested only natural and deliberate welding defects (i.e., none of the specimens were notched).

The assessment method was similar to that presented above for the A-series weld; the difference being that for some assessments a solution for an embedded defect was required.

The input data and results of each assessment are presented in Appendix I; Table I3 and Table I4, and Figure I6 to Figure I8. Presentation of the critical defect size loci with respect to the defects tested in the CWP specimens differed slightly, with multiple loci being produced per weldment; a locus for surface breaking defects, and loci based on the measured remaining ligament thickness for each CWP specimen.

8.4.2.1 Weld B03

The defects tested in the CWP specimens lay above their respective critical defect size locus (see Figure I6), suggesting the predicted failure stress of each would be less than SMYS. An individual assessment of each CWP specimen test resulted in the assessment point lying outside the FAD. The predicted critical value of failure stress for each specimen/defect configuration was less than the actual test failure stress, giving a margin between actual and critical ranging from 1.15 to 11.5. This large variation is not unexpected as the analysis is dependent on toughness, as discussed above for the A-series welds, and the idealization

of the size of the defect. For the A-series welds, the defects were machined into the specimen surface to a definite depth and length. With the natural welding defects the height and ligament dimension of the defect generally varies along its length and more often than not the defect is intermittent, but the distance between adjacent defects is so small that they are considered to interact. The defect is idealized by a containment rectangle of dimensions; maximum measured height and length, and minimum ligament dimension. The actual defect area can be much smaller than that assumed from the containment rectangle.

Specimen WP1 contained two interacting defects; lack of root penetration and lack of side wall fusion. The defect was surface breaking, at the weld root, and the dimensions of the containment rectangle were 0.179x5.94in (4.54x151mm). Despite the size of the defect, the specimen failed by plastic collapse; the deformation mode being GSY. Assessment of the idealized defect dimensions predicted a failure stress 11.5 times smaller than the actual failure stress. The predicted failure stress assuming toughness independence was found to be in much better agreement with the actual failure stress; the ratio between actual and predicted failure stress reducing to 1.25.

Specimen WP2 contained an embedded lack of side wall fusion defect, closest to the outer surface of the pipe. The dimensions of the containment rectangle were 0.067x7.95in (1.7x202mm), with a ligament dimension of 0.29in (7.3mm). The specimen failed by plastic collapse. The predicted failure stress was 1.15 times smaller than the actual failure stress.

Like WP2, specimens WP3 and WP4 also contained embedded defects, and both specimens failed by plastic collapse. The predicted failure stress for each specimen based on the measured tensile and fracture toughness properties was conservative, ratio of actual to predicted failure stress of 1.55 and 1.29, respectively. Assuming toughness independence, improved predictions of failure stress are obtained; the failure stress ratios reducing to 1.44 and 1.16 respectively.

8.4.2.2 Weld B06

The testing of specimen WP2 was terminated due to excessive strain accumulation in Pipe 1. However, when the specimen was sectioned for macro- and micro-scopic examination of the defect, no defect was found. Hence, specimen WP2 was not assessed using the BS 7910 procedure.

The test results are presented in Table I4 and Figure I7.

Specimen WP1 contained a number of defects; lack of root penetration and lack of sidewall fusion in the hot pass of pipes 1 and 2, which were considered to interact, and be equivalent to a large surface breaking root defect of dimensions 0.213x12.15in (5.41x309mm). The specimen failed by plastic collapse. Due to the size of the defect and the input material properties, it was not possible to predict a critical value of stress for failure. However, it was possible to predict a critical stress for failure assuming toughness independence; the ratio of actual to predicted failure stress was 1.32.

Specimen WP3 contained an embedded defect of dimensions 0.236x5.71in (6.0x145mm), with a minimum ligament depth to the outer surface of the pipe of 0.23in (5.8mm). Testing of the specimen was terminated due to excessive strain accumulation in Pipe 1, although the load trace did show that a load plateau had been achieved. If the specimen was loaded to failure, the specimen would have failed by plastic collapse. The predicted failure stress based on the measured tensile and fracture toughness properties was conservative; the ratio of maximum achieved to predicted failure stress was 1.55. Assuming toughness independence, an improved prediction of failure stress was obtained; the failure stress ratio reduced to 1.44.

Specimen WP4 contained an embedded defect of dimensions 0.197x5.67in (5.0x144mm), with a minimum ligament depth to the outer surface of the pipe of 0.276in (7.0mm). The specimen failed by plastic collapse. The predicted failure stress based on the measured tensile and fracture toughness properties was

conservative; the ratio of maximum achieved to predicted failure stress was 1.29. Assuming toughness independence, an improved prediction of failure stress was obtained; the failure stress ratio reduced to 1.16.

8.4.2.3 Weld B08

The testing of specimen WP2 was terminated due to excessive strain accumulation throughout the specimen. However, when the specimen was sectioned for macro- and micro-scopic examination of the defect, no defect was found. Hence, specimen WP2 was not assessed using the BS 7910 procedure.

The test results are presented in Table I4 and Figure I8.

Specimen WP1 contained a number of embedded defects, both deliberate and natural, which were considered to interact. The dimensions of the containment rectangle were 0.354x6.81in (9.0x173mm), with a minimum ligament depth to the inner surface of the pipe of 0.02in (0.5mm). The specimen failed with limited ductility, the deformation mode being LC. It was not possible to predict a critical value of stress for failure due to the measured toughness of the weldment. However, it was possible to predict a critical value of stress assuming failure to be collapse dominated, despite the specimen failing in a brittle manner. The ratio of actual to collapse failure stress was 1.2.

Specimen WP3 contained an embedded defect of dimensions 0.425x5.71in (10.8x145mm), with a minimum ligament depth to the outer surface of the pipe of 0.165in (4.2mm). The specimen failed with limited ductility, the deformation mode being LC. The predicted failure stress based on the measured tensile and fracture toughness properties was conservative; the ratio of actual to predicted failure stress was 3.88. Assuming failure to be collapse dominated, an improved prediction of failure stress was obtained; the failure stress ratio reduced to 1.54.

8.4.3 Concluding Comments

The fracture mechanics assessment procedures in BS 7910 are very versatile, enabling a number of different types of assessment to be undertaken to fully describe the behavior of the weldment. The method is dependent on three factors; applied loading, material properties and defect geometry.

Although measured tensile properties have been obtained for each weldment, the fracture toughness properties were measured using highly constrained fracture mechanics specimens which do not necessarily reflect the true material toughness of the pipe geometry. Essentially, the lower the value of toughness used in the assessment, the greater the likelihood of failure in a brittle manner. This effect was investigated with the sensitivity studies undertaken for each specimen analysis whereby the toughness was increased incrementally and a critical value of stress calculated for each new condition. While all predictions of failure stress, based on the measured material properties, gave conservative predictions of failure stress, in a number of cases the difference between actual and predicted failure stress was very large. This margin was reduced significantly when the analysis was repeated assuming failure to be collapse dominated. Again, all predictions of failure stress were conservative.

Improved accuracy in predicted failure stress could also be achieved with improvements in sizing of the defects, particularly when multiple defects with the potential to interact are contained within the weld.

The results of the analyses presented above and in Appendix I show that the BS 7910 method can reliably be used to conservatively assess the severity of defects, or develop defect acceptance criteria for girth welds in X100 pipelines. Although the girth welds tested and assessed in this program of work were associated with pipe from different sources, with different levels of mismatch between the parent and weld metal yield strength, only one diameter and thickness of pipe was investigated.

8.5 Comparison of CWP Test Results with API 579-1/ASME FFS-1

The API 579-1/ASME FFS-1 assessment procedure was very similar to that described for the BS 7910 assessments in Section 8.4. The only difference in the input values for each assessment was the assumption of as-welded residual stresses. For the API 579-1/ASME FFS-1 assessment, the through wall profile and magnitude of welding residual stress was determined using the estimation procedure given in Annex E of the document, which requires input of the weld joint profile and arc energy of the final weld pass. The weld joint was a single-V configuration and the heat input for the final weld pass was 0.4 kJ/mm (see Table 1).

The analyses were undertaken using a commercially available software package, Signal Fitness-for-Service, developed by Quest Integrity software of the US. An initiation/brittle fracture analysis was undertaken, based on a single value of fracture toughness, which was input in terms of the J-Integral. The method is that given in API 579-1/ASME FFS-1 June 2007. The Level 2 FAD was used in the analysis.

As with the BS 7910 analyses, the following assessments were undertaken for each weldment;

1. Prediction of the critical defect size locus for the weldment

The following analyses were then undertaken for each CWP test;

1. Assessment based on the global stress at failure during the test to confirm whether the assessment point lies inside or outside the FAC.
2. Criticality study – calculation of the critical failure stress for the assessment point to lay on the FAC, and determination of the margin of safety on predicted failure stress when compared with the actual test result.
3. Combined criticality and sensitivity study – investigation of the significance of material toughness on failure stress when compared with the failure stress from the test.

The assessments undertaken on the A-series welds are presented in Section 8.5.1 and the B-series welds are presented in Section 8.5.2.

8.5.1 A-Series Welds

A locus of critical height as a function of length for a surface breaking defect is presented in Figure 129 for weld A06. The analysis is based on the minimum measured tensile and fracture toughness properties of the weldment, and the maximum allowable tensile stress in the pipe longitudinal direction is limited to SMYS. The defect sizes from the CWP specimens extracted from weld A06 are also included. As can be seen, the CWP defect sizes lay above the critical defect size locus inferring that the CWP specimens would fail at a stress less than SMYS. However, each CWP specimen failed at a stress greater than SMYS, the minimum recorded failure stress was from specimen H3; 114.1 ksi (787 N/mm²). Figure 129 shows the conservatism in the API 579-1/ASME FFS-1 assessment method.

A more detailed analysis was undertaken to determine the level of conservatism in the API 579-1/ASME FFS-1 assessment method. Due to the similarity in the assessments undertaken, a detailed overview is provided of the analysis and results of CWP specimen A06-WP-H1. The remaining assessments undertaken of the A-series welds follow the same procedure. The input data and results for each assessment are presented in Appendix J.

Analysis of the test failure conditions of CWP specimen A06-WP-H1 resulted in an assessment point outside the FAC, with K_r and L_r of 1.329 and 1.175 respectively, as shown in Figure 130.

A sensitivity study was undertaken to determine the critical value of primary membrane stress (P_m) for the assessment point to lay on the FAC of Figure 130; the critical value of P_m was predicted to be 33.3 ksi (229.7 N/mm²), which compared with the actual failure stress from the test of 125.46 ksi (865 N/mm²) resulted in a conservative margin of safety of 3.77.

A further sensitivity study was undertaken to investigate the effect of material toughness on the predicted failure stress; toughness was increased in small increments and for each new toughness value a critical value of P_m was determined for the assessment point to lay on the FAC. The assessment was considered toughness independent (i.e., collapse dominated) when subsequent increases in toughness resulted in no increase in the predicted failure stress. The critical value of P_m , assuming the behavior of the weld to be toughness independent is predicted to be 111.9 ksi (771.7 N/mm²), which compared well with the actual test result, giving a conservative margin of safety between the actual and predicted failure stress of 1.12.

As discussed in Section 8.4.1, the CWP test specimen exhibited good ductility, which was also reflected in the fracture mechanics tests with each specimen exhibiting a maximum force plateau prior to failure. Furthermore, the failure stress of the CWP exceeded the yield strength of the material; hence failure was by gross scale yielding. Based on the behavior of the CWP test specimen, failure was controlled by the tensile properties across the weldment, with negligible effect of material fracture toughness.

The remaining A-series welds were analyzed in the same way as detailed above to determine a locus of critical defect height versus length of surface breaking defects. The individual CWP test specimens were then analyzed to determine a critical value of tensile failure stress, and hence margin of safety and a toughness independent value of failure stress. The input data and results for each assessment are presented in Appendix J; Table J1 and Table J2.

As presented in Section 7.6, each CWP specimen from the A-series welds failed at a global stress in excess of SMYS. Hence, as the critical defect size locus is limited to SMYS, all CWP defect sizes tested would in theory fall beneath the critical defect size locus for the particular weldment. As with the BS 7910 assessments, the critical defect size loci for each weldment are lower bounding curves, based on the minimum measured tensile properties and fracture toughness properties of the weldment. If the actual material properties at the CWP location were used the weld would be more tolerant to larger defects. As can be seen in Figure J2 to Figure J5, only three of the defects tested (CWP specimens A33-WP-H3, A46-WP-H4 and A50-WP-H2) had a defect size above the FAC, inferring that the failure stress of these specimens would be predicted to be less than SMYS. The defect size of all other CWP specimens was below its respective critical defect size loci, inferring a failure stress greater than SMYS would be predicted for these specimens.

As can be seen from the results presented in Table J2 a conservative prediction of failure stress was determined for each specimen, as the margin between actual and predicted stress was greater than 1; ranging from 1.48 up to 13.9. This large variation between actual and predicted failure stress was found to be due to the input value of fracture toughness for each assessment. The predicted failure stresses assuming toughness independence were found to be in much better agreement with the failure stresses from the CWP specimens; the predictions were conservative, ranging from 1.06 to 1.21. These toughness independent predicted values of failure stress are more representative of the actual tests as each CWP specimen failed by plastic collapse.

8.5.2 B-Series Welds

The CWP specimens from the B-series welds tested only natural and deliberate welding defects (i.e., none of the specimens were notched).

The assessment method was similar to that presented above for the A-series weld; the difference being that for some assessments a solution for an embedded defect was required.

The input data and results for each assessment are presented in Appendix J; Table J3 and Table J4, and presented in Figure J6 to Figure J8. Presentation of the critical defect size loci with respect to the defects tested in the CWP specimens differed slightly, with multiple loci being produced per weldment; a locus for surface breaking defects, and a loci based on the measured remaining ligament thickness for each CWP specimen.

8.5.2.1 Weld B03

With the exception of specimen WP2, the defects tested in CWP specimens WP1, WP3 and WP4 lay above their respective critical defect size locus (see Figure J6), suggesting that the predicted failure stress would be less than SMYS. In contrast, the defect size of CWP specimen WP2 lay below the critical defect size locus inferring a failure stress greater than SMYS. An individual assessment of each CWP specimen test resulted in the assessment point lying outside the FAD. The predicted critical value of failure stress for each specimen/defect configuration was less than the actual test failure stress, giving a margin of safety between actual and critical ranging from 1.24 to 11.35. This large variation is not unexpected as the analysis is dependent on toughness and how the size and location of the defect is idealized. For the A-series welds, the defects were machined into the specimen surface to a definite depth and length. With the natural welding defects the height and ligament dimension of the defect generally varies along its length and more often than not the defect is intermittent, but the distance between adjacent defects is so small that they are considered to interact. The defect is idealized by a containment rectangle of dimensions; maximum measured height and length, and minimum ligament dimension. The actual defect area can be much smaller than that assumed from the containment rectangle.

Specimen WP1 contained two interacting defects; lack of root penetration and lack of side wall fusion. The defect was surface breaking, at the weld root, and the dimensions of the containment rectangle were 0.179x5.94in (4.54x151mm). Despite the size of the defect, the specimen failed by plastic collapse; the deformation mode being GSY. Assessment of the idealized defect dimensions predicted a failure stress 11.35 times smaller than the actual failure stress. The predicted failure stress assuming toughness independence was found to be in much better agreement with the actual failure stress; the ratio between actual and predicted failure stress reducing to 1.25.

Specimens WP2, WP3 and WP4 contained embedded defects, and each specimen failed by plastic collapse; the deformation mode being GSY. The predicted failure stress for each specimen based on the measured tensile and fracture toughness properties was conservative, ratio of actual to predicted failure stress of 1.24, 2.92 and 1.75, respectively. Assuming toughness independence, improved predictions of failure stress are obtained; the failure stress ratios reducing to 1.15, 1.46 and 1.19 respectively.

8.5.2.2 Weld B06

The testing of specimen WP2 was terminated due to excessive strain accumulation in Pipe 1. However, when the specimen was sectioned for macro- and micro-scopic examination of the defect, no defect was found. Hence, specimen WP2 was not assessed using the API 579-1/ASME FFS-1 procedure.

The test results are presented in Table J4 and Figure J7.

Specimen WP1 contained a number of defects; lack of root penetration and lack of sidewall fusion in the hot pass of Pipe 1 and Pipe 2, which were considered to interact, and be equivalent to a large surface breaking root defect. The specimen failed by plastic collapse. Due to the size of the defect and the input material properties, it was not possible to predict a critical value of stress for failure. However, it was possible to

predict a critical stress for failure assuming toughness independence; the ratio of actual to predicted failure stress was 1.38.

Specimen WP3 contained an embedded defect. However, testing of the specimen was terminated due to excessive strain accumulation in Pipe 1, although the load trace did show that a load plateau had been achieved. If the specimen was loaded to failure, the specimen would have failed by plastic collapse. The predicted failure stress based on the measured tensile and fracture toughness properties was conservative; the ratio of maximum achieved to predicted failure stress was 2.13. Assuming toughness independence, an improved prediction of failure stress was obtained; the failure stress ratio reduced to 1.44.

Specimen WP4 also contained an embedded defect. The specimen failed in a ductile manner, the deformation mode being NSY. The predicted failure stress based on the measured tensile and fracture toughness properties was conservative; the ratio of maximum achieved to predicted failure stress was 1.73. Assuming toughness independence, an improved prediction of failure stress was obtained; the failure stress ratio reduced to 1.16.

8.5.2.3 Weld B08

The testing of specimen WP2 was terminated due to excessive strain accumulation throughout the specimen. However, when the specimen was sectioned for macro- and micro-scopic examination of the defect, no defect was found. Hence, specimen WP2 was not assessed using the API 579-1/ASME FFS-1 procedure.

The test results are presented in Table J4 and Figure J8.

Specimen WP1 contained a number of embedded defects, both deliberate and natural, which were considered to interact. The specimen failed with limited ductility, the deformation mode being LC. The predicted failure stress based on the measured tensile and fracture toughness properties was very conservative; the ratio of actual to predicted failure stress was 19.91. Assuming failure to be collapse dominated, an improved prediction of failure stress was obtained; the failure stress ratio reduced to 1.96.

Specimen WP3 contained an embedded defect. The specimen failed with limited ductility, the deformation mode being LC. The predicted failure stress based on the measured tensile and fracture toughness properties was conservative; the ratio of actual to predicted failure stress was 3.64. Assuming failure to be collapse dominated, an improved prediction of failure stress was obtained; the failure stress ratio reduced to 1.54.

9 Discussion

There are a number of methods that are commonly used for developing defect acceptance criteria for pipeline girth welds; API 1104, EPRG and CSA Z662 which are pipeline specific and BS 7910 and API 579-1/ASME FFS-1 which can be applied to a pipeline but are more generic in application.

The applicability of these methods to girth welds in higher strength steel pipelines is not yet verified. The work undertaken in this project was aimed at identifying whether these methods could potentially be used for grade X100 pipelines.

To fully assess the limitations of these methods a number of variables would need to be investigated, for example, a range of pipe sizes (diameter and wall thickness), different pipe manufacturing methods, different weld preparations and weld procedures.

BP provided the project with ten girth welds from a full-scale operational field trial of a pipeline constructed from grade X100 line pipe. Despite only one pipe size being available, 48 x 0.78in (1220 x 19.8mm) the pipe

was sourced from two different pipe mills with the original plate coming from three different suppliers. Welding of the test pipeline ensured that abutting pipes from different mill/plate sources were welded together. Furthermore, the differences in line pipe properties ensured that a range in weld metal yield strength mismatch conditions was achieved from under to over matching. Although the majority of the welds tested were produced using a main line tandem GMAW weld procedure, the project also benefitted from availability of a weld from a tie-in weld procedure which also had a different weld preparation compared with the main line weld.

Of the ten girth welds given to the project, one girth weld was sacrificed for detailed tensile testing of the weld metal; RB specimens extracted from the root, cap and mid thickness regions of the weld, and a rectangular specimen sampling almost the full weld thickness. Each data set displayed a sinusoidal trend; strength highest at the weld 3 and 9 o'clock locations and lowest at the 6 and 12 o'clock locations. The weld cap region displayed a lower strength than the weld root or full thickness specimens, which were similar.

The remaining nine welds were subjected to detailed mechanical testing of the weldment; tensile, Charpy impact and fracture mechanics tests. Based on the results of those tests, only eight of the girth welds were selected for curved wide plate testing, of which thirty tests were undertaken in total.

Each girth weld displayed a similar 'sinusoidal' trend in weld metal strength, although this was not evident in the tests undertaken on the line pipe. The strength measured throughout each weldment exceeded the minimum requirements specified in ANSI/API 5L [47] and ISO 3183 [48]. The tests undertaken clearly highlight the importance of location of specimen extraction if the data are to be used to construct defect acceptance criteria appropriate for the entire weld.

The Charpy impact specimens were notched in the through-thickness direction, sampling the HAZ/FL and weld metal centerline regions. Although significant scatter was observed in the HAZ/FL results, compared with the weld metal results, each weld achieved the minimum and average Charpy impact energy requirements of API 1104, EPRG and CSA Z662, suggesting the girth welds would behave in a ductile manner.

Contrary to the Charpy impact test results, the results from the fracture mechanics specimens varied significantly. Fifty-four tests were undertaken in total; twenty-seven specimens sampled the weld metal and a further twenty-seven specimens sampled the HAZ/FL region. Twenty-one of the weld metal specimens failed in a ductile manner, compared with only five that sampled the HAZ/FL region. The remaining specimens failed in either a brittle manner (defined as crack growth not greater than 0.008in (0.2mm) in length) or a transitional manner (defined as crack growth greater than 0.008in (0.2mm) in length, but failure occurred prior to the specimen attaining a maximum force plateau).

The mechanical test program concluded with thirty CWP tests; nineteen specimens extracted from the A-series welds, with each specimen containing a machined notch to a prescribed depth and surface length. The remaining eleven specimens that were extracted from the B-series welds contained either natural welding defects (e.g., lack of penetration, lack of side wall fusion or porosity), deliberate defects that were introduced during welding, or combinations of natural and deliberate defects.

Of the CWP specimens from the A-series welds two specimens failed by NSY where the measured strains within both pipes and across the weldment were in excess of 0.5% but the failure stress was less than the measured yield strength of the weldment. The remaining CWP specimens failed by plastic collapse with the deformation mode being GSY; the strains at failure exceeded 0.5% and the failure stress was greater than the materials measured yield strength.

The results of the CWP specimens from the B-series welds demonstrated just how tolerant a weld can be to large defects, provided the weldment achieves the specified minimum tensile properties and the Charpy

tests show the weldment to behave in a ductile manner. The results also show the weldment to be more tolerant to embedded defects, when compared with a similar sized surface breaking defect.

The results obtained from the mechanical test program provided excellent data towards verification of the five different methods for predicting girth weld defect acceptance limits, API 1104, EPRG, CSA Z662, BS 7910 and API 579-1/ASME FFS-1.

9.1 Girth Weld Defect Acceptance Criteria Performance

9.1.1 API 1104 Option 2

API 1104 Option 2 is specific to the assessment of pipeline girth welds. The method does not discriminate between surface breaking or embedded defects, but treats all as one. The method can be used provided certain limitations on material performance and pipeline axial loading are achieved; CTOD greater than 0.002in (0.05mm), weld metal strength not less than the line pipe, failure would occur in the line pipe rather than the weld/HAZ if there were no defects present, and the axial stress and/or strain in the pipeline is not greater than SMYS or 0.5%.

A unique feature to API 1104 is the addition of a procedure to take account of inspection error when using the method to develop pipe lay girth weld defect acceptance criteria.

The authors of the Option 2 method claim that it has been validated against experimental data from grade X70 to X100. However, as discussed in detail in Section 3.1.2, there are some limitations on its use, particularly for the higher strength steels.

When constructing the FAD the calculation of L_r requires input of the flow stress. Two flow stress definitions are provided, the user having the option to use either. For grade X100 the average of SMYS and SMTS should be used, rather than the alternative equation proposed, which is valid only for pipe grades up to X80.

The calculation of K_r is rather complex and requires estimation of uniform elongation (uEL) and Y/T ratio. These enable an estimation of strain hardening, which is then used in the Ramberg-Osgood equation to define the stress-strain response of the weldment and in the conversion from J to CTOD.

As discussed in Section 3.1.2, the procedure may be improved by considering replacing the current Ramberg-Osgood equation with the multi-stage Ramberg-Osgood relationship proposed by the University of Gent as the new model has the capability of predicting the 'double n' type behavior that is often seen with the higher strength steels, grade X100 in particular.

Furthermore, there are limitations to the uEL equation proposed as it can give an overestimate of strain, and if the input yield strength is high enough, a negative value of uEL can be predicted. Since development of this procedure a new method has been developed for predicting the uEL for specific ranges of Y/T, which has been validated for grades X60 up to X100+. This new method provides a lower bound fit to experimental data, rather than a mean fit which the current method provides. Again, consideration should be given to investigating the benefits from incorporating this latest estimation procedure.

Potential benefits from incorporating these new procedures within the API 1104 method may result in a reduced frequency of repair, hence maintenance of the pipe lay schedule and reduced costs.

Despite the limitations discussed above, when compared with the CWP test results generated in this work, the method performed well. A conservative prediction of failure stress was calculated for all CWP specimens, except one, although that prediction was within 3% of the actual test failure stress. Despite the CWP specimens testing a range of weld metal strength mismatch conditions, under- to over-matched, there was no clear effect of yield strength mismatch in the assessments undertaken. However, this may be due to

the inherent conservatism in the analysis procedure and the analyses being based on the lesser of the pipe and weld metal strengths on the side of the weld that the defect was located.

9.1.2 EPRG

EPRG is specific to the assessment of pipeline girth welds. The method does not discriminate between surface breaking or embedded defects, but treats all as one. The procedure is very simple to apply. It is based on the Kastner plastic collapse solution and supported by several hundred small-scale, wide plate and full-scale tests.

Application of the procedure is restricted to pipe sizes greater than 30in (762mm) with wall thickness ranging from 0.276in to 1in (7 to 25mm), constructed from line pipe up to grade X70. Furthermore, the mechanical properties of the weldment must ensure failure is by plastic collapse (requirement is for the Charpy impact energy to exceed a min(avg) of 22(30) ft-lb (30(40)J)) and that the weld metal yield strength at least matches that of the line pipe. A final requirement is for the axial loading on the pipeline not to exceed the yield strength of the pipe and/or a total strain of 0.5%.

The published guidelines have seen increasing use since their introduction and they have been included in the European standard for pipeline welding, EN 12732 and the Australian pipeline code, AS 2885.

Since early 2000 there has been much work undertaken to extend the guidance to grade X80 pipelines, defects of greater through-wall height, and assessment of adjacent defects that have the potential to interact. Despite this work being completed and presented at two major pipeline conferences (Pipeline Technology Conference held in Belgium, 2009 and IPC2010 held in Canada, 2010) a formal update of the guidelines is yet to be published.

The philosophy used to validate the guidelines for grade X80 pipelines was used in this work to assess the suitability of the approach to grade X100 pipelines, although there were significantly less tests undertaken to aid validation; 132 CWP specimens were used to help validate the approach for grade X80, but only 30 have been undertaken in this work.

An additional recommendation based on the work undertaken to extend the guidelines to grade X80 pipelines proposed that the Y/T ratio should be greater than 0.9.

The welds tested in this work achieved the min(avg) Charpy impact energy requirements to ensure failure by plastic collapse, but in many cases the Y/T ratio was much greater than 0.9 and the weld metal yield strength mismatch ranged from an under-matched to an over-matched condition. Furthermore, particularly for the defects tested from the B-series welds, the defect area exceeded 7% (based on a 12in (300mm) arc length).

Analysis of the CWP test results provided good supporting evidence of the potential use of the EPRG guidelines for grade X100 pipelines. The defect length ratios of the tests undertaken on the A-series welds was not sufficient to confirm whether the existing recommended limits for grade X80 pipelines were applicable also to grade X100 pipelines. However, the theoretical limits calculated for grade X80 pipelines were found to be sufficiently conservative to be applicable to grade X100 pipelines (note, the recommended limits for grade X80 pipelines are greater than the theoretical limits; they were extended based on the results of the CWP tests undertaken). The results of the CWP tests from the B-series welds demonstrated that a girth weld is more tolerant to larger embedded defects than surface breaking defects, upon which the EPRG limits are based. Application of the guidelines to embedded defects is therefore considered equally applicable, although with increased conservatism.

It is recommended that further tests be undertaken to investigate for example, the effects of pipe size (diameter and wall thickness) and weld preparation/procedures to provide a more robust validation of the EPRG guidelines to grade X100 pipelines.

9.1.3 CSA Z662

CSA Z662 is specific to the assessment of pipeline girth welds. Unlike API 1104 and EPRG, CSA provides a methodology for calculating maximum allowable embedded defects as well as surface breaking defects. The method can be used provided certain limitations on material performance are achieved; the measured yield strength of the weldment must not be less than SMYS of the line pipe, and the measured Charpy impact energy must not be less than 30ft-lb (40J). Although fracture mechanics testing is required, there is no lower limit on fracture toughness; the value of fracture toughness measured from the tests is used as an input into the assessment. A point to note is that CSA requires input of the *maximum effective applied tensile bending stress* which must be determined through stress analysis, and the defect is assumed to be positioned at this location around the pipe circumference.

Whether assessing for surface breaking or embedded defects, both a brittle fracture assessment and plastic collapse assessment are required to be undertaken. The intention is to estimate the critical defect length for a specified defect height, with a limit on length of 10% of the pipe circumference. For different defect heights a locus of maximum allowable defect size can be developed.

The plastic collapse analysis procedure is relatively straight forward to apply, but can be time consuming. For a given defect height (or length) the equation needs to be solved iteratively to obtain a close estimate of length (or height). This process needs to be repeated several times to construct the defect size locus.

The brittle fracture analysis procedure is more complex and requires interpretation of log-log graphs and a goodness of fit of a power law to the data. First, an effective defect size parameter (\bar{a}) must be calculated which is then normalized by the pipe wall thickness (t). A vertical line is then drawn on the log-log graph at \bar{a}/t and at the intersections with the corresponding d/L (defect depth to length) loci, horizontal lines are extended to the abscissa where the corresponding values of d/t (defect depth to pipe wall thickness) are read off. A graph is then developed of L as a function of d/t , and a power law fit to the data. The power law equation is then used to estimate a critical defect length for any specified d/t .

For the girth weld defect acceptance criteria, for a given defect height the critical length is the lesser of that calculated using the brittle fracture and plastic collapse procedures, limited to no more than 10% of the pipe circumference.

Despite the complexity of the method, it was used successfully to predict a conservative value of failure stress for each CWP test specimen. Each predicted failure stress was less than the actual test failure stress by 2% or more.

The analyses undertaken would suggest that CSA Z662 can be used to define the defect acceptance criteria for grade X100 pipelines, but as mentioned above, it is recommended that further tests be undertaken to investigate, for example, the effect of pipe size (diameter and wall thickness) and weld preparation/procedures to provide a more robust validation of the CSA Z772 approach for grade X100 pipelines.

9.1.4 Fracture Mechanics Assessment Procedures of BS 7910 and API 579-1/ASME FFS-1

API 579-1/ASME FFS-1 provides comprehensive guidance for assessing 'fitness-for-service' of 'pressure containing equipment' designed to ASME and API codes. BS 7910 provides guidance on assessing the acceptability of defects in all types of structures and components, and does not discriminate between different design codes. Neither offers a pipeline 'girth weld' specific assessment method, but the fracture

mechanics procedures therein for assessing circumferentially orientated planar, crack like defects in a pipe (or curved surface, or plate) can be applied. In comparison with the pipeline specific procedures of API 1104, EPRG and CSA Z662, BS 7910 and API 579-1/ASME FFS-1 offer more versatility to the assessment and permit a wider range of conditions to be assessed. Both procedures offer multi-levels of assessment, the choice of which depending on the materials involved the input data available and the conservatism required.

The Level 2 procedures are used in this study. The vertical axis of the FAD represents the ratio of applied stress intensity factor to the fracture toughness of the material (K_r) and the horizontal axis represents the ratio of applied load to the load required to cause failure by plastic collapse (L_r). Interaction between the two failure modes is represented by the FAC. An assessment point lying within the FAD is deemed safe; a point outside is deemed to be potentially unsafe.

Although the two FADs appear similar, there are some differences in the way each method calculates values of L_r and K_r . The biggest difference between the two is the calculation of K_r . A review of stress intensity factor solutions [49] was recently undertaken in support of the FITNET fitness for Service procedures (FITNET was a 4-year European thematic network with the objective of developing and extending the use of fitness-for-service procedures throughout Europe. The project was part of the EU's Framework 5 research program). For the case of an 'internal circumferential surface crack' the BS 7910 solution consistently gives a slightly higher value of stress intensity factor than the API 579-1/ASME FFS-1 solution.

For example, BS 7910 has a different method of estimating the magnitude and through wall distribution of welding residual stress than API 579-1/ASME FFS-1, which estimates the residual stress profile based on welding parameters (e.g., voltage, arc energy). Furthermore, the two methods have a different approach for incorporating the stress raising effect of the weld toe.

In general though, despite the differences in their approach, where an assessment was possible both BS 7910 and API 579-1/ASME FFS-1 predicted the assessment point of each CWP specimen to lie outside the FAD, and both methods predicted a conservative value of critical failure stress (i.e., a factor of safety greater than unity, when compared with the failure stress measured from the CWP test). The margin between predicted and actual failure stress increased significantly with increasing defect size (height and length). More accurate, but conservative predictions of failure stress were obtained by artificially increasing the material fracture toughness to a high value to promote failure by plastic collapse. Although the results of the Charpy impact tests showed the welds to behave in a ductile manner, this was not totally supported by the results of the fracture mechanics tests. However, as noted, the SENB specimen geometry is designed to give a lower bound value of fracture toughness due to the high crack tip constraint of the specimen geometry. In contrast, the effective toughness of the girth weld would be higher due to the reduction in constraint. To realize the increase in toughness between a girth weld and an SENB specimen, use of a SENT specimen geometry is becoming increasingly common. It is already recommended by DNV [50], and there is currently an initiative within the UK to develop an industry standard to complement the BS 7448 suite of fracture mechanics tests standards.

10 Conclusions

A comprehensive test program was undertaken to fully characterize the mechanical properties of the 10 girth welds. The main conclusions from the tests undertaken are presented below:

1. Two hundred and seventeen tensile tests were undertaken to characterize the stress-strain behavior of the girth welds. The following observations were made;

- The line pipe achieved the specified minimum yield and tensile strength requirements of the line pipe specification, ANSI/API 5L.
 - The stress-strain response of the line pipe in the pipe longitudinal direction was similar, unlike the response of the line pipe in the transverse direction, where the post yield behavior was found to vary considerably.
 - The properties were found to vary significantly depending on the type of test specimen; round bar or flat strip.
 - The properties of the weld metal varied significantly around the pipe circumference, showing a sinusoidal trend; yield strength was lowest at approximately the 6 and 12 o'clock positions and highest at approximately the 3 and 9 o'clock positions. The strength was also observed to vary through the weld thickness; the highest strength measured in the weld root and mid thickness regions, lowest at the weld cap.
 - The properties of the line pipe varied greatly between the different pipe manufacturers and plate sources; although not one consistently achieved the highest average values of yield or tensile strength, yield to tensile strength ratio or elongation.
 - The variation in strength observed between the different pipe manufacturers and plate sources resulted in a wide range of weld metal strength mismatch, ranging from 11% undermatching to 26% overmatching.
2. One hundred and eight Charpy impact tests were undertaken. The impact energy measured in each weldment achieved the minimum and average requirements stipulated within API 1104, EPRG and CSA Z662, suggesting that the girth welds would behave in a ductile manner.
 3. Fifty four fracture mechanics tests were undertaken. The results from the tests suggest the potential for failure to occur in a brittle manner; the lowest CTOD measured for the heat affect zone was 0.0016in (0.04mm), and the weld metal was 0.0031in (0.08mm).
 4. Thirty curved wide plate (CWP) tests were undertaken.
 - The CWP specimens with machined defects of varying length and height, up to 4in and 0.157in (100x4mm), with a defect area up to 6% of the specimen cross section, failed in a ductile manner, either by gross section or net section yielding.
 - The CWP specimens that contained either natural welding defects, deliberate defects introduced during welding, or combinations of natural and deliberate defects had a defect area up to 25% of the specimen cross section. The two specimens with the larger defect areas failed by local collapse (stress and strain at failure less than the yield strength and 0.5%, respectively). The remaining specimens failed in a ductile manner, either by gross section or net section yielding.
 - The results of the CWP specimens demonstrated that a girth weld is more tolerant to embedded defects when compared with an equivalent size surface breaking defect.

The results of the mechanical test program were used towards assessing the limitation of the girth weld defect acceptance procedures, API 1104, CSA Z662 and EPRG, and the more generic fracture mechanics procedures given in BS 7910 and API 579-1/ASME FFS-1. The main conclusions from the analyses undertaken are presented below;

1. Verification of the applicability of API 1104, EPRG, CSA Z662, BS 7910 and API 579-1/ASME FFS-1 assessment methods to grade X100 pipelines was based on the performance of CWP tests undertaken on one pipe size; 48in (1220mm) diameter x 0.78in (19.8mm) wall thickness.
2. The following points are concluded from the assessments undertaken to **API 1104 (Option 2)**;
 - The procedure is based on calculating limiting defect sizes for surface breaking defects. There is no distinction between surface and embedded defects. The calculated limits are considered to be equally applicable to equivalent size embedded defects.
 - The analysis procedure is complex and not all equations within the procedure are valid for grade X100.
 - Despite these limitations the procedure gave conservative predictions of failure stress for all, except one CWP specimen (the predicted failure stress was 3% lower than the actual failure stress). In many cases the ratio of predicted failure stress to actual failure stress was close to 1.0.
 - The least accurate (most conservative) predictions were for the natural/deliberate welding defects, embedded within the pipe wall.
3. The following points are concluded from **EPRG** assessments undertaken;
 - The procedure is based on calculating limiting defect sizes for surface breaking defects. There is no distinction between surface and embedded defects. The calculated limits are considered to be equally applicable to equivalent size embedded defects.
 - The defect size limits are straight forward to calculate and the criteria easy to use.
 - The limits calculated using the net-section collapse model are conservative when compared with the CWP test data.
 - The defect size limits recommended for inclusion in the EPRG guidance document for X80 grade pipelines appear suitable for grade X100 pipelines. However, the length of the defects tested did not extend to the $7t$ (t is the pipe wall thickness) limit proposed.
 - The CWP data for the natural/deliberate welding defects show that the proposed defect size limits are also applicable to equivalent sized embedded defects.
4. The following points are concluded from the assessments undertaken to **CSA Z662**;
 - The procedure can be used for calculating defect size limits for either surface breaking defects or embedded defects.
 - The analysis procedure for brittle fracture is complex and not simple to use. For example, the user is required to interpret a log-log plot to construct a table of defect height as a function of length.
 - The procedure gave conservative predictions of failure stress, 2% or more when compared with the actual test data.
5. The following points are concluded from the assessments undertaken to **BS 7910** and **API 579-1/ASME FFS-1**;
 - The procedure for calculating defect size limits for either surface breaking or embedded defects is complex and best undertaken using commercially available software.

- The defect limits calculated are specific to the pipe size, pipeline loading conditions and material properties; calculations can still be performed even if the weldment has poor toughness and/or strength as these are direct inputs into the assessment.
- The result of each CWP test was correctly predicted as a 'failure' using both methods.
- Sensitivity studies were undertaken to determine the critical failure stress;
 - i. For the BS 7910 assessments, the ratio of actual to predicted failure stress ranged from 1.15 to 6.5 for all CWP specimen except for three. The failure stress of those specimens was predicted to be very low, resulting in ratios of 11.5, 19.8 and 23.0.
 - ii. For the API 579-1/ASME FFS-1 assessments, the ratio of actual to predicted failure stress ranged from 1.48 to 5.6 for all CWP specimen except for four, which had ratios of 11.3, 11.4, 13.9 and 19.9.
- Sensitivity studies were undertaken assuming that the behavior of the girth welds was independent of fracture toughness;
 - i. For the **BS 7910** assessment, the ratio of actual to predicted failure stress ranged from 1.07 to 1.45.
 - ii. For the **API 579-1/ASME FFS-1** assessment, the ratio of actual to predicted failure stress ranged from 1.06 to 1.97.
- The differences between the BS7910 and API 579-1/ASME FFS-1 results are due to the brittle fracture assessment and treatment of welding residual stress. The plastic collapse solutions, although different, give similar results.

11 Recommendations

The principal recommendations from the work undertaken are:

1. Consideration should be given to undertaking additional testing to investigate the influence of pipe diameter and wall thickness as verification of the applicability of the different assessment methods has been based on one pipe size; 48in (1220mm) diameter x 0.78in (19.8mm) wall thickness.
2. Consideration should be given to providing more detailed guidance given in API 1104 and CSA Z662 on the type, orientation and number of tests, and the sampling position around the pipe circumference to fully characterize the behavior of the weldment.
3. Consideration should be given to including a testing plan in the EPRG guidelines to ensure sufficient testing is undertaken to fully characterize the behavior of the weldment.
4. Some equations in the API 1104 procedure are limited to grade X80 line pipe. The validity of these to grade X100 needs to be assessed or consideration should be given to updating the procedure with more appropriate models, for example those published by the University of Gent as they provide an improved fit to available experimental data and have been validated for grade X100.

12 References

- [1] R M Andrews, J Johnson and J Crossley, 'Design of pipeline damage for the BP X100 operational trial', Proceedings of the 8th International Pipeline Conference (IPC2010), 27/09-01/10 2010, Calgary, Alberta, Canada.
- [2] N A Millwood, J Johnson, M Hudson and K Armstrong, 'Construction of the X100 Operational Trial pipeline at Spadeadam, Cumbria, UK', Proceedings of the 8th International Pipeline Conference (IPC2010), 27/09-01/10 2010, Calgary, Alberta, Canada.
- [3] ASME B31.8:2003, 'Gas transmission and distribution piping systems', The American Society of Mechanical Engineers, New York, USA.
- [4] Z662:2003, 'Oil and gas pipeline systems', Canadian Standards Association, Ontario, Canada, June 2003.
- [5] API 1104, 'Welding of pipelines and related facilities', American Petroleum Institute, Twentieth Edition (October 2005), Errata/Addendum (July 2007), Errata (December 2008).
- [6] CSA Z662, 'Oil and gas pipeline systems', Canadian Standards Association, June 2007.
- [7] BS 4515-1:2009, 'Specification for welding of steel pipelines on land and offshore. Part 1 – Carbon and carbon manganese steel pipelines', British Standards Institution, London, UK, 31 December 2008.
- [8] G Knauf and P Hopkins, 'The EPRG guidelines on the assessment of defects in transmission pipeline girth welds', 3R International, Volume 35, pp.620-624, 1996.
- [9] BS 7910:2005, 'Guide to methods for assessing the acceptability of flaws in metallic structures', British Standards Institution, Incorporating amendment No.1, September 2007.
- [10] API 579-1/ASME FFS-1, 'Fitness-for-service', API 579 second edition, American Petroleum Institute and American Society for Mechanical Engineers, June 2007
- [11] R P Harrison, K Loosemore and I Milne, 'Assessment of the integrity of structures containing defects', CEGB report no. R/H/6, Nuclear Electric (formerly Central Electricity Generating Board), UK.
- [12] API 1104:1999 'Welding of pipelines and related facilities', American Petroleum Institute, Nineteenth Edition (September 1999), Errata (October 2001).
- [13] S Webster and A Bannister, 'Structural integrity assessment procedure for Europe – of the SINTAP programme overview' Engineering Fracture Mechanics, Volume 67, pp.481-514, 2000.
- [14] Anon, 'Assessment of integrity of structures containing defects', British Energy Ltd, R/H/R6, Revision 3, 1999.
- [15] Y Y Wang, M Liu, D Rudland and Y Chen, 'A comprehensive update in the evaluation of pipeline weld defects', Engineering Mechanics Corporation of Columbus, Ohio, USA, US DOT agreement DTRS56-03-T-0008 and PRCI contract PR-276-04503, May 2007.
- [16] S Hertelé, R Denys and W De Waele, 'Full stress-strain relation modeling of pipeline steels', 8th National Congress on Theoretical and Applied Mechanics (NCTAM 2009), May 2009.
- [17] R M Denys, W De Waele and A A Lefevre, 'Estimate of Y/T ratio and uniform elongation capacity of pipeline steels from yield strength', Proceedings Pipeline Technology Conference 2009, Ostend, Belgium, October 2009.

- [18] BS 4515:1984, 'Process of welding of steel pipelines on land and offshore', British Standards Institution, London, UK, 1984.
- [19] API Standard 1104, 'Welding of pipelines and related facilities', American Petroleum Institute, 17th Edition, September 1988.
- [20] PD 6493:1980, 'Guidance on some methods for the derivation of acceptance levels for defects in fusion welded joints', British Standards Institution, London, UK.
- [21] W Kastner, et. al., 'Critical crack size in ductile piping', International Journal of Pressure Vessels and Piping, Vol.9, pp.197-219, 1981.
- [22] EN 12732, 'Gas supply systems – Welding steel pipework – functional requirements', British Standards Institution, London, UK, 2000.
- [23] AS 2885.2:2001, 'Pipelines – gas and liquid petroleum. Part 2: Welding', Standards Australia, Homebush, New South Wales, Australia, 2001.
- [24] R M Denys, R M Andrews, M Zarea and G Knauf, 'Recommended revisions to the EPRG Tier 2 Guidelines for the assessment of defects in transmission pipeline girth welds', 6th International Pipeline Technology Conference, Ostend, Belgium, October 2009.
- [25] R M Denys, R M Andrews, M Zarea and G Knauf, 'EPRG Tier 2 Guidelines for the assessment of defects in transmission pipeline girth welds', Proceedings of the 8th International Pipeline Conference (IPC 2010), Calgary, Canada, 27 Sept 2010 – 01 Oct 2010.
- [26] A G Glover and R I Coote, 'Full scale fracture tests of pipeline girth welds', Proceedings of the 4th National Congress on Pressure Vessels and Piping Technology. PVP. Vol. 94. 1983.
- [27] BS 7448-2, 'Fracture mechanics toughness tests. Part 2. Method for determination of K_{Ic} , critical CTOD and critical J values of welds in metallic materials', British Standards Institution, London, UK, 1997.
- [28] ASTM E1290-08, 'Standard test method for crack tip opening displacement (CTOD) fracture toughness measurement', ASTM International, West Conshohocken, PA 19428-2959, USA.
- [29] A G Miller, 'Review of limit loads of structures containing defects', International Journal of Pressure Vessels and Piping, Vol.32, pp.197-327, 1988.
- [30] DNV-RP-F108, 'Recommended practice – Fracture control for pipeline installation methods introducing cyclic plastic strain', Det Norske Veritas, January 2006.
- [31] BS 7448-4 (incorporating corrigendum no.1), 'Fracture mechanics toughness tests. Part 4. Method for determination of fracture resistance curves and initiation values for stable crack extension in metallic materials', British Standards Institution, London, UK, 1997.
- [32] API Standard 1104, 'Welding of pipelines and related facilities', American Petroleum Institute, Washington, USA, Twentieth Edition, 2005.
- [33] GIS-43 331, 'Guidance on industry standard API 1104 for pipeline welding', BP Group, Engineering Technical Practice, 2006.
- [34] P Hopkins and R M Denys, 'The background to the European Pipeline Research Group's girth weld limits for transmission pipelines', EPRG/NG-18, 9th Biennial Joint Technical Meeting on Line Pipe Research, Houston, USA, 1993.

- [35] R M Denys, R M Andrews, M Zarea and G Knauf, 'Recommended revisions of the EPRG Tier 2 guidelines for the assessment of defects in transmission pipeline girth welds', Proceedings Pipeline Technology Conference 2009, Ostend, Belgium, October 2009.
- [36] BS EN 10002-1:2001, 'Tensile testing of metallic materials. Method of test at ambient temperature', British Standards Institution, London, UK, September 2001.
- [37] BS EN ISO 6892-1:2009, 'Metallic materials. Tensile testing. Method of test at ambient temperature', British Standards Institution, London, UK, August 2009.
- [38] R M Denys, 'Weld metal strength mismatch: past, present and future', International Symposium to celebrate Professor Masao Toyoda's retirement from Osaka University, Japan, 2008.
- [39] E Osterby, M Hauge, E Levold, A Sandvik, N Bård and C Thaulow, 'Strain capacity of SENT specimens – Influence of weld metal mismatch and ductile tearing resistance', International Offshore and Polar Engineering Conference, Vancouver, Canada, 2008.
- [40] Y Y Wang, M Liu and D Rudland, 'Strain based design of high strength pipelines' International Offshore and Polar Engineering Conference, Lisbon, Portugal, 2007.
- [41] BS EN 10045-1, 'Charpy impact tests on metallic materials. Part 1. Test method (V and U notches)', British Standards Institution, London, UK, 1990.
- [42] ASTM E23-07ae1, 'Standard test methods for notched bar impact testing of metallic materials', ASTM International, West Conshohocken, PA 19428-2959, USA.
- [43] ASTM E 1820-09e1, 'Standard test method for measurement of fracture toughness', ASTM International, West Conshohocken, PA 19428-2959, USA.
- [44] ASTM E1290-09, 'Standard test method for crack-tip opening displacement (CTOD) fracture toughness measurement', ASTM International, West Conshohocken, PA 19428-2959.
- [45] ASTM E399-09, 'Standard test method for plane strain fracture toughness of metallic materials'. ASTM International, West Conshohocken, PA 19428-2959.
- [46] BS EN ISO 15653, 'Metallic materials – Method of test for the determination of quasistatic fracture toughness of welds', British Standards Institution, London, UK, 2010.
- [47] ANSI/API Specification 5L, 'Specification for line pipe', American National Standards Institute and the American Petroleum Institute, Forty-fourth edition, 2010.
- [48] ISO 3183, 'Petroleum and natural gas industries – Steel pipe for pipeline transportation systems', International Standards Organisation, 2007.
- [49] I Hadley, M Goldthorpe and L Wei, 'Compilation of K-solutions for fitness-for-service procedures', TWI, Industrial Members Report 849/2006, May 2006.
- [50] DNV-RP-F108, 'Fracture control for pipeline installation methods introducing cyclic plastic strain', Det Norske Veritas, 2006.

Pass	Process	Travel speed (cm/min)	Arc energy (kJ/mm)
Root	P-GMAW	112 – 129	0.3 – 0.4
Hot pass	Tandem GMAW	78 – 95	0.2 – 0.3 0.2 – 0.3
Fill		65 – 115	0.2 – 0.4 0.2 – 0.3
Cap		20 - 71	0.2 – 0.4 0.2 – 0.4

Table 1 Summary of the parameters for the main line weld procedure.

Pass	Process	Wire	Travel speed (cm/min)	Arc energy (kJ/mm)
Root	STT Vertical down	Lincoln Pipeliner 80 SG	14	0.8 – 1.0
Hot pass	Mechanized FCAW Vertical up	ESAB OK Tubrod 15.09	19 - 23	1.0 – 1.4
Fill 1				
Fill				
Cap			19	1.3 – 1.4

Notes: In total nine fill and three cap passes were required.

Table 2 Summary of the parameters for the tie-in weld procedure.

Test type	Weld number									
	A06	A17	A33	A44	A46	A50	B03	B06	B08	B10
Macro	3	4	3	2	3	3	3	3	3	11
HV survey										11
Tensile tests										
AWM-cap	4	4	4	2	4	4	4	4	4	11
AWM-mid	-	-	-	-	-	-	-	-	-	11
AWM-root	2	2	2	1	2	2	2	2	2	11
AWM-pris	-	-	-	-	-	-	-	-	-	11
Pipe-L-FT	10	10	10	6	10	10	10	10	10	-
Pipe-T-FT	2	2	2	2	2	2	2	2	2	-
Pipe-T-RB	4	6	4	2	4	4	4	4	4	-
Cross weld	2	2	2	2	2	2	2	2	2	-
Charpy tests (sets of 3 specimens)										
HAZ/FL	1	1	1	1	1	1	1	1	1	-
AWM	1	1	1	1	1	1	1	1	1	-
CTOD tests (sets of 3 specimens)										
HAZ/FL	1	1	1	1	1	1	1	1	1	-
AWM	1	1	1	1	1	1	1	1	1	-
Curved wide plate tests										
HAZ/FL	3	3	3	-	3	2	-	-	-	-
AWM	1	1	1	-	1	1	-	-	-	-
Natural	-	-	-	-	-	-	4	4	3	-

Notes:

L and **T** are pipe longitudinal and transverse directions

FT and **RB** are flat tensile and round bar tensile specimen geometry

cap, **mid** and **root** are the weld cap, weld mid thickness and weld root regions sampled, respectively

pris refers to a prismatic test section

Table 3 Matrix of tests undertaken on each weld.

Test ID	Position (o'clock)	Specimen section				Yield strength				Tensile strength		Z	A	uEL	
		Diameter		Area		Upper yield		R _{p0.2}		R _m					
		in	(mm)	in ²	(mm ²)	ksi	(N/mm ²)	ksi	(N/mm ²)	ksi	(N/mm ²)				Y/T
C1	0.1 - 0.2	0.216	(5.48)	0.037	(23.59)			110	(758)	124	(856)	0.89	65	13.3	9.27
C2	1.2 - 1.3	0.216	(5.49)	0.037	(23.67)	118	(815)	118	(814)	125	(863)	0.94	69	20.6	9.60
C3	2.3 - 2.4	0.216	(5.49)	0.037	(23.67)	122	(838)	121	(834)	127	(874)	0.95	68	20.9	9.83
C4	3.4 - 3.5	0.216	(5.48)	0.037	(23.59)	124	(855)	123	(851)	129	(891)	0.96	65	20.6	9.22
C5	4.5 - 4.6	0.215	(5.47)	0.036	(23.50)	121	(834)	121	(831)	126	(872)	0.95	66	23.7	8.15
C6	5.6 - 5.7	0.216	(5.49)	0.037	(23.67)			116	(800)	125	(860)	0.93	66	17.4	8.55
C7	6.7 - 6.8	0.217	(5.50)	0.037	(23.76)			114	(785)	124	(857)	0.92	66	21.4	9.44
C8	7.8 - 7.9	0.215	(5.47)	0.036	(23.50)	120	(825)	119	(823)	126	(871)	0.94	66	19.5	9.21
C9	8.8 - 9.0	0.214	(5.44)	0.036	(23.24)	124	(852)	124	(853)	129	(888)	0.96	65	12.8	8.03
C10	9.9 - 10.1	0.213	(5.42)	0.036	(23.07)	79	(547)	121	(837)	129	(889)	0.94	66	14.3	7.84
C11	11.0 - 11.2	0.215	(5.45)	0.036	(23.33)			120	(825)	128	(885)	0.93	67	21.2	9.57

Notes: Rp0.2 is the yield strength at a non-proportional extension of 0.2% strain, Z is the percentage reduction in specimen cross section area, A is the percentage elongation of the specimen gauge length (40mm) after fracture, and uEL is the percentage uniform elongation of the specimen at fracture

Table 4 Weld B10: Tensile test results for the **weld cap region** - round bar specimens, tested at 68°F (20°C).

	Yield strength, $R_{p0.2}$		Tensile strength, R_m		Y/T ratio	uEL
	ksi	(N/mm ²)	ksi	(N/mm ²)		%
Minimum value	110	(758)	124	(856)	0.89	7.8
Maximum value	124	(853)	129	(891)	0.96	9.8
<i>Difference (max-min)</i>	14	(95)	5	(35)	0.07	2.0
Average value	119	(819)	127	(873)	0.94	9.0
Standard deviation	4	(29)	2	(13)	0.02	0.7

Table 5 Weld B10: Statistical analysis of the tensile test results for the **weld cap region** - round bar specimens, tested at 68°F (20°C).

Test ID	Position (o'clock)	Specimen section				Yield strength				Tensile strength		Z	A	uEL	
		Diameter		Area		Upper yield		R _{p0.2}		R _m					
		in	(mm)	in ²	(mm ²)	ksi	(N/mm ²)	ksi	(N/mm ²)	ksi	(N/mm ²)				Y/T
R1	0.6 - 0.7	0.215	(5.46)	0.036	(23.41)			125	(859)	130	(898)	0.96	64	18.8	7.39
R2	1.7 - 1.8	0.215	(5.45)	0.036	(23.33)	124	(857)	124	(856)	129	(891)	0.96	65	18.0	6.98
R3	2.8 - 2.9	0.216	(5.48)	0.037	(23.59)	126	(871)	126	(869)	131	(902)	0.96	52	14.3	7.00
R4	3.9 - 4.0	0.216	(5.48)	0.037	(23.59)	126	(871)	126	(870)	132	(907)	0.96	64	18.6	7.71
R5	5.0 - 5.1	0.215	(5.45)	0.036	(23.33)			121	(833)	129	(890)	0.94	65	16.8	6.43
R6	6.0 - 6.2	0.215	(5.46)	0.036	(23.41)			118	(815)	127	(876)	0.93	52	13.4	6.43
R7	7.1 - 7.3	0.216	(5.48)	0.037	(23.59)			121	(837)	129	(888)	0.94	66	14.1	5.58
R8	8.2 - 8.4	0.215	(5.47)	0.036	(23.50)	125	(862)	125	(861)	131	(903)	0.95	63	12.6	5.20
R9	9.3 - 9.5	0.216	(5.48)	0.037	(23.59)	127	(874)	127	(874)	133	(915)	0.96	65	17.7	7.09
R10	10.4 - 10.5	0.216	(5.48)	0.037	(23.59)			127	(876)	133	(919)	0.95	65	18.3	6.78
R11	11.5 - 11.6	0.216	(5.48)	0.037	(23.59)			124	(857)	130	(897)	0.96	65	14.2	6.51

Notes: Rp0.2 is the yield strength at a non-proportional extension of 0.2% strain, Z is the percentage reduction in specimen cross section area, A is the percentage elongation of the specimen gauge length (40mm) after fracture, and uEL is the percentage uniform elongation of the specimen at fracture

Table 6 Weld B10: Tensile test results for the **weld root region** - round bar specimens, tested at 68°F (20°C).

	Yield strength, $R_{p0.2}$		Tensile strength, R_m		Y/T ratio	uEL
	ksi	(N/mm ²)	ksi	(N/mm ²)		%
Minimum value	118	(815)	127	(876)	0.93	5.2
Maximum value	127	(876)	133	(919)	0.96	7.7
<i>Difference (max-min)</i>	9	(61)	6	(43)	0.03	2.5
Average value	124	(855)	130	(899)	0.95	6.6
Standard deviation	3	(19)	2	(12)	0.01	0.7

Table 7 Weld B10: Statistical analysis of the tensile test results for the **weld root region** - round bar specimens, tested at 68°F (20°C).

Test ID	Position (o'clock)	Specimen section				Yield strength				Tensile strength		Z	A	uEL	
		Diameter		Area		Upper yield		R _{p0.2}		R _m					
		in	(mm)	in ²	(mm ²)	ksi	(N/mm ²)	ksi	(N/mm ²)	ksi	(N/mm ²)				Y/T
M1	0.3 - 0.5	0.315	(8.00)	0.078	(50.27)			120	(829)	125	(865)	0.96	65	19.3	7.05
M2	1.4 - 1.6	0.312	(7.92)	0.076	(49.27)	125	(863)	124	(857)	128	(883)	0.97	63	18.6	6.72
M3	2.5 - 2.7	0.313	(7.94)	0.077	(49.51)	127	(878)	126	(867)	130	(894)	0.97	64	17.8	7.29
M4	3.6 - 3.7	0.315	(7.99)	0.078	(50.14)	127	(874)	126	(867)	130	(896)	0.97	64	19.6	7.05
M5	4.7 - 4.8	0.315	(8.00)	0.078	(50.27)	123	(846)	122	(844)	128	(880)	0.96	63	17.4	6.25
M6	5.8 - 5.9	0.315	(7.99)	0.078	(50.14)			118	(817)	125	(862)	0.95	65	16.9	5.83
M7	6.9 - 7.0	0.314	(7.97)	0.077	(49.89)	120	(824)	119	(822)	125	(860)	0.96	64	17.3	6.63
M8	8.0 - 8.1	0.314	(7.98)	0.078	(50.01)	125	(862)	125	(859)	130	(895)	0.96	63	18.7	6.59
M9	9.1 - 9.2	0.314	(7.97)	0.077	(49.89)	128	(881)	127	(878)	131	(906)	0.97	61	16.4	6.20
M10	10.2 - 10.3	0.314	(7.97)	0.077	(49.89)	127	(879)	127	(875)	131	(903)	0.97	61	17.8	6.68
M11	11.3 - 11.4	0.315	(8.00)	0.078	(50.27)	125	(859)	124	(857)	130	(894)	0.96	65	17.8	6.34

Notes: Rp0.2 is the yield strength at a non-proportional extension of 0.2% strain, Z is the percentage reduction in specimen cross section area, A is the percentage elongation of the specimen gauge length (40mm) after fracture, and uEL is the percentage uniform elongation of the specimen at fracture

Table 8 Weld B10: Tensile test results for the **weld mid-thickness region** - round bar specimens, tested at 68°F (20°C).

	Yield strength, $R_{p0.2}$		Tensile strength, R_m		Y/T ratio	uEL
	ksi	(N/mm ²)	ksi	(N/mm ²)		%
Minimum value	118	(817)	125	(860)	0.95	5.8
Maximum value	127	(878)	131	(906)	0.97	7.3
<i>Difference (max-min)</i>	9	(61)	6	(46)	0.02	1.5
Average value	124	(852)	128	(885)	0.96	6.6
Standard deviation	3	(21)	2	(17)	0.01	0.4

Table 9 Weld B10: Statistical analysis of the tensile test results for the **weld mid-thickness region** - round bar specimens, tested at 68°F (20°C).

Test ID	Position (o'clock)	Specimen section				Yield strength				Tensile strength		Y/T	A %	uEL %		
		Width		Thickness		Area		Upper yield		R _{p0.2}					R _m	
		in	(mm)	in	(mm)	in ²	(mm ²)	ksi	(N/mm ²)	ksi	(N/mm ²)				ksi	(N/mm ²)
S1	0.8 - 1.0	0.716	(18.18)	0.157	(4.00)	0.113	(72.72)	122	(838)	120	(827)	127	(877)	0.94	15.2	7.55
S2	1.9 - 2.1	0.709	(18.00)	0.157	(3.98)	0.111	(71.64)			119	(820)	128	(884)	0.93	15.7	7.12
S3	3.0 - 3.2	0.711	(18.07)	0.157	(3.99)	0.112	(72.10)			127	(879)	132	(907)	0.97	17.8	6.62
S4	4.1 - 4.3	0.708	(17.98)	0.157	(3.98)	0.111	(71.56)			124	(857)	130	(895)	0.96	18.6	6.94
S5	5.2 - 5.4	0.715	(18.17)	0.156	(3.97)	0.112	(72.13)			120	(828)	127	(876)	0.95	17.7	7.52
S6	6.3 - 6.5	0.713	(18.12)	0.156	(3.97)	0.112	(71.94)			118	(811)	127	(873)	0.93	19.0	7.46
S7	7.4 - 7.6	0.716	(18.18)	0.157	(4.00)	0.113	(72.72)			120	(830)	127	(879)	0.94	19.4	6.68
S8	8.5 - 8.7	0.712	(18.08)	0.157	(3.99)	0.112	(72.14)			124	(856)	131	(903)	0.95	19.6	7.49
S9	9.6 - 9.8	0.713	(18.10)	0.157	(3.98)	0.112	(72.04)			129	(886)	133	(914)	0.97	15.4	6.32
S10	10.7 - 10.9	0.713	(18.12)	0.158	(4.01)	0.113	(72.66)			124	(858)	130	(898)	0.96	17.5	6.70
S11	11.8 - 12.0	0.708	(17.98)	0.157	(3.98)	0.111	(71.56)			122	(838)	127	(879)	0.95	18.1	7.10

Notes: Rp0.2 is the yield strength at a non-proportional extension of 0.2% strain, A is the percentage elongation of the specimen gauge length (40mm) after fracture, and uEL is the percentage uniform elongation of the specimen at fracture

Table 10 Weld B10: Tensile test results for the **weld full-thickness** - rectangular specimens, tested at 68°F (20°C).

	Yield strength, $R_{p0.2}$		Tensile strength, R_m		Y/T ratio	uEL
	ksi	(N/mm ²)	ksi	(N/mm ²)		%
Minimum value	118	(811)	127	(873)	0.93	6.3
Maximum value	129	(886)	133	(914)	0.97	7.6
<i>Difference (max-min)</i>	<i>11</i>	<i>(75)</i>	<i>6</i>	<i>(41)</i>	<i>0.04</i>	<i>1.3</i>
Average value	122	(845)	129	(890)	0.95	7.0
Standard deviation	4	(24)	2	(14)	0.01	0.4

Table 11 Weld B10: Statistical analysis of the tensile test results for the **weld full-thickness** - round bar specimens, tested at 68°F (20°C).

Test No.	Type	Direction	Position	Location	Specimen gauge dimensions				Test results								
					d in	W in	t in	S _o in ²	R _{eH} ksi	R _{p0.2} ksi	R _{t0.5} ksi	R _m ksi	Y/T	Z %	A _{5.65} %	A _{2in} %	uEL %
Pipe 1: Source B																	
1	FT	T	7.0			0.985	0.781	0.769		115	110	130	0.88		14.6	30.7	4.4
2	RB	T	8.0		0.473			0.176	129	125	125	129	0.97	72.8	15.7		0.4
3	RB	T	10.0		0.472			0.175	124	121	121	124	0.97	74.7	11.4		0.4
4	FT	L	12.0			0.987	0.786	0.775		111	110	122	0.92		14.4	29.6	4.6
5	FT	L	3.0			0.983	0.780	0.767		112	110	124	0.91		15.8	32.6	4.2
6	FT	L	6.0			0.988	0.744	0.735		113	111	122	0.93		14.7	28.9	5.1
7	FT	L	8.0			0.983	0.789	0.775		111	110	122	0.91		15.7	32.4	5.3
8	FT	L	8.5			0.983	0.787	0.773		113	112	123	0.92		15.9	33.4	4.1
Weld metal																	
1	RB		0.6	cap	0.235			0.043	116	115	115	123	0.94	65.6	19.9		9.2
2	RB		2.8	cap	0.233			0.043	126	123	125	127	0.97	64.6	14.9		6.0
3	RB		6.2	cap	0.235			0.043		112	112	123	0.91	67.6	21.8		9.5

Notes: type **RB** and **FT** are round bar and Flat Tensile respectively, **L** and **T** are Longitudinal and Transverse specimen orientations (relative to the pipe longitudinal axis), **d**, **W** and **t** are the diameter, width and thickness of the specimen section, **S_o** is the original cross-section area, **R_{eH}** is upper yield strength, **R_{p0.2}** is the proof strength at a non-proportional extension of 0.2% strain, **R_{t0.5}** the proof strength at a total extension of 0.5% strain, **R_m** is the tensile strength, **Y/T** is the yield to tensile strength ratio ($R_{p0.2}/R_m$), **Z** is the percentage reduction in specimen cross-section, **A_{5.65}** is the percentage elongation after fracture of a gauge length of $5.65\sqrt{S_o}$, **A_{2in}** is the percentage elongation after fracture of a gauge length of 2in, and **uEL** is the specimen elongation at maximum stress

Table 12 Weld A06: Tensile test results. Specimens tested at 68°F (20°C).

Test No.	Type	Direction	Position	Location	Specimen gauge dimensions				Test results								
					d in	W in	t in	S _o in ²	R _{eH} ksi	R _{p0.2} ksi	R _{t0.5} ksi	R _m ksi	Y/T	Z %	A _{5.65} %	A _{2in} %	uEL %
Weld metal (continued from previous page)																	
4	RB		7.7	root	0.195			0.030	121	120	120	124	0.96	66.1	18.9		7.4
5	RB		8.0	cap	0.236			0.044	126	123	126	127	0.97	69.1	19.1		7.6
6	RB		9.4	root	0.195			0.030		127	128	132	0.96	65.6	14.4		5.9
Pipe 2: Source B																	
1	FT	T	7.0			0.983	0.785	0.772		112	107	124	0.90		14.6	28.8	4.2
2	RB	T	8.0		0.472			0.175	129	126	125	129	0.98	73.0	16.1		0.4
3	RB	T	10.0		0.472			0.175	131	126	127	131	0.96	76.7	11.8		0.4
4	FT	L	12.0			0.989	0.798	0.789		112	110	121	0.93		14.3	30.0	4.3
5	FT	L	3.0			0.961	0.784	0.753		112	111	120	0.94		14.6	32.1	3.5
6	FT	L	6.0			0.985	0.787	0.776		114	112	127	0.90		16.5	33.2	4.8
7	FT	L	8.0			0.987	0.791	0.781		118	114	128	0.92		12.4	26.4	2.2
8	FT	L	8.5			0.984	0.781	0.769		115	114	126	0.91		15.4	32.4	4.2

Notes: type **RB** and **FT** are round bar and Flat Tensile respectively, **L** and **T** are Longitudinal and Transverse specimen orientations (relative to the pipe longitudinal axis), **d**, **W** and **t** are the diameter, width and thickness of the specimen section, **S_o** is the original cross-section area, **R_{eH}** is upper yield strength, **R_{p0.2}** is the proof strength at a non-proportional extension of 0.2% strain, **R_{t0.5}** the proof strength at a total extension of 0.5% strain, **R_m** is the tensile strength, **Y/T** is the yield to tensile strength ratio ($R_{p0.2}/R_m$), **Z** is the percentage reduction in specimen cross-section, **A_{5.65}** is the percentage elongation after fracture of a gauge length of $5.65\sqrt{S_o}$, **A_{2in}** is the percentage elongation after fracture of a gauge length of 2in, and **uEL** is the specimen elongation at maximum stress.

Notes: type **RB** and **FT** are round bar and Flat Tensile respectively, **L** and **T** are Longitudinal and Transverse specimen orientations (relative to the pipe longitudinal axis), **d**, **W** and **t** are the diameter, width and thickness of the specimen section, **S_o** is the original cross-section area, **ReH** is upper yield strength, **Rp0.2** is the proof strength at a non-proportional extension of 0.2% strain, **Rt0.5** the proof strength at a total extension of 0.5% strain, **Rm** is the tensile strength, **Y/T** is the yield to tensile strength ratio ($R_{p0.2}/R_m$), **Z** is the percentage reduction in specimen cross-section, **A5.65** is the percentage elongation after fracture of a gauge length of $5.65\sqrt{S_o}$, **A2in** is the percentage elongation after fracture of a gauge length of 2in, and **uEL** is the specimen elongation at maximum stress

Table 12 Weld A06: Tensile test results. Specimens tested at 68°F (20°C). (continued)

Test No.	Type	Direction	Position	Location	Specimen gauge dimensions				Test results								
					d in	W in	t in	S _o in ²	R _{eH} ksi	R _{p0.2} ksi	R _{t0.5} ksi	R _m ksi	Y/T	Z %	A _{5.65} %	A _{2in} %	uEL %
Pipe 1: Source C																	
1	FT	T	7.0			0.986	0.771	0.760		104	94	129	0.81		13.8	28.8	3.9
2	RB	T	12.0		0.473			0.176		124	123	129	0.96	67.9	12.6		4.3
3	RB	T	8.0		0.469			0.172		128	128	131	0.98	66.6	15.0		3.9
4	RB	T	10.0		0.472			0.175	127	123	123	127	0.97	66.5	16.0		4.6
5	FT	L	12.0			0.984	0.773	0.761		114	113	127	0.90		16.3	28.5	4.5
6	FT	L	3.0			0.984	0.787	0.775		112	110	125	0.89		13.9	31.0	3.5
7	FT	L	6.0			0.983	0.774	0.761		113	112	125	0.90		15.7	32.8	5.2
8	FT	L	8.0			0.984	0.775	0.763		114	113	127	0.90		16.6	33.6	4.1
9	FT	L	8.5			0.984	0.770	0.758		115	113	128	0.89		15.3	32.6	5.9
Weld metal																	
1	RB		0.6	cap	0.232			0.042	111	110	110	116	0.95	66.4	22.6		6.1
2	RB		2.8	cap	0.236			0.044		110	110	115	0.96	64.6	23.1		5.7
3	RB		6.2	root	0.233			0.043	102	102	102	109	0.93	67.2	20.7		9.2

Notes: type **RB** and **FT** are round bar and Flat Tensile respectively, **L** and **T** are Longitudinal and Transverse specimen orientations (relative to the pipe longitudinal axis), **d**, **W** and **t** are the diameter, width and thickness of the specimen section, **S_o** is the original cross-section area, **R_{eH}** is upper yield strength, **R_{p0.2}** is the proof strength at a non-proportional extension of 0.2% strain, **R_{t0.5}** the proof strength at a total extension of 0.5% strain, **R_m** is the tensile strength, **Y/T** is the yield to tensile strength ratio ($R_{p0.2}/R_m$), **Z** is the percentage reduction in specimen cross-section, **A_{5.65}** is the percentage elongation after fracture of a gauge length of $5.65\sqrt{S_o}$, **A_{2in}** is the percentage elongation after fracture of a gauge length of 2in, and **uEL** is the specimen elongation at maximum stress.

Table 13 Weld A17: Tensile test results. Specimens tested at 68°F (20°C).

Test No.	Type	Direction	Position	Location	Specimen gauge dimensions				Test results								
					d in	W in	t in	S _o in ²	R _{eH} ksi	R _{p0.2} ksi	R _{t0.5} ksi	R _m ksi	Y/T	Z %	A _{5.65} %	A _{2in} %	uEL %
Weld metal (continued from previous page)																	
4	RB		7.7	cap	0.235			0.043		114	113	120	0.95	66.0	23.2		7.1
5	RB		8.4	cap	0.234			0.043		111	111	117	0.96	63.9	22.7		7.4
6	RB		9.4	root	0.233			0.043		103	104	110	0.94	68.2	21.4		7.2
Pipe 2: Source C																	
1	FT	T	7.0			0.983	0.777	0.764		113	110	125	0.90		15.0	28.6	5.1
2	RB	T	12.0		0.473			0.176	123	120	120	124	0.97	69.6	15.7		5.2
3	RB	T	8.0		0.472			0.175	126	123	123	126	0.97	68.7	13.2		0.4
4	RB	T	10.0		0.473			0.176	119	116	117	121	0.95	68.5	15.9		5.0
5	FT	L	12.0			0.985	0.776	0.764		108	108	121	0.89		17.7	33.5	4.7
6	FT	L	3.0			0.984	0.784	0.771		110	110	120	0.92		15.9	34.4	3.9
7	FT	L	6.0			0.985	0.776	0.765		110	110	122	0.90		15.9	32.7	5.1
8	FT	L	8.0			0.985	0.781	0.769		106	106	118	0.90		17.1	34.0	5.2
9	FT	L	8.5			0.985	0.776	0.765		108	107	120	0.90		17.2	32.9	4.7

Notes: type **RB** and **FT** are round bar and Flat Tensile respectively, **L** and **T** are Longitudinal and Transverse specimen orientations (relative to the pipe longitudinal axis), **d**, **W** and **t** are the diameter, width and thickness of the specimen section, **S_o** is the original cross-section area, **R_{eH}** is upper yield strength, **R_{p0.2}** is the proof strength at a non-proportional extension of 0.2% strain, **R_{t0.5}** the proof strength at a total extension of 0.5% strain, **R_m** is the tensile strength, **Y/T** is the yield to tensile strength ratio ($R_{p0.2}/R_m$), **Z** is the percentage reduction in specimen cross-section, **A_{5.65}** is the percentage elongation after fracture of a gauge length of $5.65\sqrt{S_o}$, **A_{2in}** is the percentage elongation after fracture of a gauge length of 2in, and **uEL** is the specimen elongation at maximum stress.

Table 13 Weld A17: Tensile test results. Specimens tested at 68°F (20°C). (continued)

Test No.	Type	Direction	Position	Location	Specimen gauge dimensions				Test results								
					d in	W in	t in	S _o in ²	R _{eH} ksi	R _{p0.2} ksi	R _{t0.5} ksi	R _m ksi	Y/T	Z %	A _{5.65} %	A _{2in} %	uEL %
Pipe 1: Source B																	
1	FT	T	7.0			0.983	0.785	0.772		125	123	129	0.97		12.7	28.1	1.9
2	RB	T	8.0		0.471			0.174	125	125	124	126	0.99	72.4	12.9		2.1
3	RB	T	10.0		0.470			0.174	125	120	120	125	0.96	75.0	15.5		2.5
4	FT	L	12.0			0.990	0.789	0.781		114	113	127	0.90		14.9	30.9	4.2
5	FT	L	3.0			0.985	0.778	0.766		114	112	126	0.90		15.7	31.1	4.4
6	FT	L	6.0			0.989	0.781	0.772		111	110	124	0.90		15.2	29.9	4.8
7	FT	L	8.0			0.987	0.796	0.786		112	110	121	0.92		14.6	32.5	4.7
8	FT	L	8.5			0.985	0.784	0.772		116	116	126	0.93		14.3	30.4	3.5
Weld metal																	
1	RB		0.6	cap	0.235			0.043	120	121	120	126	0.96	66.2	22.1		8.5
2	RB		2.8	cap	0.234			0.043	128	128	128	129	0.99	66.8	19.2		7.7
3	RB		6.2	cap	0.235			0.044		117	116	124	0.94	67.5	19.0		8.0

Notes: type **RB** and **FT** are round bar and Flat Tensile respectively, **L** and **T** are Longitudinal and Transverse specimen orientations (relative to the pipe longitudinal axis), **d**, **W** and **t** are the diameter, width and thickness of the specimen section, **S_o** is the original cross-section area, **R_{eH}** is upper yield strength, **R_{p0.2}** is the proof strength at a non-proportional extension of 0.2% strain, **R_{t0.5}** the proof strength at a total extension of 0.5% strain, **R_m** is the tensile strength, **Y/T** is the yield to tensile strength ratio ($R_{p0.2}/R_m$), **Z** is the percentage reduction in specimen cross-section, **A_{5.65}** is the percentage elongation after fracture of a gauge length of $5.65\sqrt{S_o}$, **A_{2in}** is the percentage elongation after fracture of a gauge length of 2in, and **uEL** is the specimen elongation at maximum stress.

Table 14 Weld A33: Tensile test results. Specimens tested at 68°F (20°C).

Test No.	Type	Direction	Position	Location	Specimen gauge dimensions				Test results								
					d in	W in	t in	S _o in ²	R _{eH} ksi	R _{p0.2} ksi	R _{t0.5} ksi	R _m ksi	Y/T	Z %	A _{5.65} %	A _{2in} %	uEL %
Weld metal (continued from previous page)																	
4	RB		7.7	root	0.197			0.031	123	121	122	126	0.96	66.5	19.4		7.5
5	RB		8.0	cap	0.233			0.043	129	127	129	130	0.98	64.6	21.0		7.7
6	RB		9.4	root	0.195			0.030	125	125	125	130	0.96	65.2	15.3		7.0
Pipe 2: Source A																	
1	FT	T	7.0			0.985	0.779	0.767		118	108	134	0.88		9.6	21.5	2.1
2	RB	T	8.0		0.471			0.174	134	132	134	134	0.98	67.2	13.9		2.6
3	RB	T	10.0		0.473			0.176	135	133	134	135	0.98	68.8	15.8		2.6
4	FT	L	12.0			0.991	0.780	0.773		114	111	131	0.87		13.9	30.2	3.9
5	FT	L	3.0			0.985	0.781	0.770		113	111	128	0.88		15.1	33.0	4.2
6	FT	L	6.0			0.983	0.780	0.767		112	111	130	0.86		14.1	30.4	3.9
7	FT	L	8.0			0.990	0.779	0.771		111	109	129	0.86		14.2	30.6	3.9
8	FT	L	8.5			0.985	0.778	0.766		114	112	132	0.87		14.8	31.7	3.1

Notes: type **RB** and **FT** are round bar and Flat Tensile respectively, **L** and **T** are Longitudinal and Transverse specimen orientations (relative to the pipe longitudinal axis), **d**, **W** and **t** are the diameter, width and thickness of the specimen section, **S_o** is the original cross-section area, **R_{eH}** is upper yield strength, **R_{p0.2}** is the proof strength at a non-proportional extension of 0.2% strain, **R_{t0.5}** the proof strength at a total extension of 0.5% strain, **R_m** is the tensile strength, **Y/T** is the yield to tensile strength ratio ($R_{p0.2}/R_m$), **Z** is the percentage reduction in specimen cross-section, **A_{5.65}** is the percentage elongation after fracture of a gauge length of $5.65\sqrt{S_o}$, **A_{2in}** is the percentage elongation after fracture of a gauge length of 2in, and **uEL** is the specimen elongation at maximum stress.

Table 14 Weld A33: Tensile test results. Specimens tested at 68°F (20°C). (continued)

Test No.	Type	Direction	Position	Location	Specimen gauge dimensions				Test results								
					d in	W in	t in	S _o in ²	R _{eH} ksi	R _{p0.2} ksi	R _{t0.5} ksi	R _m ksi	Y/T	Z %	A _{5.65} %	A _{2in} %	uEL %
Pipe 1: Source C																	
1	FT	T	7.0			0.986	0.778	0.767		121	121	129	0.94		14.9	33.3	3.2
2	RB	T	8.0		0.472			0.175	122	121	120	125	0.96	71.8	13.7		3.7
3	FT	L	12.0			0.986	0.778	0.767		109	108	120	0.91		14.9	33.3	5.3
4	FT	L	6.0			0.985	0.777	0.765		114	113	126	0.91		14.5	31.5	4.6
5	FT	L	8.0			0.984	0.776	0.764		111	110	123	0.90		15.9	32.7	6.0
Weld metal																	
1	RB		0.6	cap	0.235			0.043	116	116	116	123	0.94	64.7	20.1		8.3
2	RB		6.2	cap	0.236			0.044		118	118	125	0.95	66.8	18.2		5.8
3	RB		7.7	root	0.197			0.031	119	118	119	123	0.96	67.9	20.7		8.5
Pipe 2: Source B																	
1	FT	T	7.0			0.988	0.796	0.786		108	103	127	0.85		13.3	32.0	2.9
2	RB	T	8.0		0.471			0.174	127	126	126	127	0.99	75.5	18.0		5.0
3	FT	L	12.0			0.987	0.796	0.785		109	108	114	0.96		15.1	30.8	4.7
4	FT	L	6.0			0.989	0.785	0.776		112	110	122	0.92		15.7	30.0	4.6
5	FT	L	8.0			0.990	0.791	0.783		112	110	122	0.92		14.6	30.3	4.9

Notes: type **RB** and **FT** are round bar and Flat Tensile respectively, **L** and **T** are Longitudinal and Transverse specimen orientations (relative to the pipe longitudinal axis), **d**, **W** and **t** are the diameter, width and thickness of the specimen section, **S_o** is the original cross-section area, **R_{eH}** is upper yield strength, **R_{p0.2}** is the proof strength at a non-proportional extension of 0.2% strain, **R_{t0.5}** the proof strength at a total extension of 0.5% strain, **R_m** is the tensile strength, **Y/T** is the yield to tensile strength ratio ($R_{p0.2}/R_m$), **Z** is the percentage reduction in specimen cross-section, **A_{5.65}** is the percentage elongation after fracture of a gauge length of $5.65\sqrt{S_o}$, **A_{2in}** is the percentage elongation after fracture of a gauge length of 2in, and **uEL** is the specimen elongation at maximum stress.

Table 15 Weld A44: Tensile test results. Specimens tested at 68°F (20°C).

Test No.	Type	Direction	Position	Location	Specimen gauge dimensions				Test results								
					d in	W in	t in	S _o in ²	R _{eH} ksi	R _{p0.2} ksi	R _{t0.5} ksi	R _m ksi	Y/T	Z %	A _{5.65} %	A _{2in} %	uEL %
Pipe 1: Source C																	
1	FT	T	7.0			0.986	0.774	0.763		115	114	127	0.90		14.6	28.0	4.3
2	RB	T	8.0		0.472			0.175	123	118	118	125	0.95	68.3	16.6		5.4
3	RB	T	10.0		0.472			0.175	123	120	122	125	0.96	70.0	15.5		4.9
4	FT	L	12.0			0.984	0.782	0.770		108	107	122	0.88		17.5	34.7	5.9
5	FT	L	3.0			0.986	0.780	0.769		107	106	121	0.88		16.4	33.1	5.8
6	FT	L	6.0			0.983	0.778	0.764		111	110	122	0.91		15.1	31.3	5.1
7	FT	L	8.0			0.989	0.778	0.769		108	108	121	0.89		15.8	31.8	3.8
8	FT	L	8.5			0.984	0.781	0.768		108	105	121	0.89		16.6	32.4	5.7
Weld metal																	
1	RB		0.6	cap	0.235			0.043	126	125	126	129	0.97	64.3	19.0		7.4
2	RB		2.8	cap	0.235			0.043	135	131	131	133	0.99	63.1	11.5		3.2
3	RB		6.2	cap	0.236			0.044		121	121	128	0.94	65.0	13.7		6.8

Notes: type **RB** and **FT** are round bar and Flat Tensile respectively, **L** and **T** are Longitudinal and Transverse specimen orientations (relative to the pipe longitudinal axis), **d**, **W** and **t** are the diameter, width and thickness of the specimen section, **S_o** is the original cross-section area, **R_{eH}** is upper yield strength, **R_{p0.2}** is the proof strength at a non-proportional extension of 0.2% strain, **R_{t0.5}** the proof strength at a total extension of 0.5% strain, **R_m** is the tensile strength, **Y/T** is the yield to tensile strength ratio ($R_{p0.2}/R_m$), **Z** is the percentage reduction in specimen cross-section, **A_{5.65}** is the percentage elongation after fracture of a gauge length of $5.65\sqrt{S_o}$, **A_{2in}** is the percentage elongation after fracture of a gauge length of 2in, and **uEL** is the specimen elongation at maximum stress.

Table 16 Weld A46: Tensile test results. Specimens tested at 68°F (20°C).

Test No.	Type	Direction	Position	Location	Specimen gauge dimensions				Test results								
					d in	W in	t in	S _o in ²	R _{eH} ksi	R _{p0.2} ksi	R _{t0.5} ksi	R _m ksi	Y/T	Z %	A _{5.65} %	A _{2in} %	uEL %
Weld metal (continued from previous page)																	
4	RB		7.7	root	0.196			0.030		129	127	134	0.96	63.6	16.9		6.4
5	RB		8.0	cap	0.233			0.043	137	134	137	136	0.99	63.3	19.2		6.2
6	RB		9.4	root	0.194			0.030		130	129	135	0.96	64.8	16.5		6.2
Pipe 2: Source C																	
1	FT	T	7.0			0.987	0.779	0.769		113	112	123	0.92		15.5	31.5	3.9
2	RB	T	8.0		0.470			0.174	118	116	117	121	0.96	72.7	16.7		5.3
3	RB	T	10.0		0.472			0.175	122	121	120	124	0.97	74.2	16.6		4.8
4	FT	L	12.0			0.989	0.786	0.778		109	108	120	0.91		16.0	33.5	4.5
5	FT	L	3.0			0.984	0.783	0.771		108	108	120	0.91		16.7	31.9	4.5
6	FT	L	6.0			0.991	0.779	0.772		107	106	120	0.89		16.7	27.7	5.8
7	FT	L	8.0			0.985	0.784	0.772		107	107	119	0.90		16.2	29.2	5.2
8	FT	L	8.5			0.983	0.783	0.771		108	108	120	0.91		15.3	32.6	4.3

Notes: type **RB** and **FT** are round bar and Flat Tensile respectively, **L** and **T** are Longitudinal and Transverse specimen orientations (relative to the pipe longitudinal axis), **d**, **W** and **t** are the diameter, width and thickness of the specimen section, **S_o** is the original cross-section area, **R_{eH}** is upper yield strength, **R_{p0.2}** is the proof strength at a non-proportional extension of 0.2% strain, **R_{t0.5}** the proof strength at a total extension of 0.5% strain, **R_m** is the tensile strength, **Y/T** is the yield to tensile strength ratio ($R_{p0.2}/R_m$), **Z** is the percentage reduction in specimen cross-section, **A_{5.65}** is the percentage elongation after fracture of a gauge length of $5.65\sqrt{S_o}$, **A_{2in}** is the percentage elongation after fracture of a gauge length of 2in, and **uEL** is the specimen elongation at maximum stress.

Table 16 Weld A46: Tensile test results. Specimens tested at 68°F (20°C). (continued)

Test No.	Type	Direction	Position	Location	Specimen gauge dimensions				Test results								
					d in	W in	t in	S _o in ²	R _{eH} ksi	R _{p0.2} ksi	R _{t0.5} ksi	R _m ksi	Y/T	Z %	A _{5.65} %	A _{2in} %	uEL %
Pipe 1: Source B																	
1	FT	T	7.0			0.986	0.785	0.774		106	104	122	0.87		13.4	32.8	2.2
2	RB	T	8.0		0.470			0.174	121	121	121	126	0.96	75.8	13.6		0.4
3	RB	T	10.0		0.472			0.175	114	114	114	120	0.95	76.4	12.0		0.4
4	FT	L	12.0			0.985	0.793	0.780		111	110	116	0.96	-	15.6	33.6	3.7
5	FT	L	3.0			0.984	0.785	0.773		111	110	115	0.97		14.5	33.6	2.4
6	FT	L	6.0			0.984	0.783	0.771		112	110	121	0.93		15.6	32.6	3.7
7	FT	L	8.0			0.985	0.782	0.770		111	109	116	0.95		13.7	29.6	2.6
8	FT	L	8.5			0.986	0.781	0.770		109	108	114	0.95		14.6	33.1	2.5
Weld metal																	
1	RB		0.6	cap	0.237			0.044	121	120	121	125	0.96	67.6	19.6		8.5
2	RB		2.8	cap	0.234			0.043	128	125	127	128	0.98	63.1	18.2		8.0
3	RB		6.2	cap	0.237			0.044		120	120	127	0.95	69.7	17.6		5.7

Notes: type **RB** and **FT** are round bar and Flat Tensile respectively, **L** and **T** are Longitudinal and Transverse specimen orientations (relative to the pipe longitudinal axis), **d**, **W** and **t** are the diameter, width and thickness of the specimen section, **S_o** is the original cross-section area, **R_{eH}** is upper yield strength, **R_{p0.2}** is the proof strength at a non-proportional extension of 0.2% strain, **R_{t0.5}** the proof strength at a total extension of 0.5% strain, **R_m** is the tensile strength, **Y/T** is the yield to tensile strength ratio ($R_{p0.2}/R_m$), **Z** is the percentage reduction in specimen cross-section, **A_{5.65}** is the percentage elongation after fracture of a gauge length of $5.65\sqrt{S_o}$, **A_{2in}** is the percentage elongation after fracture of a gauge length of 2in, and **uEL** is the specimen elongation at maximum stress.

Table 17 Weld A50: Tensile test results. Specimens tested at 68°F (20°C).

Test No.	Type	Direction	Position	Location	Specimen gauge dimensions				Test results								
					d in	W in	t in	S _o in ²	R _{eH} ksi	R _{p0.2} ksi	R _{t0.5} ksi	R _m ksi	Y/T	Z %	A _{5.65} %	A _{2in} %	uEL %
Weld metal (continued from previous page)																	
4	RB		7.7	root	0.196			0.030	121	120	121	124	0.97	67.9	20.0		8.4
5	RB		8.0	cap	0.233			0.043	126	123	124	127	0.96	65.7	16.0		8.0
6	RB		9.4	root	0.195			0.030	130	130	130	134	0.97	64.4	15.8		5.5
Pipe 2: Source B																	
1	FT	T	7.0			0.986	0.776	0.765		104	103	131	0.79		15.3	30.6	4.2
2	RB	T	8.0		0.472			0.175	126	125	125	127	0.98	70.1	13.0		3.0
3	RB	T	10.0		0.472			0.175	126	124	123	126	0.98	69.2	11.3		1.3
4	FT	L	12.0			0.985	0.789	0.777		108	108	114	0.95		14.1	30.1	3.7
5	FT	L	3.0			0.967	0.782	0.756		113	112	126	0.90		16.2	28.0	4.8
6	FT	L	6.0			0.981	0.778	0.763		113	112	126	0.90		16.6	32.1	5.6
7	FT	L	8.0			0.984	0.781	0.768		115	113	128	0.89		16.3	32.8	6.0
8	FT	L	8.5			0.985	0.785	0.774		112	111	119	0.94		15.1	32.2	4.2

Notes: type **RB** and **FT** are round bar and Flat Tensile respectively, **L** and **T** are Longitudinal and Transverse specimen orientations (relative to the pipe longitudinal axis), **d**, **W** and **t** are the diameter, width and thickness of the specimen section, **S_o** is the original cross-section area, **R_{eH}** is upper yield strength, **R_{p0.2}** is the proof strength at a non-proportional extension of 0.2% strain, **R_{t0.5}** the proof strength at a total extension of 0.5% strain, **R_m** is the tensile strength, **Y/T** is the yield to tensile strength ratio ($R_{p0.2}/R_m$), **Z** is the percentage reduction in specimen cross-section, **A_{5.65}** is the percentage elongation after fracture of a gauge length of $5.65\sqrt{S_o}$, **A_{2in}** is the percentage elongation after fracture of a gauge length of 2in, and **uEL** is the specimen elongation at maximum stress.

Table 17 Weld A50: Tensile test results. Specimens tested at 68°F (20°C). (continued)

Test No.	Type	Direction	Position	Location	Specimen gauge dimensions				Test results								
					d in	W in	t in	S _o in ²	R _{eH} ksi	R _{p0.2} ksi	R _{t0.5} ksi	R _m ksi	Y/T	Z %	A _{5.65} %	A _{2in} %	uEL %
Pipe 1: Source C																	
1	FT	T	3.0			0.984	0.772	0.760		107	103	124	0.86		14.2	25.6	4.4
2	RB	T	12.0		0.472			0.175	119	121	121	126	0.96	69.1	13.7		5.5
3	RB	T	4.0		0.471			0.174	122	121	121	125	0.97	69.2	17.0		5.4
4	FT	L	12.0			0.984	0.778	0.765		108	107	121	0.89		17.5	32.1	5.5
5	FT	L	2.5			0.986	0.777	0.766		104	104	119	0.87		16.5	33.2	4.9
6	FT	L	3.0			0.983	0.777	0.764		105	105	120	0.88		17.2	32.3	5.6
7	FT	L	4.0			0.985	0.774	0.763		107	106	121	0.89		17.0	33.8	5.7
8	FT	L	7.0			0.985	0.772	0.760		108	108	120	0.90		16.0	32.6	5.3
Weld metal																	
1	RB		0.6	cap	0.235			0.043		121	121	128	0.95	67.9	14.1		5.4
2	RB		2.2	cap	0.236			0.044	133	130	133	132	0.98	63.8	17.0		6.6
3	RB		2.8	cap	0.235			0.044	132	129	132	132	0.98	63.4	17.3		6.5

Notes: type **RB** and **FT** are round bar and Flat Tensile respectively, **L** and **T** are Longitudinal and Transverse specimen orientations (relative to the pipe longitudinal axis), **d**, **W** and **t** are the diameter, width and thickness of the specimen section, **S_o** is the original cross-section area, **R_{eH}** is upper yield strength, **R_{p0.2}** is the proof strength at a non-proportional extension of 0.2% strain, **R_{t0.5}** the proof strength at a total extension of 0.5% strain, **R_m** is the tensile strength, **Y/T** is the yield to tensile strength ratio ($R_{p0.2}/R_m$), **Z** is the percentage reduction in specimen cross-section, **A_{5.65}** is the percentage elongation after fracture of a gauge length of $5.65\sqrt{S_o}$, **A_{2in}** is the percentage elongation after fracture of a gauge length of 2in, and **uEL** is the specimen elongation at maximum stress.

Table 18 Weld B03: Tensile test results. Specimens tested at 68°F (20°C).

Test No.	Type	Direction	Position	Location	Specimen gauge dimensions				Test results								
					d in	W in	t in	S _o in ²	R _{eH} ksi	R _{p0.2} ksi	R _{t0.5} ksi	R _m ksi	Y/T	Z %	A _{5.65} %	A _{2in} %	uEL %
Weld metal (continued from previous page)																	
4	RB		4.2	root	0.198			0.031		125	125	129	0.96	60.5	16.7		6.1
5	RB		6.7	cap	0.232			0.042	118	118	118	125	0.94	67.8	19.8		9.1
6	RB		9.7	root	0.195			0.030		124	123	130	0.95	63.3	16.4		6.4
Pipe 2: Source C																	
1	FT	T	3.0			0.984	0.776	0.763		110	104	127	0.86		11.8	26.6	2.9
2	RB	T	12.0		0.472			0.175	119	119	118	123	0.97	68.8	13.9		5.1
3	RB	T	4.0		0.470			0.174	123	121	121	124	0.97	70.5	15.8		4.1
4	FT	L	12.0			0.984	0.778	0.765		105	105	118	0.90		17.7	34.8	6.2
5	FT	L	2.5			0.982	0.779	0.765		108	108	120	0.90		17.0	32.5	5.2
6	FT	L	3.0			0.986	0.789	0.777		106	105	118	0.90		16.6	34.1	5.2
7	FT	L	4.0			0.984	0.778	0.765		107	106	120	0.89		17.4	32.1	5.8
8	FT	L	7.0			0.984	0.779	0.766		108	108	118	0.91		16.0	34.3	3.8

Notes: type **RB** and **FT** are round bar and Flat Tensile respectively, **L** and **T** are Longitudinal and Transverse specimen orientations (relative to the pipe longitudinal axis), **d**, **W** and **t** are the diameter, width and thickness of the specimen section, **S_o** is the original cross-section area, **R_{eH}** is upper yield strength, **R_{p0.2}** is the proof strength at a non-proportional extension of 0.2% strain, **R_{t0.5}** the proof strength at a total extension of 0.5% strain, **R_m** is the tensile strength, **Y/T** is the yield to tensile strength ratio ($R_{p0.2}/R_m$), **Z** is the percentage reduction in specimen cross-section, **A_{5.65}** is the percentage elongation after fracture of a gauge length of $5.65\sqrt{S_o}$, **A_{2in}** is the percentage elongation after fracture of a gauge length of 2in, and **uEL** is the specimen elongation at maximum stress.

Table 18 Weld B03: Tensile test results. Specimens tested at 68°F (20°C). (continued)

Test No.	Type	Direction	Position	Location	Specimen gauge dimensions				Test results								
					d in	W in	t in	S _o in ²	R _{eH} ksi	R _{p0.2} ksi	R _{t0.5} ksi	R _m ksi	Y/T	Z %	A _{5.65} %	A _{2in} %	uEL %
Pipe 1: Source A																	
1	FT	T	5.0			0.983	0.785	0.772		108	106	115	0.94		13.5	31.2	2.2
2	RB	T	12.0		0.472			0.175	125	123	125	125	0.98	73.4	16.3		4.3
3	RB	T	6.0		0.472			0.175	121	116	116	121	0.96	76.2	12.2		0.4
4	FT	L	12.0			0.985	0.781	0.770		113	112	124	0.91		15.2	32.8	3.4
5	FT	L	1.5			0.984	0.790	0.777		112	110	125	0.90		15.3	33.0	3.4
6	FT	L	4.0			0.983	0.793	0.780		105	105	110	0.95		15.5	31.4	3.6
7	FT	L	6.0			0.983	0.784	0.771		103	102	110	0.93		16.4	32.0	3.9
8	FT	L	7.0			0.984	0.787	0.775		103	103	110	0.94		15.9	29.3	4.0
Weld metal																	
1	RB		12.0	cap	0.235			0.044	119	118	118	124	0.95	62.9	22.1		8.0
2	RB		1.6	cap	0.236			0.044	124	121	122	125	0.97	68.3	16.5		7.3
3	RB		4.3	cap	0.236			0.044	122	120	122	125	0.96	66.2	18.4		7.9

Notes: type **RB** and **FT** are round bar and Flat Tensile respectively, **L** and **T** are Longitudinal and Transverse specimen orientations (relative to the pipe longitudinal axis), **d**, **W** and **t** are the diameter, width and thickness of the specimen section, **S_o** is the original cross-section area, **R_{eH}** is upper yield strength, **R_{p0.2}** is the proof strength at a non-proportional extension of 0.2% strain, **R_{t0.5}** the proof strength at a total extension of 0.5% strain, **R_m** is the tensile strength, **Y/T** is the yield to tensile strength ratio ($R_{p0.2}/R_m$), **Z** is the percentage reduction in specimen cross-section, **A_{5.65}** is the percentage elongation after fracture of a gauge length of $5.65\sqrt{S_o}$, **A_{2in}** is the percentage elongation after fracture of a gauge length of 2in, and **uEL** is the specimen elongation at maximum stress.

Table 19 Weld B06: Tensile test results. Specimens tested at 68°F (20°C).

Test No.	Type	Direction	Position	Location	Specimen gauge dimensions				Test results								
					d in	W in	t in	S _o in ²	R _{eH} ksi	R _{p0.2} ksi	R _{t0.5} ksi	R _m ksi	Y/T	Z %	A _{5.65} %	A _{2in} %	uEL %
Weld metal (continued from previous page)																	
4	RB		5.8	root	0.197			0.031		122	121	128	0.95	65.1	15.7		3.8
5	RB		7.3	cap	0.233			0.043	124	123	123	126	0.97	67.4	19.6		7.7
6	RB		8.4	root	0.197			0.031		125	125	130	0.96	67.4	17.3		7.1
Pipe 2: Source B																	
1	FT	T	5.0			0.983	0.781	0.769		114	101	127	0.90		14.7	32.0	5.0
2	RB	T	12.0		0.472			0.175	127	123	125	127	0.97	72.7	17.4		4.0
3	RB	T	6.0		0.472			0.175	126	124	124	127	0.98	74.2	17.6		5.6
4	FT	L	12.0			0.983	0.787	0.773		115	113	129	0.89		15.6	31.4	3.5
5	FT	L	1.5			0.984	0.794	0.782		115	112	129	0.89		15.4	31.2	4.5
6	FT	L	4.0			0.983	0.783	0.770		113	111	127	0.89		15.6	33.4	4.4
7	FT	L	6.0			0.985	0.787	0.775		112	110	127	0.88		16.5	27.7	5.3
8	FT	L	7.0			0.984	0.791	0.778		114	112	128	0.89		15.5	31.9	3.6

Notes: type **RB** and **FT** are round bar and Flat Tensile respectively, **L** and **T** are Longitudinal and Transverse specimen orientations (relative to the pipe longitudinal axis), **d**, **W** and **t** are the diameter, width and thickness of the specimen section, **S_o** is the original cross-section area, **R_{eH}** is upper yield strength, **R_{p0.2}** is the proof strength at a non-proportional extension of 0.2% strain, **R_{t0.5}** the proof strength at a total extension of 0.5% strain, **R_m** is the tensile strength, **Y/T** is the yield to tensile strength ratio ($R_{p0.2}/R_m$), **Z** is the percentage reduction in specimen cross-section, **A_{5.65}** is the percentage elongation after fracture of a gauge length of $5.65\sqrt{S_o}$, **A_{2in}** is the percentage elongation after fracture of a gauge length of 2in, and **uEL** is the specimen elongation at maximum stress.

Table 19 Weld B06: Tensile test results. Specimens tested at 68°F (20°C). (continued)

Test No.	Type	Direction	Position	Location	Specimen gauge dimensions				Test results								
					d in	W in	t in	S _o in ²	R _{eH} ksi	R _{p0.2} ksi	R _{t0.5} ksi	R _m ksi	Y/T	Z %	A _{5.65} %	A _{2in} %	uEL %
Pipe 1: Source C																	
1	FT	T	7.0			0.984	0.782	0.770		104	102	122	0.85		14.7	33.0	4.5
2	RB	T	12.0		0.472			0.175	121	120	120	124	0.97	67.1	15.6		4.5
3	RB	T	8.0		0.472			0.175	118	119	119	124	0.96	67.6	13.6		4.7
4	FT	L	12.0			0.984	0.780	0.768		109	109	121	0.90		16.1	33.2	4.6
5	FT	L	2.0			0.985	0.780	0.768		107	107	120	0.90		17.6	36.1	4.0
6	FT	L	3.0			0.984	0.781	0.769		108	108	121	0.90		18.0	33.1	5.0
7	FT	L	6.0			0.985	0.781	0.770		113	112	123	0.92		15.2	32.8	4.0
8	FT	L	8.0			0.983	0.778	0.765		106	106	119	0.89		16.6	33.5	5.8
Weld metal																	
1	RB		11.7	cap	0.233			0.043		121	120	127	0.95	51.2	16.3		7.9
2	RB		1.7	cap	0.234			0.043	133	130	130	133	0.98	63.5	17.0		6.4
3	RB		3.4	cap	0.237			0.044	137	133	136	135	0.98	62.5	16.7		5.9

Notes: type **RB** and **FT** are round bar and Flat Tensile respectively, **L** and **T** are Longitudinal and Transverse specimen orientations (relative to the pipe longitudinal axis), **d**, **W** and **t** are the diameter, width and thickness of the specimen section, **S_o** is the original cross-section area, **R_{eH}** is upper yield strength, **R_{p0.2}** is the proof strength at a non-proportional extension of 0.2% strain, **R_{t0.5}** the proof strength at a total extension of 0.5% strain, **R_m** is the tensile strength, **Y/T** is the yield to tensile strength ratio ($R_{p0.2}/R_m$), **Z** is the percentage reduction in specimen cross-section, **A_{5.65}** is the percentage elongation after fracture of a gauge length of $5.65\sqrt{S_o}$, **A_{2in}** is the percentage elongation after fracture of a gauge length of 2in, and **uEL** is the specimen elongation at maximum stress.

Table 20 Weld B08: Tensile test results. Specimens tested at 68°F (20°C).

Test No.	Type	Direction	Position	Location	Specimen gauge dimensions				Test results								
					d in	W in	t in	S _o in ²	R _{eH} ksi	R _{p0.2} ksi	R _{t0.5} ksi	R _m ksi	Y/T	Z %	A _{5.65} %	A _{2in} %	uEL %
Pipe 1: Source C																	
4	RB		6.5	cap	0.238			0.044		117	117	125	0.94	68.1	21.1		8.1
5	RB		7.9	root	0.195			0.030		124	124	130	0.96	65.2	16.7		5.3
6	RB		9.7	root	0.196			0.030		130	129	134	0.96	58.0	16.3		6.3
Pipe 2: Source C																	
1	FT	T	7.0			0.985	0.780	0.768		113	107	121	0.93		14.3	31.3	3.4
2	RB	T	12.0		0.472			0.175	122	118	120	122	0.97	70.2	16.2		5.0
3	RB	T	8.0		0.472			0.175	121	118	117	122	0.97	73.6	17.1		5.7
4	FT	L	12.0			0.984	0.778	0.765		105	105	118	0.89		17.8	35.6	5.4
5	FT	L	2.0			0.983	0.780	0.767		108	108	118	0.92		16.0	30.1	3.5
6	FT	L	3.0			0.985	0.779	0.767		110	109	122	0.90		16.8	34.3	5.5
7	FT	L	6.0			0.984	0.785	0.773		107	106	119	0.90		16.2	34.7	4.7
8	FT	L	8.0			0.984	0.780	0.767		108	108	120	0.90		17.3	35.9	5.5

Notes: type **RB** and **FT** are round bar and Flat Tensile respectively, **L** and **T** are Longitudinal and Transverse specimen orientations (relative to the pipe longitudinal axis), **d**, **W** and **t** are the diameter, width and thickness of the specimen section, **S_o** is the original cross-section area, **R_{eH}** is upper yield strength, **R_{p0.2}** is the proof strength at a non-proportional extension of 0.2% strain, **R_{t0.5}** the proof strength at a total extension of 0.5% strain, **R_m** is the tensile strength, **Y/T** is the yield to tensile strength ratio ($R_{p0.2}/R_m$), **Z** is the percentage reduction in specimen cross-section, **A_{5.65}** is the percentage elongation after fracture of a gauge length of $5.65\sqrt{S_o}$, **A_{2in}** is the percentage elongation after fracture of a gauge length of 2in, and **uEL** is the specimen elongation at maximum stress.

Table 20 Weld B08: Tensile test results. Specimens tested at 68°F (20°C). (continued)

	Yield strength				Tensile strength		Y/T	uEL
	$R_{p0.2}$		$R_{10.5}$		R_m			
	ksi	(N/mm ²)	ksi	(N/mm ²)	ksi	(N/mm ²)		%
Pipe from Source A								
Min	103	(709)	102	(705)	110	(757)	0.86	3.08
Max	114	(787)	112	(772)	132	(907)	0.95	4.24
Average	110	(759)	109	(748)	123	(847)	0.90	3.72
Max-Min	11	(78)	10	(67)	22	(150)	0.09	1.16
Pipe from Source B								
Min	108	(748)	108	(743)	114	(785)	0.88	2.16
Max	118	(811)	116	(797)	129	(892)	0.97	6.00
Average	113	(776)	111	(765)	123	(847)	0.92	4.19
Max-Min	9	(63)	8	(54)	16	(107)	0.09	3.84
Pipe from Source C								
Min	104	(717)	104	(717)	118	(811)	0.87	3.53
Max	115	(791)	113	(782)	128	(884)	0.92	6.18
Average	109	(749)	108	(745)	121	(834)	0.90	4.98
Max-Min	11	(74)	9	(65)	11	(73)	0.05	2.65

Notes: $R_{p0.2}$ is the proof strength at a non-proportional extension of 0.2% strain, $R_{10.5}$ the proof strength at a total extension of 0.5% strain, **Y/T** is the yield to tensile strength ratio ($R_{p0.2}/R_m$), and **uEL** is the specimen elongation at maximum stress.

Table 21 Tensile test results: Summary of **longitudinally orientated flat tensile specimens** as a function of pipe source. Specimens tested at 68°F (20°C).

	Yield strength				Tensile strength		Y/T	uEL
	$R_{p0.2}$		$R_{10.5}$		R_m			
	ksi	(N/mm ²)	ksi	(N/mm ²)	ksi	(N/mm ²)		%
Pipe from Source B (set of 6 pipes from 7 tested)								
Min	109	(749)	108	(743)	114	(785)	0.88	2.16
Max	118	(811)	116	(797)	129	(892)	0.97	5.34
Average	113	(777)	111	(765)	123	(847)	0.92	4.08
Max-Min	9	(62)	8	(54)	16	(107)	0.09	3.18
Pipe from Source C, Heat #1 (set of 5 pipes from 9 tested)								
Min	104	(717)	104	(717)	118	(813)	0.87	3.53
Max	115	(791)	113	(782)	128	(884)	0.92	6.03
Average	109	(755)	109	(749)	122	(843)	0.90	5.03
Max-Min	11	(74)	9	(65)	10	(71)	0.04	2.50
Pipe from Source C, Heat #2 (set of 2 pipes from 9 tested)								
Min	105	(727)	105	(721)	118	(811)	0.89	3.84
Max	113	(781)	112	(770)	123	(847)	0.92	6.18
Average	108	(743)	107	(740)	120	(824)	0.90	4.96
Max-Min	8	(54)	7	(49)	5	(36)	0.03	2.34
Pipe from Source C, Heat #3 (set of 2 pipes from 9 tested)								
Min	105	(727)	105	(725)	118	(813)	0.89	3.54
Max	110	(756)	109	(751)	122	(840)	0.92	5.82
Average	108	(743)	107	(739)	119	(824)	0.90	4.90
Max-Min	4	(29)	4	(26)	4	(27)	0.03	2.28

Notes: $R_{p0.2}$ is the proof strength at a non-proportional extension of 0.2% strain, $R_{10.5}$ the proof strength at a total extension of 0.5% strain, Y/T is the yield to tensile strength ratio ($R_{p0.2}/R_m$), and uEL is the specimen elongation at maximum stress.

Table 22 Tensile test results: Summary of **longitudinally orientated flat tensile specimens** as a function of pipe heat. Specimens tested at 68°F (20°C).

	Yield strength				Tensile strength		Y/T	uEL
	$R_{p0.2}$		$R_{10.5}$		R_m			
	ksi	(N/mm ²)	ksi	(N/mm ²)	ksi	(N/mm ²)		%
Pipe from Source A								
Min	116	(798)	116	(800)	121	(832)	0.96	0.40
Max	133	(915)	134	(926)	135	(931)	0.98	4.34
Average	126	(868)	127	(878)	129	(888)	0.98	2.47
Max-Min	17	(117)	18	(126)	14	(99)	0.03	3.94
Pipe from Source B								
Min	114	(784)	114	(785)	120	(825)	0.95	0.38
Max	126	(868)	127	(875)	131	(903)	0.99	5.64
Average	123	(848)	123	(848)	126	(872)	0.97	2.00
Max-Min	12	(84)	13	(90)	11	(78)	0.04	5.26
Pipe from Source C								
Min	116	(798)	117	(805)	121	(835)	0.95	0.39
Max	128	(884)	128	(883)	131	(903)	0.98	5.66
Average	120	(830)	120	(830)	125	(860)	0.97	4.60
Max-Min	12	(86)	11	(78)	10	(68)	0.03	5.27

Notes: $R_{p0.2}$ is the proof strength at a non-proportional extension of 0.2% strain, $R_{10.5}$ the proof strength at a total extension of 0.5% strain, **Y/T** is the yield to tensile strength ratio ($R_{p0.2}/R_m$), and **uEL** is the specimen elongation at maximum stress.

Table 23 Tensile test results: Summary of **transverse orientated round bar specimens** as a function of pipe source. Specimens tested at 68°F (20°C).

	Yield strength				Tensile strength		Y/T	uEL
	$R_{p0.2}$		$R_{10.5}$		R_m			
	ksi	(N/mm ²)	ksi	(N/mm ²)	ksi	(N/mm ²)		%
Pipe from Source B (set of 6 pipes from 7 tested)								
Min	114	(784)	114	(785)	120	(825)	0.95	0.38
Max	126	(868)	127	(875)	131	(903)	0.99	5.64
Average	123	(846)	123	(847)	126	(872)	0.97	1.98
Max-Min	12	(84)	13	(90)	11	(78)	0.04	5.26
Pipe from Source C, Heat #1 (set of 5 pipes from 9 tested)								
Min	116	(798)	117	(806)	121	(837)	0.95	0.39
Max	128	(884)	128	(883)	131	(903)	0.98	5.50
Average	121	(837)	121	(837)	126	(868)	0.96	4.40
Max-Min	12	(86)	11	(77)	10	(66)	0.03	5.11
Pipe from Source C, Heat #2 (set of 2 pipes from 9 tested)								
Min	119	(821)	118	(817)	123	(851)	0.96	4.06
Max	121	(834)	121	(834)	124	(856)	0.97	5.12
Average	120	(826)	120	(824)	124	(854)	0.97	4.59
Max-Min	2	(13)	2	(17)	1	(5)	0.02	1.06
Pipe from Source C, Heat #3 (set of 2 pipes from 9 tested)								
Min	116	(803)	117	(805)	121	(835)	0.96	4.78
Max	121	(834)	120	(830)	124	(857)	0.97	5.66
Average	118	(816)	119	(818)	122	(844)	0.97	5.17
Max-Min	4	(31)	4	(25)	3	(22)	0.01	0.88

Notes: $R_{p0.2}$ is the proof strength at a non-proportional extension of 0.2% strain, $R_{10.5}$ the proof strength at a total extension of 0.5% strain, Y/T is the yield to tensile strength ratio ($R_{p0.2}/R_m$), and uEL is the specimen elongation at maximum stress.

Table 24 Tensile test results: Summary of **transverse orientated round bar specimens** as a function of pipe heat. Specimens tested at 68°F (20°C).

Test ID	Position (o'clock)	Notch location	Charpy Impact Energy, ft-lb (J)				Shear Area, %			Lateral Expansion, in (mm)		
			Individual	Min	Avg	STDV	Individual	Min	Avg	Individual	Min	Avg
61	6.4 - 6.5	WMC	131 (178)	121 (164)	133 (181)	13 (18)	100	100	100	0.075 (1.90)	0.075 (1.90)	0.079 (2.00)
62	6.4 - 6.5		121 (164)				100			0.076 (1.92)		
63	6.4 - 6.5		148 (200)				100			0.085 (2.17)		
64	6.6 - 6.7	Pipe 2 HAZ/FL	115 (156)	51 (69)	112 (152)	60 (81)	70	50	73	0.071 (1.81)	0.038 (0.96)	0.067 (1.70)
65	6.6 - 6.7		51 (69)				50			0.038 (0.96)		
66	6.6 - 6.7		170 (231)				100			0.092 (2.33)		
121	0.2 - 0.3	WMC	100 (136)	100 (136)	113 (154)	11 (16)	90	90	93	0.067 (1.69)	0.067 (1.69)	0.070 (1.78)
122	0.2 - 0.3		122 (165)				95			0.073 (1.85)		
123	0.2 - 0.3		118 (160)				95			0.071 (1.81)		
124	0.4 - 0.5	Pipe 1 HAZ/FL	44 (60)	44 (60)	63 (86)	23 (31)	50	50	62	0.032 (0.82)	0.032 (0.82)	0.044 (1.13)
125	0.4 - 0.5		57 (77)				55			0.041 (1.04)		
126	0.4 - 0.5		89 (120)				80			0.060 (1.52)		

Notes: All specimens are full size; 0.394x0.394in (10x10mm), extracted from the root region of the girth weld. All specimens are orientated perpendicular to the girth weld, notched in the through-thickness direction. All HAZ/FL specimens are notched 50/50. Test temperature of -4°F (-20°C)

Table 25 Charpy Impact test results: Weld A06.

Test ID	Position (o'clock)	Notch location	Charpy Impact Energy, ft-lb (J)				Shear Area, %			Lateral Expansion, in (mm)			
			Individual	Min	Avg	STDV	Individual	Min	Avg	Individual	Min	Avg	
71	6.4 - 6.6	WMC	63 (85)	58 (79)	60 (81)	3 (3)	95	85	90	0.047 (1.20)		0.044 (1.13)	0.046 (1.16)
72	6.4 - 6.6		58 (79)				90			0.046 (1.16)			
73	6.4 - 6.6		58 (79)				85			0.044 (1.13)			
74	6.6 - 6.7	Pipe 2 HAZ/FL	139 (189)	139 (188)	142 (192)	5 (7)	100	100	100	0.083 (2.10)		0.083 (2.10)	0.086 (2.17)
75	6.6 - 6.7		148 (200)				100			0.089 (2.25)			
76	6.6 - 6.7		139 (188)				100			0.085 (2.17)			
121	0.2 - 0.3	WMC	73 (99)	62 (84)	67 (90)	6 (8)	100	85	95	0.050 (1.26)		0.046 (1.18)	0.048 (1.21)
122	0.2 - 0.3		65 (88)				100			0.046 (1.18)			
123	0.2 - 0.3		62 (84)				85			0.047 (1.19)			
124	0.3 - 0.5	Pipe 1 HAZ/FL	95 (129)	95 (129)	103 (140)	13 (18)	85	85	88	0.065 (1.64)		0.065 (1.64)	0.072 (1.83)
125	0.3 - 0.5		96 (130)				85			0.069 (1.76)			
126	0.3 - 0.5		118 (160)				95			0.083 (2.10)			

Notes: All specimens are full size; 0.394x0.394in (10x10mm), extracted from the root region of the girth weld. All specimens are orientated perpendicular to the girth weld, notched in the through-thickness direction. All HAZ/FL specimens are notched 50/50. Test temperature of -4°F (-20°C)

Table 26 Charpy Impact test results: Weld A17.

Test ID	Position (o'clock)	Notch location	Charpy Impact Energy, ft-lb (J)				Shear Area, %			Lateral Expansion, in (mm)		
			Individual	Min	Avg	STDV	Individual	Min	Avg	Individual	Min	Avg
61	6.4 - 6.5	WMC	149 (202)	122 (165)	134 (182)	14 (19)	100	100	100	0.080 (2.03)	0.075 (1.91)	0.078 (1.99)
62	6.4 - 6.5		122 (165)				100			0.075 (1.91)		
63	6.4 - 6.5		131 (178)				100			0.080 (2.02)		
64	6.6 - 6.7	Pipe 2 HAZ/FL	176 (239)	33 (45)	127 (172)	81 (110)	100	40	80	0.094 (2.39)	0.026 (0.65)	0.072 (1.83)
65	6.6 - 6.7		33 (45)				40			0.026 (0.65)		
66	6.6 - 6.7		172 (233)				100			0.096 (2.44)		
121	0.2 - 0.3	WMC	132 (179)	107 (145)	123 (167)	14 (19)	100	100	100	0.080 (2.04)	0.067 (1.69)	0.078 (1.99)
122	0.2 - 0.3		130 (176)				100			0.088 (2.24)		
123	0.2 - 0.3		107 (145)				100			0.067 (1.69)		
124	0.4 - 0.5	Pipe 1 HAZ/FL	81 (110)	72 (97)	111 (150)	60 (81)	80	55	78	0.056 (1.42)	0.049 (1.24)	0.069 (1.74)
125	0.4 - 0.5		179 (243)				100			0.101 (2.56)		
126	0.4 - 0.5		72 (97)				55			0.049 (1.24)		

Notes: All specimens are full size; 0.394x0.394in (10x10mm), extracted from the root region of the girth weld. All specimens are orientated perpendicular to the girth weld, notched in the through-thickness direction. All HAZ/FL specimens are notched 50/50. Test temperature of -4°F (-20°C)

Table 27 Charpy Impact test results: Weld A33.

Test ID	Position (o'clock)	Notch location	Charpy Impact Energy, ft-lb (J)				Shear Area, %			Lateral Expansion, in (mm)		
			Individual	Min	Avg	STDV	Individual	Min	Avg	Individual	Min	Avg
61	6.4 - 6.5	WMC	142 (193)	142 (193)	160 (216)	15 (21)	100	100	100	0.083 (2.12)	0.083 (2.11)	0.085 (2.17)
62	6.4 - 6.5		164 (223)				100			0.083 (2.11)		
63	6.4 - 6.5		172 (233)				100			0.090 (2.28)		
64	6.6 - 6.7	Pipe 2 HAZ/FL	185 (251)	185 (251)	187 (254)	2 (3)	100	100	100	0.100 (2.54)	0.100 (2.53)	0.101 (2.56)
65	6.6 - 6.7		188 (255)				100			0.103 (2.61)		
66	6.6 - 6.7		189 (256)				100			0.100 (2.53)		
121	0.2 - 0.3	WMC	128 (173)	114 (155)	131 (177)	18 (25)	100	95	98	0.077 (1.96)	0.067 (1.69)	0.077 (1.96)
122	0.2 - 0.3		114 (155)				95			0.067 (1.69)		
123	0.2 - 0.3		150 (204)				100			0.087 (2.22)		
124	0.4 - 0.5	Pipe 1 HAZ/FL	199 (270)	68 (92)	153 (208)	74 (101)	100	60	87	0.099 (2.51)	0.045 (1.14)	0.080 (2.03)
125	0.4 - 0.5		193 (262)				100			0.096 (2.44)		
126	0.4 - 0.5		68 (92)				60			0.045 (1.14)		

Notes: All specimens are full size; 0.394x0.394in (10x10mm), extracted from the root region of the girth weld. All specimens are orientated perpendicular to the girth weld, notched in the through-thickness direction. All HAZ/FL specimens are notched 50/50. Test temperature of -4°F (-20°C)

Table 28 Charpy Impact test results: Weld A44.

Test ID	Position (o'clock)	Notch location	Charpy Impact Energy, ft-lb (J)				Shear Area, %			Lateral Expansion, in (mm)		
			Individual	Min	Avg	STDV	Individual	Min	Avg	Individual	Min	Avg
61	6.4 - 6.5	WMC	122 (165)	107 (145)	132 (178)	31 (42)	100	100	100	0.076 (1.93)	0.071 (1.80)	0.077 (1.94)
62	6.4 - 6.5		107 (145)				100			0.071 (1.80)		
63	6.4 - 6.5		166 (225)				100			0.083 (2.10)		
64	6.6 - 6.7	Pipe 2 HAZ/FL	167 (227)	163 (221)	168 (227)	5 (7)	100	100	100	0.090 (2.29)	0.090 (2.29)	0.093 (2.36)
65	6.6 - 6.7		163 (221)				100			0.093 (2.37)		
66	6.6 - 6.7		173 (234)				100			0.096 (2.43)		
121	0.2 - 0.3	WMC	91 (123)	91 (123)	117 (159)	23 (31)	85	85	95	0.058 (1.47)	0.058 (1.47)	0.072 (1.83)
122	0.2 - 0.3		132 (179)				100			0.080 (2.02)		
123	0.2 - 0.3		128 (174)				100			0.079 (2.00)		
124	0.4 - 0.5	Pipe 1 HAZ/FL	180 (244)	180 (244)	184 (249)	4 (6)	100	100	100	0.102 (2.60)	0.098 (2.49)	0.101 (2.56)
125	0.4 - 0.5		188 (255)				100			0.098 (2.49)		
126	0.4 - 0.5		184 (249)				100			0.102 (2.58)		

Notes: All specimens are full size; 0.394x0.394in (10x10mm), extracted from the root region of the girth weld. All specimens are orientated perpendicular to the girth weld, notched in the through-thickness direction. All HAZ/FL specimens are notched 50/50. Test temperature of -4°F (-20°C)

Table 29 Charpy Impact test results: Weld A46.

Test ID	Position (o'clock)	Notch location	Charpy Impact Energy, ft-lb (J)				Shear Area, %			Lateral Expansion, in (mm)		
			Individual	Min	Avg	STDV	Individual	Min	Avg	Individual	Min	Avg
61	6.4 - 6.5	WMC	97 (132)	97 (132)	105 (142)	7 (9)	100	90	97	0.073 (1.86)	0.073 (1.86)	0.078 (1.97)
62	6.4 - 6.5		107 (145)				90			0.079 (2.00)		
63	6.4 - 6.5		111 (150)				100			0.081 (2.05)		
64	6.6 - 6.7	Pipe 2 HAZ/FL	56 (76)	56 (76)	124 (168)	64 (86)	100	100	100	0.098 (2.48)	0.098 (2.48)	0.101 (2.56)
65	6.6 - 6.7		134 (181)				100			0.102 (2.60)		
66	6.6 - 6.7		182 (247)				100			0.102 (2.60)		
121	0.2 - 0.3	WMC	121 (164)	121 (164)	127 (173)	7 (9)	95	95	98	0.065 (1.66)	0.065 (1.66)	0.068 (1.72)
122	0.2 - 0.3		134 (182)				100			0.069 (1.75)		
123	0.2 - 0.3		127 (172)				100			0.069 (1.74)		
124	0.4 - 0.5	Pipe 1 HAZ/FL	184 (249)	184 (249)	195 (264)	11 (15)	55	55	78	0.039 (1.00)	0.039 (1.00)	0.072 (1.82)
125	0.4 - 0.5		195 (265)				80			0.080 (2.02)		
126	0.4 - 0.5		206 (279)				100			0.096 (2.45)		

Notes: All specimens are full size; 0.394x0.394in (10x10mm), extracted from the root region of the girth weld. All specimens are orientated perpendicular to the girth weld, notched in the through-thickness direction. All HAZ/FL specimens are notched 50/50. Test temperature of -4°F (-20°C)

Table 30 Charpy Impact test results: Weld A50.

Test ID	Position (o'clock)	Notch location	Charpy Impact Energy, ft-lb (J)				Shear Area, %			Lateral Expansion, in (mm)			
			Individual	Min	Avg	STDV	Individual	Min	Avg	Individual	Min	Avg	
31	6.4 - 6.5	WMC	80 (109)	80 (109)	94 (128)	16 (21)	95	90	95	0.050 (1.26)		0.050 (1.26)	0.056 (1.42)
32	6.4 - 6.5		91 (124)				100			0.052 (1.32)			
33	6.4 - 6.5		111 (151)				90			0.067 (1.69)			
34	6.6 - 6.7	Pipe 2 HAZ/FL	136 (184)	63 (85)	126 (170)	59 (79)	90	75	88	0.078 (1.98)		0.047 (1.19)	0.076 (1.92)
35	6.6 - 6.7		63 (85)				75			0.047 (1.19)			
36	6.6 - 6.7		178 (242)				100			0.102 (2.60)			
121	0.2 - 0.3	WMC	140 (190)	124 (168)	137 (186)	12 (17)	100	100	100	0.079 (2.00)		0.068 (1.73)	0.077 (1.95)
122	0.2 - 0.3		124 (168)				100			0.068 (1.73)			
123	0.2 - 0.3		148 (201)				100			0.083 (2.11)			
124	0.4 - 0.5	Pipe 1 HAZ/FL	108 (147)	71 (96)	121 (164)	58 (78)	80	55	78	0.068 (1.73)		0.047 (1.20)	0.071 (1.81)
125	0.4 - 0.5		184 (250)				100			0.098 (2.49)			
126	0.4 - 0.5		71 (96)				55			0.047 (1.20)			

Notes: All specimens are full size; 0.394x0.394in (10x10mm), extracted from the root region of the girth weld. All specimens are orientated perpendicular to the girth weld, notched in the through-thickness direction. All HAZ/FL specimens are notched 50/50. Test temperature of -4°F (-20°C)

Table 31 Charpy Impact test results: Weld B03.

Test ID	Position (o'clock)	Notch location	Charpy Impact Energy, ft-lb (J)				Shear Area, %			Lateral Expansion, in (mm)		
			Individual	Min	Avg	STDV	Individual	Min	Avg	Individual	Min	Avg
41	4.2 - 4.4	WMC	86 (117)	86 (117)	96 (130)	12 (16)	100	75	92	0.056 (1.43)	0.056 (1.41)	0.057 (1.45)
42	4.2 - 4.4		109 (148)				100			0.056 (1.41)		
43	4.2 - 4.4		92 (125)				75			0.059 (1.50)		
44	4.4 - 4.6	Pipe 2 HAZ/FL	43 (58)	35 (48)	74 (100)	60 (81)	55	50	63	0.033 (0.85)	0.022 (0.57)	0.044 (1.11)
45	4.4 - 4.6		35 (48)				50			0.022 (0.57)		
46	4.4 - 4.6		142 (193)				85			0.075 (1.91)		
121	12.0 - 0.2	WMC	127 (172)	63 (86)	97 (132)	32 (43)	100	85	93	0.082 (2.08)	0.042 (1.06)	0.061 (1.55)
122	12.0 - 0.2		101 (137)				95			0.059 (1.51)		
123	12.0 - 0.2		63 (86)				85			0.042 (1.06)		
124	0.2 - 0.3	Pipe 1 HAZ/FL	86 (117)	33 (45)	66 (89)	28 (39)	65	45	55	0.051 (1.29)	0.023 (0.58)	0.041 (1.04)
125	0.2 - 0.3		33 (45)				45			0.023 (0.58)		
126	0.2 - 0.3		77 (105)				55			0.049 (1.24)		

Notes: All specimens are full size; 0.394x0.394in (10x10mm), extracted from the root region of the girth weld. All specimens are orientated perpendicular to the girth weld, notched in the through-thickness direction. All HAZ/FL specimens are notched 50/50. Test temperature of -4°F (-20°C)

Table 32 Charpy Impact test results: Weld B06.

Test ID	Position (o'clock)	Notch location	Charpy Impact Energy, ft-lb (J)				Shear Area, %			Lateral Expansion, in (mm)		
			Individual	Min	Avg	STDV	Individual	Min	Avg	Individual	Min	Avg
71	6.6 - 6.8	WMC	121 (164)	111 (151)	137 (186)	36 (49)	100	100	100	0.070 (1.78)	0.059 (1.50)	0.072 (1.82)
72	6.6 - 6.8		111 (151)				100			0.059 (1.50)		
73	6.6 - 6.8		178 (242)				100			0.086 (2.19)		
74	6.8 - 6.9	Pipe 2 HAZ/FL	187 (253)	187 (253)	192 (260)	7 (10)	100	100	100	0.099 (2.52)	0.097 (2.47)	0.099 (2.52)
75	6.8 - 6.9		189 (256)				100			0.097 (2.47)		
76	6.8 - 6.9		200 (271)				100			0.101 (2.57)		
121	11.6 - 11.8	WMC	117 (158)	93 (126)	108 (147)	13 (18)	95	95	95	0.070 (1.78)	0.049 (1.25)	0.063 (1.59)
122	11.6 - 11.8		93 (126)				95			0.049 (1.25)		
123	11.6 - 11.8		115 (156)				95			0.069 (1.74)		
124	11.8 - 12.0	Pipe 1 HAZ/FL	178 (241)	89 (120)	131 (178)	45 (61)	100	55	77	0.095 (2.42)	0.061 (1.56)	0.076 (1.94)
125	11.8 - 12.0		89 (120)				55			0.061 (1.56)		
126	11.8 - 12.0		127 (172)				75			0.072 (1.83)		

Notes: All specimens are full size; 0.394x0.394in (10x10mm), extracted from the root region of the girth weld. All specimens are orientated perpendicular to the girth weld, notched in the through-thickness direction. All HAZ/FL specimens are notched 50/50. Test temperature of -4°F (-20°C)

Table 33 Charpy Impact test results: Weld B08.

Weld ID	Notch location	Position (o'clock)	Charpy Impact Energy, ft-lb (J)			Shear Area, %		Supplier	Heat
			Min	Max	Avg	Min	Avg		
B 06	P2 HAZ/FL	4.00	35 (48)	142 (193)	74 (100)	50	63	B	#1
A 06	P2 HAZ/FL	6.00	51 (69)	170 (231)	112 (152)	50	73	B	#1
A 44	P2 HAZ/FL	6.00	185 (251)	189 (256)	187 (254)	100	100	B	#1
A 06	P1 HAZ/FL	12.00	44 (60)	89 (120)	63 (86)	50	62	B	#1
A 33	P1 HAZ/FL	12.00	72 (97)	179 (243)	111 (150)	55	78	B	#1
A 50	P1 HAZ/FL	12.00	184 (249)	206 (279)	195 (264)	55	78	B	#1
A 17	P2 HAZ/FL	6.00	139 (188)	148 (200)	142 (192)	100	100	C	#2
A 17	P1 HAZ/FL	12.00	95 (129)	118 (160)	103 (140)	85	88	C	#2
A 44	P1 HAZ/FL	12.00	68 (92)	199 (270)	153 (208)	60	87	C	#2
A 46	P1 HAZ/FL	12.00	180 (244)	188 (255)	184 (249)	100	100	C	#2
B 03	P1 HAZ/FL	12.00	71 (96)	184 (250)	121 (164)	55	78	C	#2
A 46	P2 HAZ/FL	6.00	163 (221)	173 (234)	168 (227)	100	100	C	#3
B 08	P2 HAZ/FL	6.00	187 (253)	200 (271)	192 (260)	100	100	C	#3
B 03	P2 HAZ/FL	6.00	63 (85)	178 (242)	126 (170)	75	88	C	#4
B 08	P1 HAZ/FL	12.00	89 (120)	178 (241)	131 (178)	55	77	C	#4

Notes: A17 was welded using a Tie-in weld procedure; the remaining welds were produced using the main-line welding procedure.

Table 34 Charpy Impact test results: Comparison of HAZ/FL results from welds produced from pipes from the same source and same production heat.

Weld ID	Charpy Impact Energy, ft-lb (J)						Shear Area, %	
	Min		Max		Avg		Min	Avg
4 o'clock position (approximate)								
B 06	86	(117)	109	(148)	96	(130)	75	92
6 o'clock position (approximate)								
A 06	121	(164)	148	(200)	133	(181)	100	100
A 17	58	(79)	63	(85)	60	(81)	85	90
A 33	122	(165)	149	(202)	134	(182)	100	100
A 44	142	(193)	172	(233)	160	(216)	100	100
A 46	107	(145)	166	(225)	132	(178)	100	100
A 50	97	(132)	111	(150)	105	(142)	90	97
B 03	80	(109)	111	(151)	94	(128)	90	95
B 08	111	(151)	178	(242)	137	(186)	100	100
12 o'clock position (approximate)								
A 06	100	(136)	122	(165)	113	(154)	90	93
A 17	62	(84)	73	(99)	67	(90)	85	95
A 33	107	(145)	132	(179)	123	(167)	100	100
A 44	114	(155)	150	(204)	131	(177)	95	98
A 46	91	(123)	132	(179)	117	(159)	85	95
A 50	121	(164)	134	(182)	127	(173)	95	98
B 03	124	(168)	148	(201)	137	(186)	100	100
B 06	63	(86)	127	(172)	97	(132)	85	93
B 08	93	(126)	117	(158)	108	(147)	95	95

Notes: A17 was welded using a Tie-in weld procedure; the remaining welds were produced using the main-line welding procedure

Table 35 Charpy Impact test results: Comparison of weld metal results.

Test ID	Position	Material	Specimen dimensions				Max. Force		Final crack length, a_f		Yield strength		Failure type	Test results				
			B		W		a_o/W	F		in (mm)	σ_y			K	CTOD		J	
			in	(mm)	in	(mm)		lbf	(kN)		ksi	(N/mm ²)			MPa√m	in		(mm)
A06-7-C1	7.00	WMC	0.694	(17.6)	1.417	(36.0)	0.51	8,780	(39.1)	0.761	(19.34)	124.7	(860)	m	127.9	0.006	(0.15)	166.2
A06-7-C2	7.00	WMC	0.693	(17.6)	1.417	(36.0)	0.50	8,935	(39.7)	0.781	(19.84)	124.7	(860)	c ^{\$}	125.1	0.005	(0.12)	130.5
A06-7-C3	7.00	WMC	0.691	(17.5)	1.417	(36.0)	0.51	8,912	(39.6)	0.768	(19.50)	124.7	(860)	m	130.0	0.007	(0.17)	181.6
A06-7-C4	7.00	HAZ	0.687	(17.5)	1.417	(36.0)	0.49	7,484	(33.3)	0.698	(17.72)	124.7	(860)	c	104.0	0.002	(0.05)	64.5
A06-7-C5	7.00	HAZ	0.693	(17.6)	1.417	(36.0)	0.51	8,241	(36.7)	0.728	(18.50)	124.7	(860)	c	121.2	0.005	(0.12)	126.2
A06-7-C6	7.00	HAZ	0.693	(17.6)	1.418	(36.0)	0.50	8,300	(36.9)	0.725	(18.43)	124.7	(860)	u	119.6	0.003	(0.09)	100.6

Notes: **B** and **W** are specimen thickness and width, a_o is initial crack length, F_{max} is the maximum force during the test at the point of fracture, a_f is the post test crack length, σ_y is the material yield strength at the test temperature. Failure type 'c' is the critical value of fracture toughness at the onset of brittle crack extension (or pop-in) when the average stable crack extension is less than 0.008in (0.2mm); type 'u' is the critical value of fracture toughness at the onset of brittle crack extension (or pop-in) when the average stable crack extension is equal to or greater than 0.008in (0.2mm); type 'm' is the value of fracture toughness at the first attainment of a maximum force plateau for fully plastic behavior. Superscript \$ signifies a critical pop-in event.

Dual units are provided for consistency with the requirements of the testing standards; ASTM E1820 and B 7448:Part 2

Table 36 Fracture mechanics test results: Weld A06.

Test ID	Position	Material	Specimen dimensions				Max. Force		Final crack length, a_f		Yield strength		Failure type	Test results				
			B		W		a_o/W	F		in (mm)	σ_y			K	CTOD		J	
			in	(mm)	in	(mm)		lbf	(kN)		ksi	(N/mm ²)			MPa√m	in		(mm)
A 17-1-C1	1.00	WMC	0.660	(16.8)	1.340	(34.0)	0.48	7,977	(35.5)	0.699	(17.74)	113.0	(779)	m	114.7	0.005	(0.13)	130.9
A 17-1-C2	1.00	WMC	0.652	(16.6)	1.339	(34.0)	0.48	8,212	(36.5)	0.699	(17.75)	113.0	(779)	m	118.8	0.006	(0.14)	146.1
A 17-1-C3	1.00	WMC	0.656	(16.7)	1.339	(34.0)	0.47	8,238	(36.6)	0.708	(17.97)	113.0	(779)	m	117.3	0.004	(0.11)	118.3
A 17-2-C4	2.00	HAZ	0.662	(16.8)	1.337	(34.0)	0.47	9,048	(40.2)	0.668	(16.96)	118.2	(815)	m	126.8	0.007	(0.17)	183.4
A 17-2-C5	2.00	HAZ	0.661	(16.8)	1.336	(33.9)	0.46	9,911	(44.1)	0.654	(16.62)	118.2	(815)	m	135.9	0.012	(0.30)	312.0
A 17-2-C6	2.00	HAZ	0.667	(16.9)	1.336	(33.9)	0.46	9,544	(42.5)	0.699	(17.74)	118.2	(815)	m	128.9	0.009	(0.22)	223.5

Notes: **B** and **W** are specimen thickness and width, a_o is initial crack length, F_{max} is the maximum force during the test at the point of fracture, a_f is the post test crack length, σ_y is the material yield strength at the test temperature. Failure type 'c' is the critical value of fracture toughness at the onset of brittle crack extension (or pop-in) when the average stable crack extension is less than 0.008in (0.2mm); type 'u' is the critical value of fracture toughness at the onset of brittle crack extension (or pop-in) when the average stable crack extension is equal to or greater than 0.008in (0.2mm); type 'm' is the value of fracture toughness at the first attainment of a maximum force plateau for fully plastic behavior. Superscript \$ signifies a critical pop-in event.

Dual units are provided for consistency with the requirements of the testing standards; ASTM E1820 and B 7448:Part 2

Table 37 Fracture mechanics test results: Weld A17.

Test ID	Position	Material	Specimen dimensions				Max. Force		Final crack length, a_f		Yield strength		Failure type	Test results				
			B		W		a_o/W	F		in (mm)	σ_y			K	CTOD		J	
			in	(mm)	in	(mm)		lbf	(kN)		ksi	(N/mm ²)		MPa√m	in	(mm)	kJ/m ²	
A33-7-C1	7.00	WMC	0.697	(17.7)	1.420	(36.1)	0.51	9,148	(40.7)	0.758	(19.26)	127.5	(879)	m	132.3	0.008	(0.19)	212.1
A33-7-C2	7.00	WMC	0.694	(17.6)	1.419	(36.1)	0.49	9,029	(40.2)	0.726	(18.44)	127.5	(879)	c ^{\$}	124.0	0.004	(0.10)	115.0
A33-7-C3	7.00	WMC	0.691	(17.5)	1.417	(36.0)	0.50	9,075	(40.4)	0.763	(19.38)	127.5	(879)	m	130.0	0.008	(0.19)	207.8
A33-7-C4	7.00	HAZ	0.695	(17.7)	1.418	(36.0)	0.51	8,267	(36.8)	0.734	(18.64)	127.5	(879)	u	119.9	0.003	(0.09)	101.0
A33-7-C5	7.00	HAZ	0.687	(17.5)	1.419	(36.0)	0.50	10,081	(44.8)	0.725	(18.41)	127.5	(879)	c ^{\$}	145.1	0.008	(0.19)	225.8
A33-7-C6	7.00	HAZ	0.690	(17.5)	1.419	(36.1)	0.50	9,344	(41.6)	0.715	(18.15)	127.5	(879)	u	132.7	0.005	(0.12)	139.6

Notes: **B** and **W** are specimen thickness and width, a_o is initial crack length, F_{max} is the maximum force during the test at the point of fracture, a_f is the post test crack length, σ_y is the material yield strength at the test temperature. Failure type 'c' is the critical value of fracture toughness at the onset of brittle crack extension (or pop-in) when the average stable crack extension is less than 0.008in (0.2mm); type 'u' is the critical value of fracture toughness at the onset of brittle crack extension (or pop-in) when the average stable crack extension is equal to or greater than 0.008in (0.2mm); type 'm' is the value of fracture toughness at the first attainment of a maximum force plateau for fully plastic behavior. Superscript \$ signifies a critical pop-in event.

Dual units are provided for consistency with the requirements of the testing standards; ASTM E1820 and B 7448:Part 2

Table 38 Fracture mechanics test results: Weld A33.

Test ID	Position	Material	Specimen dimensions				Max. Force		Final crack length, a_f		Yield strength		Failure type	Test results				
			B		W		a_o/W	F		in (mm)	σ_y			K	CTOD		J	
			in	(mm)	in	(mm)		lbf	(kN)		ksi	(N/mm ²)			MPa√m	in		(mm)
A44-7-C1	7.00	WMC	0.691	(17.6)	1.417	(36.0)	0.51	8,453	(37.6)	0.772	(19.61)	121.9	(841)	m	124.0	0.006	(0.16)	172.2
A44-7-C2	7.00	WMC	0.688	(17.5)	1.419	(36.0)	0.50	8,780	(39.1)	0.754	(19.15)	121.9	(841)	m	125.0	0.006	(0.15)	162.8
A44-7-C3	7.00	WMC	0.689	(17.5)	1.419	(36.0)	0.50	8,691	(38.7)	0.766	(19.45)	121.9	(841)	m	124.4	0.006	(0.16)	168.6
A44-7-C4	7.00	HAZ	0.692	(17.6)	1.419	(36.0)	0.51	7,174	(31.9)	0.731	(18.57)	121.9	(841)	c	106.7	0.003	(0.07)	74.2
A44-7-C5	7.00	HAZ	0.691	(17.6)	1.418	(36.0)	0.50	9,551	(42.5)	0.719	(18.27)	121.9	(841)	u	136.3	0.007	(0.19)	203.9
A44-7-C6	7.00	HAZ	0.693	(17.6)	1.417	(36.0)	0.50	9,729	(43.3)	0.730	(18.54)	121.9	(841)	m	136.6	0.010	(0.26)	282.1

Notes: **B** and **W** are specimen thickness and width, a_o is initial crack length, F_{max} is the maximum force during the test at the point of fracture, a_f is the post test crack length, σ_y is the material yield strength at the test temperature. Failure type 'c' is the critical value of fracture toughness at the onset of brittle crack extension (or pop-in) when the average stable crack extension is less than 0.008in (0.2mm); type 'u' is the critical value of fracture toughness at the onset of brittle crack extension (or pop-in) when the average stable crack extension is equal to or greater than 0.008in (0.2mm); type 'm' is the value of fracture toughness at the first attainment of a maximum force plateau for fully plastic behavior. Superscript \$ signifies a critical pop-in event.

Dual units are provided for consistency with the requirements of the testing standards; ASTM E1820 and B 7448:Part 2

Table 39 Fracture mechanics test results: Weld A44.

Test ID	Position	Material	Specimen dimensions				Max. Force		Final crack length, a_f		Yield strength		Failure type	Test results				
			B		W		a_o/W	F		in (mm)	σ_y			K	CTOD		J	
			in	(mm)	in	(mm)		lbf	(kN)		ksi	(N/mm ²)		MPa√m	in	(mm)	kJ/m ²	
A46-7-C1	7.00	WMC	0.689	(17.5)	1.417	(36.0)	0.50	9,000	(40.0)	0.745	(18.93)	132.7	(915)	m	126.6	0.009	(0.24)	242.8
A46-7-C2	7.00	WMC	0.691	(17.6)	1.418	(36.0)	0.49	7,969	(35.4)	0.763	(19.39)	132.7	(915)	c ^{\$}	109.9	0.003	(0.07)	82.3
A46-7-C3	7.00	WMC	0.690	(17.5)	1.418	(36.0)	0.50	8,420	(37.5)	0.731	(18.57)	132.7	(915)	m	119.8	0.006	(0.15)	153.9
A46-7-C4	7.00	HAZ	0.691	(17.6)	1.419	(36.0)	0.50	8,446	(37.6)	0.719	(18.26)	132.7	(915)	u	120.3	0.004	(0.10)	115.1
A46-7-C5	7.00	HAZ	0.692	(17.6)	1.419	(36.0)	0.50	8,759	(39.0)	0.724	(18.40)	132.7	(915)	u	123.4	0.004	(0.10)	115.5
A46-7-C6	7.00	HAZ	0.691	(17.6)	1.419	(36.0)	0.52	9,469	(42.1)	0.753	(19.13)	132.7	(915)	m	144.1	0.014	(0.36)	403.1

Notes: **B** and **W** are specimen thickness and width, a_o is initial crack length, F_{max} is the maximum force during the test at the point of fracture, a_f is the post test crack length, σ_y is the material yield strength at the test temperature. Failure type 'c' is the critical value of fracture toughness at the onset of brittle crack extension (or pop-in) when the average stable crack extension is less than 0.008in (0.2mm); type 'u' is the critical value of fracture toughness at the onset of brittle crack extension (or pop-in) when the average stable crack extension is equal to or greater than 0.008in (0.2mm); type 'm' is the value of fracture toughness at the first attainment of a maximum force plateau for fully plastic behavior. Superscript \$ signifies a critical pop-in event.

Dual units are provided for consistency with the requirements of the testing standards; ASTM E1820 and B 7448:Part 2

Table 40 Fracture mechanics test results: Weld A46.

Test ID	Position	Material	Specimen dimensions				Max. Force		Final crack length, a_f		Yield strength		Failure type	Test results				
			B		W		F				σ_y			K	CTOD		J	
			in	(mm)	in	(mm)	a_o/W	lbf	(kN)	in	(mm)	ksi		(N/mm ²)	MPa√m	in	(mm)	kJ/m ²
A50-7-C1	7.00	WMC	0.687	(17.5)	1.417	(36.0)	0.50	8,901	(39.6)	0.761	(19.33)	127.5	(879)	m	126.4	0.006	(0.15)	159.2
A50-7-C2	7.00	WMC	0.692	(17.6)	1.418	(36.0)	0.49	9,633	(42.9)	0.734	(18.64)	127.5	(879)	m	133.4	0.007	(0.19)	206.3
A50-7-C3	7.00	WMC	0.691	(17.6)	1.419	(36.1)	0.50	8,747	(38.9)	0.774	(19.65)	127.5	(879)	m	125.7	0.007	(0.17)	182.5
A50-7-C4	7.00	HAZ	0.691	(17.6)	1.419	(36.0)	0.50	6,290	(28.0)	0.714	(18.14)	127.5	(879)	c ^{\$}	89.8	0.001	(0.04)	43.4
A50-7-C5	7.00	HAZ	0.694	(17.6)	1.417	(36.0)	0.50	8,583	(38.2)	0.711	(18.05)	127.5	(879)	c	121.7	0.003	(0.09)	101.3
A50-7-C6	7.00	HAZ	0.694	(17.6)	1.419	(36.0)	0.50	9,873	(43.9)	0.709	(18.01)	127.5	(879)	u	139.2	0.006	(0.16)	180.8

Notes: **B** and **W** are specimen thickness and width, a_o is initial crack length, F_{max} is the maximum force during the test at the point of fracture, a_f is the post test crack length, σ_y is the material yield strength at the test temperature. Failure type 'c' is the critical value of fracture toughness at the onset of brittle crack extension (or pop-in) when the average stable crack extension is less than 0.008in (0.2mm); type 'u' is the critical value of fracture toughness at the onset of brittle crack extension (or pop-in) when the average stable crack extension is equal to or greater than 0.008in (0.2mm); type 'm' is the value of fracture toughness at the first attainment of a maximum force plateau for fully plastic behavior. Superscript \$ signifies a critical pop-in event.

Dual units are provided for consistency with the requirements of the testing standards; ASTM E1820 and B 7448:Part 2

Table 41 Fracture mechanics test results: Weld A50.

Test ID	Position	Material	Specimen dimensions				Max. Force		Final crack length, a_f		Yield strength		Failure type	Test results				
			B		W		a_o/W	F		in (mm)	σ_y			K	CTOD		J	
			in	(mm)	in	(mm)		lbf	(kN)		ksi	(N/mm ²)		MPa√m	in	(mm)	kJ/m ²	
B03-6-C1	6.00	WMC	0.695	(17.7)	1.419	(36.0)	0.50	8,493	(37.8)	0.752	(19.11)	128.8	(888)	c ^{\$}	119.6	0.003	(0.07)	85.4
B03-6-C2	6.00	WMC	0.696	(17.7)	1.419	(36.0)	0.50	9,836	(43.8)	0.753	(19.13)	128.8	(888)	m	138.5	0.009	(0.22)	242.5
B03-6-C3	6.00	WMC	0.695	(17.7)	1.418	(36.0)	0.50	9,506	(42.3)	0.776	(19.72)	128.8	(888)	m	136.0	0.009	(0.22)	243.4
B03-6-C4	6.00	HAZ	0.705	(17.9)	1.413	(35.9)	0.50	10,611	(47.2)	0.715	(18.17)	128.8	(888)	u	150.3	0.008	(0.19)	235.9
B03-5-C5	5.00	HAZ	0.707	(18.0)	1.417	(36.0)	0.50	10,013	(44.5)	0.743	(18.86)	128.8	(888)	c ^{\$}	140.0	0.005	(0.13)	161.0
B03-5-C6	5.00	HAZ	0.698	(17.7)	1.419	(36.0)	0.51	8,022	(35.7)	0.724	(18.40)	128.8	(888)	c	116.1	0.002	(0.06)	77.9

Notes: **B** and **W** are specimen thickness and width, a_o is initial crack length, F_{max} is the maximum force during the test at the point of fracture, a_f is the post test crack length, σ_y is the material yield strength at the test temperature. Failure type 'c' is the critical value of fracture toughness at the onset of brittle crack extension (or pop-in) when the average stable crack extension is less than 0.008in (0.2mm); type 'u' is the critical value of fracture toughness at the onset of brittle crack extension (or pop-in) when the average stable crack extension is equal to or greater than 0.008in (0.2mm); type 'm' is the value of fracture toughness at the first attainment of a maximum force plateau for fully plastic behavior. Superscript \$ signifies a critical pop-in event.

Dual units are provided for consistency with the requirements of the testing standards; ASTM E1820 and B 7448:Part 2

Table 42 Fracture mechanics test results: Weld B03.

Test ID	Position	Material	Specimen dimensions				Max. Force		Final crack length, a_f		Yield strength		Failure type	Test results				
			B		W		a_o/W	F		in (mm)	σ_y			K	CTOD		J	
			in	(mm)	in	(mm)		lbf	(kN)		ksi	(N/mm ²)		MPa√m	in	(mm)	kJ/m ²	
B06-3-C1	3.00	WMC	0.698	(17.7)	1.416	(36.0)	0.50	10,364	(46.1)	0.723	(18.36)	126.0	(869)	m	144.3	0.006	(0.15)	188.0
B06-3-C2	3.00	WMC	0.697	(17.7)	1.416	(36.0)	0.48	10,623	(47.3)	0.706	(17.93)	126.0	(869)	u	138.9	0.005	(0.14)	162.6
B06-3-C3	3.00	WMC	0.699	(17.8)	1.418	(36.0)	0.47	11,795	(52.5)	0.710	(18.04)	126.0	(869)	m	152.1	0.008	(0.20)	243.0
B06-3-C4	3.00	HAZ	0.696	(17.7)	1.417	(36.0)	0.50	9,158	(40.7)	0.710	(18.04)	126.0	(869)	c	128.3	0.003	(0.08)	104.2
B06-11-C5	11.00	HAZ	0.705	(17.9)	1.418	(36.0)	0.47	12,385	(55.1)	0.669	(16.98)	126.0	(869)	u	156.7	0.007	(0.17)	218.2
B06-11-C6	11.00	HAZ	0.698	(17.7)	1.417	(36.0)	0.50	8,982	(40.0)	0.708	(17.98)	126.0	(869)	c	125.6	0.003	(0.08)	96.7

Notes: **B** and **W** are specimen thickness and width, a_o is initial crack length, F_{max} is the maximum force during the test at the point of fracture, a_f is the post test crack length, σ_y is the material yield strength at the test temperature. Failure type 'c' is the critical value of fracture toughness at the onset of brittle crack extension (or pop-in) when the average stable crack extension is less than 0.008in (0.2mm); type 'u' is the critical value of fracture toughness at the onset of brittle crack extension (or pop-in) when the average stable crack extension is equal to or greater than 0.008in (0.2mm); type 'm' is the value of fracture toughness at the first attainment of a maximum force plateau for fully plastic behavior. Superscript \$ signifies a critical pop-in event.

Dual units are provided for consistency with the requirements of the testing standards; ASTM E1820 and B 7448:Part 2

Table 43 Fracture mechanics test results: Weld B06.

Test ID	Position	Material	Specimen dimensions				Max. Force		Final crack length, a_f		Yield strength		Failure type	Test results				
			B		W		a_o/W	F		in (mm)	ksi (N/mm ²)	K		CTOD		J		
			in	(mm)	in	(mm)		lbf	(kN)					MPa√m	in		(mm)	kJ/m ²
B08-11-C1	11.00	WMC	0.703	(17.9)	1.417	(36.0)	0.49	10,292	(45.8)	0.733	(18.61)	130.1	(897)	m	140.0	0.011	(0.27)	306.3
B08-11-C2	11.00	WMC	0.699	(17.8)	1.418	(36.0)	0.50	9,508	(42.3)	0.725	(18.41)	130.1	(897)	u	132.9	0.005	(0.12)	143.8
B08-11-C3	11.00	WMC	0.704	(17.9)	1.417	(36.0)	0.49	10,531	(46.8)	0.736	(18.69)	130.1	(897)	m	140.9	0.006	(0.16)	186.9
B08-11-C4	11.00	HAZ	0.701	(17.8)	1.419	(36.1)	0.50	11,597	(51.6)	0.719	(18.26)	130.1	(897)	u	160.8	0.015	(0.38)	454.2
B08-5-C5	5.00	HAZ	0.702	(17.8)	1.420	(36.1)	0.50	9,585	(42.6)	0.712	(18.09)	130.1	(897)	u	133.6	0.004	(0.10)	126.4
B08-6-C6	6.00	HAZ	0.690	(17.5)	1.419	(36.1)	0.50	9,344	(41.6)	0.715	(18.15)	130.1	(897)	c	132.7	0.005	(0.12)	141.5

Notes: **B** and **W** are specimen thickness and width, a_o is initial crack length, F_{max} is the maximum force during the test at the point of fracture, a_f is the post test crack length, σ_y is the material yield strength at the test temperature. Failure type 'c' is the critical value of fracture toughness at the onset of brittle crack extension (or pop-in) when the average stable crack extension is less than 0.008in (0.2mm); type 'u' is the critical value of fracture toughness at the onset of brittle crack extension (or pop-in) when the average stable crack extension is equal to or greater than 0.008in (0.2mm); type 'm' is the value of fracture toughness at the first attainment of a maximum force plateau for fully plastic behavior. Superscript \$ signifies a critical pop-in event.

Dual units are provided for consistency with the requirements of the testing standards; ASTM E1820 and B 7448:Part 2

Table 44 Fracture mechanics test results: Weld B08.

Test ID	Position	Material	Specimen dimension				Defect dimensions				Defect area	
			Thickness (<i>t</i>)		Gross cross section		Depth (<i>d</i>)		Length (<i>l</i>)		<i>lxd</i>	actual
			in	(mm)	in ²	(mm ²)	in	(mm)	in	(mm)	%	%
WP-H1	4.8-5.8	HAZ	0.78	(19.78)	9.47	(6,109)	0.118	(3.00)	1.97	(50)	2.46	1.97
WP-H2	8.3-9.2	HAZ	0.78	(19.89)	9.48	(6,117)	0.118	(3.00)	3.94	(100)	4.90	4.42
WP-H3	1.2-2.2	HAZ	0.78	(19.76)	9.52	(6,139)	0.157	(4.00)	3.94	(100)	6.52	5.87
WP-W	3.0-4.0	WMC	0.78	(19.80)	9.44	(6,091)	0.118	(3.00)	1.97	(50)	2.46	1.97

Table 45 Weld A06: CWP specimens – general dimensions.

Test ID	Position	Notch location	Maximum stress at failure				CMOD	Remote strain at failure			Deformation mode	
			Gross		Net Section			Pipe 1	Pipe 2	Plate		
			ksi	(N/mm ²)	ksi	(N/mm ²)		in	(mm)	%		%
WP-H1	4.8-5.8	HAZ	125.5	(865)	128.6	(887)	0.120	(3.04)	3.28	2.44	2.87	GSY
WP-H2	8.3-9.2	HAZ	117.5	(810)	123.5	(852)	0.057	(1.46)	1.28	0.69	0.87	GSY
WP-H3	1.2-2.2	HAZ	114.1	(787)	122.1	(842)	0.034	(0.86)	0.55	0.58	0.53	NSY
WP-W	3.0-4.0	WMC	124.3	(857)	127.5	(879)	0.101	(2.57)	2.62	2.14	2.25	GSY

Notes: Net Section Stress is calculated based on the hypothesized containment rectangle for the defect(s).

Table 46 Weld A06: CWP test results.

Test ID	Position	Material	Specimen dimension				Defect dimensions				Defect area	
			Thickness (<i>t</i>)		Gross cross section		Depth (<i>d</i>)		Length (<i>l</i>)		<i>lxd</i>	actual
			in	(mm)	in ²	(mm ²)	in	(mm)	in	(mm)	%	%
WP-H1	4.8-5.8	HAZ	0.78	(19.78)	9.47	(6,109)	0.118	(3.00)	1.97	(50)	2.46	1.97
WP-H2	8.3-9.2	HAZ	0.78	(19.73)	9.42	(6,077)	0.118	(3.00)	3.94	(100)	4.94	4.50
WP-H3	1.2-2.2	HAZ	0.78	(19.74)	9.44	(6,090)	0.118	(3.00)	3.94	(100)	4.93	4.49
WP-W	3.0-4.0	WMC	0.78	(19.79)	9.45	(6,094)	0.118	(3.00)	1.97	(50)	2.46	2.03

Table 47 Weld A17: CWP specimens – general dimensions.

Test ID	Position	Notch location	Maximum stress at failure				CMOD	Remote strain at failure			Deformation mode	
			Gross		Net Section			Pipe 1	Pipe 2	Plate		
			ksi	(N/mm ²)	ksi	(N/mm ²)		in	(mm)	%		%
WP-H1	4.8-5.8	HAZ	120.2	(829)	123.2	(850)	0.140	(3.56)	0.83	3.57	1.84	GSY
WP-H2	8.3-9.2	HAZ	115.3	(795)	121.3	(836)	0.107	(2.73)	0.58	1.75	0.91	GSY
WP-H3	1.2-2.2	HAZ	113.4	(782)	119.3	(822)	0.095	(2.42)	0.52	0.87	0.57	GSY
WP-W	3.0-4.0	WMC	118.5	(817)	121.5	(837)	0.137	(3.49)	1.58	2.23	1.61	GSY

Notes: Net Section Stress is calculated based on the hypothesized containment rectangle for the defect(s).

Table 48 Weld A17: CWP test results.

Test ID	Position	Material	Specimen dimension				Defect dimensions				Defect area	
			Thickness (<i>t</i>)		Gross cross section		Depth (<i>d</i>)		Length (<i>l</i>)		<i>lxd</i>	actual
			in	(mm)	in ²	(mm ²)	in	(mm)	in	(mm)	%	%
WP-H1	4.8-5.8	HAZ	0.78	(19.75)	9.44	(6,091)	0.118	(3.00)	1.97	(50)	2.46	1.97
WP-H2	8.3-9.2	HAZ	0.78	(19.79)	9.38	(6,050)	0.118	(3.00)	3.94	(100)	4.96	4.52
WP-H3	1.2-2.2	HAZ	0.78	(19.86)	9.49	(6,120)	0.157	(4.00)	3.94	(100)	6.54	5.88
WP-W	3.0-4.0	WMC	0.78	(19.79)	9.45	(6,094)	0.118	(3.00)	1.97	(50)	2.46	1.97

Table 49 Weld A33: CWP specimens – general dimensions.

Test ID	Position	Notch location	Maximum stress at failure				CMOD	Remote strain at failure			Deformation mode	
			Gross		Net Section			Pipe 1	Pipe 2	Plate		
			ksi	(N/mm ²)	ksi	(N/mm ²)		in	(mm)	%		%
WP-H1	4.8-5.8	HAZ	123.0	(848)	126.1	(870)	0.049	(1.24)	1.84	1.11	1.60	GSY
WP-H2	8.3-9.2	HAZ	117.6	(811)	123.7	(853)	0.082	(2.08)	1.18	0.87	0.93	GSY
WP-H3	1.2-2.2	HAZ	114.8	(791)	122.8	(847)	0.031	(0.80)	0.57	0.65	0.60	GSY
WP-W	3.0-4.0	WMC	125.1	(862)	128.2	(884)	0.082	(2.09)	2.33	1.34	1.83	GSY

Notes: Net Section Stress is calculated based on the hypothesized containment rectangle for the defect(s).

Table 50 Weld A33: CWP test results.

Test ID	Position	Material	Specimen dimension				Defect dimensions				Defect area	
			Thickness (<i>t</i>)		Gross cross section		Depth (<i>d</i>)		Length (<i>l</i>)		<i>lxd</i>	actual
			in	(mm)	in ²	(mm ²)	in	(mm)	in	(mm)	%	%
WP-H1	4.8-5.8	HAZ	0.78	(19.72)	9.44	(6,091)	0.118	(3.00)	1.97	(50)	2.46	1.97
WP-H2	8.3-9.2	HAZ	0.78	(19.74)	9.45	(6,095)	0.118	(3.00)	2.95	(75)	3.69	3.20
WP-H3	3.0-4.0	HAZ	0.77	(19.66)	9.40	(6,062)	0.118	(3.00)	3.94	(100)	4.95	4.46
WP-H4	1.4-2.4	HAZ	0.78	(19.83)	9.50	(6,127)	0.157	(4.00)	3.94	(100)	6.53	5.88

Table 51 Weld A46: CWP specimens – general dimensions.

Test ID	Position	Notch location	Maximum stress at failure				CMOD	Remote strain at failure			Deformation mode	
			Gross		Net Section			Pipe 1	Pipe 2	Plate		
			ksi	(N/mm ²)	ksi	(N/mm ²)		in	(mm)	%		%
WP-H1	4.8-5.8	HAZ	119.4	(823)	122.4	(844)	0.153	(3.89)	2.04	3.55	2.63	GSY
WP-H2	8.3-9.2	HAZ	115.0	(793)	119.4	(823)	0.088	(2.23)	1.07	1.37	1.09	GSY
WP-H3	3.0-4.0	HAZ	113.6	(783)	119.5	(824)	0.059	(1.50)	0.96	0.88	0.81	GSY
WP-H4	1.4-2.4	HAZ	108.8	(750)	116.4	(802)	0.038	(0.97)	0.48	0.66	0.49	NSY

Notes: Net Section Stress is calculated based on the hypothesized containment rectangle for the defect(s).

Table 52 Weld A46: CWP test results.

Test ID	Position	Material	Specimen dimension				Defect dimensions				Defect area	
			Thickness (<i>t</i>)		Gross cross section		Depth (<i>d</i>)		Length (<i>l</i>)		<i>lxd</i>	actual
			in	(mm)	in ²	(mm ²)	in	(mm)	in	(mm)	%	%
WP-H1	4.8-5.8	HAZ	0.78	(19.73)	9.43	(6,082)	0.118	(3.00)	1.97	(50)	2.47	1.97
WP-H2	8.3-9.2	HAZ	0.78	(19.79)	9.46	(6,103)	0.157	(4.00)	3.94	(100)	6.55	5.90
WP-W	3.0-4.0	WMC	0.78	(19.79)	9.46	(6,101)	0.118	(3.00)	1.97	(50)	2.46	1.97

Table 53 Weld A50: CWP specimens – general dimensions.

Test ID	Position	Notch location	Maximum stress at failure				CMOD	Remote strain at failure			Deformation mode	
			Gross		Net Section			Pipe 1	Pipe 2	Plate		
			ksi	(N/mm ²)	ksi	(N/mm ²)		in	(mm)	%		%
WP-H1*	4.8-5.8	HAZ	121.5	(838)	124.6	(859)	0.044	(1.13)	5.14	2.28	2.70	GSY
WP-H2	8.3-9.2	HAZ	115.5	(797)	123.6	(852)	0.056	(1.43)	2.28	1.04	1.14	GSY
WP-W*	3.0-4.0	WMC	119.0	(820)	122.0	(841)	0.032	(0.81)	5.43	1.54	2.40	GSY

Notes: Net Section Stress is calculated based on the hypothesized containment rectangle for the defect(s)

* Testing of WP-H1 and WP-W was terminated without failure of the specimen due to excessive strain in Pipe 1.

Table 54 Weld A50: CWP test results.

Test ID	Position	Specimen dimension				Defect dimensions					Defect area		
		Thickness (<i>t</i>)		Gross cross section		Depth (<i>d</i>)		Length (<i>l</i>)		Ligament (ρ)		<i>lxd</i>	
		in	(mm)	in ²	(mm ²)	in	(mm)	in	(mm)	in	(mm)	Surface*	%
WP1	1.0-2.0	0.78	(19.70)	9.42	(6,075)	0.179	(4.54)	5.94	(151)	Surface breaking defect		11.28	
WP2	5.0-6.0	0.78	(19.77)	9.56	(6,165)	0.067	(1.70)	7.95	(202)	0.29	(7.3)	Outer	5.57
WP3	6.9-7.9	0.78	(19.76)	9.45	(6,097)	0.256	(6.50)	4.55	(116)	0.21	(5.4)	Inner	12.31
WP4	9.9-10.9	0.78	(19.73)	9.44	(6,091)	0.173	(4.40)	5.77	(147)	0.30	(7.6)	Outer	10.58

Notes: * For ligament dimension, surface refers to the inner or outer pipe surface that the minimum ligament dimension is measured

Table 55 Weld B03: CWP specimens – general dimensions.

Test ID	Position	Maximum stress at failure				Remote strain at failure			Deformation mode	Comment
		Gross		Net Section		Pipe 1	Pipe 2	Plate		
		ksi	(N/mm ²)	ksi	(N/mm ²)	%	%	%		
WP1	1.0-2.0	119.1	(821)	134.2	(925)	2.27	2.40	2.32	GSY	
WP2	5.0-6.0	123.5	(852)	130.8	(902)	4.76	5.02	4.43	GSY	
WP3	6.9-7.9	121.3	(836)	138.3	(954)	3.15	3.91	3.65	GSY	
WP4	9.9-10.9	112.2	(774)	125.5	(865)	0.91	0.59	0.75	GSY	

Notes: **Net Section Stress** is calculated based on the hypothesized containment rectangle for the defect(s).

Table 56 Weld B03: CWP test results.

Test ID	Position	Specimen dimension				Defect dimensions					Defect area		
		Thickness (<i>t</i>)		Gross cross section		Depth (<i>d</i>)		Length (<i>l</i>)		Ligament (ρ)		<i>lxd</i>	
		in	(mm)	in ²	(mm ²)	in	(mm)	in	(mm)	in	(mm)	Surface*	%
WP1	1.8-2.9	0.79	(20.00)	9.57	(6,177)	0.213	(5.41)	12.15	(309)	Surface breaking defect		27.04	
WP2	6.2-7.2	0.79	(19.99)	9.55	(6,161)	No defect found							
WP3	8.8-9.8	0.79	(19.97)	9.56	(6,166)	0.236	(6.00)	5.71	(145)	0.23	(5.8)	Outer	14.11
WP4	10.2-11.2	0.79	(20.12)	9.63	(6,214)	0.197	(5.00)	5.67	(144)	0.28	(7.0)	Outer	11.59

Notes: * For ligament dimension, surface refers to the inner or outer pipe surface that the minimum ligament dimension is measured

Table 57 Weld B06: CWP specimens – general dimensions.

Test ID	Position	Maximum stress at failure				Remote strain at failure			Deformation mode	Comment
		Gross		Net Section		Pipe 1	Pipe 2	Plate		
		ksi	(N/mm ²)	ksi	(N/mm ²)	%	%	%		
WP1	1.8-2.9	118.6	(818)	162.6	(1121)	2.40	0.83	1.44	GSY	
WP2	6.2-7.2	111.0	(765)	No defect		5.33	0.47	2.52	GSY	Test terminated, no failure
WP3	8.8-9.8	115.9	(799)	135.0	(931)	5.25	0.75	2.37	GSY	Test terminated, no failure
WP4	10.2-11.2	112.1	(773)	126.8	(874)	0.88	0.55	0.69	NSY	

Notes: **Net Section Stress** is calculated based on the hypothesized containment rectangle for the defect(s).

Table 58 Weld B06: CWP test results.

Test ID	Position	Specimen dimension				Defect dimensions					Defect area		
		Thickness (<i>t</i>)		Gross cross section		Depth (<i>d</i>)		Length (<i>l</i>)		Ligament (ρ)		<i>lxd</i>	
		in	(mm)	in ²	(mm ²)	in	(mm)	in	(mm)	in	(mm)	Surface*	%
WP1	2.0-2.9	0.78	(19.82)	9.50	(6,129)	0.354	(9.00)	6.81	(173)	0.02	(0.5)	Inner	25.40
WP2	5.0-6.0	0.78	(19.83)	9.50	(6,126)	No defect found							
WP3	9.9-10.9	0.78	(19.85)	9.52	(6,139)	0.425	(10.80)	5.71	(145)	0.17	(4.2)	Outer	25.51

Notes: * For ligament dimension, surface refers to the inner or outer pipe surface that the minimum ligament dimension is measured

Table 59 Weld B08: CWP specimens – general dimensions.

Test ID	Position	Maximum stress at failure				Remote strain at failure			Deformation mode	Comment
		Gross		Net Section		Pipe 1	Pipe 2	Plate		
		ksi	(N/mm ²)	ksi	(N/mm ²)	%	%	%		
WP1	2.0-2.9	89.5	(617)	120.0	(827)	0.30	0.30	0.29	LC	
WP2	5.0-6.0	121.4	(837)			4.49	4.30	4.31	GSY	Test terminated, no failure
WP3	9.9-10.9	91.0	(627)	122.1	(842)	0.35	0.34	0.34	LC	

Notes: Net Section Stress is calculated based on the hypothesized containment rectangle for the defect(s).

Table 60 Weld B08: CWP test results.

Weld ID	Pipe size		Defect dimensions		Material properties			CWP assessment		Critical stress assessment			
	Diameter OD in	Thickness t in	Length 2c in	Height a in	Yield σ_y ksi	Tensile σ_t ksi	CTOD in	K_r	L_r	Critical stress σ_{crit} ksi	Factor of safety	K_r	L_r
WP-H1	48.0	0.78	1.97	0.118	115.6	126.6	0.0034	0.640	1.111	113.0	1.110	0.576	1.001
WP-H2	48.0	0.78	3.94	0.118	115.6	126.6	0.0034	0.636	1.065	109.0	1.078	0.590	0.988
WP-H3	48.0	0.79	3.94	0.157	115.6	126.6	0.0034	0.729	1.050	102.5	1.114	0.654	0.943
WP1	48.0	0.78	1.97	0.118	115.6	126.6	0.0057	0.491	1.101	118.5	1.049	0.468	1.050

(a) US Customary Units

Weld ID	Pipe size		Defect dimensions		Material properties			CWP assessment		Critical stress assessment			
	Diameter OD mm	Thickness t mm	Length 2c mm	Height a mm	Yield σ_y N/mm ²	Tensile σ_t N/mm ²	CTOD mm	K_r	L_r	Critical stress σ_{crit} N/mm ²	Factor of safety	K_r	L_r
WP-H1	1220.0	19.8	50.0	3.0	796.8	872.7	0.09	0.640	1.111	779	1.110	0.576	1.001
WP-H2	1220.0	19.9	100.0	3.0	796.8	872.7	0.09	0.636	1.065	752	1.078	0.590	0.988
WP-H3	1220.0	20.0	100.0	4.0	796.8	872.7	0.09	0.729	1.050	707	1.114	0.654	0.943
WP1	1220.0	19.9	50.0	3.0	796.8	872.7	0.15	0.491	1.101	817	1.049	0.468	1.050

(b) SI Units

Table 61 Weld A06: API 1104 Option 2 analysis results.

Weld ID	Pipe size		Defect dimensions		Material properties			CWP assessment		Critical stress assessment			
	Diameter OD in	Thickness t in	Length 2c in	Height a in	Yield σ_y ksi	Tensile σ_t ksi	CTOD in	K_r	L_r	Critical stress σ_{crit} ksi	Factor of safety	K_r	L_r
WP-H1	48.0	0.78	1.97	0.118	106.3	113.7	0.0091	0.403	1.158	107.0	1.124	0.359	1.031
WP-H2	48.0	0.78	3.94	0.118	110.5	122.9	0.0091	0.386	1.093	111.0	1.039	0.372	1.052
WP-H3	48.0	0.78	3.94	0.118	106.3	113.7	0.0091	0.404	1.118	105.0	1.080	0.374	1.035
WP1	48.0	0.78	1.97	0.118	106.3	113.7	0.0050	0.537	1.141	107.5	1.102	0.487	1.035

(a) US Customary Units

Weld ID	Pipe size		Defect dimensions		Material properties			CWP assessment		Critical stress assessment			
	Diameter OD mm	Thickness t mm	Length 2c mm	Height a mm	Yield σ_y N/mm ²	Tensile σ_t N/mm ²	CTOD mm	K_r	L_r	Critical stress σ_{crit} N/mm ²	Factor of safety	K_r	L_r
WP-H1	1220.0	19.8	50.0	3.0	732.8	783.9	0.23	0.403	1.158	738	1.124	0.359	1.031
WP-H2	1220.0	19.8	100.0	3.0	761.8	847.2	0.23	0.386	1.093	765	1.039	0.372	1.052
WP-H3	1220.0	19.8	100.0	3.0	732.8	783.9	0.23	0.404	1.118	724	1.080	0.374	1.035
WP1	1220.0	19.8	50.0	3.0	732.8	783.9	0.13	0.537	1.141	741	1.102	0.487	1.035

(b) SI Units

Table 62 Weld A17: API 1104 Option 2 analysis results.

Weld ID	Pipe size		Defect dimensions		Material properties			CWP assessment		Critical stress assessment			
	Diameter OD in	Thickness t in	Length 2c in	Height a in	Yield σ_y ksi	Tensile σ_t ksi	CTOD in	K_r	L_r	Critical stress σ_{crit} ksi	Factor of safety	K_r	L_r
WP-H1	48.0	0.78	1.97	0.118	115.9	129.1	0.0052	0.474	1.087	120.0	1.025	0.462	1.060
WP-H2	48.0	0.78	3.94	0.118	115.9	129.1	0.0052	0.481	1.063	117.0	1.005	0.478	1.058
WP-H3	48.0	0.78	3.94	0.157	115.9	129.1	0.0052	0.554	1.053	112.0	1.024	0.541	1.028
WP1	48.0	0.78	1.97	0.118	115.6	133.8	0.0064	0.414	1.107	122.0	1.025	0.404	1.081

(a) US Customary Units

Weld ID	Pipe size		Defect dimensions		Material properties			CWP assessment		Critical stress assessment			
	Diameter OD mm	Thickness t mm	Length 2c mm	Height a mm	Yield σ_y N/mm ²	Tensile σ_t N/mm ²	CTOD mm	K_r	L_r	Critical stress σ_{crit} N/mm ²	Factor of safety	K_r	L_r
WP-H1	1220.0	19.8	50.0	3.0	798.8	890.3	0.13	0.474	1.087	827	1.025	0.462	1.060
WP-H2	1220.0	19.8	100.0	3.0	798.8	890.3	0.13	0.481	1.063	807	1.005	0.478	1.058
WP-H3	1220.0	19.9	100.0	4.0	798.8	890.3	0.13	0.554	1.053	772	1.024	0.541	1.028
WP1	1220.0	19.8	50.0	3.0	796.8	922.6	0.16	0.414	1.107	841	1.025	0.404	1.081

(b) SI Units

Table 63 Weld A33: API 1104 Option 2 analysis results.

Weld ID	Pipe size		Defect dimensions		Material properties			CWP assessment		Critical stress assessment			
	Diameter OD in	Thickness t in	Length 2c in	Height a in	Yield σ_y ksi	Tensile σ_t ksi	CTOD in	K_r	L_r	Critical stress σ_{crit} ksi	Factor of safety	K_r	L_r
WP-H1	48.0	0.777	1.97	0.118	112	126	0.0074	0.410	1.094	114.5	1.04	0.394	1.050
WP-H2	48.0	0.778	2.95	0.118	112	126	0.0074	0.410	1.067	115.0	1.00	0.410	1.067
WP-H3	48.0	0.775	3.94	0.118	112	126	0.0074	0.415	1.066	113.0	1.00	0.413	1.061
WP-H4	48.0	0.781	3.94	0.157	112	126	0.0074	0.469	1.036	112.0	0.97	0.483	1.067

(a) US Customary Units

Weld ID	Pipe size		Defect dimensions		Material properties			CWP assessment		Critical stress assessment			
	Diameter OD mm	Thickness t mm	Length 2c mm	Height a mm	Yield σ_y N/mm ²	Tensile σ_t N/mm ²	CTOD mm	K_r	L_r	Critical stress σ_{crit} N/mm ²	Factor of safety	K_r	L_r
WP-H1	1220.0	19.7	50.0	3.0	769.8	871.9	0.19	0.410	1.094	789	1.043	0.394	1.050
WP-H2	1220.0	19.8	75.0	3.0	769.8	871.9	0.19	0.410	1.067	793	1.000	0.410	1.067
WP-H3	1220.0	19.7	100.0	3.0	769.8	871.9	0.19	0.415	1.066	779	1.005	0.413	1.061
WP-H4	1220.0	19.9	100.0	4.0	769.8	871.9	0.19	0.469	1.036	772	0.971	0.483	1.067

(b) SI Units

Table 64 Weld A46: API 1104 Option 2 analysis results.

Weld ID	Pipe size		Defect dimensions		Material properties			CWP assessment		Critical stress assessment			
	Diameter OD in	Thickness t in	Length 2c in	Height a in	Yield σ_y ksi	Tensile σ_t ksi	CTOD in	K_r	L_r	Critical stress σ_{crit} ksi	Factor of safety	K_r	L_r
WP-H1	48.0	0.780	1.97	0.118	113	119	0.0037	0.617	1.100	111.0	1.09	0.563	1.005
WP-H2	48.0	0.780	3.94	0.157	113	119	0.0037	0.736	1.087	101.0	1.14	0.643	0.950
WP1	48.0	0.784	1.97	0.118	113	119	0.0067	0.448	1.076	113.0	1.05	0.425	1.023

(a) US Customary Units

Weld ID	Pipe size		Defect dimensions		Material properties			CWP assessment		Critical stress assessment			
	Diameter OD mm	Thickness t mm	Length 2c mm	Height a mm	Yield σ_y N/mm ²	Tensile σ_t N/mm ²	CTOD mm	K_r	L_r	Critical stress σ_{crit} N/mm ²	Factor of safety	K_r	L_r
WP-H1	1220.0	19.8	50.0	3.0	779.8	817.3	0.09	0.617	1.100	765	1.095	0.563	1.005
WP-H2	1220.0	19.8	100.0	4.0	779.8	817.3	0.09	0.736	1.087	696	1.145	0.643	0.950
WP1	1220.0	19.9	50.0	3.0	779.8	817.3	0.17	0.448	1.076	779	1.052	0.425	1.023

(b) SI Units

Table 65 Weld A50: API 1104 Option 2 analysis results.

Weld ID	Pipe size		Defect dimensions		Material properties			CWP assessment		Critical stress assessment			
	Diameter OD in	Thickness t in	Length 2c in	Height a in	Yield σ_y ksi	Tensile σ_t ksi	CTOD in	K_r	L_r	Critical stress σ_{crit} ksi	Factor of safety	K_r	L_r
WP1	48.0	0.777	5.94	0.179	108	124	0.0024	1.032	1.216	85.0	1.40	0.737	0.868
WP2	48.0	0.779	7.95	0.067	108	124	0.0024	0.602	1.201	106.0	1.17	0.517	1.031
WP3	48.0	0.779	4.55	0.256	108	124	0.0024	1.272	1.249	77.7	1.56	0.815	0.800
WP4	48.0	0.778	5.77	0.173	108	124	0.0024	0.950	1.140	86.5	1.30	0.732	0.878

(a) US Customary Units

Weld ID	Pipe size		Defect dimensions		Material properties			CWP assessment		Critical stress assessment			
	Diameter OD mm	Thickness t mm	Length 2c mm	Height a mm	Yield σ_y N/mm ²	Tensile σ_t N/mm ²	CTOD mm	K_r	L_r	Critical stress σ_{crit} N/mm ²	Factor of safety	K_r	L_r
WP1	1220.0	19.7	151.0	4.5	747.8	858.3	0.06	1.032	1.216	586	1.401	0.737	0.868
WP2	1220.0	19.8	202.0	1.7	747.8	858.3	0.06	0.602	1.201	731	1.166	0.517	1.031
WP3	1220.0	19.8	115.5	6.5	747.8	858.3	0.06	1.272	1.249	536	1.561	0.815	0.800
WP4	1220.0	19.8	146.5	4.4	747.8	858.3	0.06	0.950	1.140	596	1.298	0.732	0.878

(b) SI Units

Table 66 Weld B03: API 1104 Option 2 analysis results.

Weld ID	Pipe size		Defect dimensions		Material properties			CWP assessment		Critical stress assessment			
	Diameter OD in	Thickness t in	Length 2c in	Height a in	Yield σ_y ksi	Tensile σ_t ksi	CTOD in	K_r	L_r	Critical stress σ_{crit} ksi	Factor of safety	K_r	L_r
WP1	48.0	0.788	12.15	0.213	107	115	0.0030	1.214	1.368	74.0	1.603	0.757	0.853
WP3	48.0	0.791	5.71	0.236	107	115	0.0030	1.122	1.223	80.0	1.449	0.775	0.845
WP4	48.0	0.793	5.67	0.197	107	115	0.0030	0.962	1.161	85.0	1.319	0.729	0.880

(a) US Customary Units

Weld ID	Pipe size		Defect dimensions		Material properties			CWP assessment		Critical stress assessment			
	Diameter OD mm	Thickness t mm	Length 2c mm	Height a mm	Yield σ_y N/mm ²	Tensile σ_t N/mm ²	CTOD mm	K_r	L_r	Critical stress σ_{crit} N/mm ²	Factor of safety	K_r	L_r
WP1	1220.0	20.0	308.7	5.4	739.8	792.0	0.08	1.214	1.368	510	1.603	0.757	0.853
WP3	1220.0	20.1	145.0	6.0	739.8	792.0	0.08	1.122	1.223	552	1.449	0.775	0.845
WP4	1220.0	20.1	144.0	5.0	739.8	792.0	0.08	0.962	1.161	586	1.319	0.729	0.880

(b) SI Units

Table 67 Weld B06: API 1104 Option 2 analysis results.

Weld ID	Pipe size		Defect dimensions		Material properties			CWP assessment		Critical stress assessment			
	Diameter OD in	Thickness t in	Length 2c in	Height a in	Yield σ_y ksi	Tensile σ_t ksi	CTOD in	K_r	L_r	Critical stress σ_{crit} ksi	Factor of safety	K_r	L_r
WP1	48.0	0.781	6.81	0.354	110	123	0.0043	0.964	0.998	73.5	1.218	0.792	0.820
WP2	48.0	0.782	0.00	0.000	110	123	0.0043	0.000	1.104	116.5	1.042	0.000	1.059
WP3	48.0	0.782	5.71	0.425	110	123	0.0043	1.075	1.015	70.0	1.299	0.827	0.781

(a) US Customary Units

Weld ID	Pipe size		Defect dimensions		Material properties			CWP assessment		Critical stress assessment			
	Diameter OD mm	Thickness t mm	Length 2c mm	Height a mm	Yield σ_y N/mm ²	Tensile σ_t N/mm ²	CTOD mm	K_r	L_r	Critical stress σ_{crit} N/mm ²	Factor of safety	K_r	L_r
WP1	1220.0	19.8	173.0	9.0	757.8	850.5	0.11	0.964	0.998	507	1.218	0.792	0.820
WP2	1220.0	19.9	0.0	0.0	757.8	850.5	0.11	0.000	1.104	803	1.042	0.000	1.059
WP3	1220.0	19.9	145.0	10.8	757.8	850.5	0.11	1.075	1.015	483	1.299	0.827	0.781

(b) SI Units

Table 68 Weld B08: API 1104 Option 2 analysis results.

Weld ID	Pipe size		Defect dimensions		Material properties			Analysis			
	Diameter OD in	Thickness t in	Length L in	Height d in	Yield σ_y ksi	Tensile σ_t ksi	CTOD in	Critical stress σ_a ksi	Actual stress σ_{actual} ksi	Factor of safety	Predicted failure type
WP-H1	48.0	0.78	1.97	0.118	115.6	126.6	0.0034	116	125	1.08	Plastic collapse
WP-H2	48.0	0.78	3.94	0.118	115.6	126.6	0.0034	100	117	1.17	Brittle fracture
WP-H3	48.0	0.79	3.94	0.157	115.6	126.6	0.0034	86	114	1.33	Brittle fracture
WP1	48.0	0.78	1.97	0.118	115.6	126.6	0.0057	116	124	1.07	Plastic collapse

(a) US Customary Units

Weld ID	Pipe size		Defect dimensions		Material properties			Analysis			
	Diameter OD mm	Thickness t mm	Length L mm	Height d mm	Yield σ_y N/mm ²	Tensile σ_t N/mm ²	CTOD mm	Critical stress σ_a N/mm ²	Actual stress σ_{actual} N/mm ²	Factor of safety	Predicted failure type
WP-H1	1220	19.8	50	3.0	797	873	0.09	798	865	1.08	Plastic collapse
WP-H2	1220	19.9	100	3.0	797	873	0.09	690	810	1.17	Brittle fracture
WP-H3	1220	20.0	100	4.0	797	873	0.09	591	787	1.33	Brittle fracture
W	1220	19.9	50	3.0	797	873	0.15	798	857	1.07	Plastic collapse

(b) SI Units

Table 69 Weld A06: CSA Z662 analysis results.

Weld ID	Pipe size		Defect dimensions		Material properties			Analysis			
	Diameter OD in	Thickness t in	Length L in	Height d in	Yield σ_y ksi	Tensile σ_t ksi	CTOD in	Critical stress σ_a ksi	Actual stress σ_{actual} ksi	Factor of safety	Predicted failure type
WP-H1	48.0	0.78	1.97	0.118	106.3	113.7	0.0091	106	120	1.13	Plastic collapse
WP-H2	48.0	0.78	3.94	0.118	106.3	113.7	0.0091	104	115	1.11	Plastic collapse
WP-H3	48.0	0.78	3.94	0.118	106.3	113.7	0.0091	104	113	1.09	Plastic collapse
W	48.0	0.78	1.97	0.118	106.3	113.7	0.0091	106	118	1.11	Plastic collapse

(a) US Customary Units

Weld ID	Pipe size		Defect dimensions		Material properties			Analysis			
	Diameter OD mm	Thickness t mm	Length L mm	Height d mm	Yield σ_y N/mm ²	Tensile σ_t N/mm ²	CTOD mm	Critical stress σ_a N/mm ²	Actual stress σ_{actual} N/mm ²	Factor of safety	Predicted failure type
WP-H1	1220	19.8	50	3.0	733	784	0.23	734	829	1.13	Plastic collapse
WP-H2	1220	19.8	100	3.0	733	784	0.23	715	795	1.11	Plastic collapse
WP-H3	1220	19.8	100	3.0	733	784	0.23	715	782	1.09	Plastic collapse
W	1220	19.8	50	3.0	733	784	0.23	734	817	1.11	Plastic collapse

(b) SI Units

Table 70 Weld A17: CSA Z662 analysis results.

Weld ID	Pipe size		Defect dimensions		Material properties			Analysis			
	Diameter OD in	Thickness t in	Length L in	Height d in	Yield σ_y ksi	Tensile σ_t ksi	CTOD in	Critical stress σ_a ksi	Actual stress σ_{actual} ksi	Factor of safety	Predicted failure type
WP-H1	48.0	0.78	1.97	0.118	115.9	129.1	0.0051	116	123	1.06	Plastic collapse
WP-H2	48.0	0.78	3.94	0.118	115.9	129.1	0.0051	113	118	1.04	Plastic collapse
WP-H3	48.0	0.78	3.94	0.157	115.9	129.1	0.0051	99	115	1.15	Brittle fracture
W	48.0	0.78	1.97	0.118	115.9	129.1	0.0051	116	125	1.08	Plastic collapse

(a) US Customary Units

Weld ID	Pipe size		Defect dimensions		Material properties			Analysis			
	Diameter OD mm	Thickness t mm	Length L mm	Height d mm	Yield σ_y N/mm ²	Tensile σ_t N/mm ²	CTOD mm	Critical stress σ_a N/mm ²	Actual stress σ_{actual} N/mm ²	Factor of safety	Predicted failure type
WP-H1	1220	19.8	50	3.0	799	890	0.13	800	848	1.06	Plastic collapse
WP-H2	1220	19.8	100	3.0	799	890	0.13	779	811	1.04	Plastic collapse
WP-H3	1220	19.8	100	4.0	799	890	0.13	686	791	1.15	Brittle fracture
W	1220	19.8	50	3.0	799	890	0.13	800	862	1.08	Plastic collapse

(b) SI Units

Table 71 Weld A33: CSA Z662 analysis results.

Weld ID	Pipe size		Defect dimensions		Material properties			Analysis			
	Diameter OD in	Thickness t in	Length L in	Height d in	Yield σ_y ksi	Tensile σ_t ksi	CTOD in	Critical stress σ_a ksi	Actual stress σ_{actual} ksi	Factor of safety	Predicted failure type
WP-H1	48.0	0.78	1.97	0.118	111.7	126.5	0.0075	112	119	1.07	Plastic collapse
WP-H2	48.0	0.78	2.95	0.118	111.7	126.5	0.0075	110	115	1.04	Plastic collapse
WP-H3	48.0	0.78	3.94	0.118	111.7	126.5	0.0075	109	114	1.04	Plastic collapse
WP-H4	48.0	0.78	3.94	0.157	111.7	126.5	0.0075	107	109	1.02	Plastic collapse

(a) US Customary Units

Weld ID	Pipe size		Defect dimensions		Material properties			Analysis			
	Diameter OD mm	Thickness t mm	Length L mm	Height d mm	Yield σ_y N/mm ²	Tensile σ_t N/mm ²	CTOD mm	Critical stress σ_a N/mm ²	Actual stress σ_{actual} N/mm ²	Factor of safety	Predicted failure type
WP-H1	1220	19.8	50	3.0	770	872	0.19	771	823	1.07	Plastic collapse
WP-H2	1220	19.8	75	3.0	770	872	0.19	761	793	1.04	Plastic collapse
WP-H3	1220	19.8	100	3.0	770	872	0.19	751	783	1.04	Plastic collapse
WP-H4	1220	19.8	100	4.0	770	872	0.19	737	750	1.02	Plastic collapse

(b) SI Units

Table 72 Weld A46: CSA Z662 analysis results.

Weld ID	Pipe size		Defect dimensions		Material properties			Analysis			
	Diameter OD in	Thickness t in	Length L in	Height d in	Yield σ_y ksi	Tensile σ_t ksi	CTOD in	Critical stress σ_a ksi	Actual stress σ_{actual} ksi	Factor of safety	Predicted failure type
WP-H1	48.0	0.78	1.97	0.118	113.1	118.5	0.0035	113	122	1.07	Plastic collapse
WP-H2	48.0	0.78	3.94	0.157	113.1	118.5	0.0035	83	116	1.38	Brittle fracture
W	48.0	0.78	1.97	0.118	113.1	118.5	0.0035	113	119	1.05	Plastic collapse

(a) US Customary Units

Weld ID	Pipe size		Defect dimensions		Material properties			Analysis			
	Diameter OD mm	Thickness t mm	Length L mm	Height d mm	Yield σ_y N/mm ²	Tensile σ_t N/mm ²	CTOD mm	Critical stress σ_a N/mm ²	Actual stress σ_{actual} N/mm ²	Factor of safety	Predicted failure type
WP-H1	1220	19.8	50	3.0	780	817	0.09	781	838	1.07	Plastic collapse
WP-H2	1220	19.8	100	4.0	780	817	0.09	576	797	1.38	Brittle fracture
W	1220	19.8	50	3.0	780	817	0.09	781	820	1.05	Plastic collapse

(b) SI Units

Table 73 Weld A50: CSA Z662 analysis results.

Weld ID	Pipe size		Defect dimensions			Material properties			Analysis			
	Diameter OD in	Thickness t in	Length L in	Height d in	Ligament ρ in	Yield σ_y ksi	Tensile σ_t ksi	CTOD in	Critical stress σ_a ksi	Actual stress σ_{actual} ksi	Factor of safety	Predicted failure type
WP1	48.0	0.78	5.9	0.179	N/A	108.5	124.5	0.0024	51.6	119.1	2.31	Brittle fracture
WP2	48.0	0.78	8.0	0.067	0.287	108.5	124.5	0.0024	104.9	123.6	1.18	Plastic collapse
WP3	48.0	0.78	4.5	0.256	0.213	108.5	124.5	0.0024	97.6	121.3	1.24	Plastic collapse
WP4	48.0	0.78	5.8	0.173	0.299	108.5	124.5	0.0024	99.5	112.3	1.13	Plastic collapse

(a) US Customary Units

Weld ID	Pipe size		Defect dimensions			Material properties			Analysis			
	Diameter OD mm	Thickness t mm	Length L mm	Height d mm	Ligament ρ mm	Yield σ_y N/mm ²	Tensile σ_t N/mm ²	CTOD mm	Critical stress σ_a N/mm ²	Actual stress σ_{actual} N/mm ²	Factor of safety	Predicted failure type
WP1	1220	19.8	151	4.5	N/A	748	858	0.06	356	821	2.31	Brittle fracture
WP2	1220	19.8	202	1.7	7.3	748	858	0.06	724	852	1.18	Plastic collapse
WP3	1220	19.8	116	6.5	5.4	748	858	0.06	673	836	1.24	Plastic collapse
WP4	1220	19.8	147	4.4	7.6	748	858	0.06	686	774	1.13	Plastic collapse

(b) SI Units

Table 74 Weld B03: CSA Z662 analysis results.

Weld ID	Pipe size		Defect dimensions			Material properties			Analysis			
	Diameter OD in	Thickness t in	Length L in	Height d in	Ligament ρ in	Yield σ_y ksi	Tensile σ_t ksi	CTOD in	Critical stress σ_a ksi	Actual stress σ_{actual} ksi	Factor of safety	Predicted failure type
WP1	48.0	0.78	12.2	0.213		107.3	114.9	0.0031	98.8	118.6	1.20	Plastic collapse
WP2	48.0	0.78	No defect present			107.3	114.9	0.0031	Test terminated without failure of the specimen			
WP3	48.0	0.78	5.7	0.236	0.228	107.3	114.9	0.0031	94.6	>115.9*	>1.22*	Plastic collapse
WP4	48.0	0.78	5.7	0.197	0.276	107.3	114.9	0.0031	97.1	112.1	1.15	Plastic collapse

(a) US Customary Units

Weld ID	Pipe size		Defect dimensions			Material properties			Analysis			
	Diameter OD mm	Thickness t mm	Length L mm	Height d mm	Ligament ρ mm	Yield σ_y N/mm ²	Tensile σ_t N/mm ²	CTOD mm	Critical stress σ_a N/mm ²	Actual stress σ_{actual} N/mm ²	Factor of safety	Predicted failure type
WP1	1220	19.8	309	5.4		740	792	0.08	681	818	1.20	Plastic collapse
WP2	1220	19.8	No defect present			740	792	0.08	Test terminated without failure of the specimen			
WP3	1220	19.8	145	6.0	5.8	740	792	0.08	653	>799*	>1.22*	Plastic collapse
WP4	1220	19.8	144	5.0	7.0	740	792	0.08	670	773	1.15	Plastic collapse

(b) SI Units

Notes: * The testing of CWP specimen WP3 was terminated without failure of the specimens

Table 75 Weld B06: CSA Z662 analysis results.

Weld ID	Pipe size		Defect dimensions			Material properties			Analysis			
	Diameter OD in	Thickness t in	Length L in	Height d in	Ligament ρ in	Yield σ_y ksi	Tensile σ_t ksi	CTOD in	Critical stress σ_a ksi	Actual stress σ_{actual} ksi	Factor of safety	Predicted failure type
WP1	48.0	0.78	6.8	0.354	0.021	109.9	123.4	0.0043	78.4	89.5	1.14	Brittle fracture
WP2	48.0	0.78	No defect present			109.9	123.4	0.0043	Test terminated without failure of the specimen			
WP3	48.0	0.78	5.7	0.425	0.165	109.9	123.4	0.0043	86.2	90.9	1.05	Plastic collapse

(a) US Customary Units

Weld ID	Pipe size		Defect dimensions			Material properties			Analysis			
	Diameter OD mm	Thickness t mm	Length L mm	Height d mm	Ligament ρ mm	Yield σ_y N/mm ²	Tensile σ_t N/mm ²	CTOD mm	Critical stress σ_a N/mm ²	Actual stress σ_{actual} N/mm ²	Factor of safety	Predicted failure type
WP1	1220	19.8	173	9.0	0.5	758	851	0.11	540	617	1.14	Brittle fracture
WP2	1220	19.8	No defect present			758	851	0.11	Test terminated without failure of the specimen			
WP3	1220	19.8	145	10.8	4.2	758	851	0.11	595	627	1.05	Plastic collapse

(b) SI Units

Table 76 Weld B08: CSA Z662 analysis results.

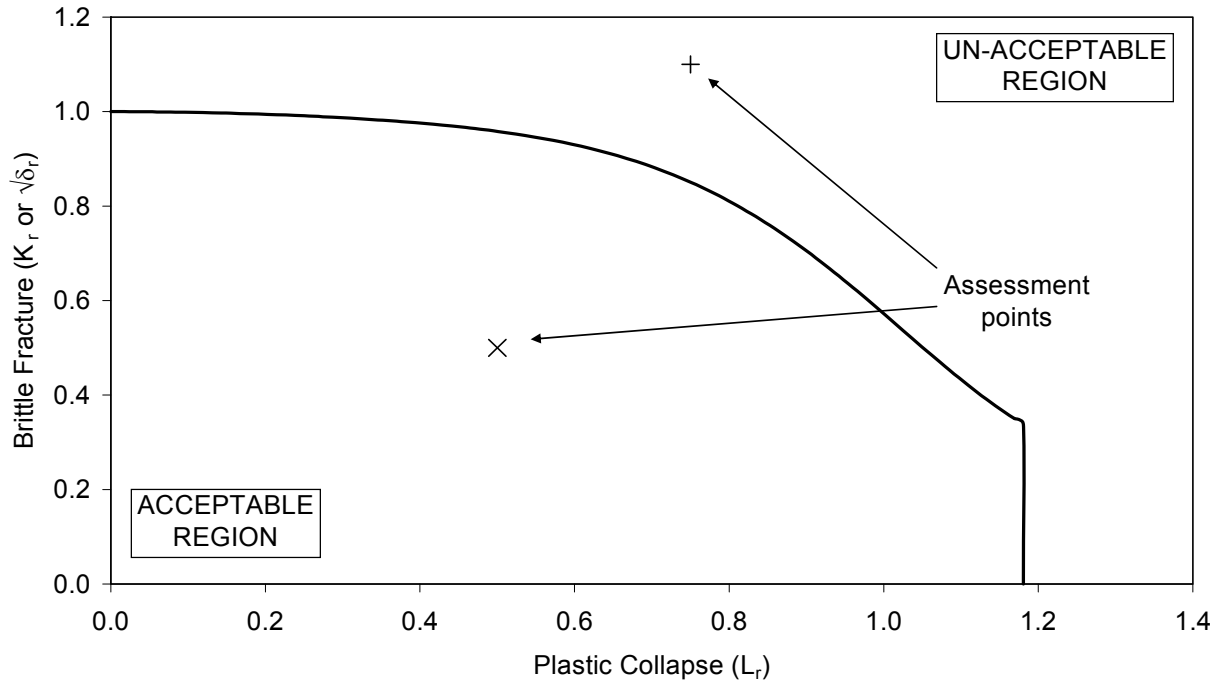


Figure 1 Example of a Failure Assessment Diagram (FAD): Level 2 FAD shown.

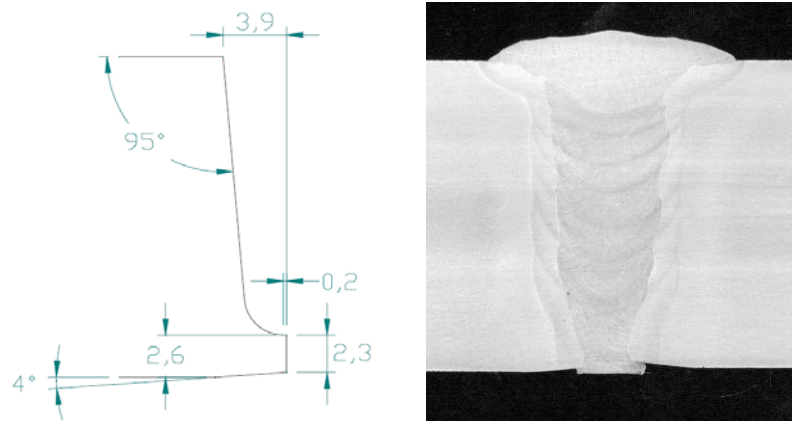
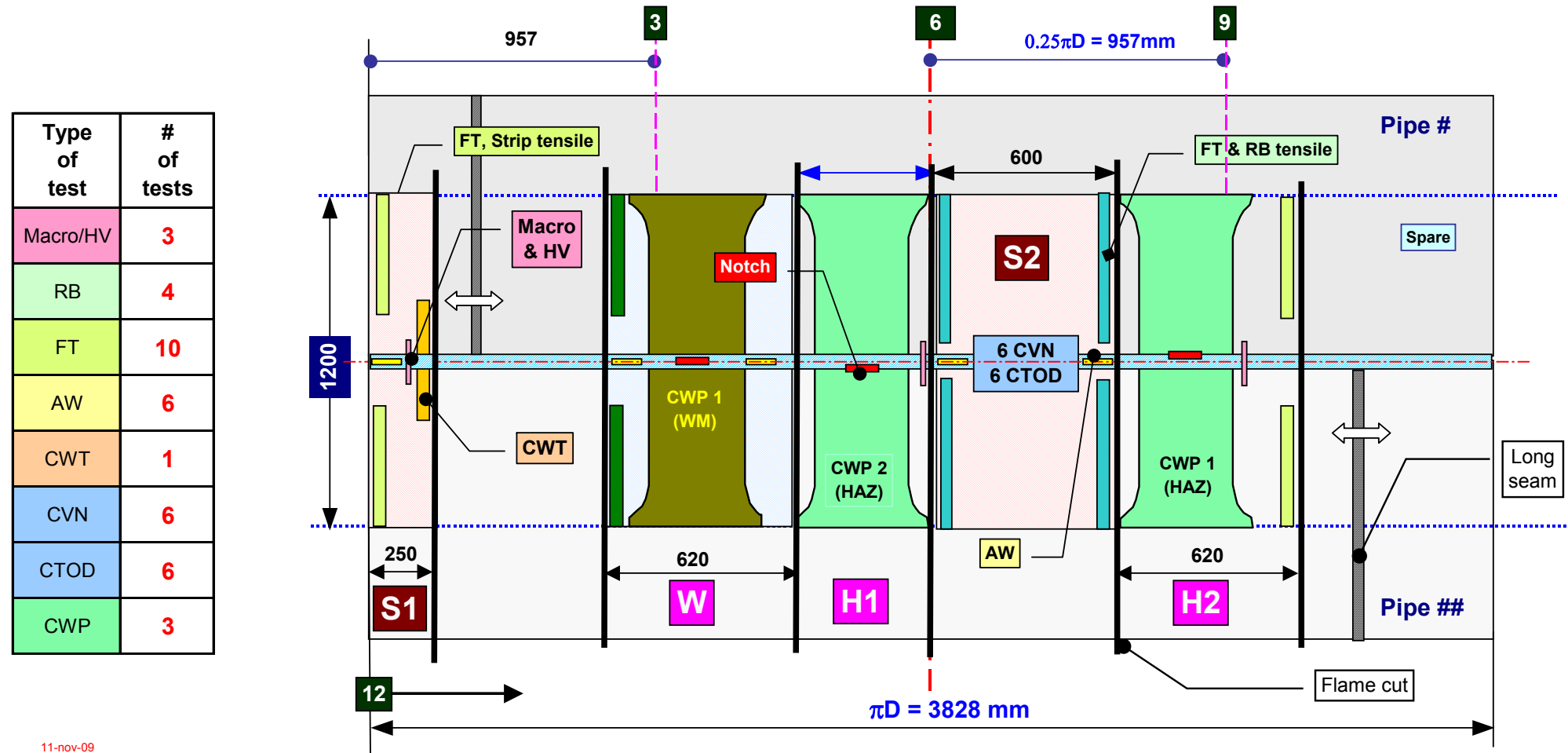


Figure 2 Weld bevel design and weld macro.



11-nov-09

Figure 3 Typical specimen sampling / weld cutting plan (as provided by University of Gent).

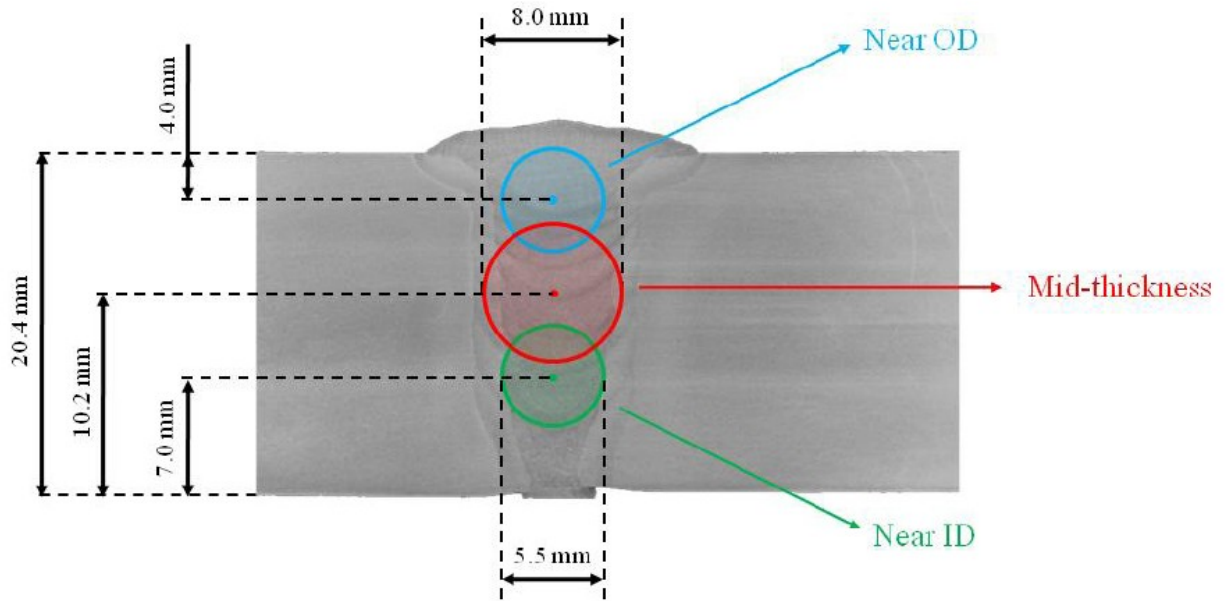


Figure 4 **Weld B10:** Through wall sampling plan for the round bar specimens.

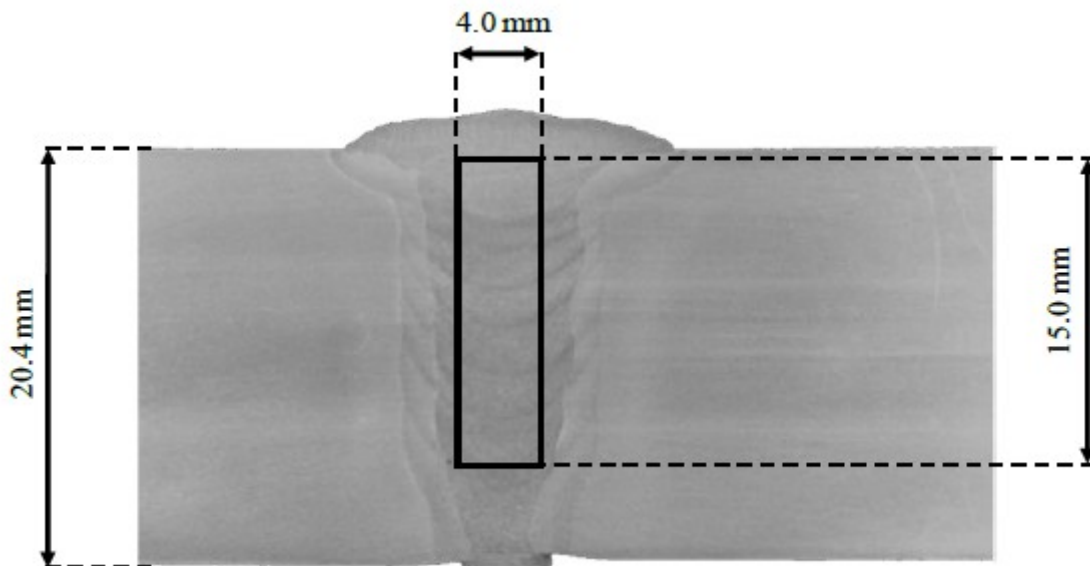
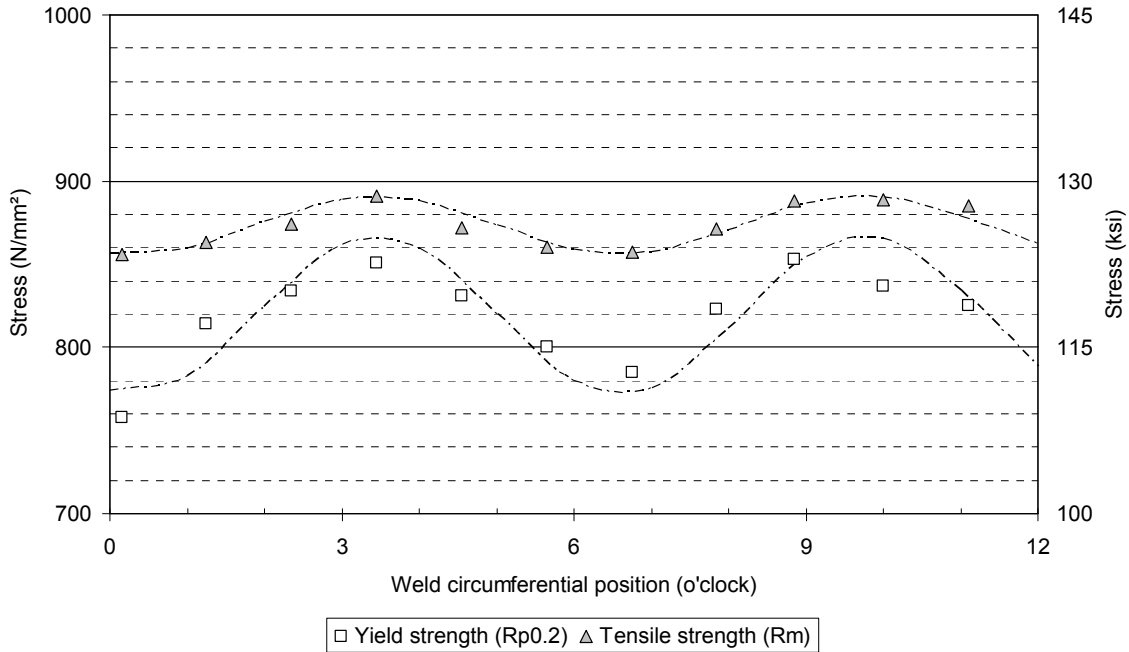
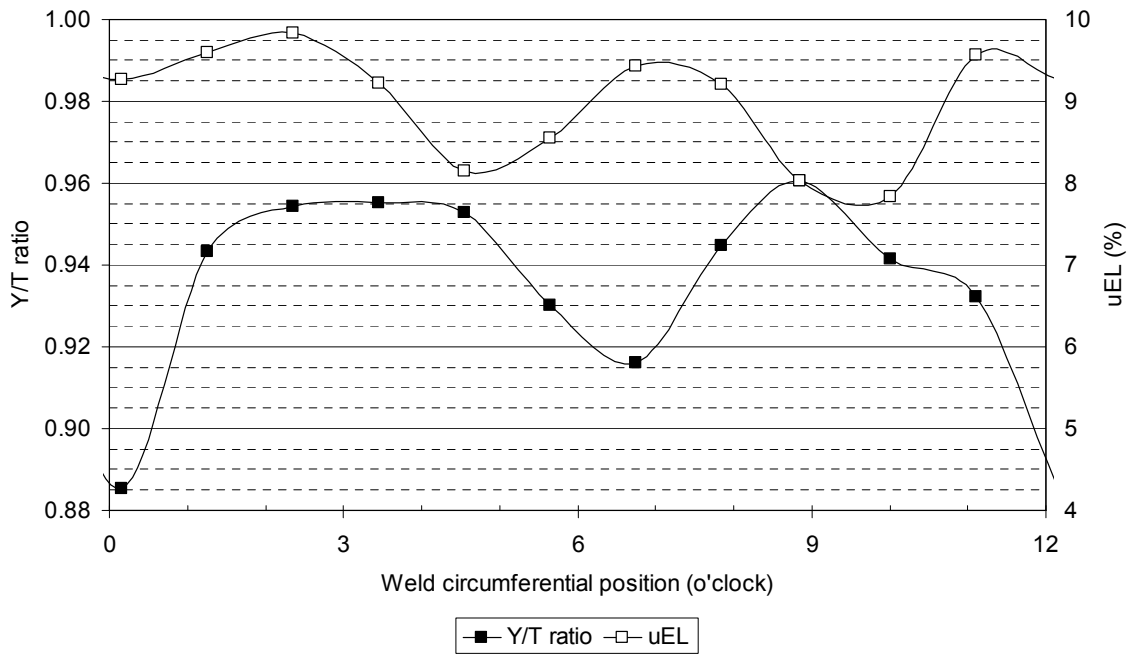


Figure 5 **Weld B10:** Through wall location of rectangular section tensile specimen.

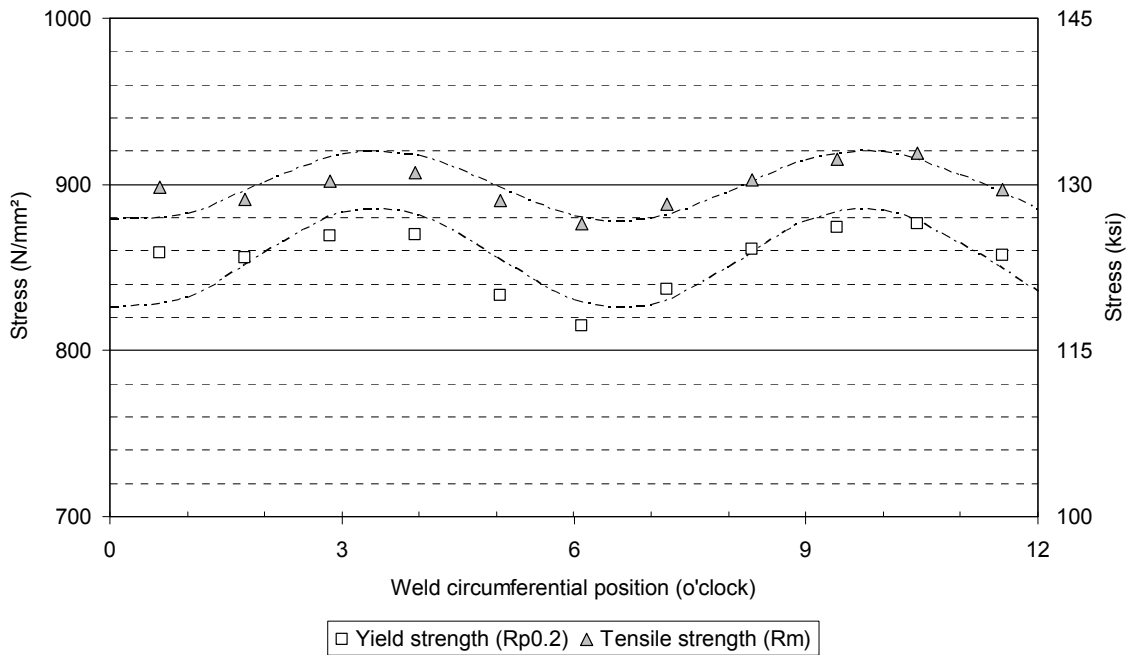


(a) Yield and tensile strength

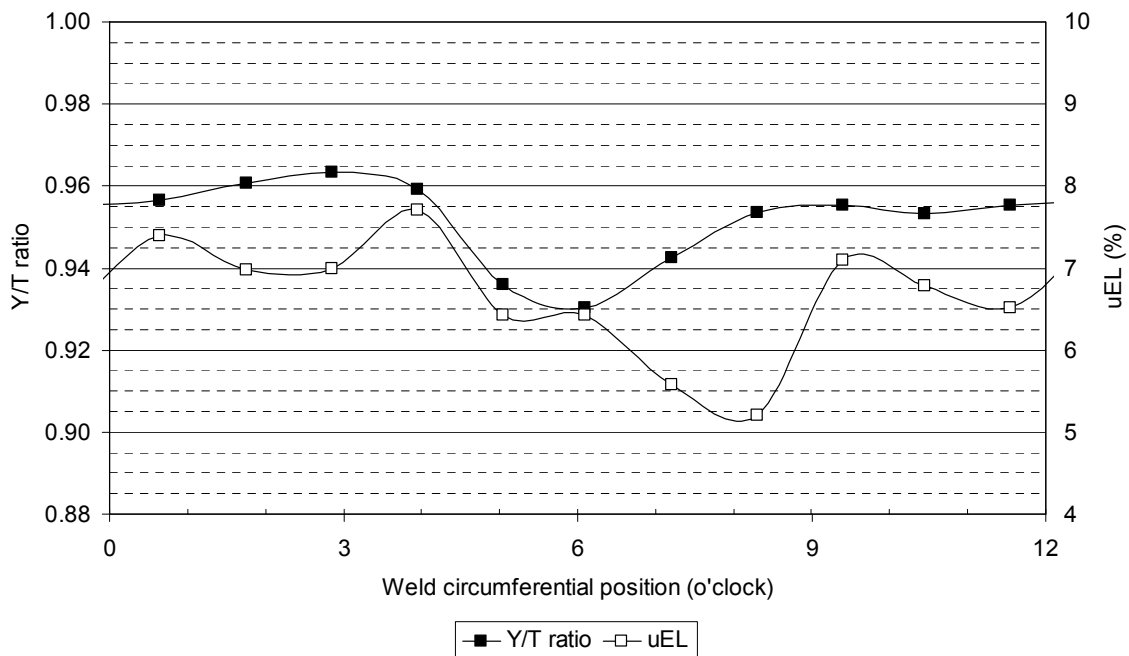


(b) Y/T ratio and uEL

Figure 6 **Weld B10:** Circumferential variation in tensile properties in the **weld cap region** – round bar specimens, tested at 68°F (20°C).

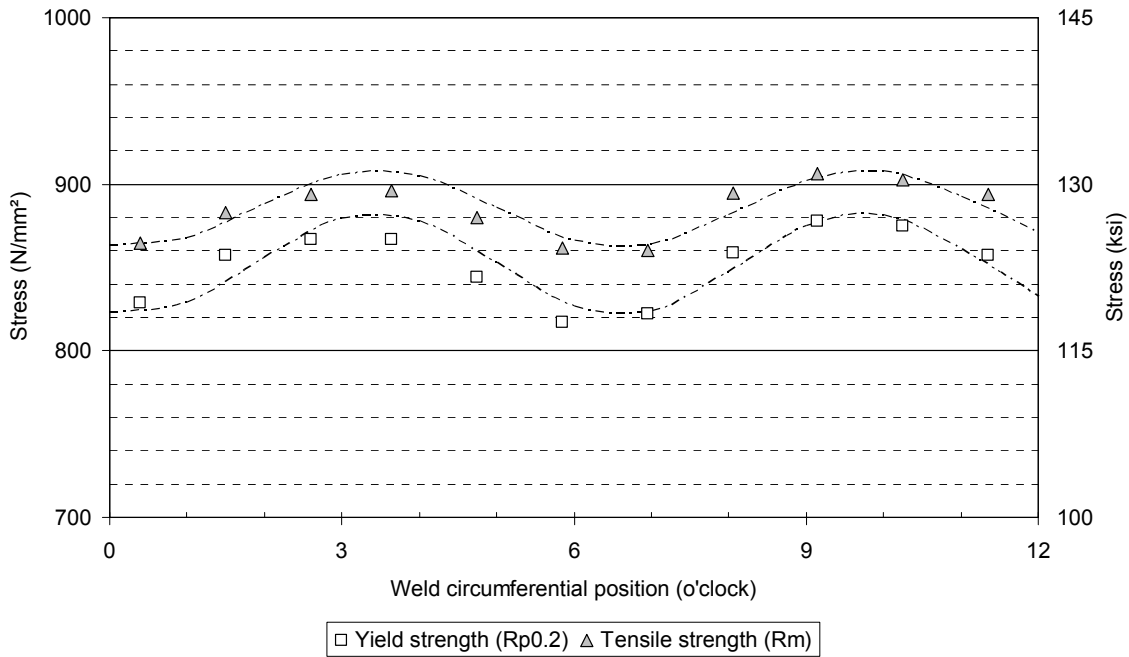


(a) Yield and tensile strength

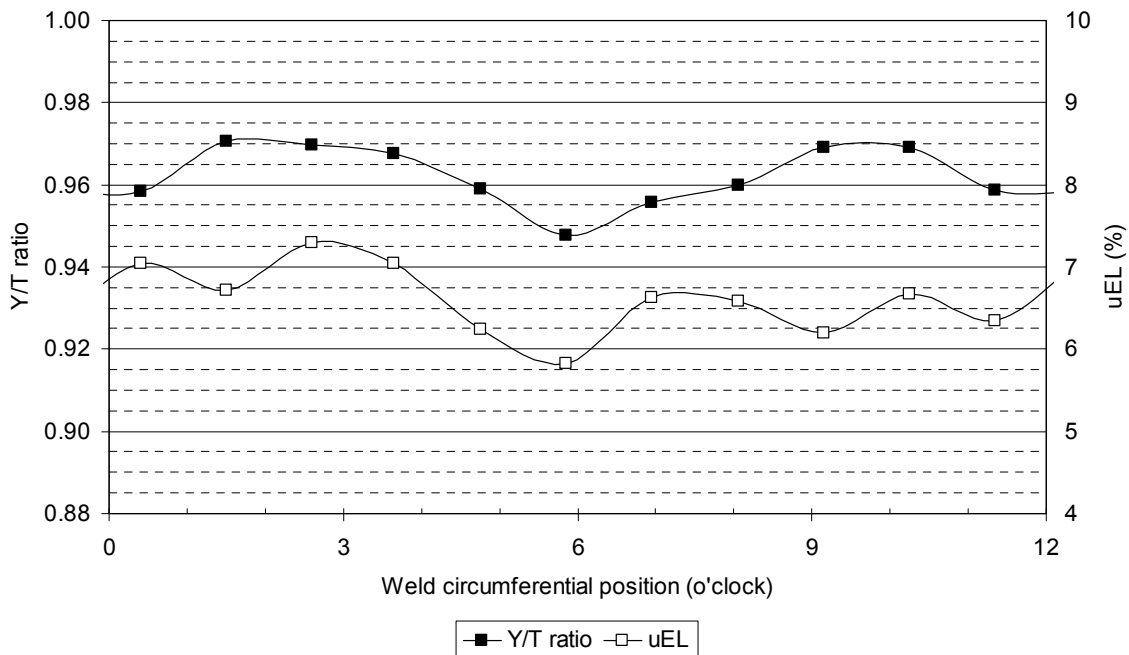


(b) Y/T ratio and uEL

Figure 7 **Weld B10:** Circumferential variation in tensile properties in the **weld root region** – round bar specimens, tested at 68°F (20°C).

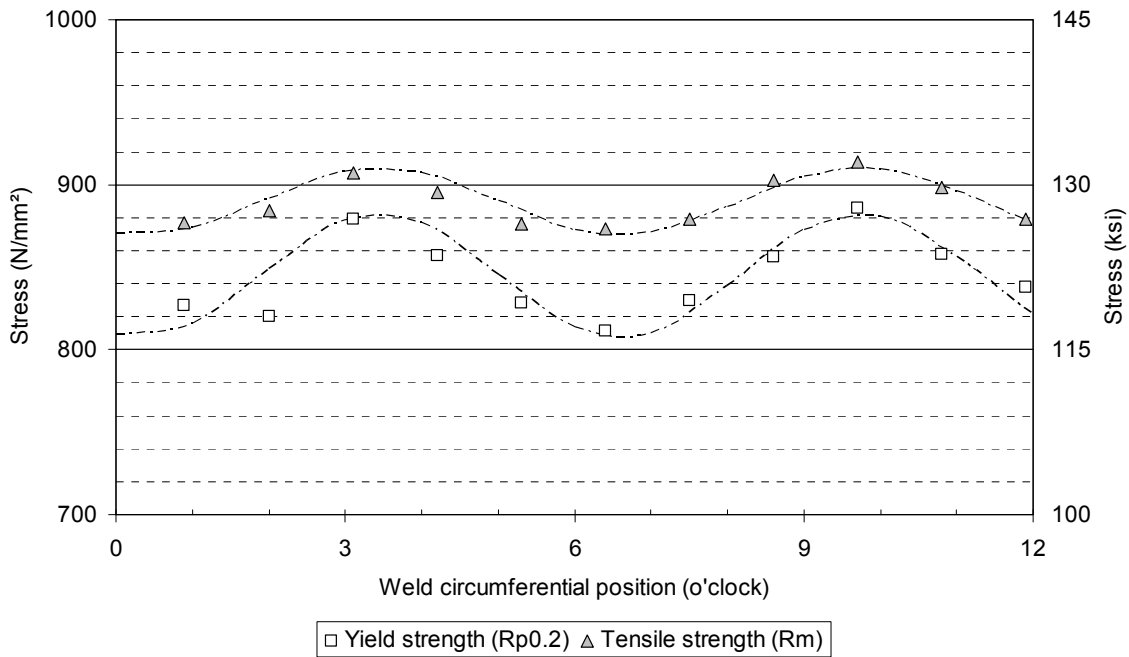


(a) Yield and tensile strength

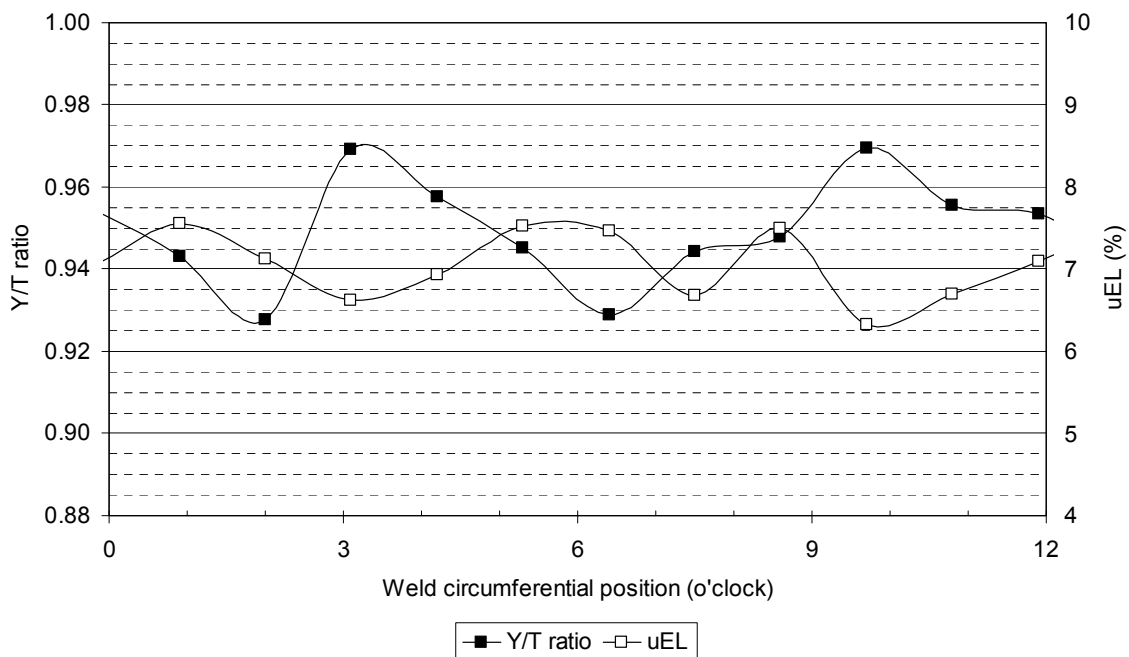


(b) Y/T ratio and uEL

Figure 8 **Weld B10**: Circumferential variation in tensile properties in the **weld mid-thickness region** – round bar specimens, tested at 68°F (20°C).



(a) Yield and tensile strength



(b) Y/T ratio and uEL

Figure 9 **Weld B10:** Circumferential variation in tensile properties for the **weld full-thickness** – rectangular specimens, tested at 68°F (20°C).

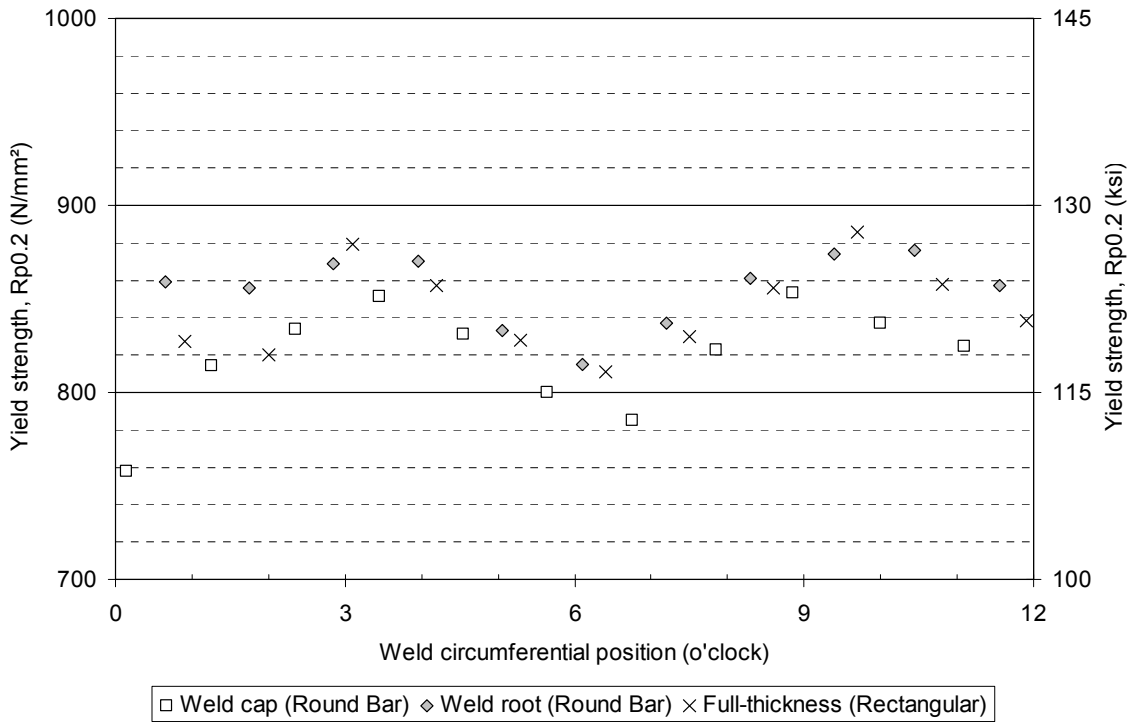


Figure 10 **Weld B10:** through thickness variation in yield strength around the pipe circumference.

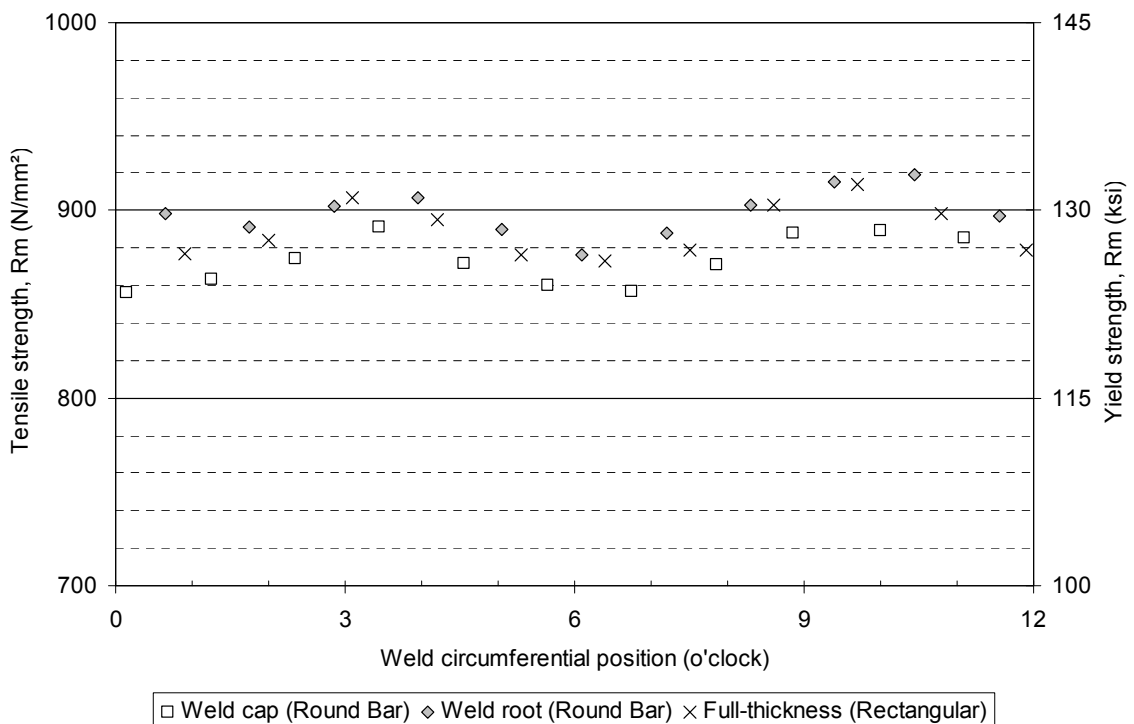


Figure 11 **Weld B10:** through thickness variation in tensile strength around the pipe circumference.

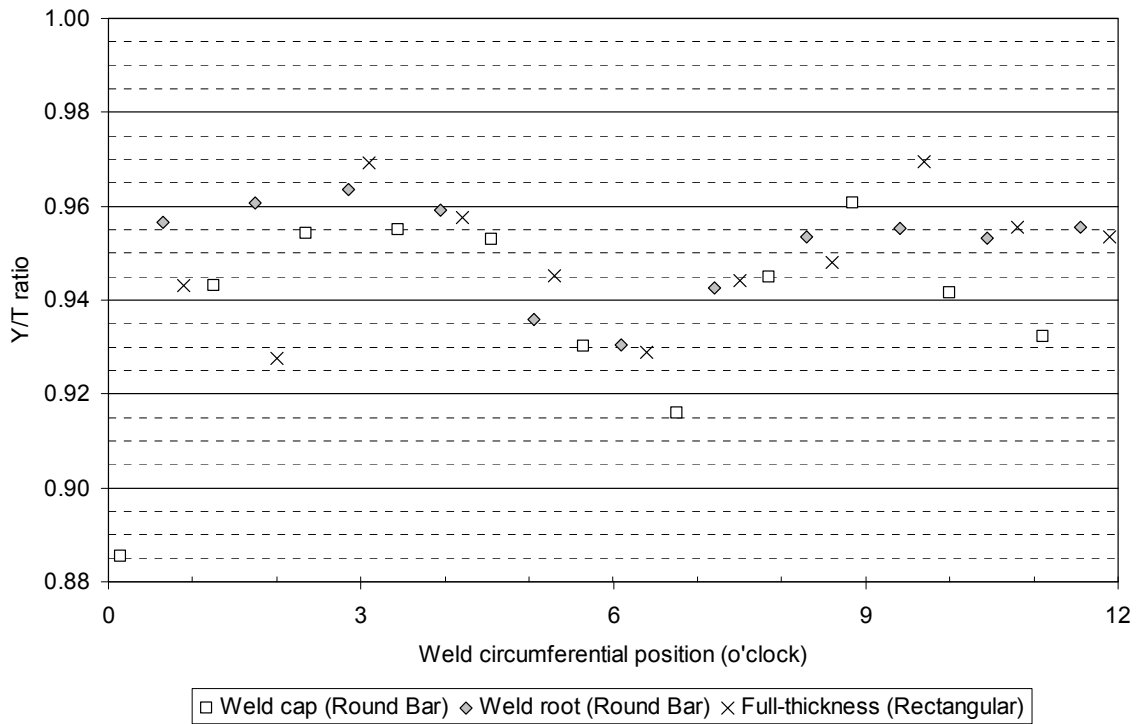


Figure 12 **Weld B10**: through thickness variation in Y/T ratio around the pipe circumference.

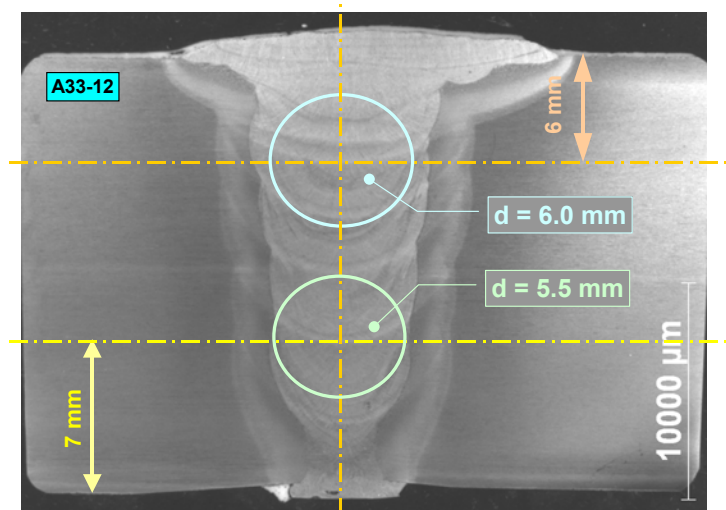


Figure 13 Through wall sampling plan for the all weld metal round bar specimens for all welds, except B10.

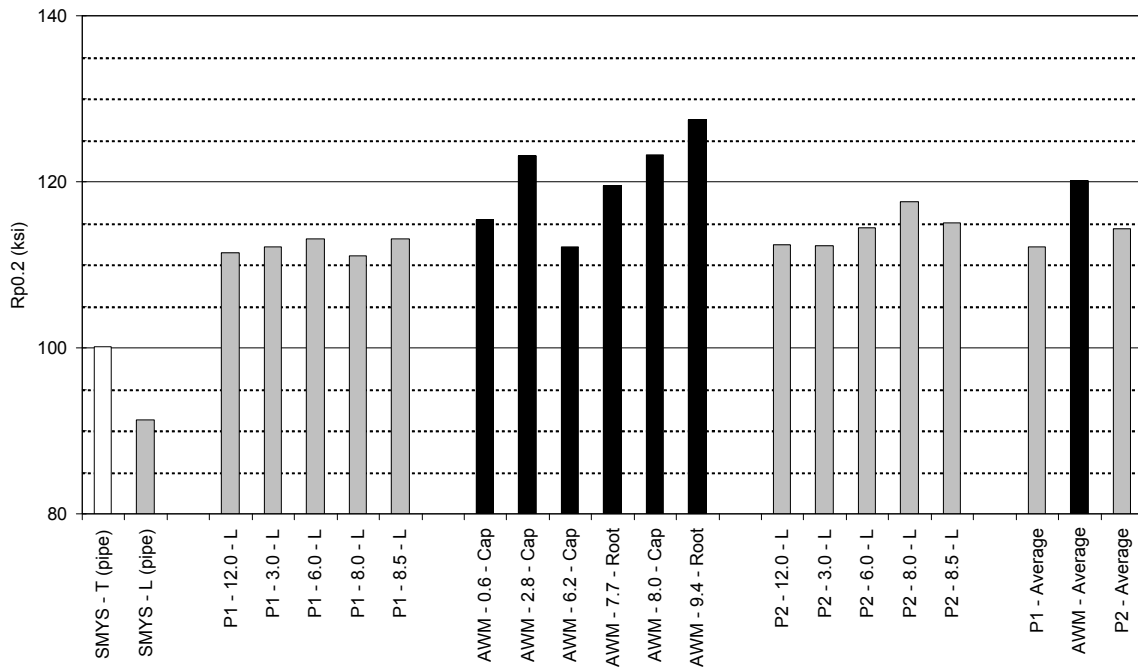


Figure 14 **Weld A06:** Comparison of yield strength of the pipe in the *longitudinal* direction with the all weld metal yield strength. Tested at 68°F (20°C).

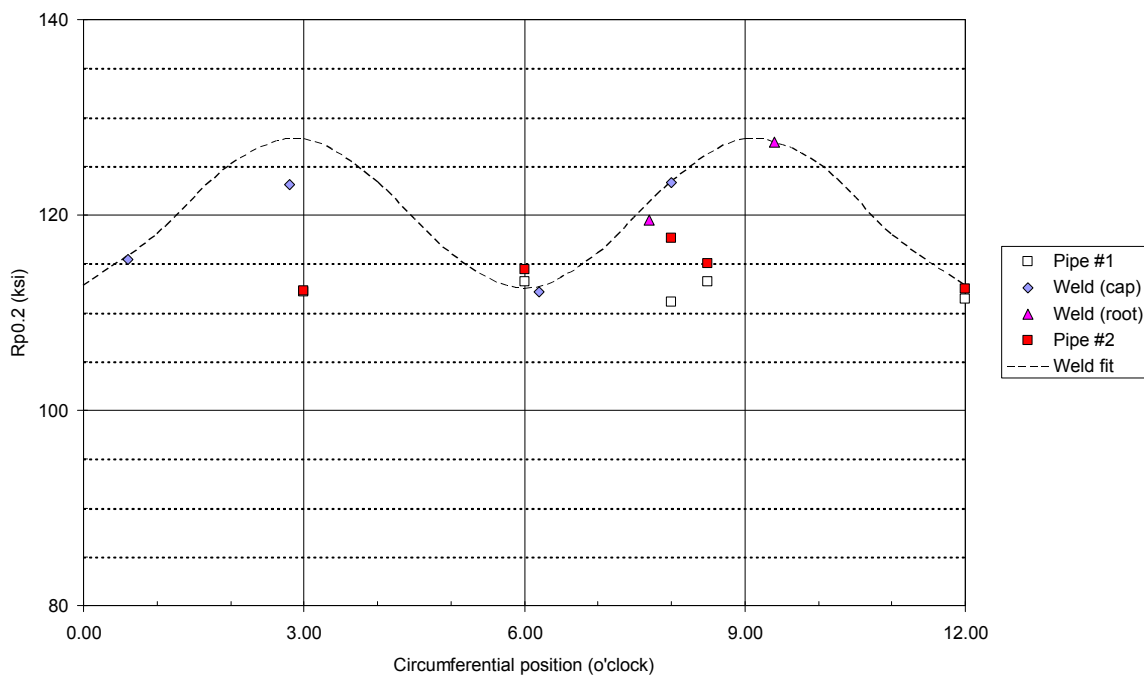


Figure 15 **Weld A06:** Comparison of yield strength (pipe *longitudinal* direction and all weld metal tests) in relation to the pipe circumferential position. Tested at 68°F (20°C).

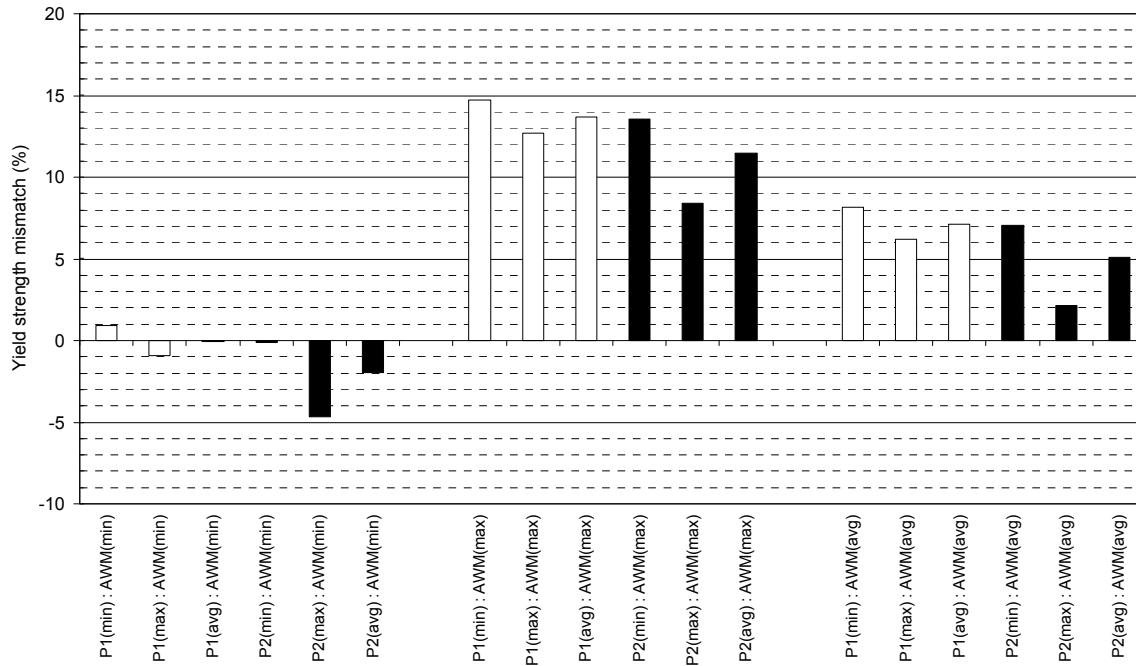


Figure 16 **Weld A06:** Comparison of the weld metal yield strength to the pipe yield strength in the *longitudinal* direction. Tested at 68°F (20°C).

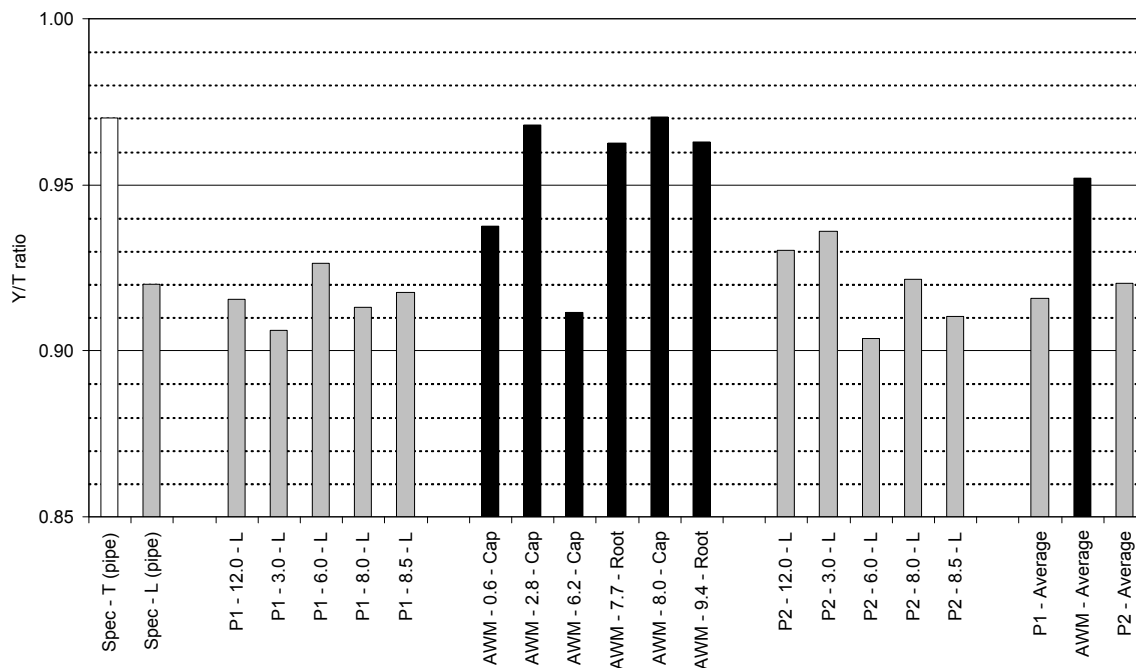


Figure 17 **Weld A06:** Comparison of yield to tensile strength ratio of the pipe in the *longitudinal* direction with the weld metal. Tested at 68°F (20°C).

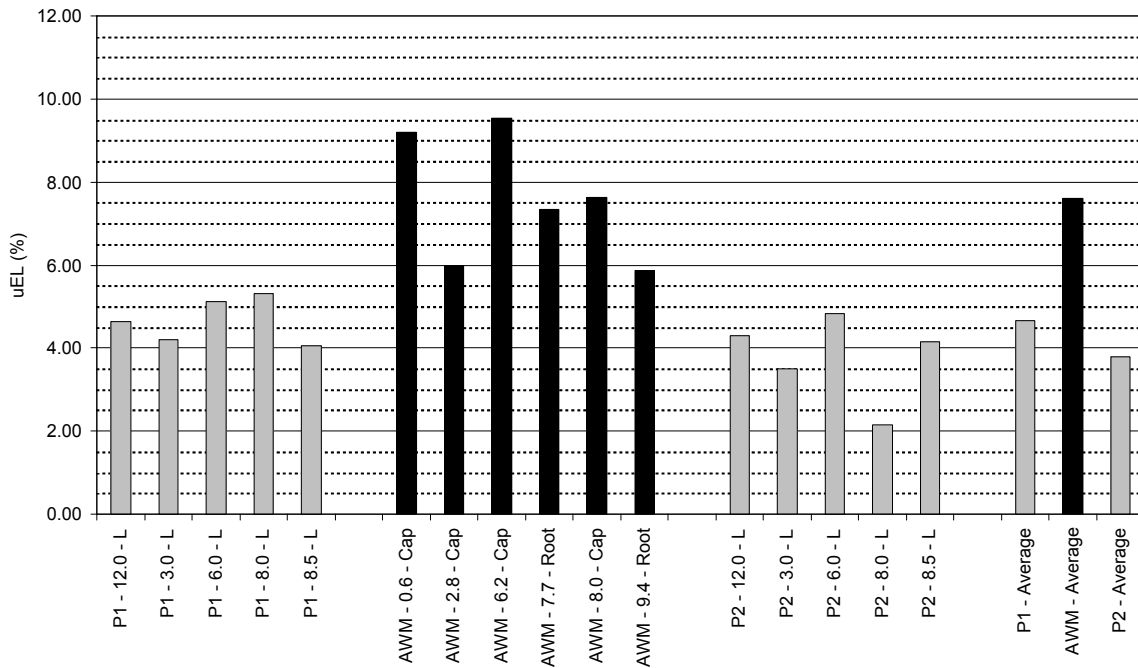
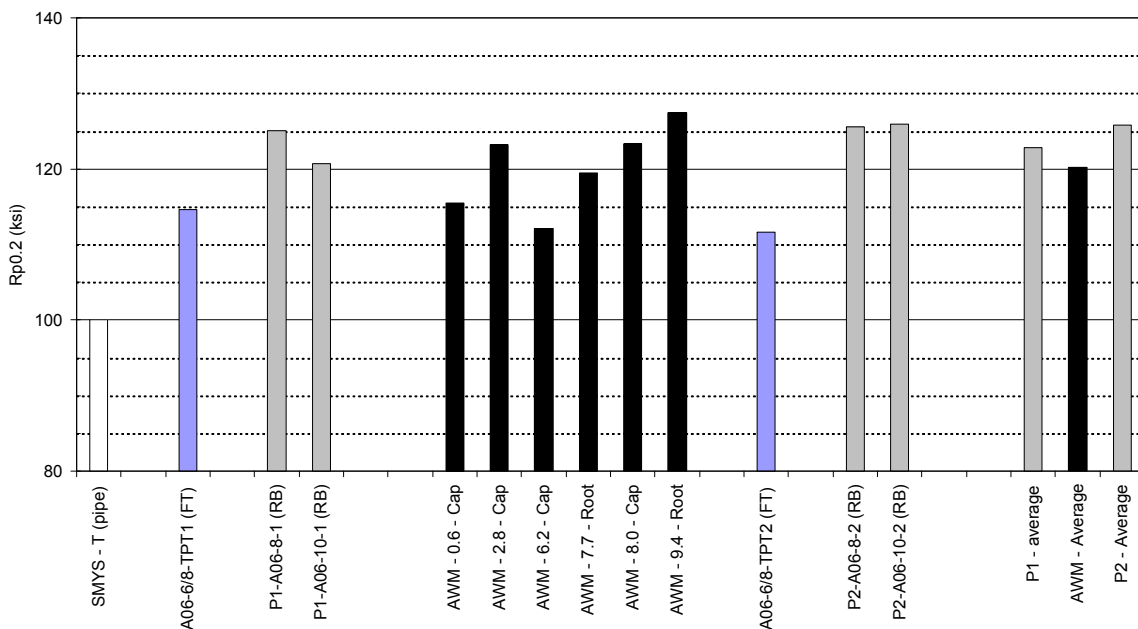
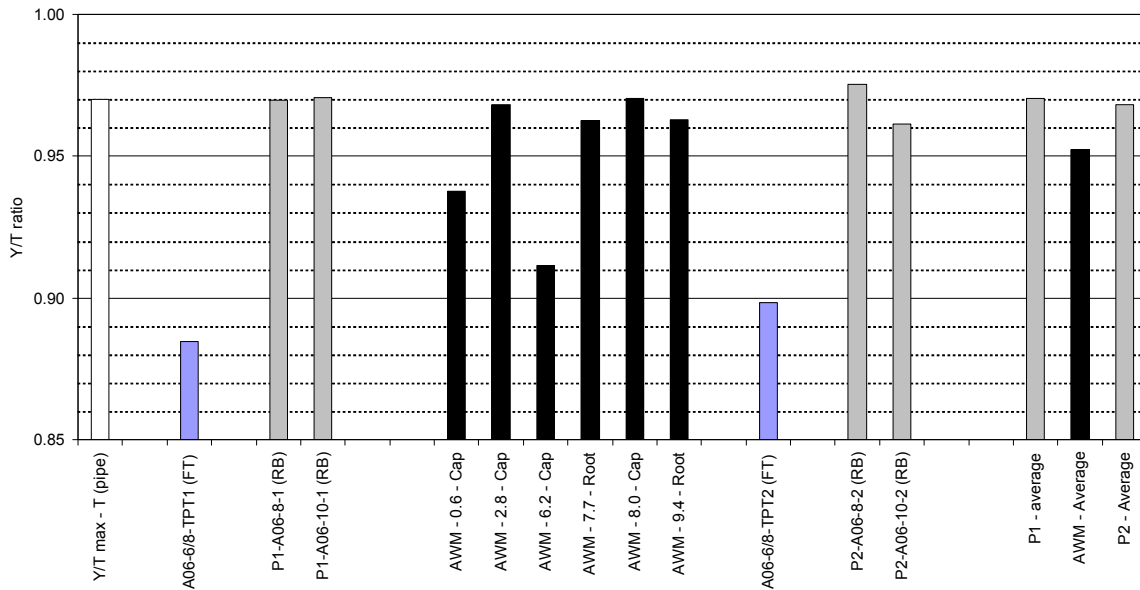


Figure 18 **Weld A06:** Comparison of the strain capacity of the pipe in the *longitudinal* direction with the all weld metal tests. Tested at 68°F (20°C).



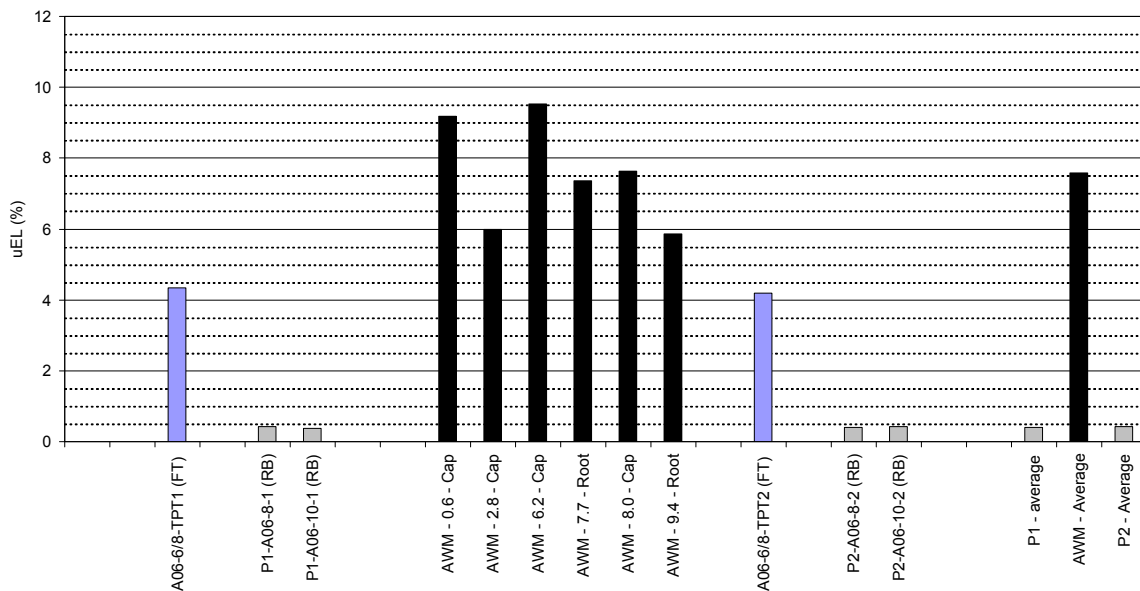
Notes: FT and RB are Flat Tensile and Round Bar specimens respectively

Figure 19 **Weld A06:** Comparison of yield strength of the pipe in the *transverse* direction with the all weld metal yield strength. Tested at 68°F (20°C).



Notes: FT and RB are Flat Tensile and Round Bar specimens respectively

Figure 20 **Weld A06:** Comparison of the weld metal yield strength to the pipe yield strength in the *transverse* direction. Tested at 68°F (20°C).



Notes: FT and RB are Flat Tensile and Round Bar specimens respectively

Figure 21 **Weld A06:** Comparison of the strain capacity of the pipe in the *transverse* direction with the all weld metal tests. Tested at 68°F (20°C).

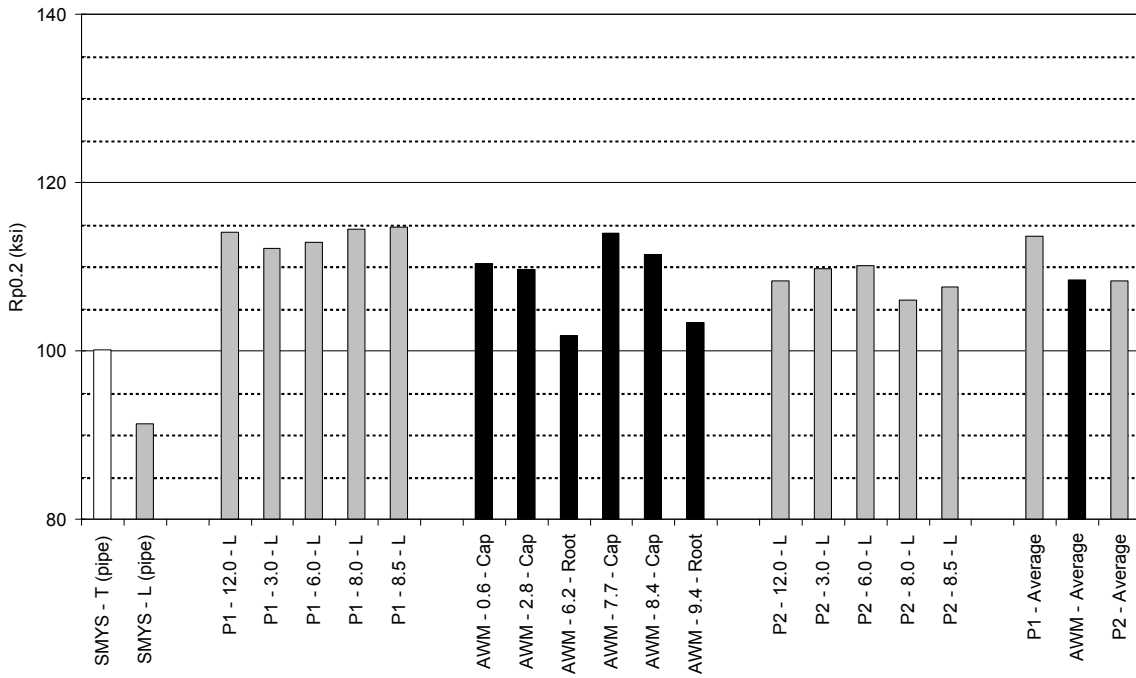


Figure 22 **Weld A17:** Comparison of yield strength of the pipe in the *longitudinal* direction with the all weld metal yield strength. Tested at 68°F (20°C).

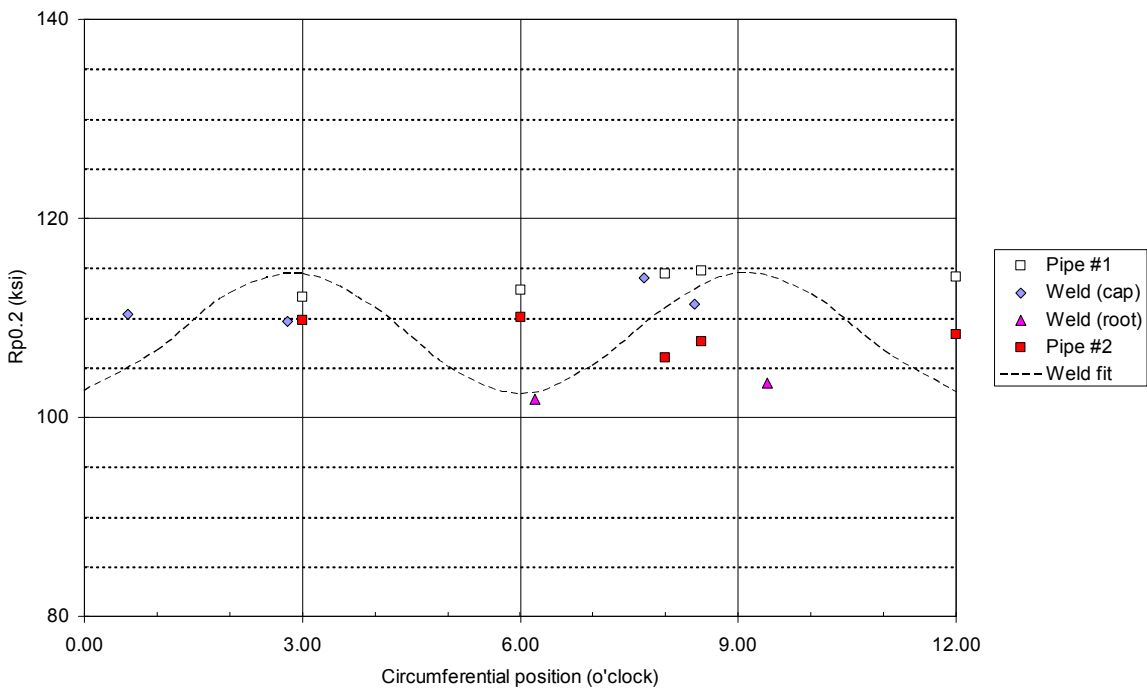


Figure 23 **Weld A17:** Comparison of yield strength (pipe *longitudinal* direction and all weld metal tests) in relation to the pipe circumferential position. Tested at 68°F (20°C).

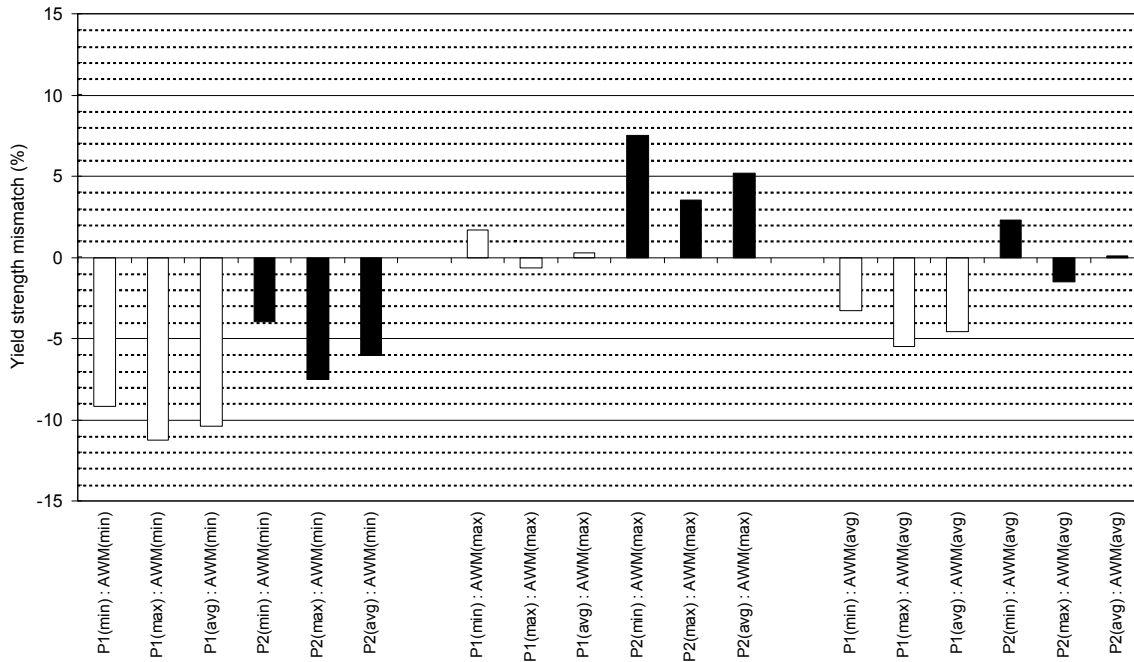


Figure 24 **Weld A17:** Comparison of the weld metal yield strength to the pipe yield strength in the *longitudinal* direction. Tested at 68°F (20°C).

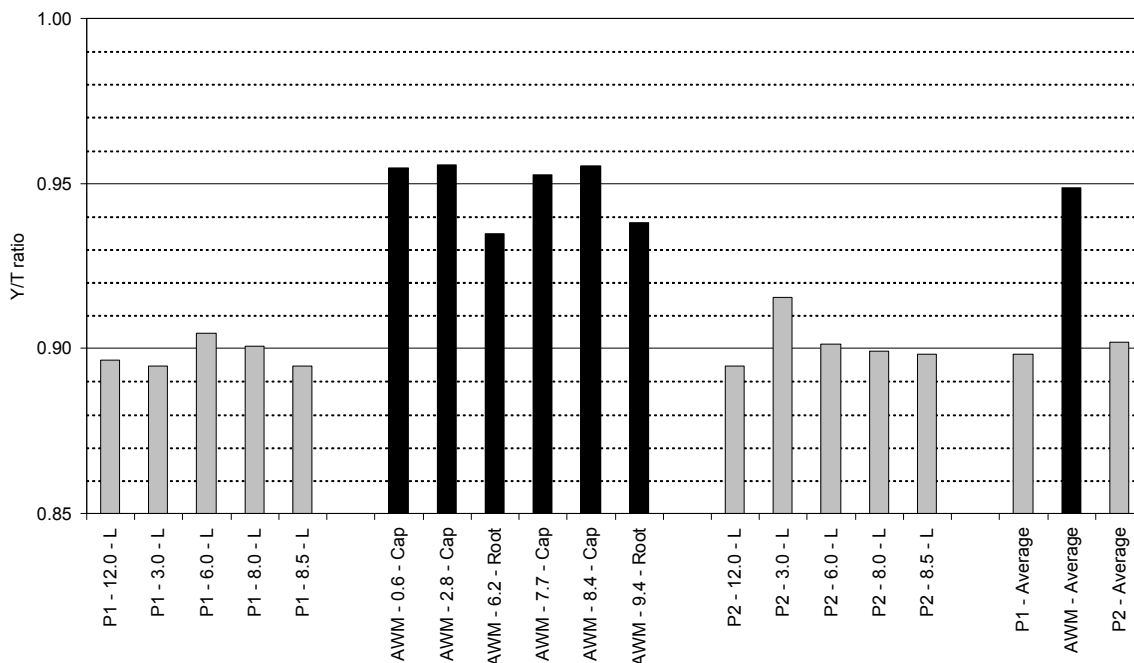


Figure 25 **Weld A17:** Comparison of yield to tensile strength ratio of the pipe in the *longitudinal* direction with the weld metal. Tested at 68°F (20°C).

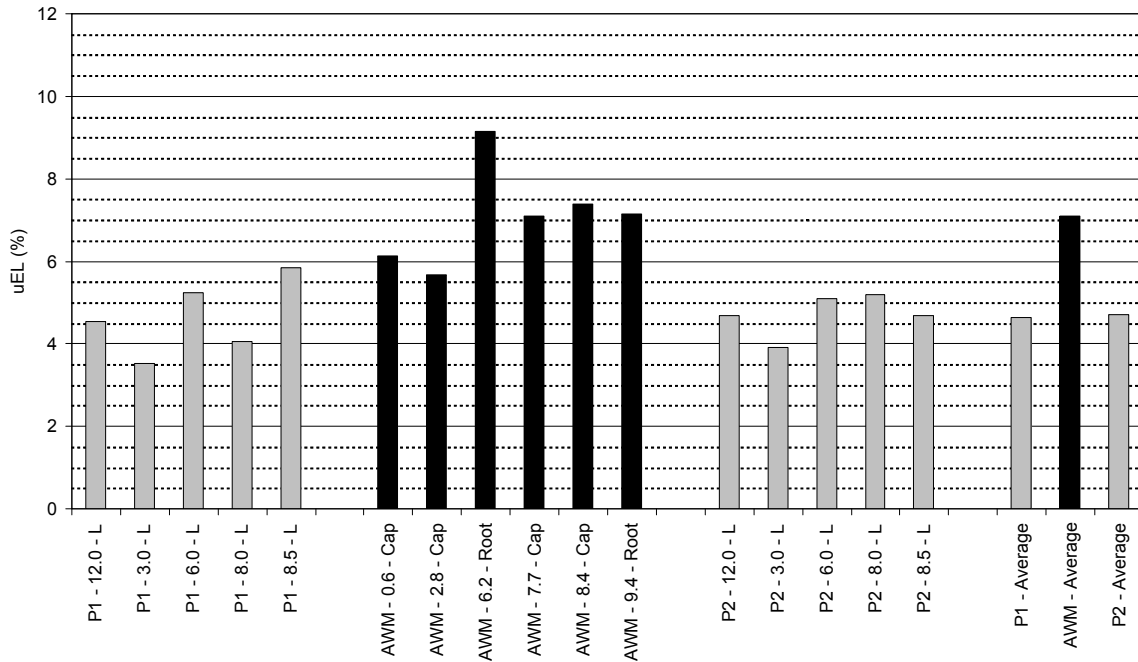
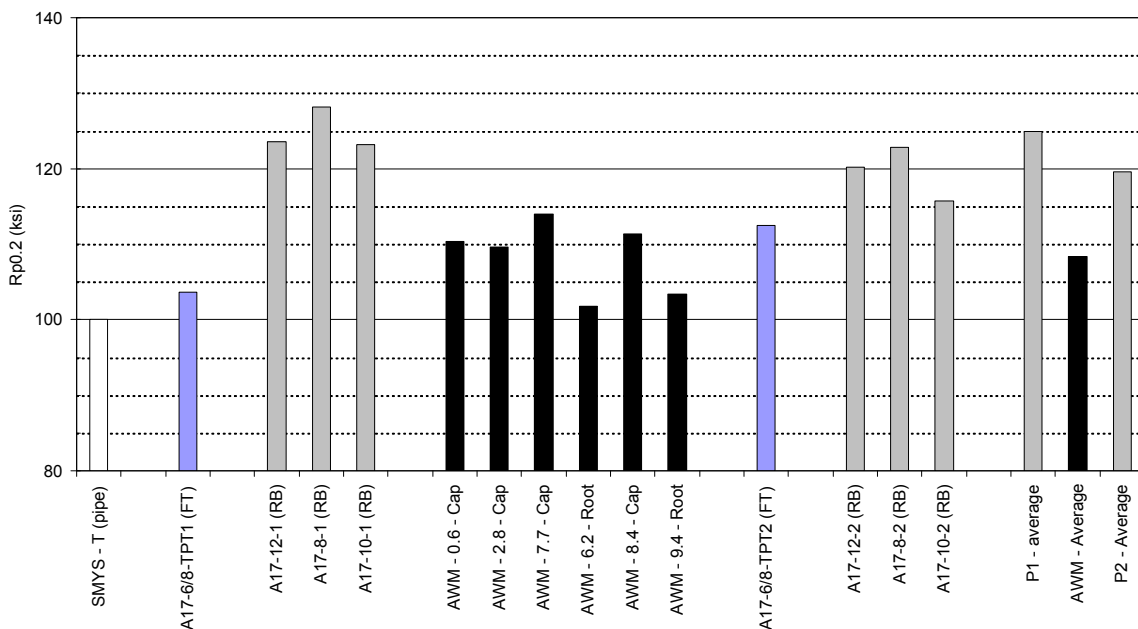
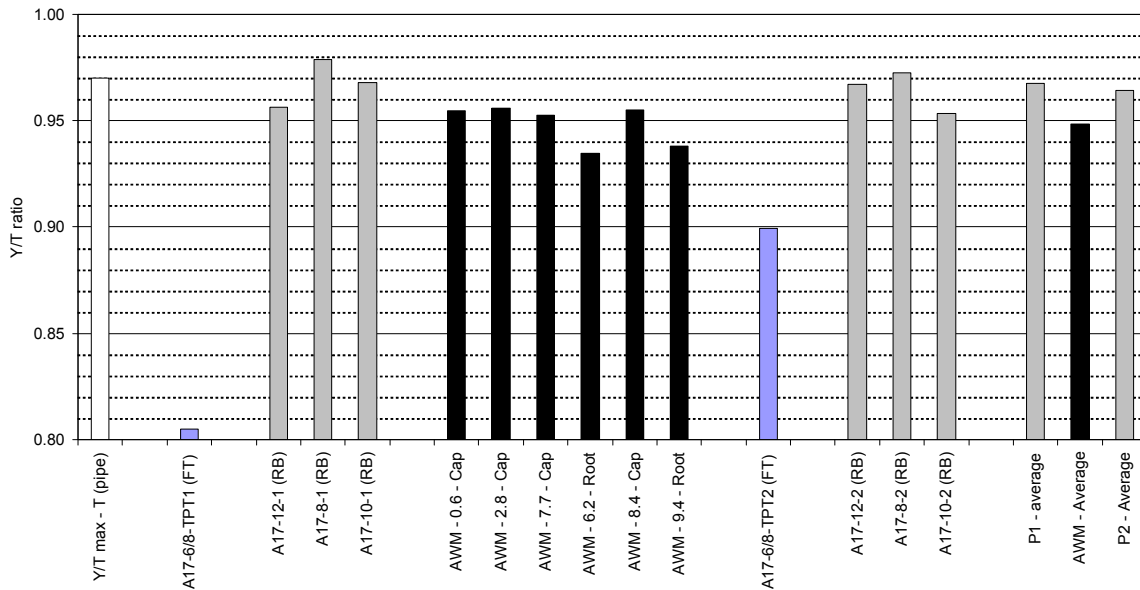


Figure 26 **Weld A17:** Comparison of the strain capacity of the pipe in the *longitudinal* direction with the all weld metal tests. Tested at 68°F (20°C).



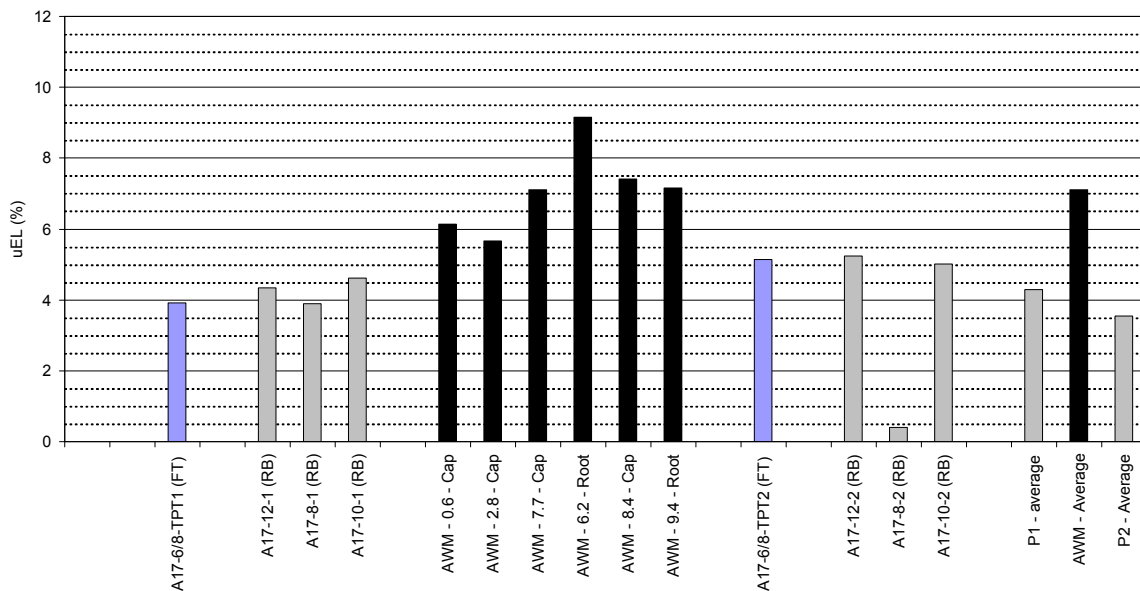
Notes: FT and RB are Flat Tensile and Round Bar specimens respectively

Figure 27 **Weld A17:** Comparison of yield strength of the pipe in the *transverse* direction with the all weld metal yield strength. Tested at 68°F (20°C).



Notes: FT and RB are Flat Tensile and Round Bar specimens respectively

Figure 28 **Weld A17:** Comparison of the weld metal yield strength to the pipe yield strength in the *transverse* direction. Tested at 68°F (20°C).



Notes: FT and RB are Flat Tensile and Round Bar specimens respectively

Figure 29 **Weld A17:** Comparison of the strain capacity of the pipe in the *transverse* direction with the all weld metal tests. Tested at 68°F (20°C).

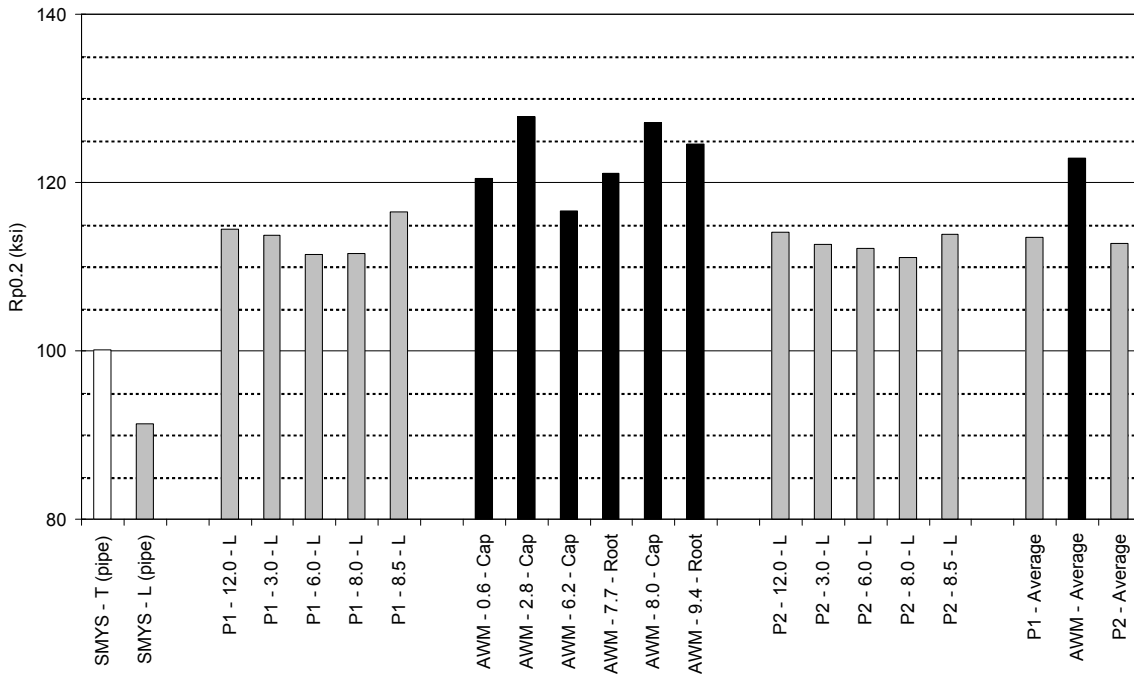


Figure 30 **Weld A33:** Comparison of yield strength of the pipe in the *longitudinal* direction with the all weld metal yield strength. Tested at 68°F (20°C).

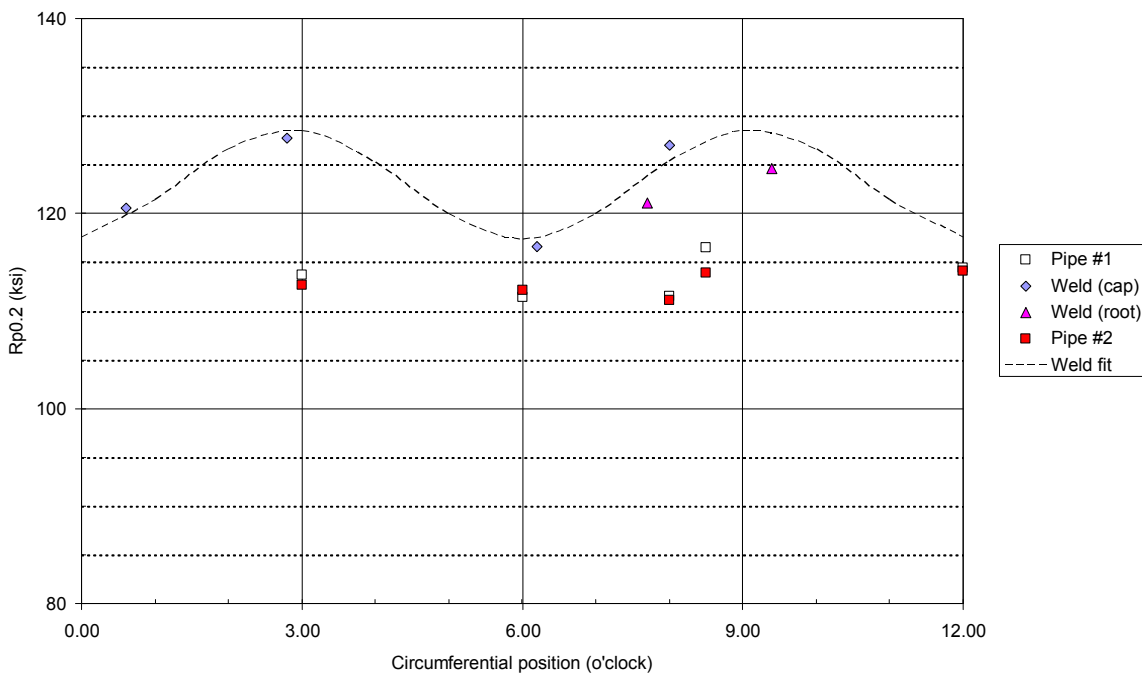


Figure 31 **Weld A33:** Comparison of yield strength (pipe *longitudinal* direction and all weld metal tests) in relation to the pipe circumferential position. Tested at 68°F (20°C).

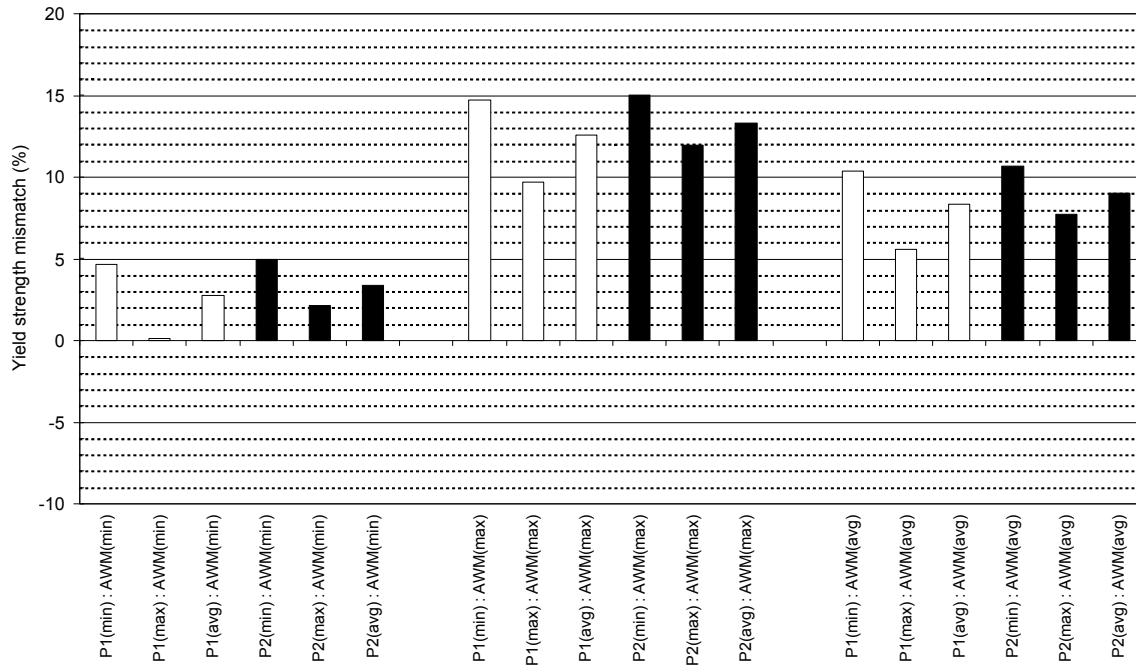


Figure 32 **Weld A33:** Comparison of the weld metal yield strength to the pipe yield strength in the *longitudinal* direction. Tested at 68°F (20°C).

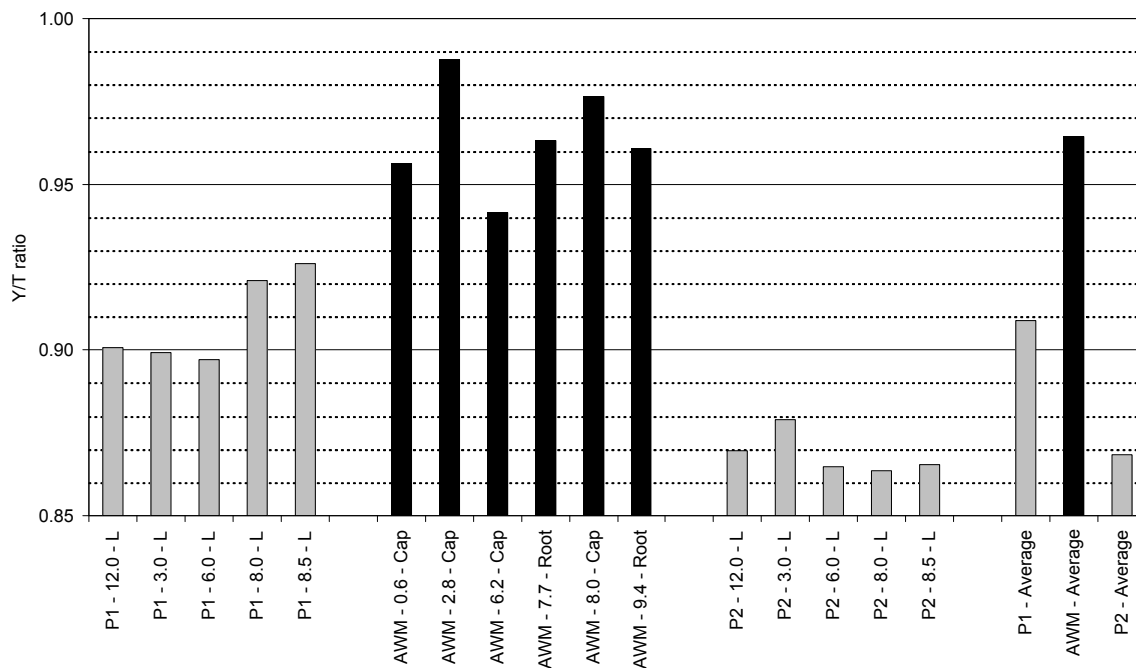


Figure 33 **Weld A33:** Comparison of yield to tensile strength ratio of the pipe in the *longitudinal* direction with the weld metal. Tested at 68°F (20°C).

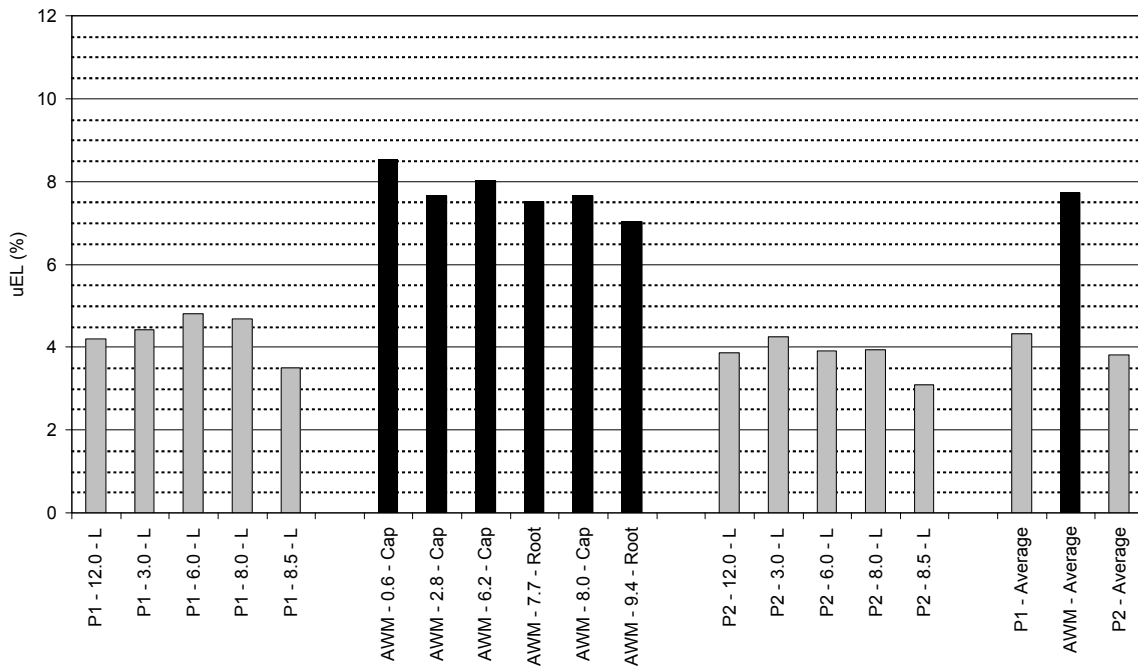
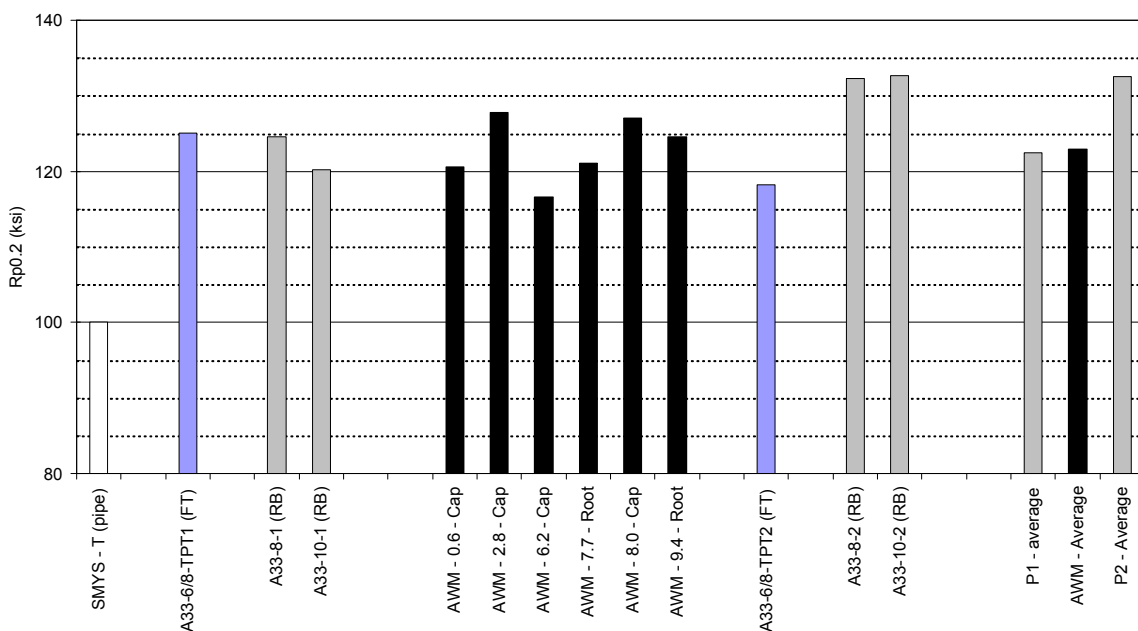
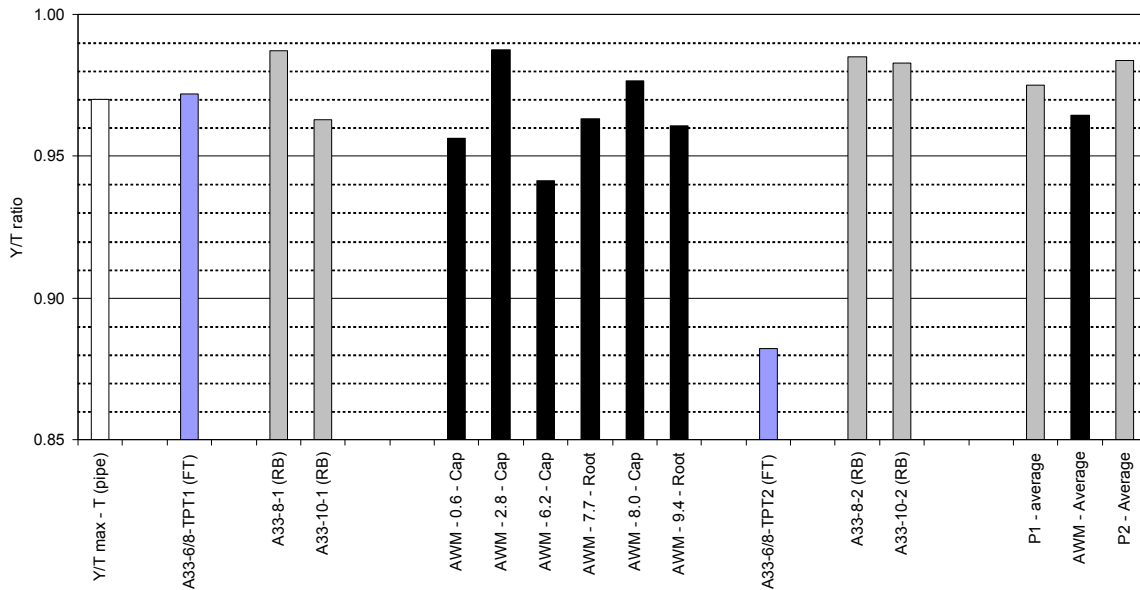


Figure 34 **Weld A33:** Comparison of the strain capacity of the pipe in the *longitudinal* direction with the all weld metal tests. Tested at 68°F (20°C).



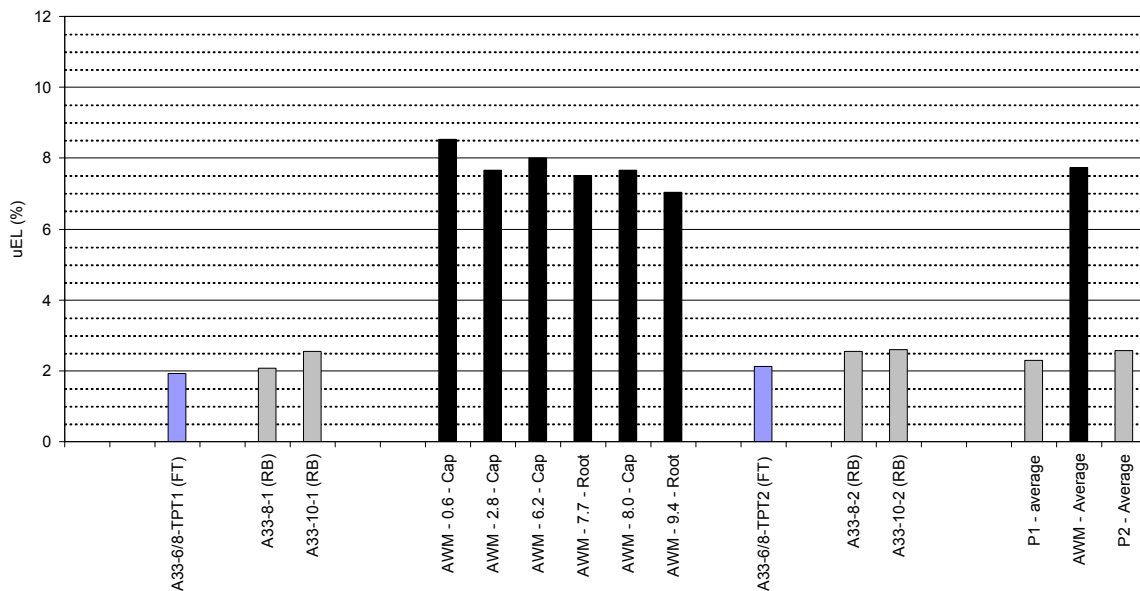
Notes: FT and RB are Flat Tensile and Round Bar specimens respectively

Figure 35 **Weld A33:** Comparison of yield strength of the pipe in the *transverse* direction with the all weld metal yield strength. Tested at 68°F (20°C).



Notes: FT and RB are Flat Tensile and Round Bar specimens respectively

Figure 36 **Weld A33:** Comparison of the weld metal yield strength to the pipe yield strength in the *transverse* direction. Tested at 68°F (20°C).



Notes: FT and RB are Flat Tensile and Round Bar specimens respectively

Figure 37 **Weld A33:** Comparison of the strain capacity of the pipe in the *transverse* direction with the all weld metal tests. Tested at 68°F (20°C).

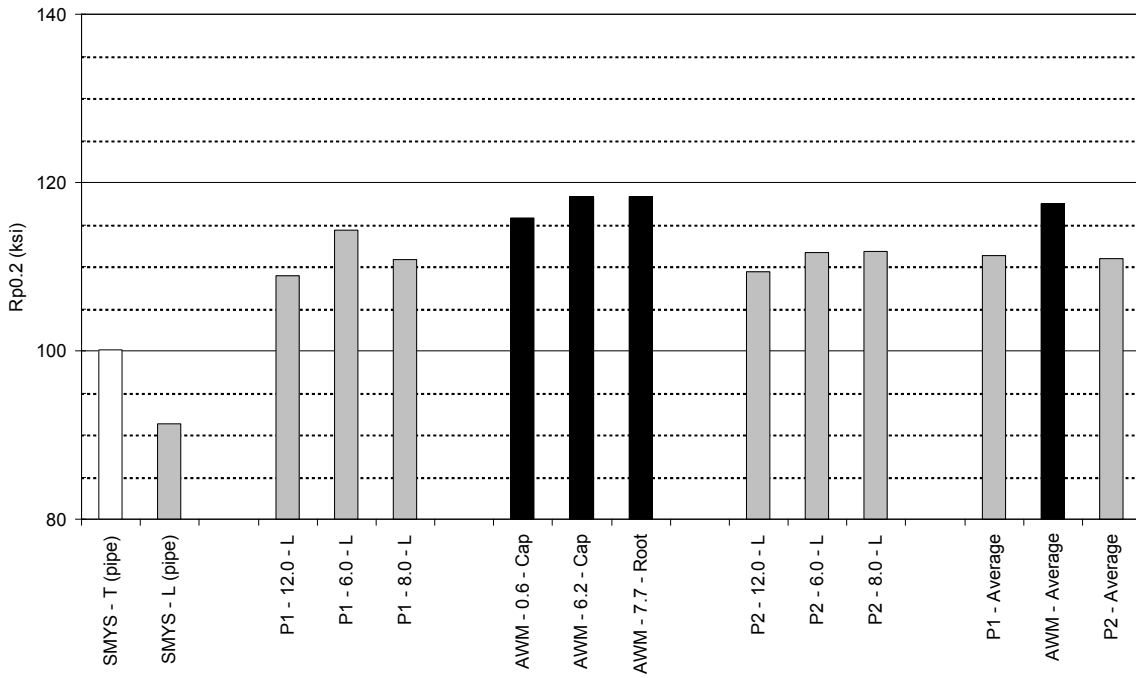


Figure 38 **Weld A44:** Comparison of yield strength of the pipe in the *longitudinal* direction with the all weld metal yield strength. Tested at 68°F (20°C).

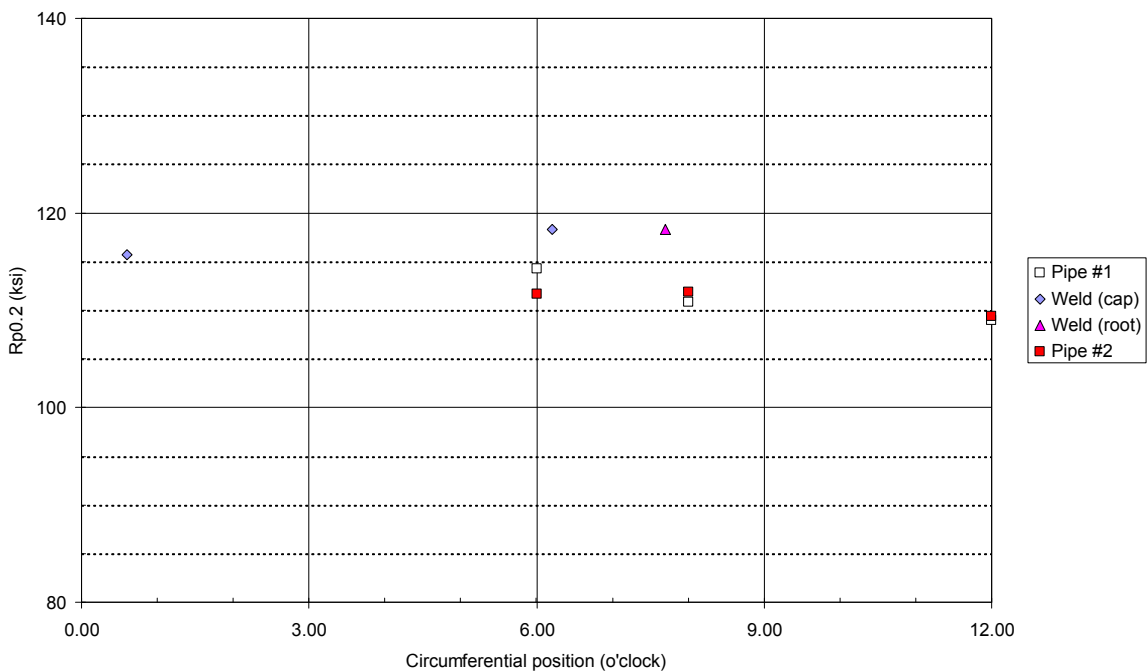


Figure 39 **Weld A44:** Comparison of yield strength (pipe *longitudinal* direction and all weld metal tests) in relation to the pipe circumferential position. Tested at 68°F (20°C).

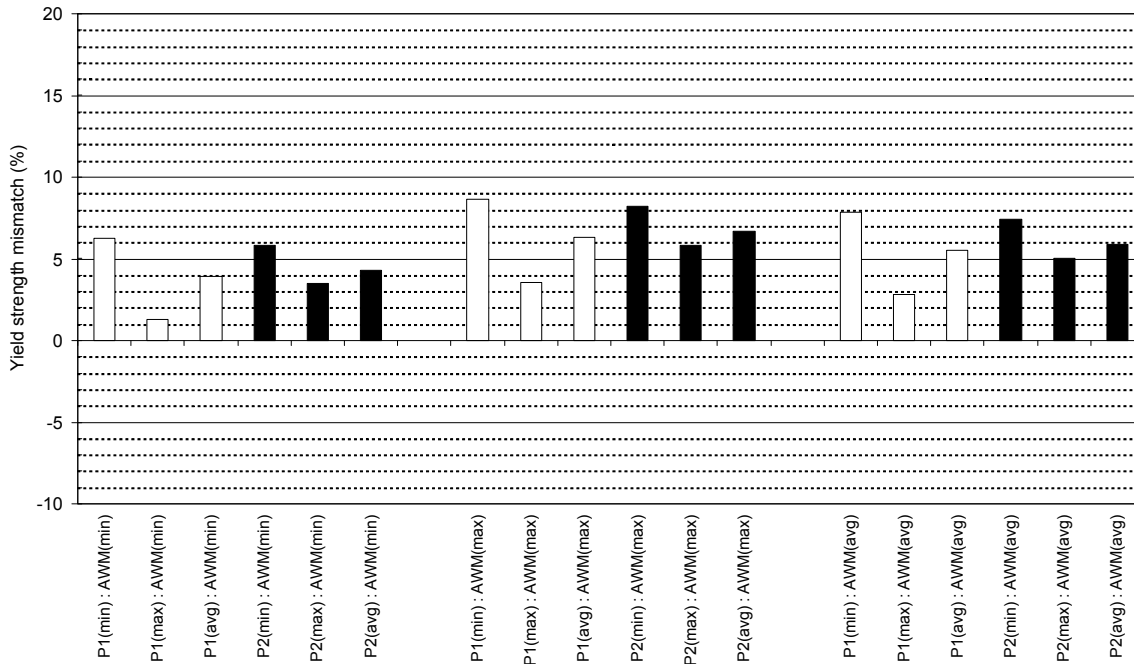


Figure 40 **Weld A44:** Comparison of the weld metal yield strength to the pipe yield strength in the *longitudinal* direction. Tested at 68°F (20°C).

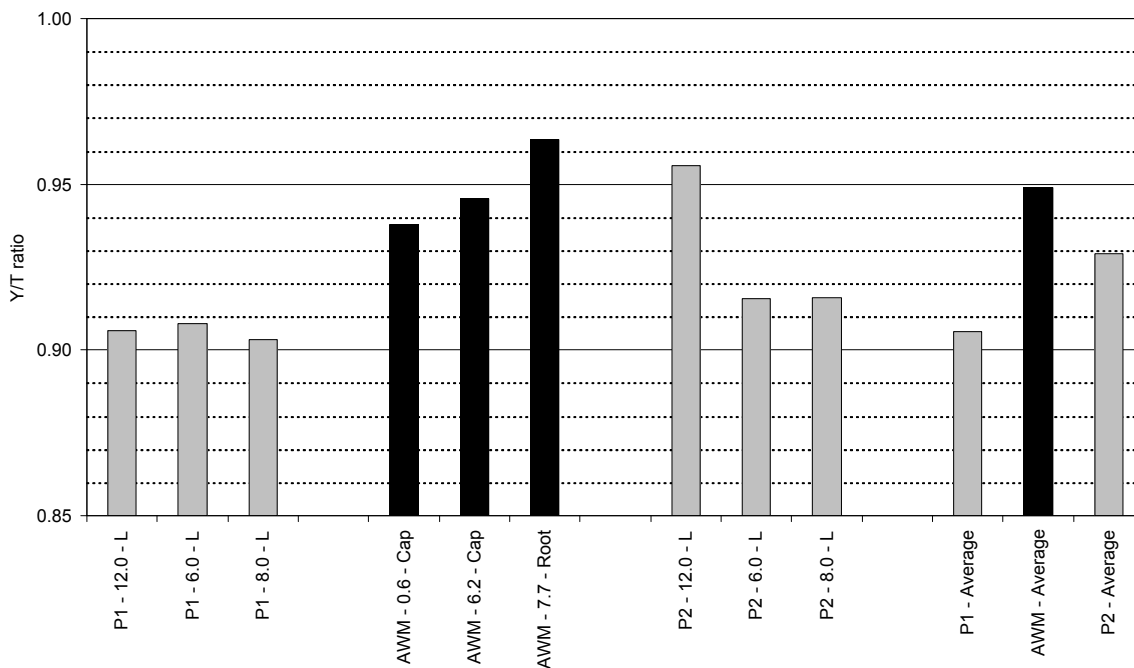


Figure 41 **Weld A44:** Comparison of yield to tensile strength ratio of the pipe in the *longitudinal* direction with the weld metal. Tested at 68°F (20°C).

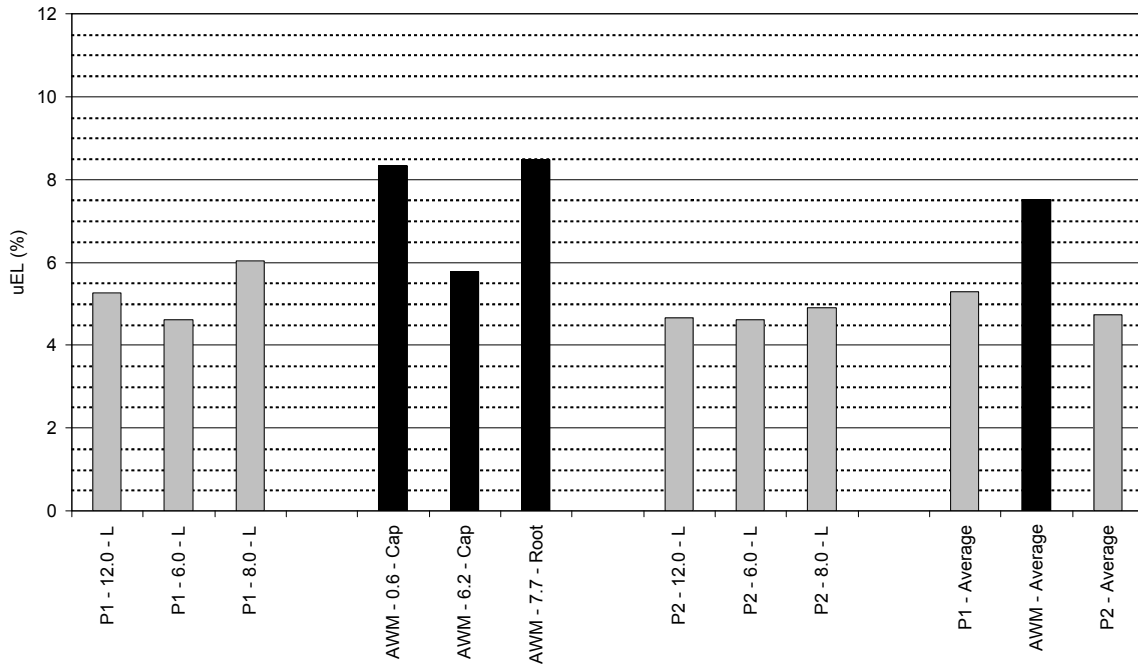
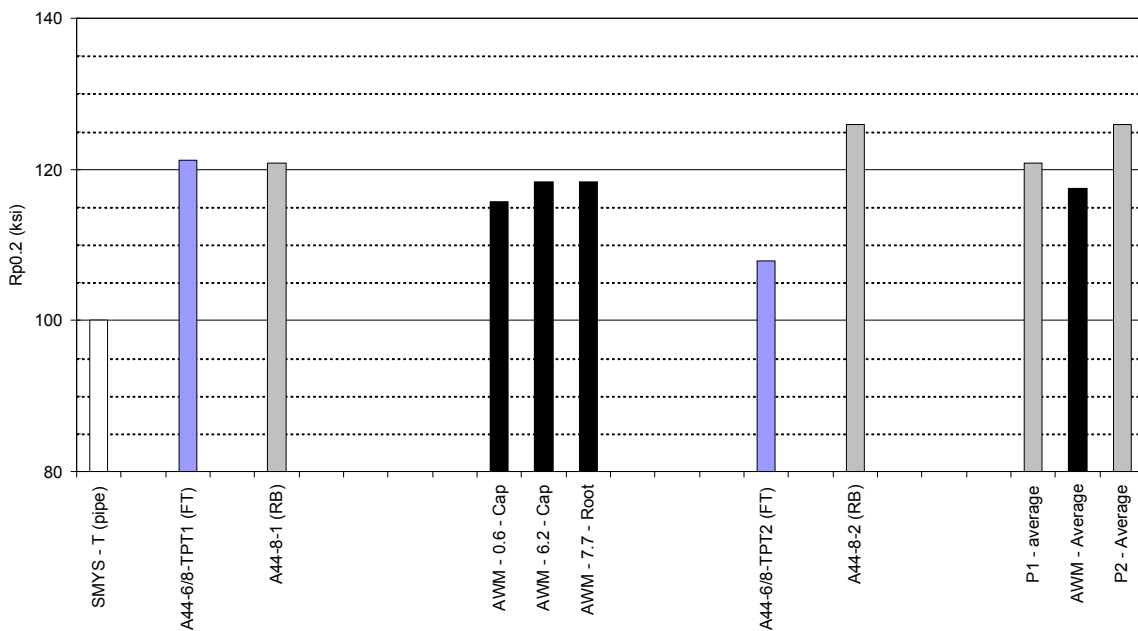
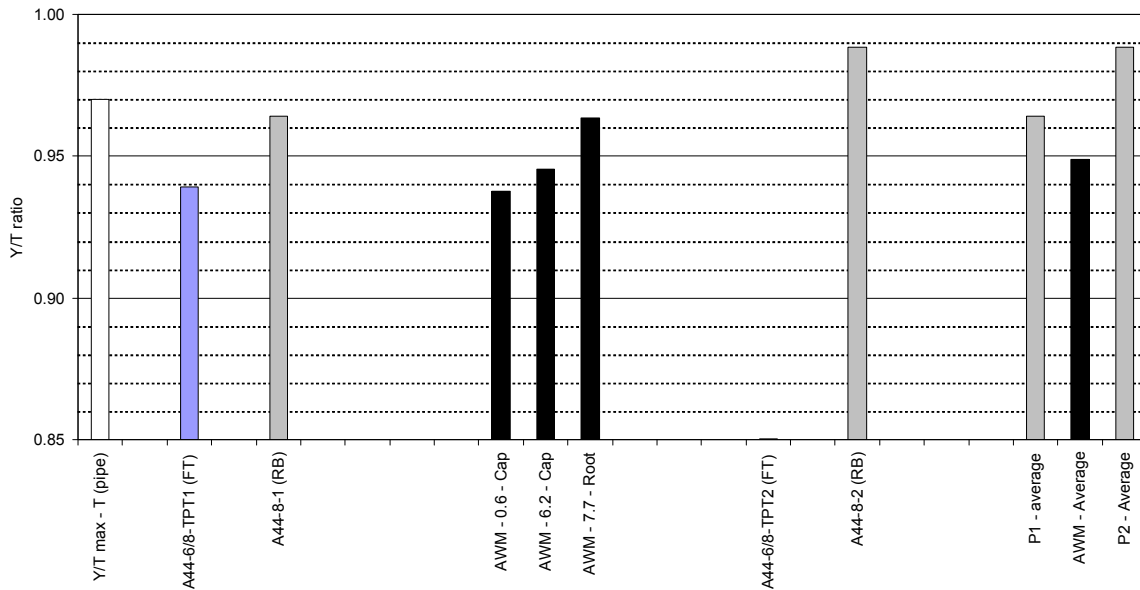


Figure 42 **Weld A44:** Comparison of the strain capacity of the pipe in the *longitudinal* direction with the all weld metal tests. Tested at 68°F (20°C).



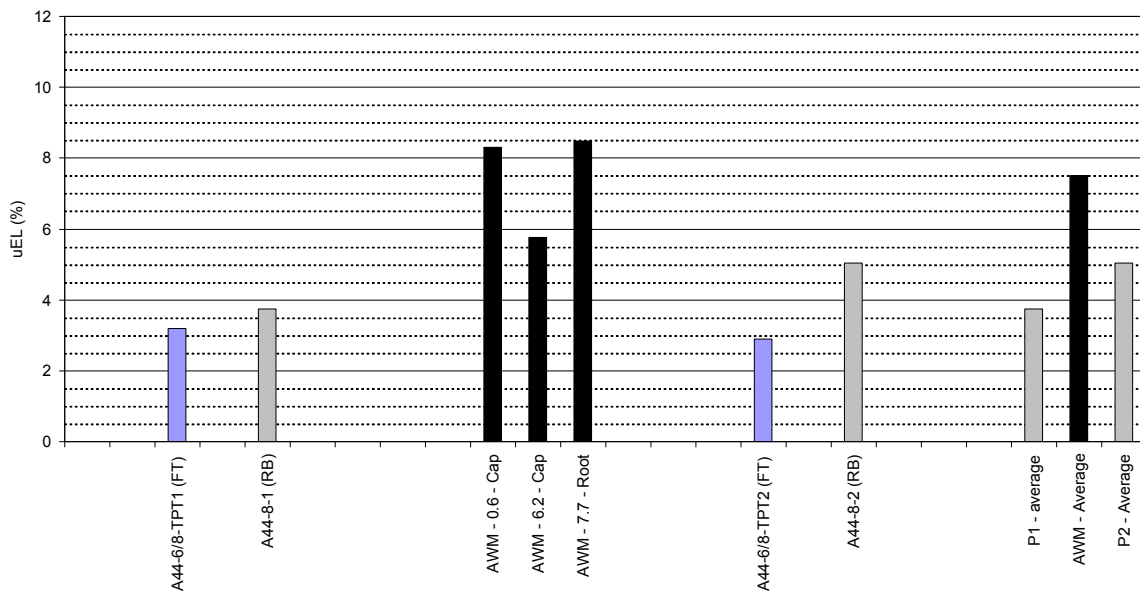
Notes: FT and RB are Flat Tensile and Round Bar specimens respectively

Figure 43 **Weld A44:** Comparison of yield strength of the pipe in the *transverse* direction with the all weld metal yield strength. Tested at 68°F (20°C).



Notes: FT and RB are Flat Tensile and Round Bar specimens respectively

Figure 44 **Weld A44:** Comparison of the weld metal yield strength to the pipe yield strength in the *transverse* direction. Tested at 68°F (20°C).



Notes: FT and RB are Flat Tensile and Round Bar specimens respectively

Figure 45 **Weld A44:** Comparison of the strain capacity of the pipe in the *transverse* direction with the all weld metal tests. Tested at 68°F (20°C).

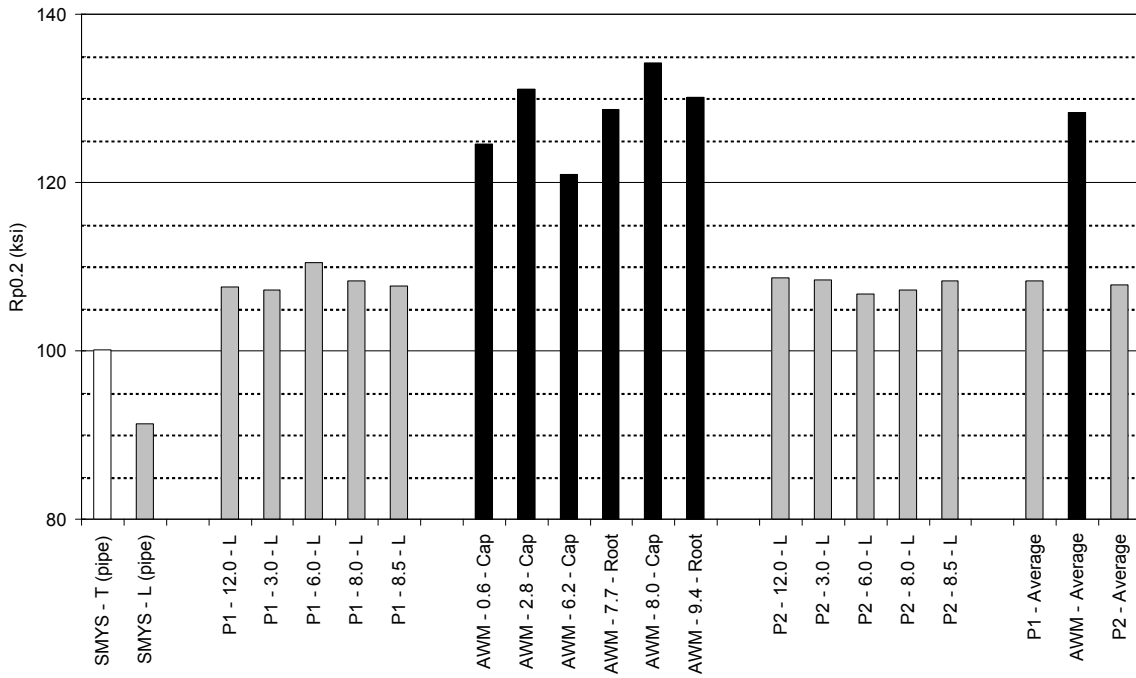


Figure 46 **Weld A46:** Comparison of yield strength of the pipe in the *longitudinal* direction with the all weld metal yield strength. Tested at 68°F (20°C).

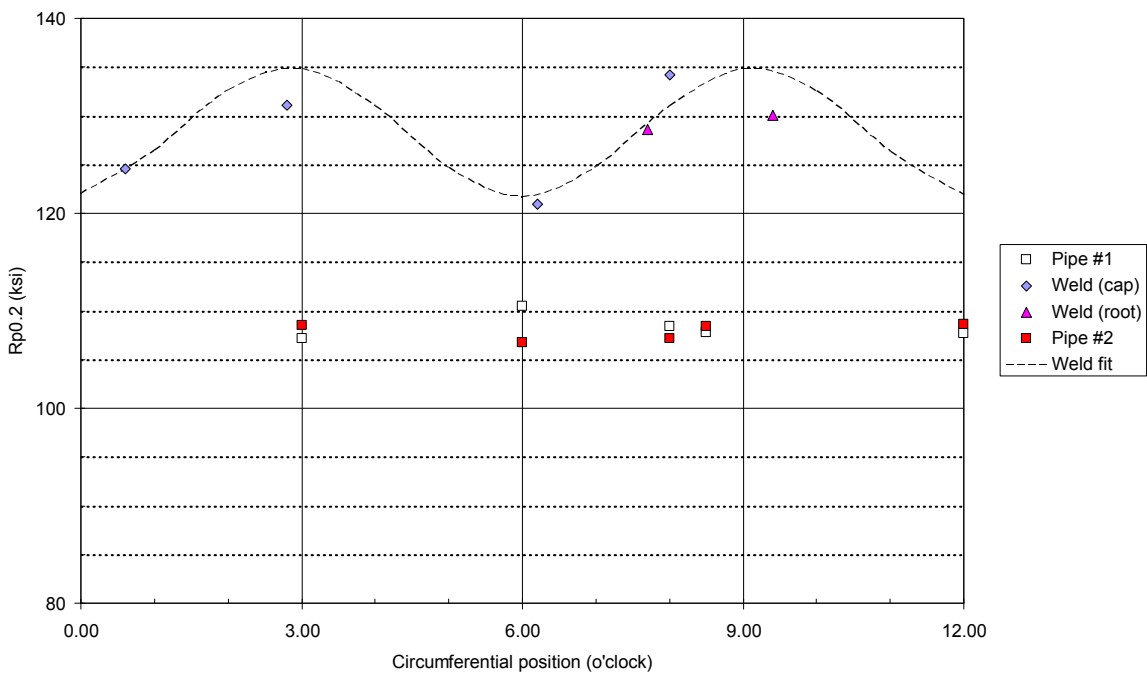


Figure 47 **Weld A46:** Comparison of yield strength (pipe *longitudinal* direction and all weld metal tests) in relation to the pipe circumferential position. Tested at 68°F (20°C).

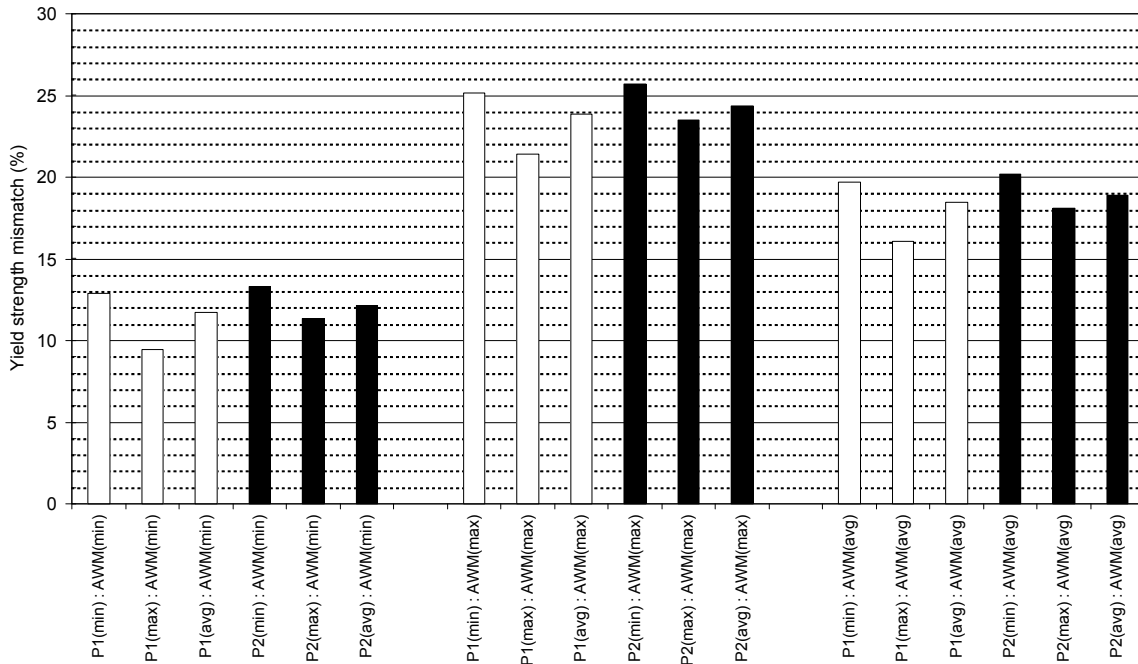


Figure 48 **Weld A46:** Comparison of the weld metal yield strength to the pipe yield strength in the *longitudinal* direction. Tested at 68°F (20°C).

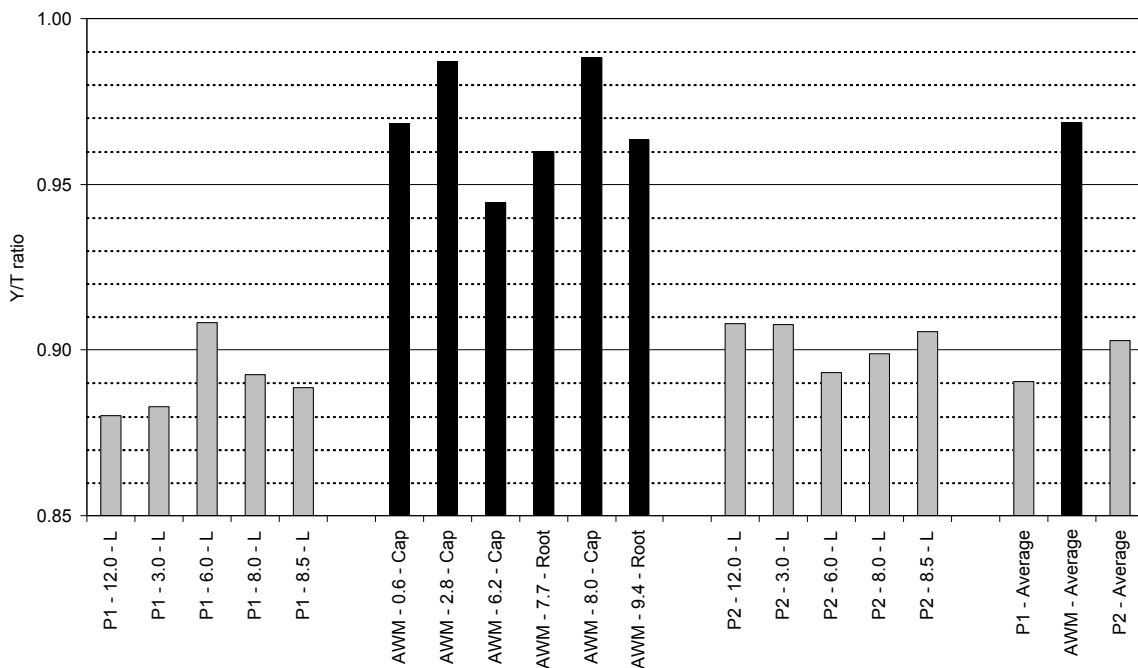


Figure 49 **Weld A46:** Comparison of yield to tensile strength ratio of the pipe in the *longitudinal* direction with the weld metal. Tested at 68°F (20°C).

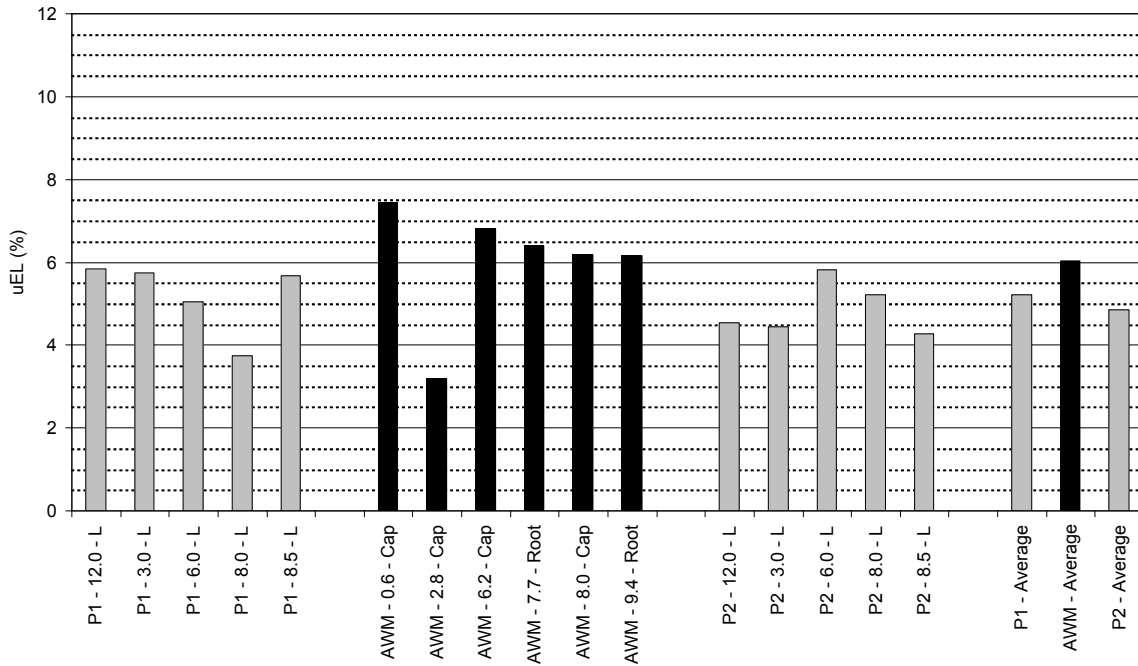
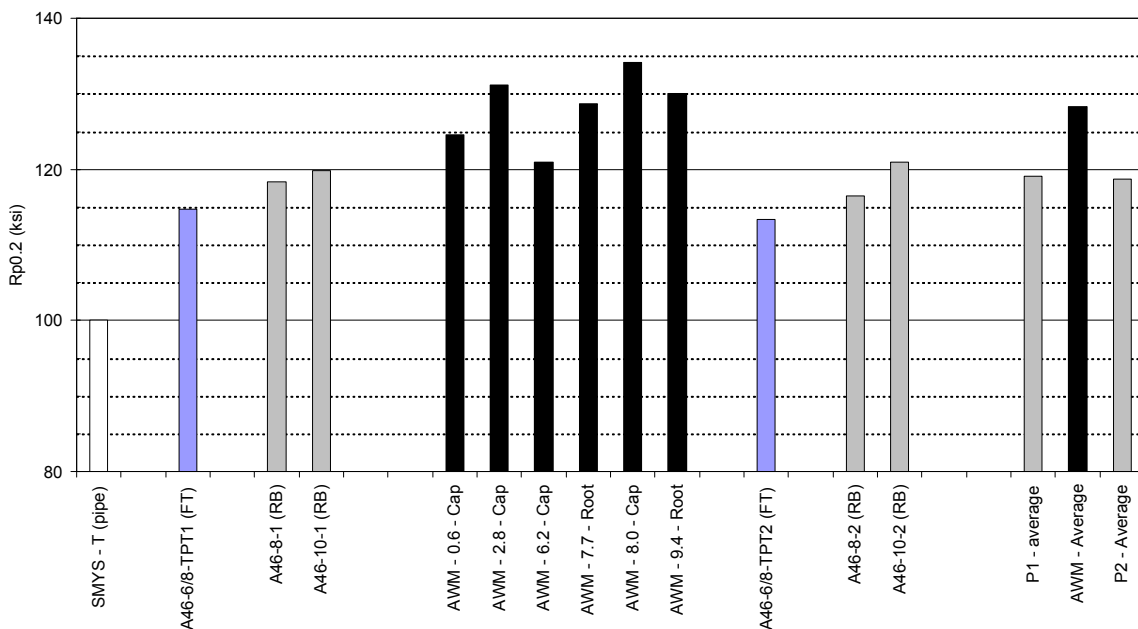
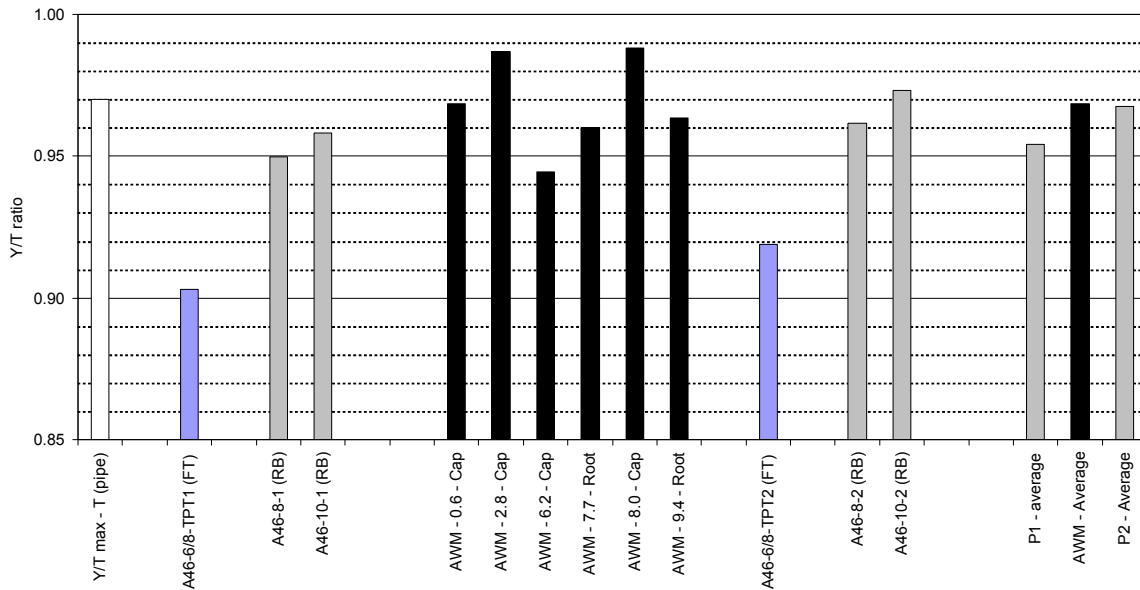


Figure 50 **Weld A46:** Comparison of the strain capacity of the pipe in the *longitudinal* direction with the all weld metal tests. Tested at 68°F (20°C).



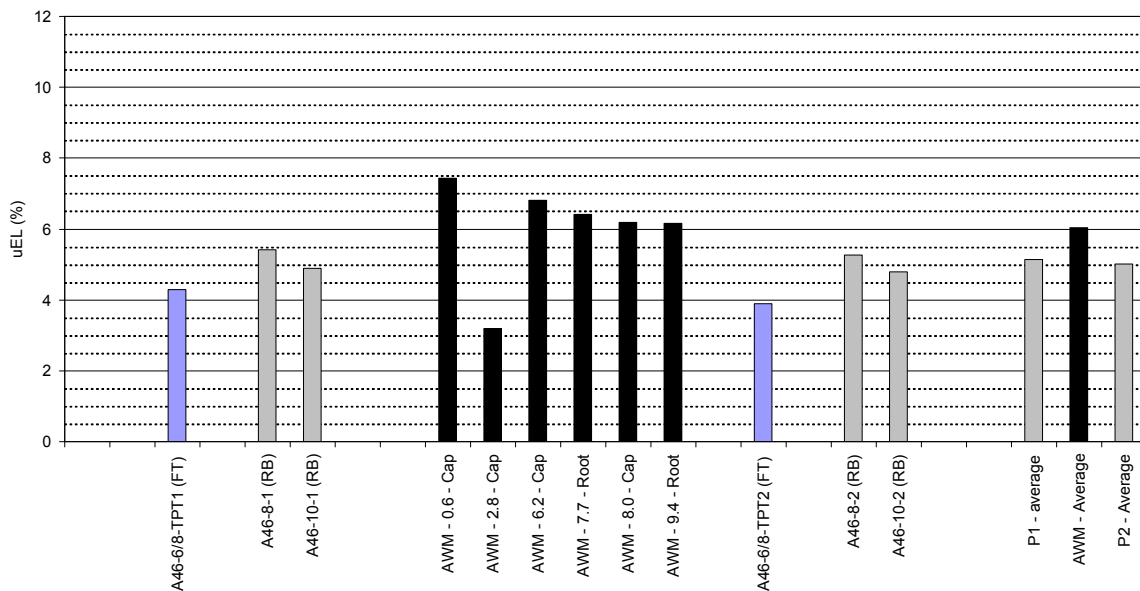
Notes: FT and RB are Flat Tensile and Round Bar specimens respectively

Figure 51 **Weld A46:** Comparison of yield strength of the pipe in the *transverse* direction with the all weld metal yield strength. Tested at 68°F (20°C).



Notes: FT and RB are Flat Tensile and Round Bar specimens respectively

Figure 52 **Weld A46:** Comparison of the weld metal yield strength to the pipe yield strength in the *transverse* direction. Tested at 68°F (20°C).



Notes: FT and RB are Flat Tensile and Round Bar specimens respectively

Figure 53 **Weld A46:** Comparison of the strain capacity of the pipe in the *transverse* direction with the all weld metal tests. Tested at 68°F (20°C).

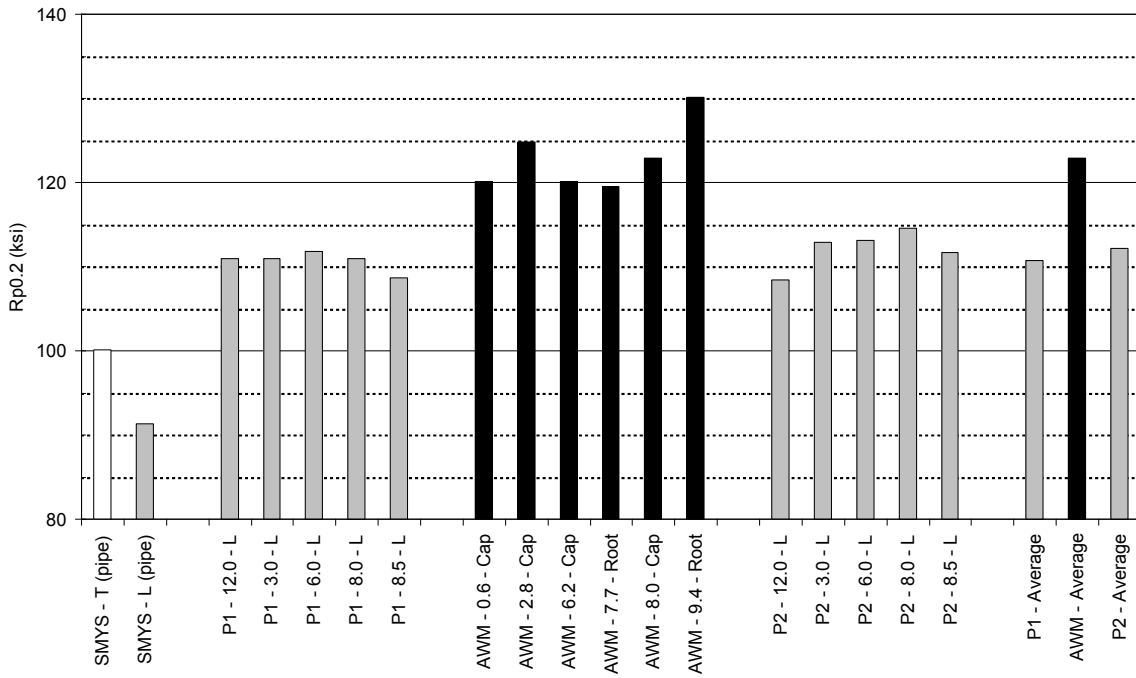


Figure 54 **Weld A50:** Comparison of yield strength of the pipe in the *longitudinal* direction with the all weld metal yield strength. Tested at 68°F (20°C).

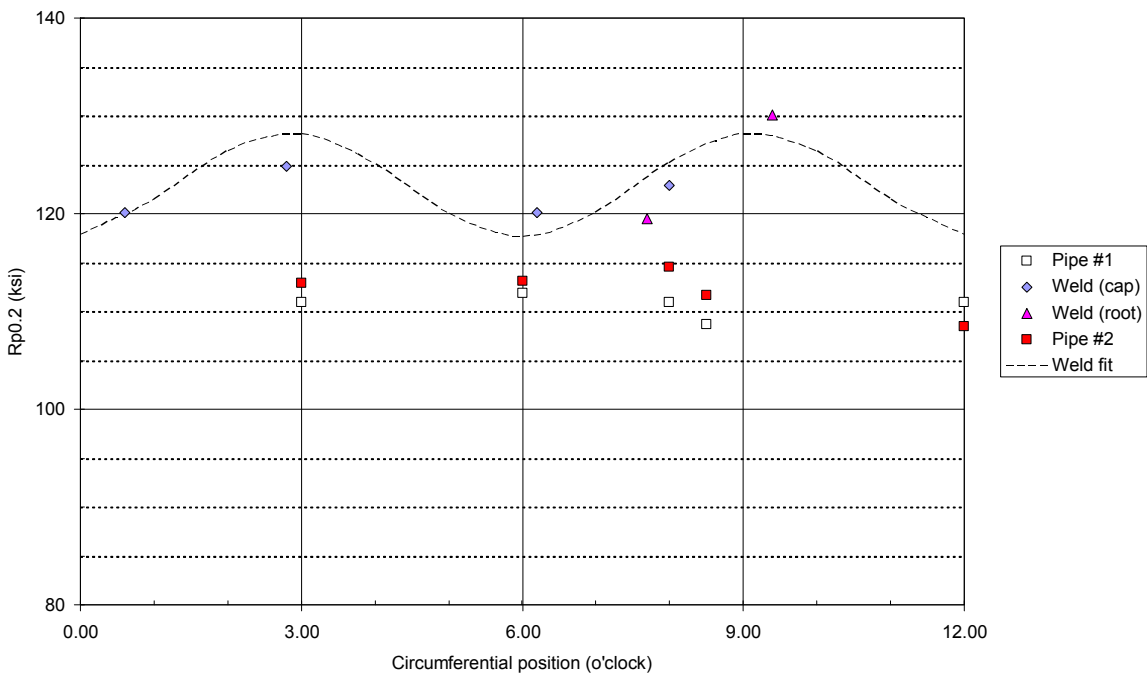


Figure 55 **Weld A50:** Comparison of yield strength (pipe *longitudinal* direction and all weld metal tests) in relation to the pipe circumferential position. Tested at 68°F (20°C).

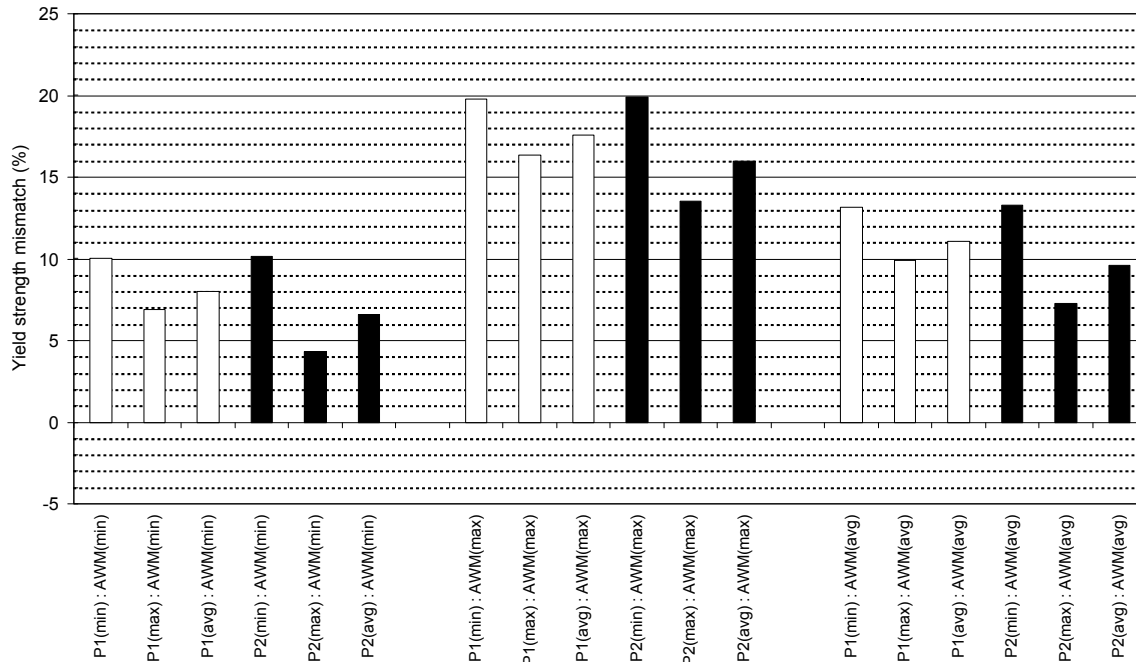


Figure 56 **Weld A50:** Comparison of the weld metal yield strength to the pipe yield strength in the *longitudinal* direction. Tested at 68°F (20°C).

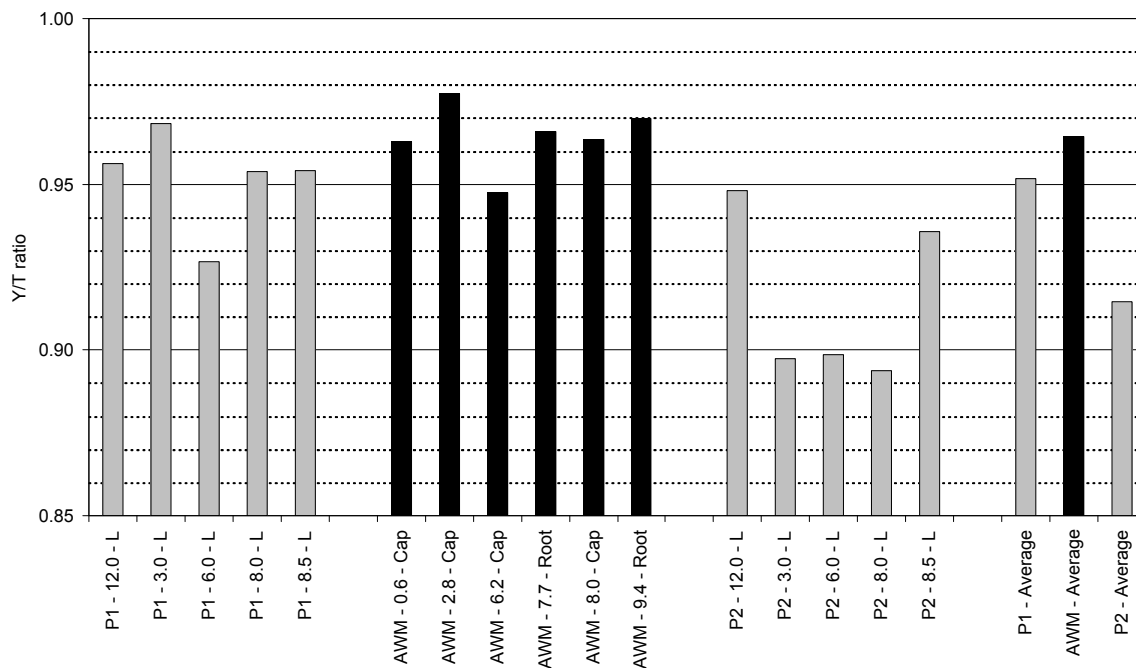


Figure 57 **Weld A50:** Comparison of yield to tensile strength ratio of the pipe in the *longitudinal* direction with the weld metal. Tested at 68°F (20°C).

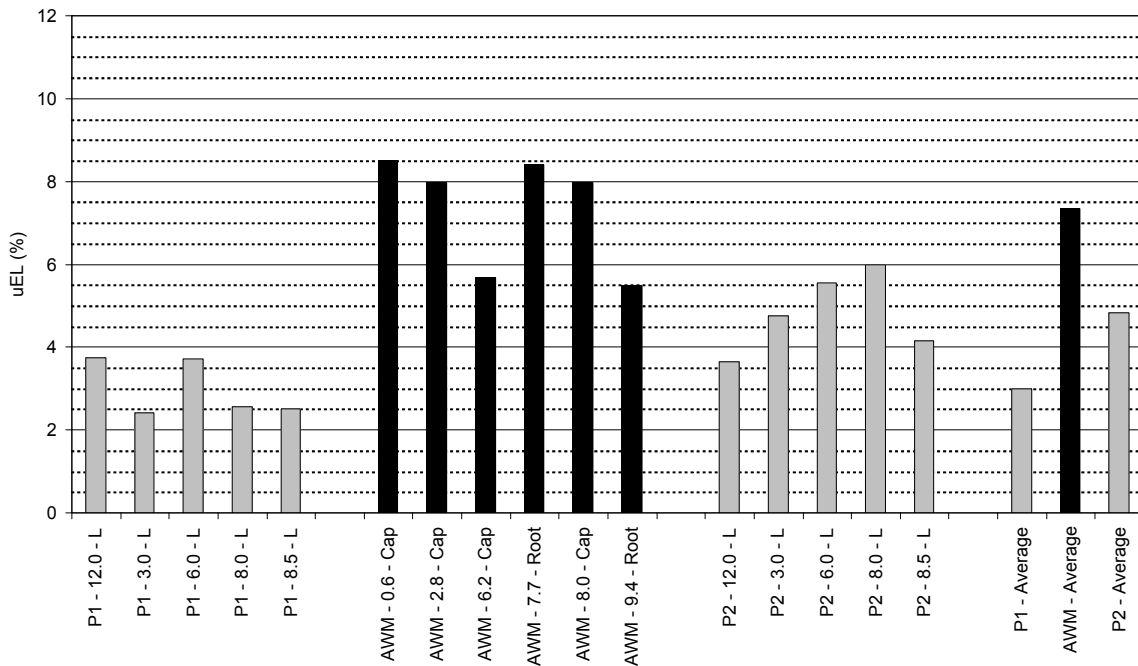
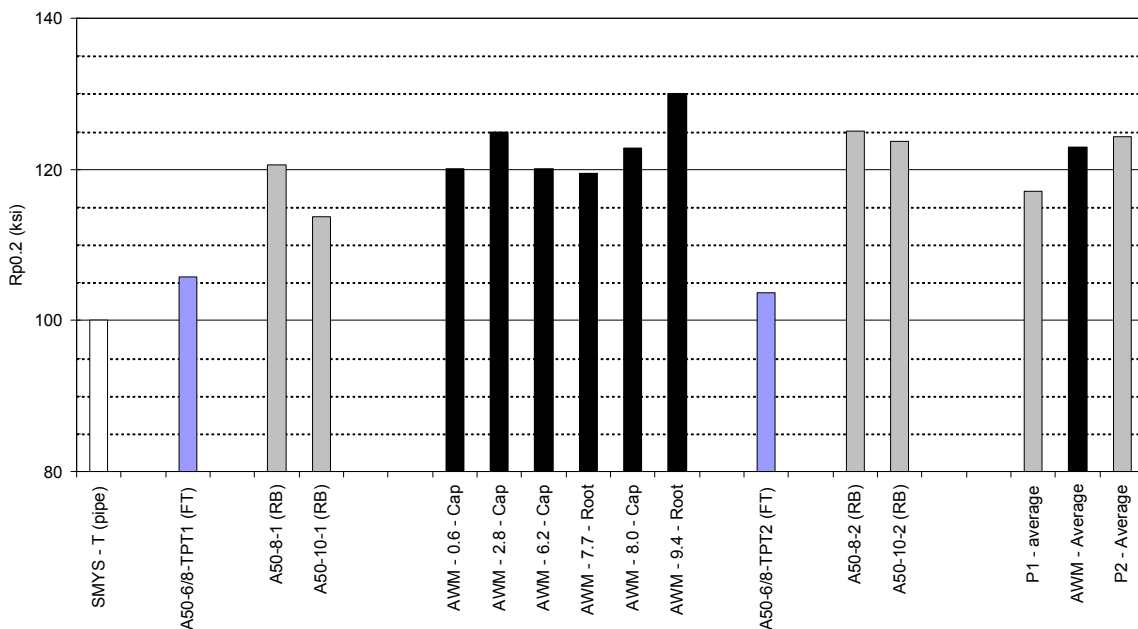
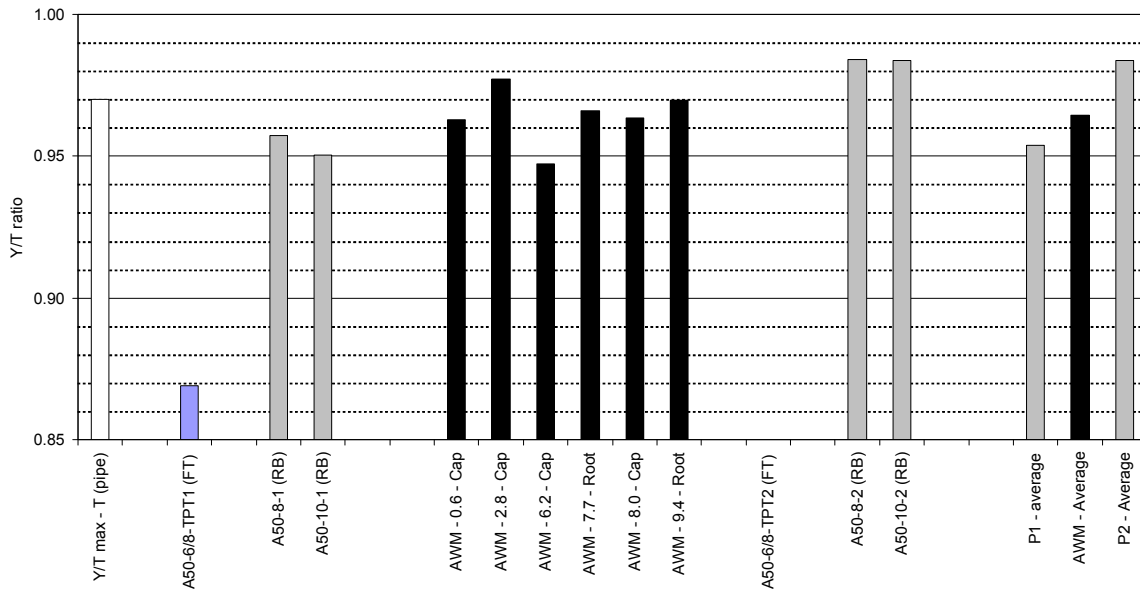


Figure 58 **Weld A50:** Comparison of the strain capacity of the pipe in the *longitudinal* direction with the all weld metal tests. Tested at 68°F (20°C).



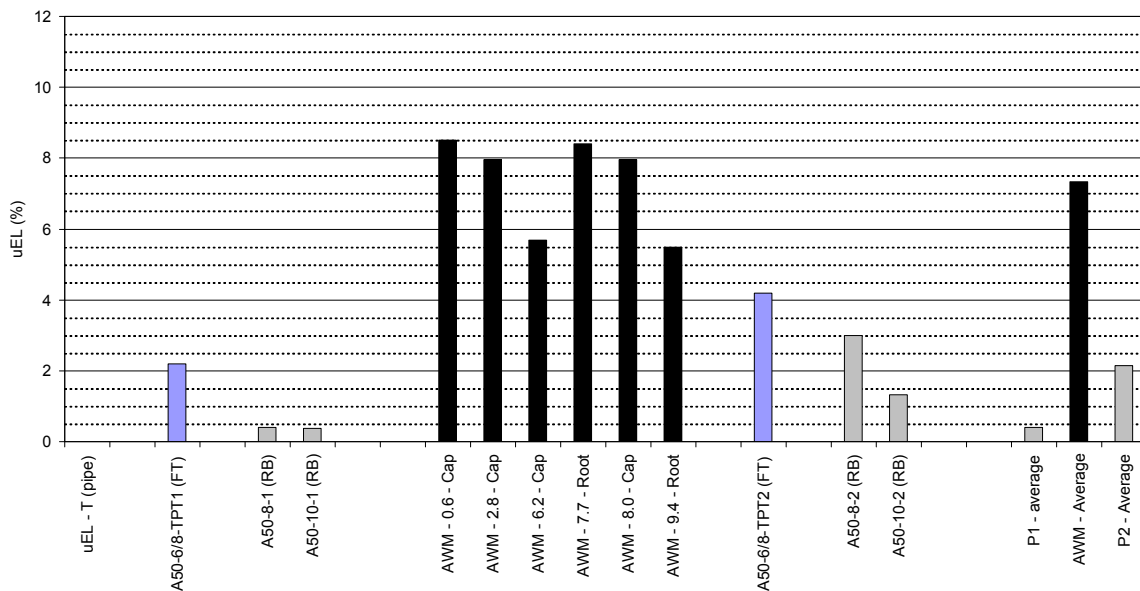
Notes: FT and RB are Flat Tensile and Round Bar specimens respectively

Figure 59 **Weld A50:** Comparison of yield strength of the pipe in the *transverse* direction with the all weld metal yield strength. Tested at 68°F (20°C).



Notes: FT and RB are Flat Tensile and Round Bar specimens respectively

Figure 60 **Weld A50:** Comparison of the weld metal yield strength to the pipe yield strength in the *transverse* direction. Tested at 68°F (20°C).



Notes: FT and RB are Flat Tensile and Round Bar specimens respectively

Figure 61 **Weld A50:** Comparison of the strain capacity of the pipe in the *transverse* direction with the all weld metal tests. Tested at 68°F (20°C).

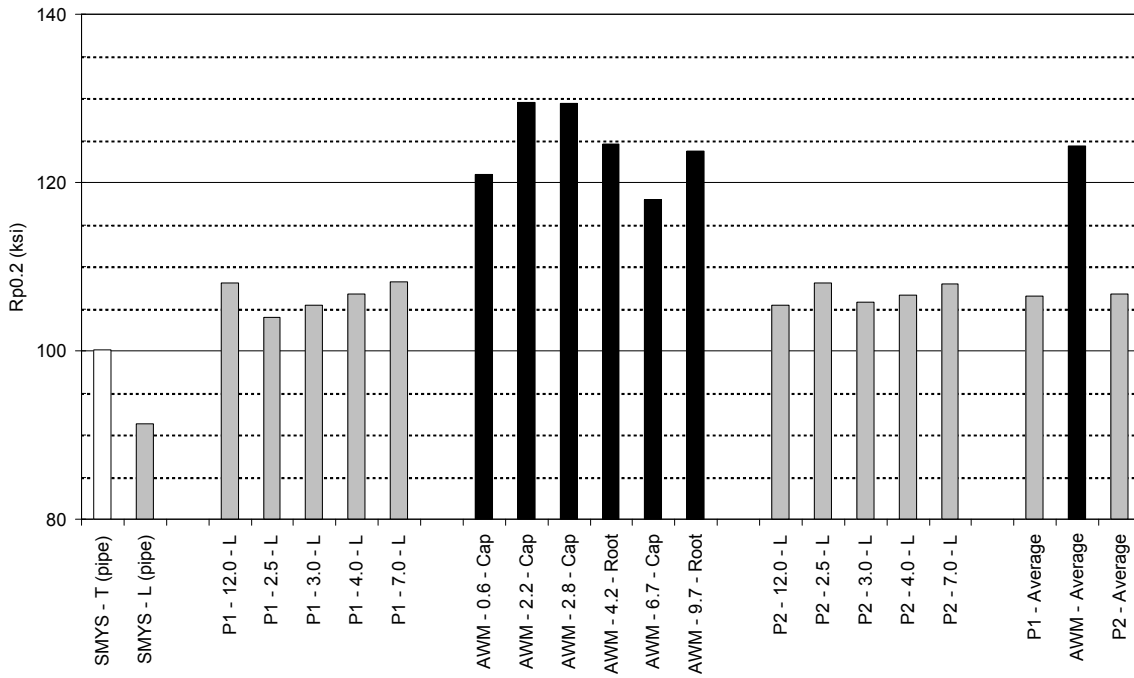


Figure 62 **Weld B03:** Comparison of yield strength of the pipe in the *longitudinal* direction with the all weld metal yield strength. Tested at 68°F (20°C).

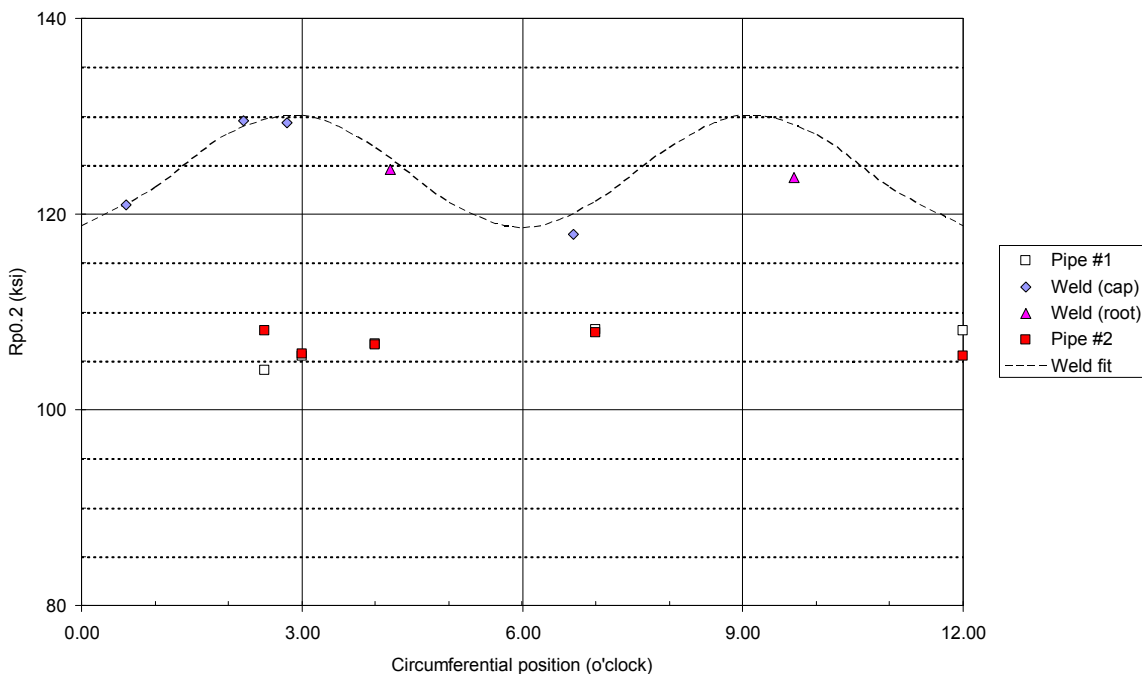


Figure 63 **Weld B03:** Comparison of yield strength (pipe *longitudinal* direction and all weld metal tests) in relation to the pipe circumferential position. Tested at 68°F (20°C).

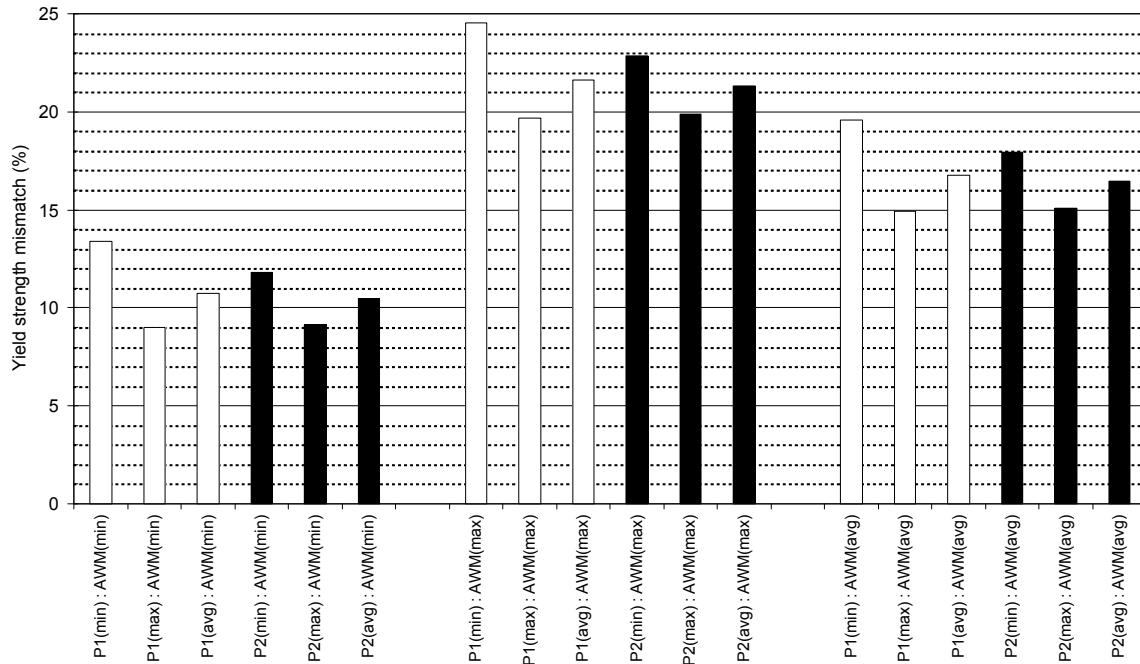


Figure 64 **Weld B03:** Comparison of the weld metal yield strength to the pipe yield strength in the *longitudinal* direction. Tested at 68°F (20°C).

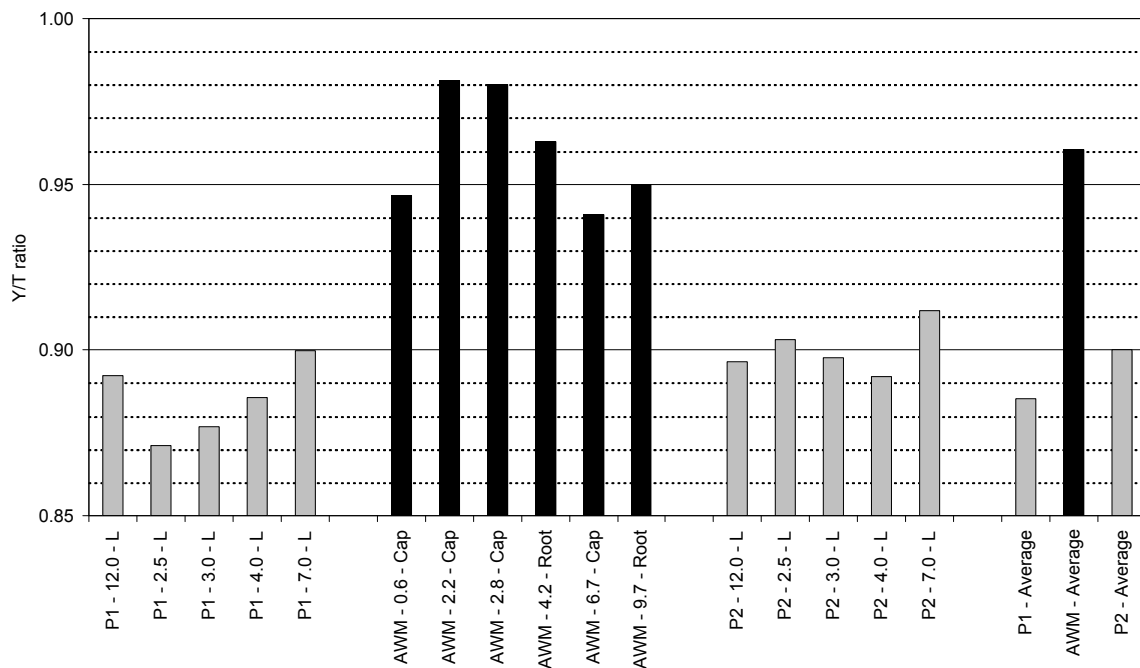


Figure 65 **Weld B03:** Comparison of yield to tensile strength ratio of the pipe in the *longitudinal* direction with the weld metal. Tested at 68°F (20°C).

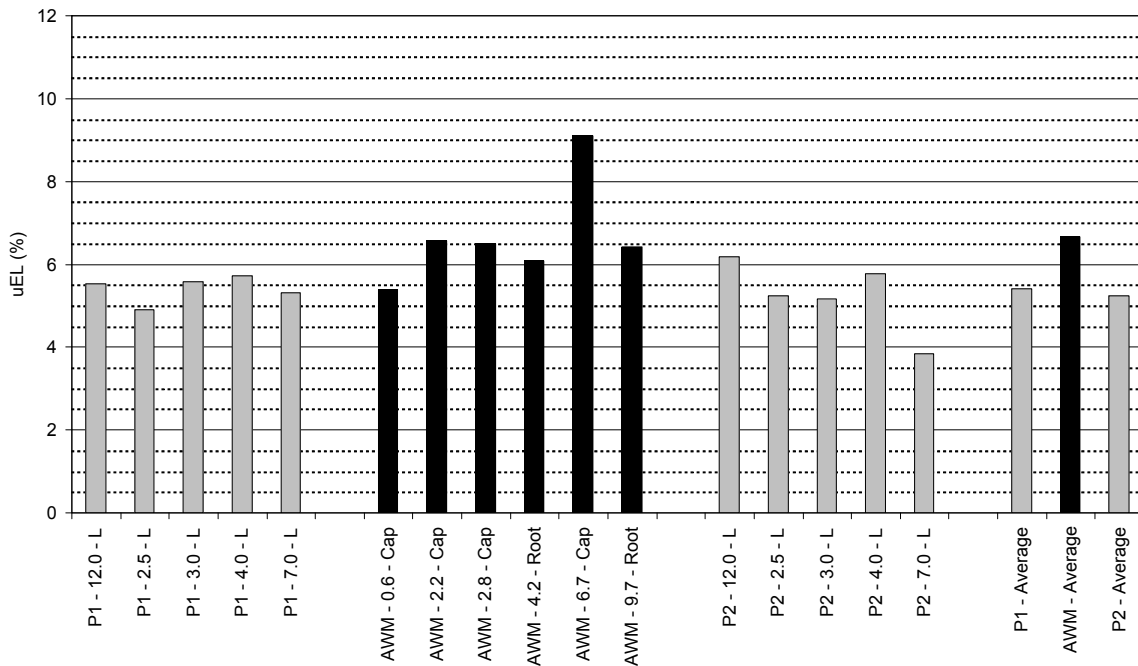
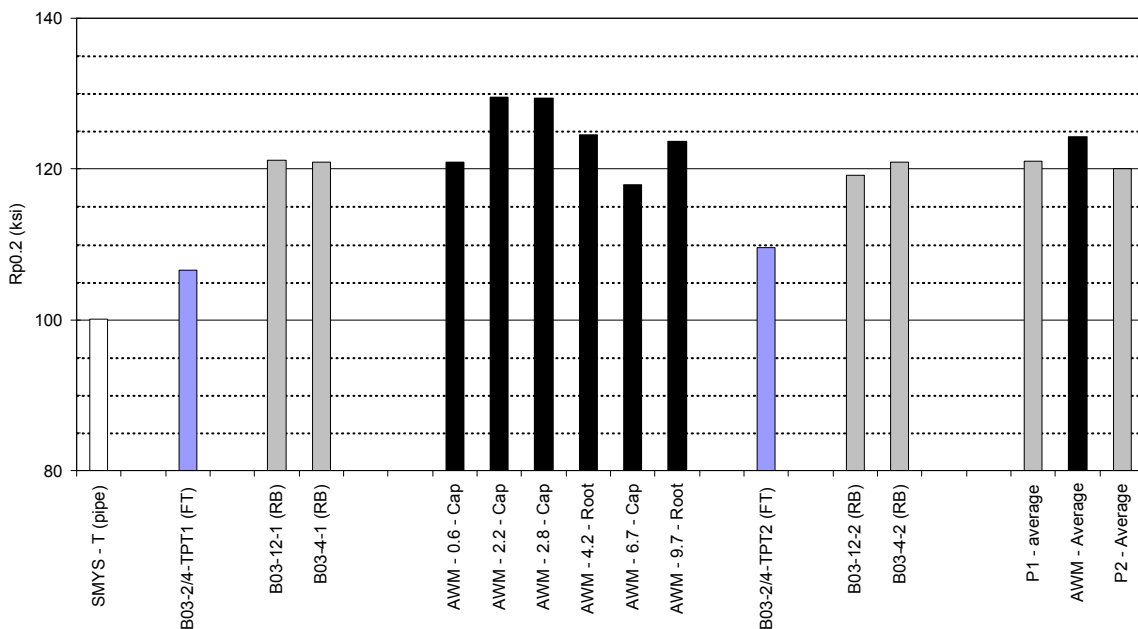
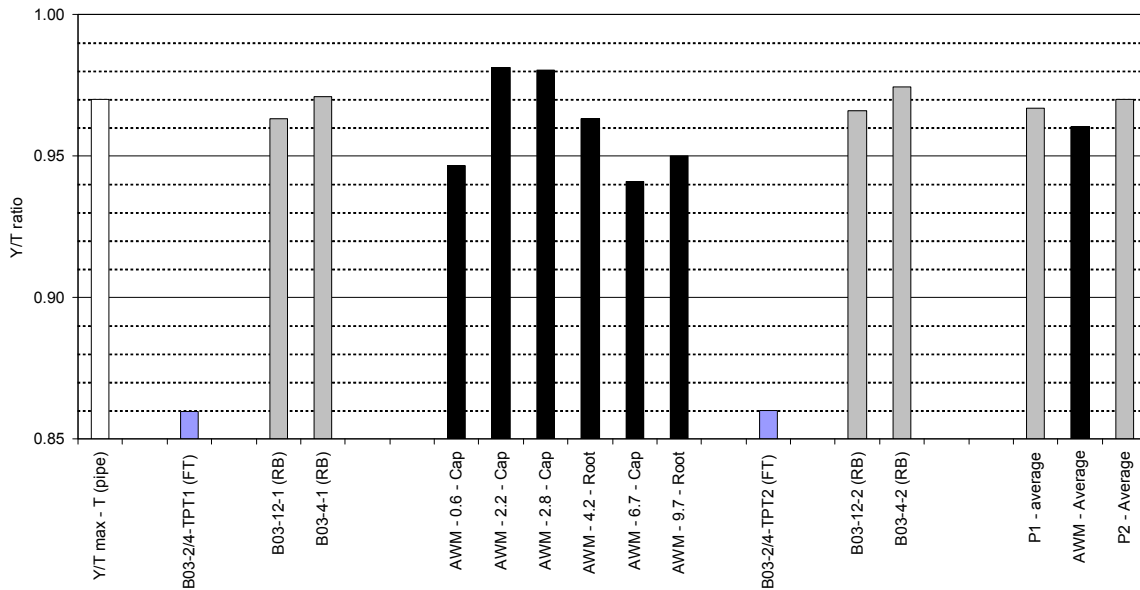


Figure 66 **Weld B03:** Comparison of the strain capacity of the pipe in the *longitudinal* direction with the all weld metal tests. Tested at 68°F (20°C).



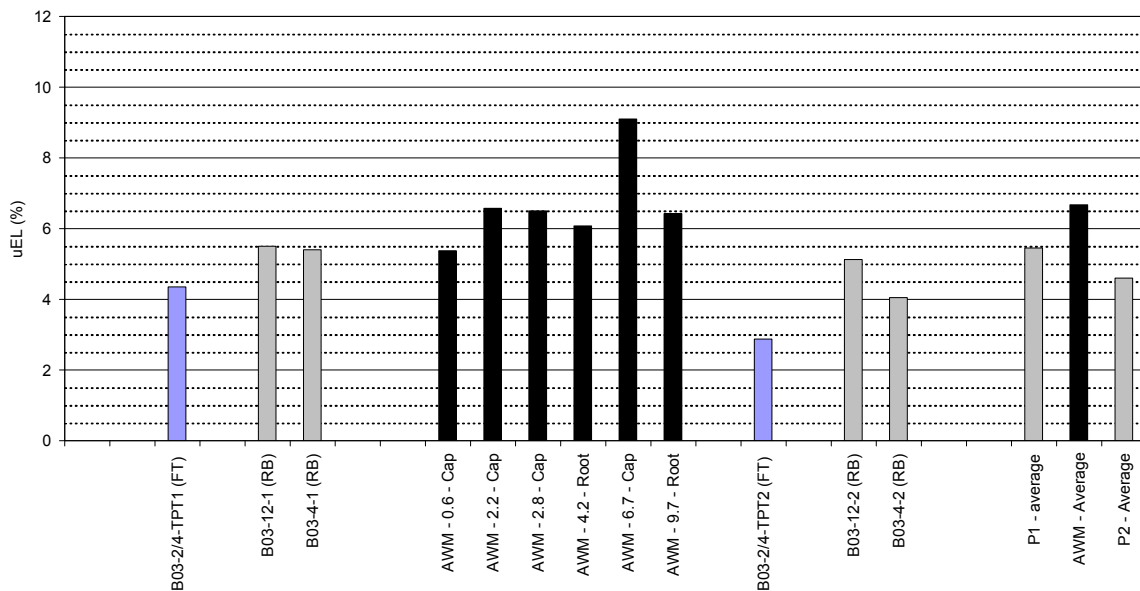
Notes: FT and RB are Flat Tensile and Round Bar specimens respectively

Figure 67 **Weld B03:** Comparison of yield strength of the pipe in the *transverse* direction with the all weld metal yield strength. Tested at 68°F (20°C).



Notes: FT and RB are Flat Tensile and Round Bar specimens respectively

Figure 68 **Weld B03:** Comparison of the weld metal yield strength to the pipe yield strength in the *transverse* direction. Tested at 68°F (20°C).



Notes: FT and RB are Flat Tensile and Round Bar specimens respectively

Figure 69 **Weld B03:** Comparison of the strain capacity of the pipe in the *transverse* direction with the all weld metal tests. Tested at 68°F (20°C).

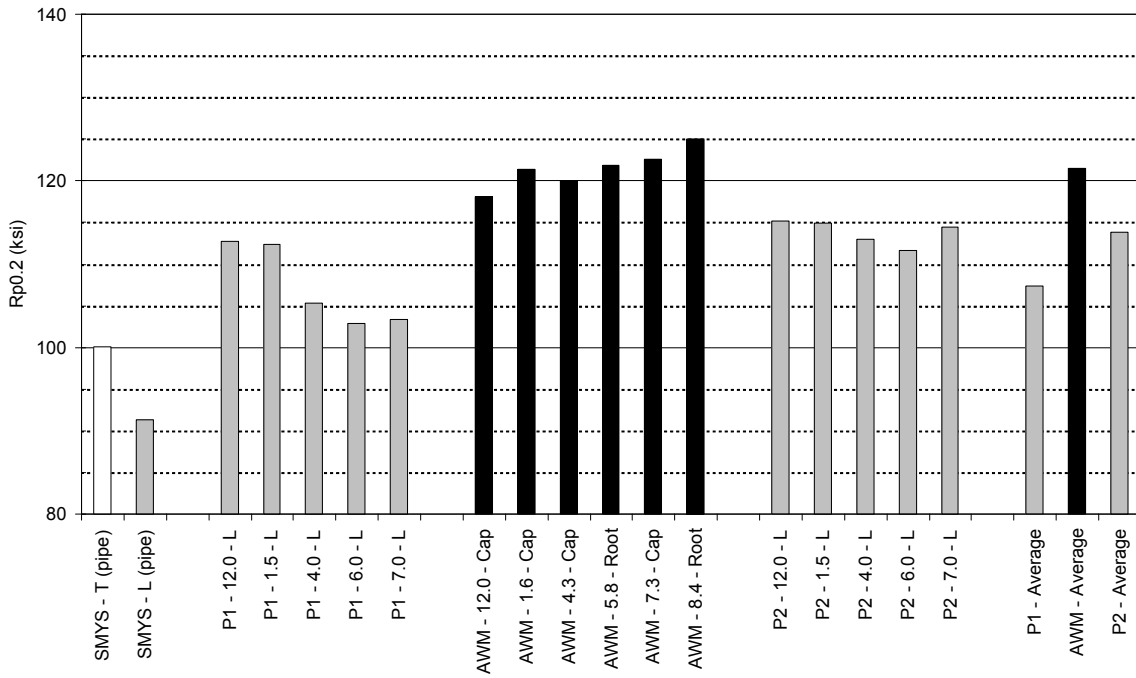


Figure 70 **Weld B06:** Comparison of yield strength of the pipe in the *longitudinal* direction with the all weld metal yield strength. Tested at 68°F (20°C).

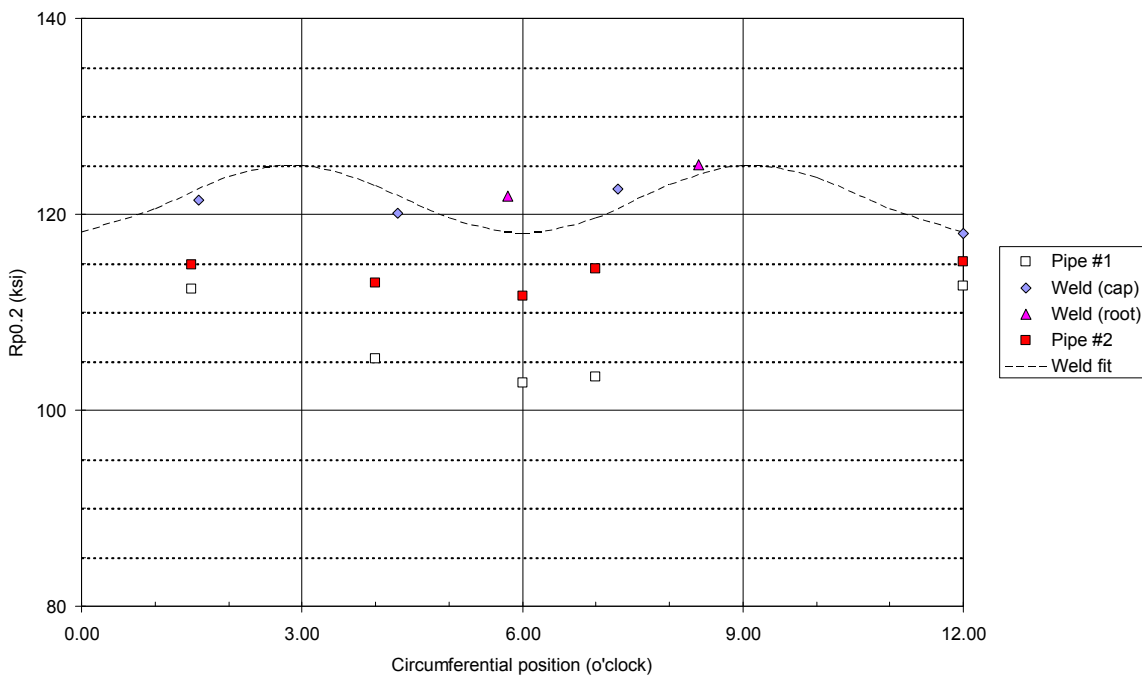


Figure 71 **Weld B06:** Comparison of yield strength (pipe *longitudinal* direction and all weld metal tests) in relation to the pipe circumferential position. Tested at 68°F (20°C).

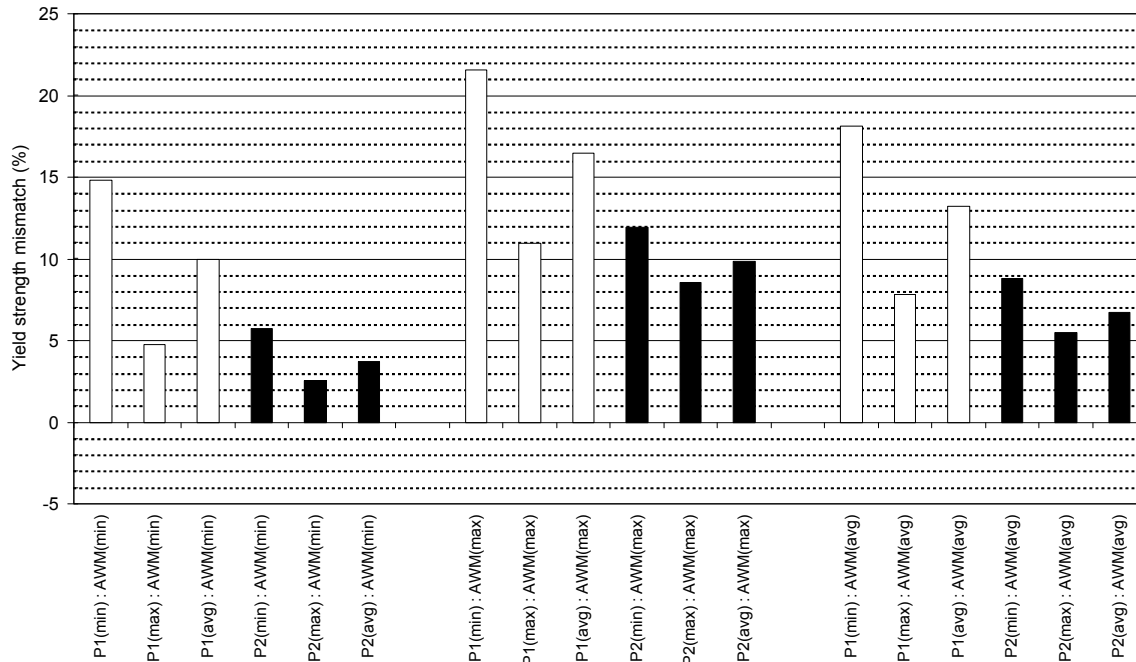


Figure 72 **Weld B06:** Comparison of the weld metal yield strength to the pipe yield strength in the *longitudinal* direction. Tested at 68°F (20°C).

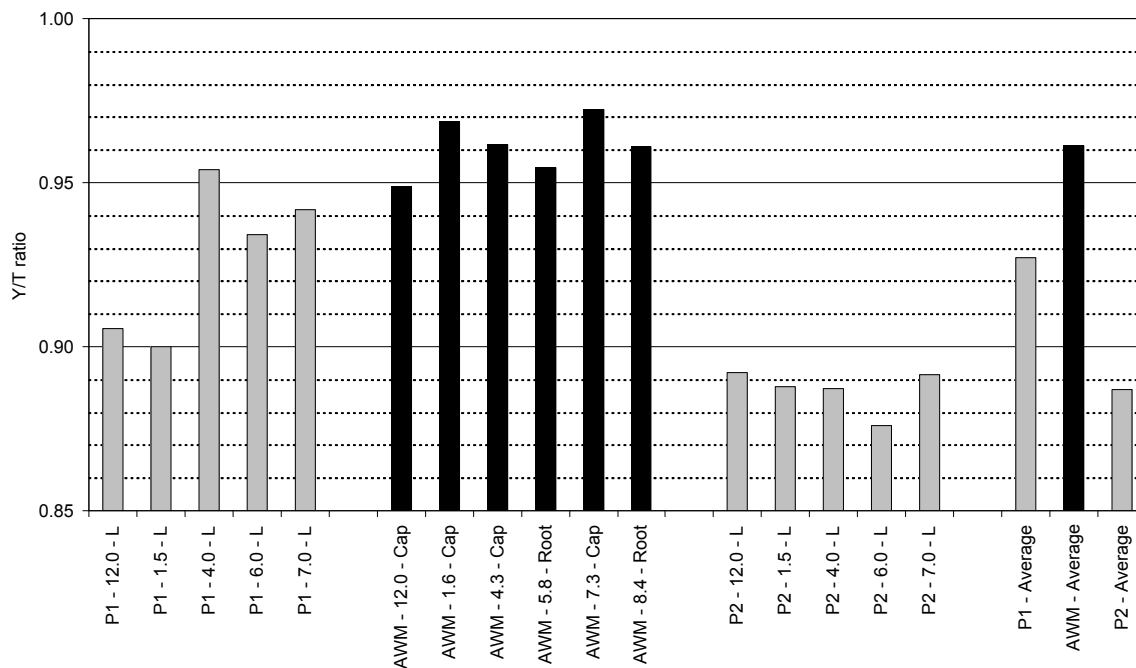


Figure 73 **Weld B06:** Comparison of yield to tensile strength ratio of the pipe in the *longitudinal* direction with the weld metal. Tested at 68°F (20°C).

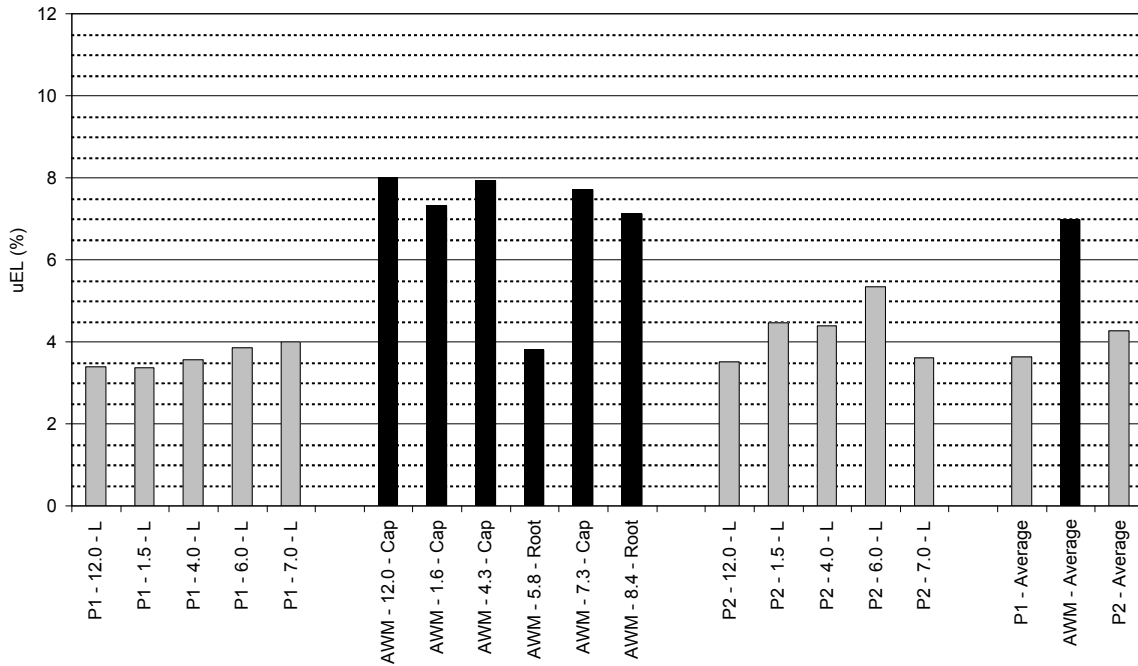
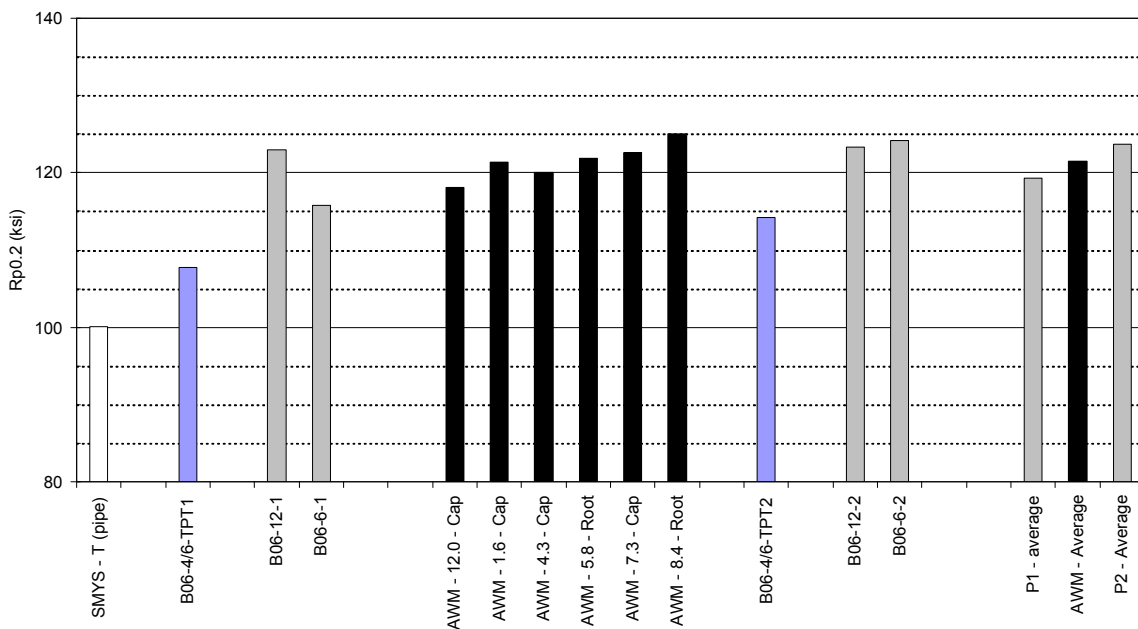
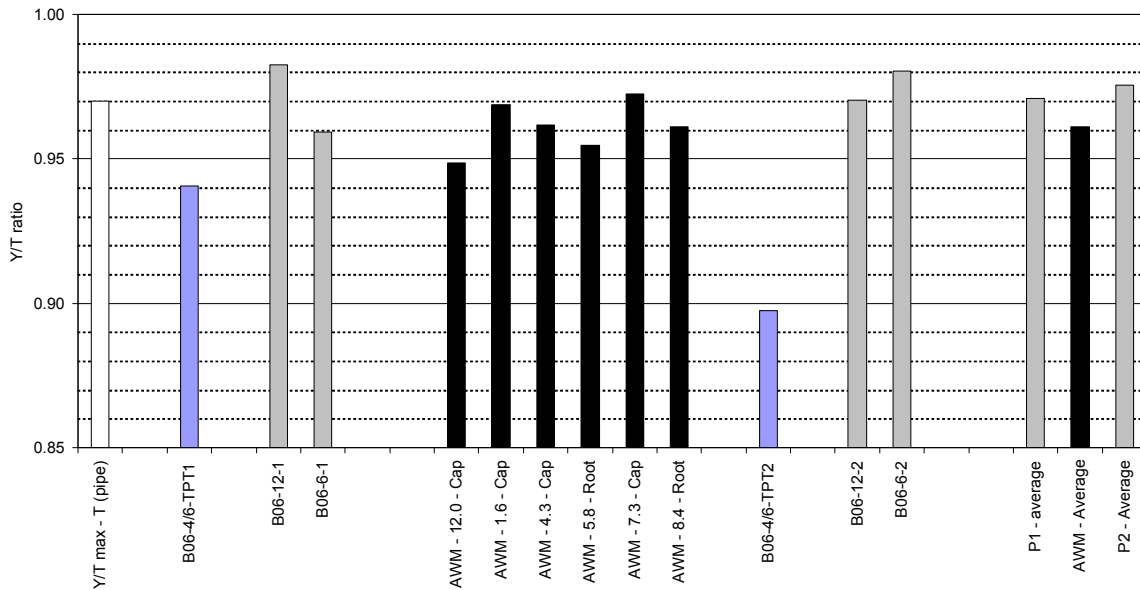


Figure 74 **Weld B06:** Comparison of the strain capacity of the pipe in the *longitudinal* direction with the all weld metal tests. Tested at 68°F (20°C).



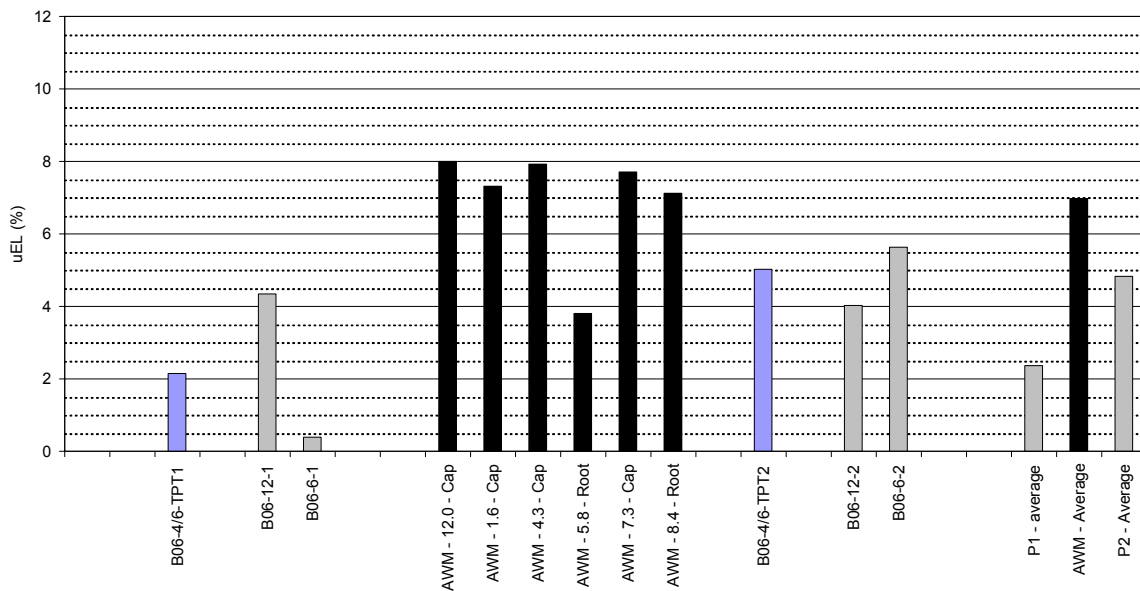
Notes: FT and RB are Flat Tensile and Round Bar specimens respectively

Figure 75 **Weld B06:** Comparison of yield strength of the pipe in the *transverse* direction with the all weld metal yield strength. Tested at 68°F (20°C).



Notes: FT and RB are Flat Tensile and Round Bar specimens respectively

Figure 76 **Weld B06:** Comparison of the weld metal yield strength to the pipe yield strength in the *transverse* direction. Tested at 68°F (20°C).



Notes: FT and RB are Flat Tensile and Round Bar specimens respectively

Figure 77 **Weld B06:** Comparison of the strain capacity of the pipe in the *transverse* direction with the all weld metal tests. Tested at 68°F (20°C).

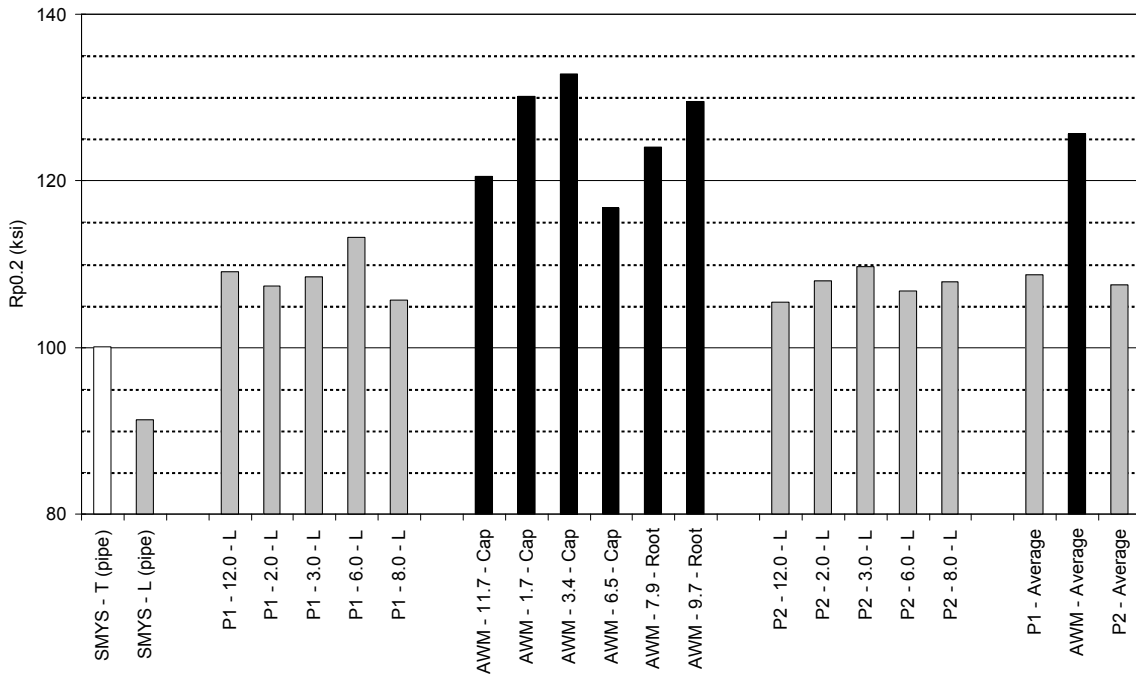


Figure 78 **Weld B08:** Comparison of yield strength of the pipe in the *longitudinal* direction with the all weld metal yield strength. Tested at 68°F (20°C).

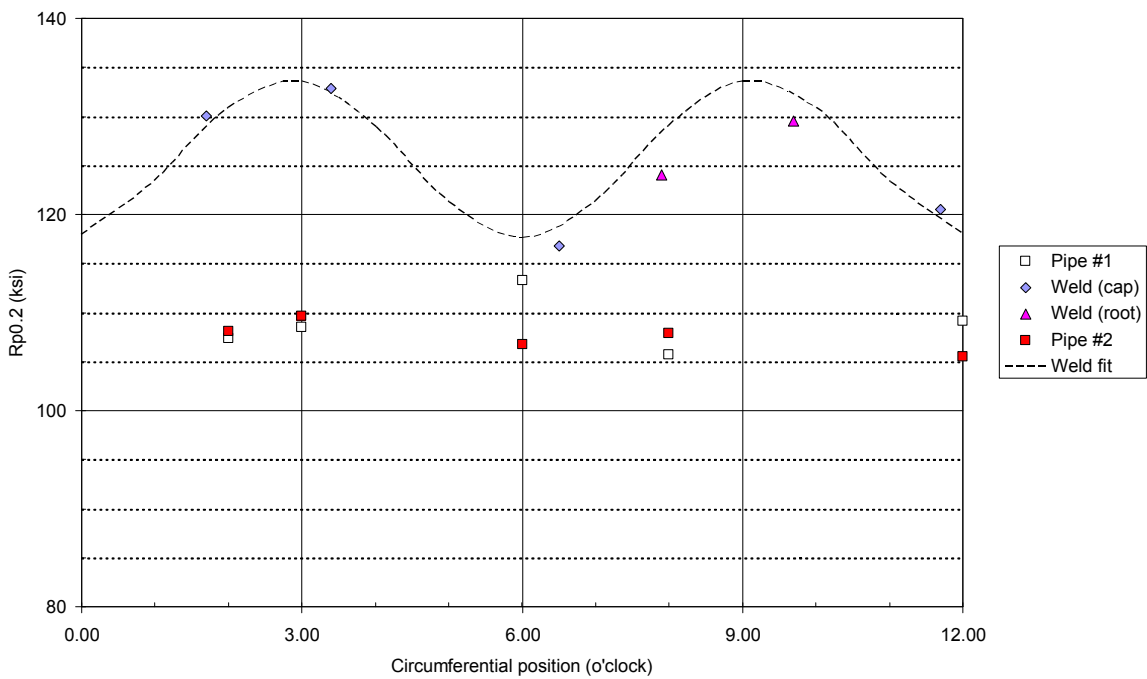


Figure 79 **Weld B08:** Comparison of yield strength (pipe *longitudinal* direction and all weld metal tests) in relation to the pipe circumferential position. Tested at 68°F (20°C).

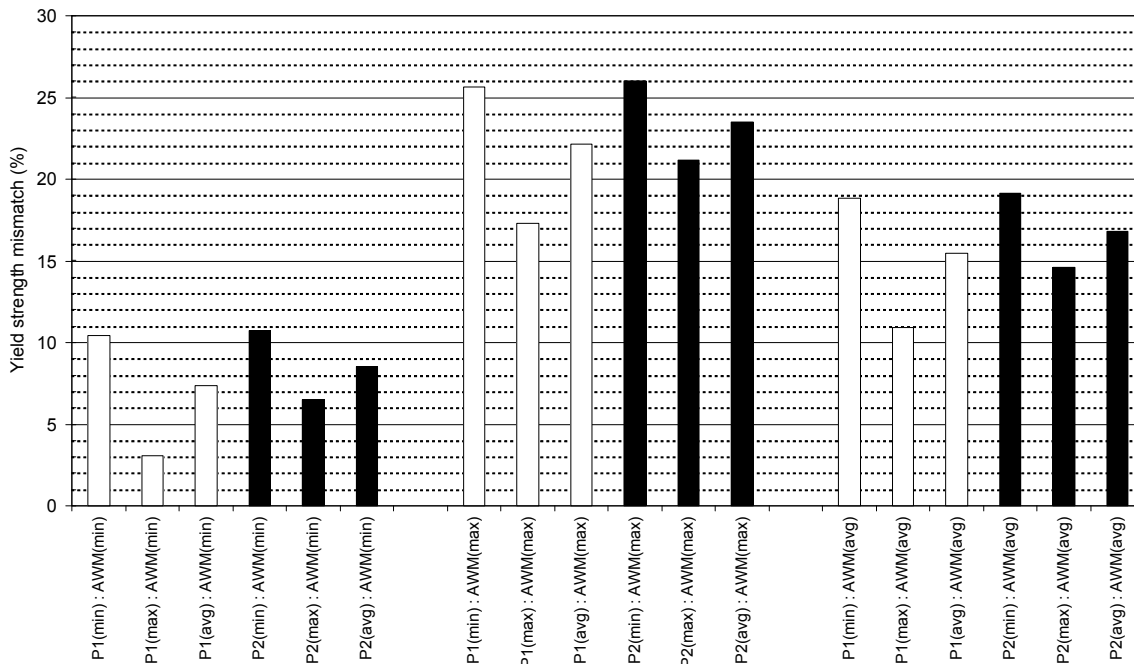


Figure 80 **Weld B08:** Comparison of the weld metal yield strength to the pipe yield strength in the *longitudinal* direction. Tested at 68°F (20°C).

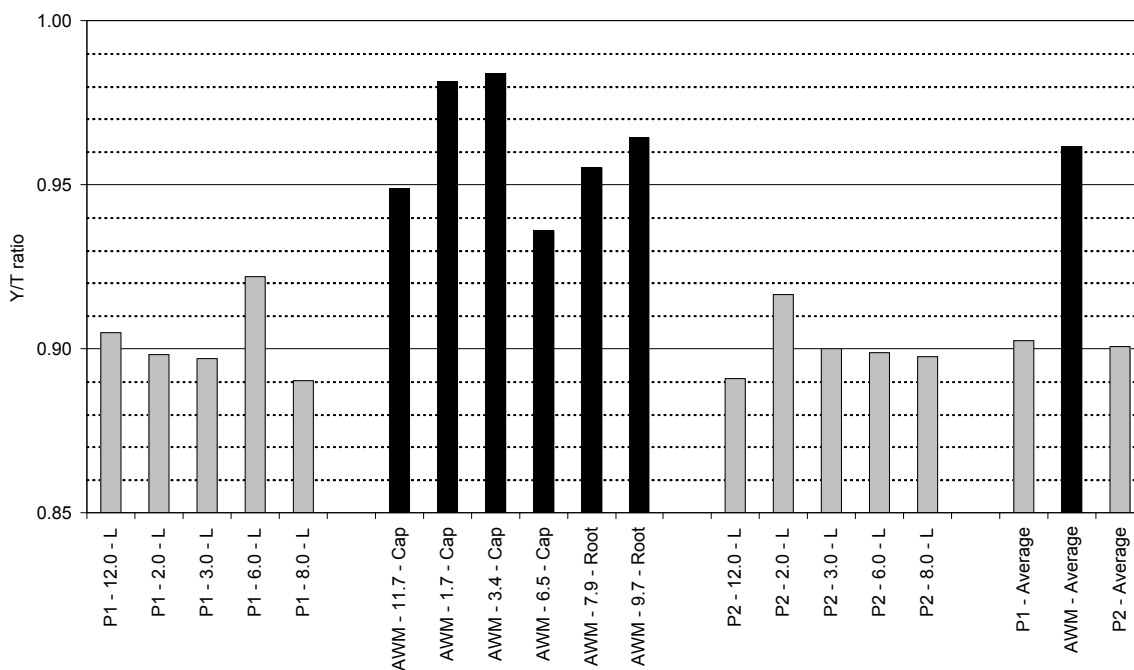


Figure 81 **Weld B08:** Comparison of yield to tensile strength ratio of the pipe in the *longitudinal* direction with the weld metal. Tested at 68°F (20°C).

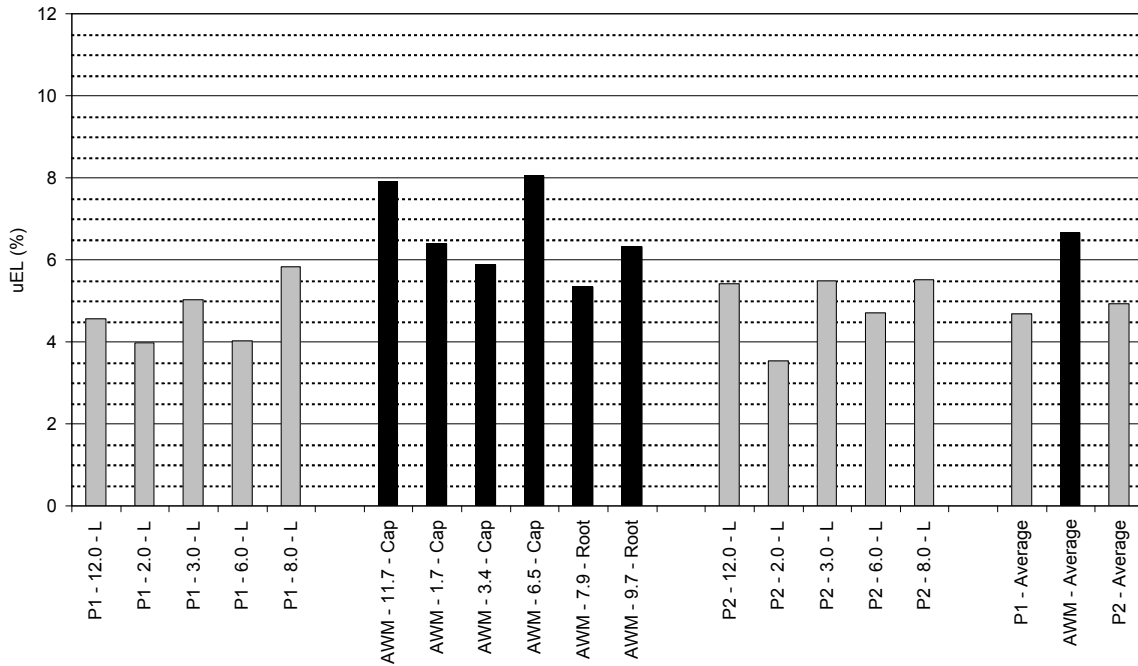
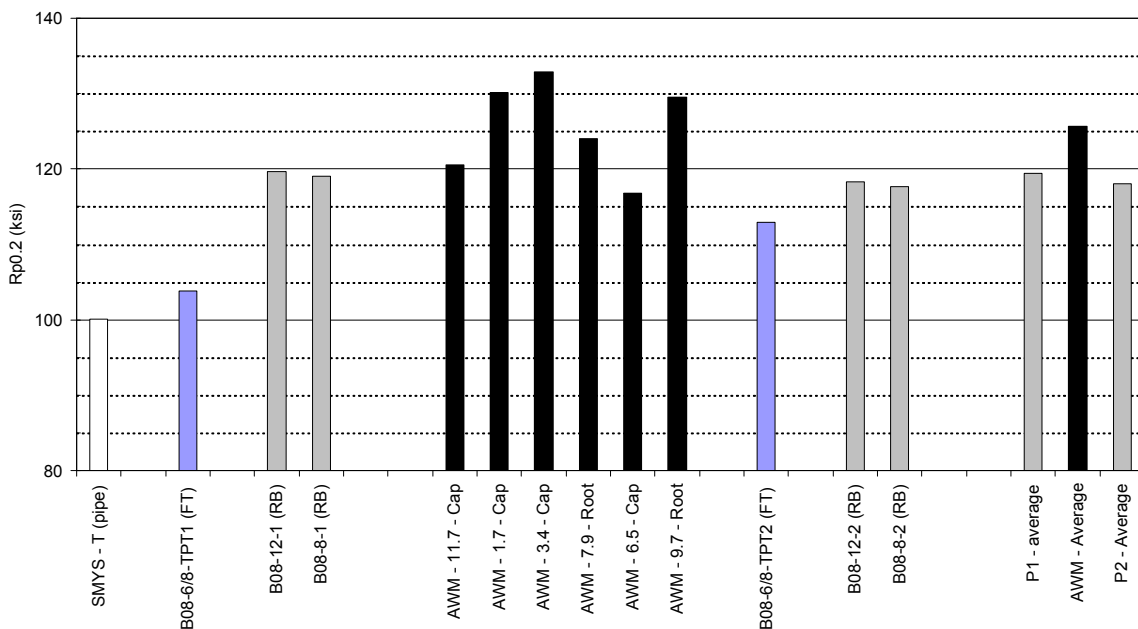
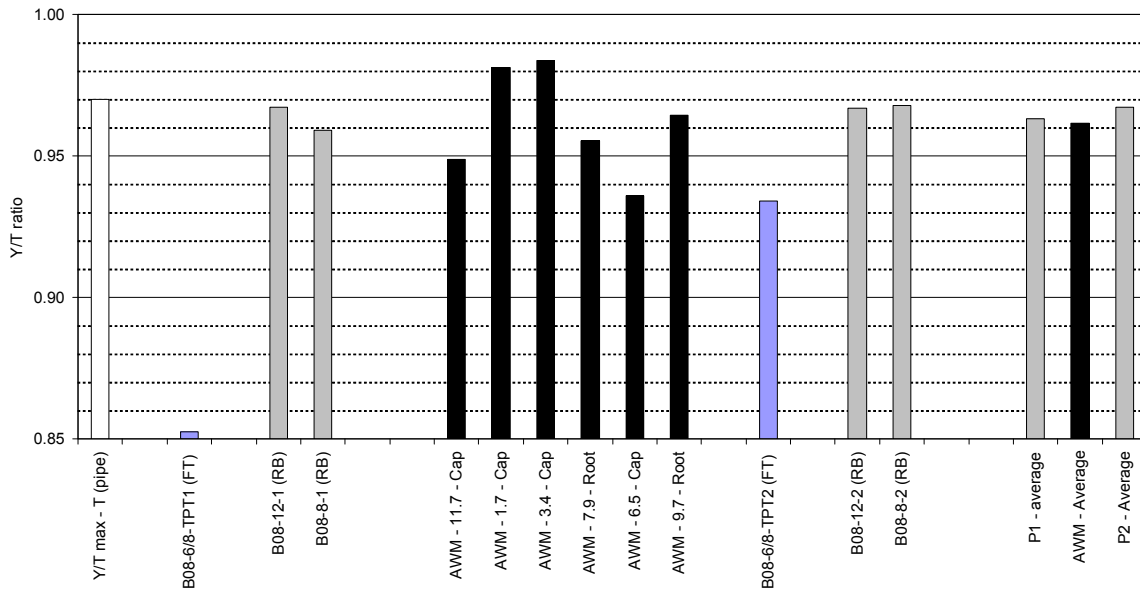


Figure 82 **Weld B08:** Comparison of the strain capacity of the pipe in the *longitudinal* direction with the all weld metal tests. Tested at 68°F (20°C).



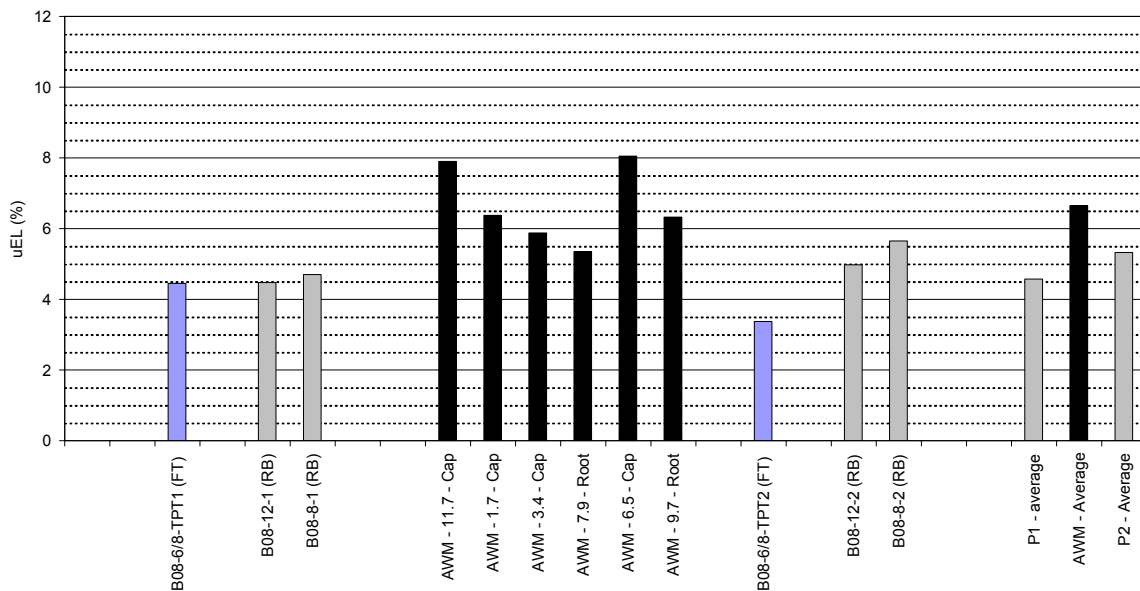
Notes: FT and RB are Flat Tensile and Round Bar specimens respectively

Figure 83 **Weld B08:** Comparison of yield strength of the pipe in the *transverse* direction with the all weld metal yield strength. Tested at 68°F (20°C).



Notes: FT and RB are Flat Tensile and Round Bar specimens respectively

Figure 84 **Weld B08:** Comparison of the weld metal yield strength to the pipe yield strength in the *transverse* direction. Tested at 68°F (20°C).



Notes: FT and RB are Flat Tensile and Round Bar specimens respectively

Figure 85 **Weld B08:** Comparison of the strain capacity of the pipe in the *transverse* direction with the all weld metal tests. Tested at 68°F (20°C).

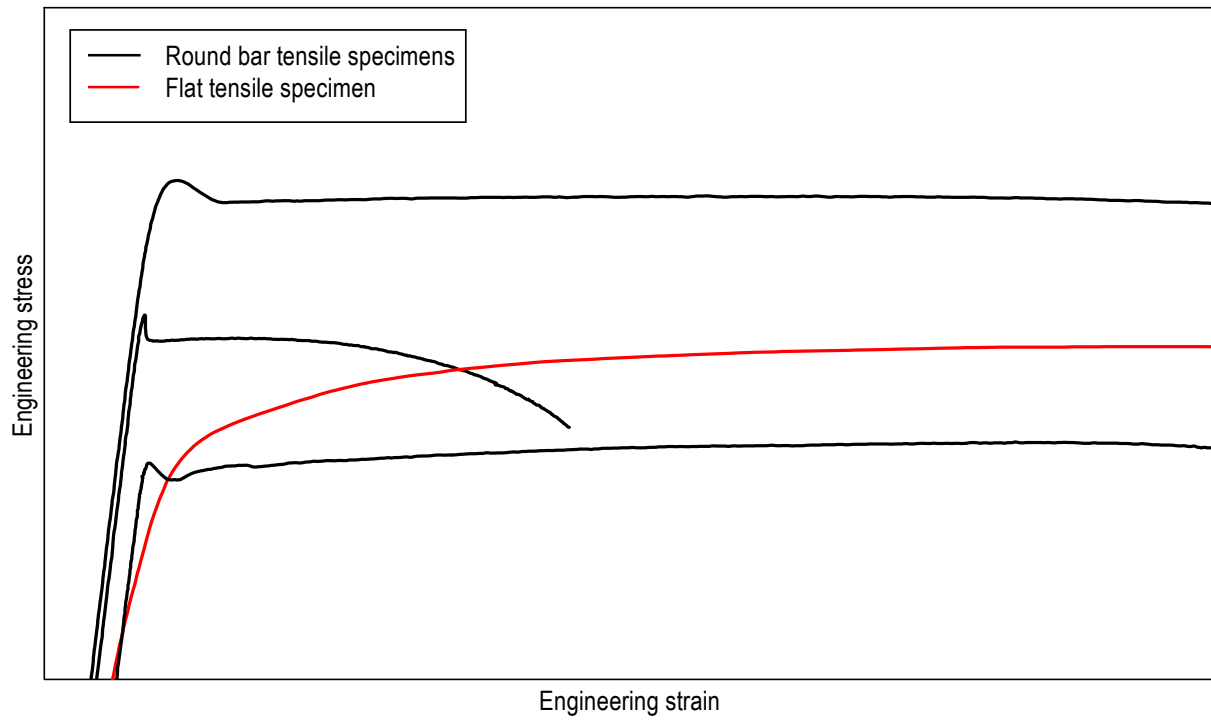
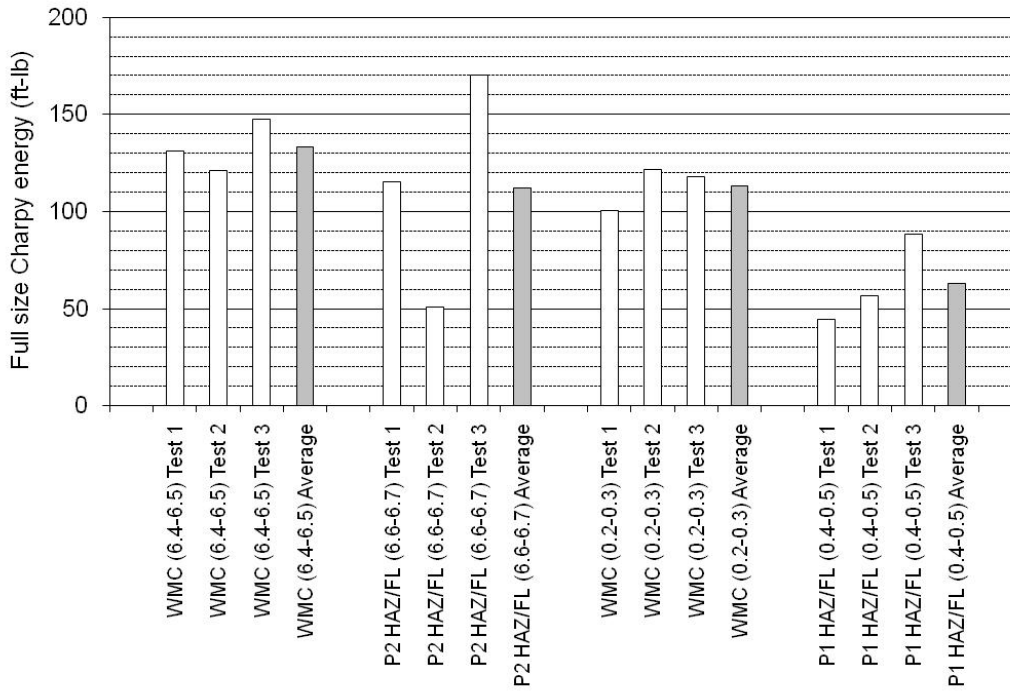
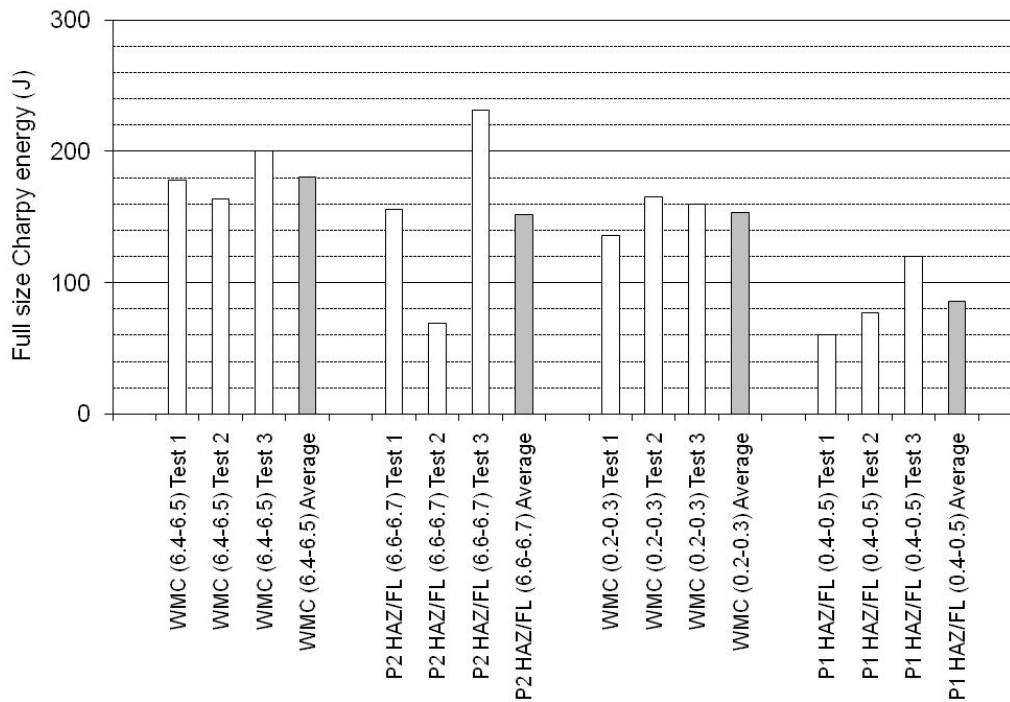


Figure 86 Engineering stress-strain responses from specimens extracted from the pipe transverse direction.



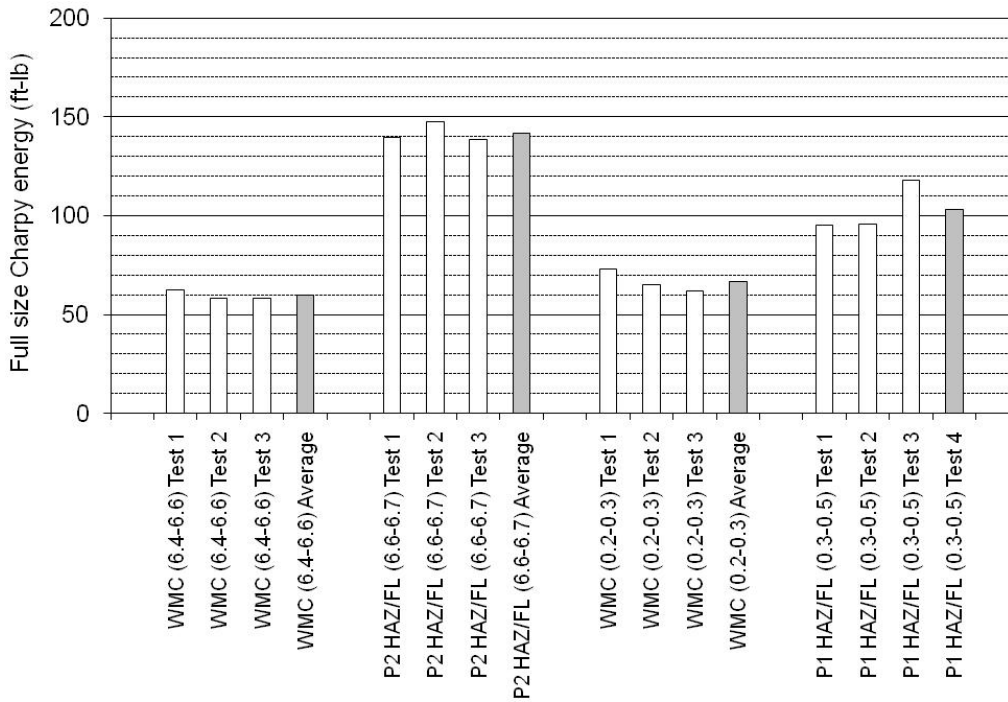
(a) US customary units



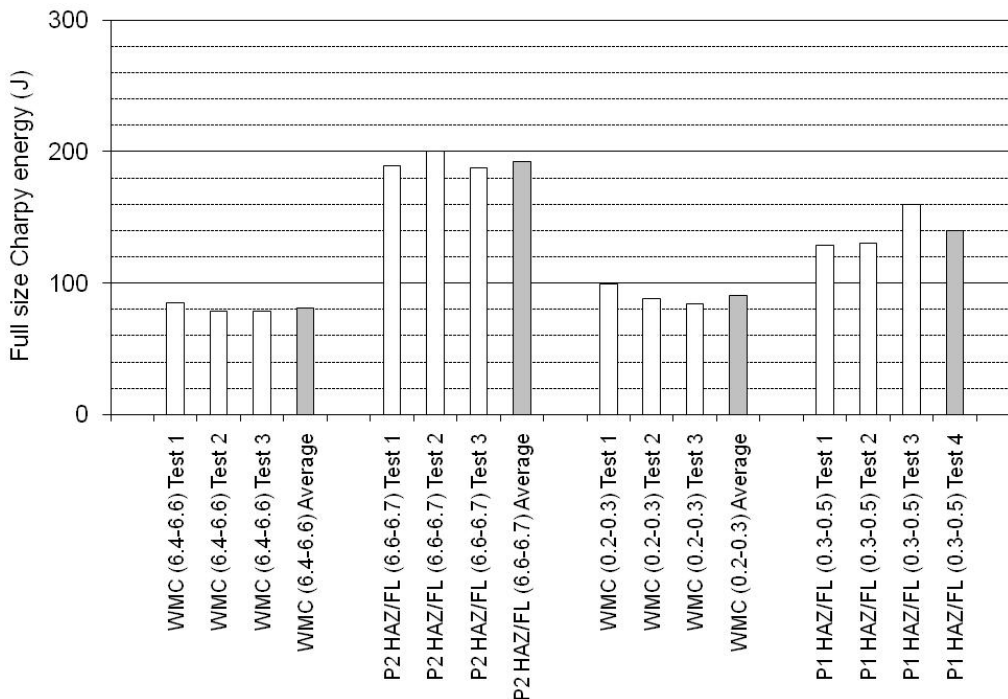
(b) SI units

Notes: Labeling is 'notch location (specimen o'clock position)'. P1 and P2 are Pipe 1 and Pipe 2, WMC, HAZ and FL are weld metal centerline, heat affected zone and fusion line, respectively.

Figure 87 Charpy Impact test results: Weld A06.



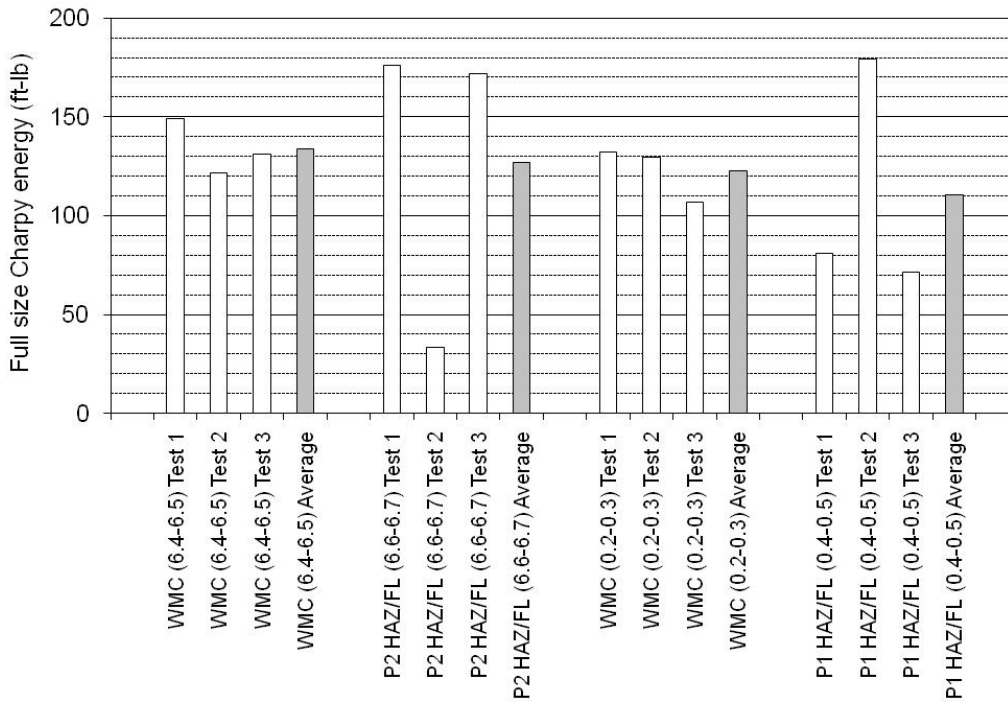
(a) US customary units



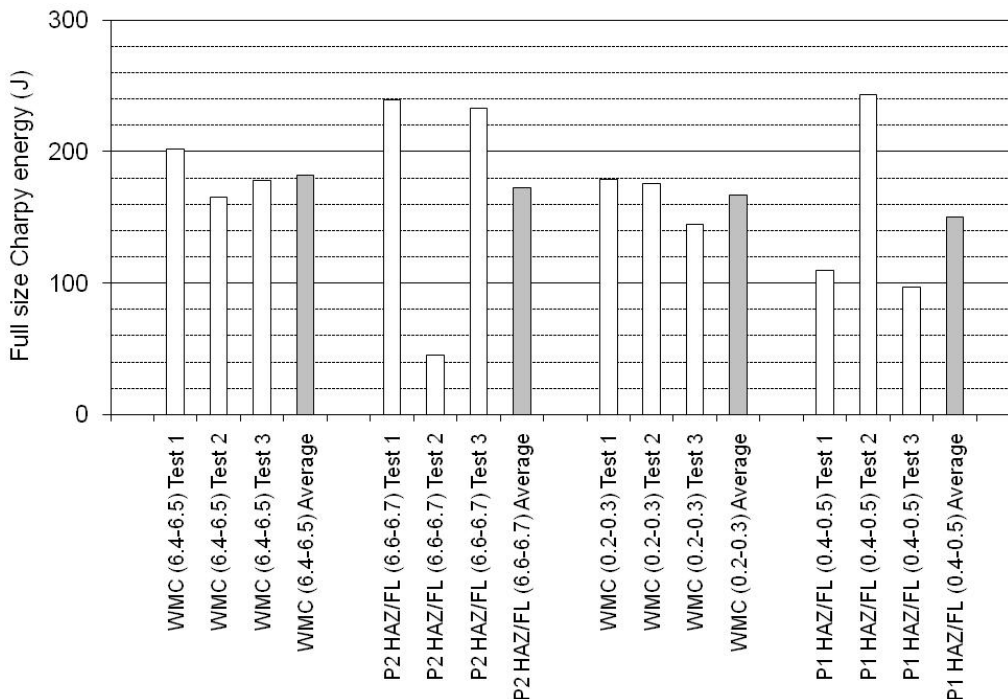
(b) SI units

Notes: Labeling is 'notch location (specimen o'clock position)'. P1 and P2 are Pipe 1 and Pipe 2, WMC, HAZ and FL are weld metal centerline, heat affected zone and fusion line, respectively.

Figure 88 Charpy Impact test results: Weld A17.



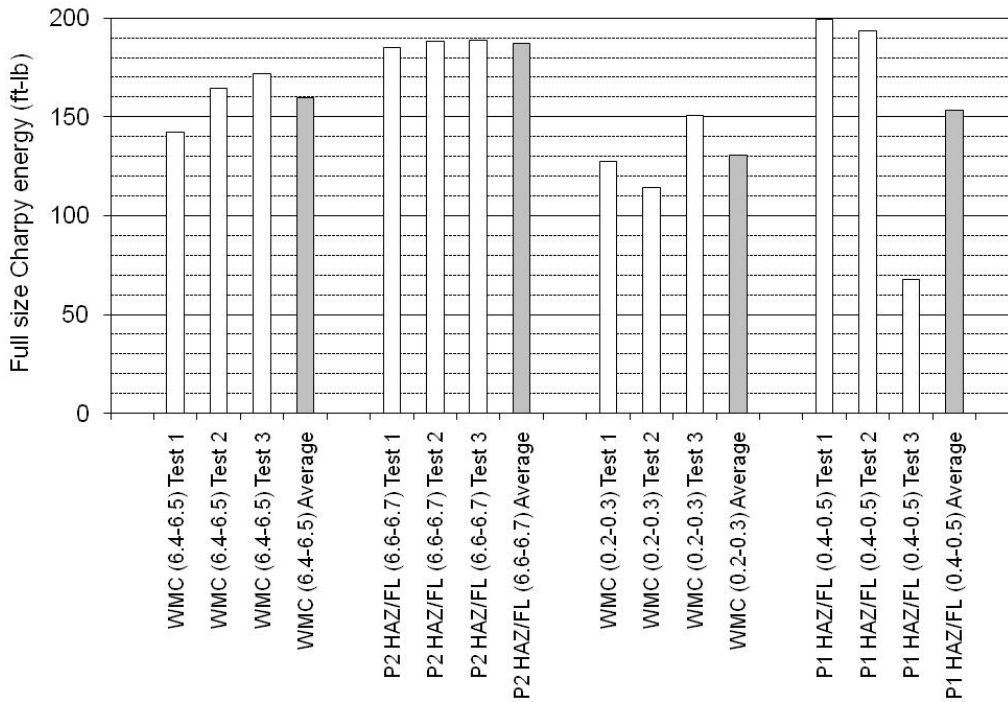
(a) US customary units



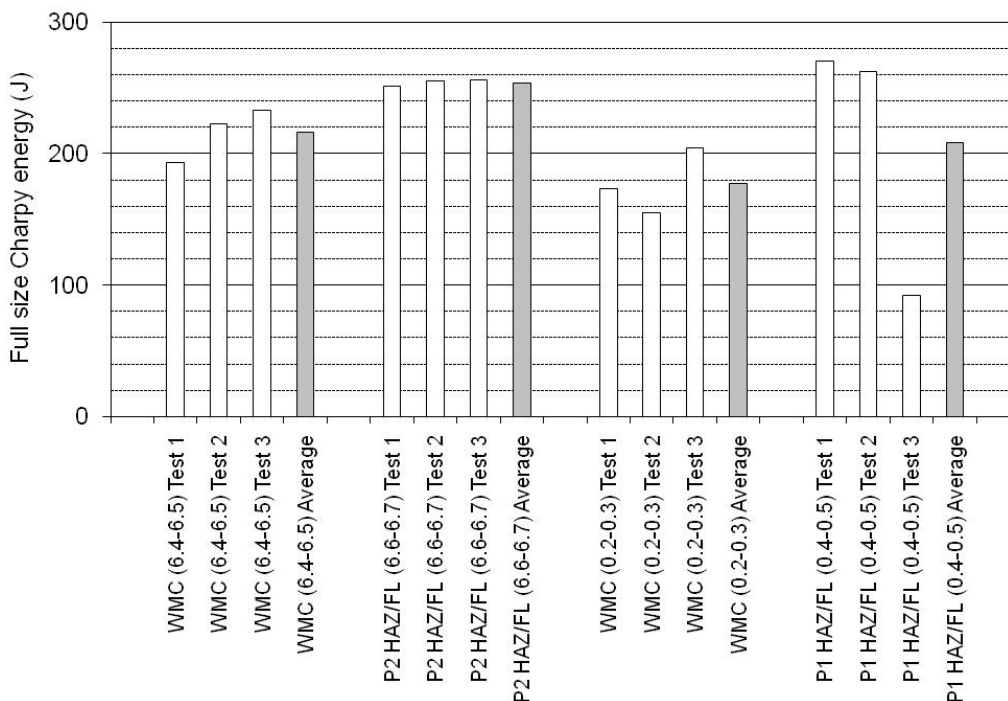
(b) SI units

Notes: Labeling is 'notch location (specimen o'clock position)'. P1 and P2 are Pipe 1 and Pipe 2, WMC, HAZ and FL are weld metal centerline, heat affected zone and fusion line, respectively.

Figure 89 Charpy Impact test results: Weld A33.



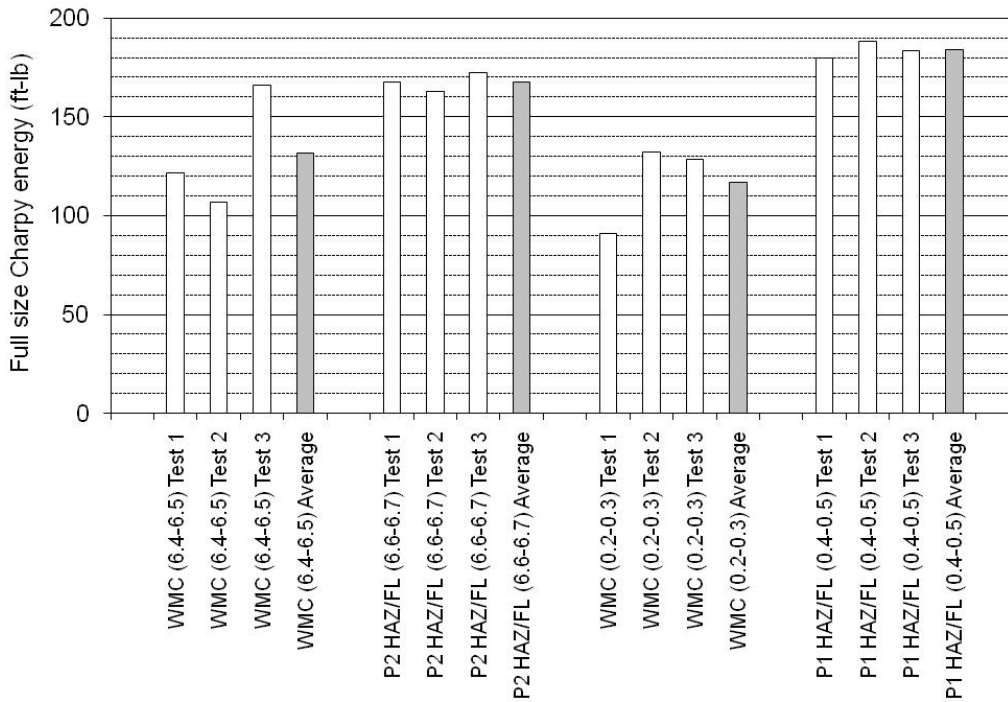
(a) US customary units



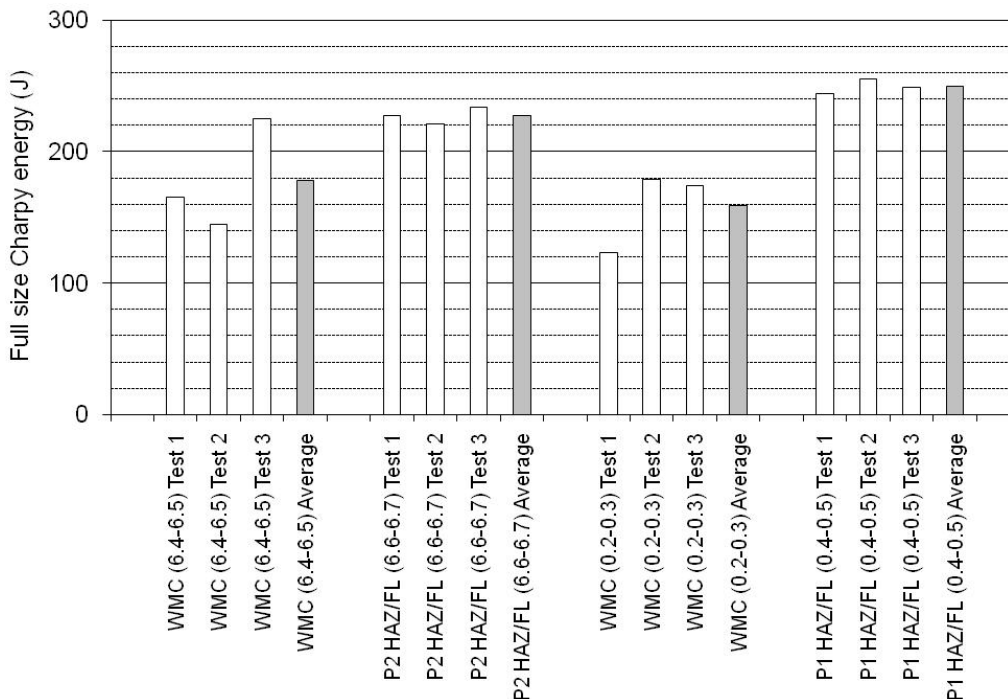
(b) SI units

Notes: Labeling is 'notch location (specimen o'clock position)'. P1 and P2 are Pipe 1 and Pipe 2, WMC, HAZ and FL are weld metal centerline, heat affected zone and fusion line, respectively.

Figure 90 Charpy Impact test results: Weld A44.



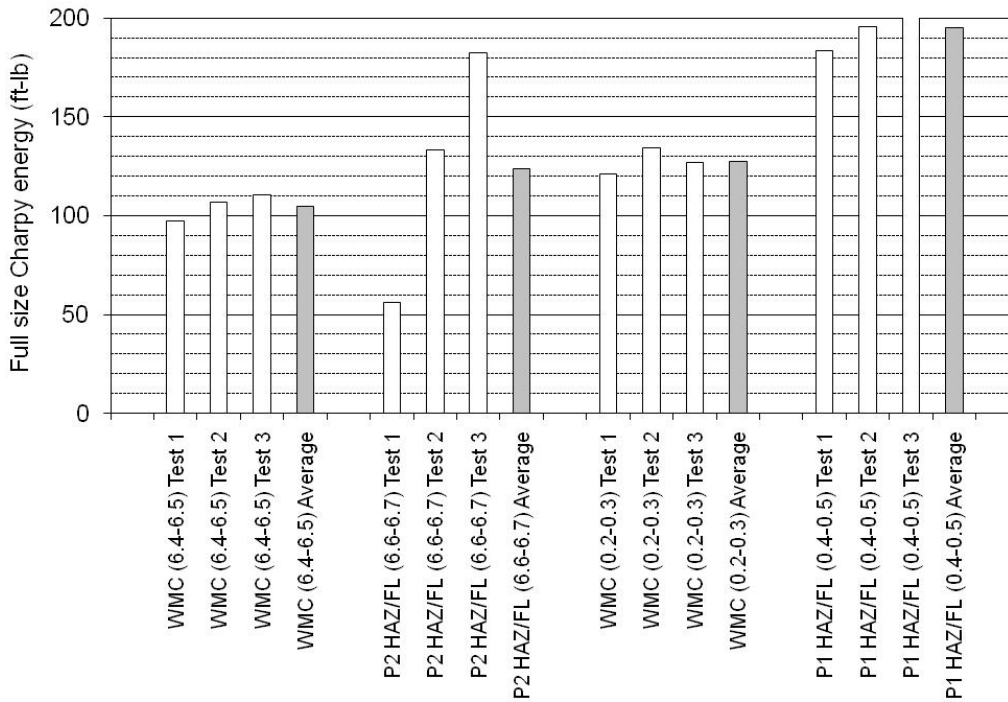
(a) US customary units



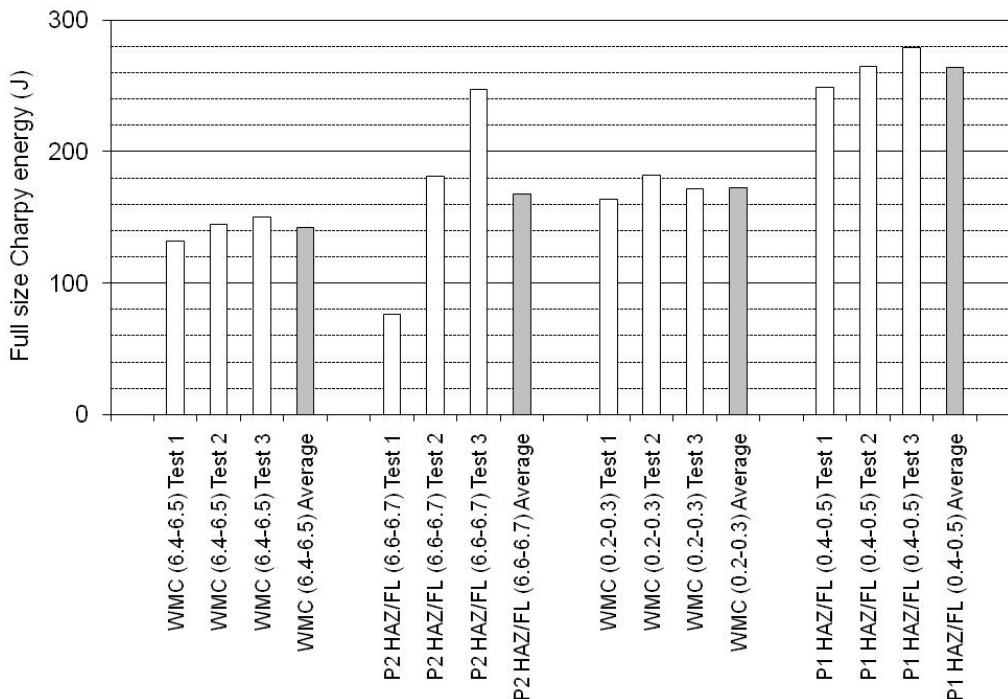
(b) SI units

Notes: Labeling is 'notch location (specimen o'clock position)'. P1 and P2 are Pipe 1 and Pipe 2, WMC, HAZ and FL are weld metal centerline, heat affected zone and fusion line, respectively.

Figure 91 Charpy Impact test results: Weld A46.



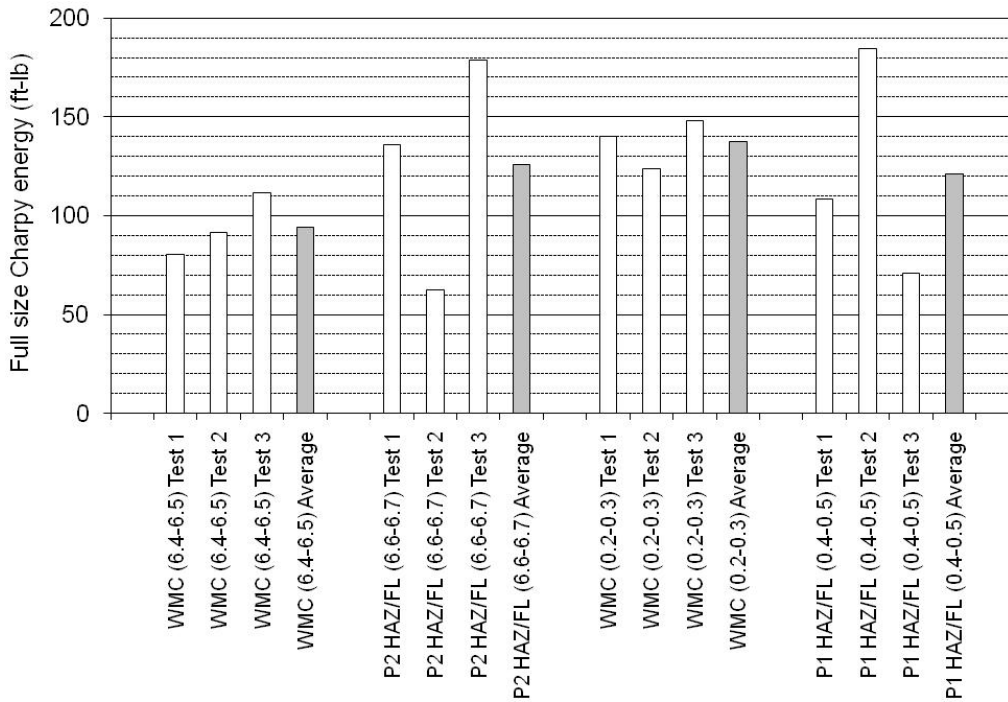
(a) US customary units



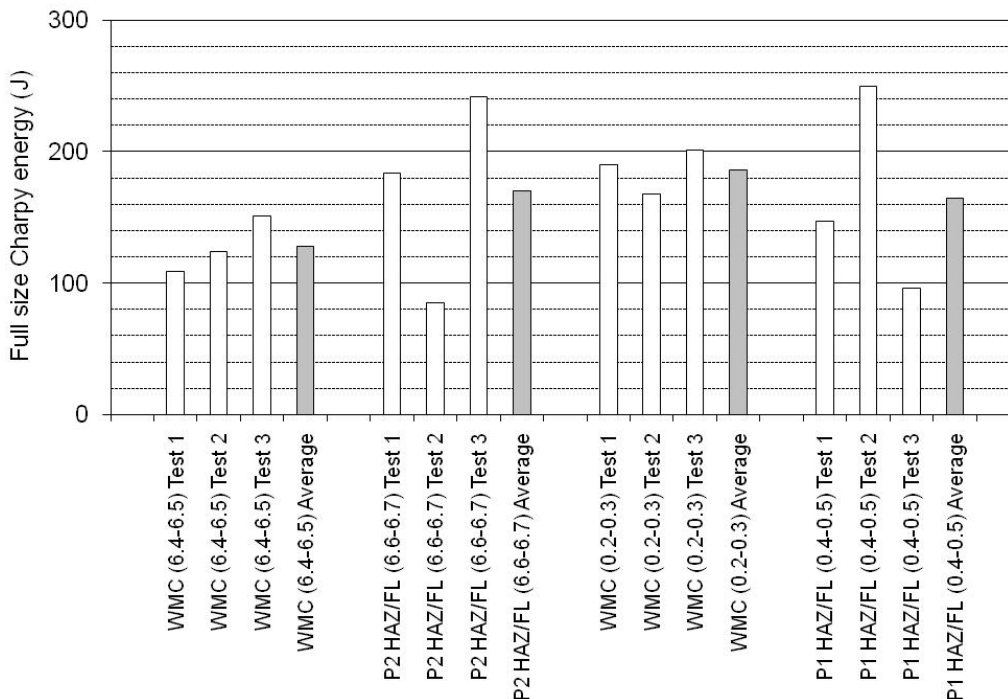
(b) SI units

Notes: Labeling is 'notch location (specimen o'clock position)'. P1 and P2 are Pipe 1 and Pipe 2, WMC, HAZ and FL are weld metal centerline, heat affected zone and fusion line, respectively.

Figure 92 Charpy Impact test results: Weld A50.



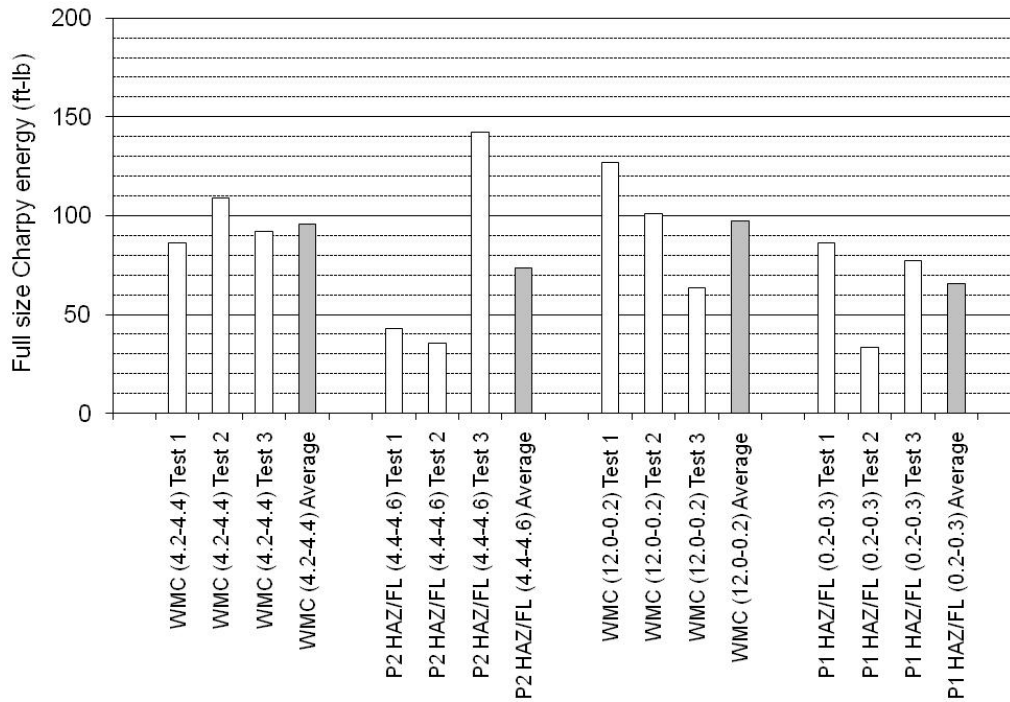
(a) US customary units



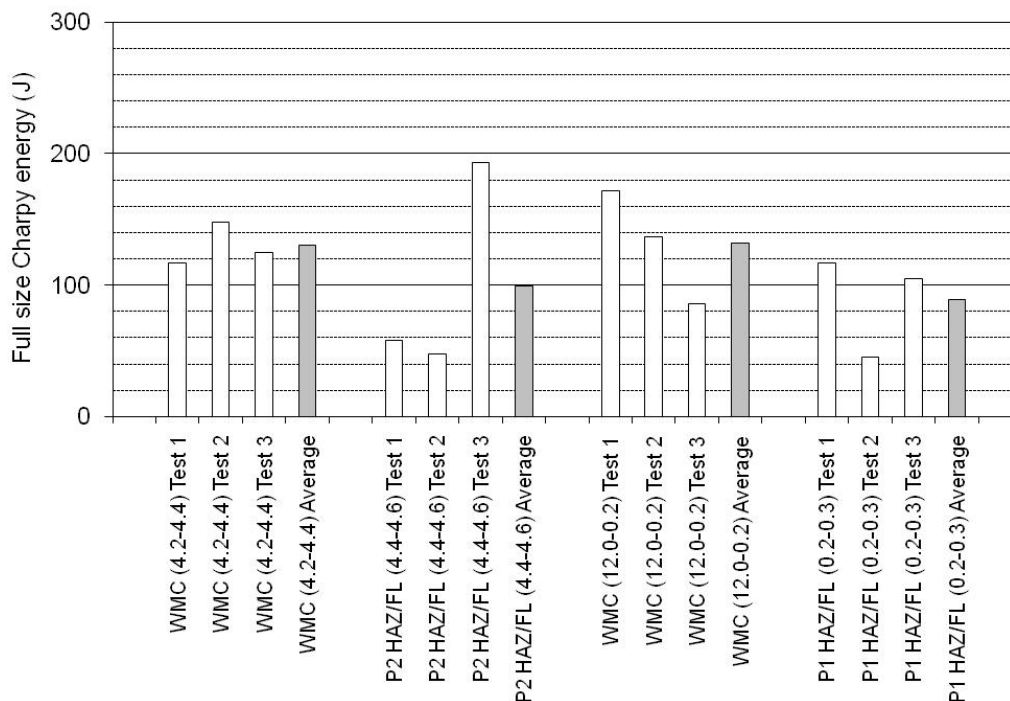
(b) SI units

Notes: Labeling is 'notch location (specimen o'clock position)'. P1 and P2 are Pipe 1 and Pipe 2, WMC, HAZ and FL are weld metal centerline, heat affected zone and fusion line, respectively.

Figure 93 Charpy Impact test results: Weld B03.



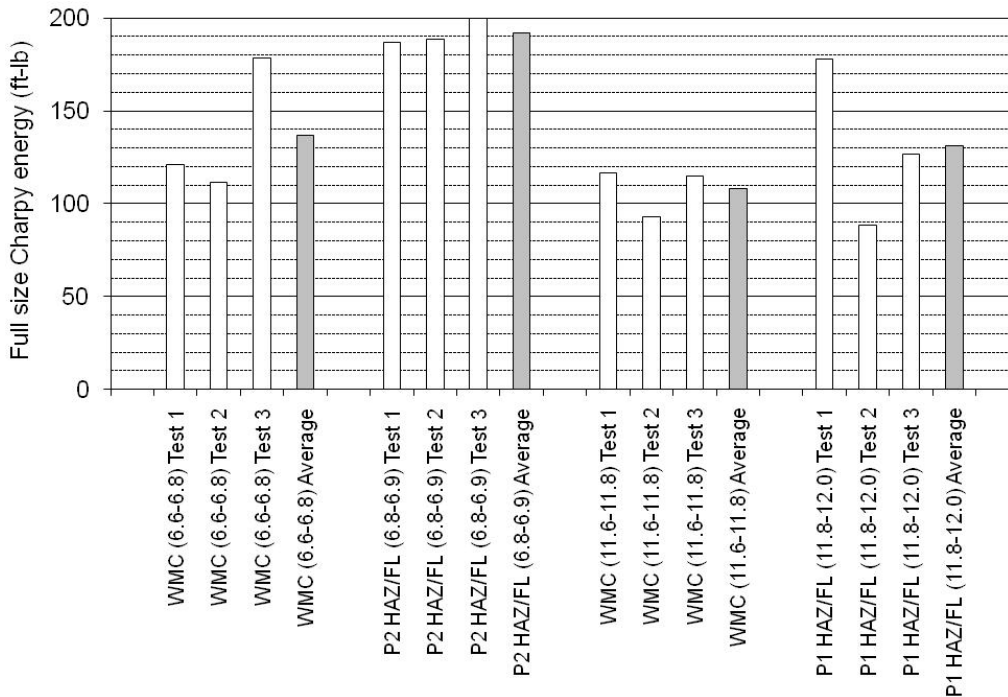
(a) US customary units



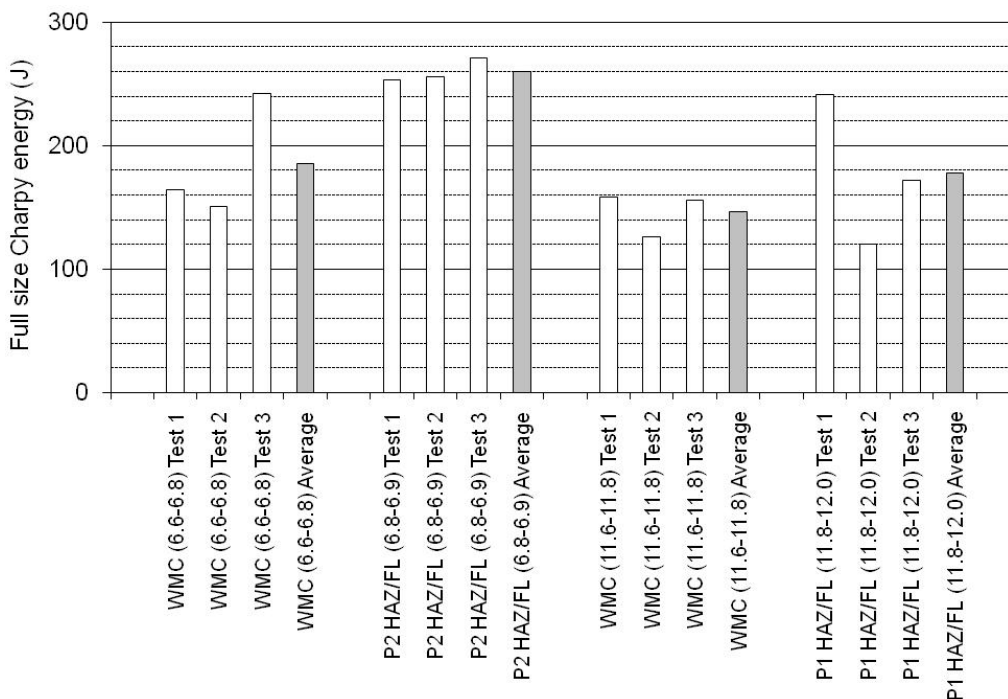
(b) SI units

Notes: Labeling is 'notch location (specimen o'clock position)'. P1 and P2 are Pipe 1 and Pipe 2, WMC, HAZ and FL are weld metal centerline, heat affected zone and fusion line, respectively.

Figure 94 Charpy Impact test results: Weld B06.



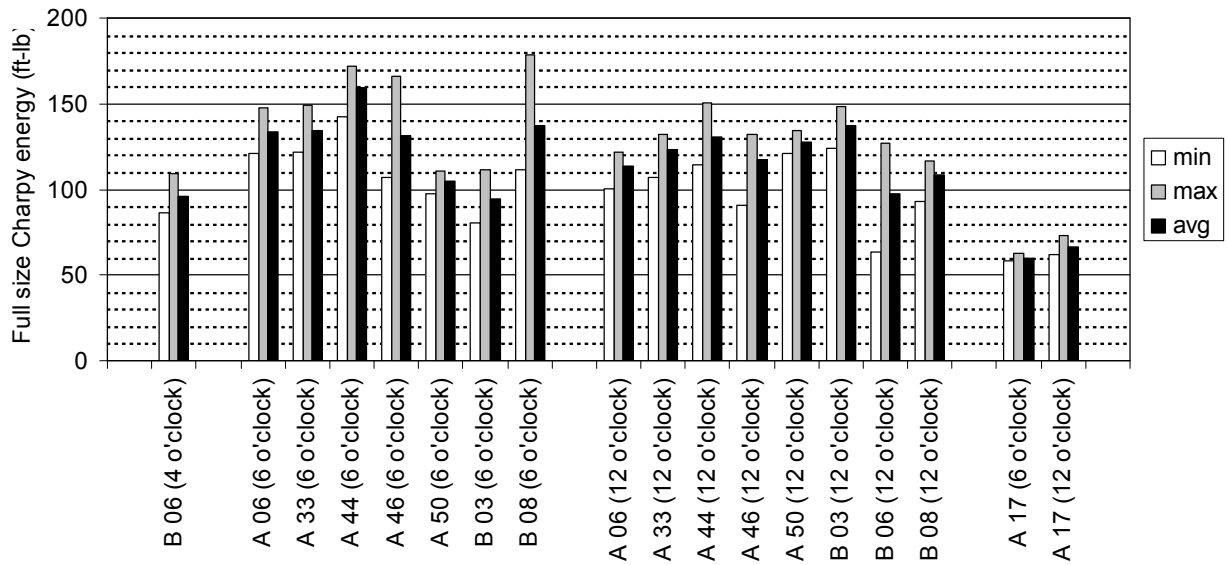
(a) US customary units



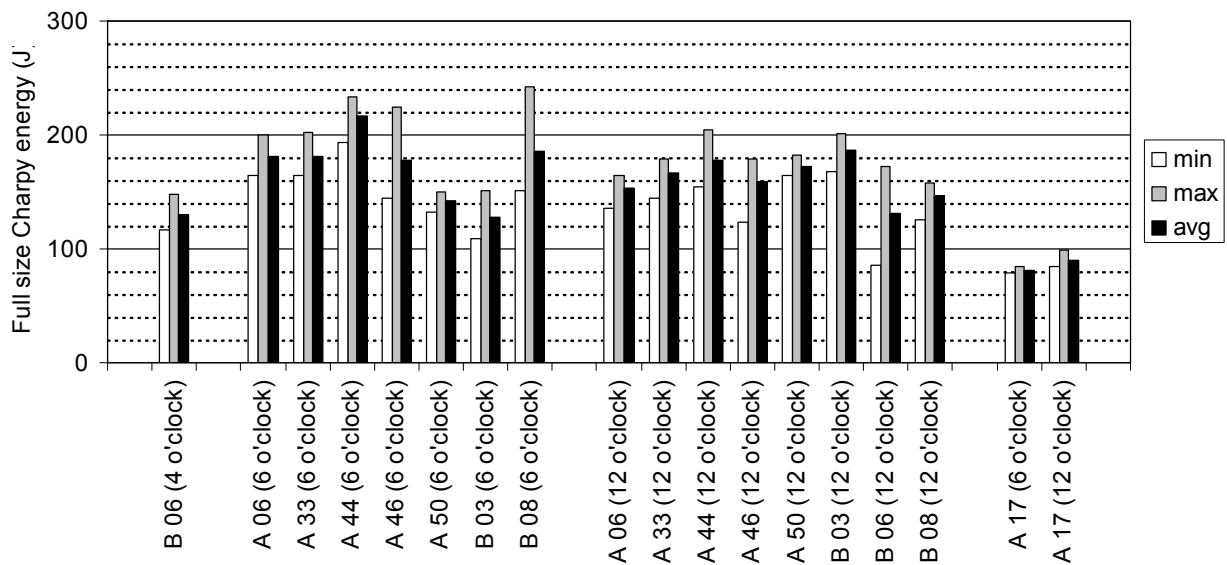
(b) SI units

Notes: Labeling is 'notch location (specimen o'clock position)'. P1 and P2 are Pipe 1 and Pipe 2, WMC, HAZ and FL are weld metal centerline, heat affected zone and fusion line, respectively.

Figure 95 Charpy Impact test results: Weld B08.



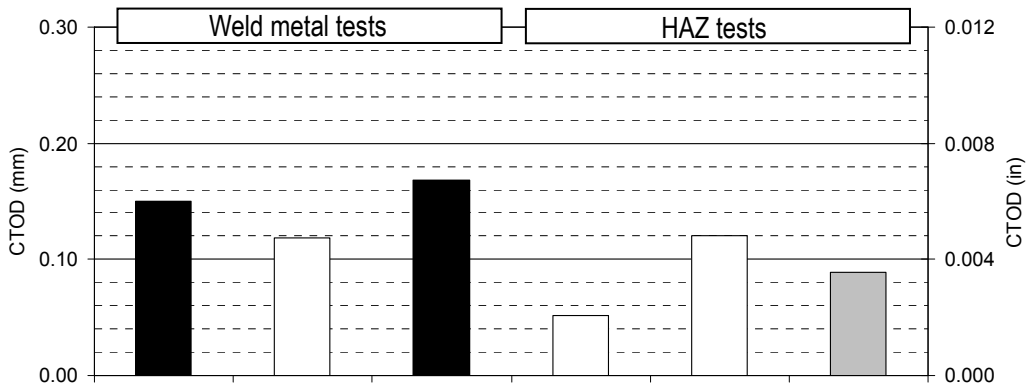
(a) US customary units



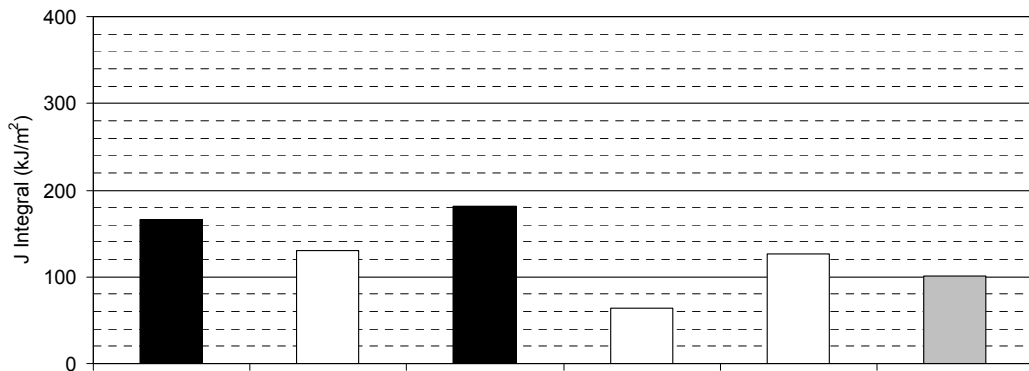
(b) SI units

Notes: Labeling is 'weld ID (specimen o'clock position)'. Weld **A17** was welded using a Tie-in weld procedure; the remaining welds were produced using the main-line welding procedure.

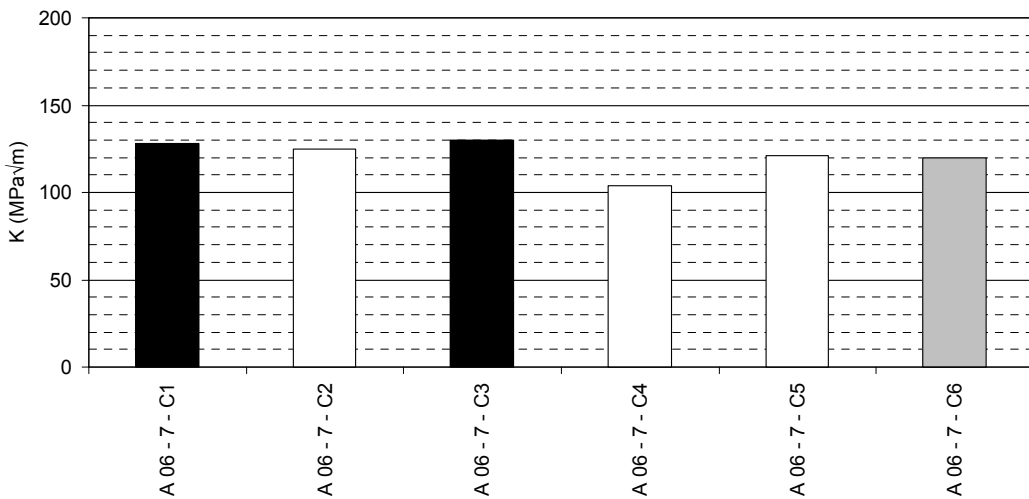
Figure 96 Charpy Impact test results: Comparison of weld metal results.



(a) CTOD test results



(b) J-Integral test results

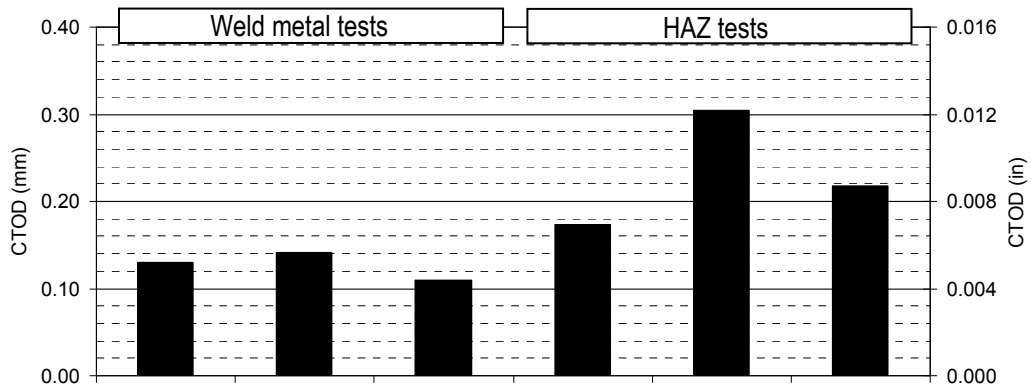


(c) K test results

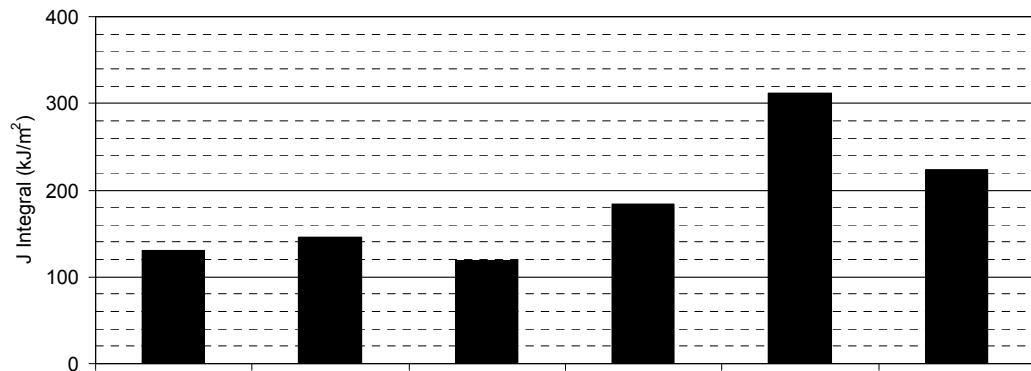
Failure type 'c'
 Failure type 'u'
 Failure type 'm'

Weld metal test specimens: C1, C2 and C3 HAZ test specimens: C4, C5 and C6

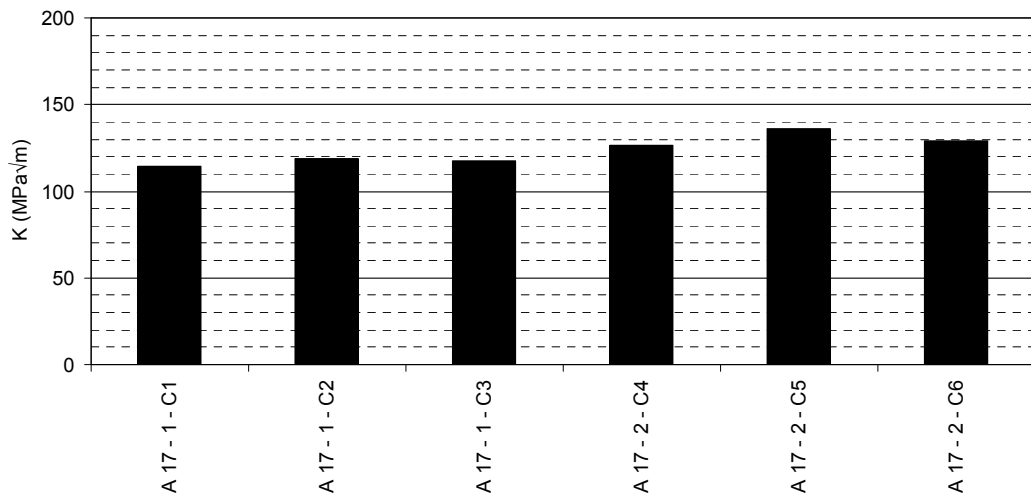
Figure 97 Fracture mechanics test: Weld A06.



(a) CTOD test results



(b) J-Integral test results



(c) K test results

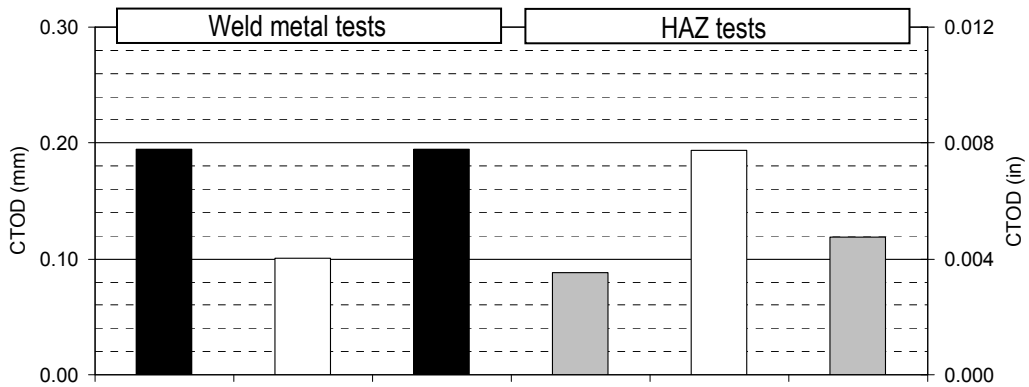


Failure type 'm'

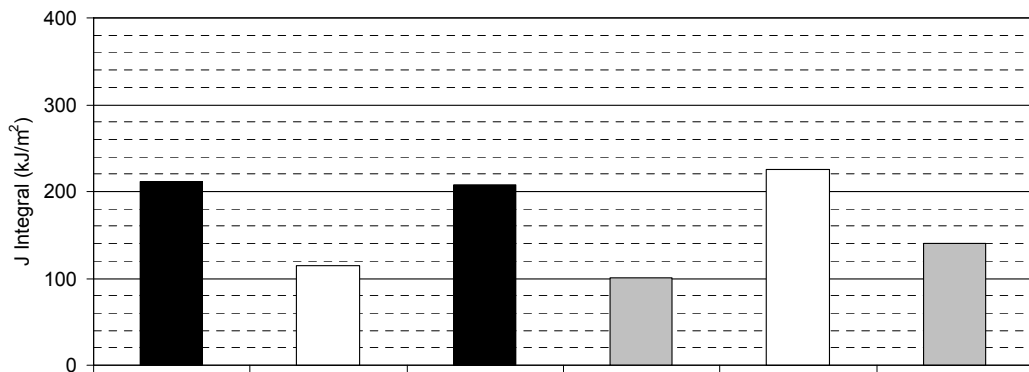
Weld metal test specimens: C1, C2 and C3

HAZ test specimens: C4, C5 and C6

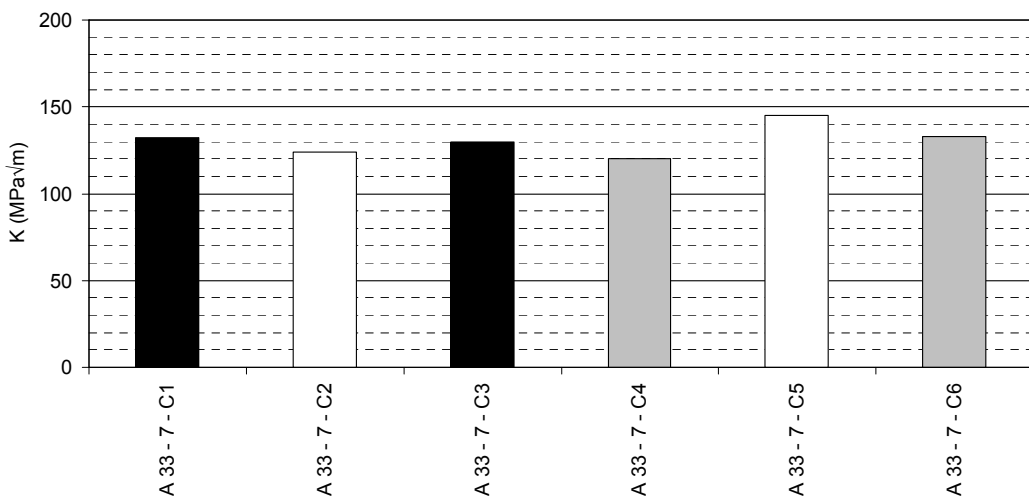
Figure 98 Fracture mechanics test: Weld A17.



(a) CTOD test results



(b) J-Integral test results



(c) K test results

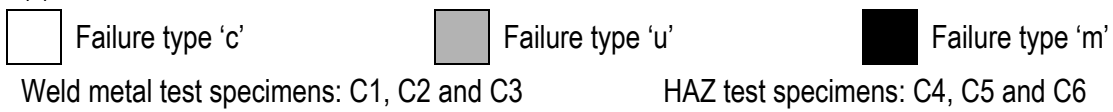
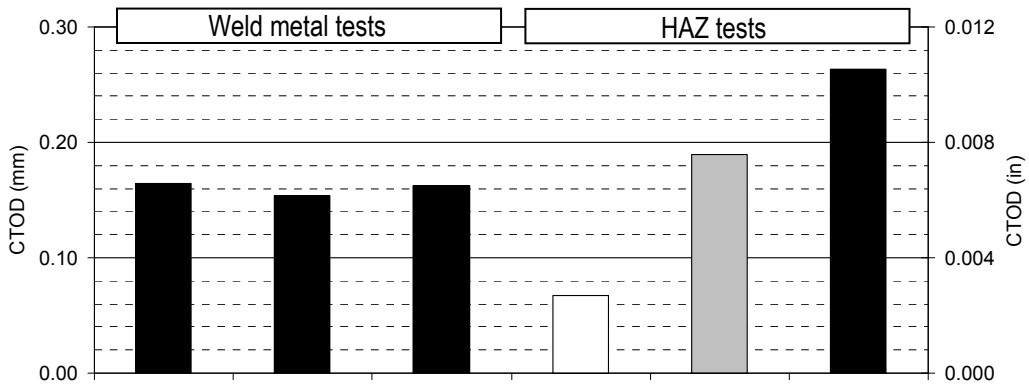
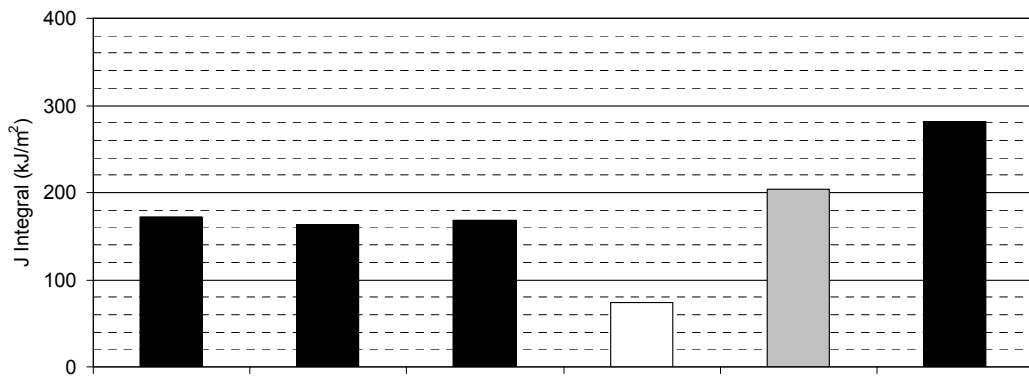


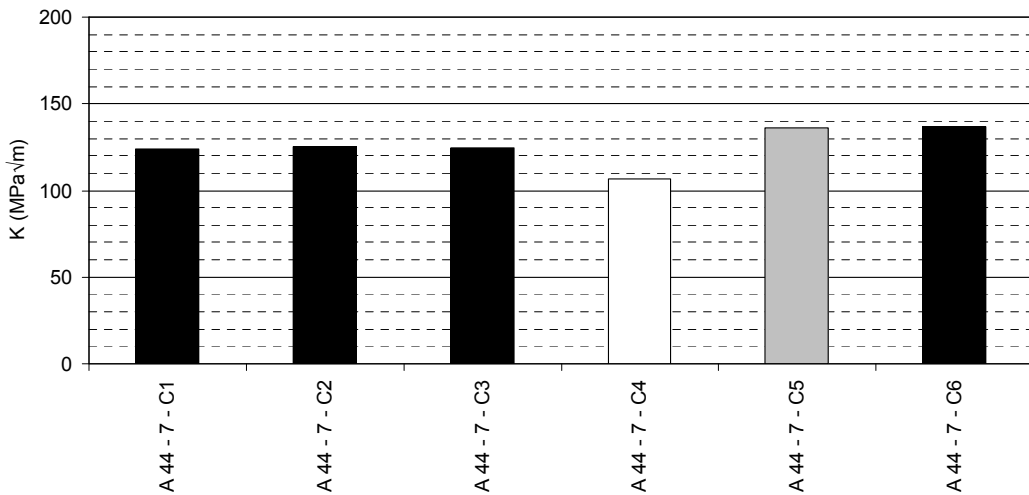
Figure 99 Fracture mechanics test: Weld A33.



(a) CTOD test results



(b) J-Integral test results



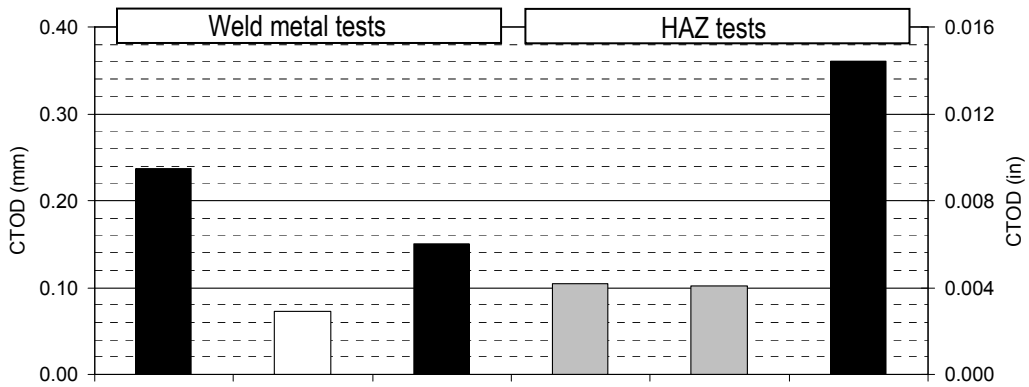
(c) K test results

Failure type 'c'
 Failure type 'u'
 Failure type 'm'

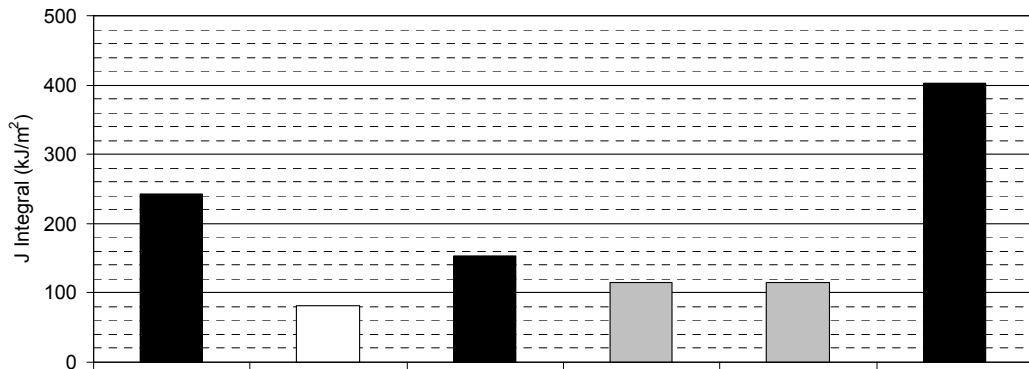
Weld metal test specimens: C1, C2 and C3

HAZ test specimens: C4, C5 and C6

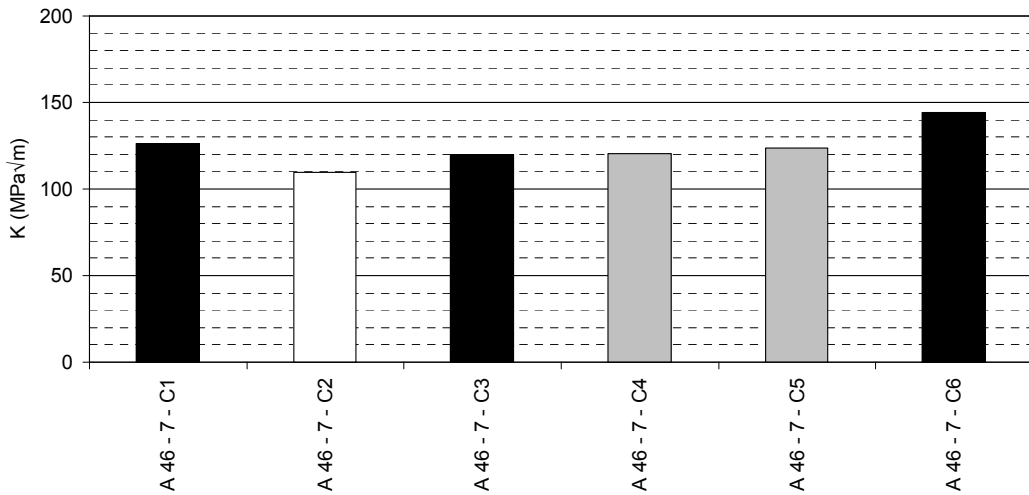
Figure 100 Fracture mechanics test: Weld A44.



(a) CTOD test results



(b) J-Integral test results

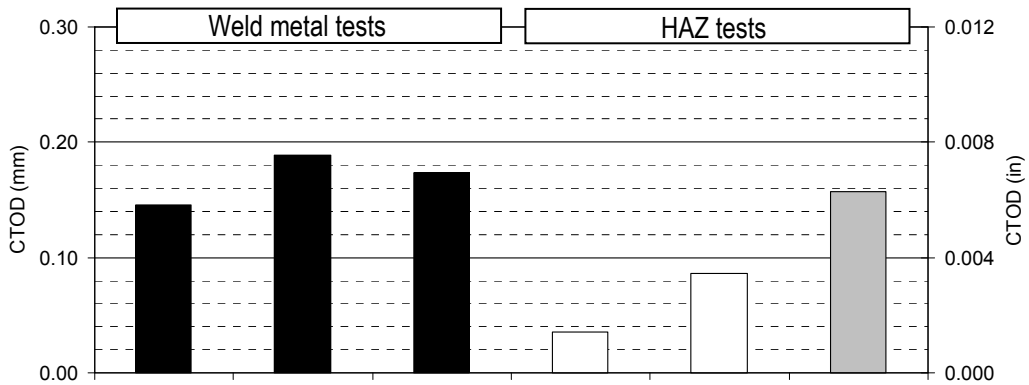


(c) K test results

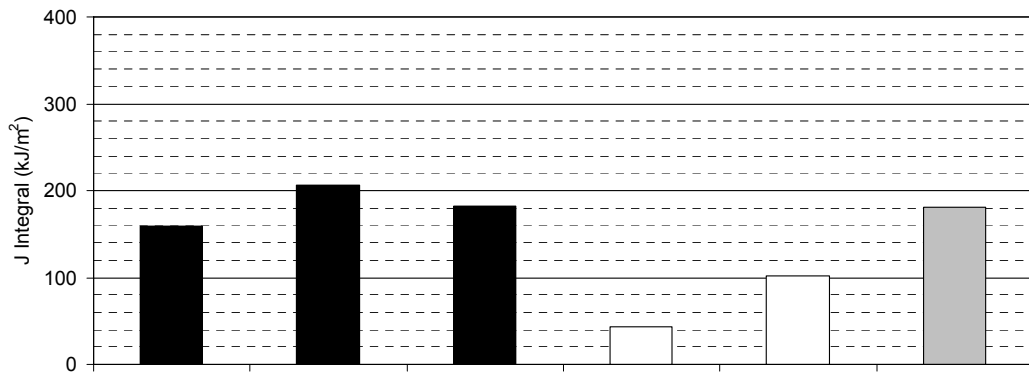
Failure type 'c'
 Failure type 'u'
 Failure type 'm'

Weld metal test specimens: C1, C2 and C3
 HAZ test specimens: C4, C5 and C6

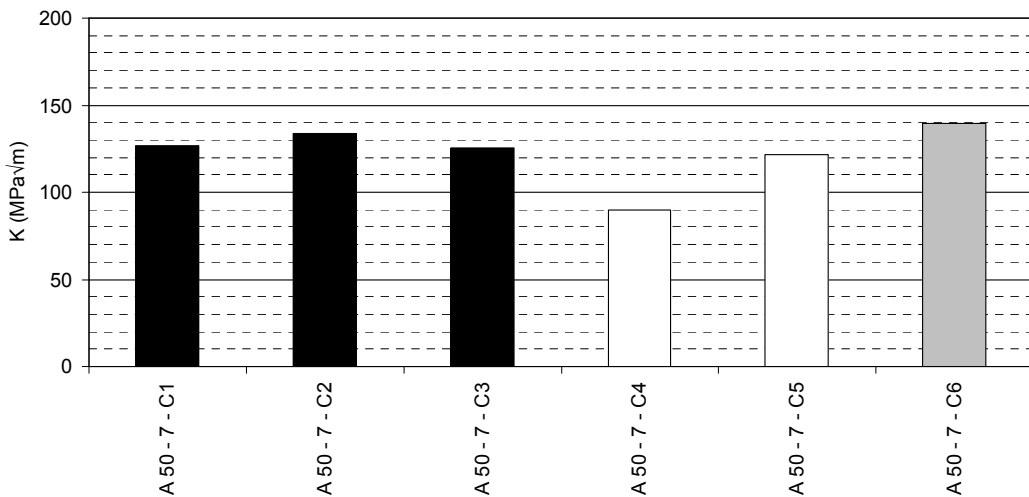
Figure 101 Fracture mechanics test: Weld A46.



(a) CTOD test results



(b) J-Integral test results



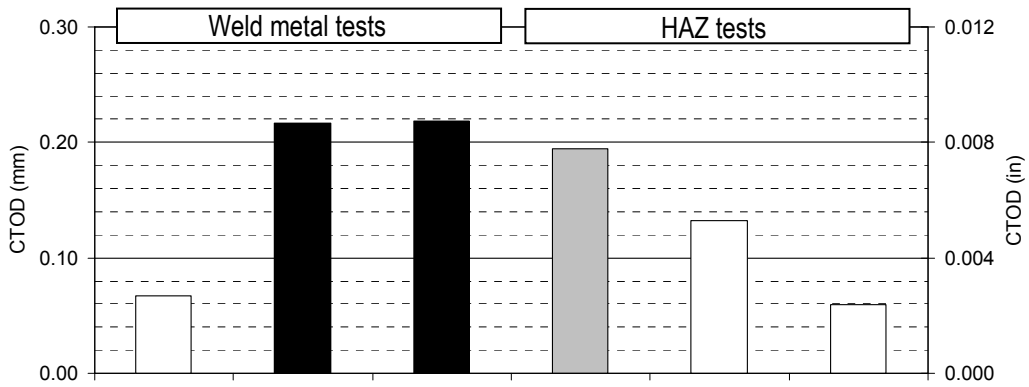
(c) K test results

Failure type 'c'
 Failure type 'u'
 Failure type 'm'

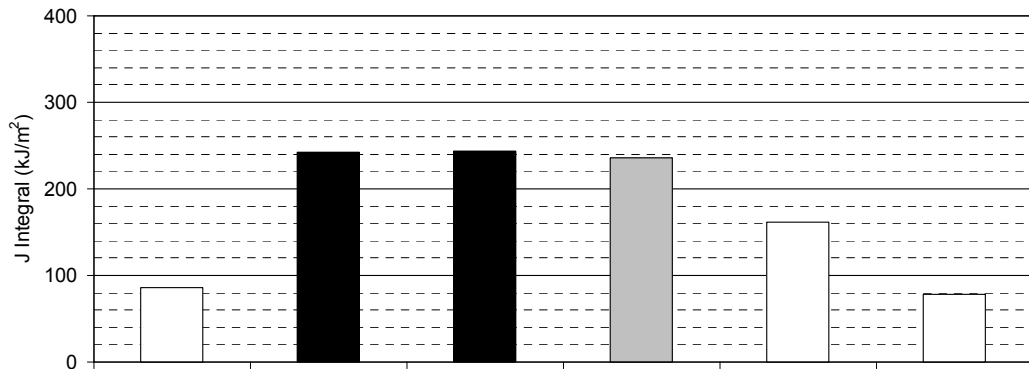
Weld metal test specimens: C1, C2 and C3

HAZ test specimens: C4, C5 and C6

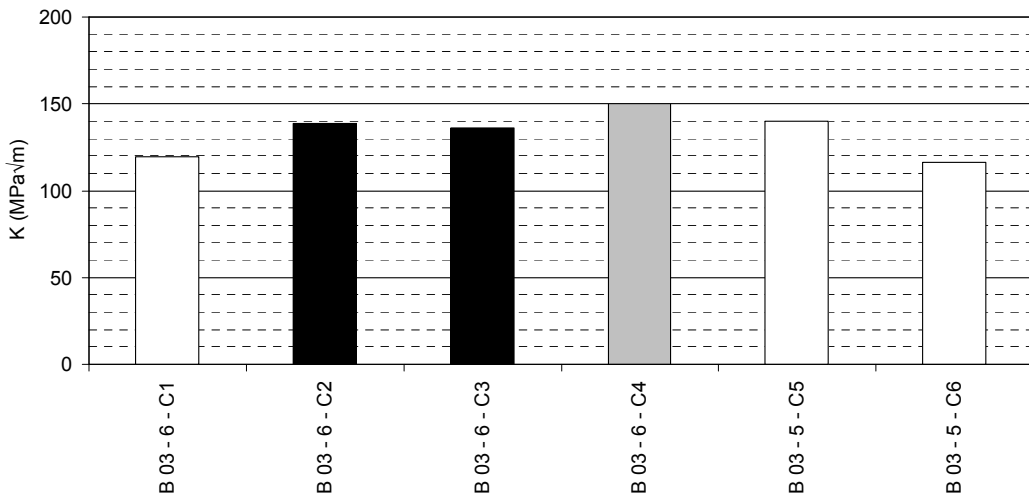
Figure 102 Fracture mechanics test: Weld A50.



(a) CTOD test results



(b) J-Integral test results



(c) K test results

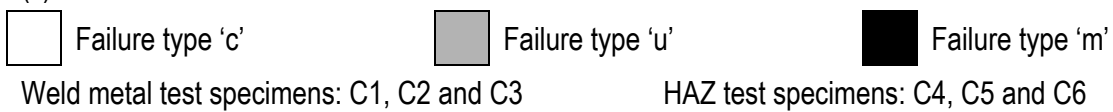
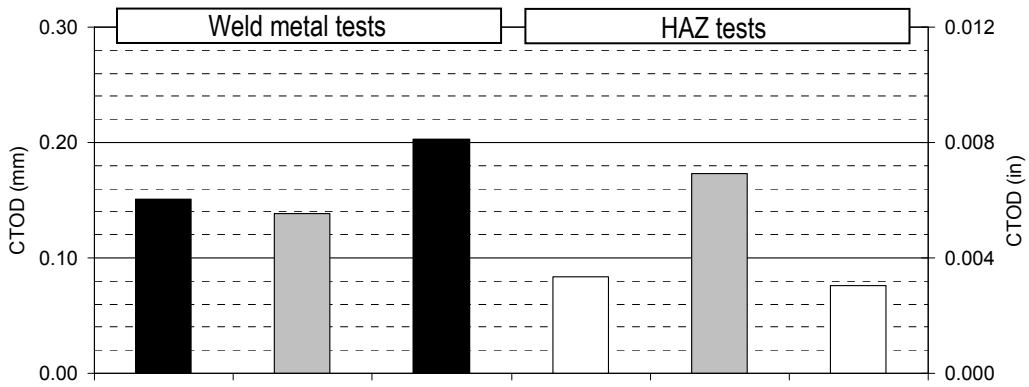
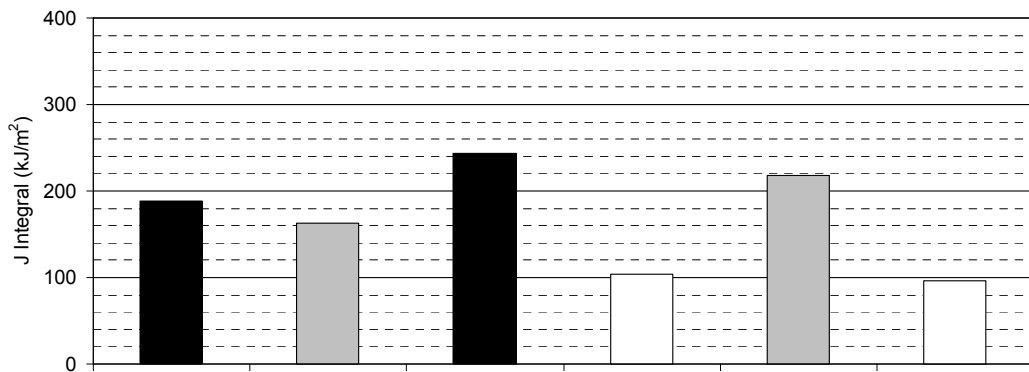


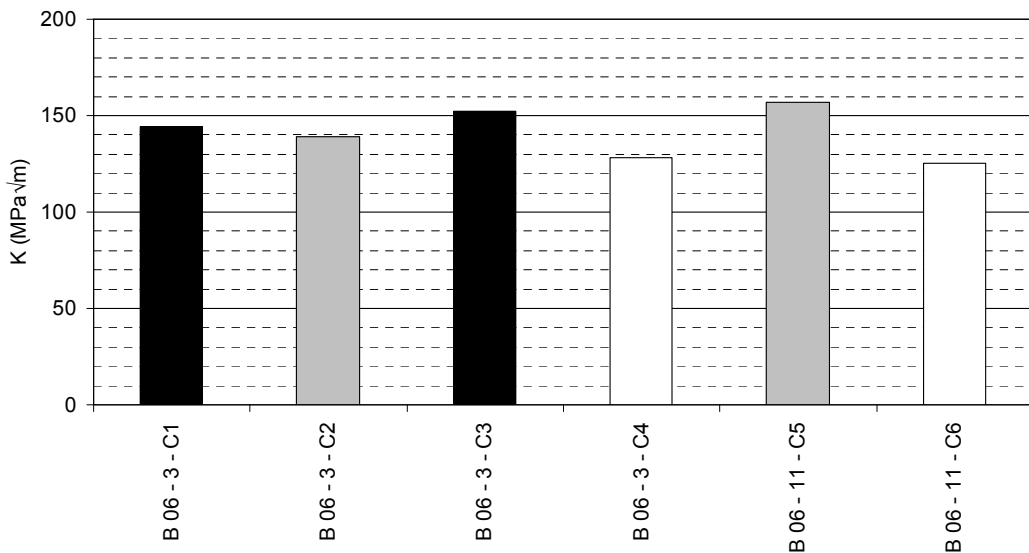
Figure 103 Fracture mechanics test: Weld B03.



(a) CTOD test results



(b) J-Integral test results



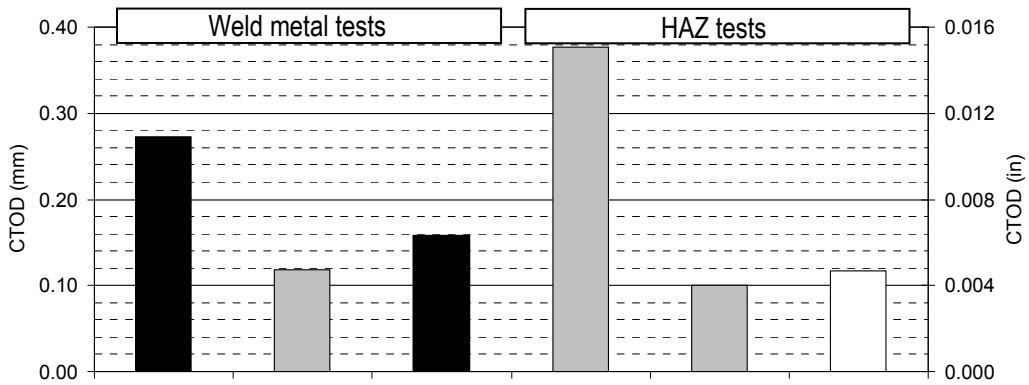
(c) K test results



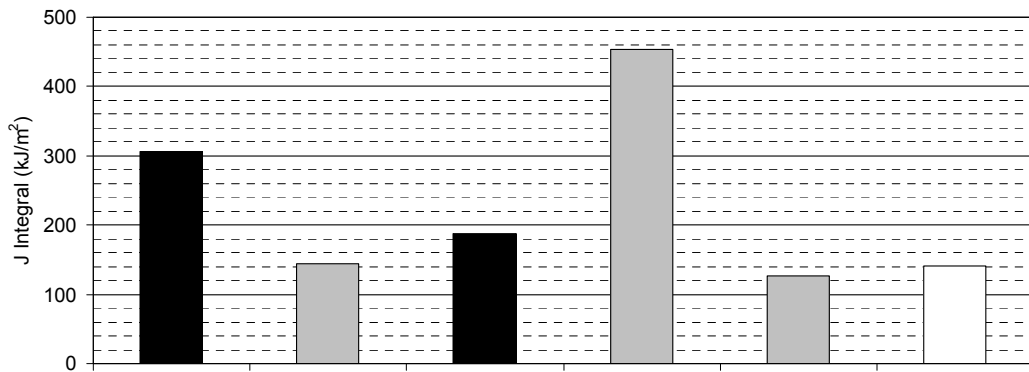
Weld metal test specimens: C1, C2 and C3

HAZ test specimens: C4, C5 and C6

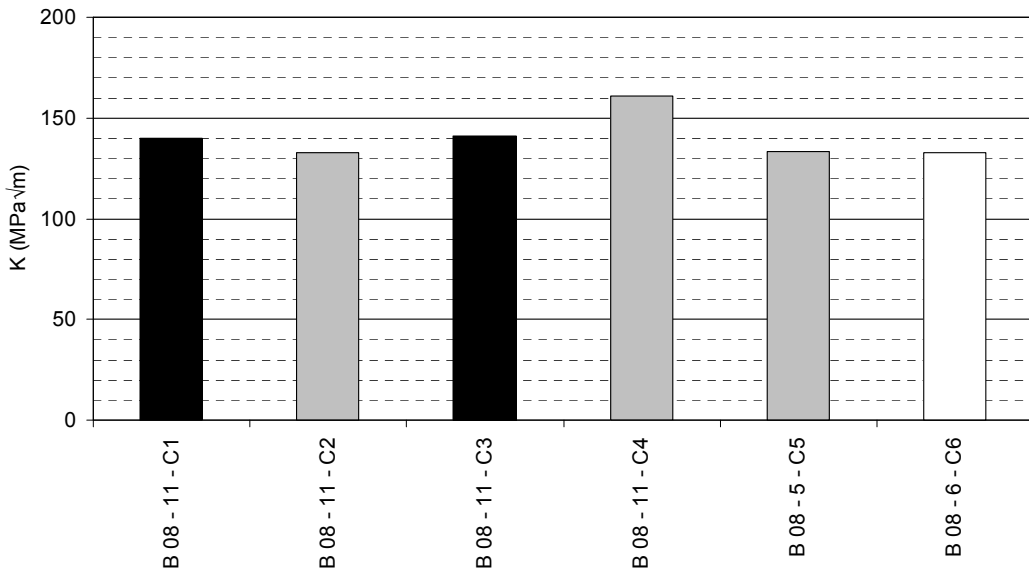
Figure 104 Fracture mechanics test: Weld B06.



(a) CTOD test results



(b) J-Integral test results



(c) K test results

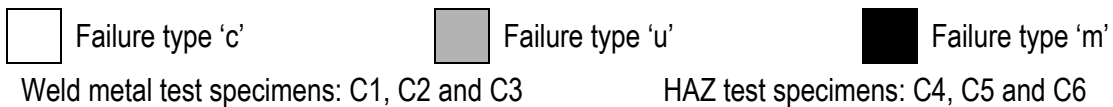
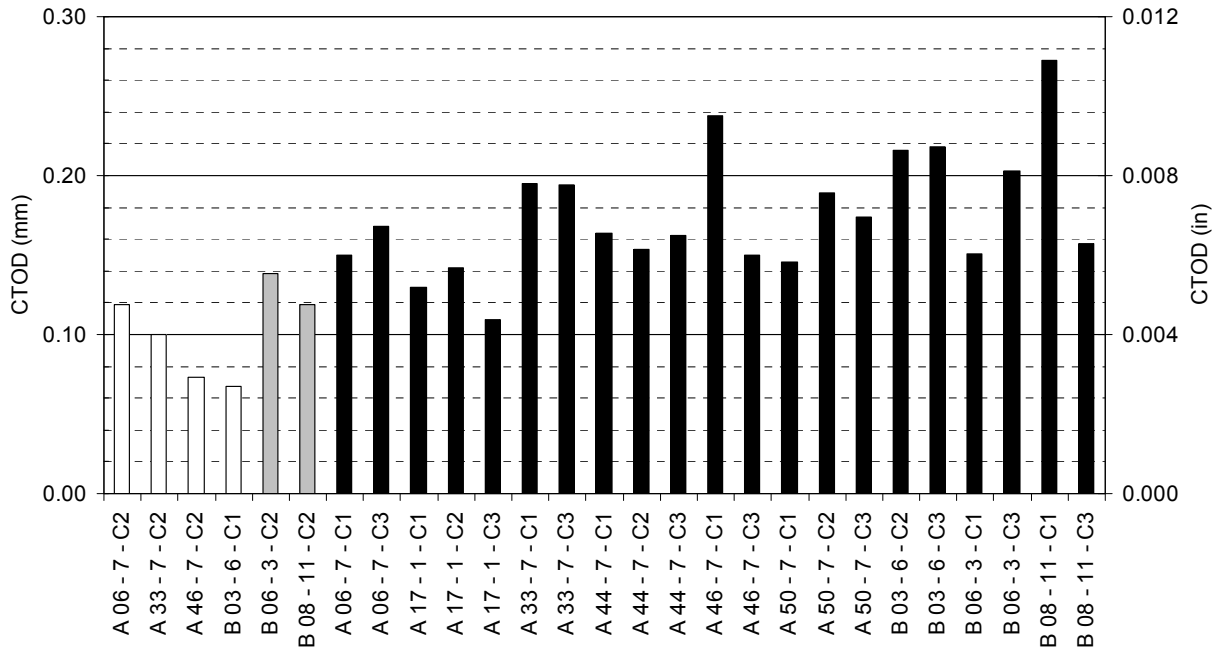
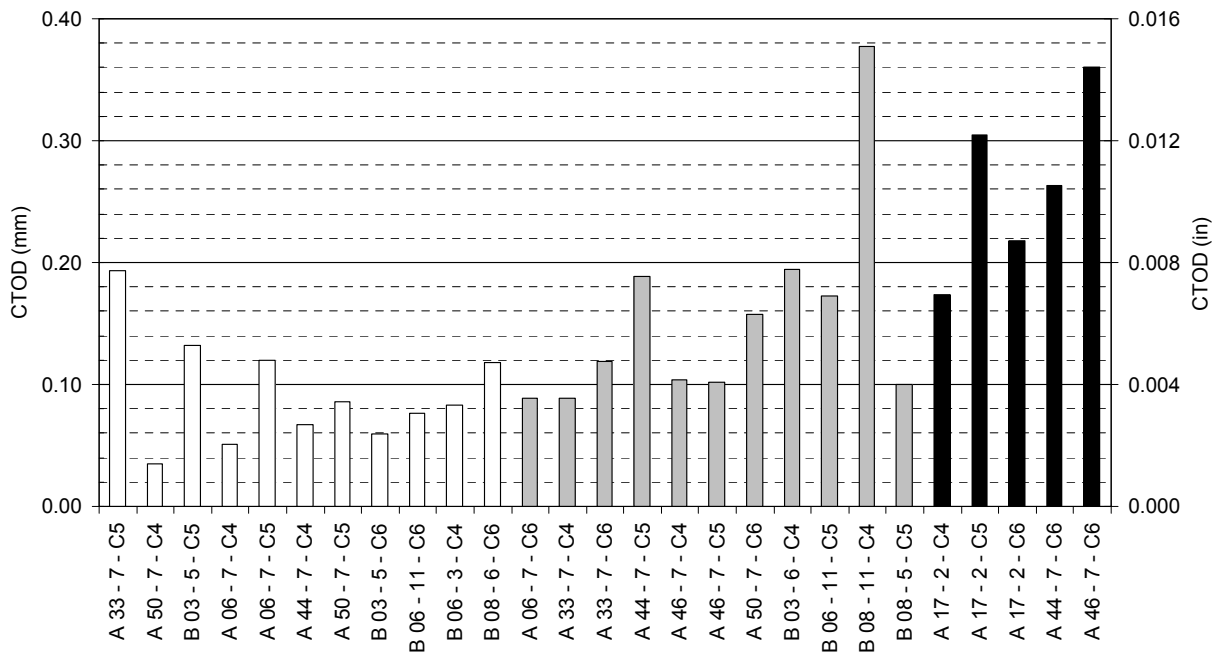


Figure 105 Fracture mechanics test: Weld B08.



(a) Specimens notched at the weld metal centerline



(b) Specimens notched at the fusion line 50/50 (HAZ/weld metal)

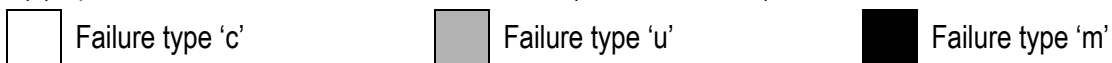
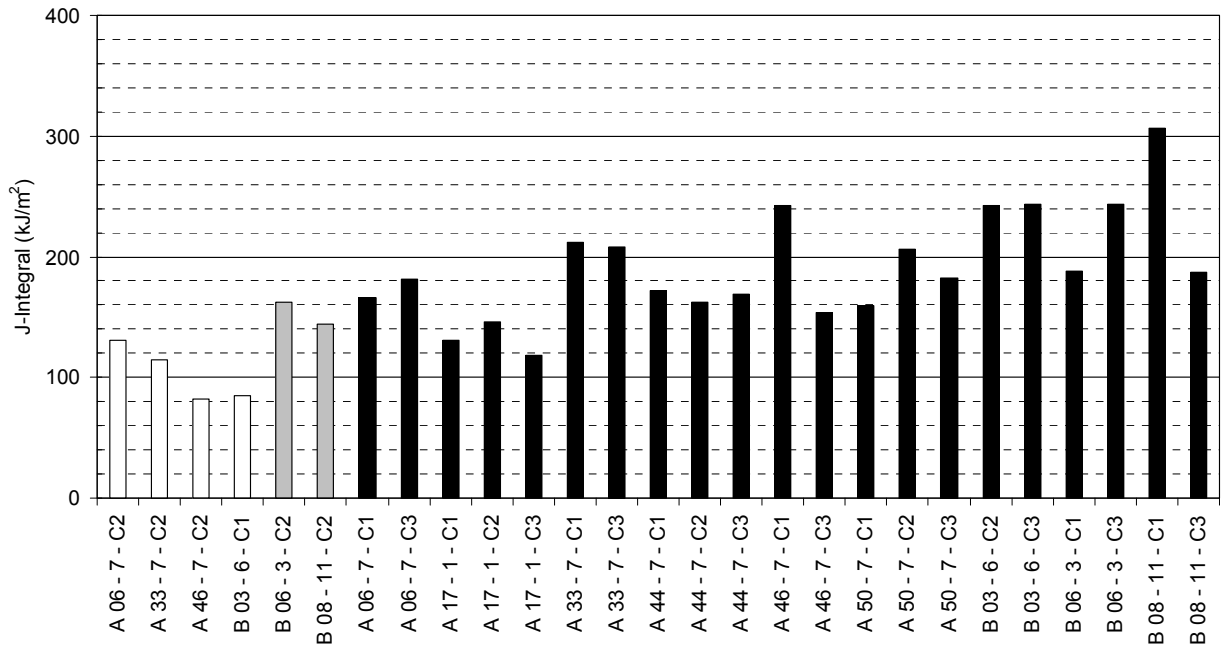
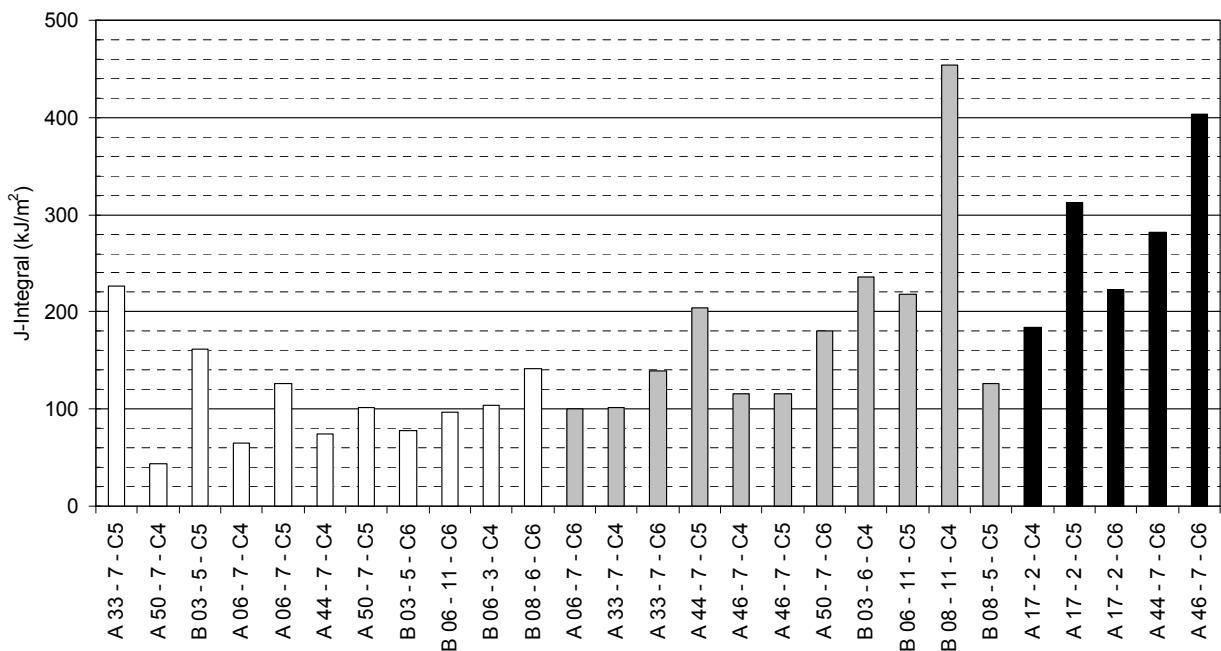


Figure 106 Fracture mechanics test results: CTOD.



(a) Specimens notched at the weld metal centerline



(b) Specimens notched at the fusion line 50/50 (HAZ/weld metal)

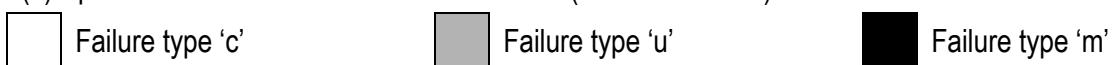
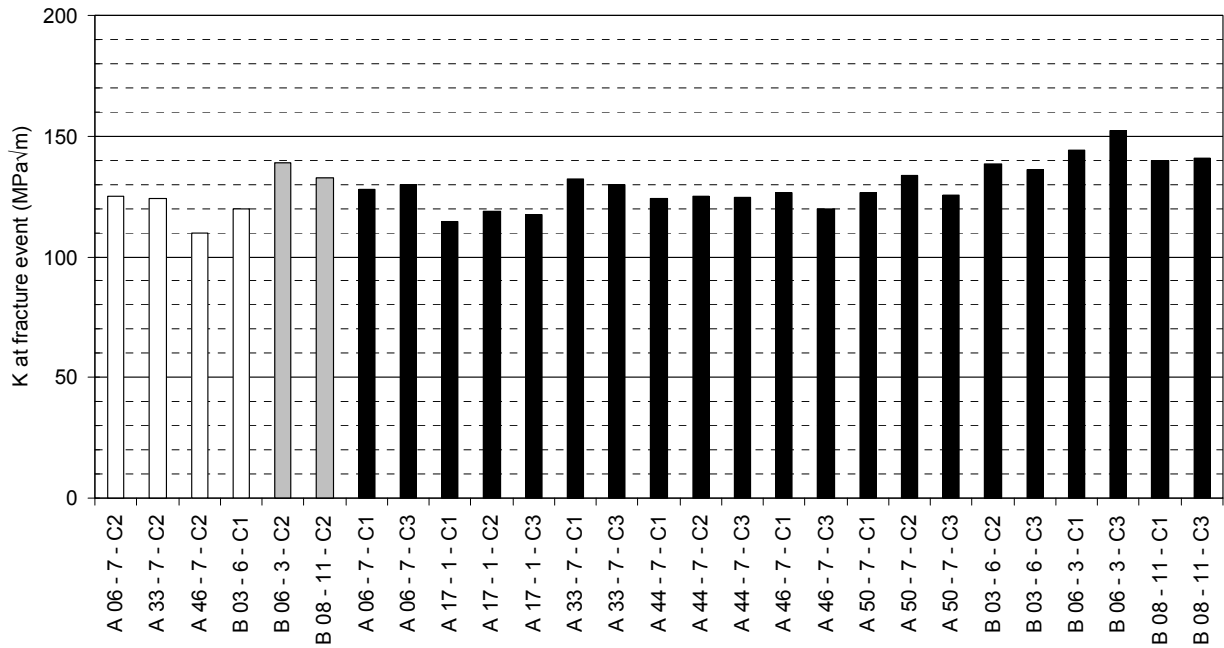
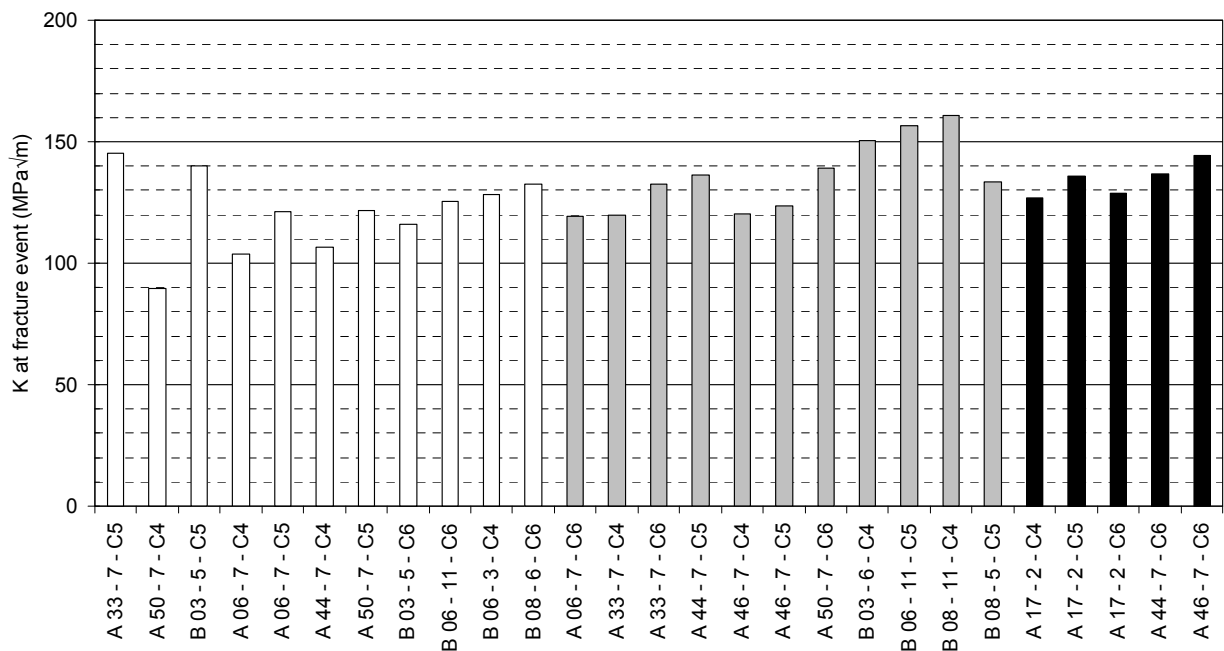


Figure 107 Fracture mechanics test results: J-Integral.



(a) Specimens notched at the weld metal centerline



(b) Specimens notched at the fusion line 50/50 (HAZ/weld metal)

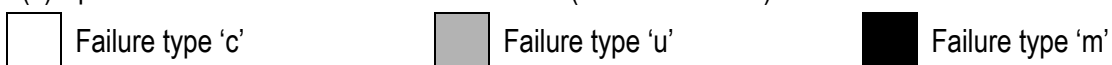
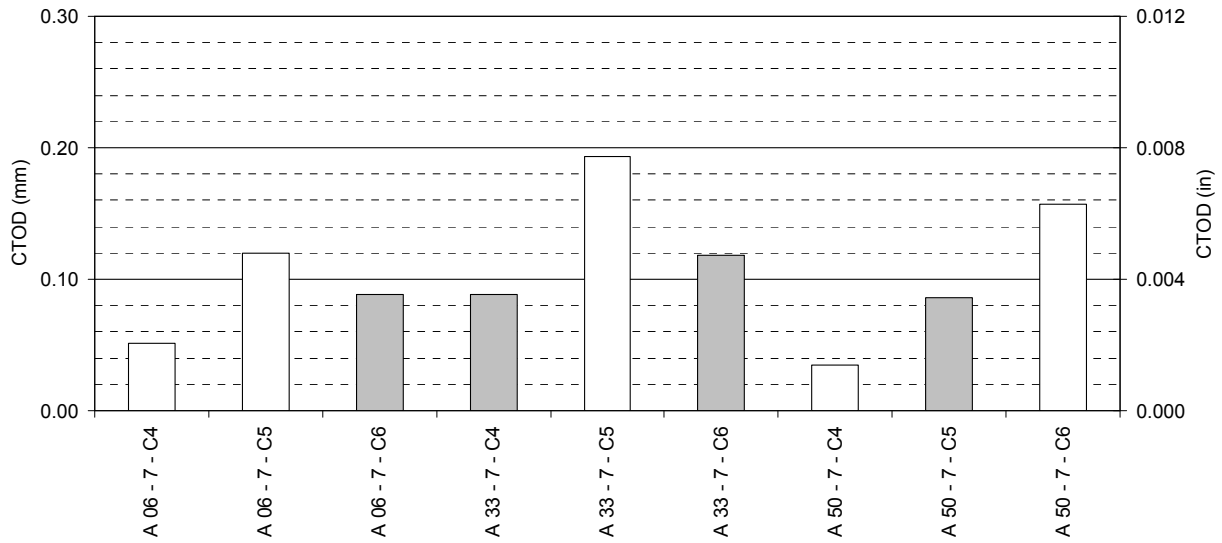
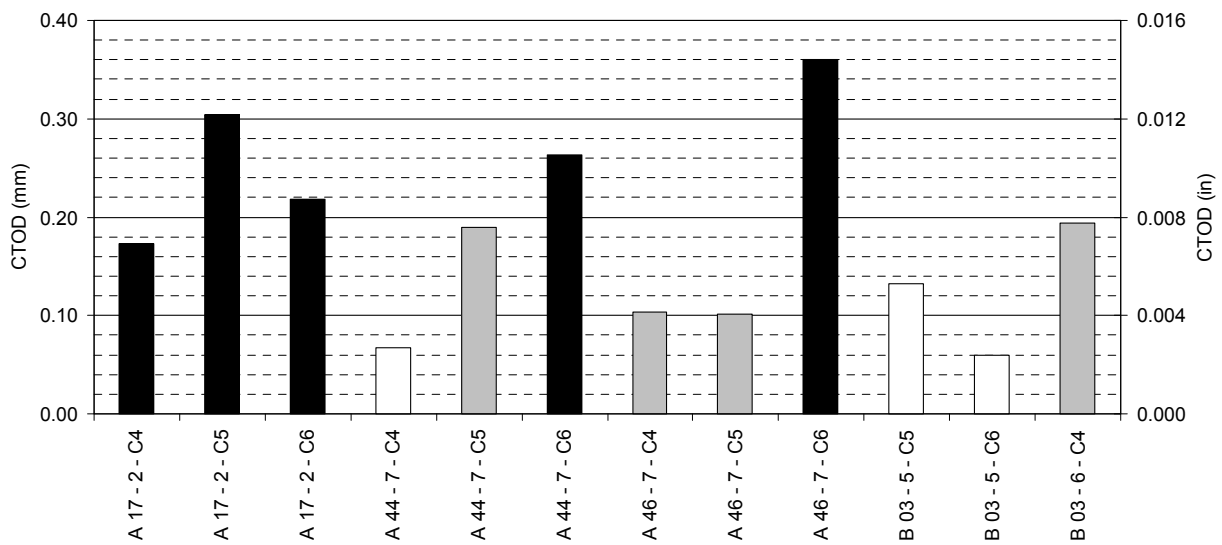


Figure 108 Fracture mechanics test results: K at the critical fracture event.



(a) Pipes from Source B



(b) Pipes from Source C

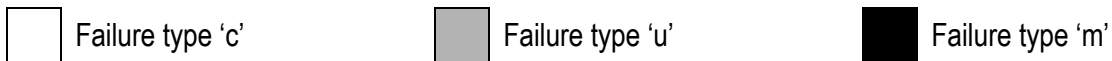
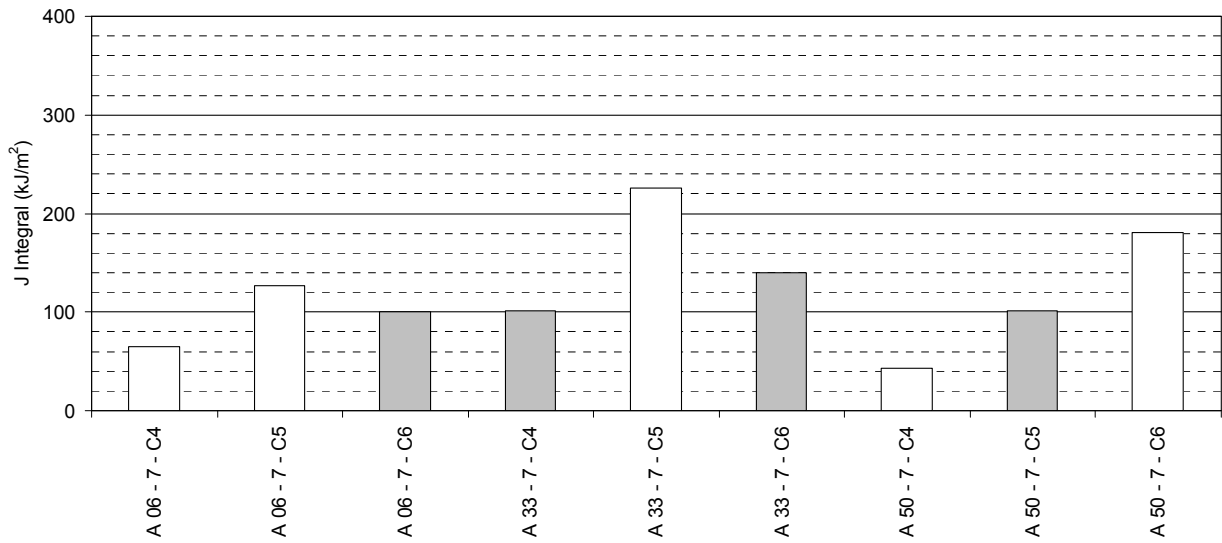
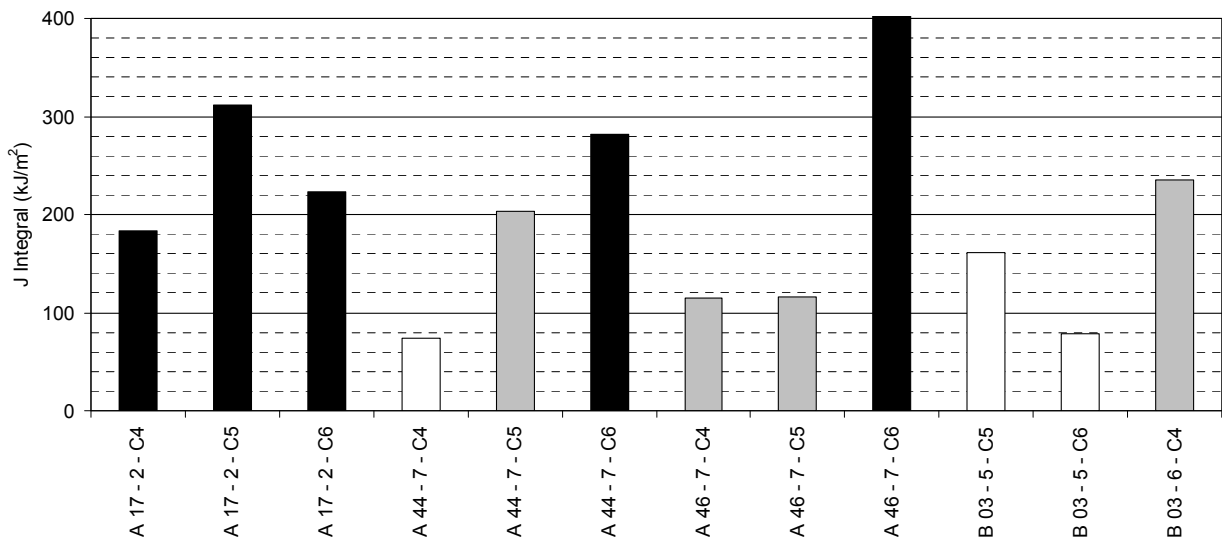


Figure 109 Comparison of HAZ fracture toughness for pipes from the same source and production heat: CTOD.



(a) Pipes from Source B



(b) Pipes from Source C

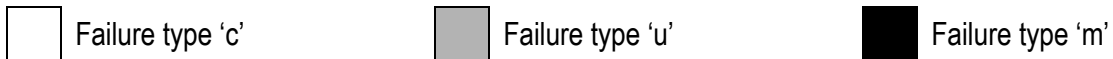
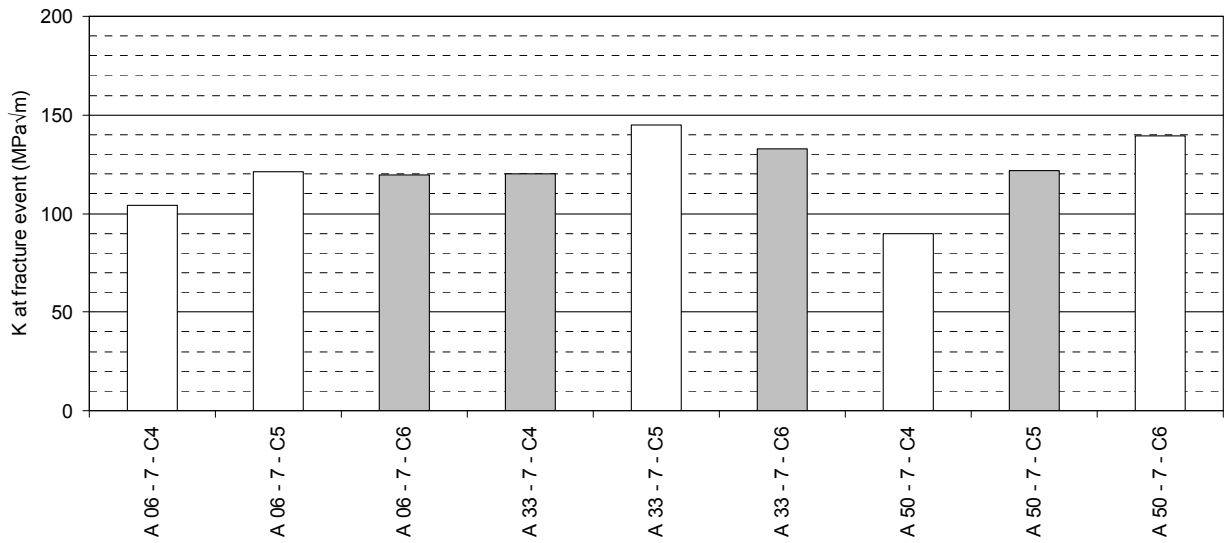
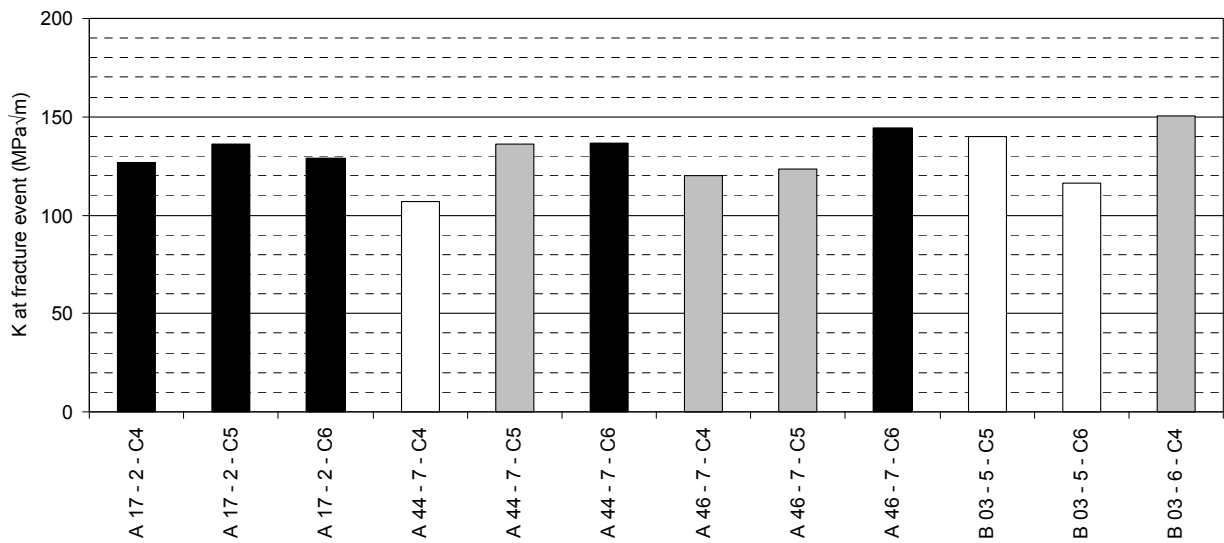


Figure 110 Comparison of HAZ fracture toughness for pipes from the same source and production heat: J.



(a) Pipes from Source B



(b) Pipes from Source C

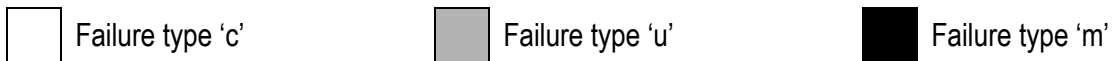
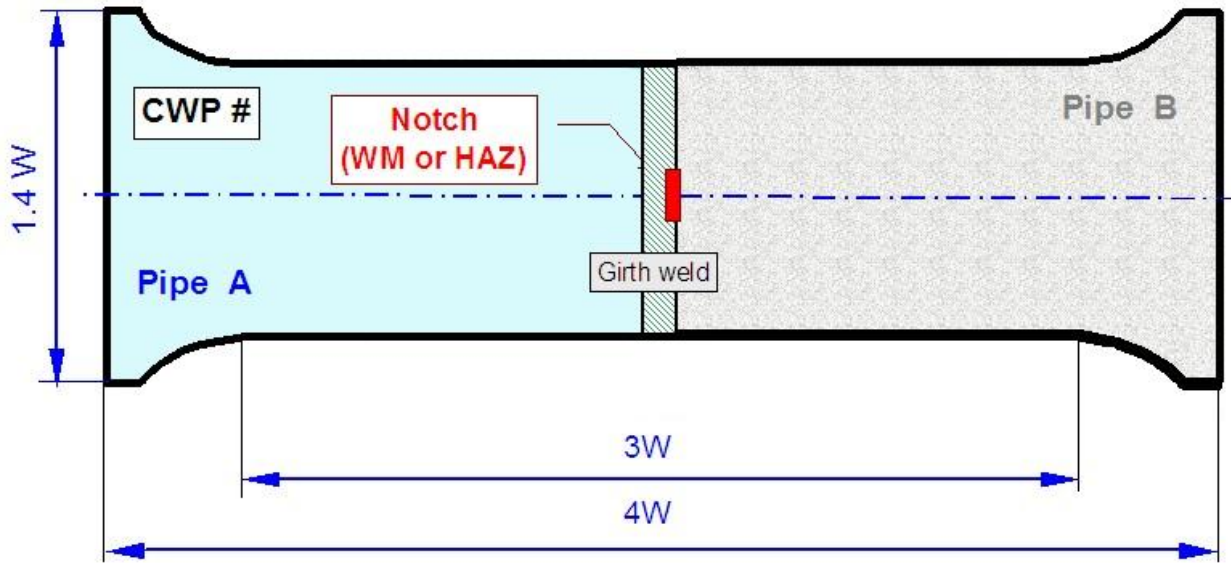


Figure 111 Comparison of HAZ fracture toughness for pipes from the same source and production heat: K.



Notes: W is the width of the CWP specimen, approximately 12in (300mm)

Figure 112 Curved wide plate test specimen: General dimensions.

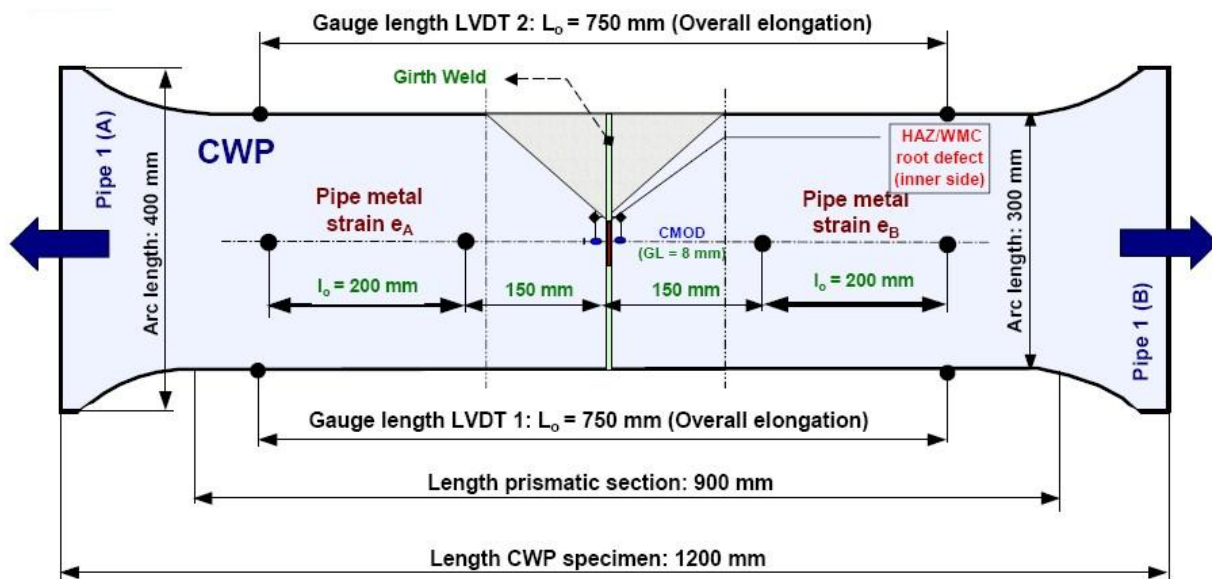
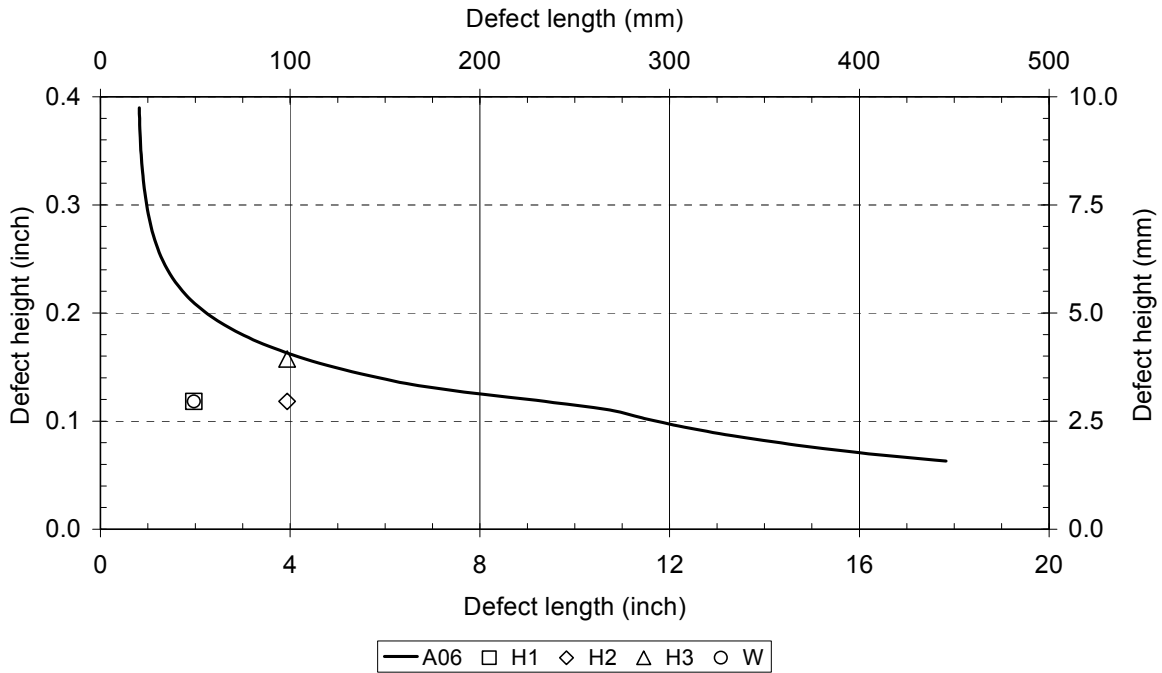


Figure 113 Curved wide plate test specimen: layout of instrumentation.



Note: The locus of maximum allowable defect size does not include an allowance for defect sizing error

Figure 114 Weld A06: Comparison of maximum allowable defect sizes predicted by API 1104 Option 2 with the CWP test specimen defects.

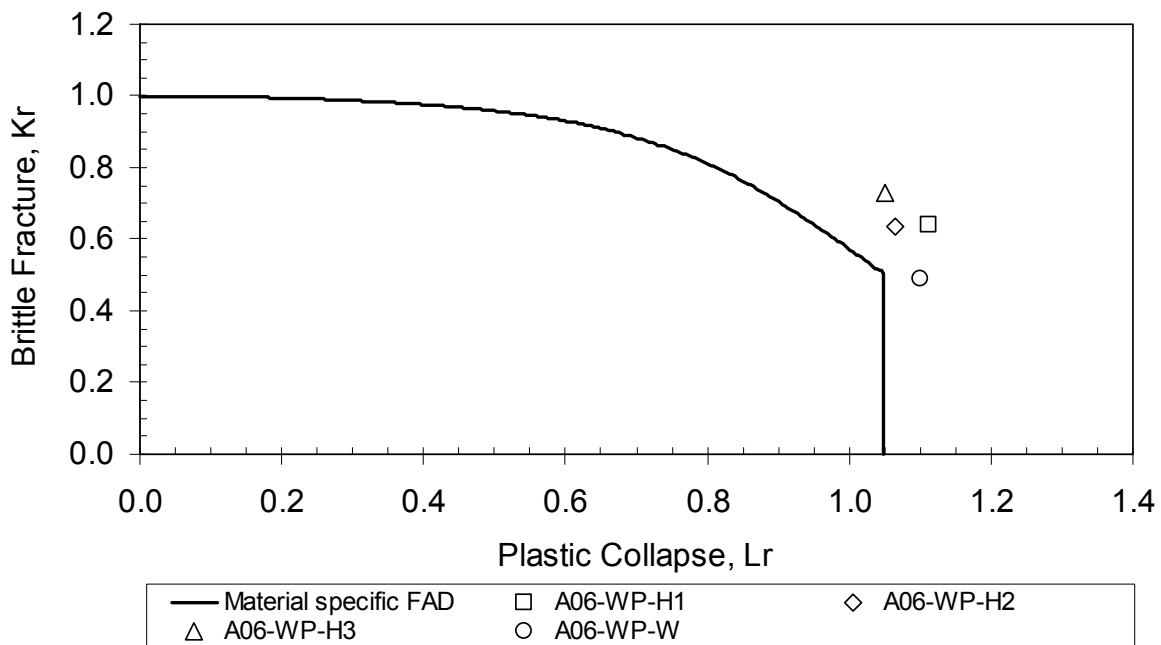


Figure 115 Weld A06: Comparison of CWP test results with the API 1104 Option 2 FAD specific for the weldment.

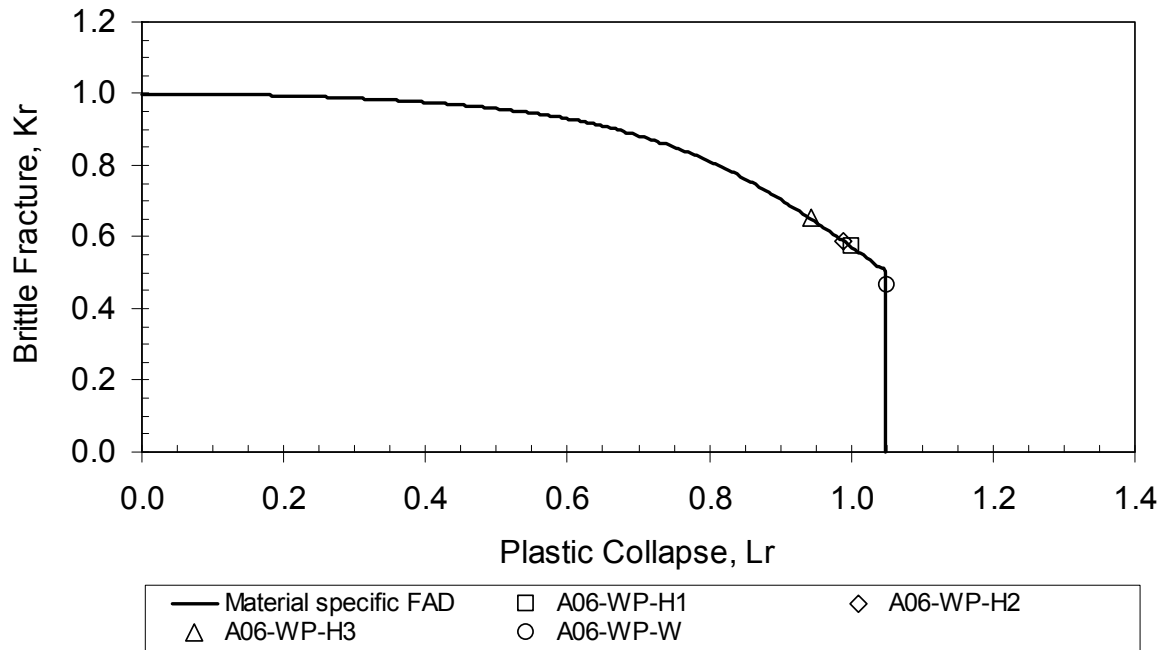
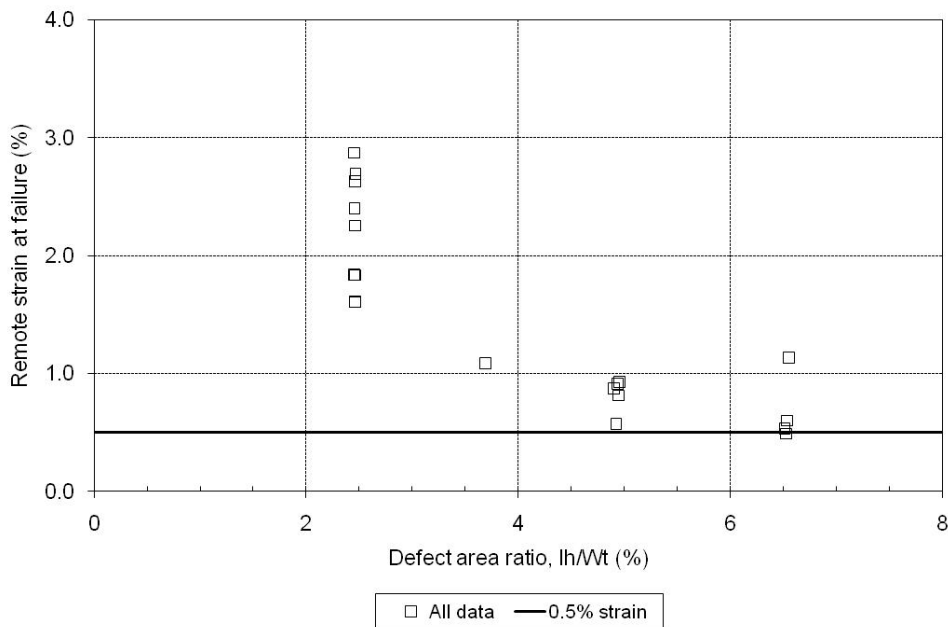
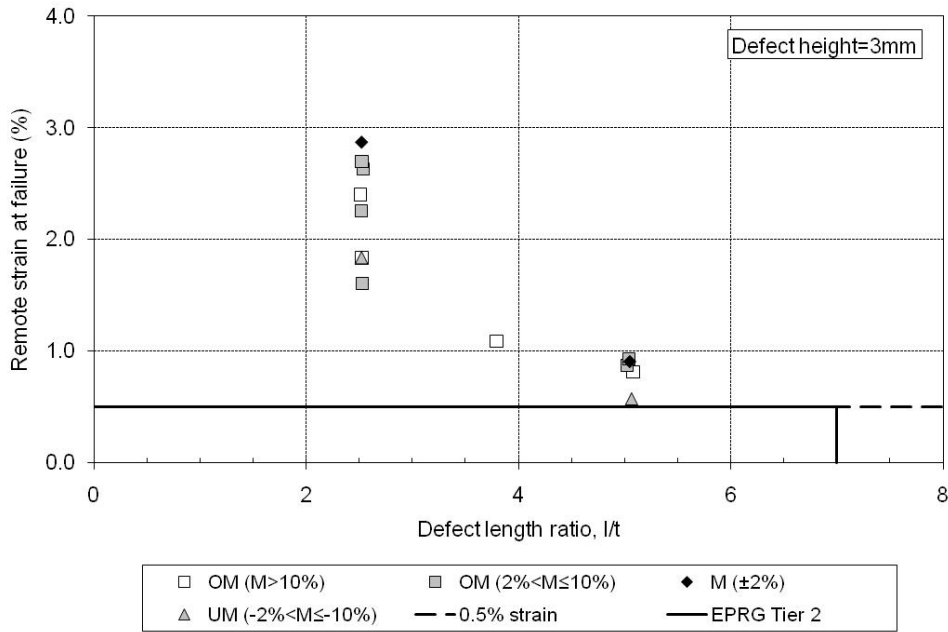


Figure 116 Weld A06: API 1104 Option 2 analysis to predict the critical failure stress for each CWP test specimen.



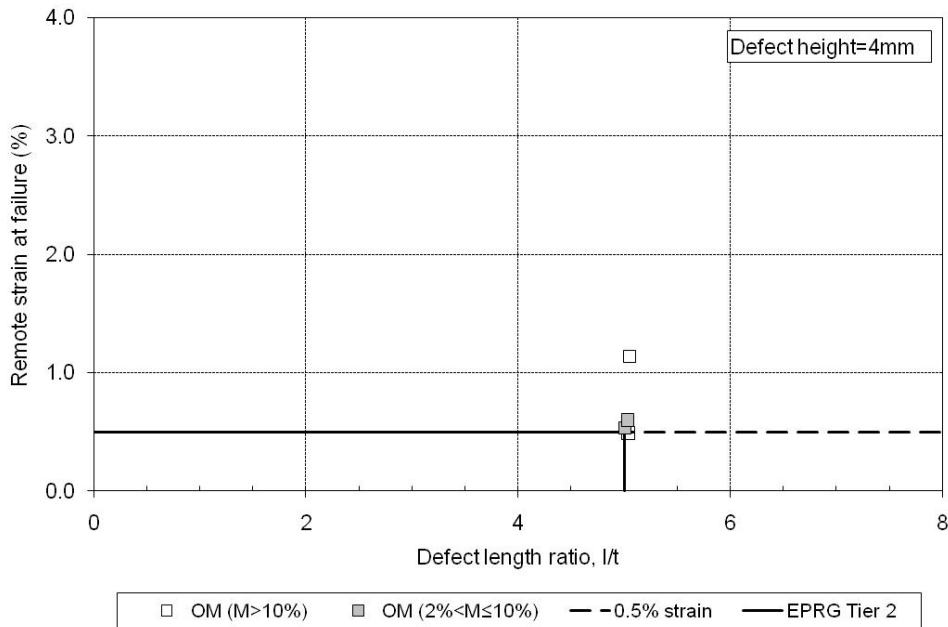
Notes: l and h are defect length and height, and W and t are CWP specimen width and thickness

Figure 117 A-series welds, CWP test results: remote failure strain as a function of defect area (all data).



Notes: l and t are defect length and CWP specimen thickness

Figure 118 A-series welds, CWP test results: remote failure strain as a function of defect length ratio (0.118in (3mm) high defects).



Notes: l and t are defect length and CWP specimen thickness

Figure 119 A-series welds, CWP test results: remote failure strain as a function of defect length ratio (0.157in (4mm) high defects).

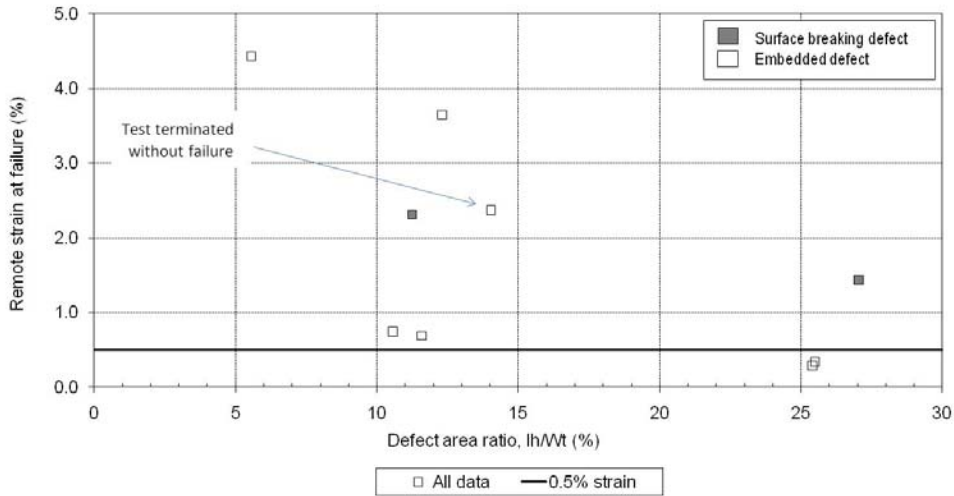
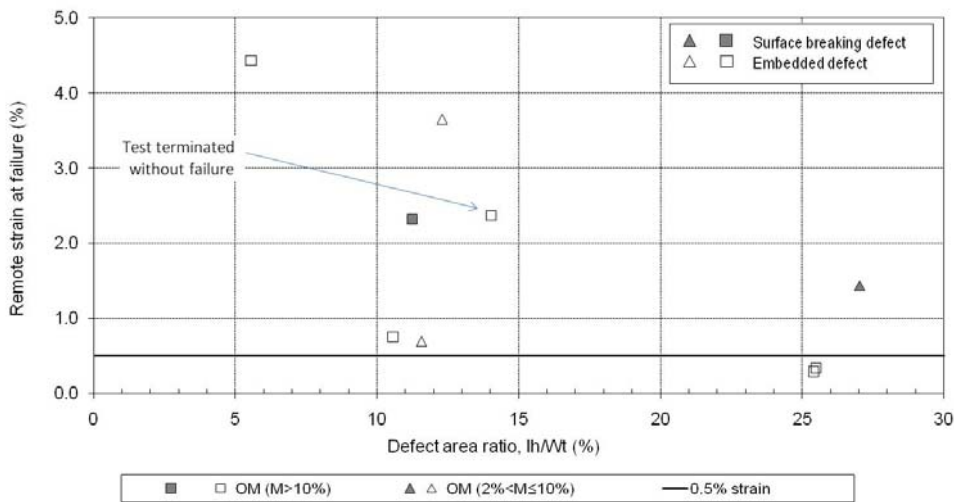
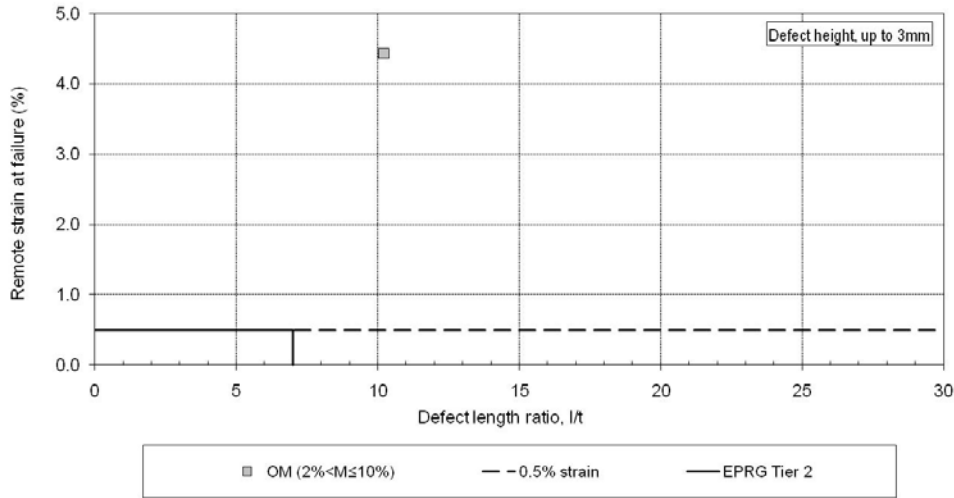


Figure 120 B-series welds, CWP test results: remote failure strain as a function of defect area (all data).



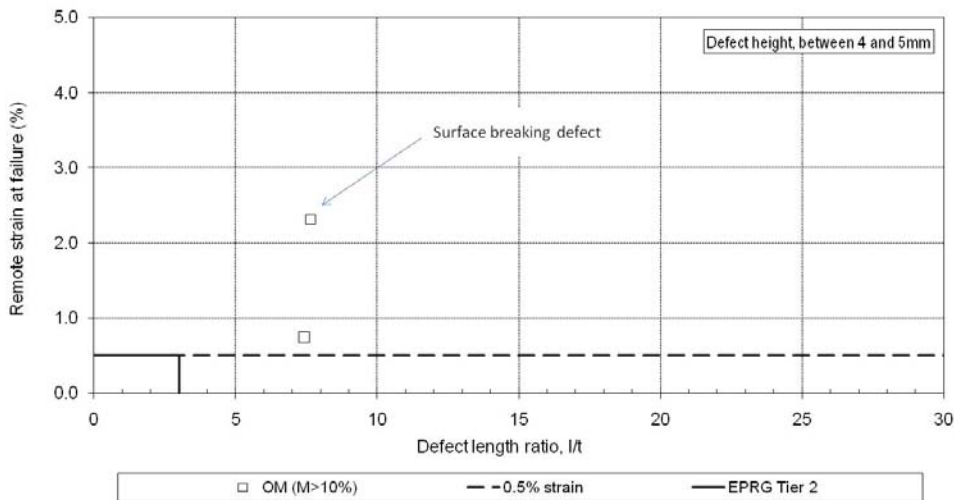
Notes: l and t are defect length and CWP specimen thickness

Figure 121 B-series welds, CWP test results: remote failure strain as a function of defect area ratio for different levels of weld metal yield strength overmatch.



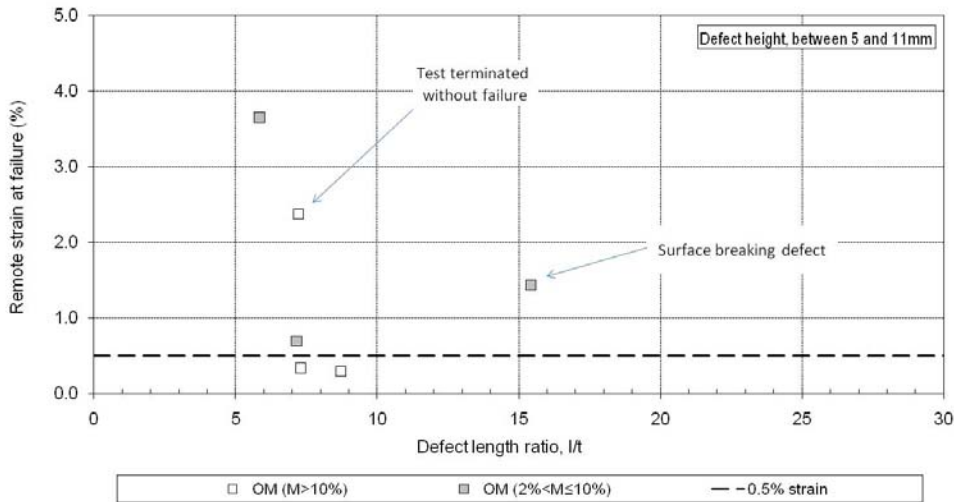
Notes: l and t are defect length and CWP specimen thickness

Figure 122 B-series welds, CWP test results: remote failure strain as a function of defect length ratio (defect height up to 0.118in (3mm)).



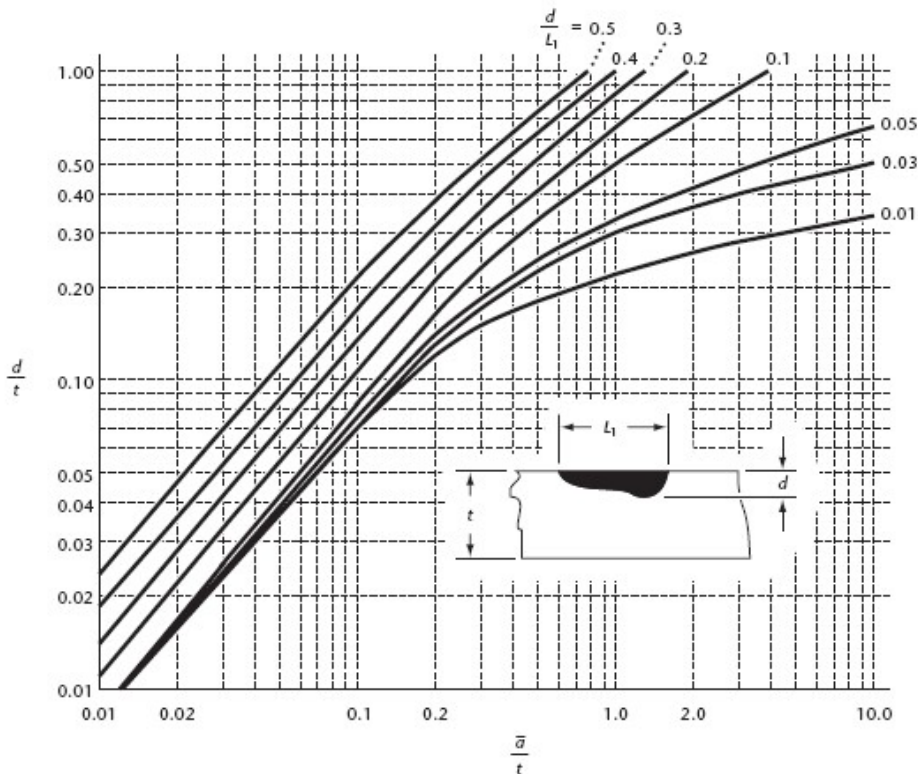
Notes: l and t are defect length and CWP specimen thickness

Figure 123 B-series welds, CWP test results: remote failure strain as a function of defect length ratio (defect height from 0.157 to 0.197in (4 to 5mm)).



Notes: l and t are defect length and CWP specimen thickness

Figure 124 B-series welds, CWP test results: remote failure strain as a function of defect length ratio (defect height greater than 0.197in (5mm)).



Note: \bar{a} is the effective defect size parameter, t is the thickness of the pipe, and a and L are defect height and length

Figure 125 Relationship between actual dimensions and \bar{a}/t for surface breaking defects (Figure K.4 from CSA Z662).

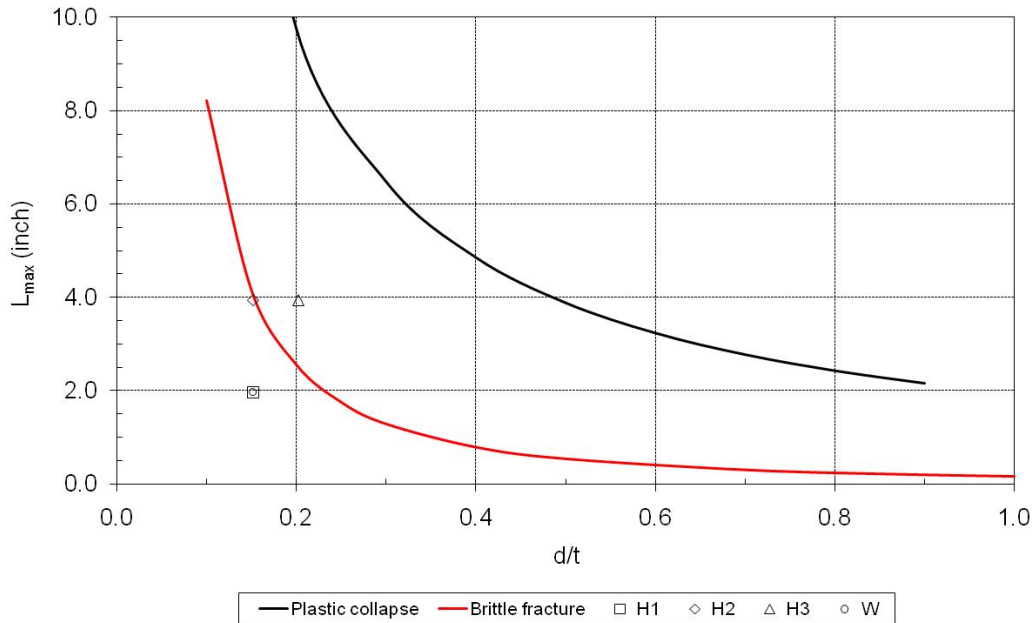
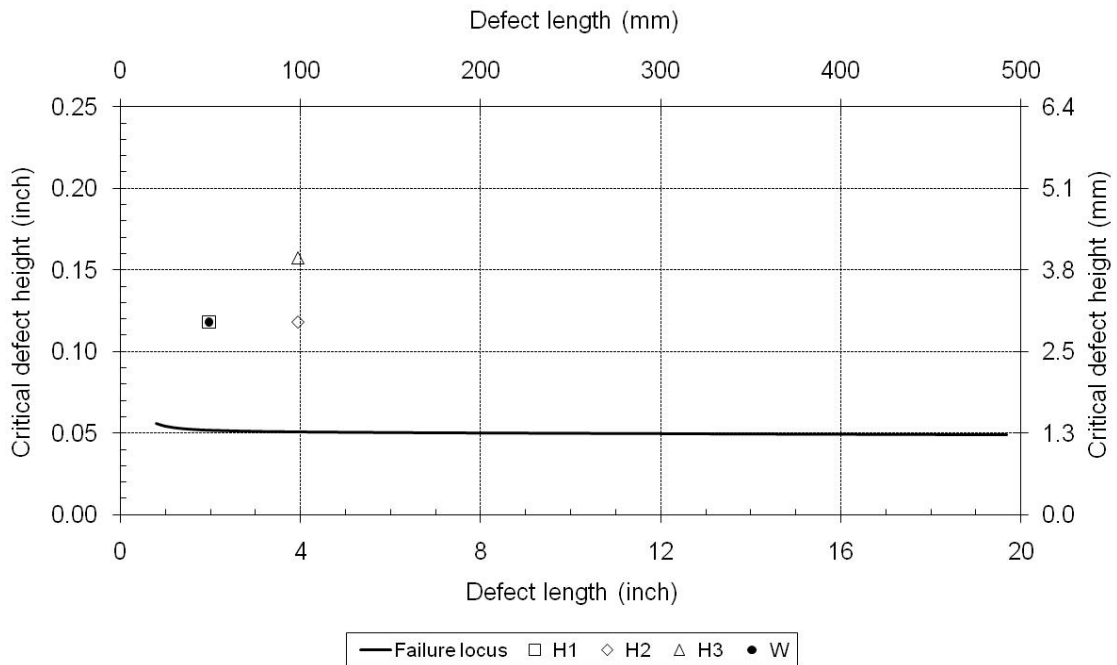


Figure 126 Weld A06: Comparison of maximum allowable defect sizes calculated using CSA Z662 with the CWP test specimen defects.



Notes: Analysis based on the minimum measured tensile properties and fracture toughness for the weldment, and the maximum pipeline longitudinal stress is assumed equal to SMYS

Figure 127 BS 7910 assessment: Locus of critical surface breaking defect size for Weld A06.

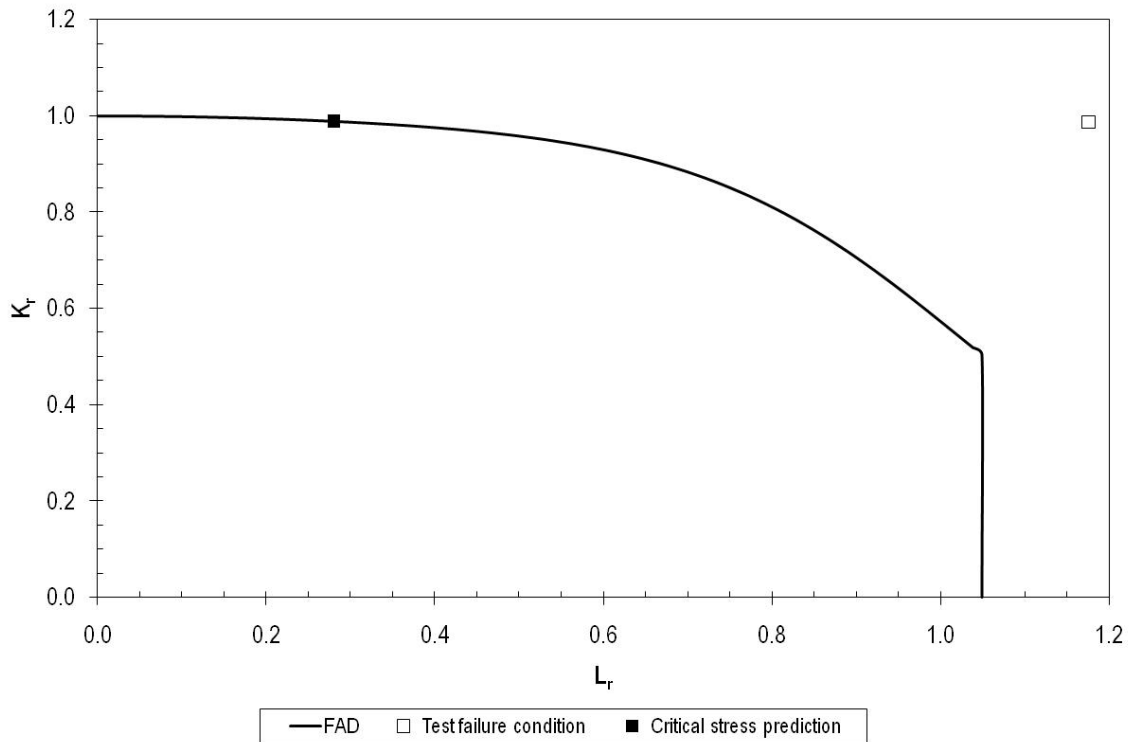
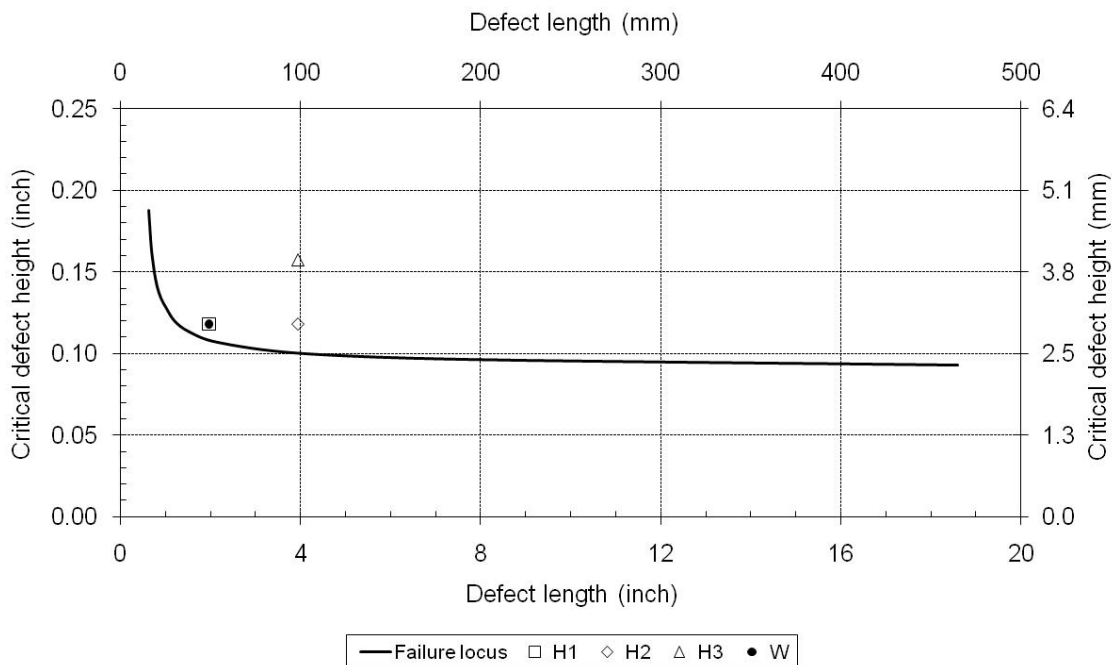


Figure 128 BS 7910 assessment of CWP specimen A06-WP-H1, extracted from Weld A06.



Notes: Analysis based on the minimum measured tensile properties and fracture toughness for the weldment, and the maximum pipeline longitudinal stress is assumed equal to SMYS

Figure 129 API 579-1/ASME FFS-1 assessment: Locus of critical surface breaking defect size for Weld A06.

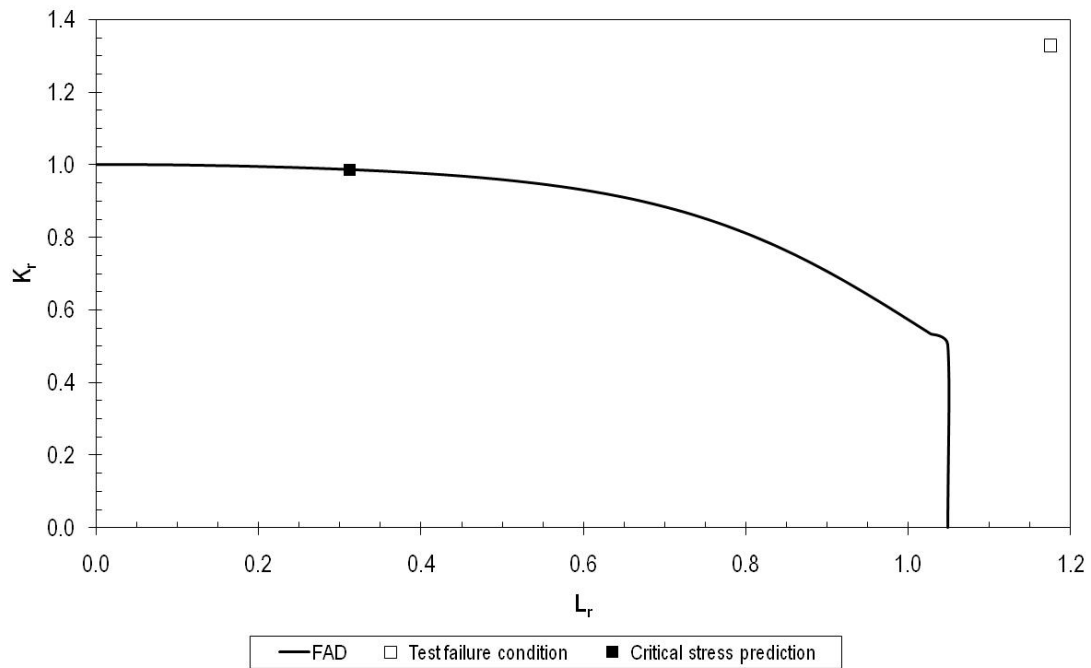


Figure 130 API 579-1/ASME FFS-1 assessment of CWP specimen A06-WP-H1, extracted from Weld A06 (plots output from Quest, Signal FFS software).

Appendix A Weld Macro Sections and Vickers Hardness Surveys

Vickers hardness surveys were undertaken on each prepared weld macro-section. Measurements were undertaken 0.06in (1.5mm) below the weld cap, at the pipe mid-wall thickness and 0.06in (1.5mm) up from the weld root. Eleven measurements were taken at each location, as shown in Figure A1.

For each weld, the macro-sections are presented first, followed by the results of the hardness surveys.

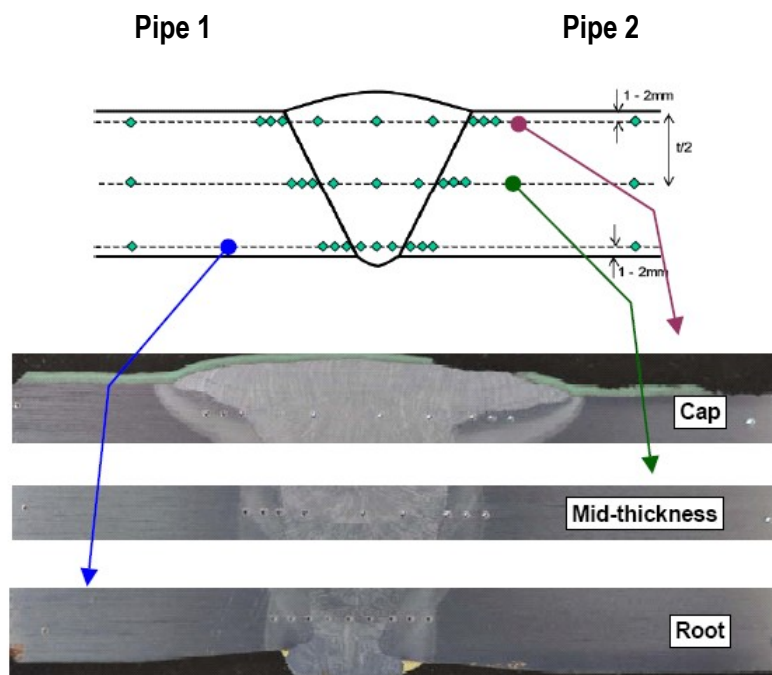
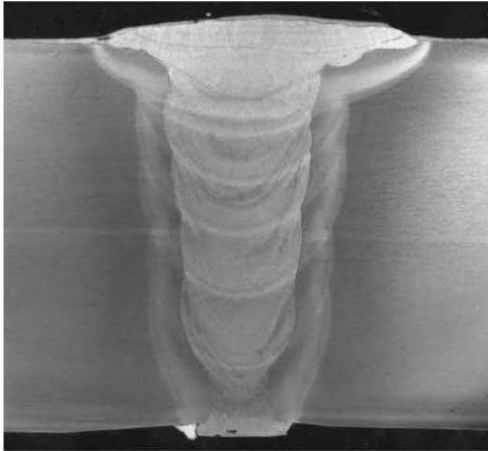
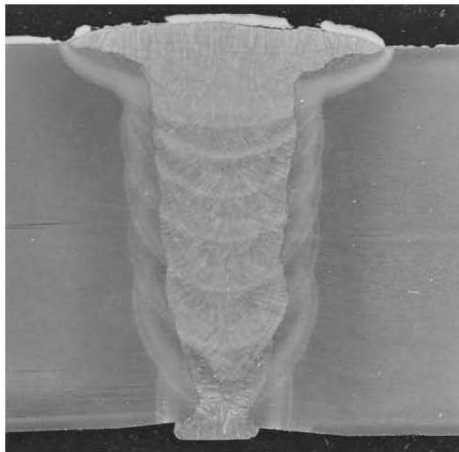


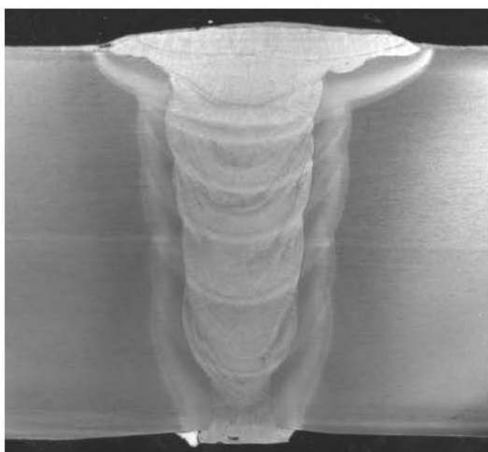
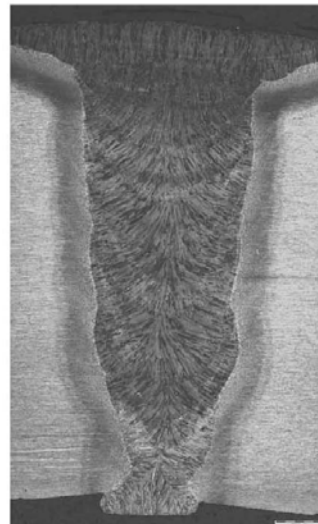
Figure A1 Hardness measurement locations for welds A06 through to B08.



Macro section # A06-12-M
Sampling position: 0.5 o'clock



Macro section # A06-3-M
Sampling position: 2.8 o'clock



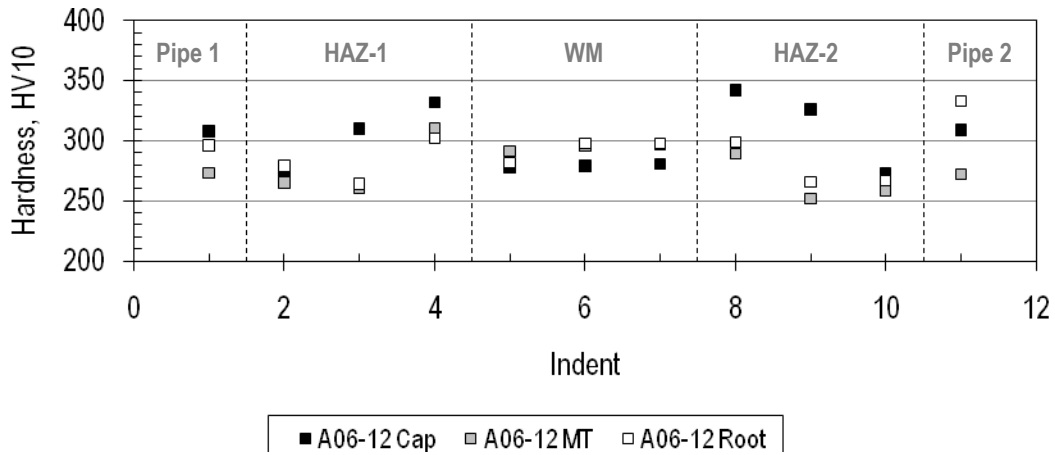
Macro section # A06-7-M
Sampling position: 6.7 o'clock

Figure A2 Weld A06: Macro sections (approximate positions: 0.5, 2.8 and 6.7 o'clock).

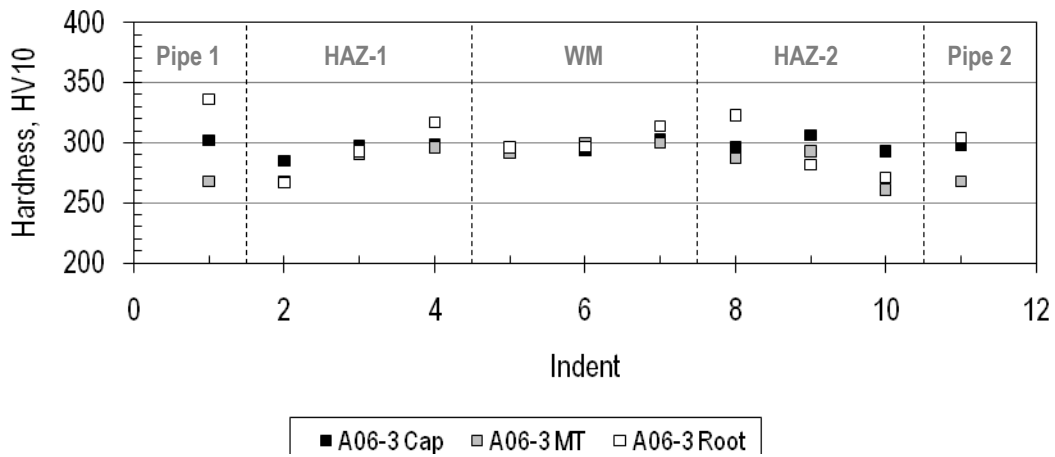
Indent	Material	Source	Vickers hardness measurements, HV10								
			0.5 o'clock			2.8 o'clock			6.7 o'clock		
			Cap	MT	Root	Cap	MT	Root	Cap	MT	Root
1	PM-1	B	308	273	296	302	268	336	275	280	304
2	HAZ-1		273	265	279	285	268	267	272	265	268
3			310	261	264	298	290	293	280	280	261
4			332	310	302	299	296	317	282	279	287
5	WM	B	278	291	282	293	292	296	291	290	294
6			279	296	298	294	300	297	284	285	292
7			281	297	298	303	300	314	284	293	298
8	HAZ-2		342	289	299	296	287	323	294	280	303
9		326	252	266	306	293	282	279	273	266	
10		273	258	267	293	261	271	275	269	289	
11	PM-2		309	272	333	298	268	304	292	281	300

Notes: measurements taken 0.06in (1.5mm) below weld **Cap**, at the pipe mid-wall thickness **MT** and 0.06in (1.5mm) up from the weld **Root**

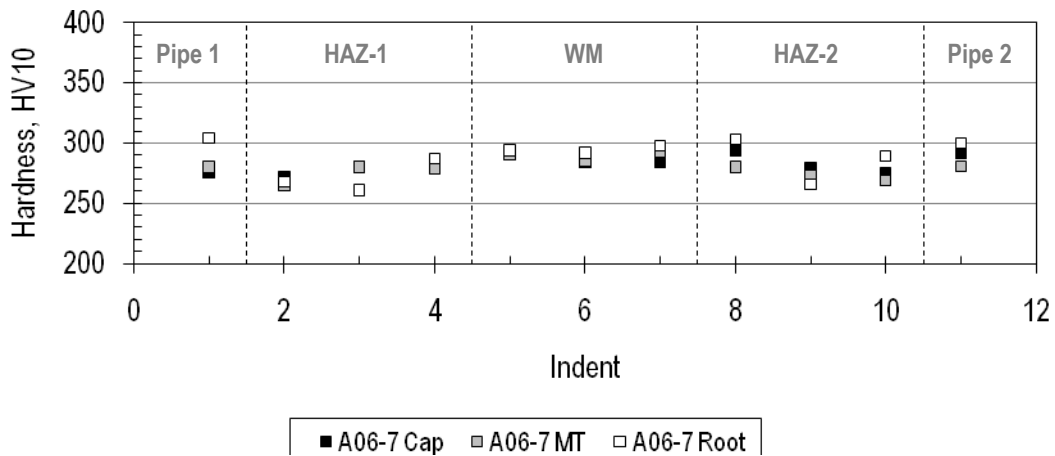
Table A1 Weld A06: Individual Vickers hardness measurements, HV10.



Sampling position: 0.5 o'clock



Sampling position: 2.8 o'clock

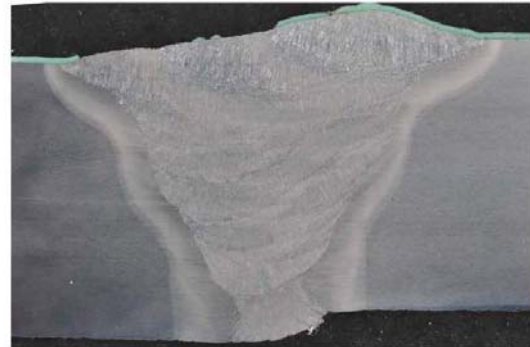


Sampling position: 6.7 o'clock

Figure A3 Weld A06: Vickers hardness surveys (undertaken on macro sections shown in Figure A2)



Macro section # A17-3-M
Sampling position: 2.9 o'clock



Macro section # A17-7-M
Sampling position: 6.7 o'clock



Macro section # A17-8.5-M
Sampling position: 8.2 o'clock



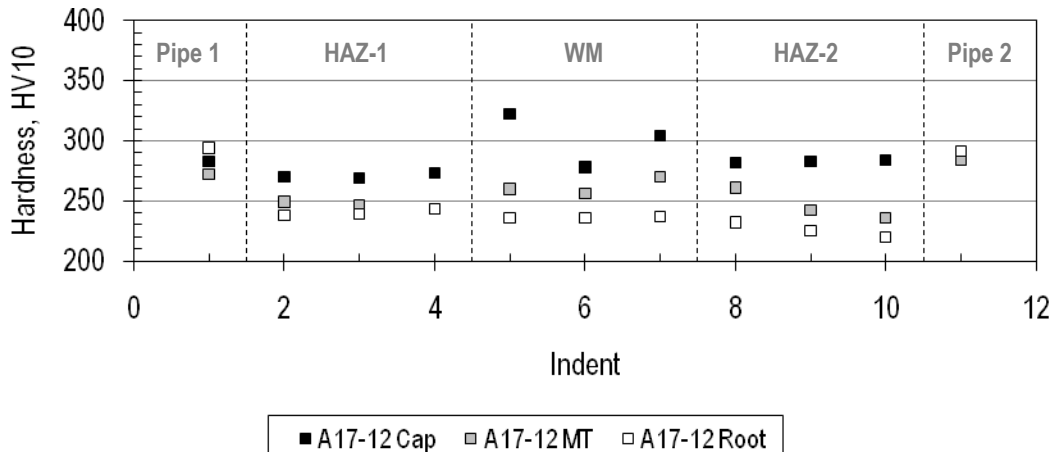
Macro section # A17-12-M
Sampling position: 0.4 o'clock

Figure A4 Weld A17: Macro sections (approximate positions: 0.4, 2.9, 6.7 and 8.2 o'clock)

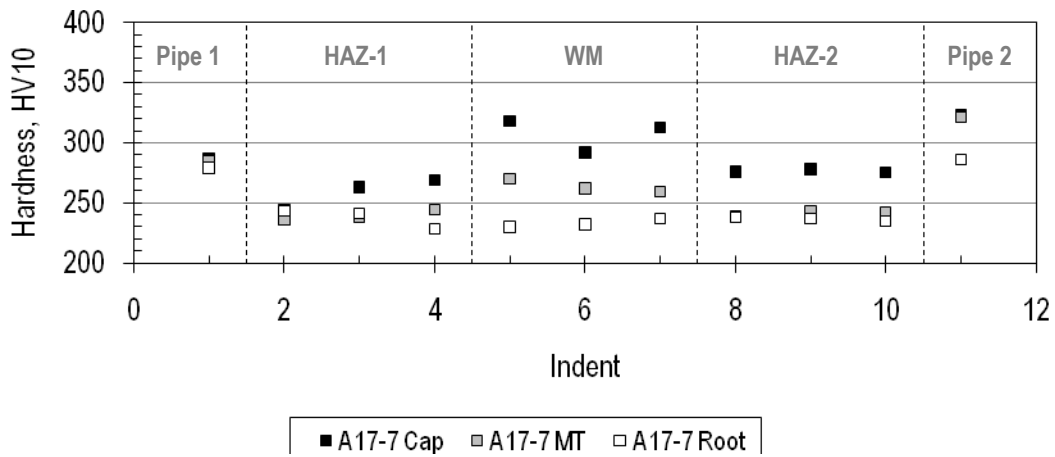
Indent	Material	Source	Vickers hardness measurements, HV10								
			0.4 o'clock			6.7 o'clock			8.2 o'clock		
			Cap	MT	Root	Cap	MT	Root	Cap	MT	Root
1	PM-1	C	283	272	294	287	285	279	319	293	305
2	HAZ-1		270	249	238	244	236	243	252	243	241
3			269	246	239	263	238	241	263	229	238
4			273	243	243	269	244	228	282	240	237
5	WM	C	322	260	236	318	270	230	304	276	229
6			278	256	236	292	262	232	285	274	233
7			304	270	237	313	259	237	283	289	231
8	HAZ-2		282	261	232	276	239	238	269	232	248
9		283	242	225	278	243	237	269	232	254	
10		284	236	220	275	242	235	254	241	249	
11	PM-2		285	284	291	323	321	286	255	253	283

Notes: measurements taken 0.06in (1.5mm) below weld **Cap**, at the pipe mid-wall thickness **MT** and 0.06in (1.5mm) up from the weld **Root**

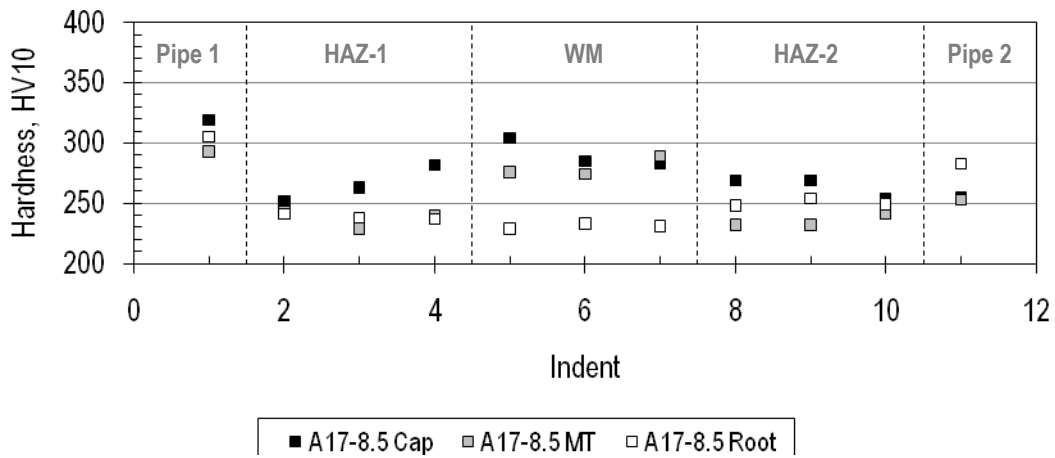
Table A2 Weld A17: Individual Vickers hardness measurements, HV10.



Sampling position: 0.4 o'clock

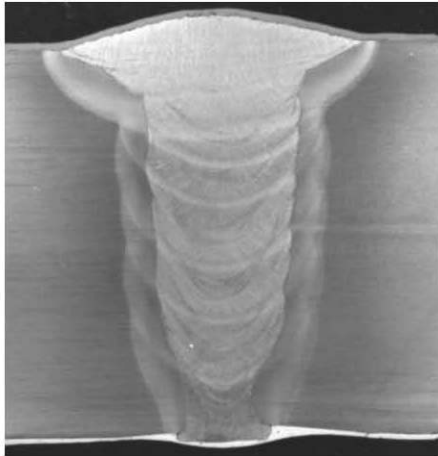


Sampling position: 6.7 o'clock

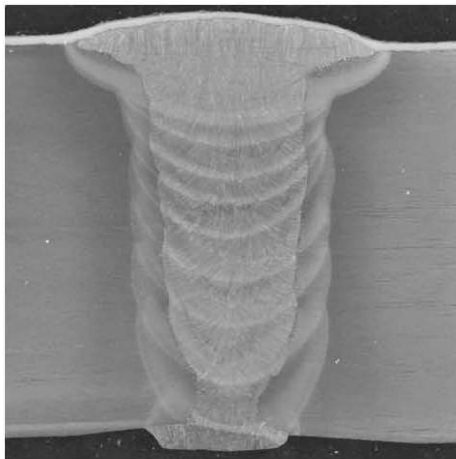


Sampling position: 8.2 o'clock

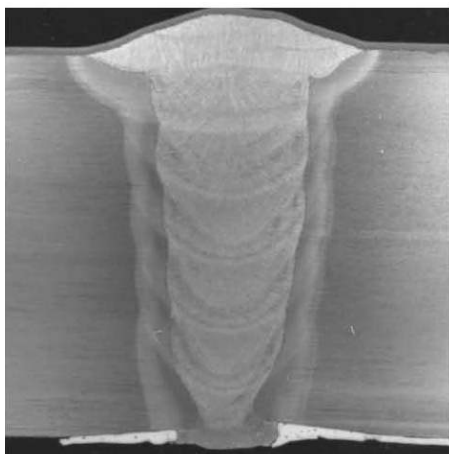
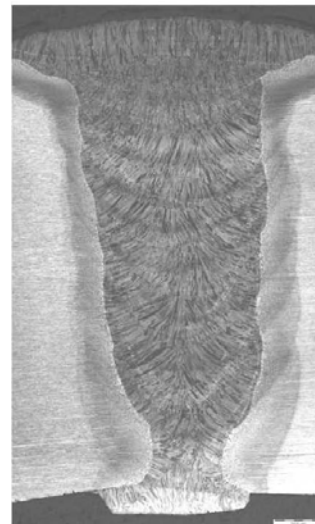
Figure A5 Weld A17: Vickers hardness surveys (undertaken on macro sections shown in Figure A4)



Macro section # A33-12-M
Sampling position: 0.5 o'clock



Macro section # A33-3-M
Sampling position: 2.8 o'clock



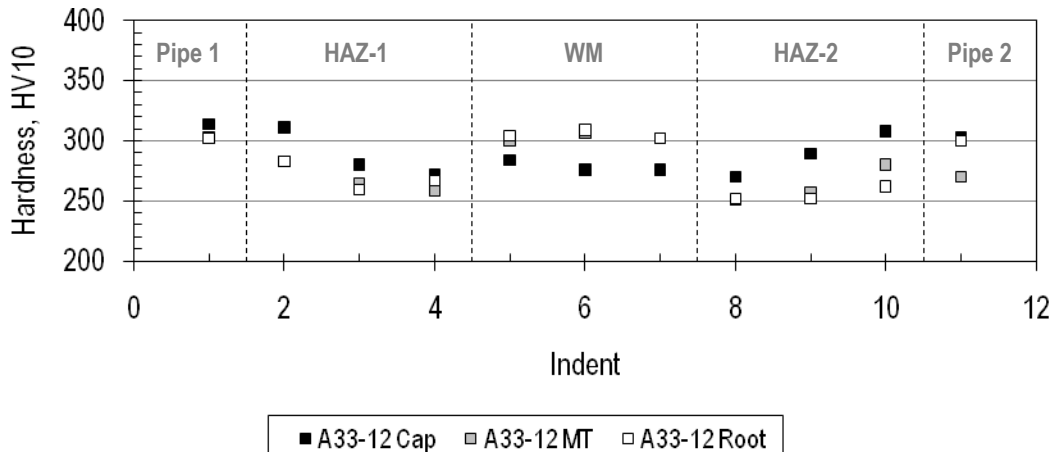
Macro section # A33-7-M
Sampling position: 6.7 o'clock

Figure A6 Weld A33: Macro sections (approximate positions: 0.5, 2.8 and 6.7 o'clock).

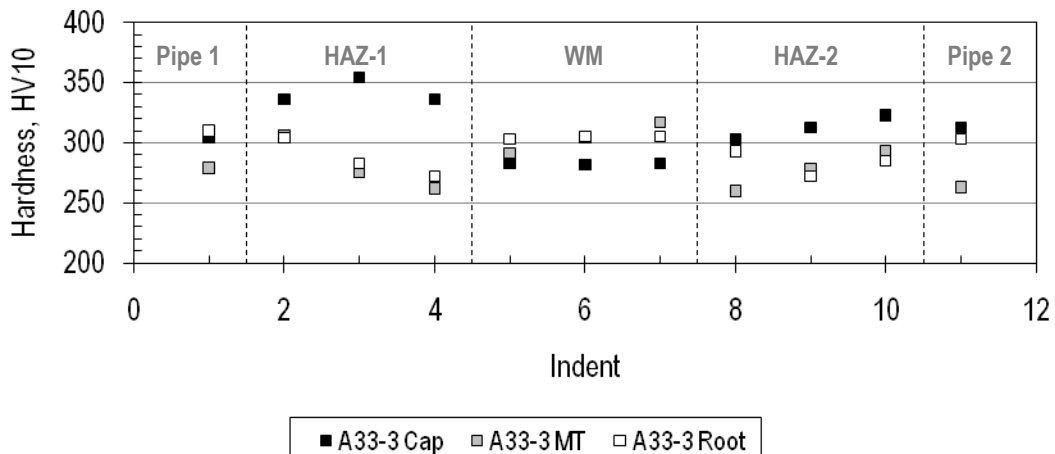
Indent	Material	Source	Vickers hardness measurements, HV10								
			0.5 o'clock			2.8 o'clock			6.7 o'clock		
			Cap	MT	Root	Cap	MT	Root	Cap	MT	Root
1	PM-1	B	314	303	302	304	279	310	299	268	322
2	HAZ-1		311	283	283	336	306	304	332	332	297
3			280	264	259	354	275	283	306	303	272
4			272	258	267	336	262	272	283	294	268
5	WM	A	284	300	304	283	291	303	303	304	283
6			276	306	309	282	304	305	298	302	287
7			276	302	302	283	317	305	291	299	290
8	HAZ-2		270	251	252	303	260	293	275	251	256
9		289	257	252	313	278	272	291	251	256	
10		308	280	262	323	293	285	315	294	290	
11	PM-2		303	270	300	313	263	303	322	276	319

Notes: measurements taken 0.06in (1.5mm) below weld **Cap**, at the pipe mid-wall thickness **MT** and 0.06in (1.5mm) up from the weld **Root**

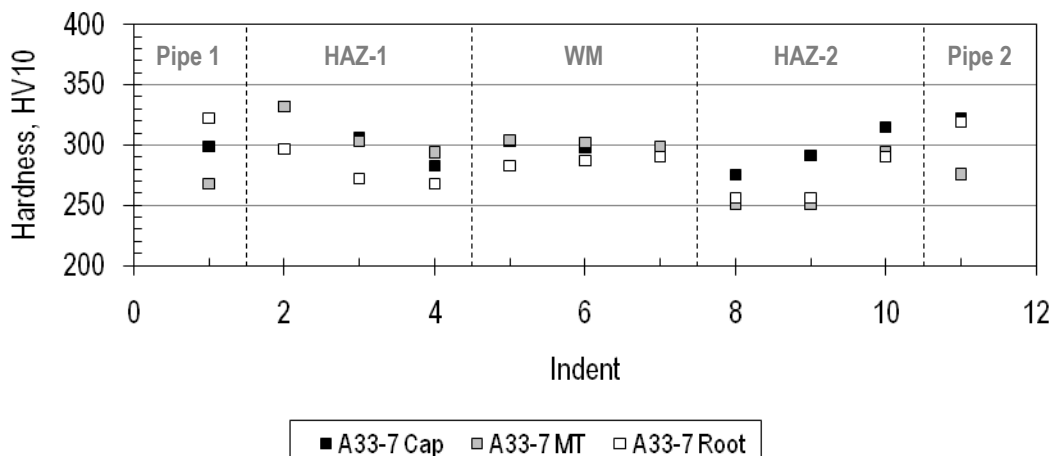
Table A3 Weld A33: Individual Vickers hardness measurements, HV10.



Sampling position: 0.5 o'clock

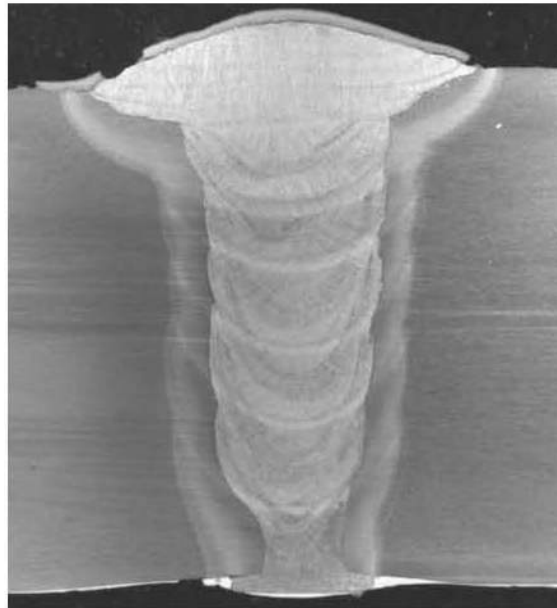


Sampling position: 2.8 o'clock

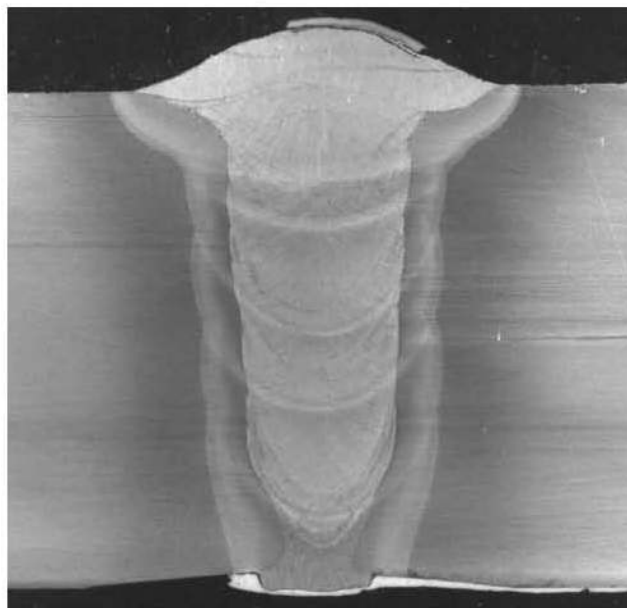


Sampling position: 6.7 o'clock

Figure A7 Weld A33: Vickers hardness surveys (undertaken on macro sections shown in Figure A6)



Macro section # A44-12-M
Sampling position: 0.5 o'clock



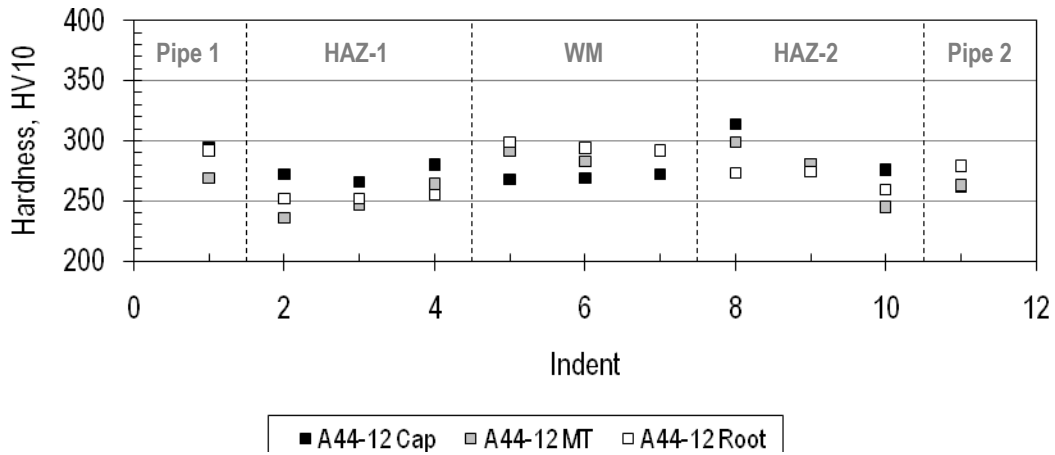
Macro section # A44-7-M
Sampling position: 6.7 o'clock

Figure A8 Weld A44: Macro sections (approximate positions: 0.5 and 6.7 o'clock)

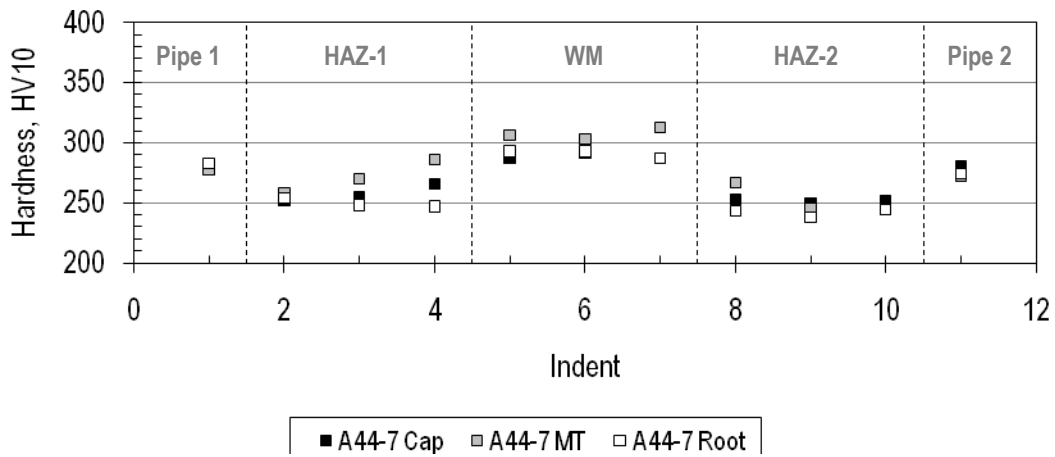
Indent	Material	Source	Vickers hardness measurements, HV10					
			0.5 o'clock			6.7 o'clock		
			Cap	MT	Root	Cap	MT	Root
1	PM-1	C	294	269	292	280	278	283
2	HAZ-1		272	236	252	252	258	254
3			266	247	252	255	270	248
4			280	264	255	266	286	247
5	WM		268	292	299	287	306	293
6			269	283	294	292	303	293
7			272	291	292	287	313	287
8	HAZ-2	B	314	299	273	253	267	243
9			281	281	274	249	245	238
10			276	245	259	252	244	244
11	PM-2		262	263	279	281	272	274

Notes: measurements taken 0.06in (1.5mm) below weld **Cap**, at the pipe mid-wall thickness **MT** and 0.06in (1.5mm) up from the weld **Root**

Table A4 Weld A44: Individual Vickers hardness measurements, HV10.

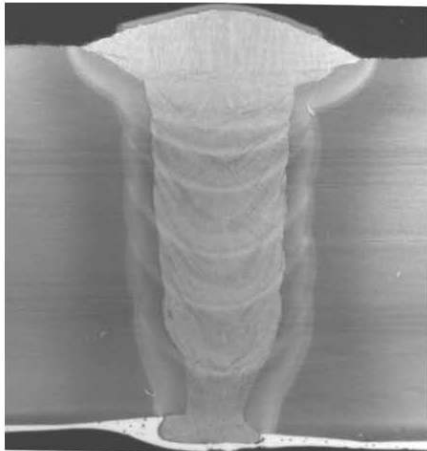


Sampling position: 0.5 o'clock

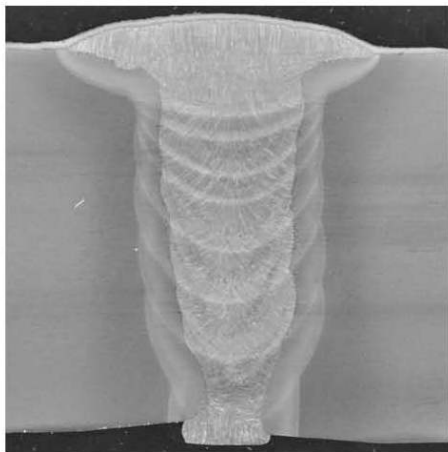


Sampling position: 6.7 o'clock

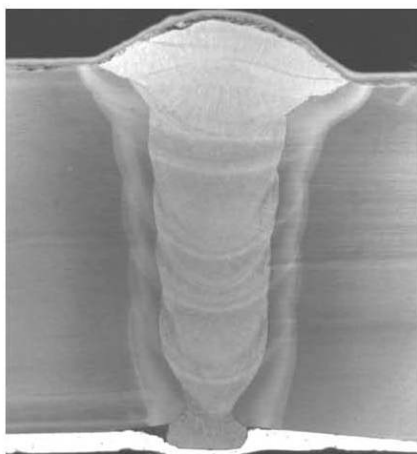
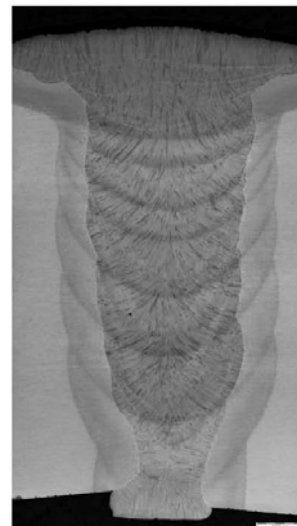
Figure A9 Weld A44: Vickers hardness surveys (undertaken on macro sections shown in Figure A8)



Macro section # A46-12-M
Sampling position: 0.5 o'clock



Macro section # A46-3-M
Sampling position: 2.8 o'clock



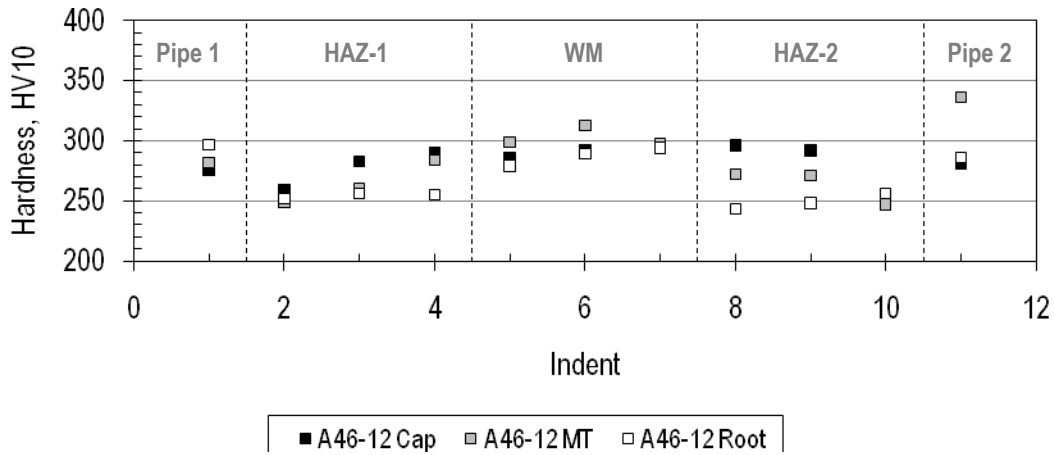
Macro section # A46-7-M
Sampling position: 6.7 o'clock

Figure A10 Weld A46: Macro sections (approximate positions: 0.5, 2.8 and 6.7 o'clock)

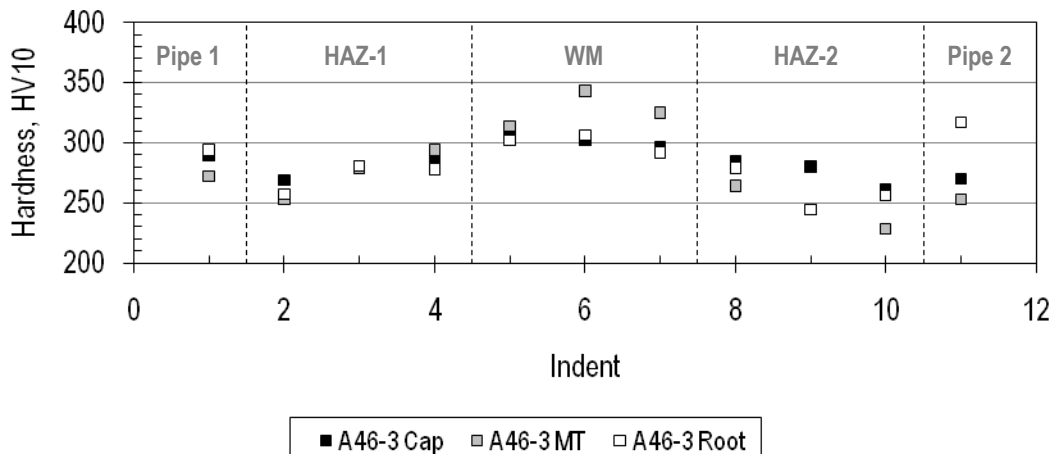
Indent	Material	Source	Vickers hardness measurements, HV10								
			0.5 o'clock			2.8 o'clock			6.7 o'clock		
			Cap	MT	Root	Cap	MT	Root	Cap	MT	Root
1	PM-1	C	276	282	297	289	272	294	297	280	305
2	HAZ-1		259	249	252	269	253	257	267	265	267
3			283	260	256	280	279	281	278	276	266
4			290	284	255	287	294	278	282	291	285
5	WM	C	286	299	279	305	314	302	282	289	292
6			292	313	289	302	343	306	273	292	292
7			294	298	294	296	325	292	275	287	291
8	HAZ-2		296	272	243	285	264	279	283	284	262
9		292	271	248	280	244	244	284	266	260	
10		255	247	256	261	228	256	258	253	252	
11	PM-2		281	336	286	270	253	317	285	267	321

Notes: measurements taken 0.06in (1.5mm) below weld **Cap**, at the pipe mid-wall thickness **MT** and 0.06in (1.5mm) up from the weld **Root**

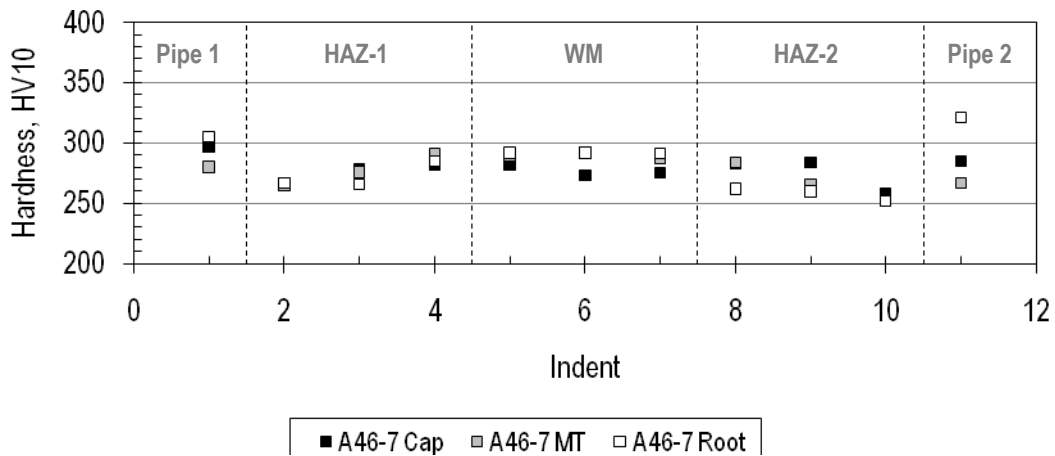
Table A5 Weld A46: Individual Vickers hardness measurements, HV10.



Sampling position: 0.5 o'clock

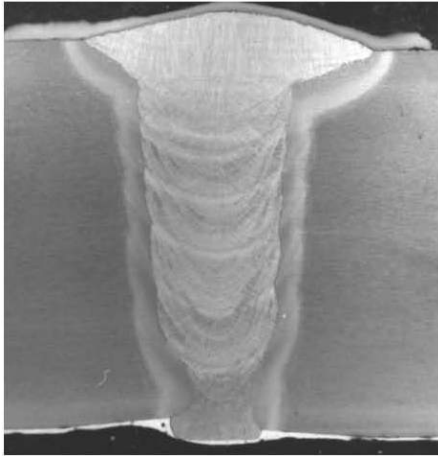


Sampling position: 2.8 o'clock

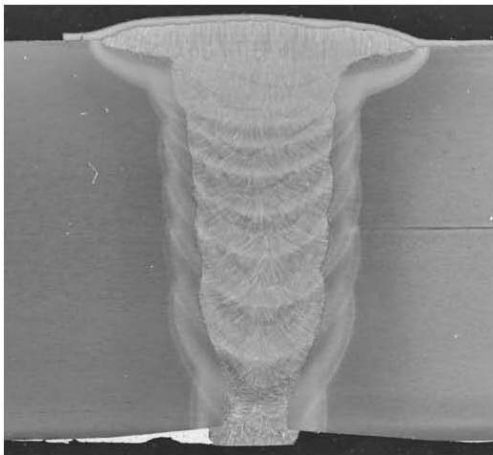


Sampling position: 6.7 o'clock

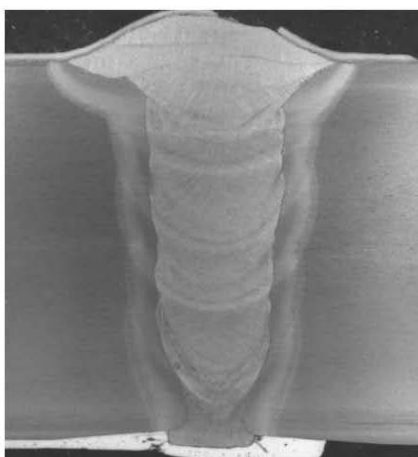
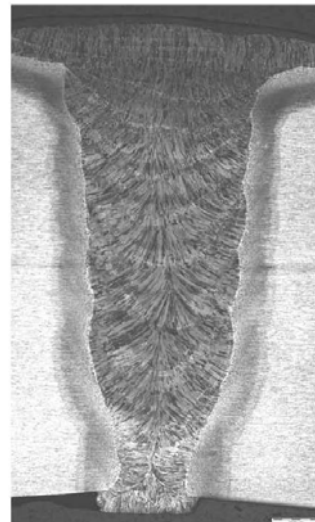
Figure A11 Weld A46: Vickers hardness surveys (undertaken on macro sections shown in Figure A10)



Macro section # A50-12-M
Sampling position: 0.5 o'clock



Macro section # A50-3-M
Sampling position: 2.8 o'clock



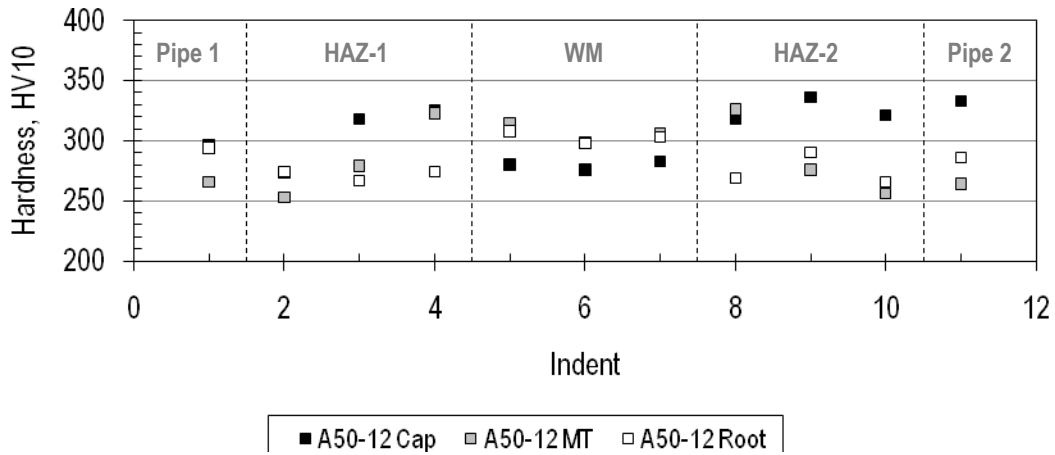
Macro section # A50-7-M
Sampling position: 6.7 o'clock

Figure A12 Weld A50: Macro sections (approximate positions: 0.5, 2.8 and 6.7 o'clock)

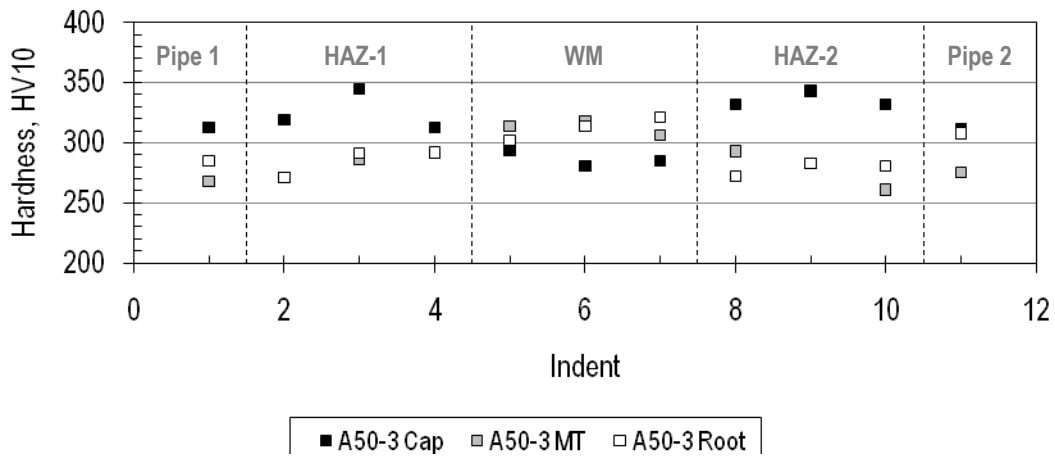
Indent	Material	Source	Vickers hardness measurements, HV10								
			0.5 o'clock			2.8 o'clock			6.7 o'clock		
			Cap	MT	Root	Cap	MT	Root	Cap	MT	Root
1	PM-1	B	297	266	294	313	268	285	302	298	285
2	HAZ-1		273	253	274	319	271	271	279	261	275
3			318	279	267	345	286	291	283	263	276
4			325	323	274	313	291	292	283	282	302
5	WM	B	280	315	308	294	314	302	289	284	296
6			276	299	298	281	318	314	285	283	296
7			283	306	303	285	306	321	285	287	294
8	HAZ-2		318	326	269	332	293	272	274	278	294
9		336	276	290	343	283	283	271	265	271	
10		321	256	266	332	261	281	278	268	280	
11	PM-2		333	264	286	311	275	308	271	323	294

Notes: measurements taken 0.06in (1.5mm) below weld **Cap**, at the pipe mid-wall thickness **MT** and 0.06in (1.5mm) up from the weld **Root**

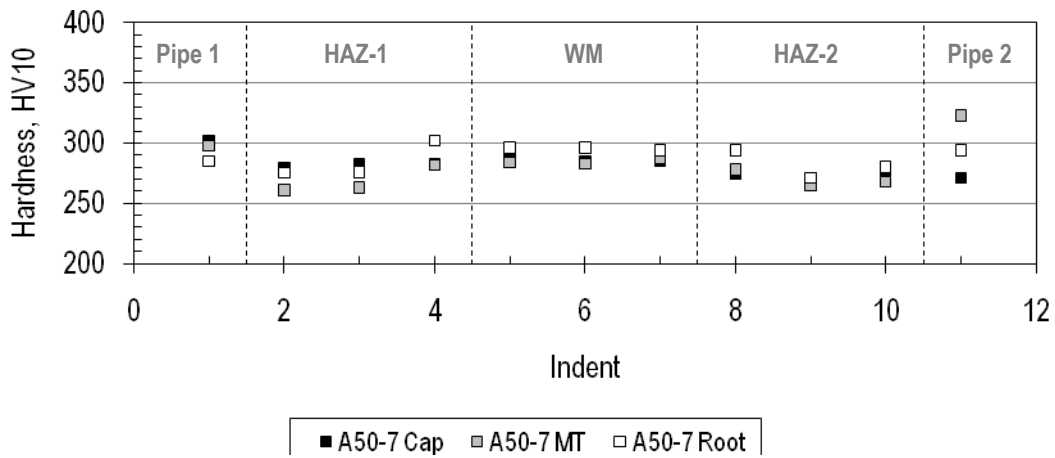
Table A6 Weld A50: Individual Vickers hardness measurements, HV10.



Sampling position: 0.5 o'clock

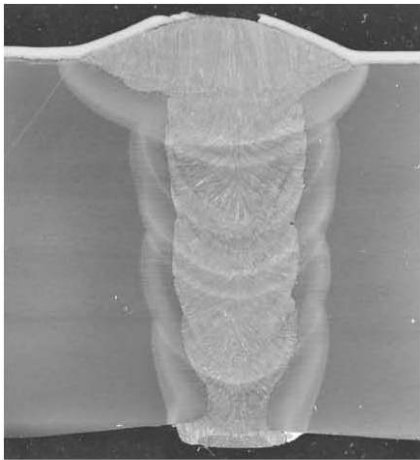


Sampling position: 2.8 o'clock

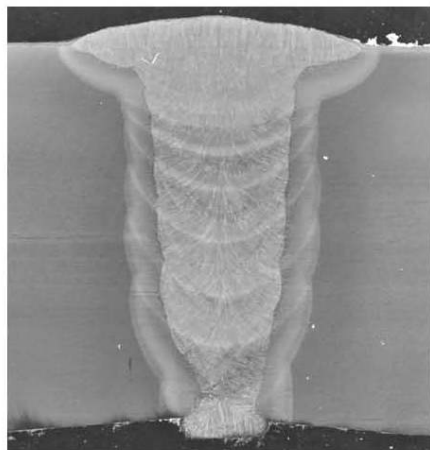
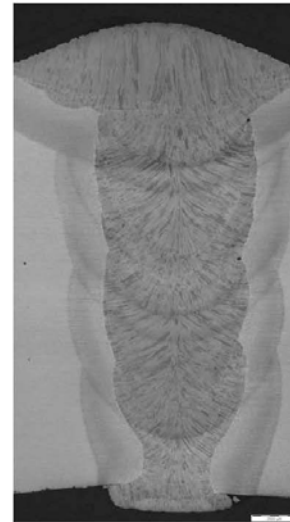


Sampling position: 6.7 o'clock

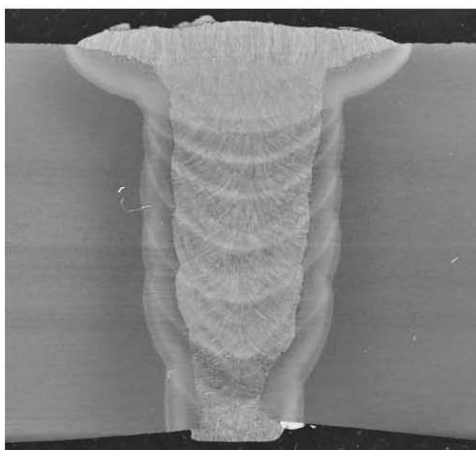
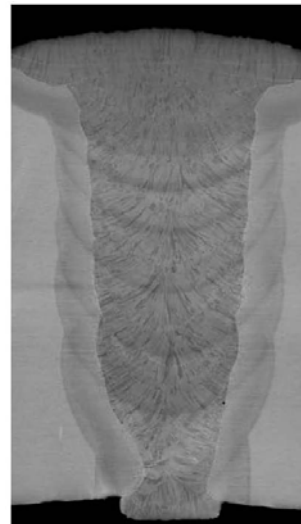
Figure A13 Weld A50: Vickers hardness surveys (undertaken on macro sections shown in Figure A12)



Macro section # B03-12-M
Sampling position: 12.0 o'clock



Macro section # B03-2.5-M
Sampling position: 2.3 o'clock



Macro section # B03-3-M
Sampling position: 3.3 o'clock

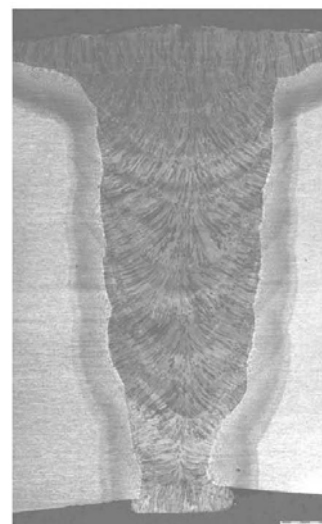
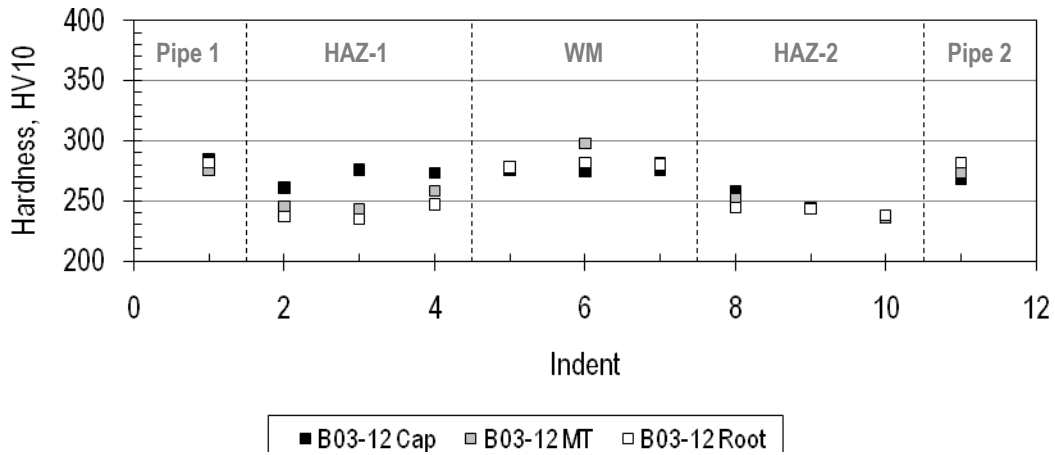


Figure A14 Weld B03: Macro sections (approximate positions: 12, 2.3 and 3.3 o'clock)

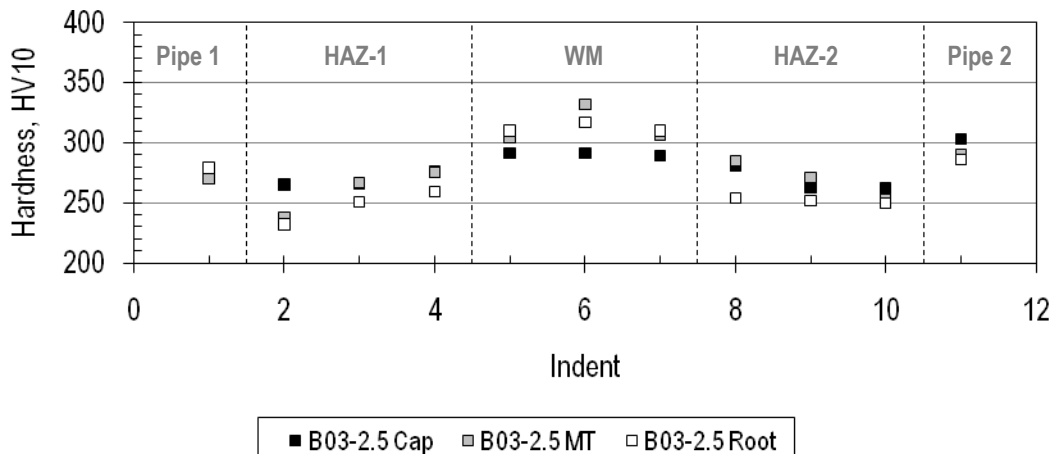
Incident	Material	Source	Vickers hardness measurements, HV10								
			12.0 o'clock			2.3 o'clock			3.3 o'clock		
			Cap	MT	Root	Cap	MT	Root	Cap	MT	Root
1	PM-1	C	285	275	282	273	270	279	285	286	272
2	HAZ-1		261	245	237	265	238	232	262	251	237
3			276	243	235	266	267	251	268	274	248
4			273	258	247	276	275	259	270	298	272
5	WM	C	275	278	278	291	304	310	291	298	305
6			274	298	282	291	332	317	297	297	305
7			275	282	280	289	306	310	294	293	306
8	HAZ-2		258	252	244	281	285	254	273	284	254
9		243	244	243	263	271	252	263	263	243	
10		236	236	238	262	253	250	262	254	244	
11	PM-2		268	273	282	303	290	286	281	285	278

Notes: measurements taken 0.06in (1.5mm) below weld **Cap**, at the pipe mid-wall thickness **MT** and 0.06in (1.5mm) up from the weld **Root**

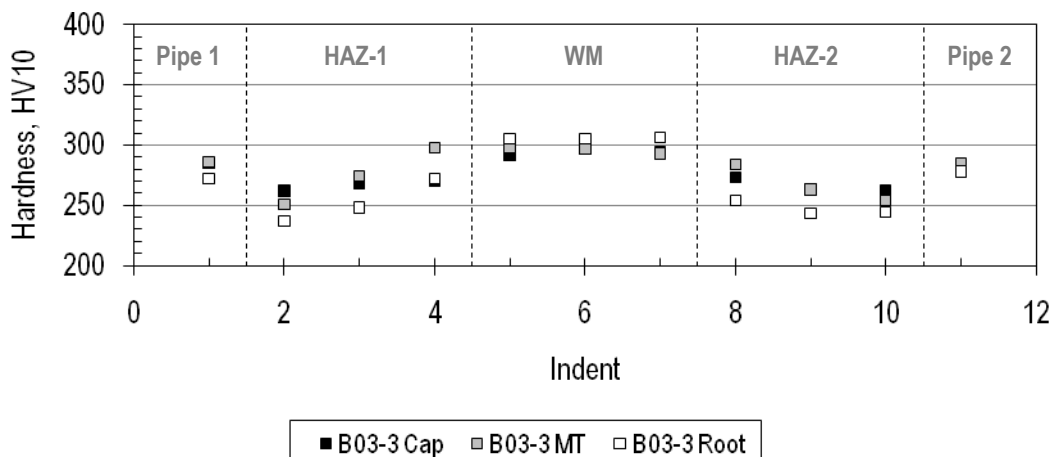
Table A7 Weld B03: Individual Vickers hardness measurements, HV10.



Sampling position: 12.0 o'clock

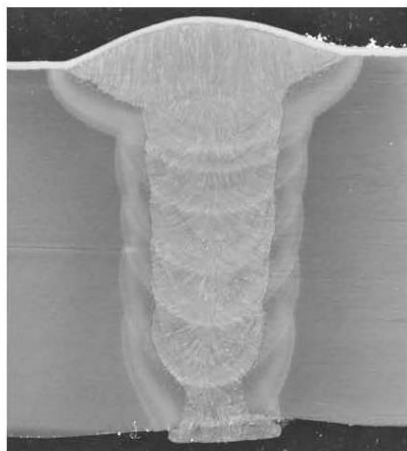


Sampling position: 2.3 o'clock

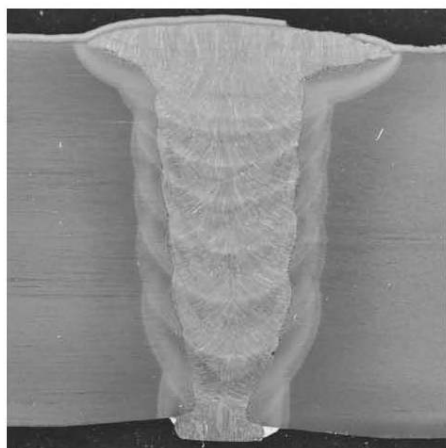
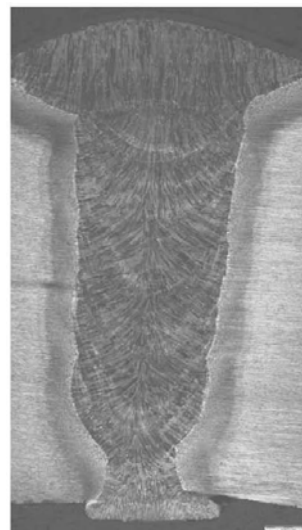


Sampling position: 3.3 o'clock

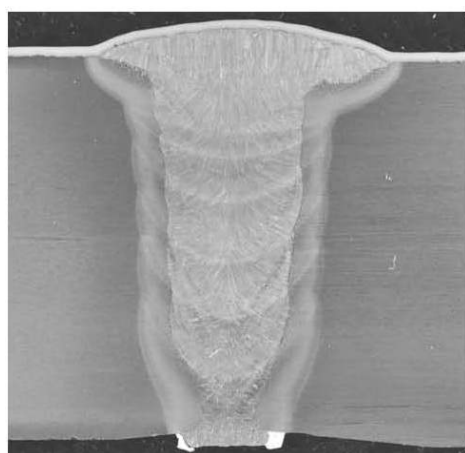
Figure A15 Weld B03: Vickers hardness surveys (undertaken on macro sections shown in Figure A14)



Macro section # B06-12-M
Sampling position: 0.3 o'clock



Macro section # B06-1.5-M
Sampling position: 1.7 o'clock



Macro section # B06-5-M
Sampling position: 4.8 o'clock

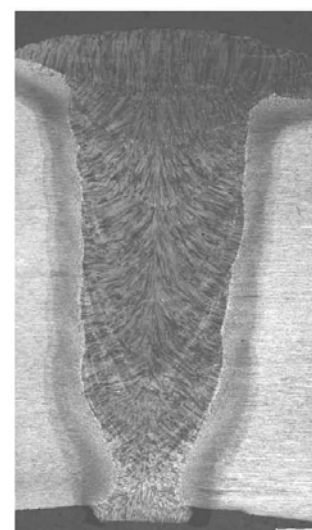
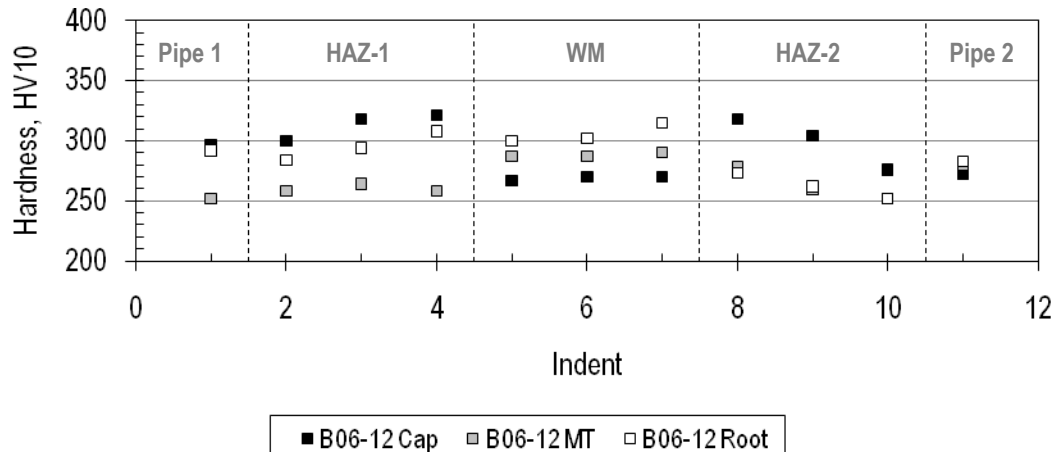


Figure A16 Weld B06: Macro sections (approximate positions: 0.3, 1.7 and 4.8 o'clock)

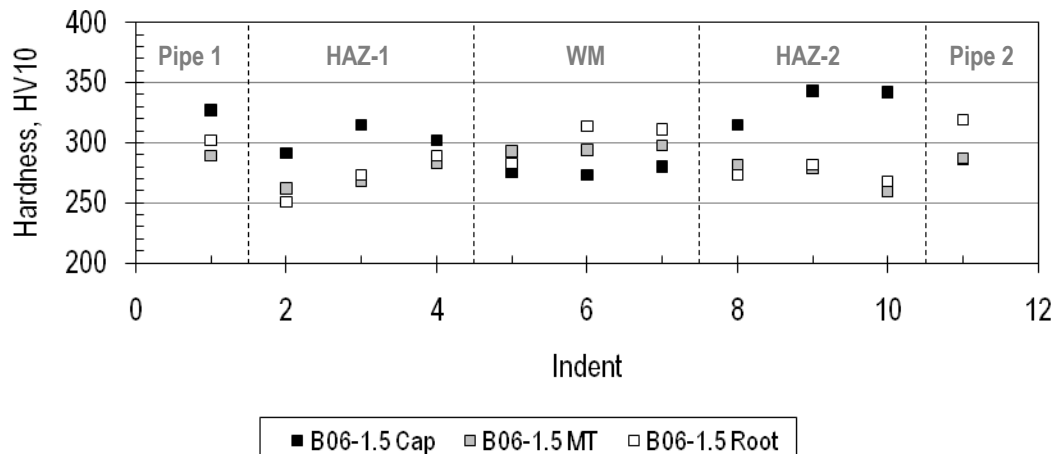
Indent	Material	Source	Vickers hardness measurements, HV10								
			0.3 o'clock			1.7 o'clock			4.8 o'clock		
			Cap	MT	Root	Cap	MT	Root	Cap	MT	Root
1	PM-1	A	296	252	292	327	289	302	305	286	309
2	HAZ-1		300	258	284	291	262	251	284	279	269
3			318	264	294	315	268	273	275	273	269
4			321	258	308	302	283	289	285	272	281
5	WM	B	267	287	300	276	293	283	294	293	294
6			270	287	302	273	294	314	292	310	296
7			270	290	315	280	298	311	294	309	298
8	HAZ-2		318	278	273	315	282	273	282	240	279
9		304	260	262	343	279	282	269	236	251	
10		276	252	252	342	260	268	268	233	263	
11	PM-2		272	280	283	286	287	319	273	259	285

Notes: measurements taken 0.06in (1.5mm) below weld **Cap**, at the pipe mid-wall thickness **MT** and 0.06in (1.5mm) up from the weld **Root**

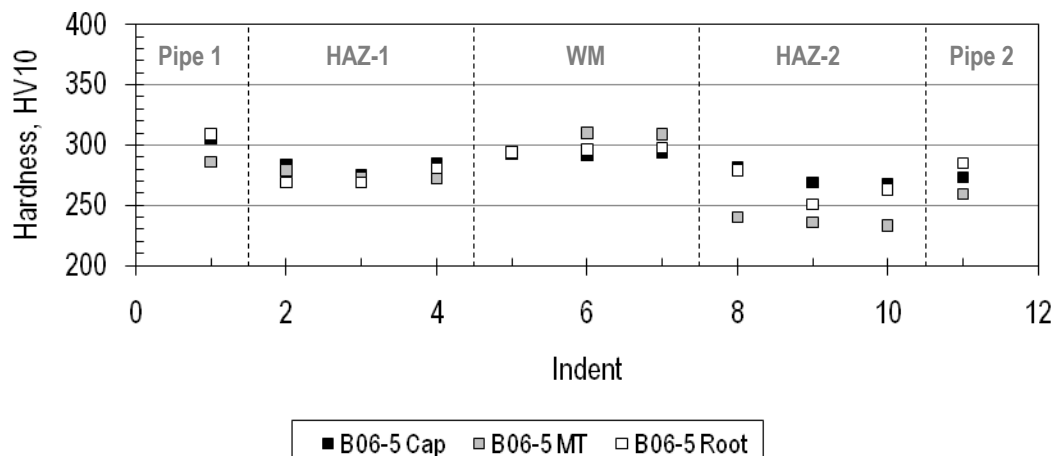
Table A8 Weld B06: Individual Vickers hardness measurements, HV10.



Sampling position: 0.3 o'clock

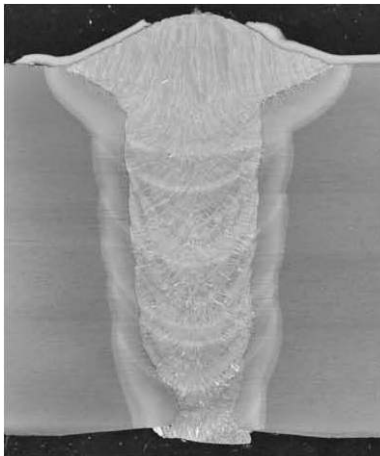


Sampling position: 1.7 o'clock

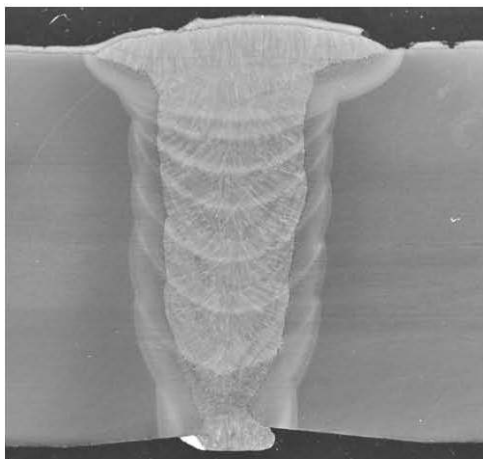
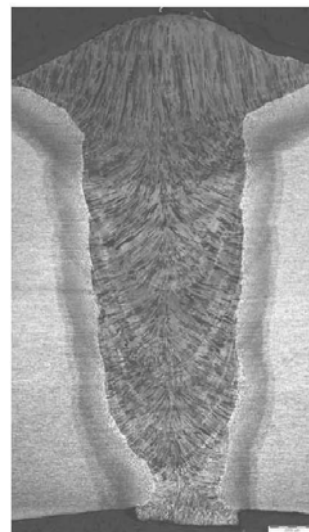


Sampling position: 4.8 o'clock

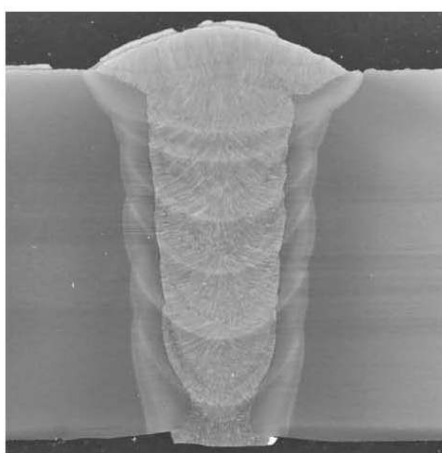
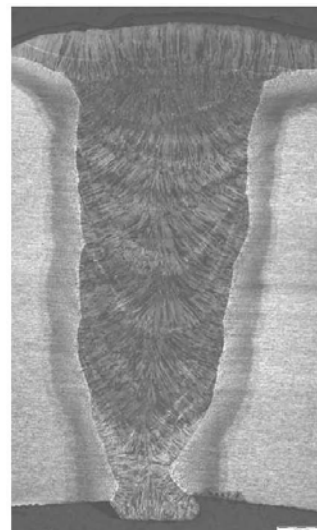
Figure A17 Weld B06: Vickers hardness surveys (undertaken on macro sections shown in Figure A16)



Macro section # B08-12-M
Sampling position: 12.0 o'clock



Macro section # B08-2-M
Sampling position: 1.8 o'clock



Macro section # B08-7-M
Sampling position: 6.9 o'clock

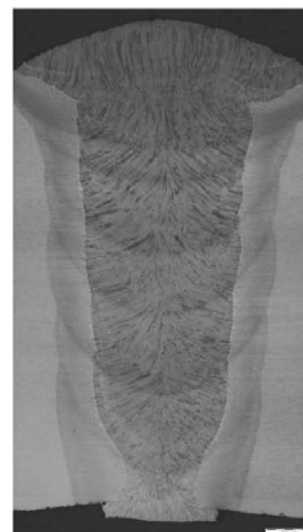
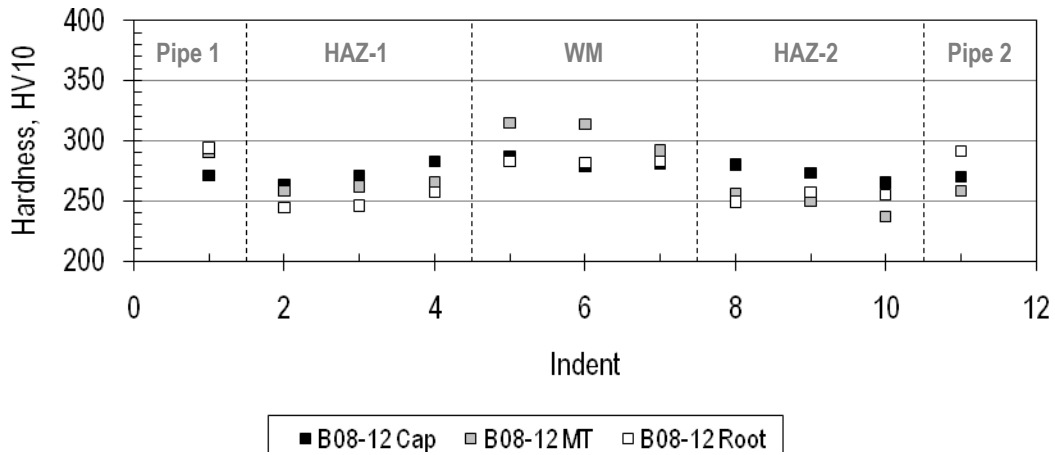


Figure A18 Weld B08: Macro sections (approximate positions: 12, 1.8 and 6.9 o'clock).

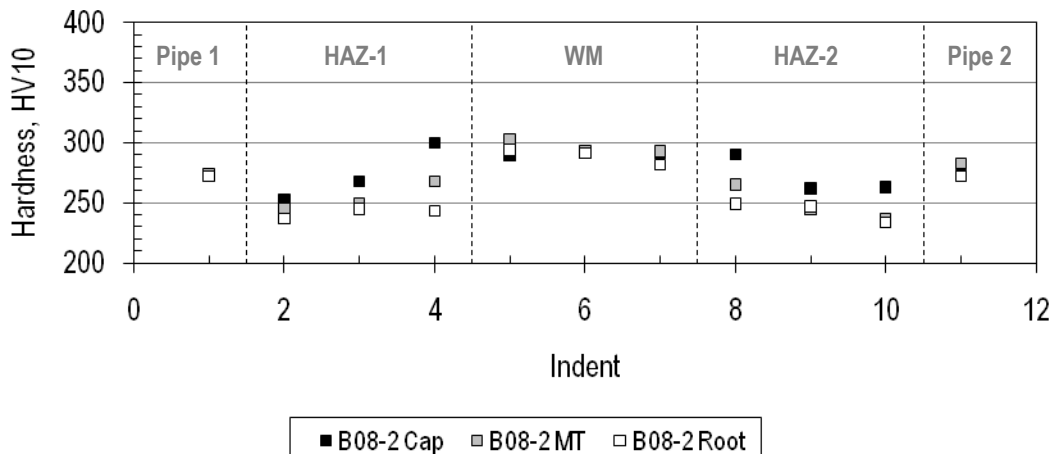
Incident	Material	Source	Vickers hardness measurements, HV10								
			12.0 o'clock			1.8 o'clock			6.9 o'clock		
			Cap	MT	Root	Cap	MT	Root	Cap	MT	Root
1	PM-1	C	271	290	294	273	274	272	272	275	291
2	HAZ-1		263	258	244	253	245	237	240	247	239
3			271	262	246	268	250	245	250	255	243
4			283	265	257	300	268	243	257	259	246
5	WM	C	287	315	283	289	303	294	284	309	298
6			279	314	282	291	293	291	286	306	297
7			281	292	283	291	293	282	285	298	292
8	HAZ-2		280	256	249	290	265	249	259	235	248
9		273	250	257	262	244	247	253	232	241	
10		265	237	255	263	237	234	244	228	243	
11	PM-2		270	258	291	273	283	272	282	243	271

Notes: measurements taken 0.06in (1.5mm) below weld **Cap**, at the pipe mid-wall thickness **MT** and 0.06in (1.5mm) up from the weld **Root**

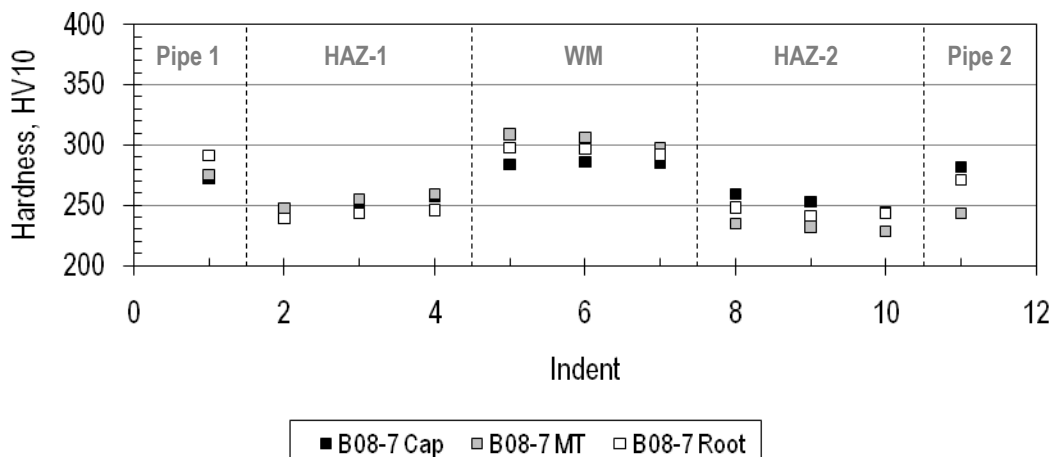
Table A9 Weld B08: Individual Vickers hardness measurements, HV10.



Sampling position: 12.0 o'clock



Sampling position: 1.8 o'clock



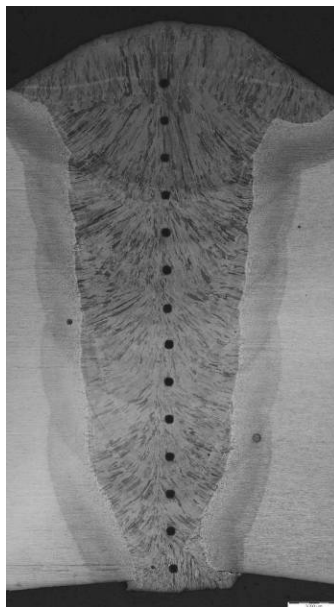
Sampling position: 6.9 o'clock

Figure A19 Weld B08: Vickers hardness surveys (undertaken on macro sections shown in Figure A18)

	Weld ID								
	A06	A17*	A33	A44	A46	A50	B03	B06	B08
Source (Pipe 1)	B	C	B	C	C	B	C	A	C
Pipe 1 _{avg}	294	291	300	283	288	290	279	295	279
Pipe 1 HAZ _{avg}	285	248	292	259	272	288	259	282	255
WM _{avg}	293	267	296	290	296	296	295	292	293
Pipe 2 HAZ _{avg}	286	251	279	263	264	290	256	276	252
Pipe 2 _{avg}	295	287	297	272	291	296	283	283	271
Source (Pipe 2)	B	C	A	B	C	B	C	B	C

Notes: * is a tie in weld; all others are main line welds. **HAZ** is heat affected zone, **WM** is weld metal and **avg** is average

Table A10 Average hardness properties as a function of pipe source and weld number

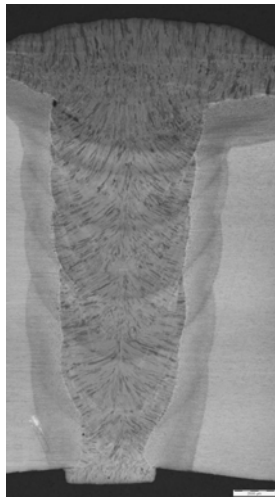


Notes: indents taken 1mm up from the weld root, then at 1.5mm increments

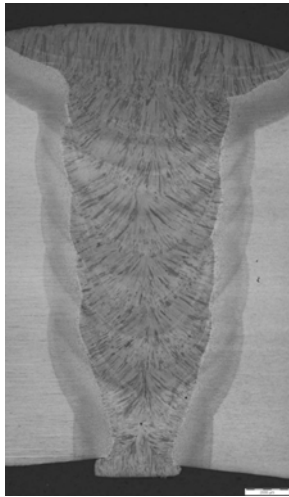
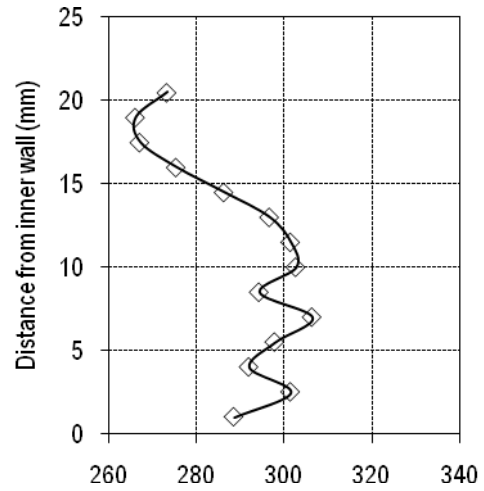
Figure A20 Weld B10: example of a through thickness hardness traverse at the weld metal centre-line

Position (o'clock)	Through wall thickness indent location, from weld root inch (mm)													
	0.04 (1.0)	0.10 (2.5)	0.16 (4.0)	0.22 (5.5)	0.28 (7.0)	0.33 (8.5)	0.39 (10.0)	0.45 (11.5)	0.51 (13.0)	0.57 (14.5)	0.63 (16.0)	0.69 (17.5)	0.75 (19.0)	0.81 (20.5)
12.0	289	301	292	298	306	294	303	301	297	286	275	267	266	273
1.1	329	299	311	309	300	304	314	305	309	285	285	280	281	
2.2	327	297	295	318	284	315	301	308	310	291	271	291	285	
3.3	325	293	306	319	300	329	301	314	315	300	274	295	297	
4.4	317	310	295	310	297	308	305	300	313	292	293	276	287	
5.5	290	297	297	295	299	292	308	300	304	283	285	279	277	289
6.6	305	294	293	300	287	297	286	295	283	276	286	283	287	275
7.7	315	300	303	304	305	317	297	300	295	299	283	286	286	273
8.8	308	314	293	321	295	309	305	319	321	295	295	277	290	
9.9	317	308	293	322	281	300	331	315	319	291	275	300	297	
11.0	295	303	295	314	311	313	314	305	314	276	279	286	279	

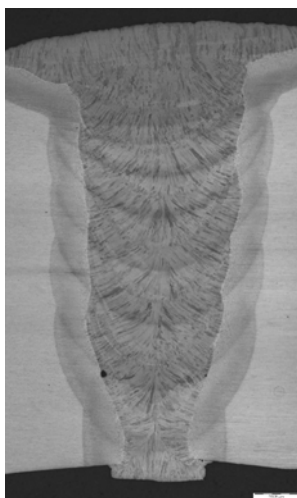
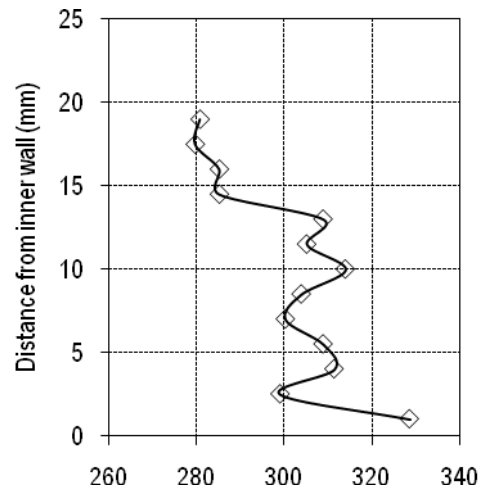
Table A11 Weld B10: Individual Vickers hardness measurements, HV10.



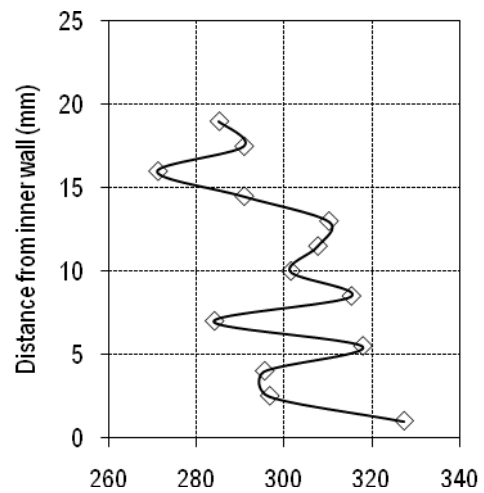
12 o'clock position



1.1 o'clock position



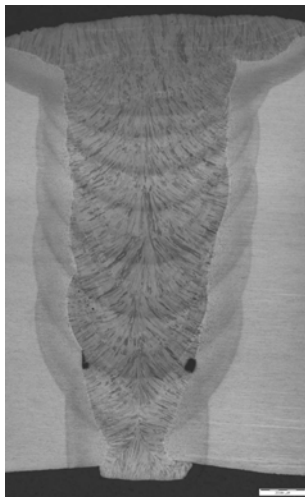
2.2 o'clock position



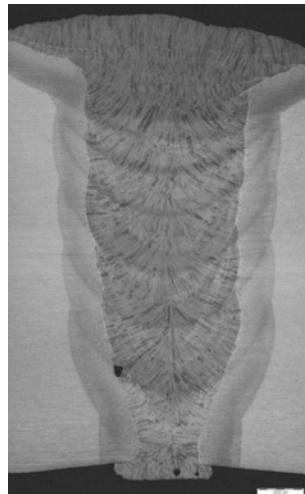
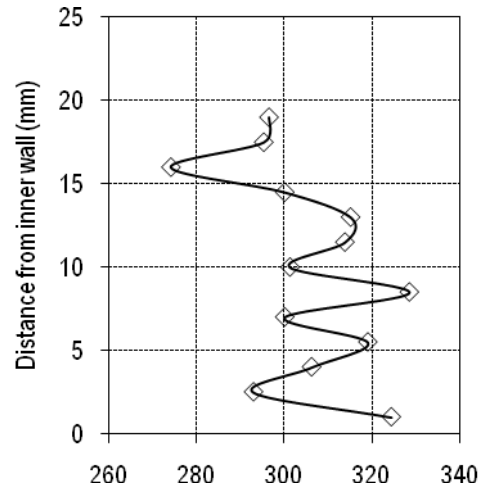
Macro-Sections

Hardness profiles (HV10)

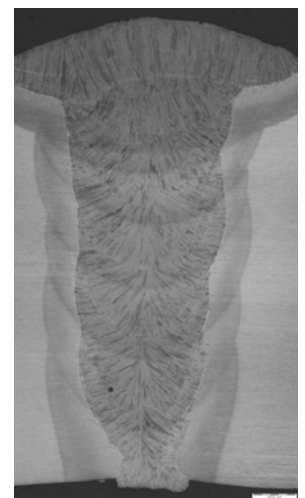
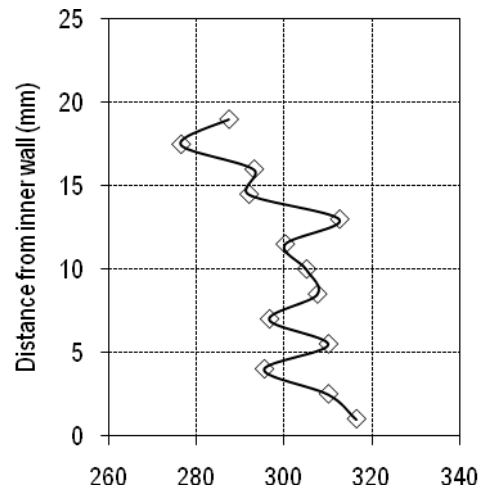
Figure A21 Weld B10: Macro sections and hardness profiles around the pipe circumference (continued over).



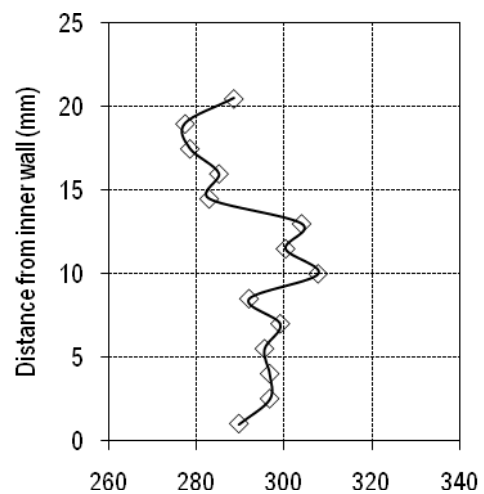
3.3 o'clock position



4.4 o'clock position



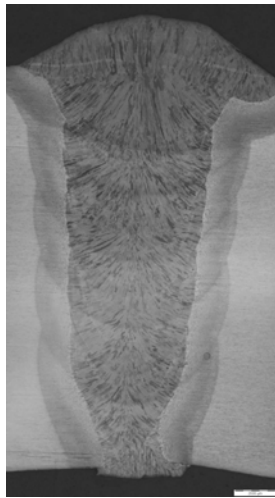
5.5 o'clock position



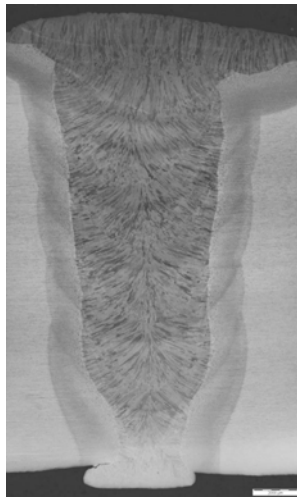
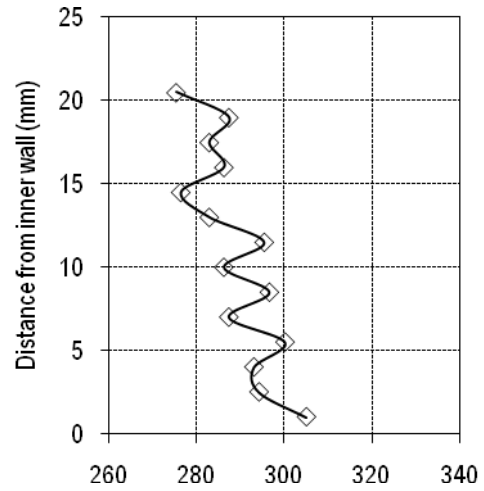
Macro-Sections

Hardness profiles (HV10)

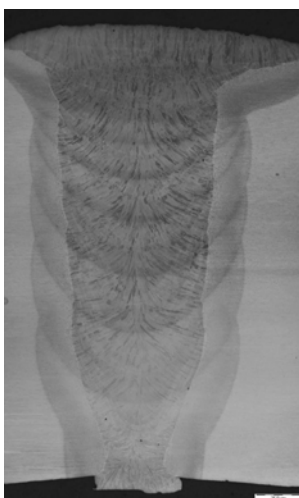
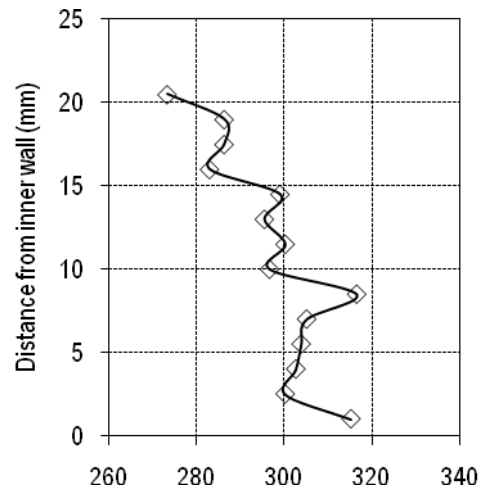
Figure A22 Weld B10: Macro sections and hardness profiles around the pipe circumference (continued over).



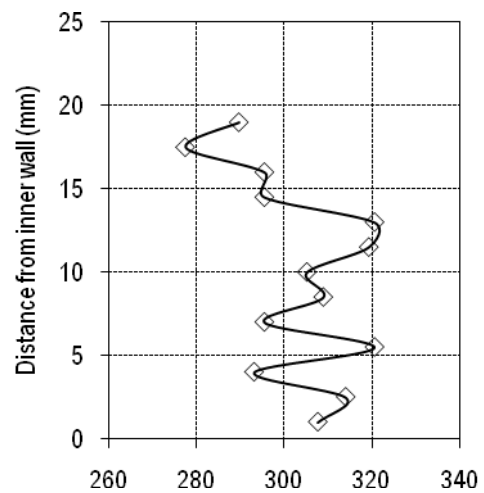
6.6 o'clock position



7.7 o'clock position



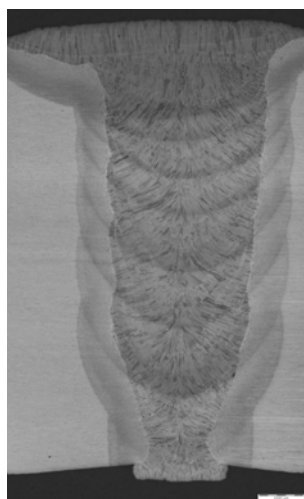
8.8 o'clock position



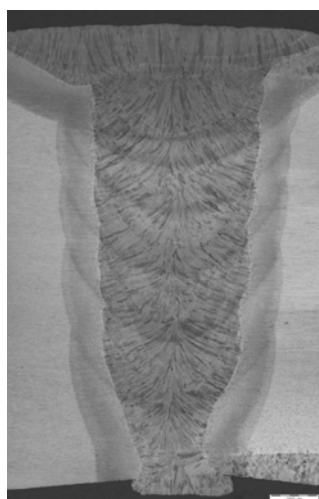
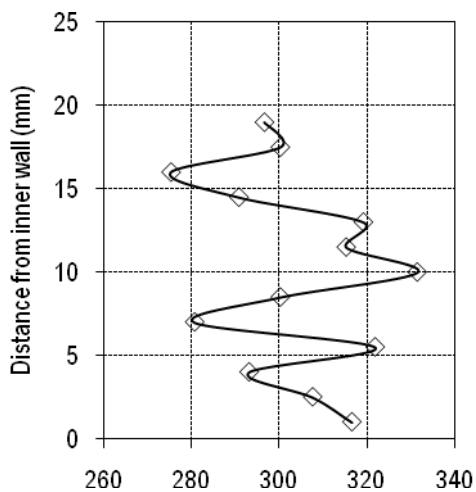
Macro-Sections

Hardness profiles (HV10)

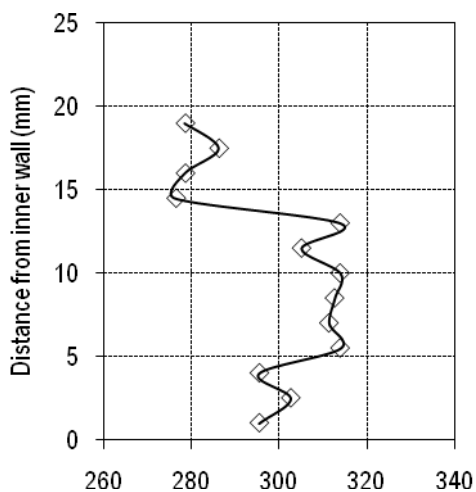
Figure A23 Weld B10: Macro sections and hardness profiles around the pipe circumference (continued over).



9.9 o'clock position



11.0 o'clock position



Macro-Sections

Hardness profiles (HV10)

Figure A24 Weld B10: Macro sections and hardness profiles around the pipe circumference.

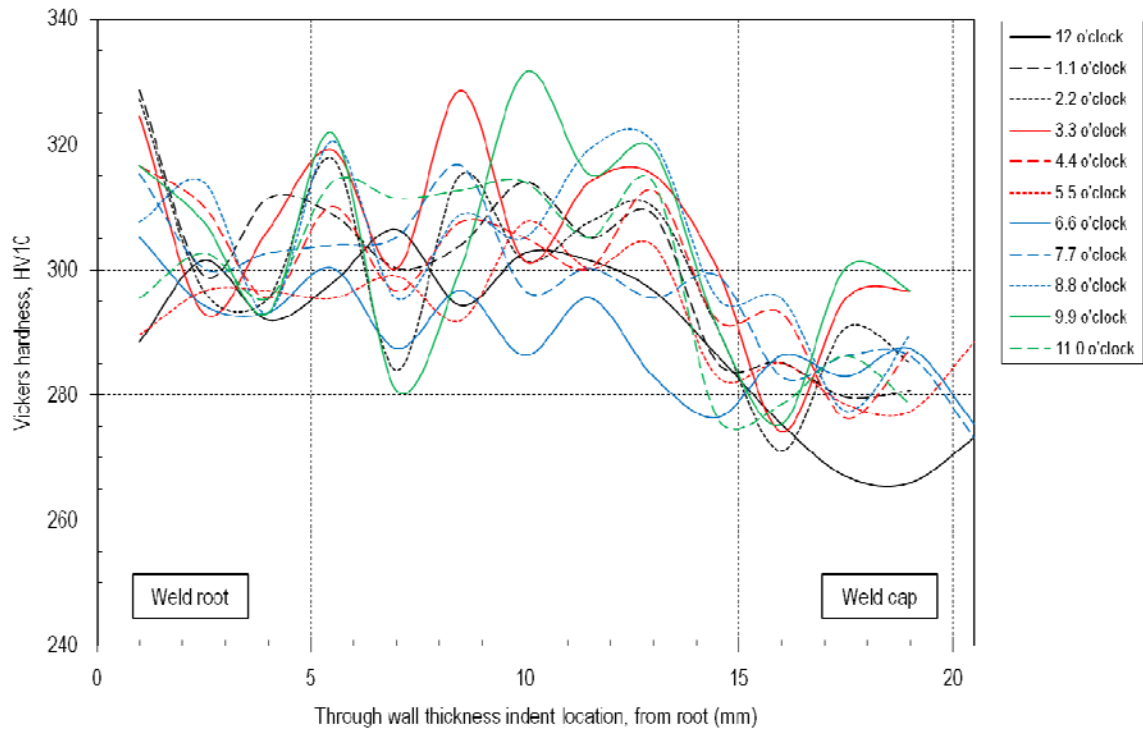


Figure A25 Weld B10: Hardness summary.

Appendix B Tensile Test Results: Stress-Strain Curves

This appendix presents the individual engineering stress-strain curves for each weld that was utilized for curved wide plate testing.

The parent material test results are from flat tensile specimens that sampled the full pipe wall thickness. Each specimen was extracted from the pipe longitudinal direction.

The all weld metal test results are from round bar specimens that sampled the weld cap and root regions (the different regions are color coded).

All tests were undertaken at ambient laboratory temperature, approximately 68°F (20°C).

The legends are formatted as follows 'material sampled'-'circumferential position'-'orientation', for example:

P1 – 12.0 - L : means the specimen was extracted from Pipe 1, at the 12 o'clock position, orientated in the pipe longitudinal direction

AWM - 8.0 – cap : means the specimen was extracted from the weld metal, at the 8 o'clock position, sampling the weld cap region.

The following table provides reference to which supplier provided which pipe and whether the abutting pipes were from the same production heat.

	Weld type	P1 (Pipe 1)	P2 (Pipe 2)	Production Heat
Weld A06	Main line	Source B	Source B	Same
Weld A17	Repair	Source C	Source C	Same
Weld A33	Main line	Source B	Source A	Different
Weld A44	Main line	Source C	Source B	Different
Weld A46	Main line	Source C	Source C	Different
Weld A50	Main line	Source B	Source B	Different
Weld B03	Main line	Source C	Source C	Different
Weld B06	Main line	Source A	Source B	Different
Weld B08	Main line	Source C	Source C	Different

Table B1 Weld and pipe source cross reference

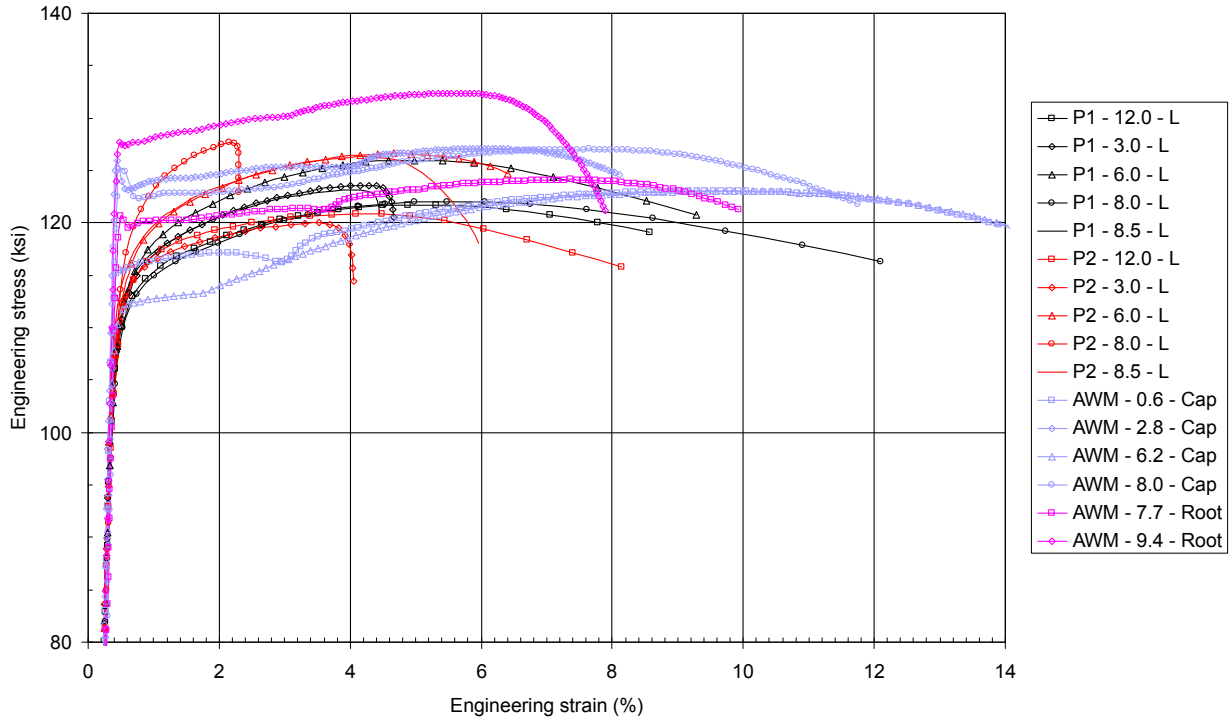


Figure B1 Weld A06: Tensile test results, all curves.

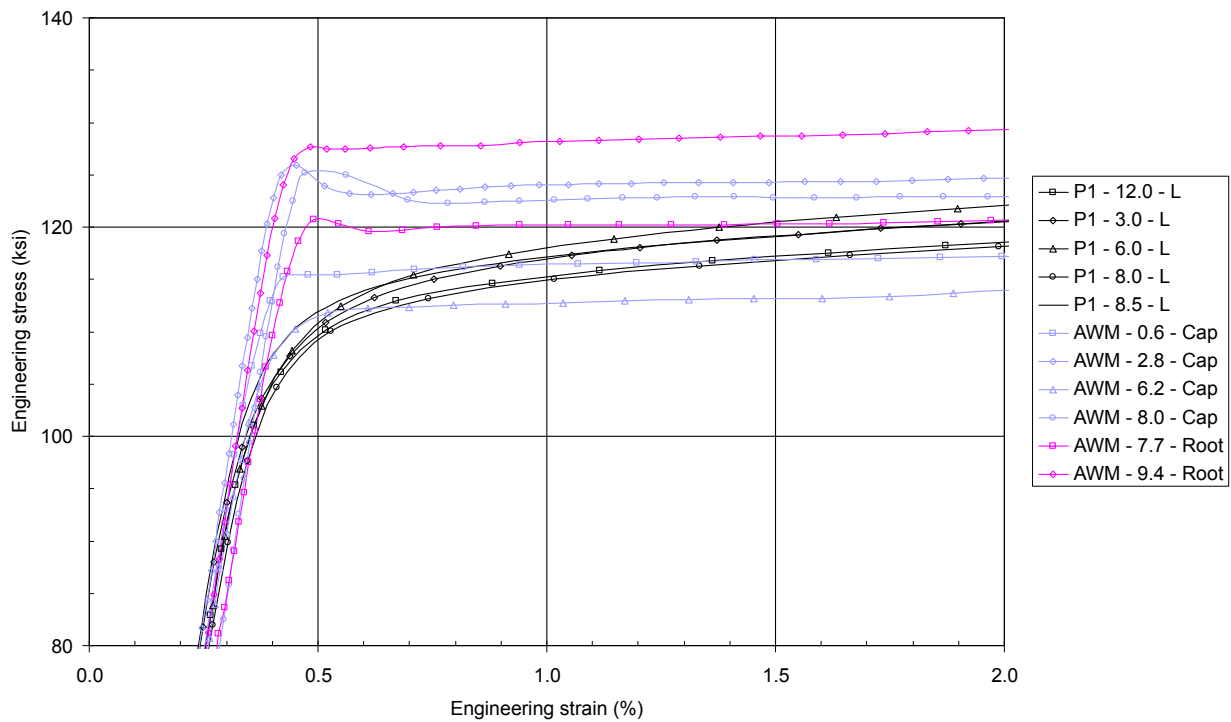


Figure B2 Weld A06: Tensile test results, yielding behaviour of Pipe 1 and all weld metal tests.

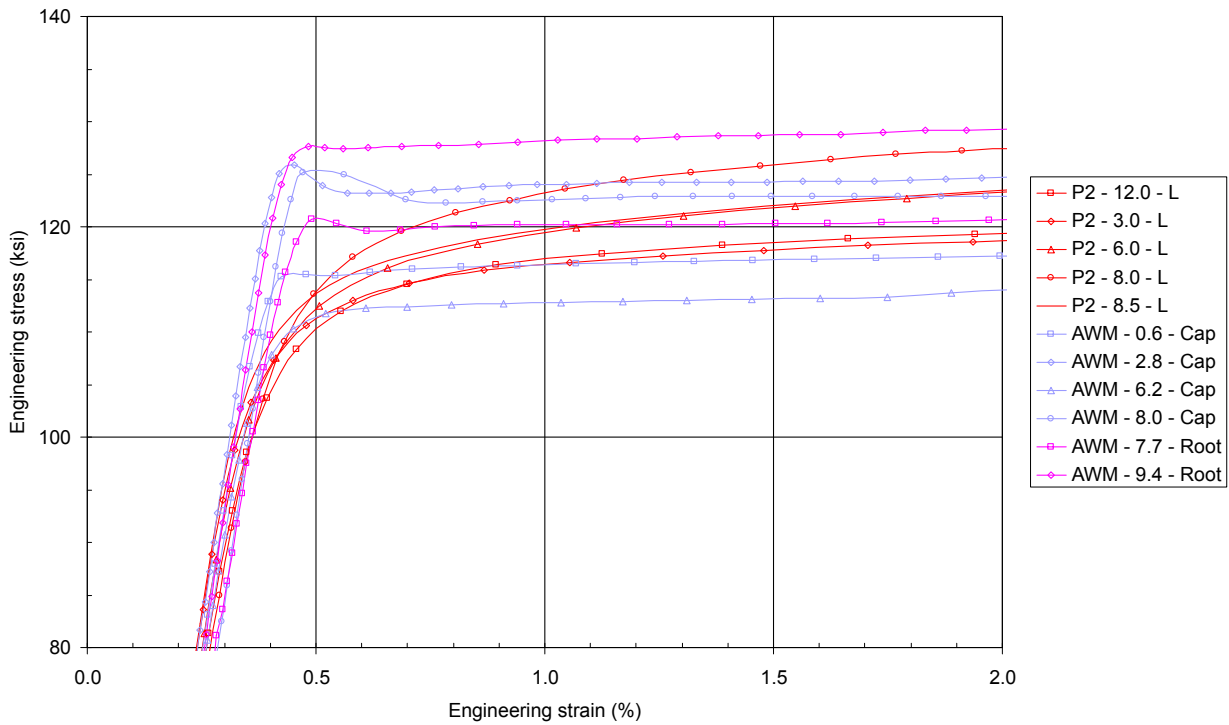


Figure B3 Weld A06: Tensile test results, yielding behaviour of Pipe 2 and all weld metal tests.

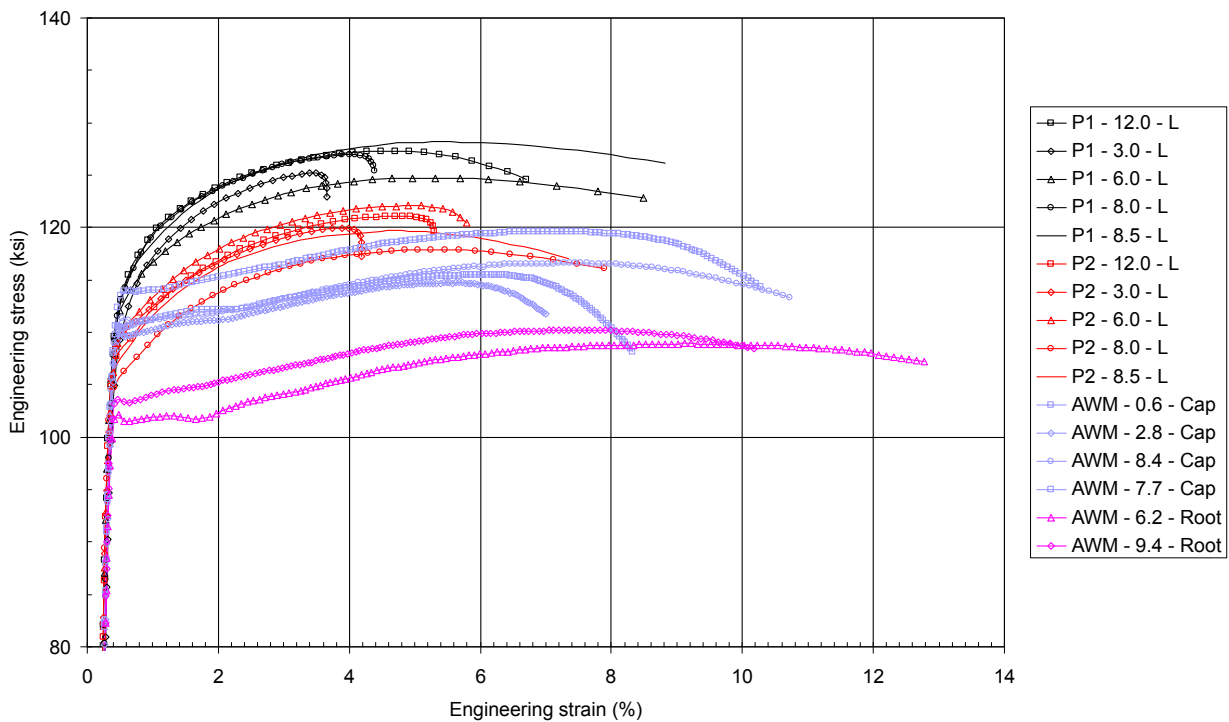


Figure B4 Weld A17: Tensile test results, all curves.

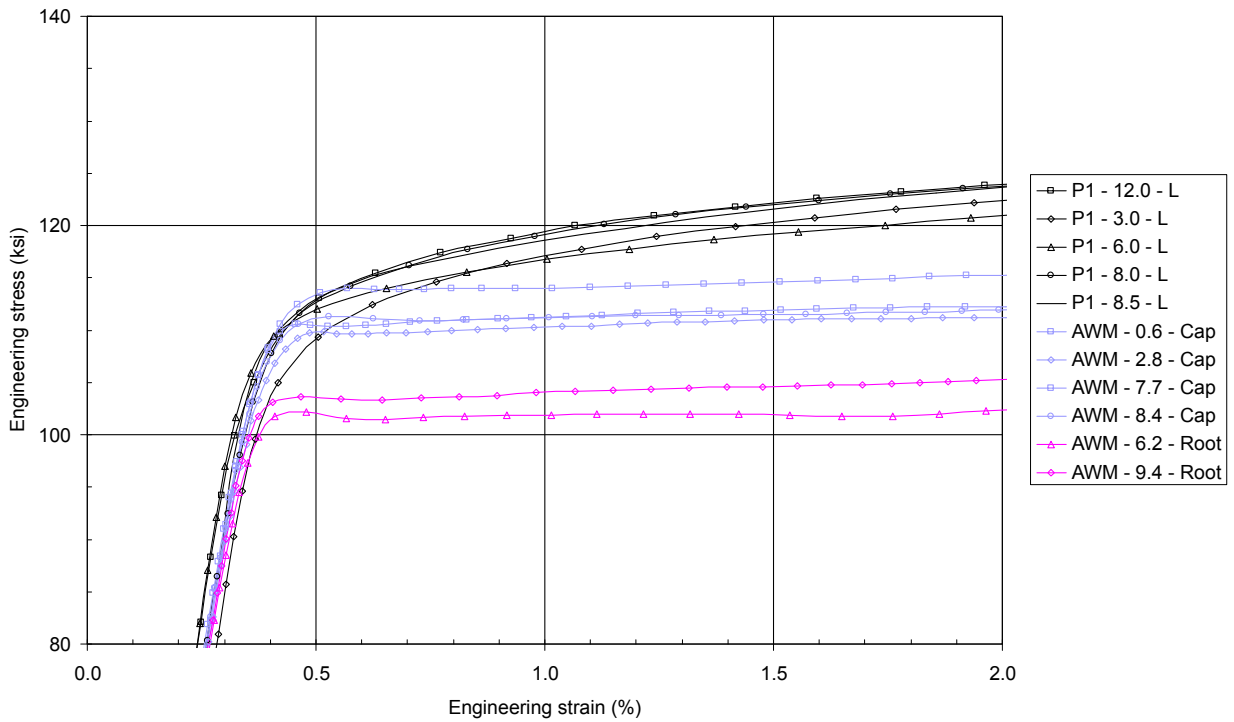


Figure B5 Weld A17: Tensile test results, yielding behaviour of **Pipe 1** and **all weld metal** tests.

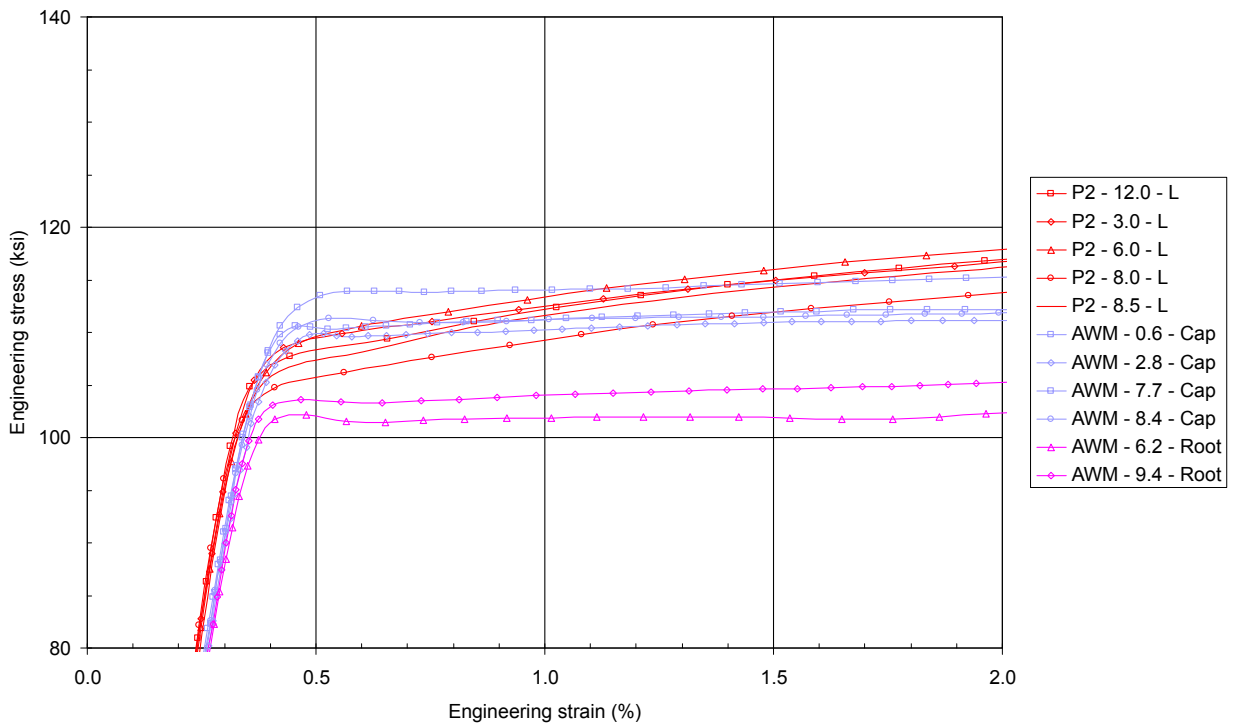


Figure B6 Weld A17: Tensile test results, yielding behaviour of **Pipe 2** and **all weld metal** tests.

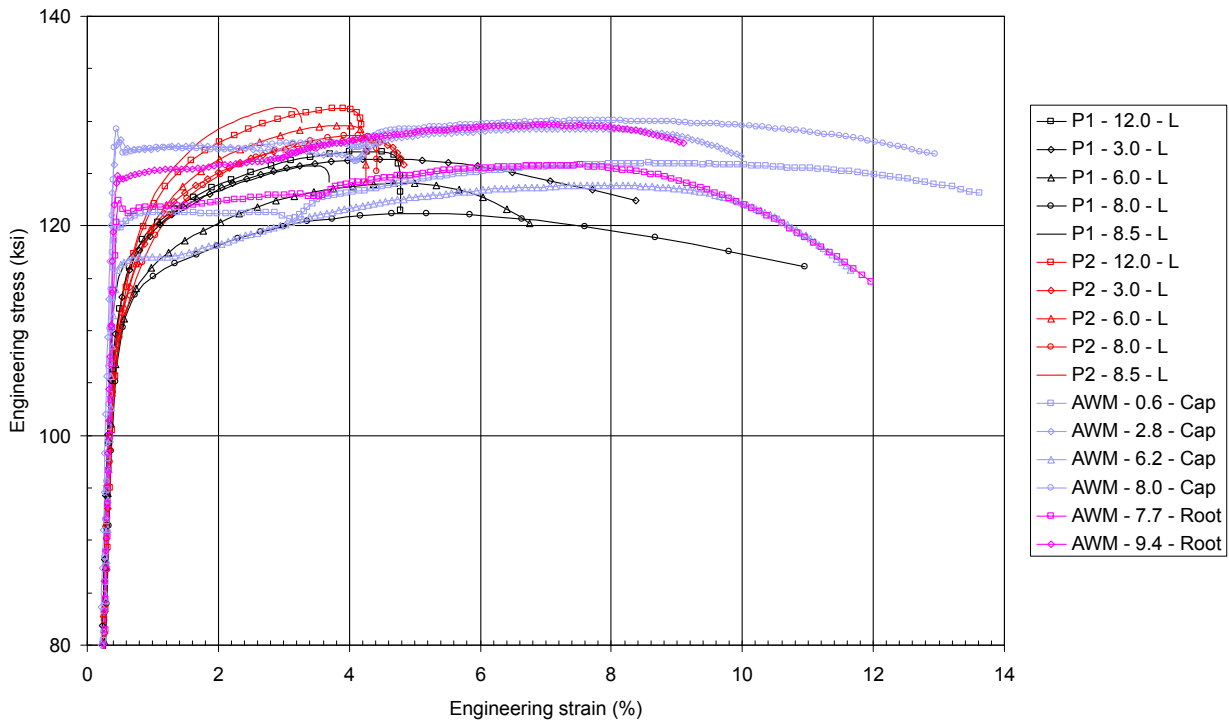


Figure B7 Weld A33: Tensile test results, all curves.

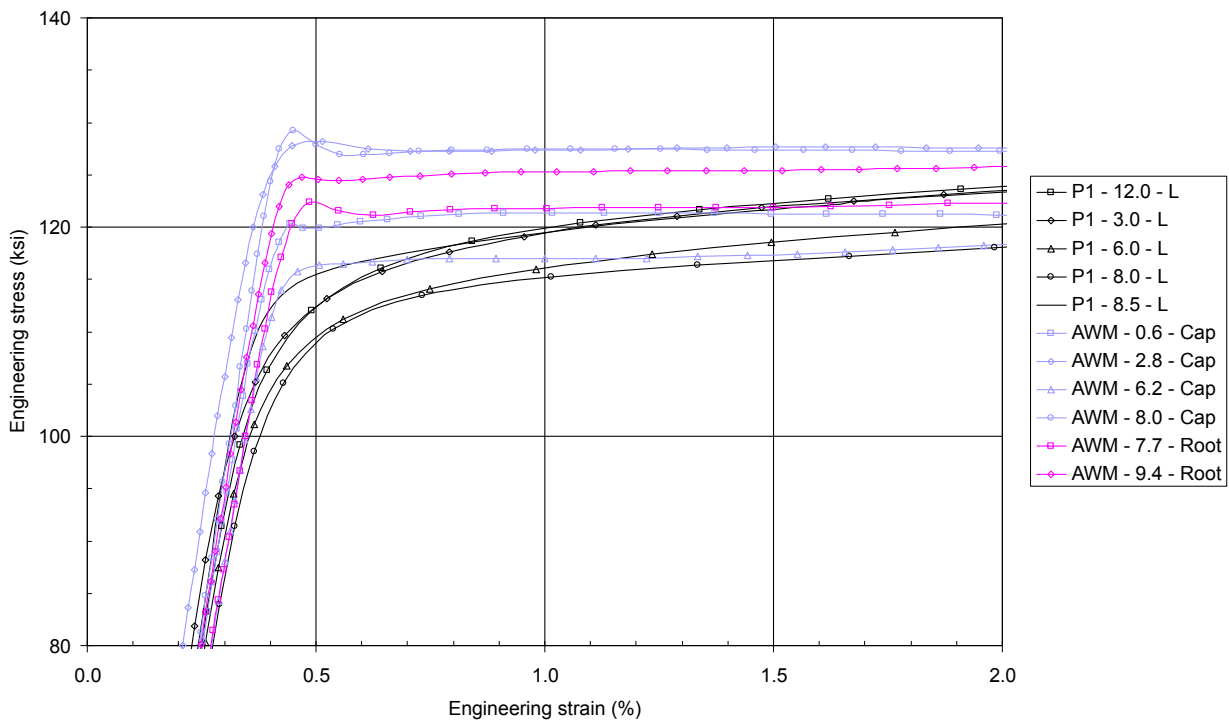


Figure B8 Weld A33: Tensile test results, yielding behaviour of Pipe 1 and all weld metal tests.

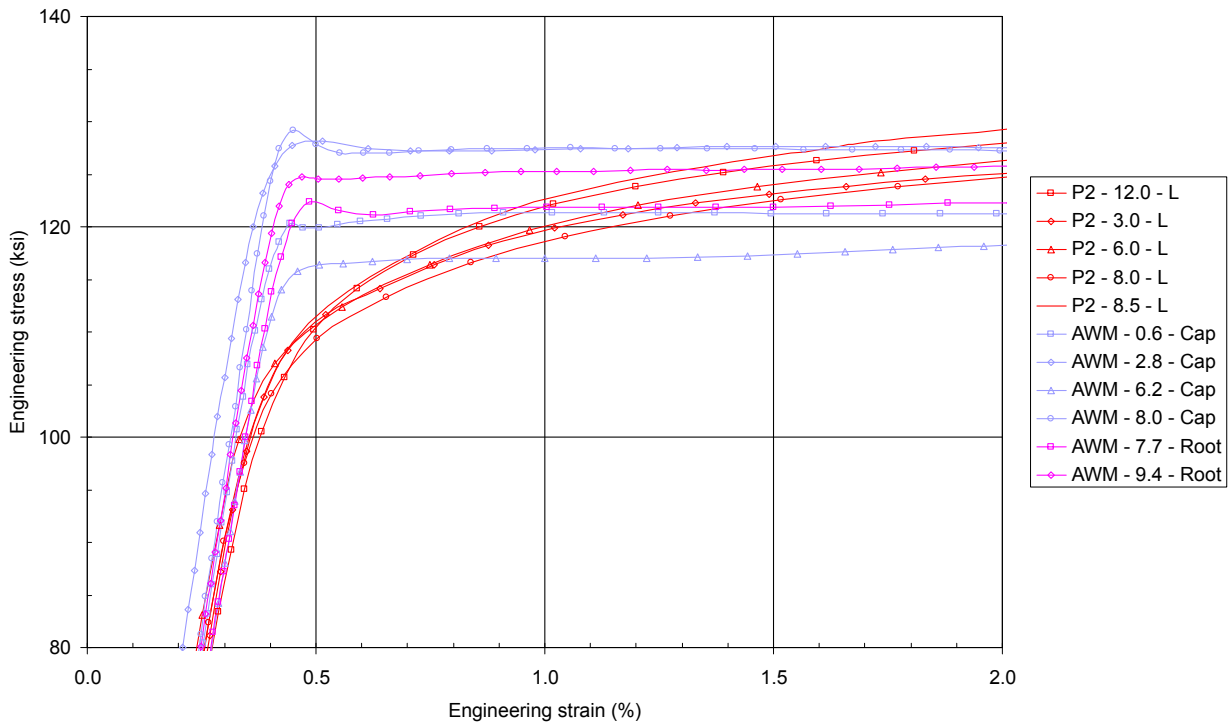


Figure B9 Weld A33: Tensile test results, yielding behaviour of Pipe 2 and all weld metal tests.

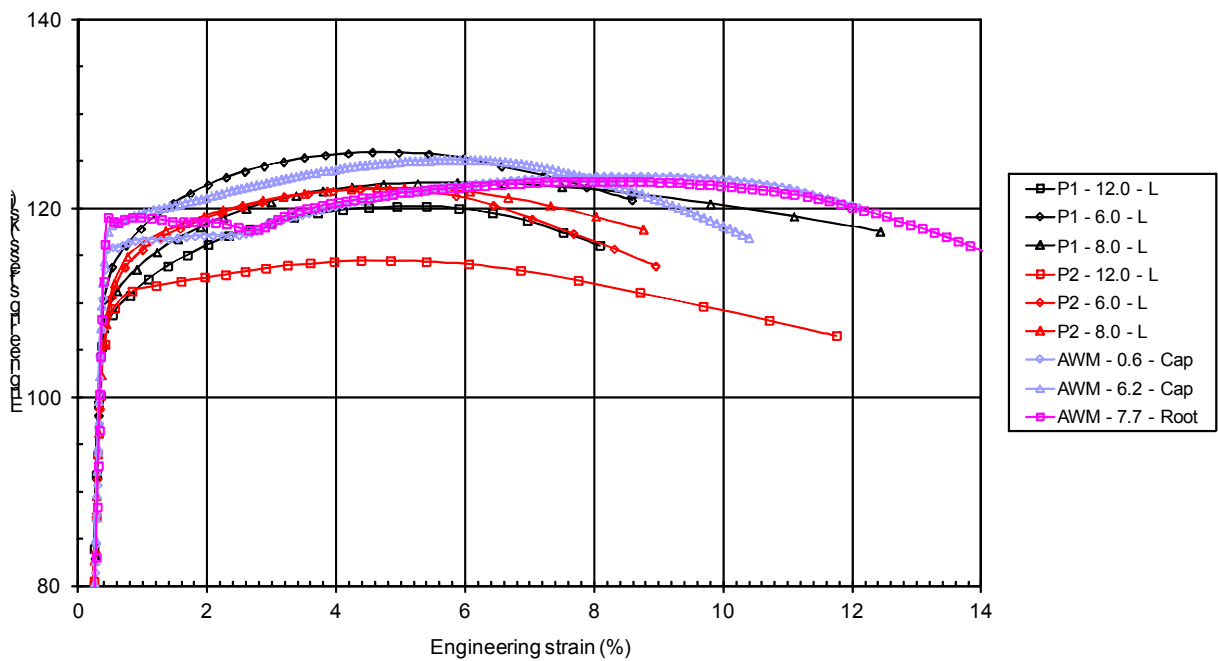


Figure B10 Weld A44: Tensile test results, all curves.

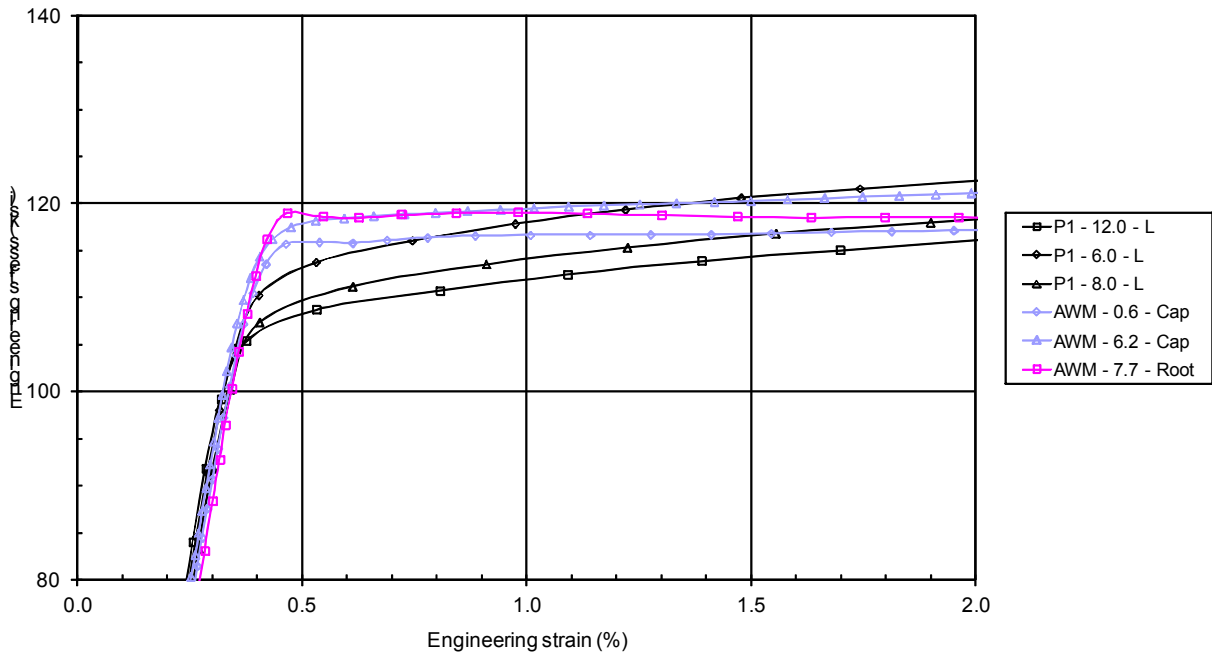


Figure B11 Weld A44: Tensile test results, yielding behaviour of **Pipe 1** and **all weld metal** tests.

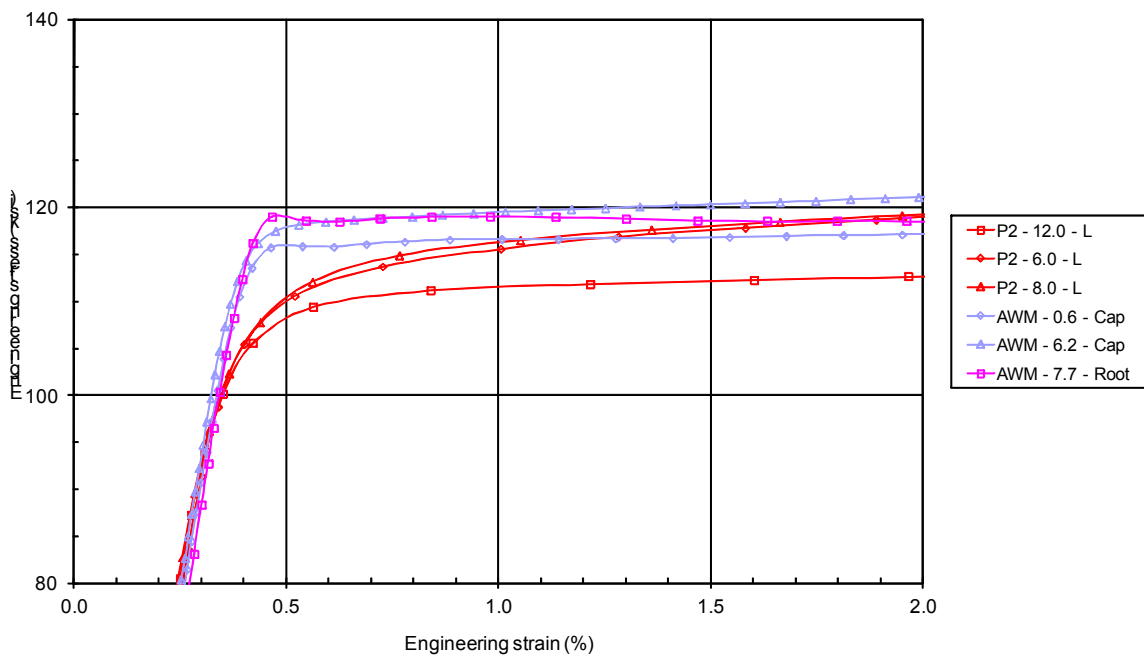


Figure B12 Weld A44: Tensile test results, yielding behaviour of **Pipe 2** and **all weld metal** tests.

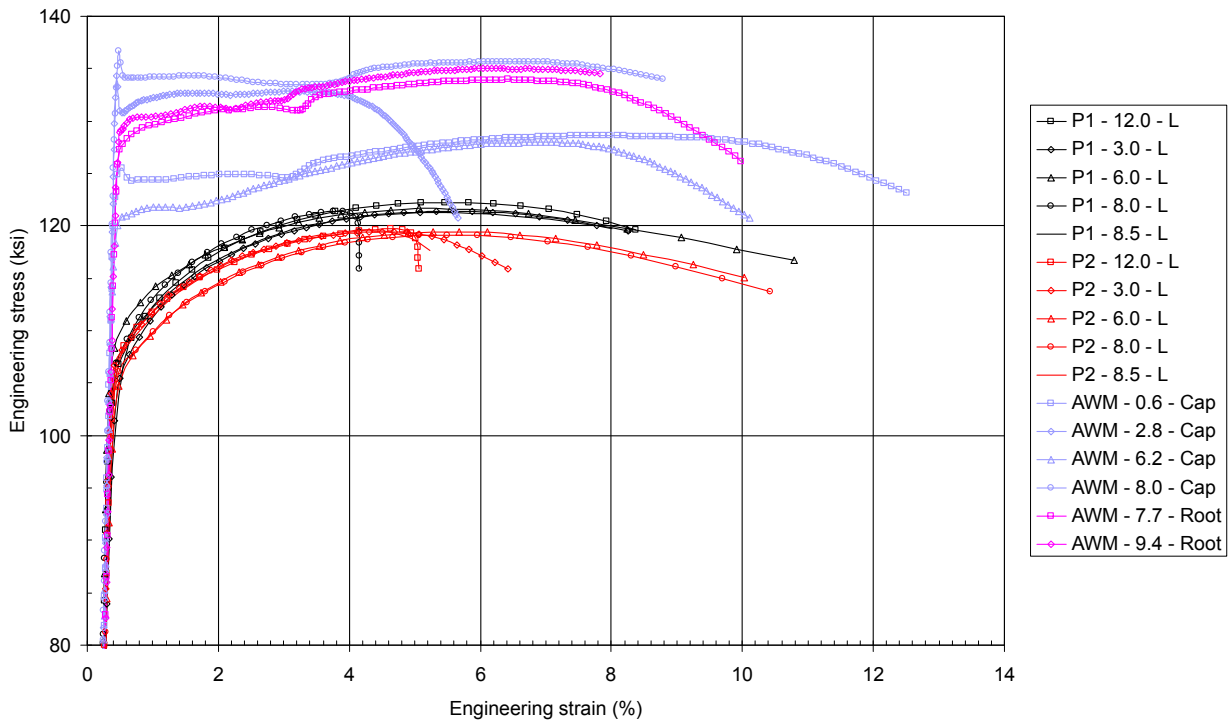


Figure B13 Weld A46: Tensile test results, all curves.

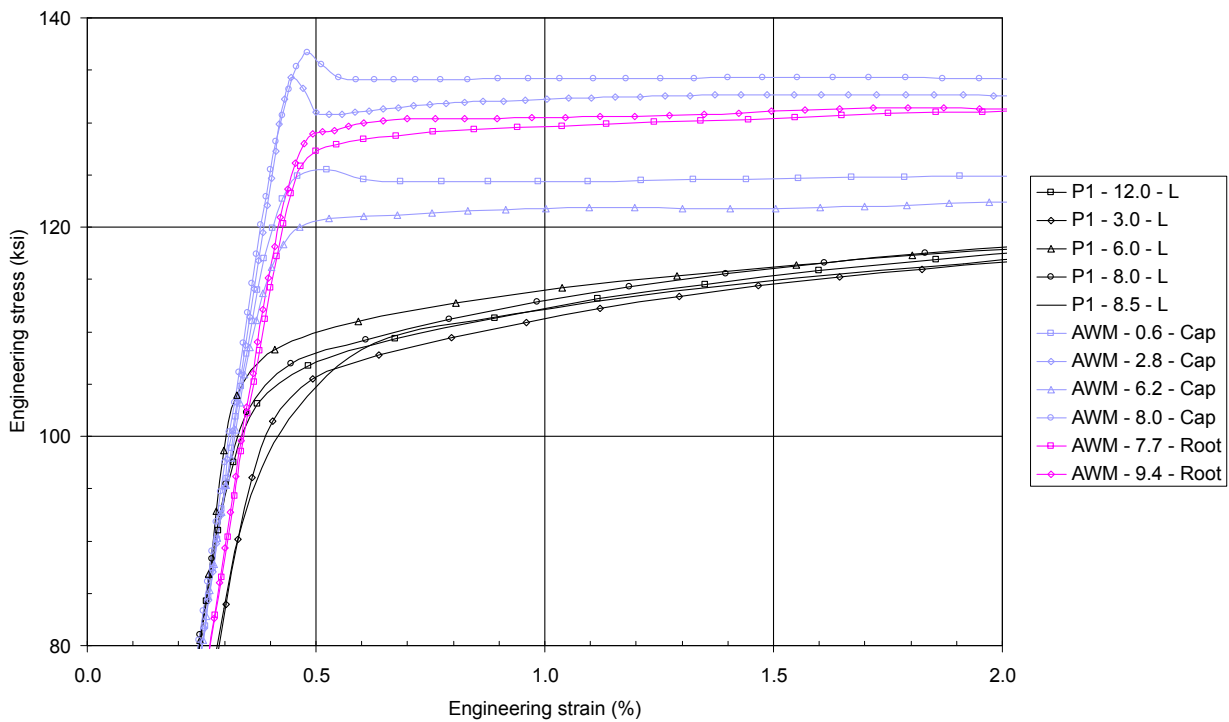


Figure B14 Weld A46: Tensile test results, yielding behaviour of Pipe 1 and all weld metal tests.

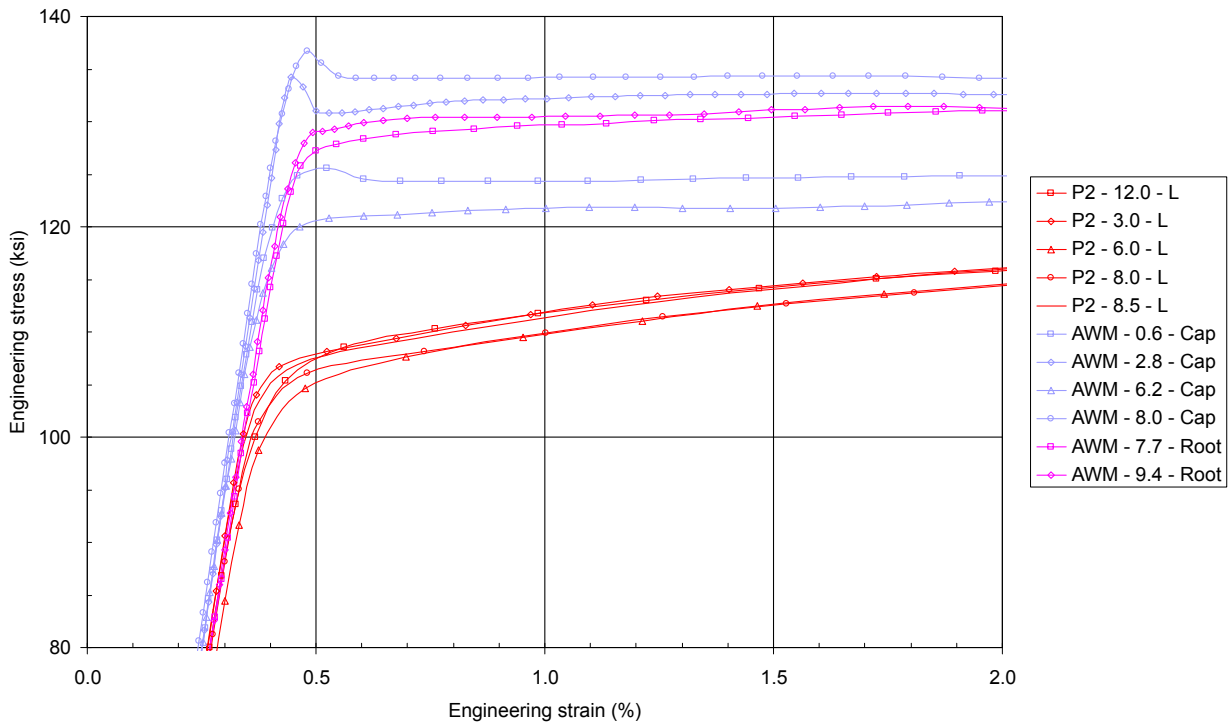


Figure B15 Weld A46: Tensile test results, yielding behaviour of Pipe 2 and all weld metal tests.

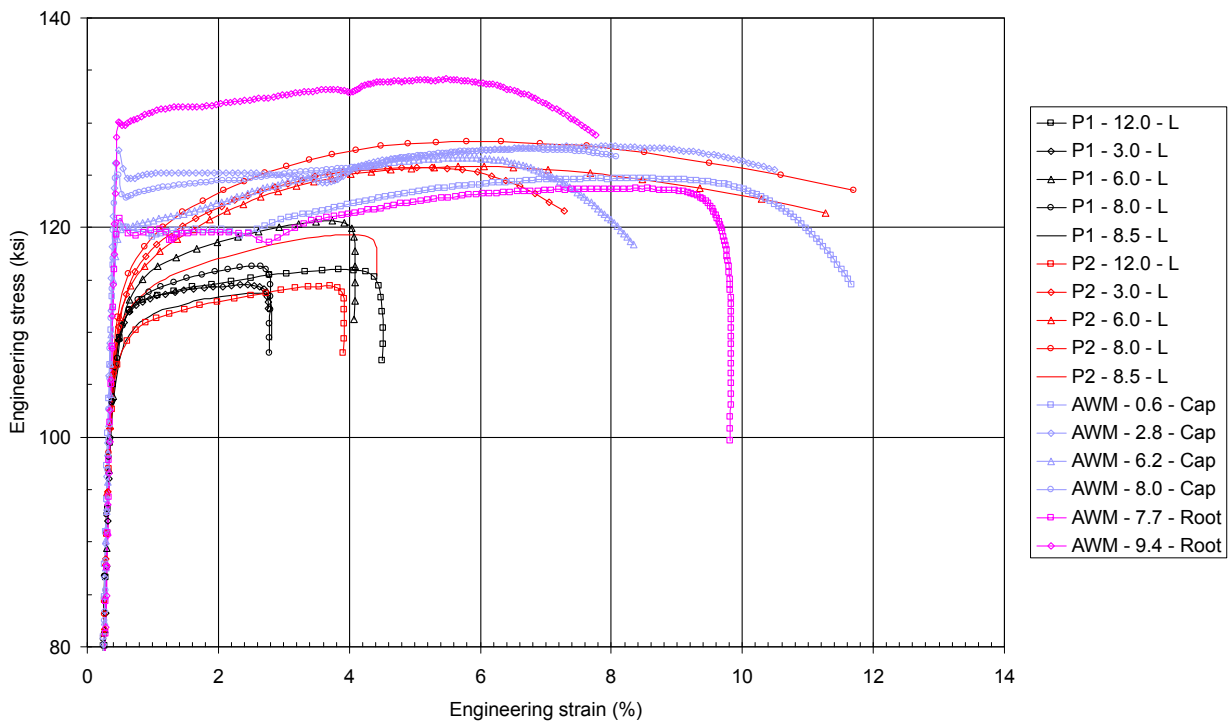


Figure B16 Weld A50: Tensile test results, all curves.

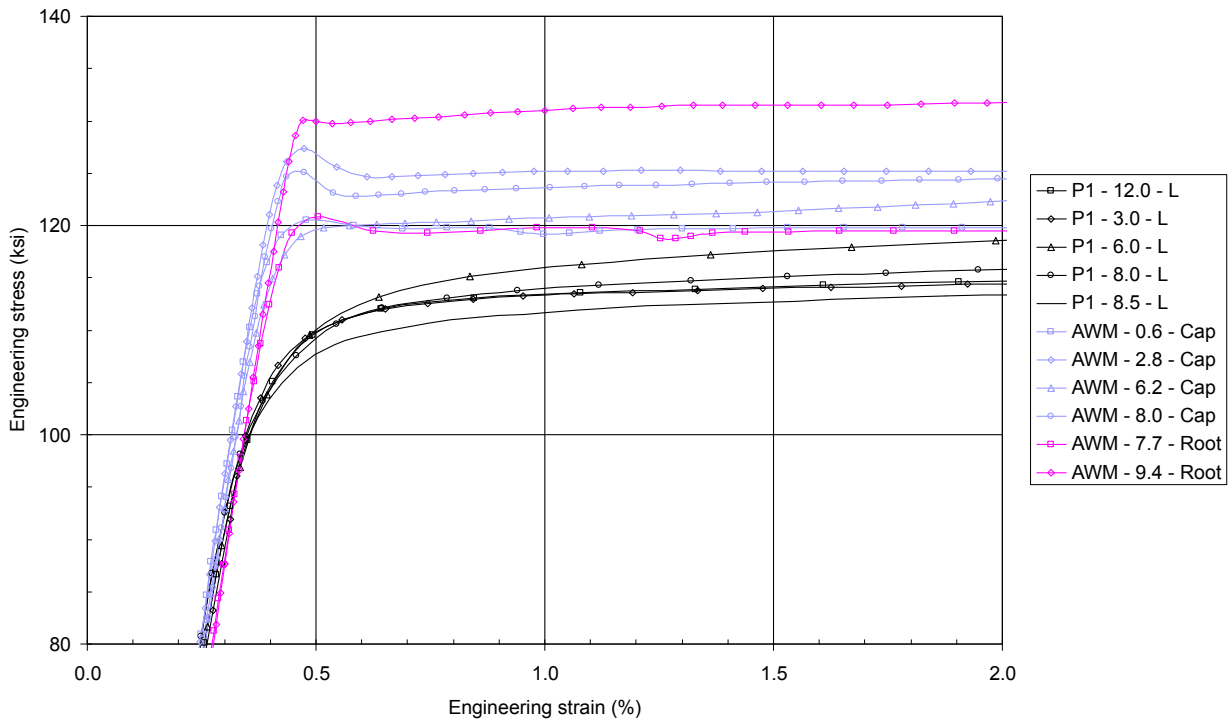


Figure B17 Weld A50: Tensile test results, yielding behaviour of **Pipe 1** and **all weld metal** tests.

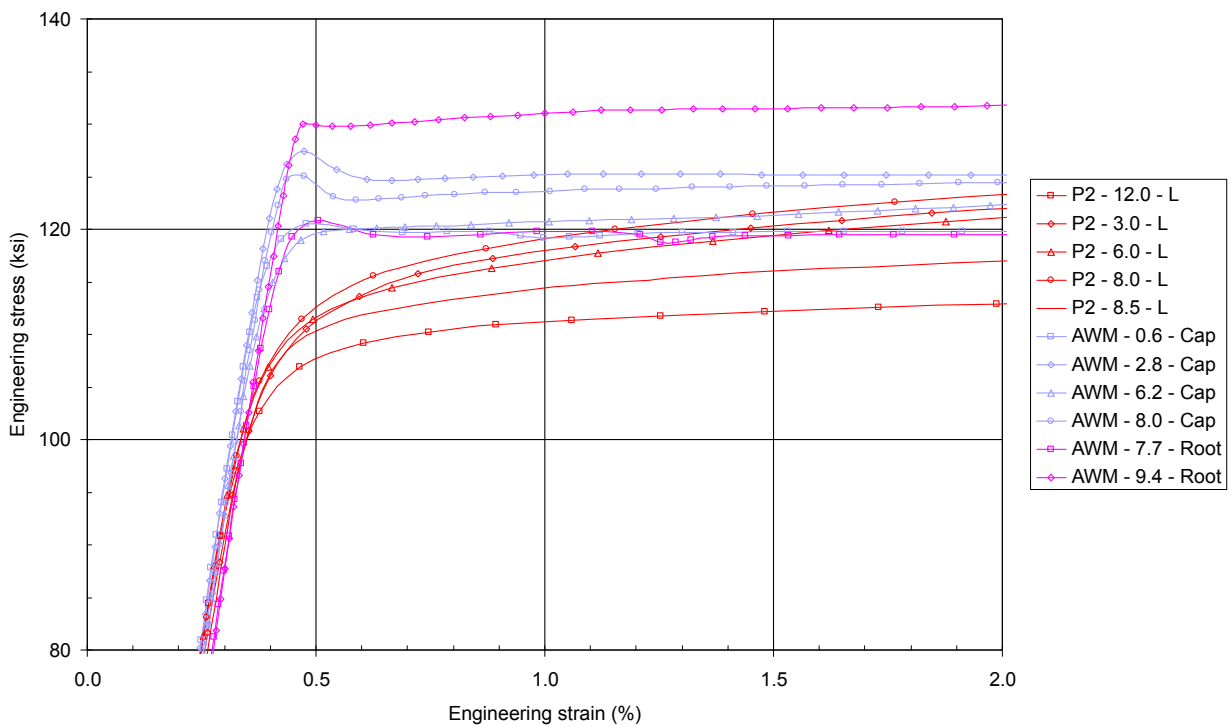


Figure B18 Weld A50: Tensile test results, yielding behaviour of **Pipe 2** and **all weld metal** tests.

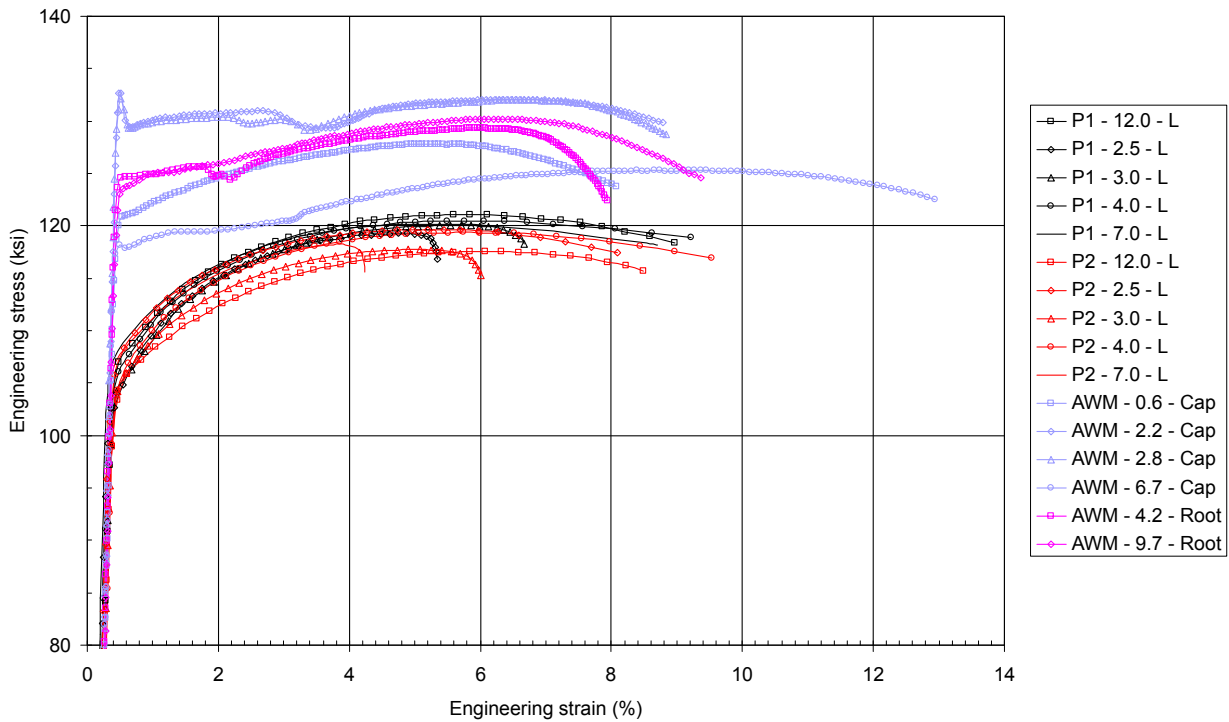


Figure B19 Weld B03: Tensile test results, all curves.

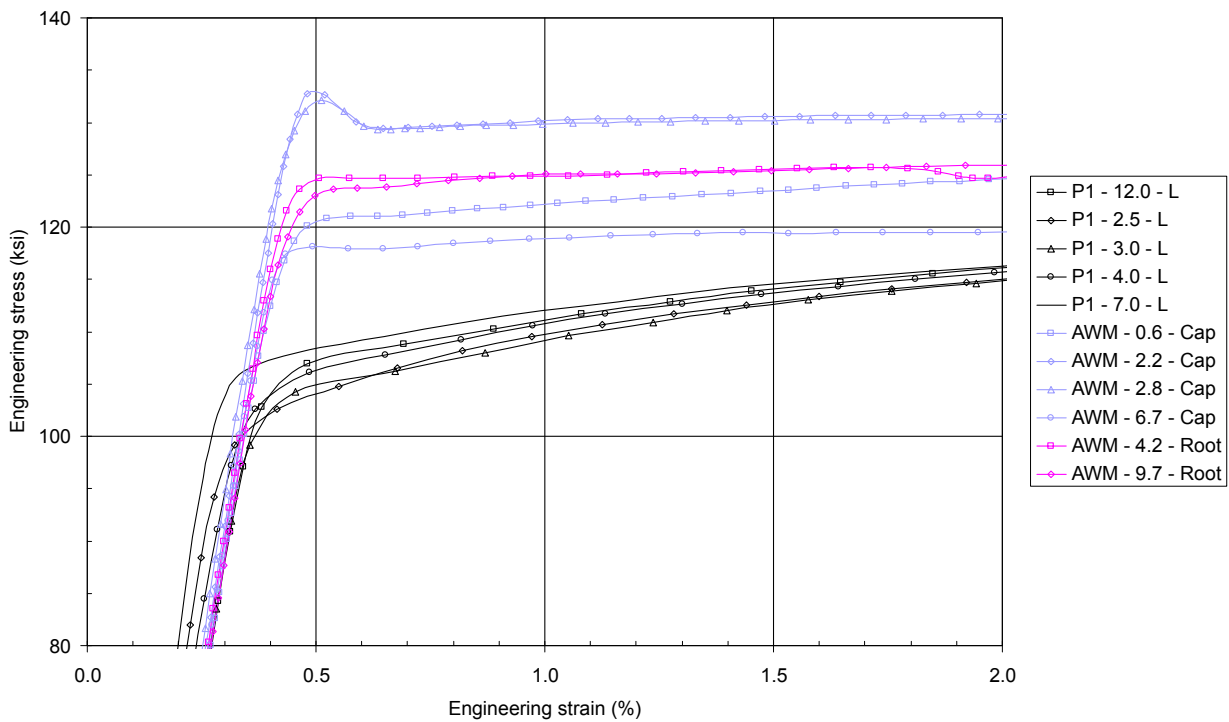


Figure B20 Weld B03: Tensile test results, yielding behaviour of Pipe 1 and all weld metal tests.

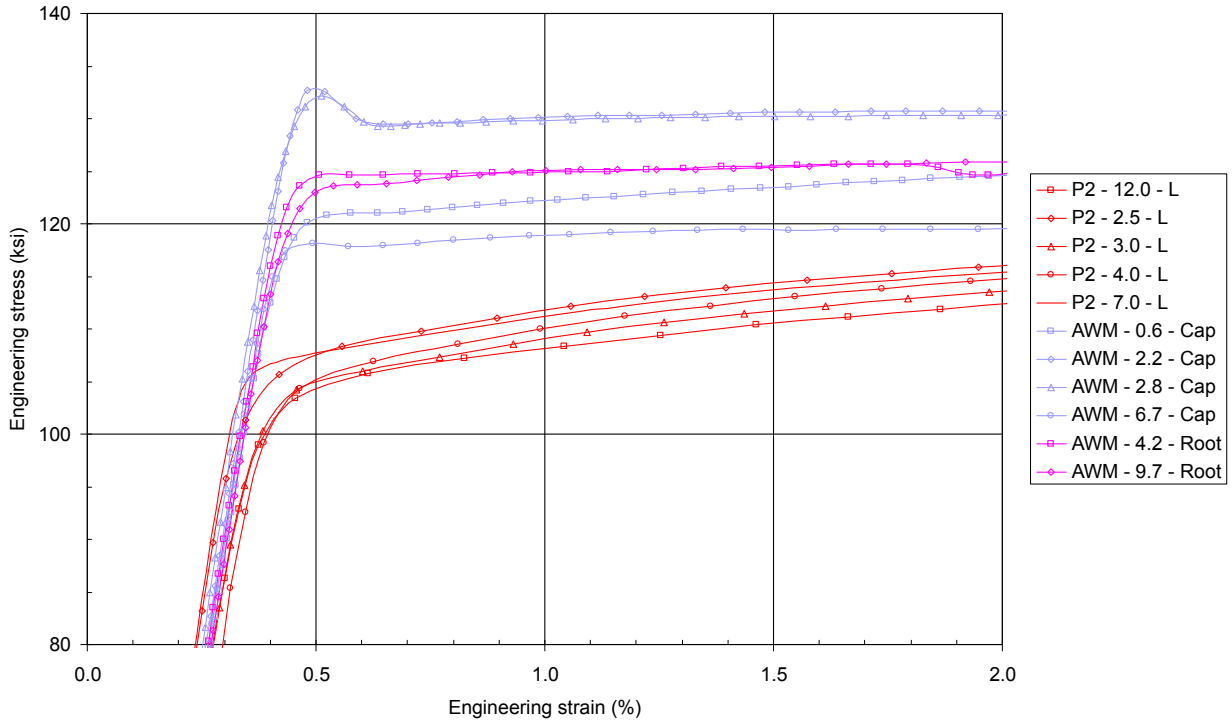


Figure B21 Weld B03: Tensile test results, yielding behaviour of Pipe 2 and all weld metal tests.

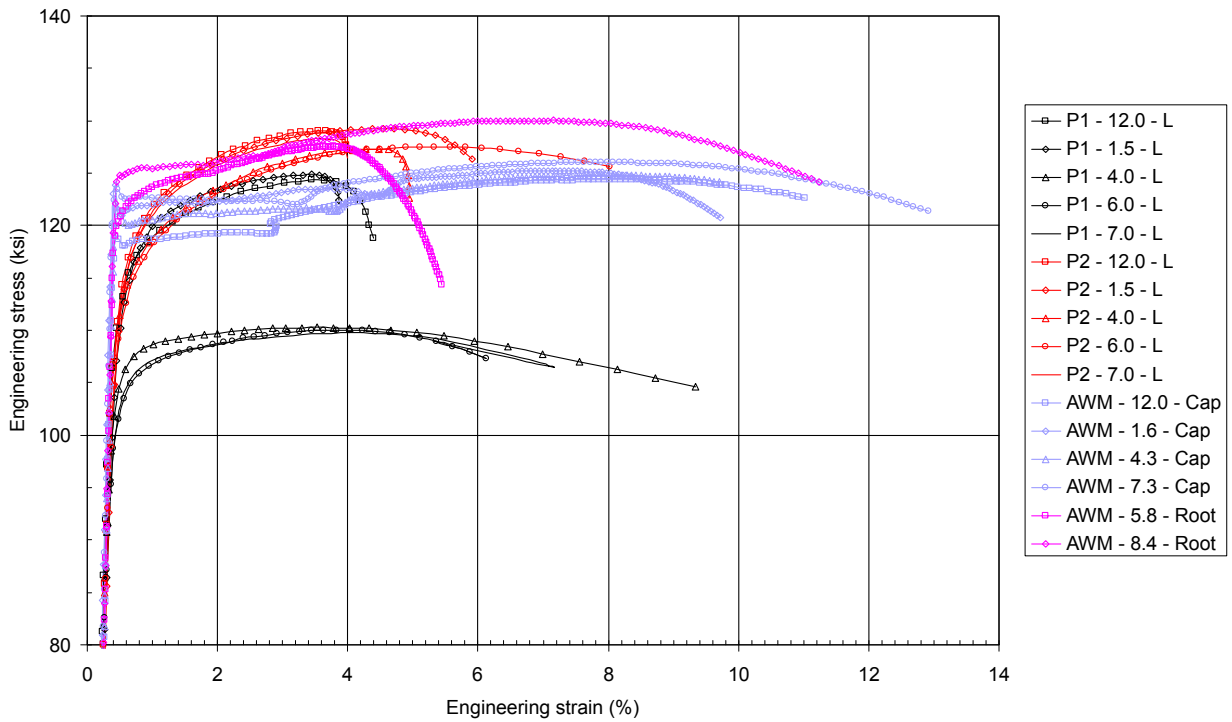


Figure B22 Weld B06: Tensile test results, all curves.

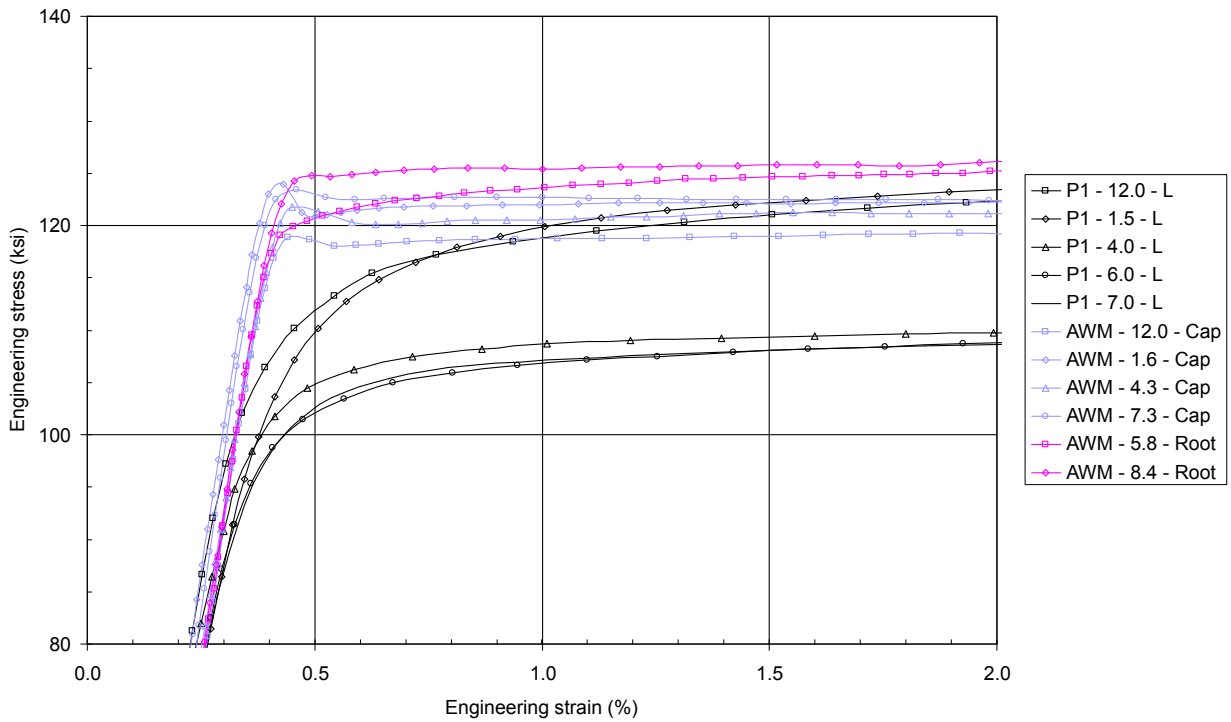


Figure B23 Weld B06: Tensile test results, yielding behaviour of **Pipe 1** and **all weld metal** tests.

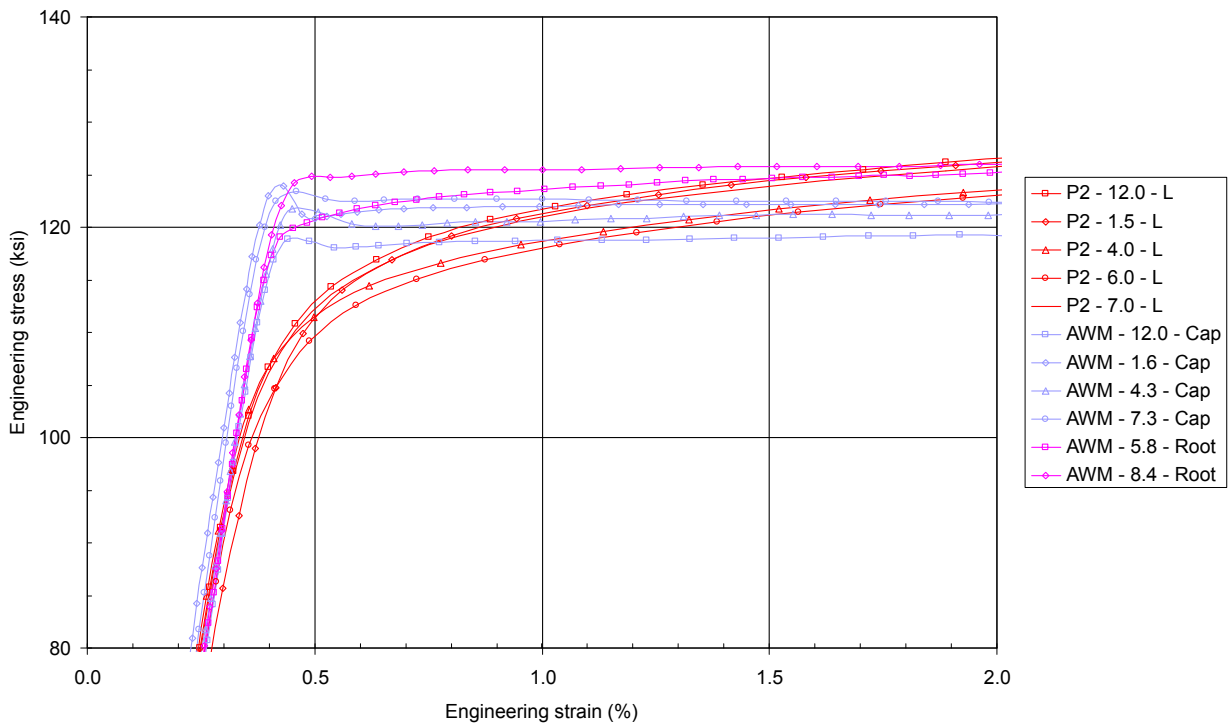


Figure B24 Weld B06: Tensile test results, yielding behaviour of **Pipe 2** and **all weld metal** tests.

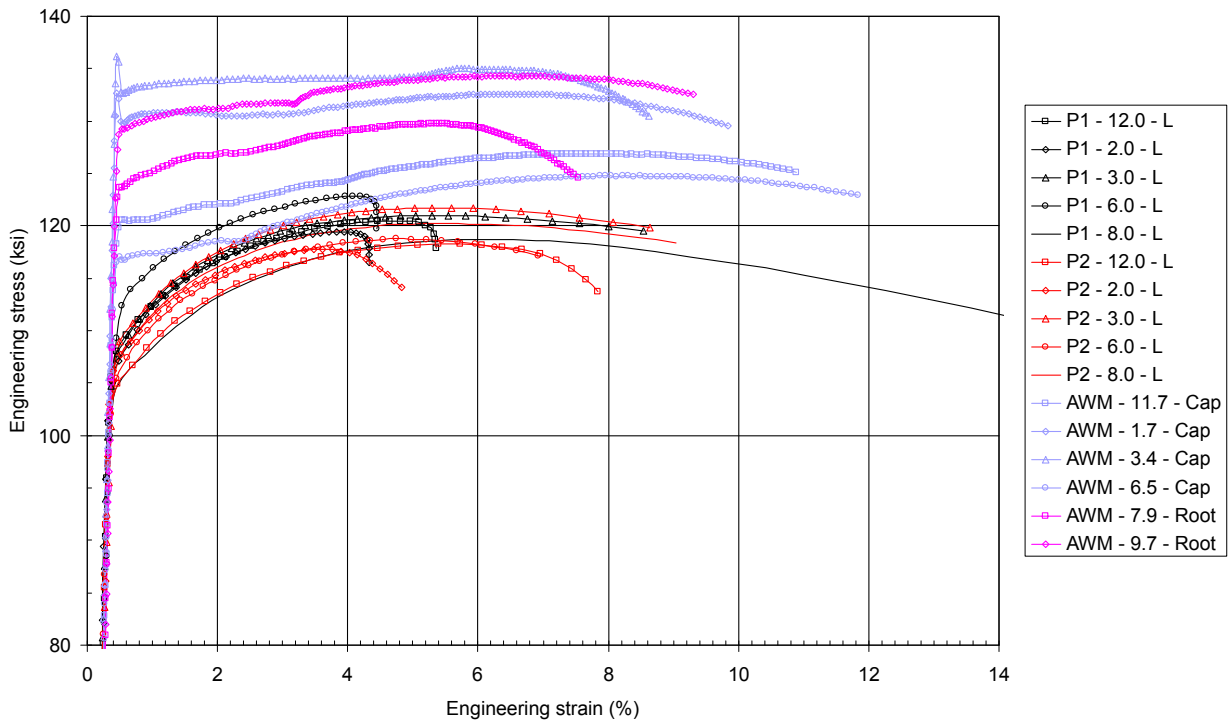


Figure B25 Weld B08: Tensile test results, all curves.

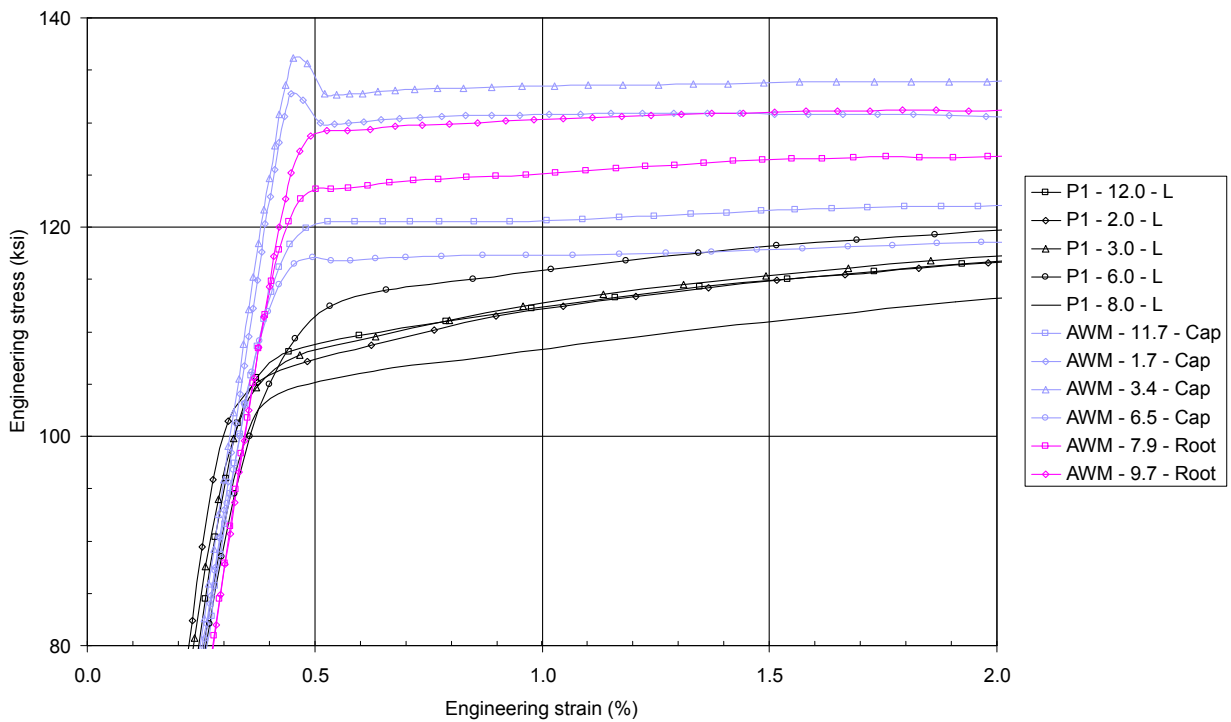


Figure B26 Weld B08: Tensile test results, yielding behaviour of Pipe 1 and all weld metal tests.

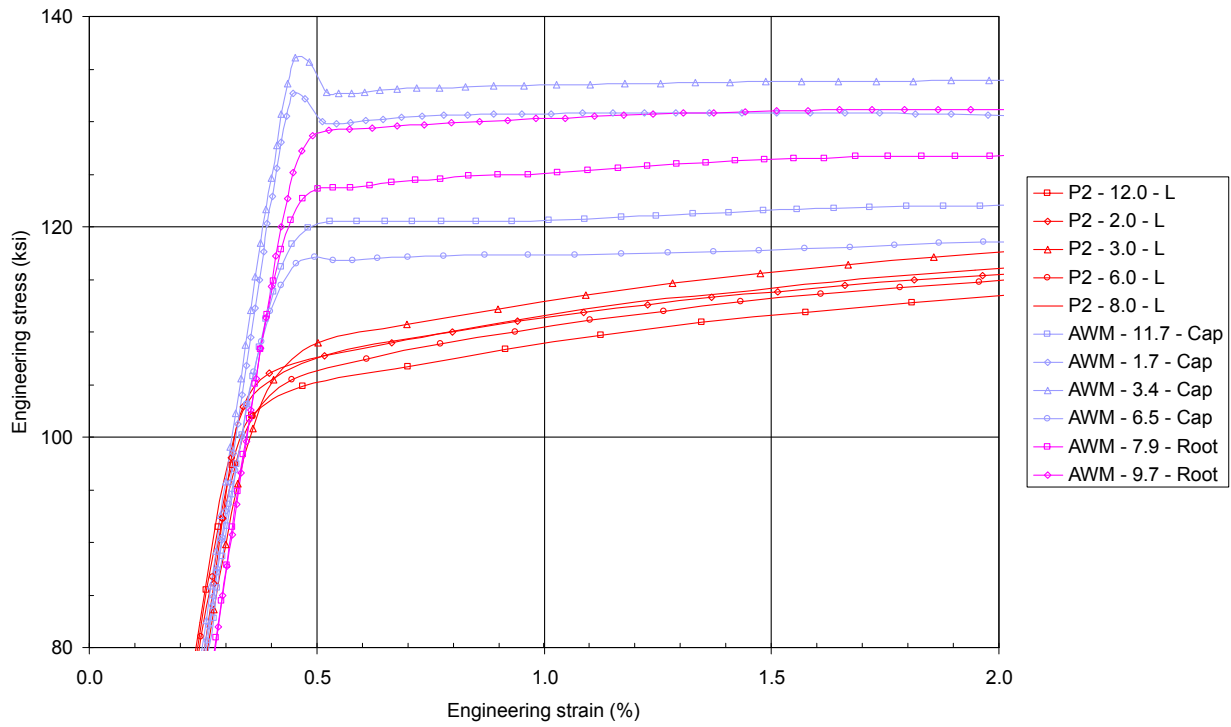


Figure B27 Weld B08: Tensile test results, yielding behaviour of Pipe 2 and all weld metal tests.

Appendix C Calculation of Fracture Toughness: CTOD, J and K

C.1 Calculation of CTOD

$$CTOD = \left[\frac{FS}{BW^{1.5}} f\left(\frac{a_o}{W}\right) \right]^2 \frac{(1-\nu^2)}{2\sigma_{ys}E} + \frac{0.4(W-a_o)V_p}{0.4W+0.6a_o+z} \quad [C1]$$

- Where:
- F = Applied force (units: N)
 - S = Span between the outer loading points (units: mm)
 - B = Specimen thickness (units: mm)
 - W = Specimen width (units: mm)
 - a_o = Average 'original' crack length (units: mm)
 - $f(a_o/W)$ = Geometry function
 - ν = Poisson's ratio
 - σ_{ys} = 0.2% proof stress at the fracture test temperature (units: N/mm²)
 - E = Young's modulus of elasticity at the fracture test temperature (units: N/mm²)
 - V_p = Plastic component of the notch opening displacement (units: mm)
 - z = Knife edge height from the specimen surface (units: mm)

For specimens loaded in three-point-bending S is equal to $4W$.

The geometry function, $f(a_o/W)$ is given by:

$$f\left(\frac{a_o}{W}\right) = \frac{3\left(\frac{a_o}{W}\right)^{0.5} \left[1.99 - \left(\frac{a_o}{W}\right) \left(1 - \frac{a_o}{W}\right) \left(2.15 - \frac{3.93a_o}{W} + \frac{2.7a_o^2}{W^2} \right) \right]}{2\left(1 + \frac{2a_o}{W}\right) \left(1 - \frac{a_o}{W}\right)^{1.5}} \quad [C2]$$

C.2 Calculation of J

$$J = \left[\frac{FS}{BW^{1.5}} f\left(\frac{a_o}{W}\right) \right]^2 \frac{(1-\nu^2)}{E} + \frac{2U_p}{B(W-a_o)} \quad [C3]$$

Where: U_p = Plastic component of area beneath the force versus clip opening plot (units: Nmm)

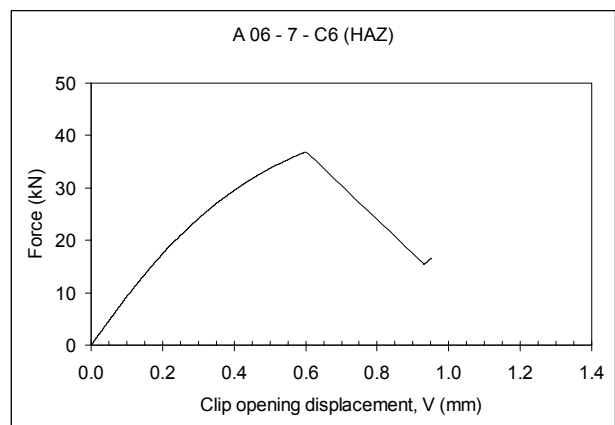
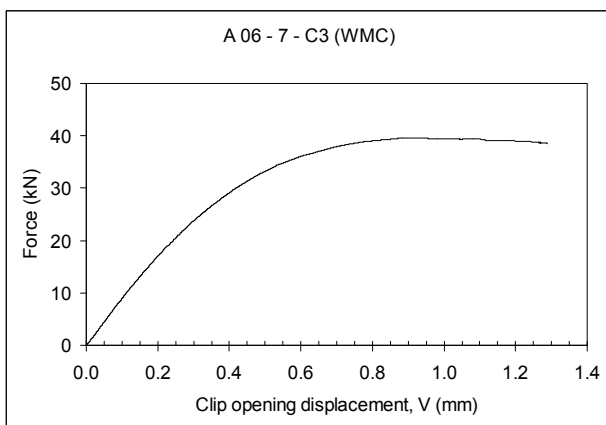
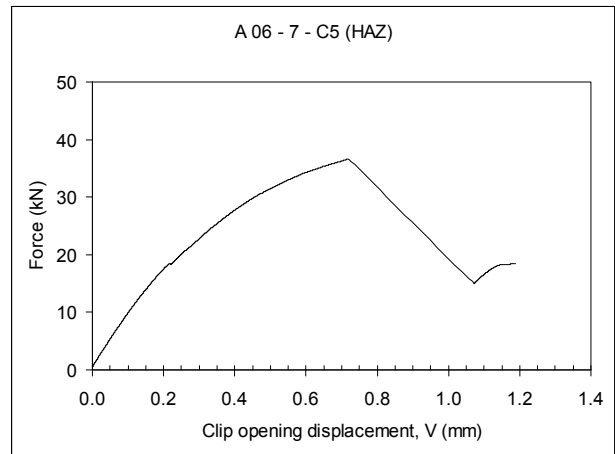
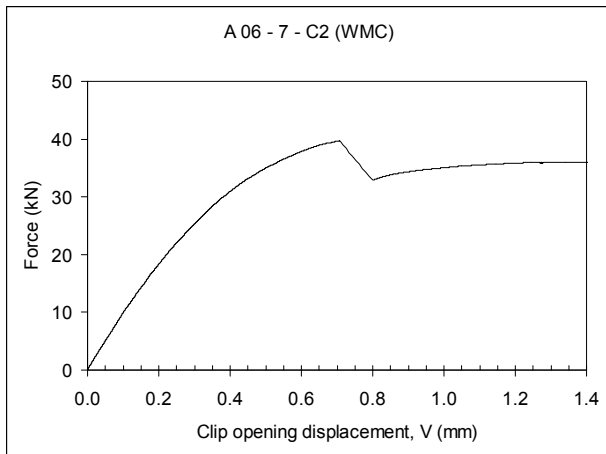
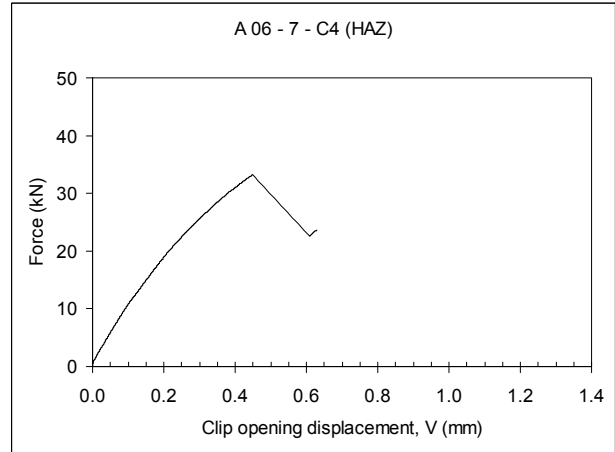
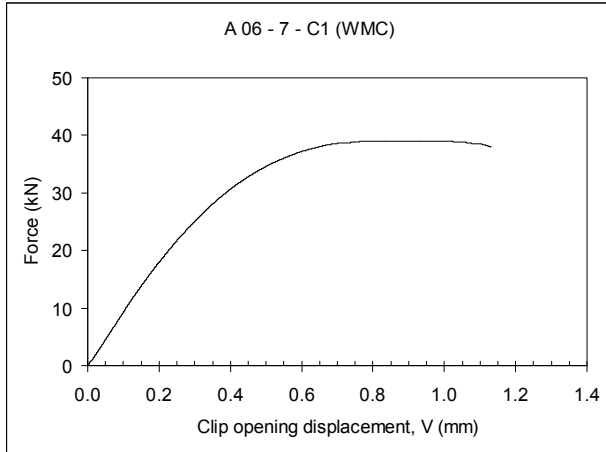
The function $f(a_o/W)$ is given by equation [C2].

C.3 Calculation of K

$$K = \frac{FS}{BW^{1.5}} f\left(\frac{a_o}{W}\right) \quad [C4]$$

The function $f(a_o/W)$ is given by equation [C2].

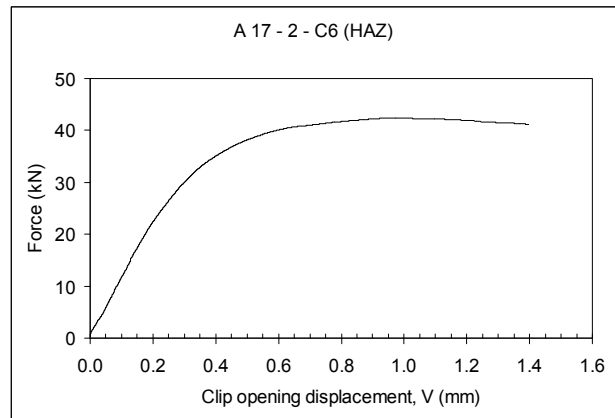
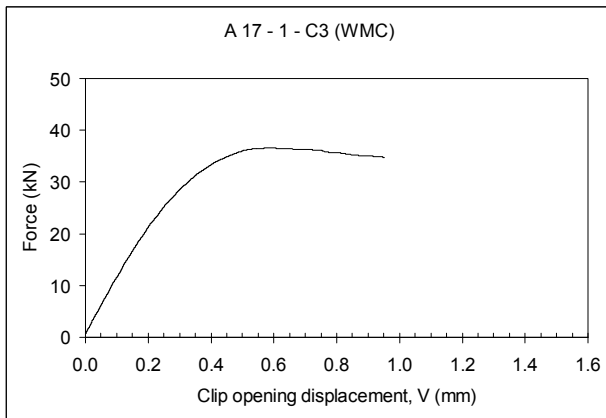
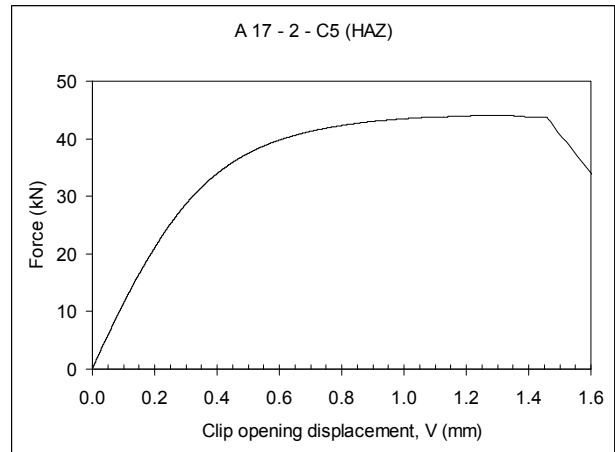
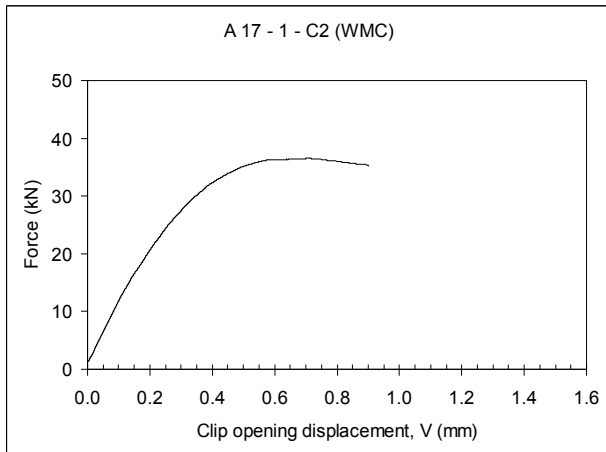
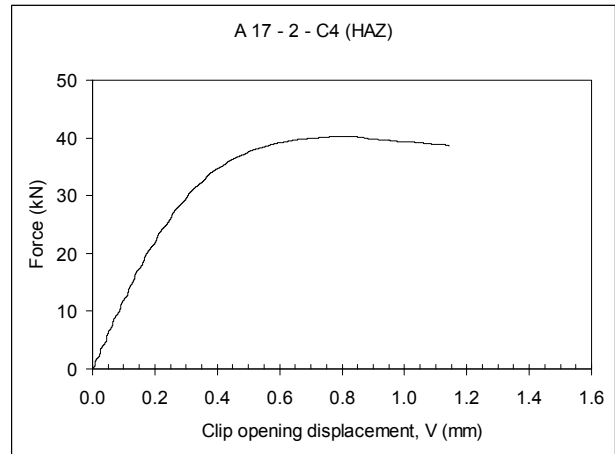
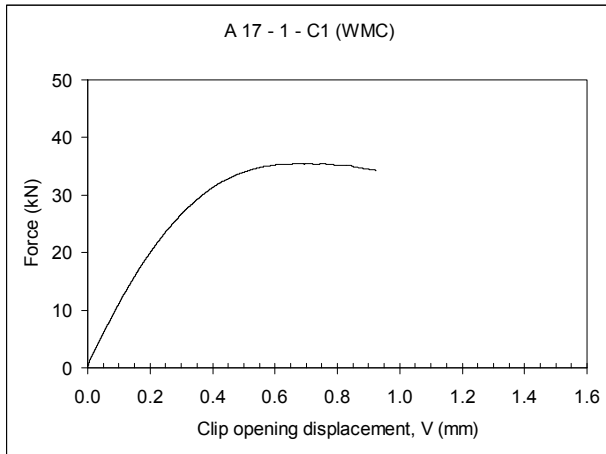
Appendix D Fracture Mechanics Test Results: Force versus Clip Opening



Notch location:
Weld metal centerline

Notch location:
Fusion line 50/50
Side - pipe 'Source B'

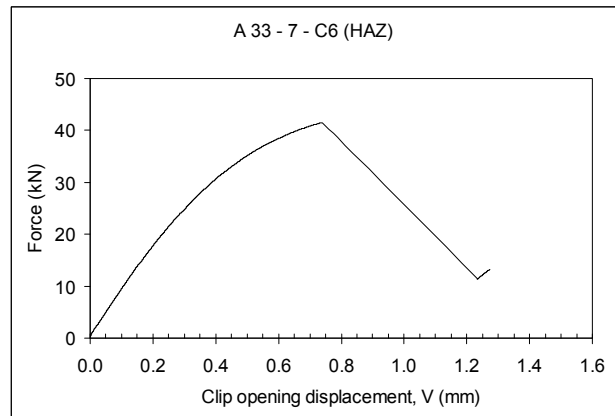
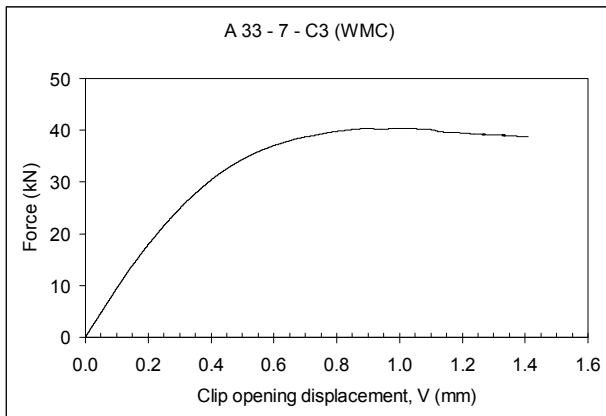
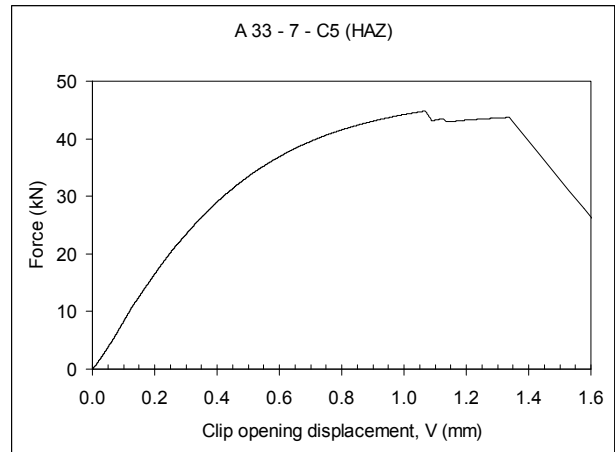
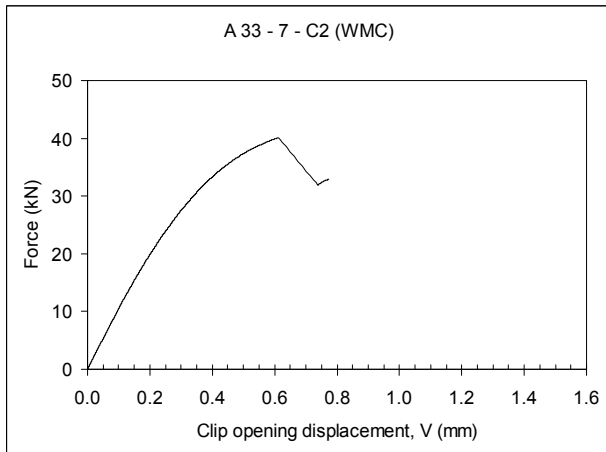
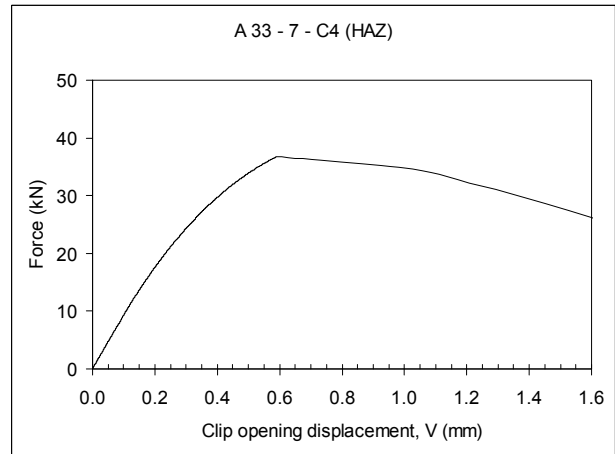
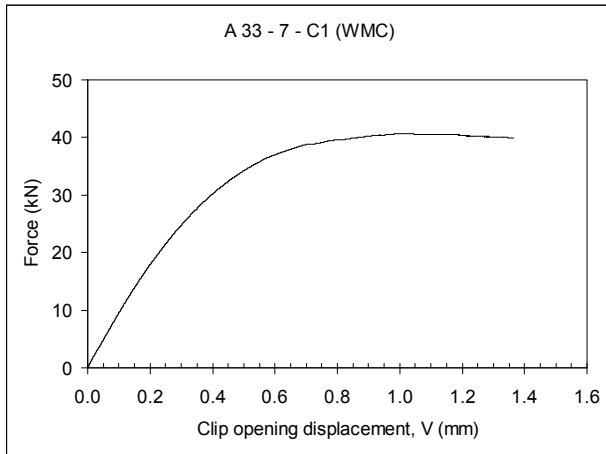
Figure D1 Weld A06: Force versus clip opening displacement plots



Notch location:
Weld metal centerline

Notch location:
Fusion line 50/50
Side - pipe 'Source C'

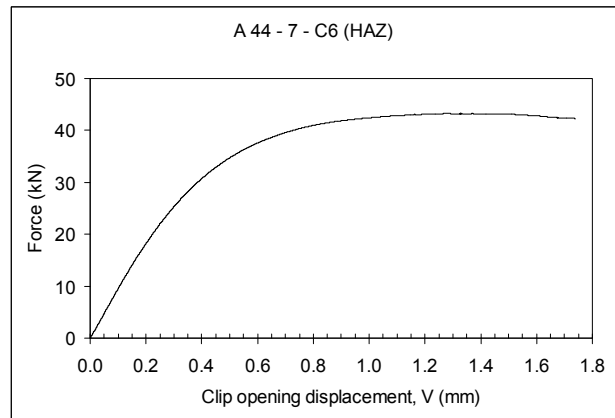
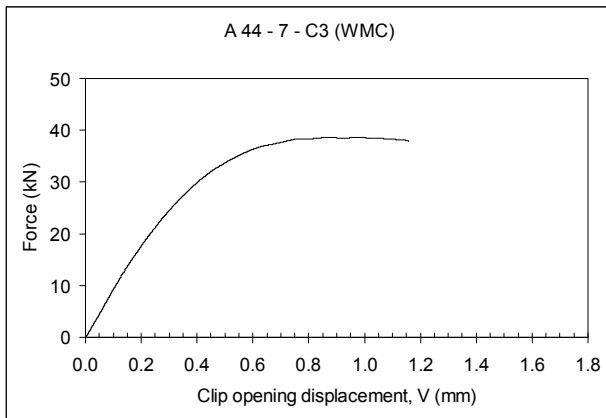
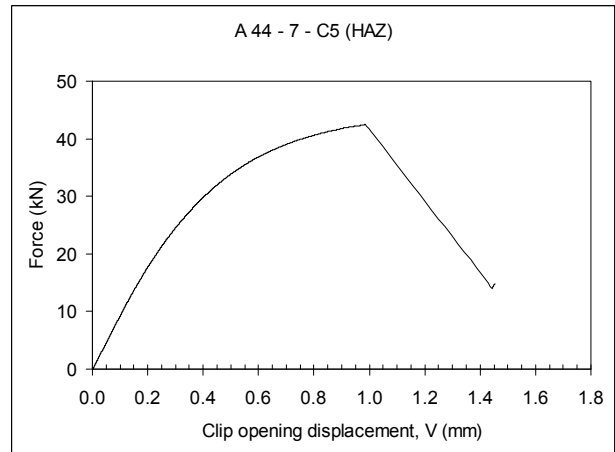
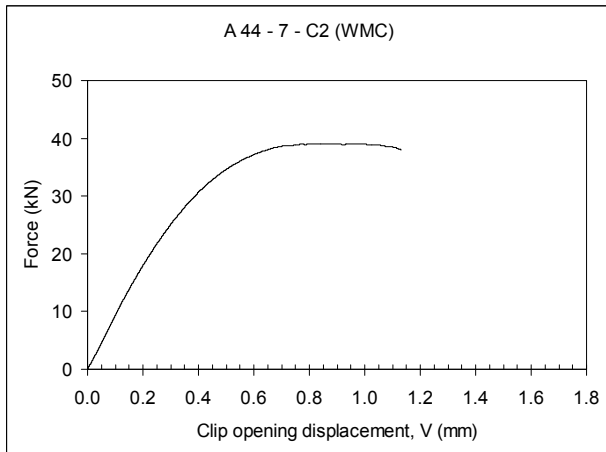
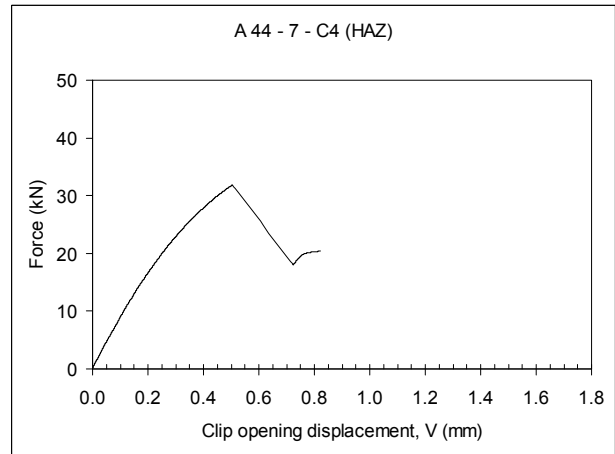
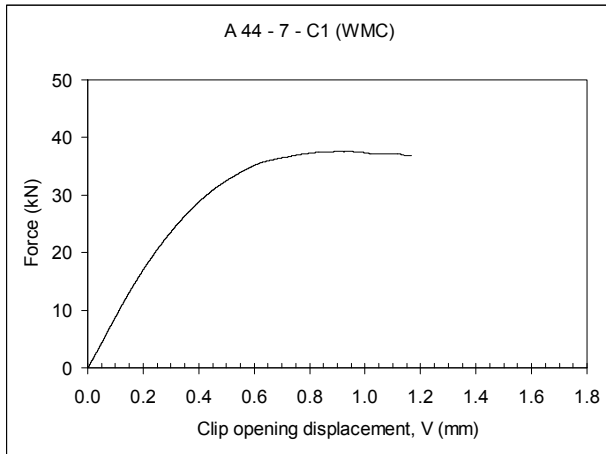
Figure D2 Weld A17: Force versus clip opening displacement plots



Notch location:
Weld metal centerline

Notch location:
Fusion line 50/50
Side - pipe 'Source B'

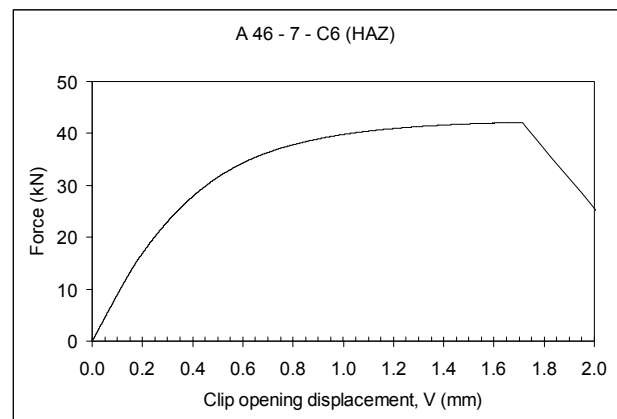
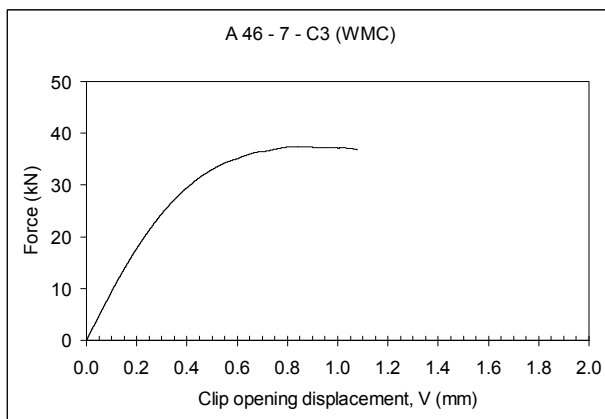
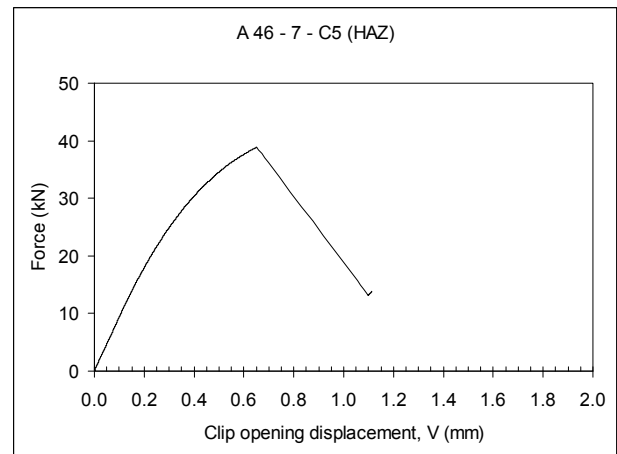
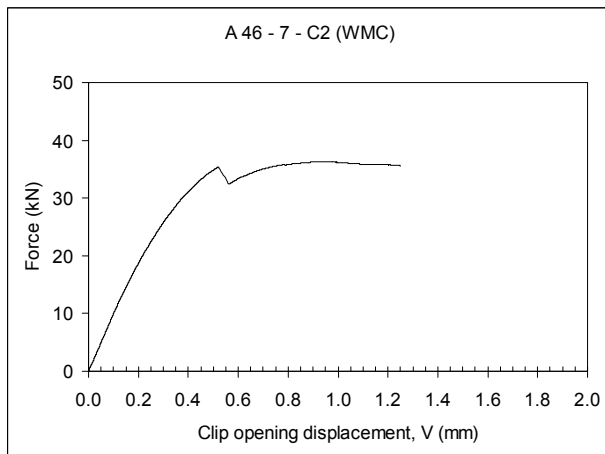
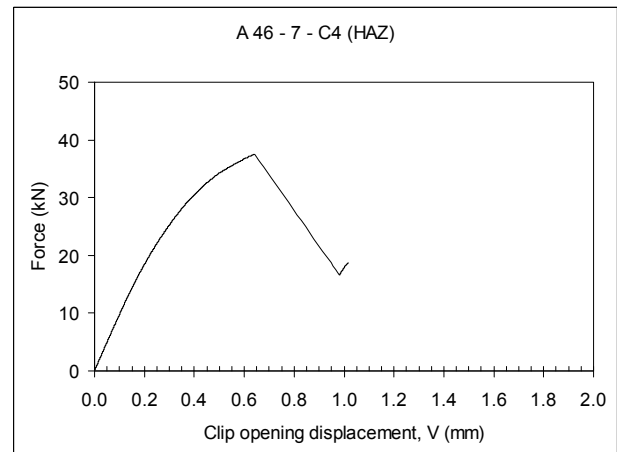
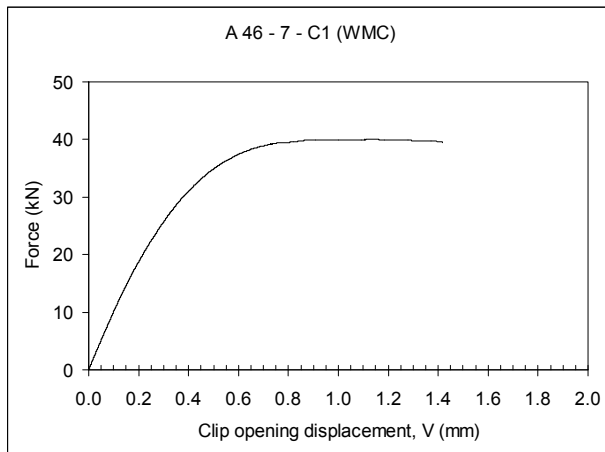
Figure D3 Weld A33: Force versus clip opening displacement plots



Notch location:
Weld metal centerline

Notch location:
Fusion line 50/50
Side - pipe 'Source C'

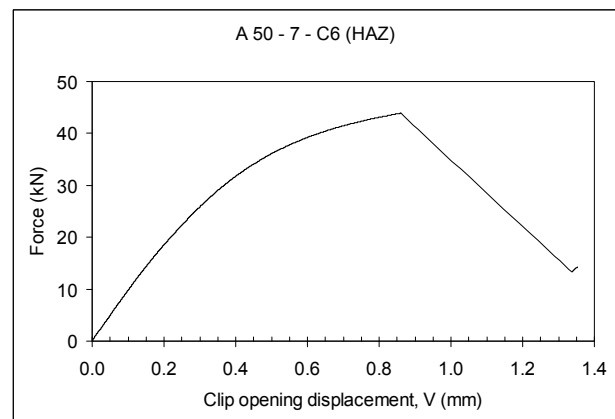
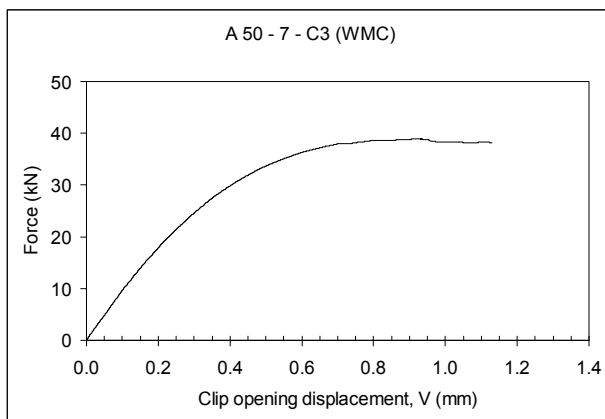
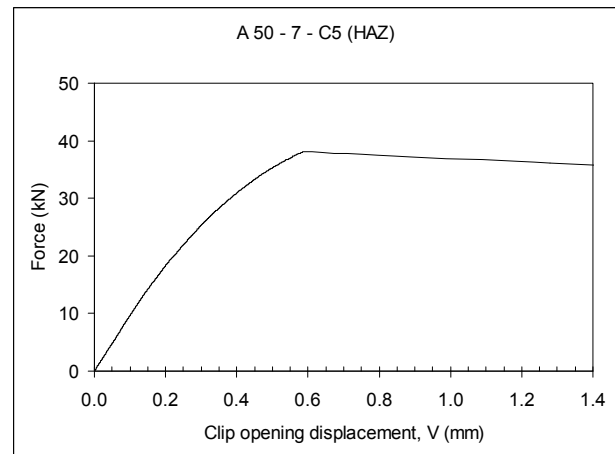
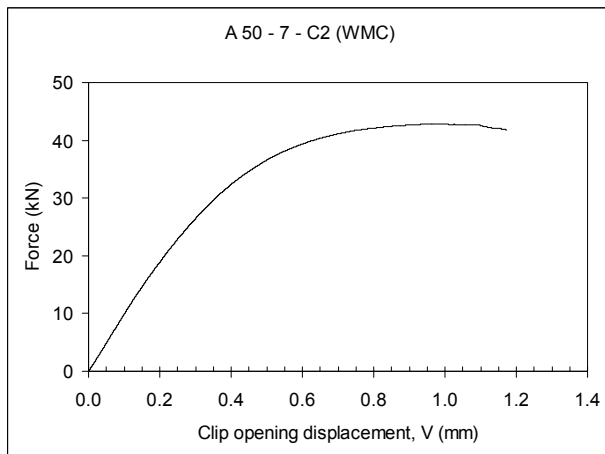
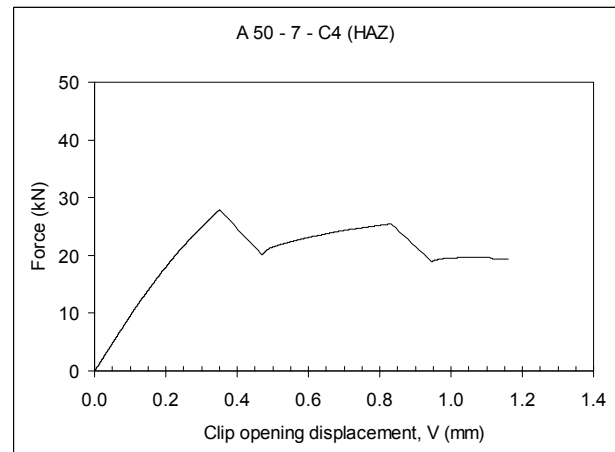
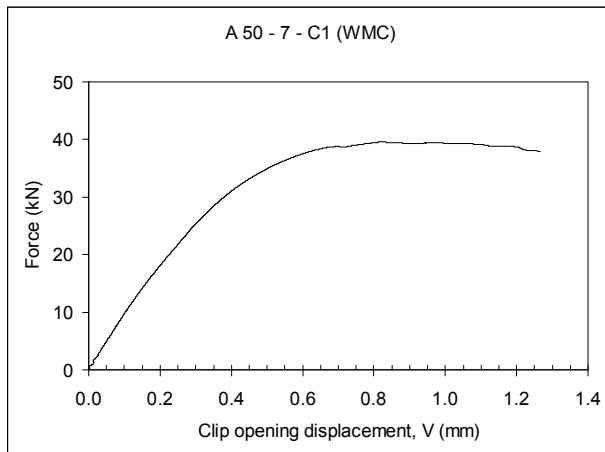
Figure D4 Weld A44: Force versus clip opening displacement plots



Notch location:
Weld metal centerline

Notch location:
Fusion line 50/50
Side - pipe 'Source C'

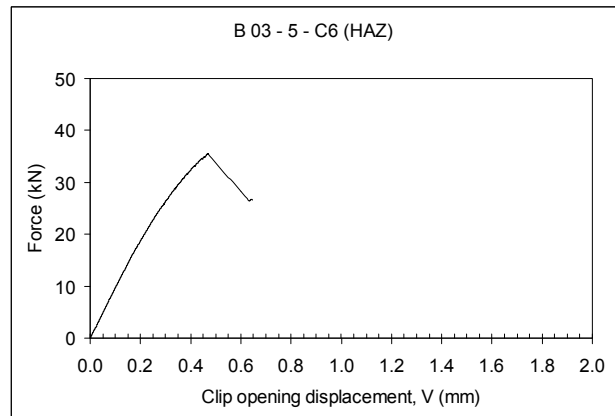
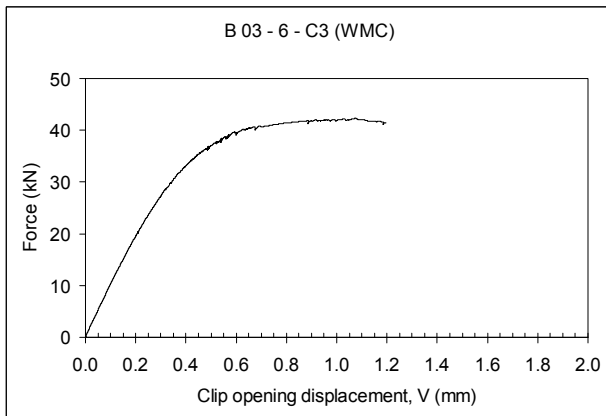
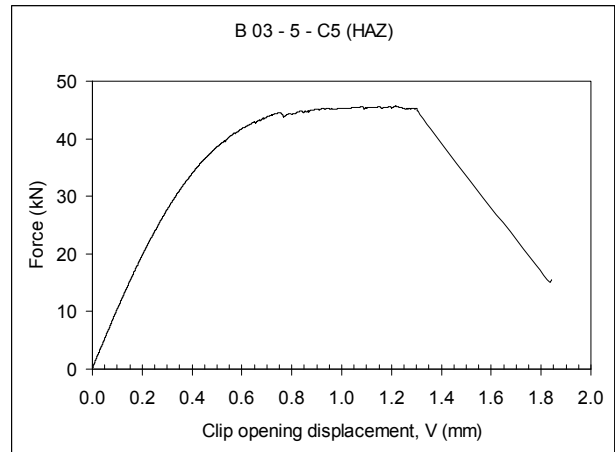
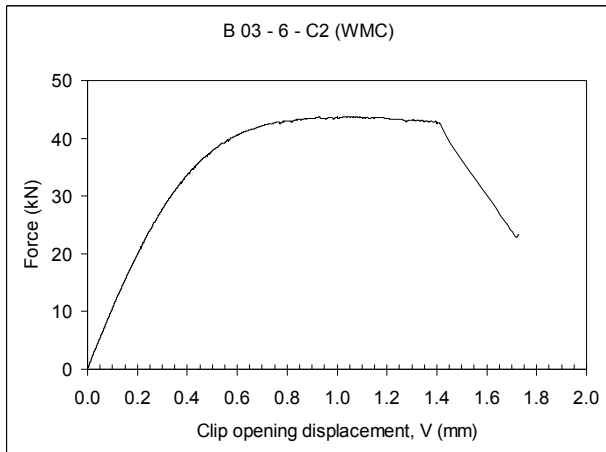
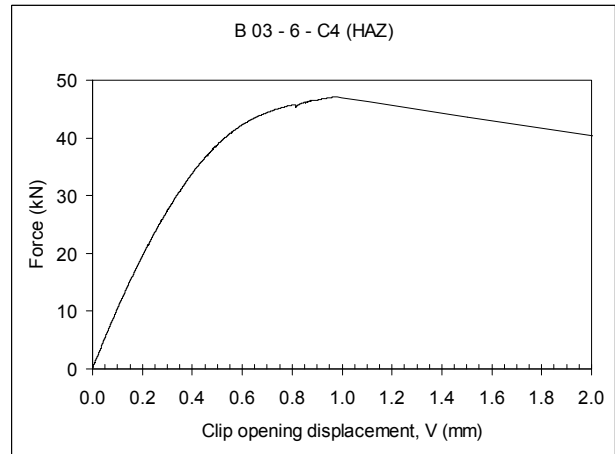
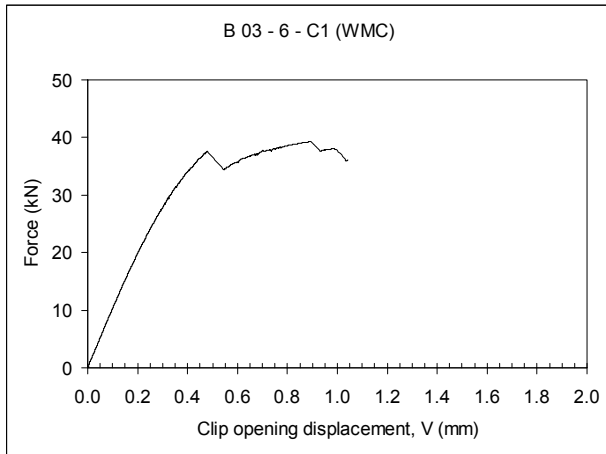
Figure D5 Weld A46: Force versus clip opening displacement plots



Notch location:
Weld metal centerline

Notch location:
Fusion line 50/50
Side - pipe 'Source B'

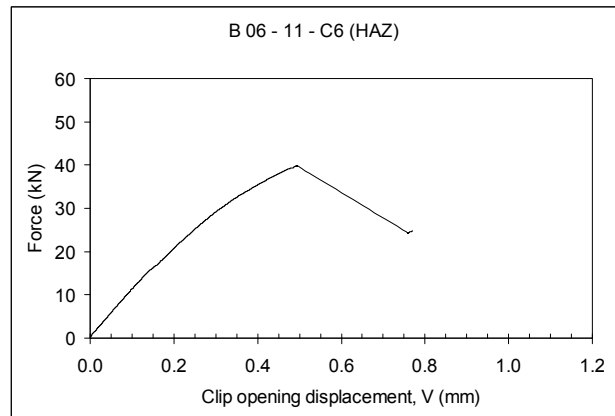
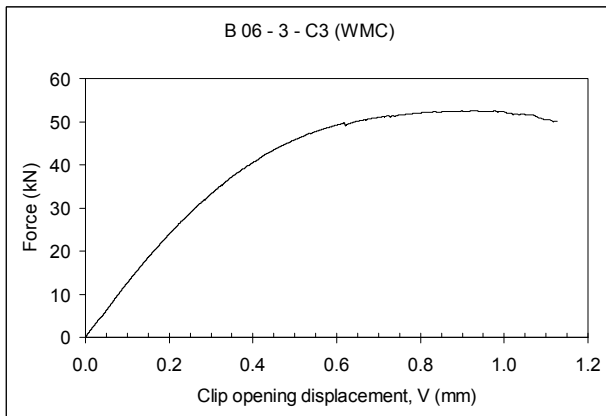
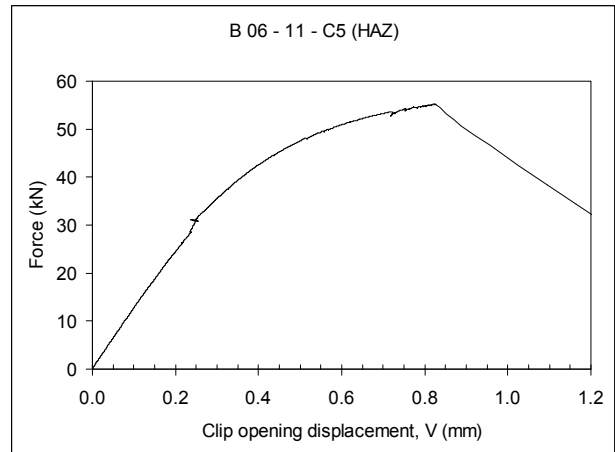
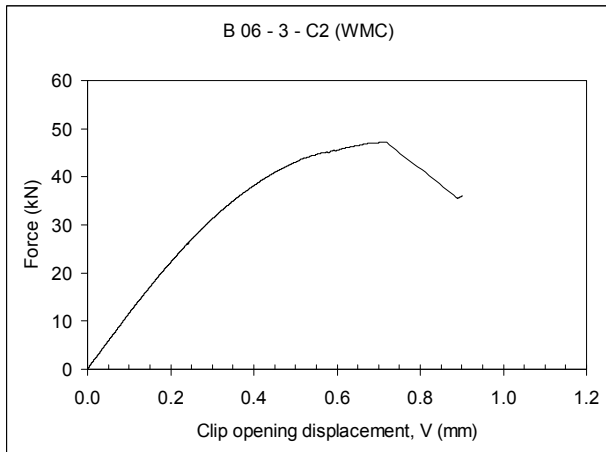
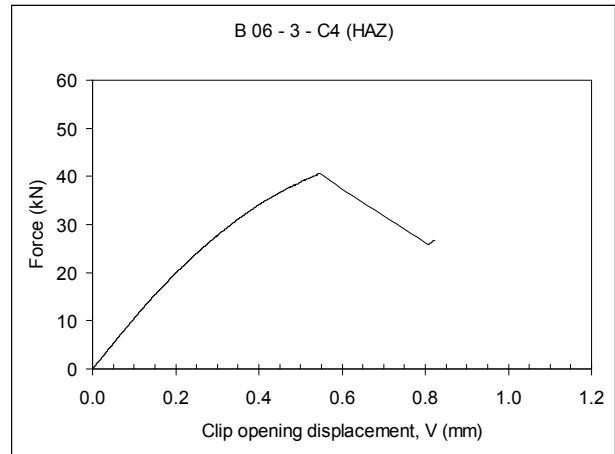
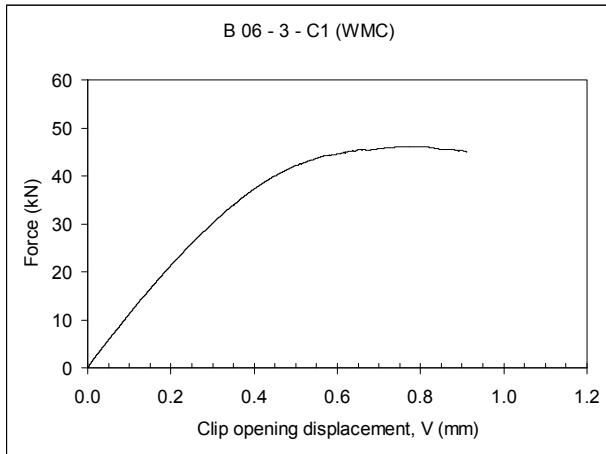
Figure D6 Weld A50: Force versus clip opening displacement plots



Notch location:
Weld metal centerline

Notch location:
Fusion line 50/50
Side - pipe 'Source C'

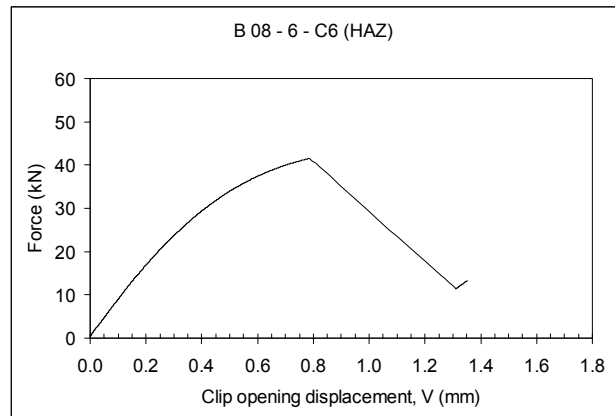
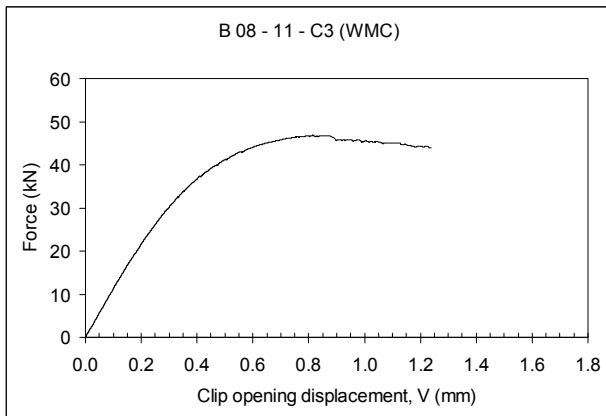
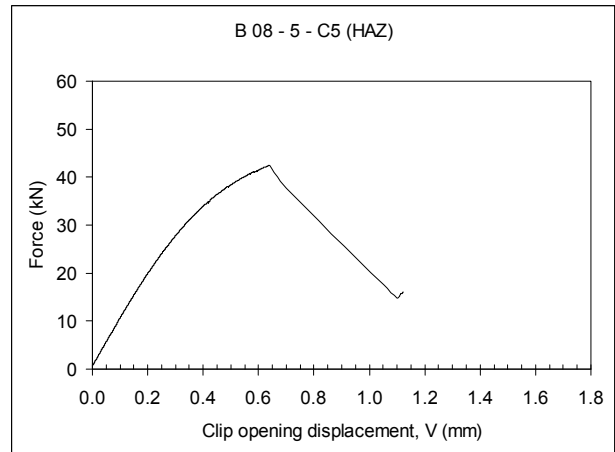
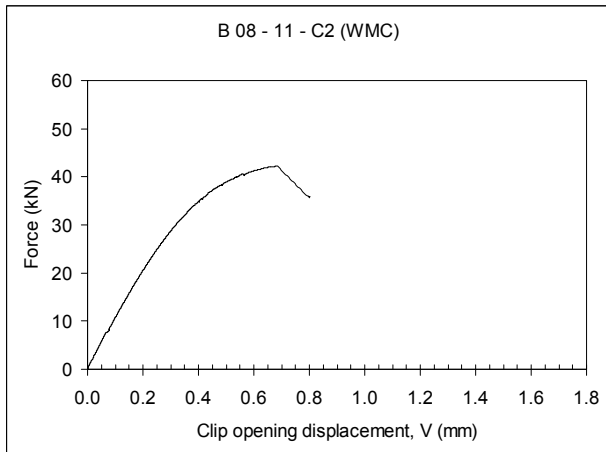
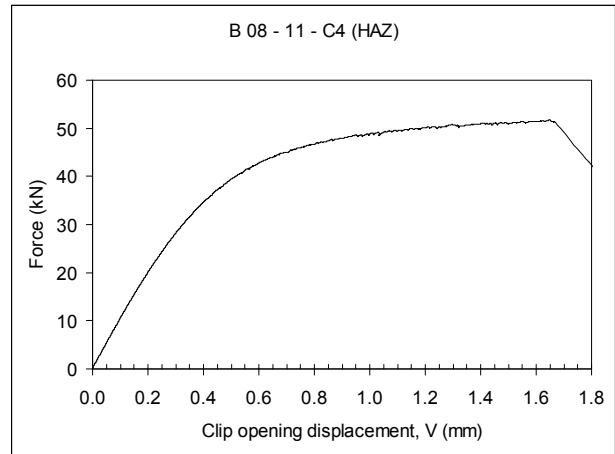
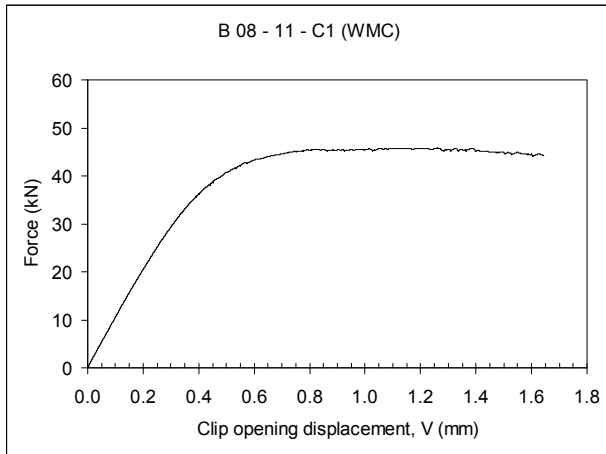
Figure D7 Weld B03: Force versus clip opening displacement plots



Notch location:
Weld metal centerline

Notch location:
Fusion line 50/50
Side - pipe 'Source A'

Figure D8 Weld B06: Force versus clip opening displacement plots



Notch location:
Weld metal centerline

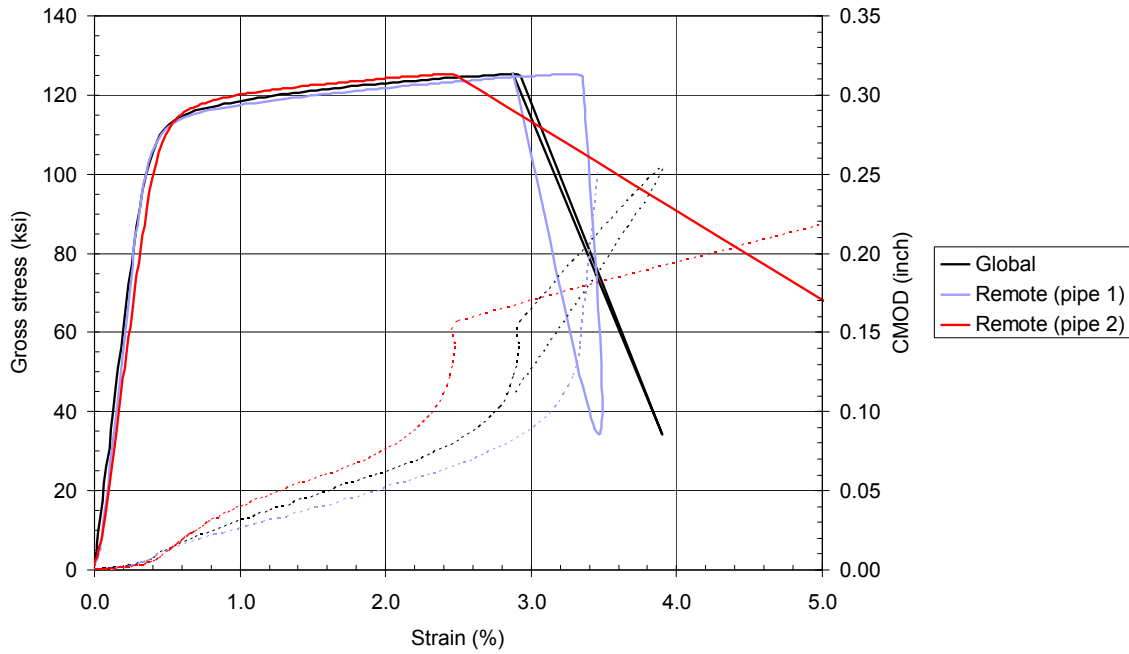
Notch location:
Fusion line 50/50
Side - pipe 'Source C'

Figure D9 Weld B08: Force versus clip opening displacement plots

Appendix E Curved Wide Plate Test Results

This appendix contains the following detail for each tested CWP specimen:

- Plot of gross stress versus strain; strain is recorded for each pipe (Pipe 1 and Pipe 2) and across the weldment.
- Macro-photograph of the tested specimen showing the fracture path on the outside and inside pipe surfaces.
- Macro-photographs of the fracture surfaces.
- Micro-photograph transverse weld section at the fracture initiation point, showing the microstructure sampled by the tip of the defect.



Notes: Surface notch at the weld root, sampling the HAZ of Pipe 1, with dimensions length x height; 2 x 0.118in (50 x 3mm). Tested at -4°F (-20°C)

Figure E1 Weld A06: CWP specimen A06-WP-H1



U-Gent photo ID: dsc-0980-1

(a) Side: weld cap



U-Gent photo ID: dsc-0978-1

(b) Side: weld root

Figure E2 Weld A06: Macro photograph of tested CWP specimen A06-WP-H1



U-Gent photo ID: dsc-327-1

(a) Side: weld



U-Gent photo ID: dsc-332-1

(b) Side: pipe

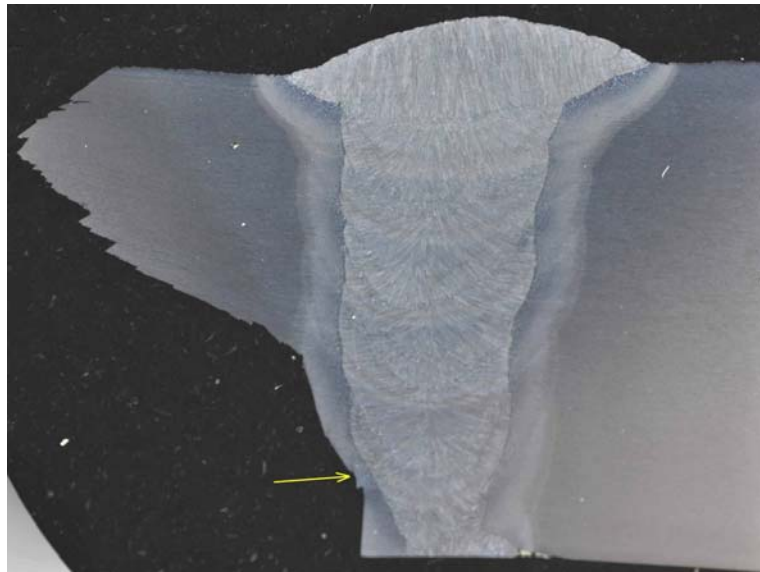
Figure E3 Weld A06: Macro photograph showing fracture faces of tested CWP specimen A06-WP-H1



U-Gent photo ID: dsc-9819-1 (Magnification: x 2.0)

Notes: No clear fracture initiation point

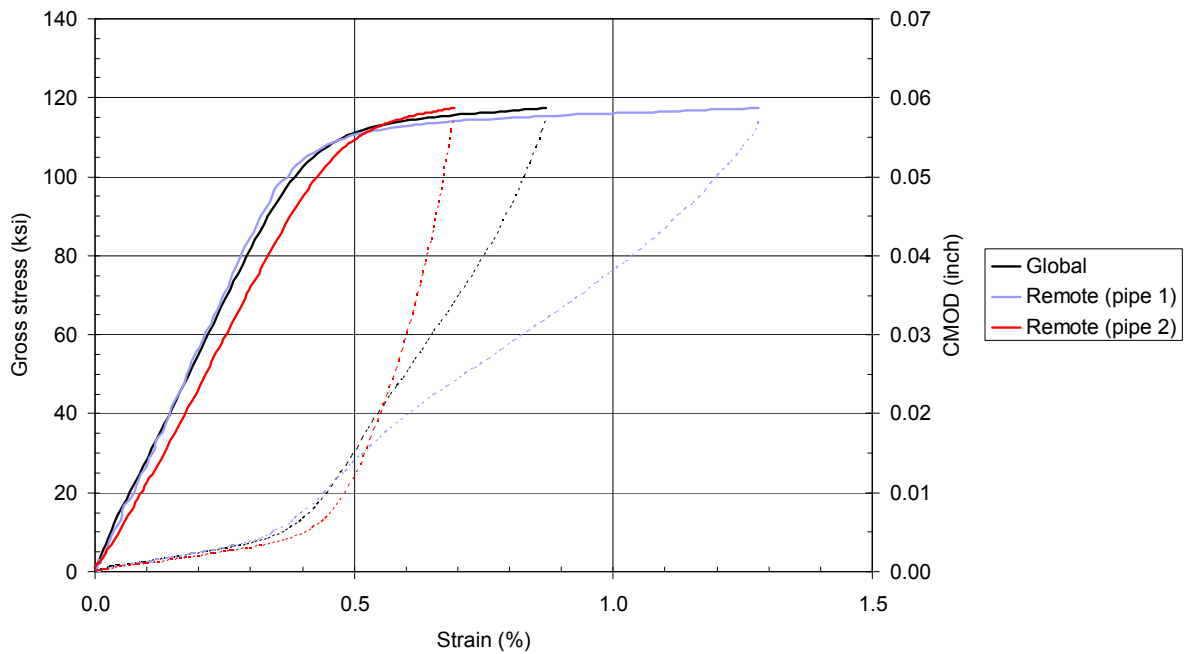
Figure E4 Weld A06, CWP specimen A06-WP-H1: Fracture face, weld metal side showing section location



U-Gent photo ID: dsc-1233 (Magnification: x 5.0)

Notes: Defect tip located in the coarse / fine grained (CG / FG) HAZ microstructure, +0.024in (+0.60mm) from the fusion line.

Figure E5 Weld A06, CWP specimen A06-WP-H1: Position of tip of machined defect (sectioned taken mid-way along the length of the defect)



Notes: Surface notch at the weld root, sampling the HAZ of Pipe 1, with dimensions length x height; 4 x 0.118in (100 x 3mm). Tested at -4°F (-20°C)

Figure E6 Weld A06: CWP specimen A06-WP-H2



U-Gent photo ID: dsc-558-1

(a) Side: weld cap



U-Gent photo ID: dsc-555-1

(b) Side: weld root

Figure E7 Weld A06: Macro photograph of tested CWP specimen A06-WP-H2



U-Gent photo ID: dsc-560-1

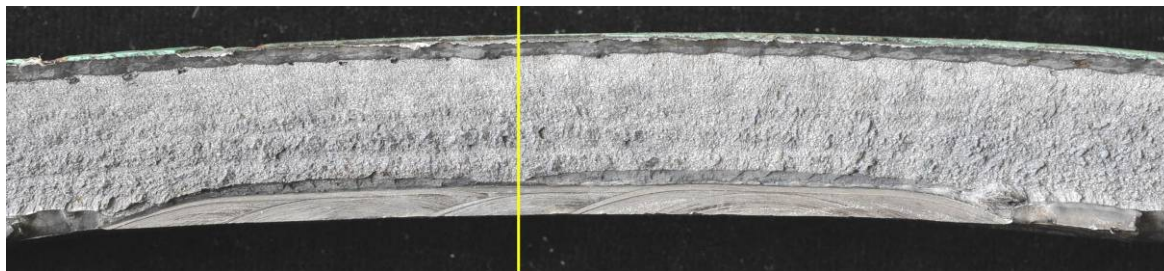
(a) Side: weld



U-Gent photo ID: dsc-565-1

(b) Side: pipe

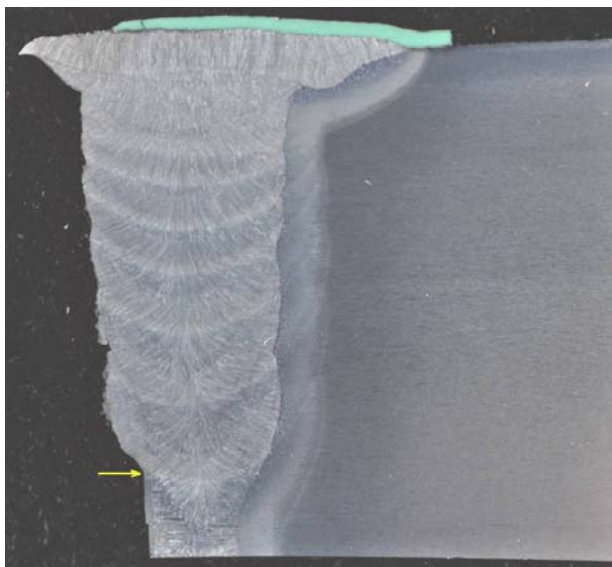
Figure E8 Weld A06: Macro photograph showing fracture faces of tested CWP specimen A06-WP-H2



U-Gent photo ID: dsc-562-2 (Magnification: x 1.2)

Notes: Section taken through fracture initiation point

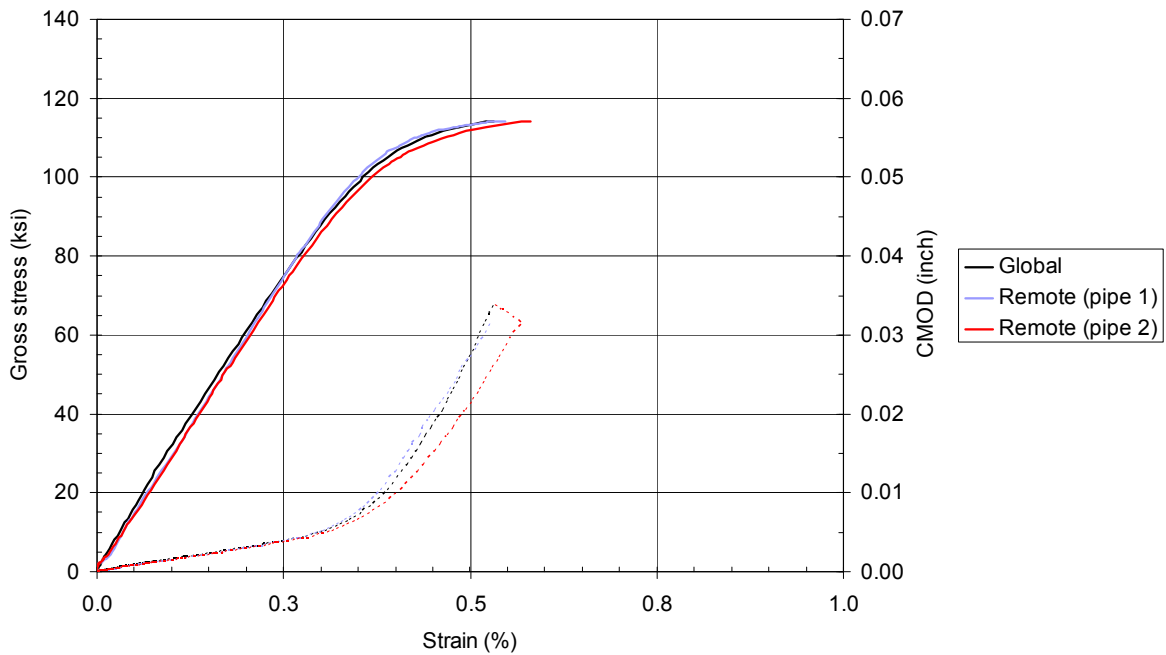
Figure E9 Weld A06, CWP specimen A06-WP-H2: Fracture face, weld metal side showing section location



U-Gent photo ID: dsc-1253 (Magnification: x 5.0)

Notes: Defect tip located in the coarse grained (CG) HAZ microstructure, on the fusion line.

Figure E10 Weld A06, CWP specimen A06-WP-H2: Position of tip of machined defect (sectioned taken at fracture initiation point)



Notes: Surface notch at the weld root, sampling the HAZ of Pipe 1, with dimensions length x height; 4 x 0.157in (100 x 4mm). Tested at -4°F (-20°C)

Figure E11 Weld A06: CWP specimen A06-WP-H3



U-Gent photo ID: dsc-583-1

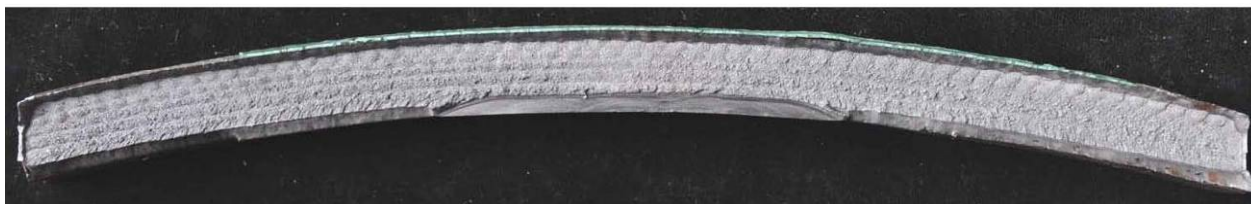
(a) Side: weld cap



U-Gent photo ID: dsc-580-1

(b) Side: weld root

Figure E12 Weld A06: Macro photograph of tested CWP specimen A06-WP-H3



U-Gent photo ID: dsc-587-1

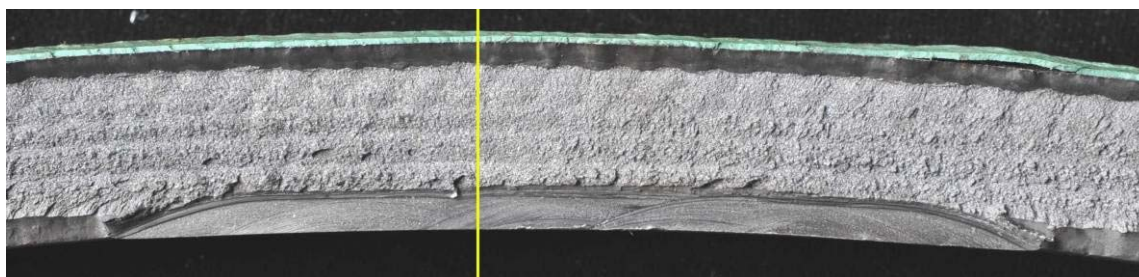
(a) Side: weld



U-Gent photo ID: dsc-591-1

(b) Side: pipe

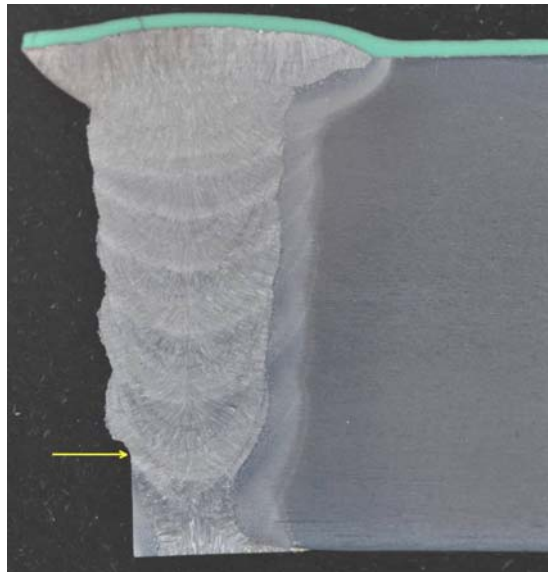
Figure E13 Weld A06: Macro photograph showing fracture faces of tested CWP specimen A06-WP-H3



U-Gent photo ID: dsc-586-2 (Magnification: x 1.2)

Notes: Section taken through fracture initiation point

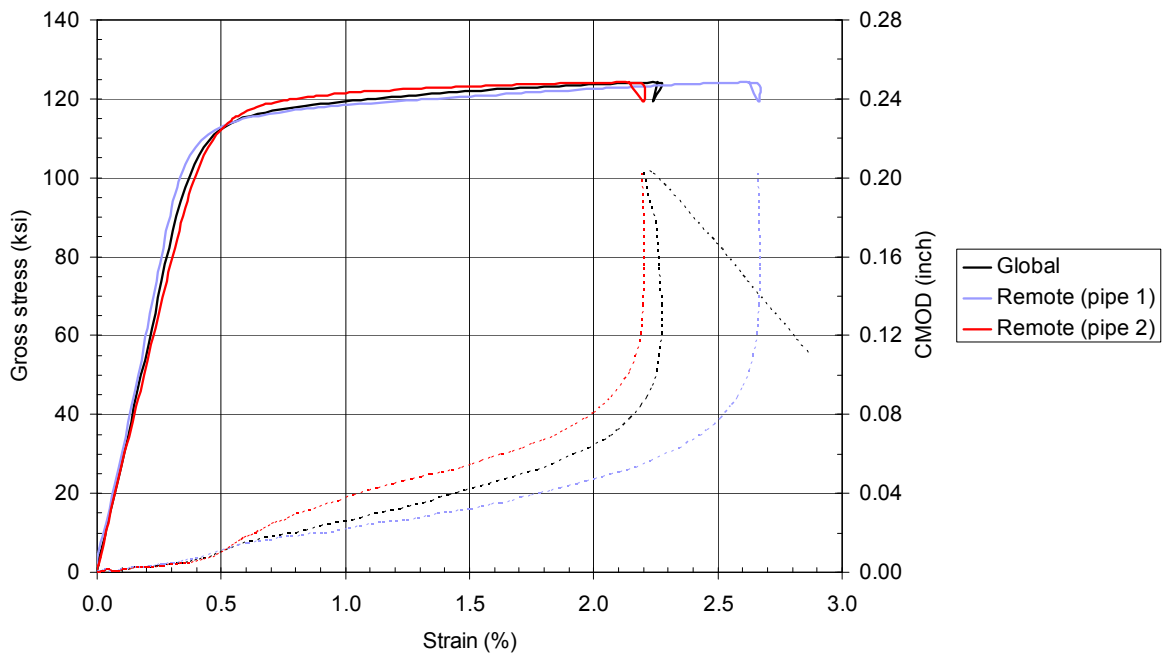
Figure E14 Weld A06, CWP specimen A06-WP-H3: Fracture face, weld metal side showing section location



U-Gent photo ID: dsc-1236 (Magnification: x 5.0)

Notes: Defect tip located in the coarse grained (CG) HAZ microstructure, on the fusion line.

Figure E15 Weld A06, CWP specimen A06-WP-H3: Position of tip of machined defect (sectioned taken at fracture initiation point)



Notes: Surface notch at the weld root, sampling all weld metal, with dimensions length x height; 2 x 0.118in (50 x 3mm). Tested at -4°F (-20°C)

Figure E16 Weld A06: CWP specimen A06-WP-W



U-Gent photo ID: dsc-961-1

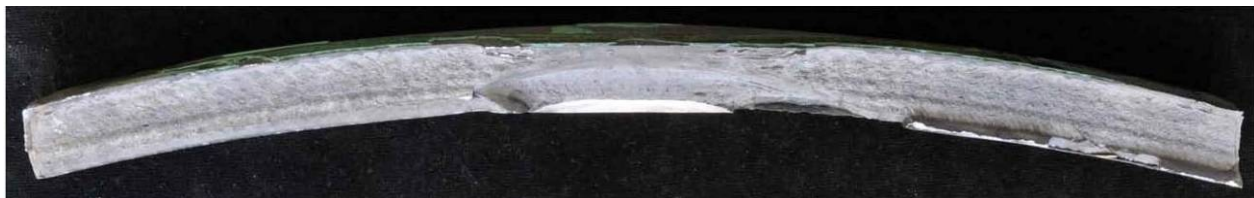
(a) Side: weld cap



U-Gent photo ID: dsc-958-1

(b) Side: weld root

Figure E17 Weld A06: Macro photograph of tested CWP specimen A06-WP-W



U-Gent photo ID: dsc-320-1

(a) Side: weld



U-Gent photo ID: dsc-325-1

(b) Side: pipe

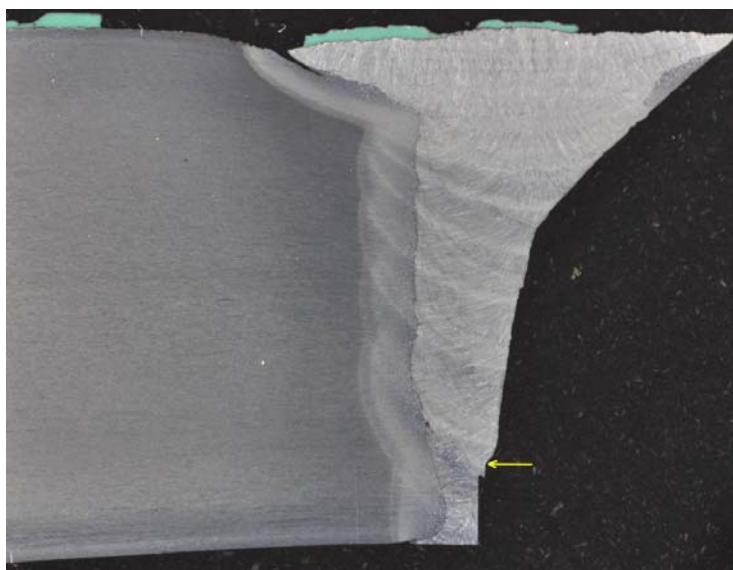
Figure E18 Weld A06: Macro photograph showing fracture faces of tested CWP specimen A06-WP-W



U-Gent photo ID: dsc-998-2 (Magnification: x 2.0)

Notes: No clear fracture initiation point

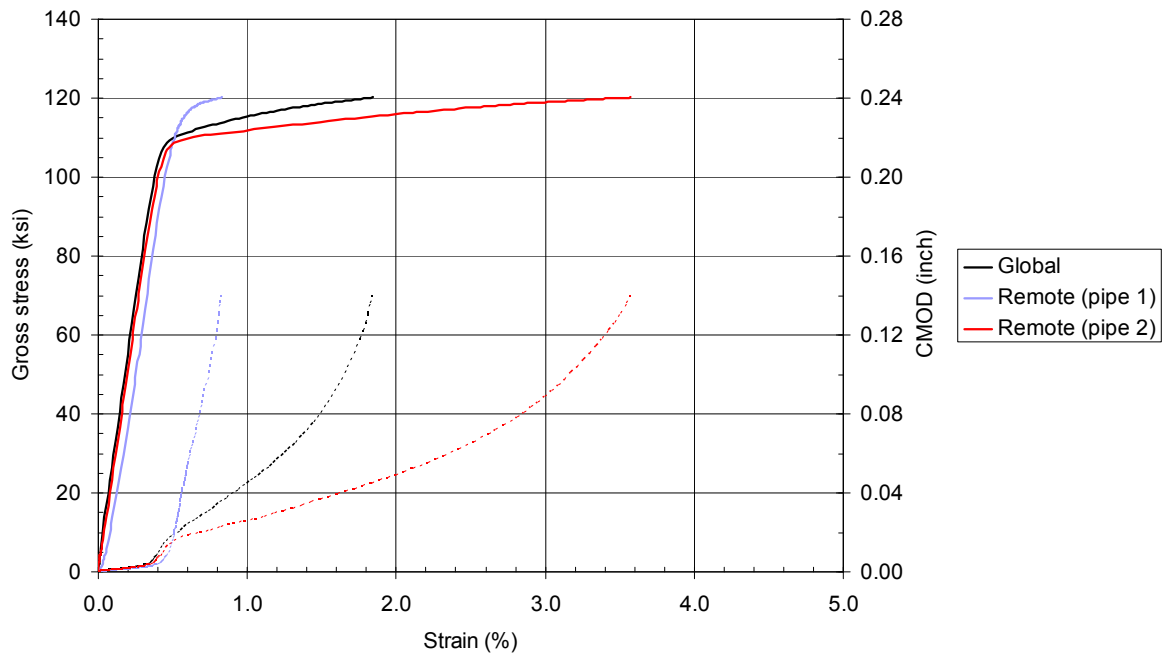
Figure E19 Weld A06, CWP specimen A06-WP-W: Fracture face, weld metal side showing section location



U-Gent photo ID: dsc-1231 (Magnification: x 5.0)

Notes: Defect tip located in the coarse grained (columnar) weld metal.

Figure E20 Weld A06, CWP specimen A06-WP-W: Position of tip of machined defect (sectioned taken mid-way along the length of the defect)



Notes: Surface notch at the weld root, sampling the HAZ of Pipe 1, with dimensions length x height; 2 x 0.118in (50 x 3mm). Tested at -4°F (-20°C)

Figure E21 Weld A17: CWP specimen A17-WP-H1



U-Gent photo ID: dsc-648-1

(a) Side: weld cap



U-Gent photo ID: dsc-645-1

(b) Side: weld root

Figure E22 Weld A17: Macro photograph of tested CWP specimen A17-WP-H1



U-Gent photo ID: dsc-652-1

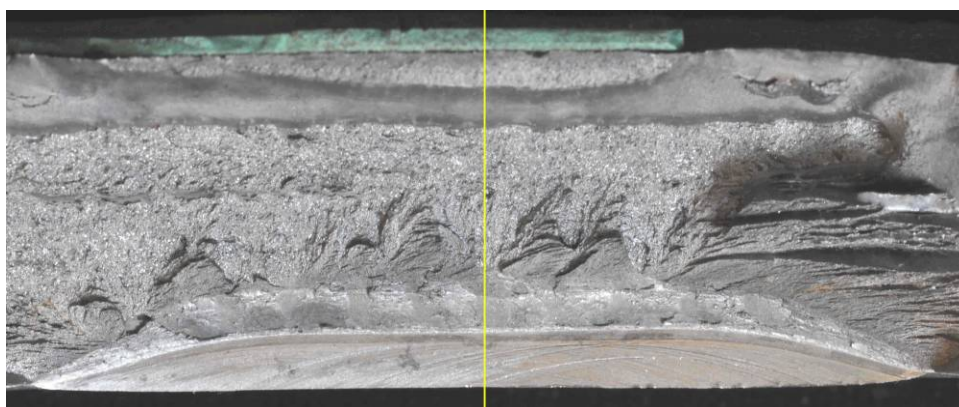
(a) Side: weld



U-Gent photo ID: dsc-656-1

(b) Side: pipe

Figure E23 Weld A17: Macro photograph showing fracture faces of tested CWP specimen A17-WP-H1



U-Gent photo ID: dsc-1011-2 (Magnification: x 2.0)

Notes: No clear fracture initiation point

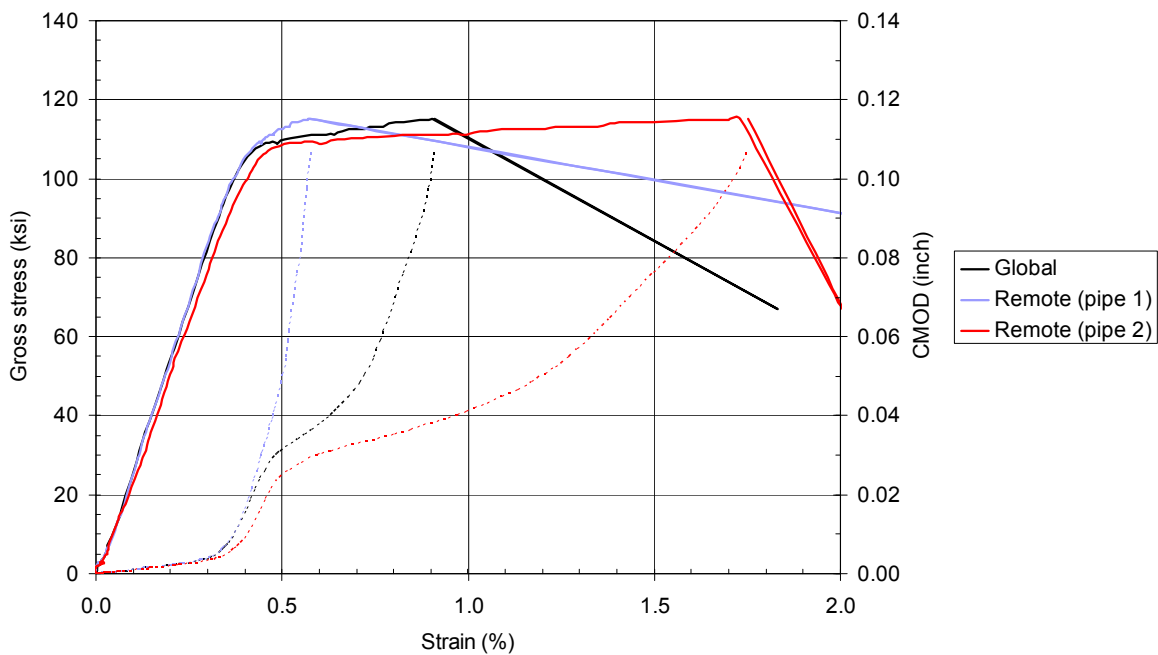
Figure E24 Weld A17, CWP specimen A17-WP-H1: Fracture face, weld metal side showing section location



U-Gent photo ID: dsc-1225 (Magnification: x 3.75)

Notes: Defect tip located in the coarse grained (CG) HAZ microstructure, +0.006in (+0.16mm) from the fusion line.

Figure E25 Weld A17, CWP specimen A17-WP-H1: Position of tip of machined defect (sectioned taken mid-way along the length of the defect)



Notes: Surface notch at the weld root, sampling the HAZ of Pipe 1, with dimensions length x height; 4 x 0.118in (100 x 3mm). Tested at -4°F (-20°C)

Figure E26 Weld A17: CWP specimen A17-WP-H2



U-Gent photo ID: dsc-899-1

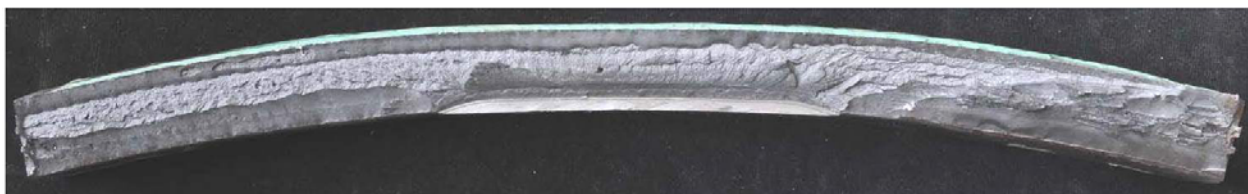
(a) Side: weld cap



U-Gent photo ID: dsc-684-1

(b) Side: weld root

Figure E27 Weld A17: Macro photograph of tested CWP specimen A17-WP-H2



U-Gent photo ID: dsc-695-1

(a) Side: weld

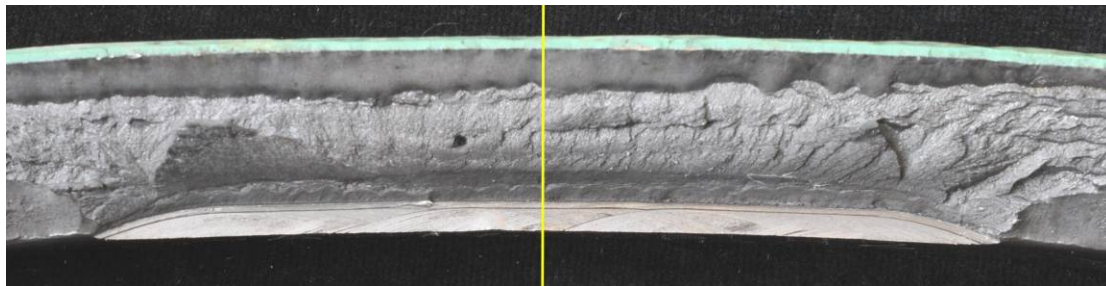


U-Gent photo ID: dsc-697-1

(b) Side: pipe

Figure E28 Weld A17: Macro photograph showing fracture faces of tested CWP specimen A17-WP-H2

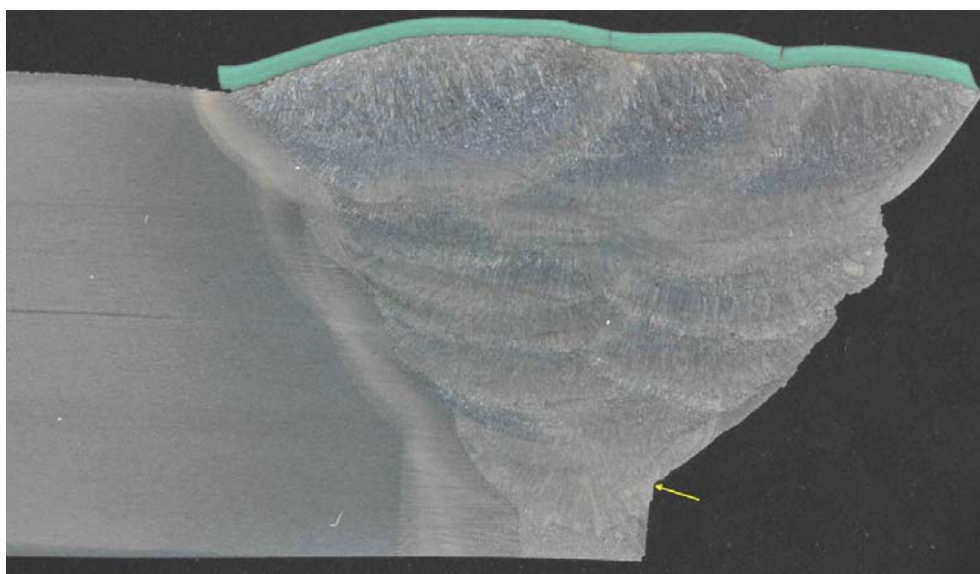
Report Number: 10361
Issue: 1.0



U-Gent photo ID: dsc-691-2 (Magnification: x 2.0)

Notes: No clear fracture initiation point

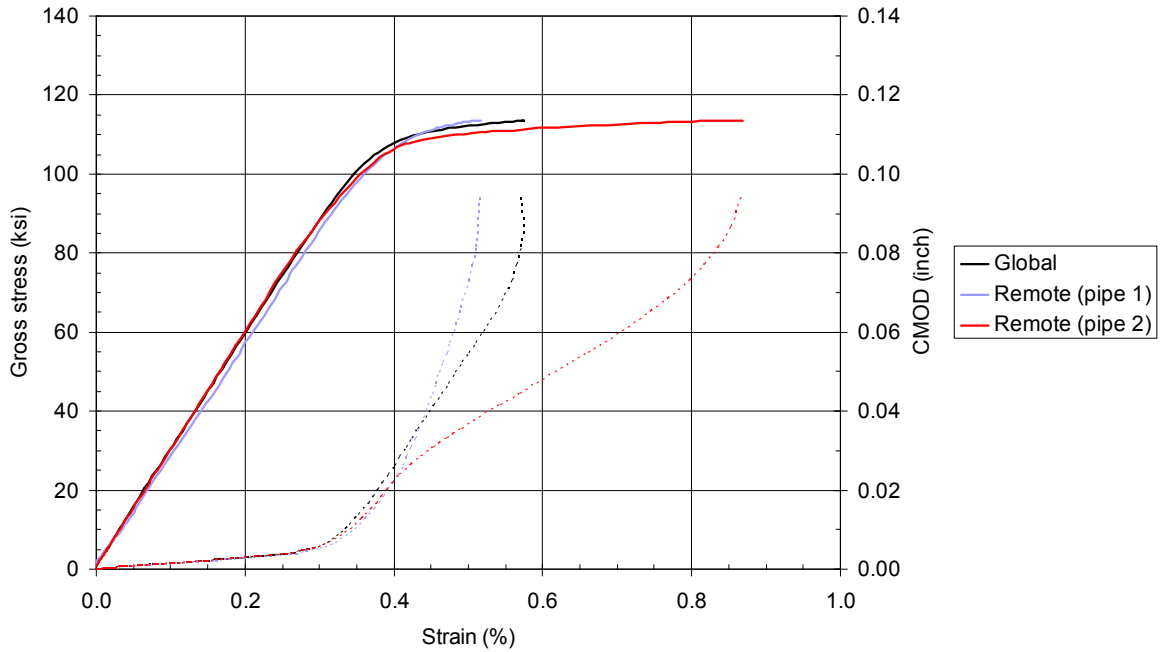
Figure E29 Weld A17, CWP specimen A17-WP-H2: Fracture face, weld metal side showing section location



U-Gent photo ID: dsc-1226 (Magnification: x 3.9)

Notes: Defect tip located in the coarse grained (columnar) weld metal, -0.02in (-0.50mm) from the fusion line. Slow stable crack growth in the weld metal, propagating towards the fusion line

Figure E30 Weld A17, CWP specimen A06-WP-H2: Position of tip of machined defect (sectioned taken mid-way along the length of the defect)



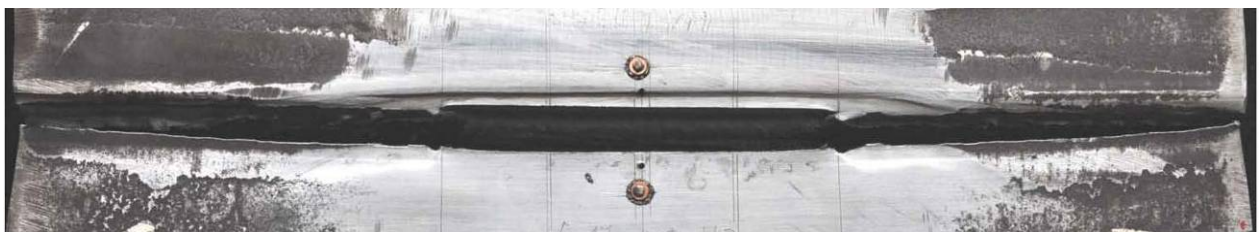
Notes: Surface notch at the weld root, sampling the HAZ of Pipe 1, with dimensions length x height; 4 x 0.118in (100 x 3mm). Tested at -4°F (-20°C)

Figure E31 Weld A17: CWP specimen A17-WP-H3



U-Gent photo ID: dsc-890-1

(a) Side: weld cap



U-Gent photo ID: dsc-887-1

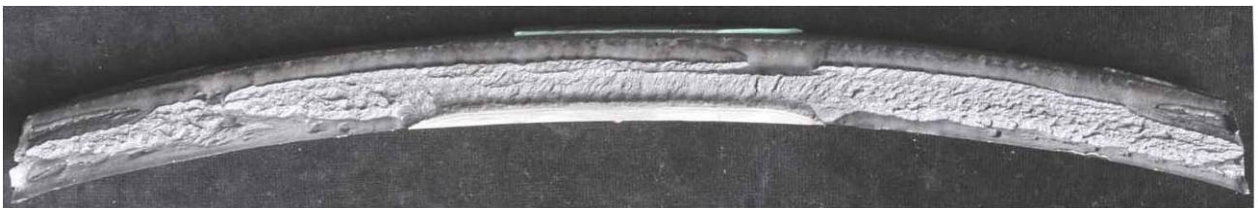
(b) Side: weld root

Figure E32 Weld A17: Macro photograph of tested CWP specimen A17-WP-H3



U-Gent photo ID: dsc-900-1

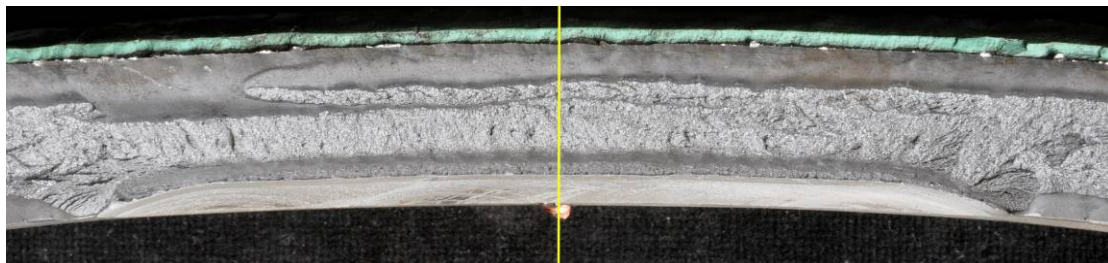
(a) Side: weld



U-Gent photo ID: dsc-905-1

(b) Side: pipe

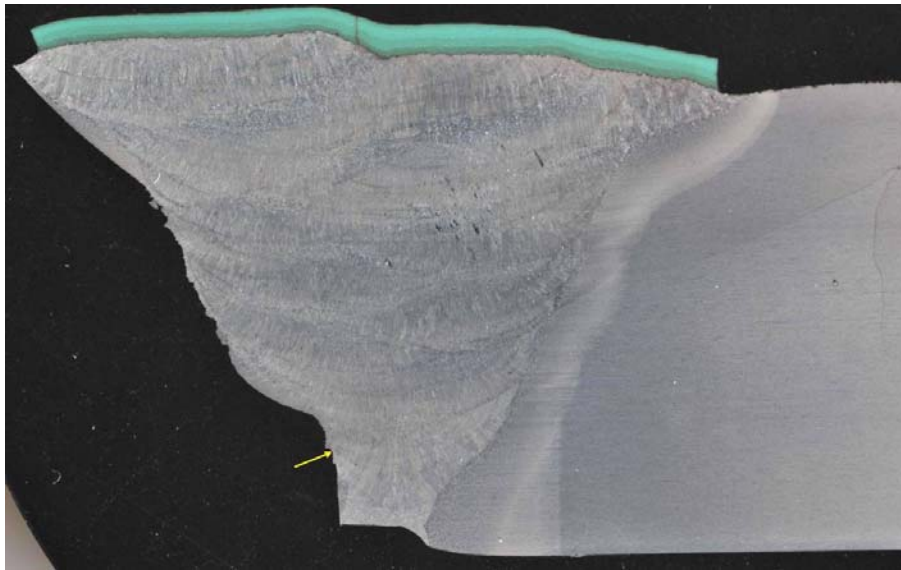
Figure E33 Weld A17: Macro photograph showing fracture faces of tested CWP specimen A17-WP-H3



U-Gent photo ID: dsc-903-2 (Magnification: x 2.0)

Notes: No clear fracture initiation point

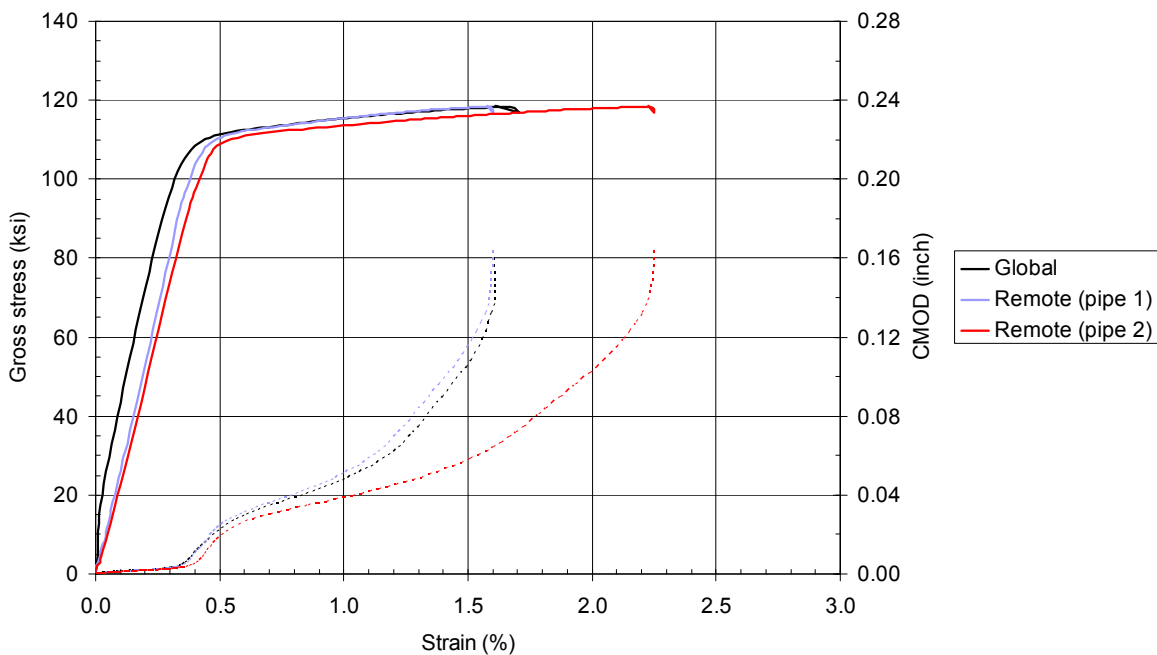
Figure E34 Weld A17, CWP specimen A17-WP-H3: Fracture face, weld metal side showing section location



U-Gent photo ID: dsc-1227 (Magnification: x 4.0)

Notes: Defect tip located in the coarse grained (columnar) weld metal, -0.018in (-0.45mm) from the fusion line. Slow stable crack growth in the weld metal, propagating towards the fusion line

Figure E35 Weld A17, CWP specimen A06-WP-H3: Position of tip of machined defect (sectioned taken mid-way along the length of the defect)



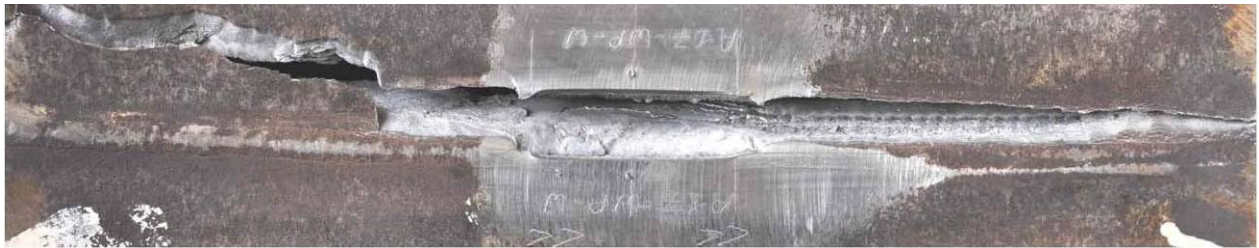
Notes: Surface notch at the weld root, sampling all weld metal, with dimensions length x height; 2 x 0.118in (50 x 3mm). Tested at -4°F (-20°C)

Figure E36 Weld A17: CWP specimen A17-WP-W



U-Gent photo ID: dsc-597-1

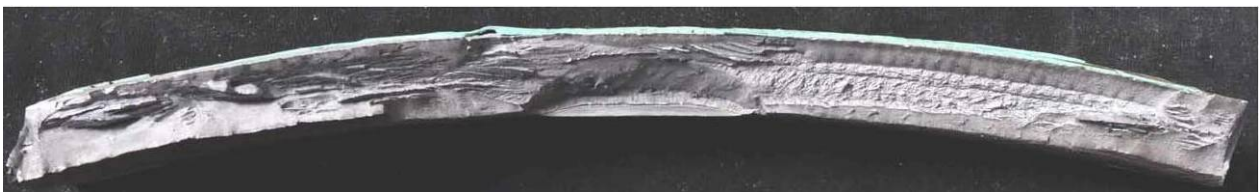
(a) Side: weld cap



U-Gent photo ID: dsc-592-1

(b) Side: weld root

Figure E37 Weld A17: Macro photograph of tested CWP specimen A17-WP-W



U-Gent photo ID: dsc-602-1

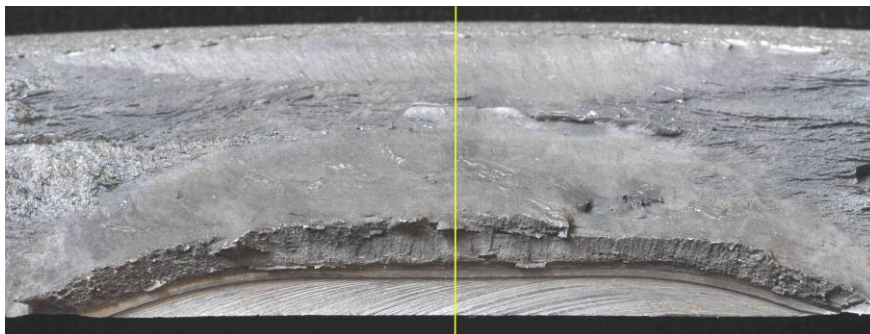
(a) Side: weld



U-Gent photo ID: dsc-606-1

(b) Side: pipe

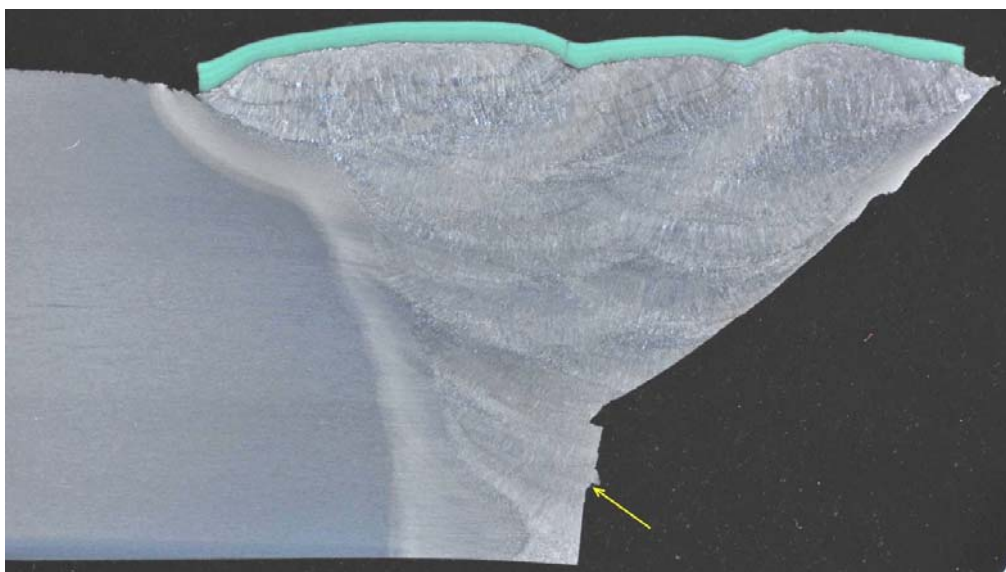
Figure E38 Weld A17: Macro photograph showing fracture faces of tested CWP specimen A17-WP-W



U-Gent photo ID: dsc-1009-2 (Magnification: x 2.0)

Notes: No clear fracture initiation point

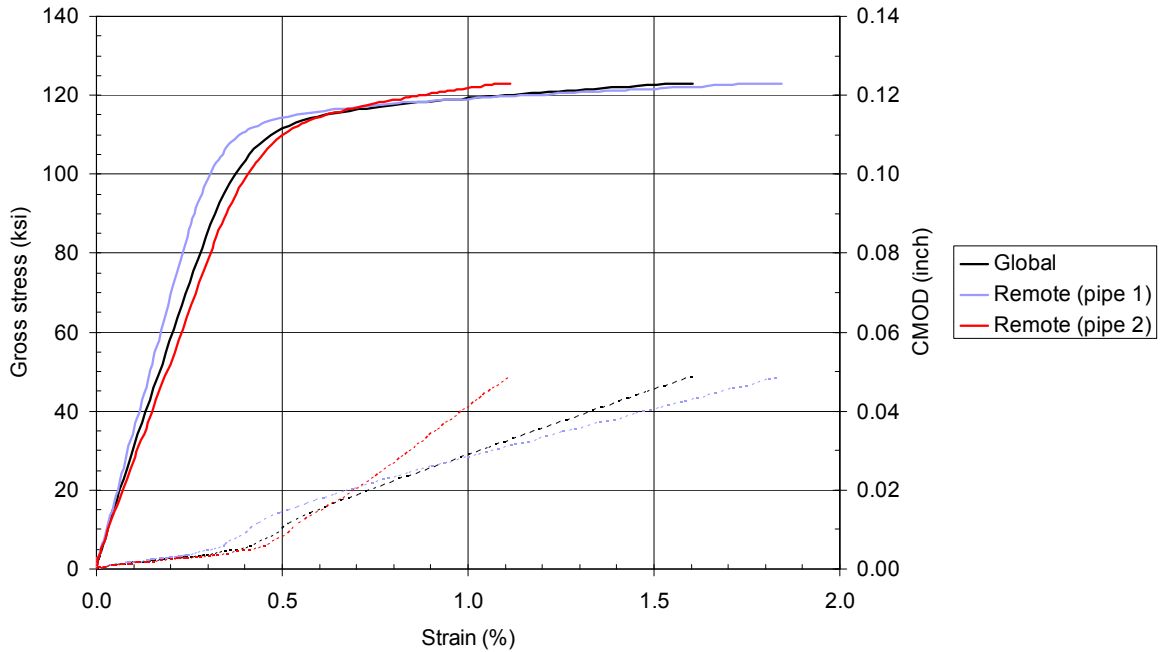
Figure E39 Weld A17, CWP specimen A17-WP-W: Fracture face, weld metal side showing section location



U-Gent photo ID: dsc-1224 (Magnification: x 4.0)

Notes: Defect tip located in the coarse grained (columnar) and grain refined weld metal.

Figure E40 Weld A17, CWP specimen A06-WP-W: Position of tip of machined defect (sectioned taken mid-way along the length of the defect)



Notes: Surface notch at the weld root, sampling the HAZ of Pipe 1, with dimensions length x height; 2 x 0.118in (50 x 3mm). Tested at -4°F (-20°C)

Figure E41 Weld A33: CWP specimen A33-WP-H1



U-Gent photo ID: dsc-957-1

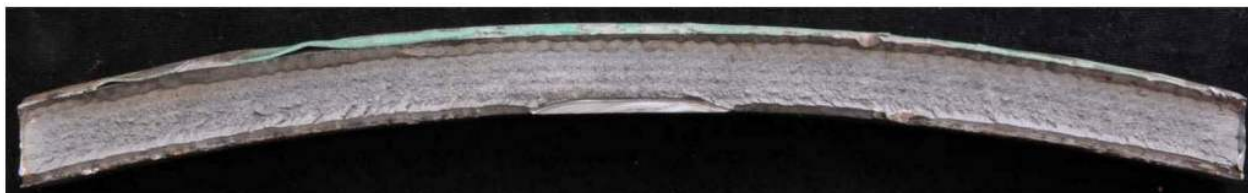
(a) Side: weld cap



U-Gent photo ID: dsc-954-1

(b) Side: weld root

Figure E42 Weld A33: Macro photograph of tested CWP specimen A33-WP-H1



U-Gent photo ID: dsc-291-1

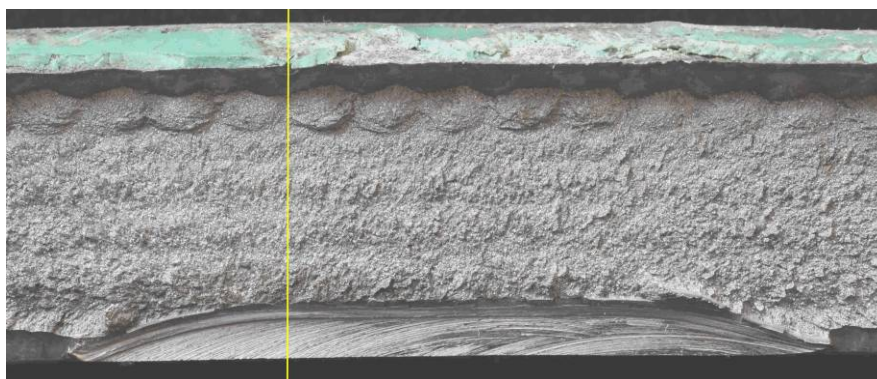
(a) Side: weld



U-Gent photo ID: dsc-288-1

(b) Side: pipe

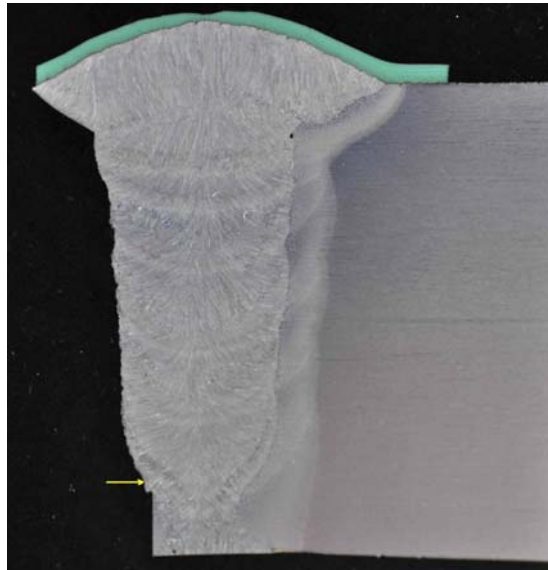
Figure E43 Weld A33: Macro photograph showing fracture faces of tested CWP specimen A33-WP-H1



U-Gent photo ID: dsc-986-2 (Magnification: x 2.0)

Notes: Section taken through fracture initiation point

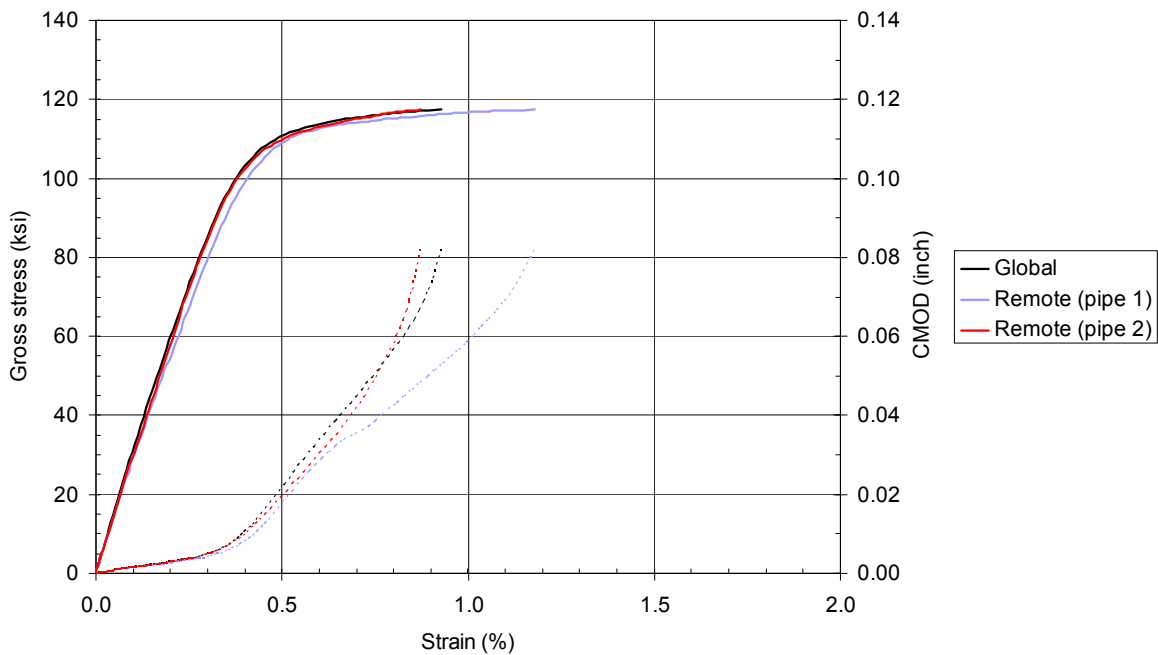
Figure E44 Weld A33, CWP specimen A33-WP-H1: Fracture face, weld metal side showing section location



U-Gent photo ID: dsc-1247 (Magnification: x 5.0)

Notes: Defect tip located in the coarse grained (CG) HAZ microstructure, +0.005in (+0.13mm) from the fusion line.

Figure E45 Weld A33, CWP specimen A33-WP-H1: Position of tip of machined defect (sectioned taken at fracture initiation point)



Notes: Surface notch at the weld root, sampling the HAZ of Pipe 1, with dimensions length x height; 4 x 0.118in (100 x 3mm). Tested at -4°F (-20°C)

Figure E46 Weld A33: CWP specimen A33-WP-H2



U-Gent photo ID: dsc-570-1

(a) Side: weld cap



U-Gent photo ID: dsc-567-1

(b) Side: weld root

Figure E47 Weld A33: Macro photograph of tested CWP specimen A33-WP-H2



U-Gent photo ID: dsc-575-1

(a) Side: weld



U-Gent photo ID: dsc-576-1

(b) Side: pipe

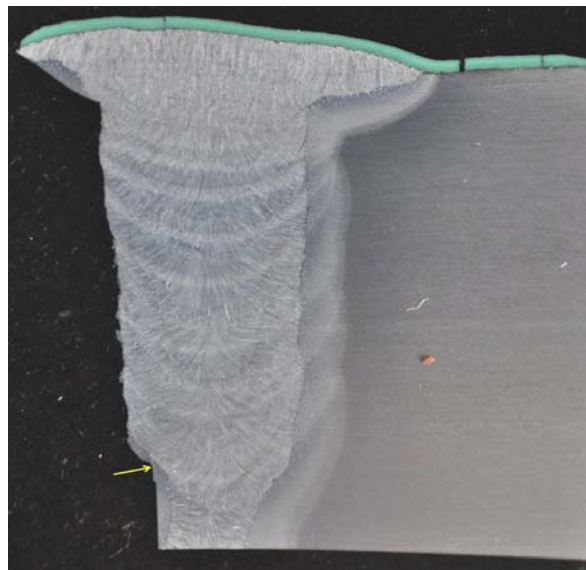
Figure E48 Weld A33: Macro photograph showing fracture faces of tested CWP specimen A33-WP-H2



U-Gent photo ID: dsc-573-2 (Magnification: x 1.2)

Notes: Section taken through fracture initiation point

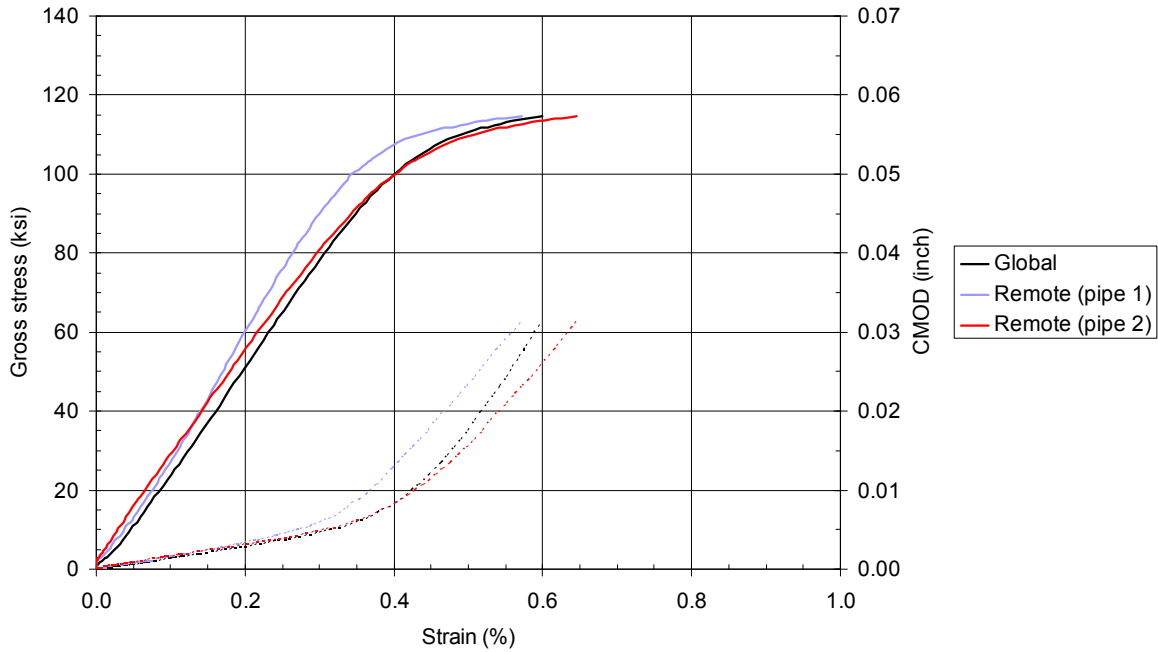
Figure E49 Weld A33, CWP specimen A33-WP-H2: Fracture face, weld metal side showing section location



U-Gent photo ID: dsc-1249 (Magnification: x 5.0)

Notes: Defect tip located in the coarse / fine grained (CG / FG) HAZ microstructure, +0.018in (+0.45mm) from the fusion line. Initial crack extension towards the coarse grained HAZ microstructure.

Figure E50 Weld A33, CWP specimen A33-WP-H2: Position of tip of machined defect (sectioned taken at fracture initiation point)



Notes: Surface notch at the weld root, sampling the HAZ of Pipe 1, with dimensions length x height; 4 x 0.157in (100 x 4mm). Tested at -4°F (-20°C)

Figure E51 Weld A33: CWP specimen A33-WP-H3



U-Gent photo ID: dsc-700-1

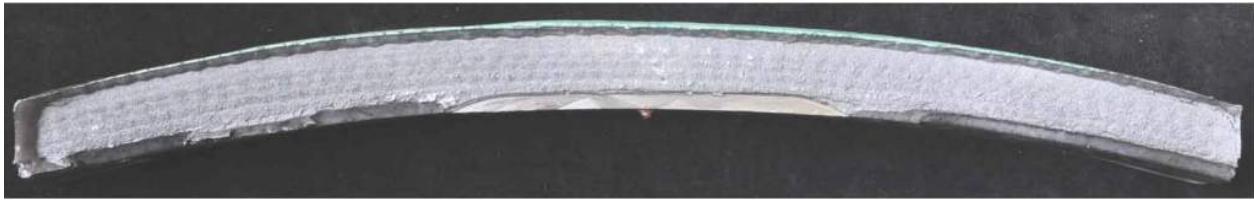
(a) Side: weld cap



U-Gent photo ID: dsc-698-1

(b) Side: weld root

Figure E52 Weld A33: Macro photograph of tested CWP specimen A33-WP-H3



U-Gent photo ID: dsc-706-1

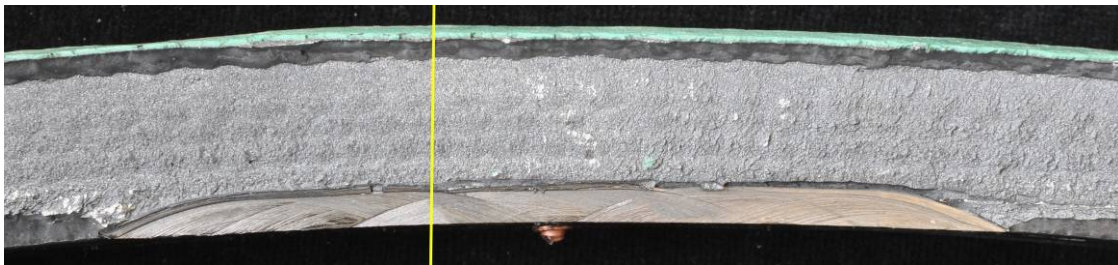
(a) Side: weld



U-Gent photo ID: dsc-707-1

(b) Side: pipe

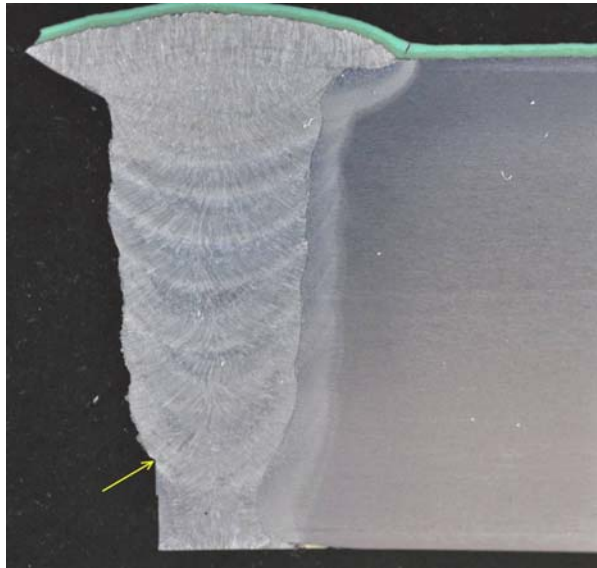
Figure E53 Weld A33: Macro photograph showing fracture faces of tested CWP specimen A33-WP-H3



U-Gent photo ID: dsc-705-2 (Magnification: x 1.2)

Notes: Section taken through fracture initiation point

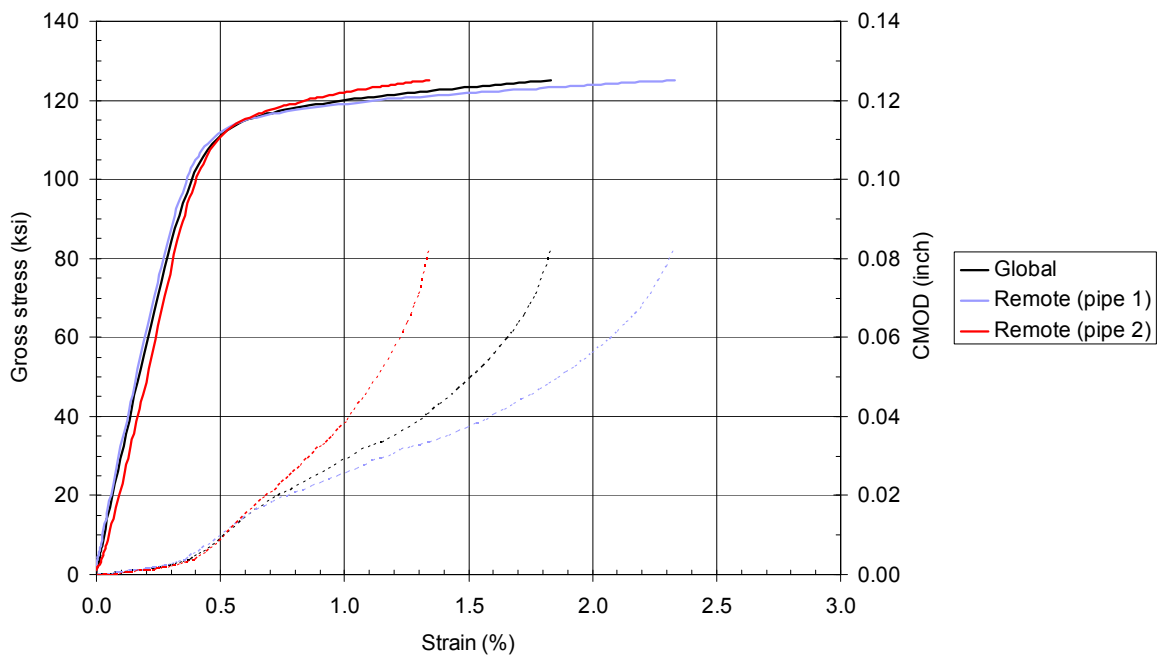
Figure E54 Weld A33, CWP specimen A33-WP-H3: Fracture face, weld metal side showing section location



U-Gent photo ID: dsc-1251 (Magnification: x 5.0)

Notes: Defect tip located in the coarse grained (CG) HAZ microstructure, on the fusion line.

Figure E55 Weld A33, CWP specimen A33-WP-H3: Position of tip of machined defect (sectioned taken at fracture initiation point)



Notes: Surface notch at the weld root, sampling all weld metal, with dimensions length x height; 2 x 0.118in (50 x 3mm). Tested at -4°F (-20°C)

Figure E56 Weld A33: CWP specimen A33-WP-W



U-Gent photo ID: dsc-941-1

(a) Side: weld cap



U-Gent photo ID: dsc-938-1

(b) Side: weld root

Figure E57 Weld A33: Macro photograph of tested CWP specimen A33-WP-W



U-Gent photo ID: dsc-314-1

(a) Side: weld



U-Gent photo ID: dsc-315-1

(b) Side: pipe

Figure E58 Weld A33: Macro photograph showing fracture faces of tested CWP specimen A33-WP-W

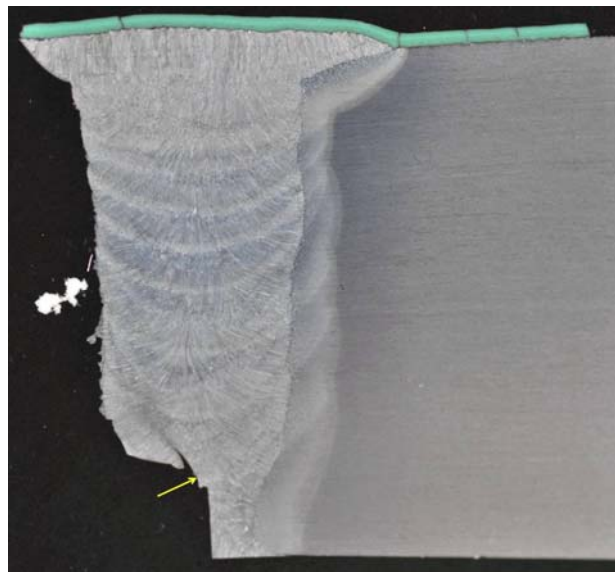
Report Number: 10361
Issue: 1.0



U-Gent photo ID: dsc-9858-2 (Magnification: x 2.0)

Notes: Section taken through fracture initiation point

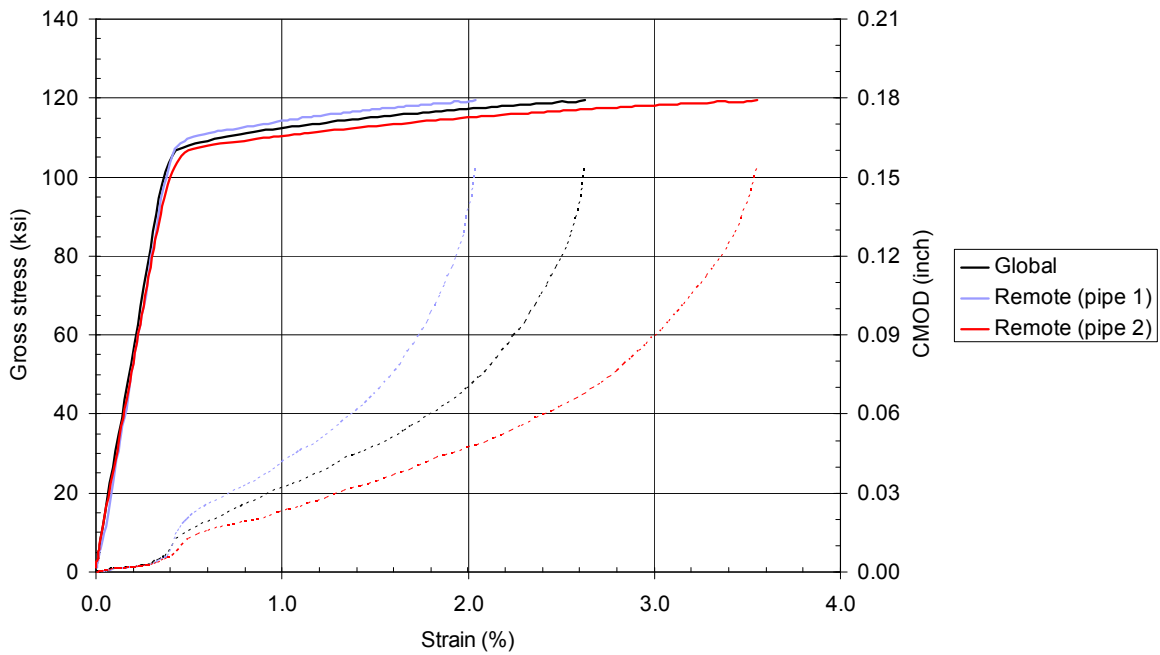
Figure E59 Weld A33, CWP specimen A33-WP-W: Fracture face, weld metal side showing section location



U-Gent photo ID: dsc-1246 (Magnification: x 6.0)

Notes: Defect tip located in the coarse grained (columnar) weld metal. Slow stable crack growth in the weld metal, propagating towards the fusion line. Unstable fracture along the fusion line (CG HAZ microstructure)

Figure E60 Weld A33, CWP specimen A33-WP-W: Position of tip of machined defect (sectioned taken at fracture initiation point)



Notes: Surface notch at the weld root, sampling the HAZ of Pipe 1, with dimensions length x height; 2 x 0.118in (50 x 3mm). Tested at -4°F (-20°C)

Figure E61 Weld A46: CWP specimen A46-WP-H1



U-Gent photo ID: dsc-948-1

(a) Side: weld cap



U-Gent photo ID: dsc-946-1

(b) Side: weld root

Figure E62 Weld A46: Macro photograph of tested CWP specimen A46-WP-H1



U-Gent photo ID: dsc-301-1

(a) Side: weld



U-Gent photo ID: dsc-303-1

(b) Side: pipe

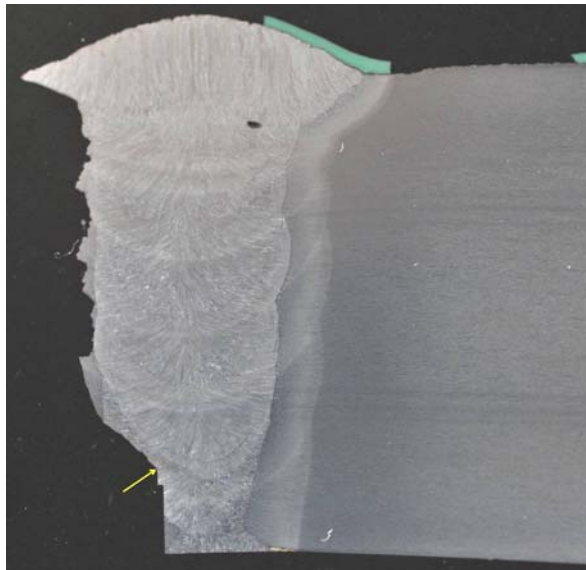
Figure E63 Weld A46: Macro photograph showing fracture faces of tested CWP specimen A46-WP-H1



U-Gent photo ID: dsc-995-2 (Magnification: x 2.0)

Notes: No clear fracture initiation point

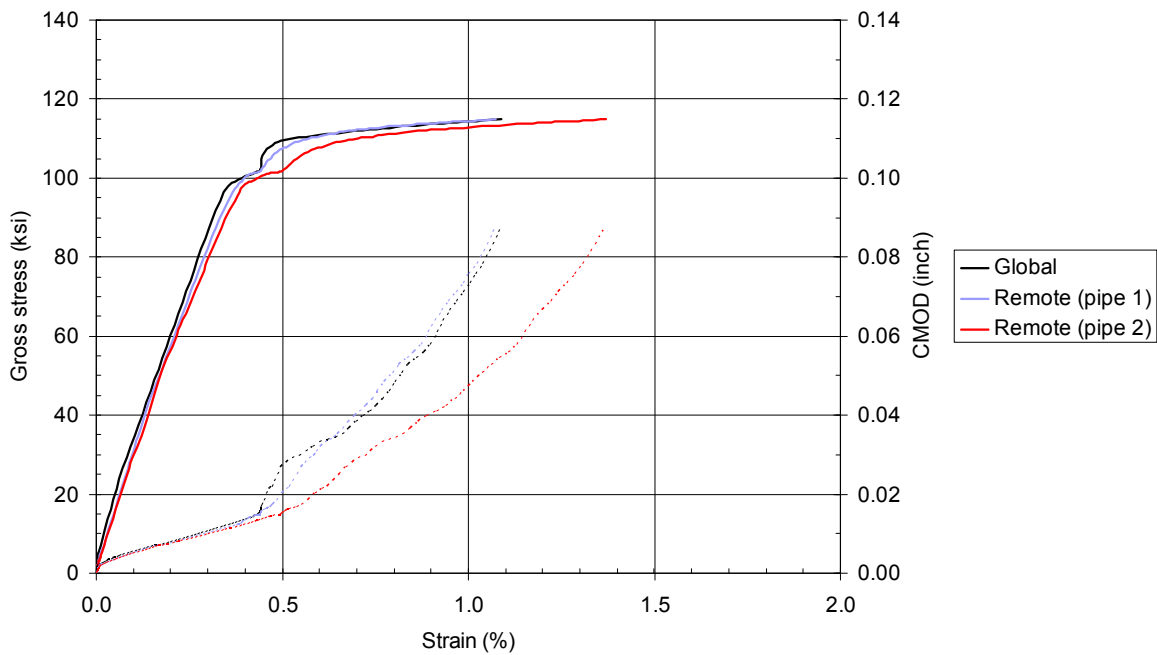
Figure E64 Weld A46, CWP specimen A46-WP-H1: Fracture face, weld metal side showing section location



U-Gent photo ID: dsc-1238 (Magnification: x 5.0)

Notes: Defect tip located in the coarse grained (columnar) weld metal, -0.030in (-0.75mm) from the fusion line. Slow stable crack growth in the weld metal, propagating towards the fusion line.

Figure E65 Weld A46, CWP specimen A46-WP-H1: Position of tip of machined defect (sectioned taken mid-way along the length of the defect)



Notes: Surface notch at the weld root, sampling the HAZ of Pipe 1, with dimensions length x height; 3 x 0.118in (75 x 3mm). Tested at -4°F (-20°C)

Figure E66 Weld A46: CWP specimen A46-WP-H2



U-Gent photo ID: dsc-953-1

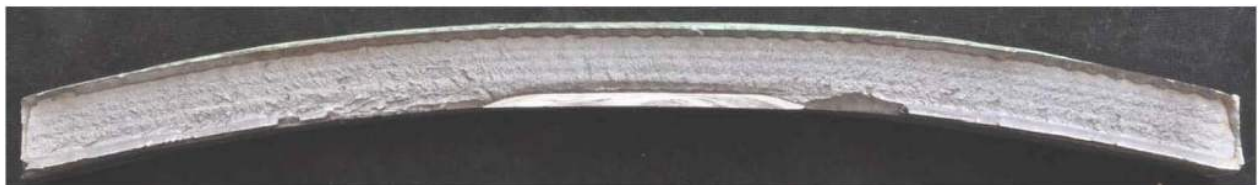
(a) Side: weld cap



U-Gent photo ID: dsc-950-1

(b) Side: weld root

Figure E67 Weld A46: Macro photograph of tested CWP specimen A46-WP-H2



U-Gent photo ID: dsc-295-1

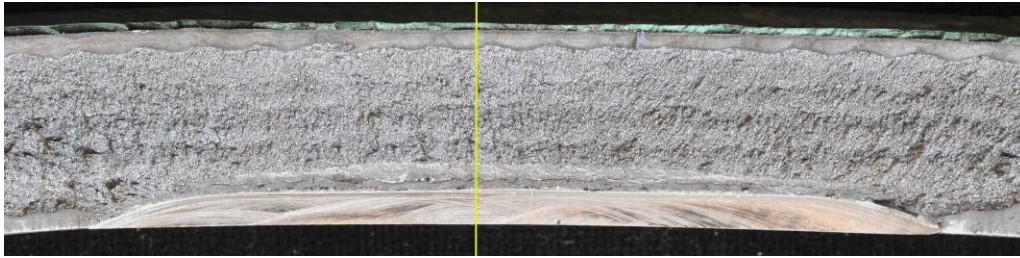
(a) Side: weld



U-Gent photo ID: dsc-296-1

(b) Side: pipe

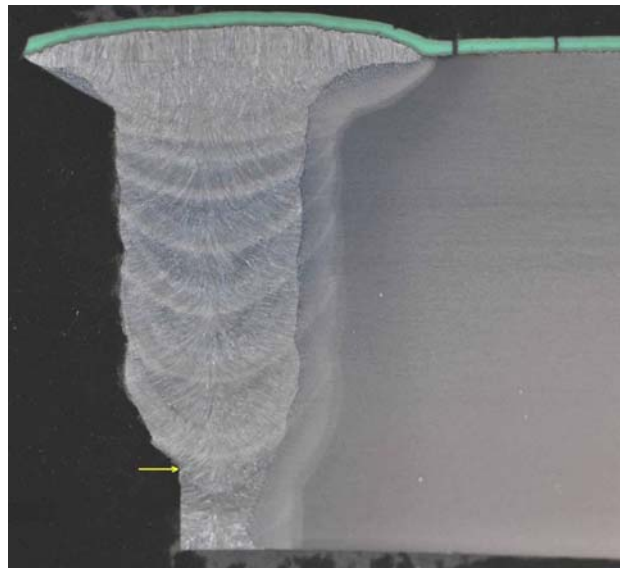
Figure E68 Weld A46: Macro photograph showing fracture faces of tested CWP specimen A46-WP-H2



U-Gent photo ID: dsc-982-2 (Magnification: x 1.5)

Notes: Section through fracture initiation point

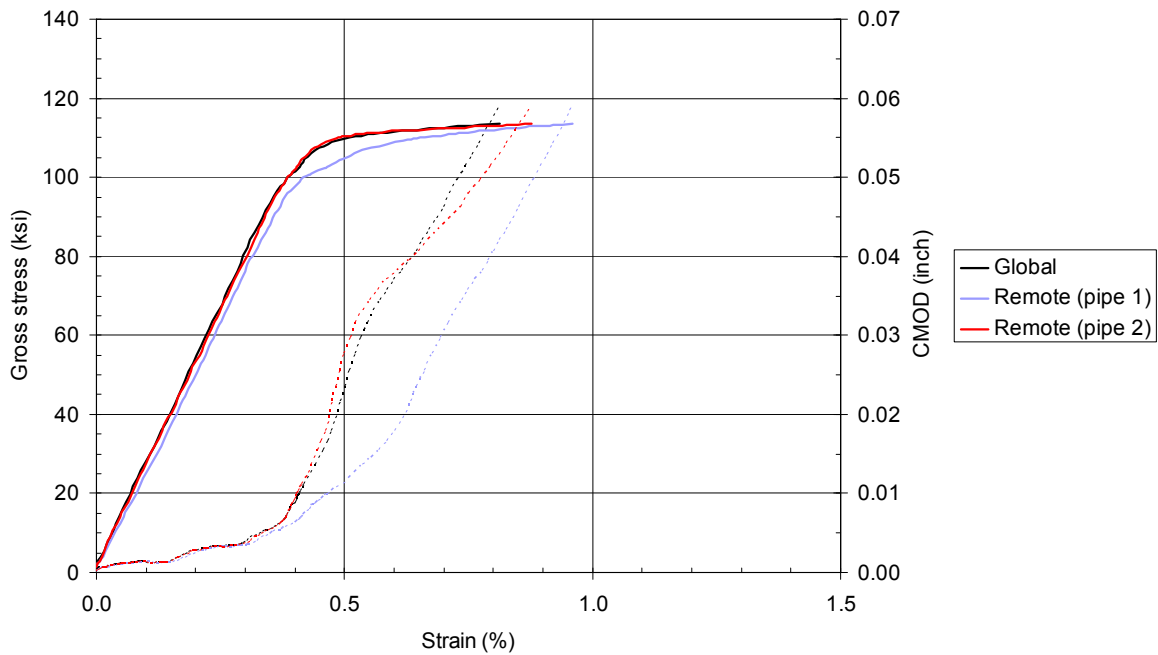
Figure E69 Weld A46, CWP specimen A46-WP-H2: Fracture face, weld metal side showing section location



U-Gent photo ID: dsc-1240 (Magnification: x 4.0)

Notes: Defect tip located in the coarse grained (columnar) weld metal, -0.008in (-0.20mm) from the fusion line. Slow stable crack growth in the weld metal, propagating towards the fusion line.

Figure E70 Weld A46, CWP specimen A46-WP-H2: Position of tip of machined defect (sectioned taken at fracture initiation point)



Notes: Surface notch at the weld root, sampling the HAZ of Pipe 1, with dimensions length x height; 4 x 0.118in (100 x 3mm). Tested at -4°F (-20°C)

Figure E71 Weld A46: CWP specimen A46-WP-H3



U-Gent photo ID: dsc-945-1

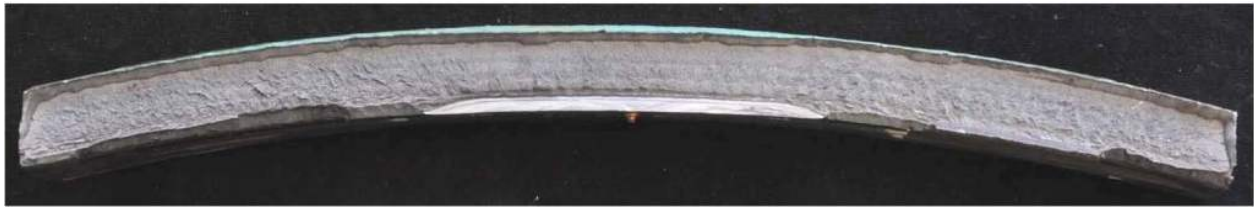
(a) Side: weld cap



U-Gent photo ID: dsc-942-1

(b) Side: weld root

Figure E72 Weld A46: Macro photograph of tested CWP specimen A46-WP-H3



U-Gent photo ID: dsc-309-1

(a) Side: weld



U-Gent photo ID: dsc-310-1

(b) Side: pipe

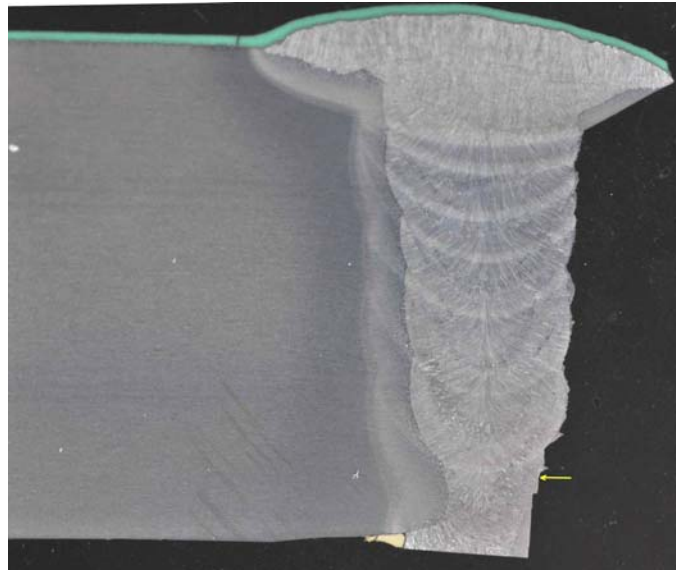
Figure E73 Weld A46: Macro photograph showing fracture faces of tested CWP specimen A46-WP-H3



U-Gent photo ID: dsc-308-2 (Magnification: x 1.2)

Notes: Section through fracture initiation point

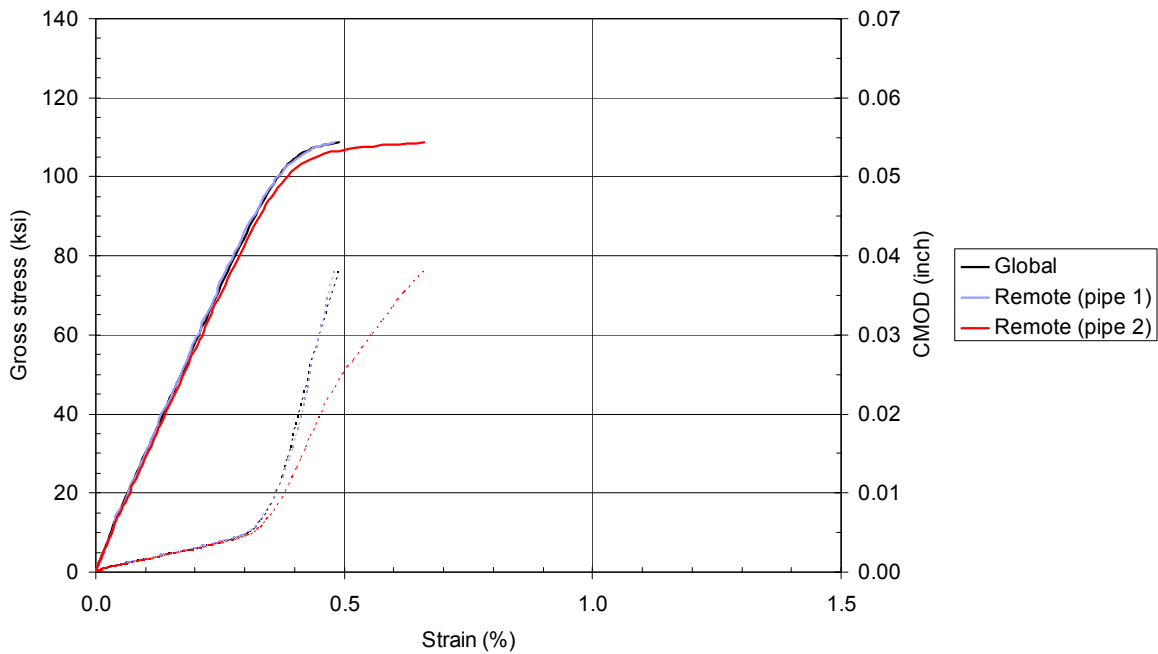
Figure E74 Weld A46, CWP specimen A46-WP-H3: Fracture face, weld metal side showing section location



U-Gent photo ID: dsc-1242 (Magnification: x 5.0)

Notes: Defect tip located in the coarse grained (CG) HAZ microstructure, on the fusion line.

Figure E75 Weld A46, CWP specimen A46-WP-H3: Position of tip of machined defect (sectioned taken at fracture initiation point)



Notes: Surface notch at the weld root, sampling the HAZ of Pipe 1, with dimensions length x height; 4 x 0.157in (100 x 4mm). Tested at -4°F (-20°C)

Figure E76 Weld A46: CWP specimen A46-WP-H4



U-Gent photo ID: dsc-538-1

(a) Side: weld cap



U-Gent photo ID: dsc-535-1

(b) Side: weld root

Figure E77 Weld A46: Macro photograph of tested CWP specimen A46-WP-H4



U-Gent photo ID: dsc-545-1

(a) Side: weld



U-Gent photo ID: dsc-552-1

(b) Side: pipe

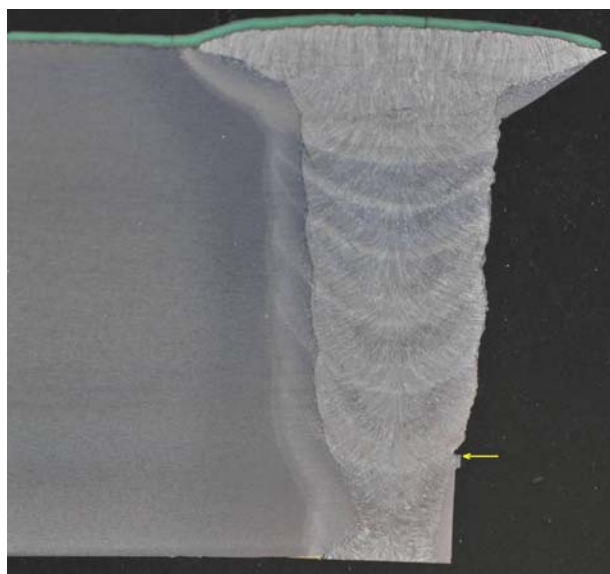
Figure E78 Weld A46: Macro photograph showing fracture faces of tested CWP specimen A46-WP-H4



U-Gent photo ID: dsc-544-2 (Magnification: x 1.2)

Notes: Section through fracture initiation point

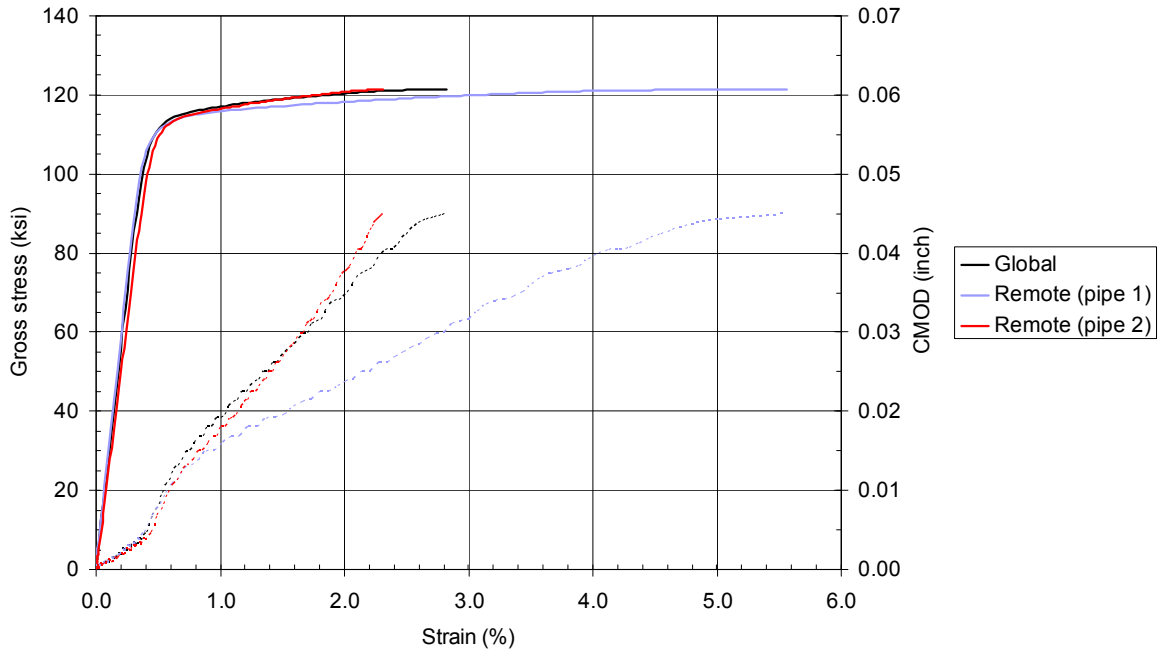
Figure E79 Weld A46, CWP specimen A46-WP-H4: Fracture face, weld metal side showing section location



U-Gent photo ID: dsc-1244 (Magnification: x 5.0)

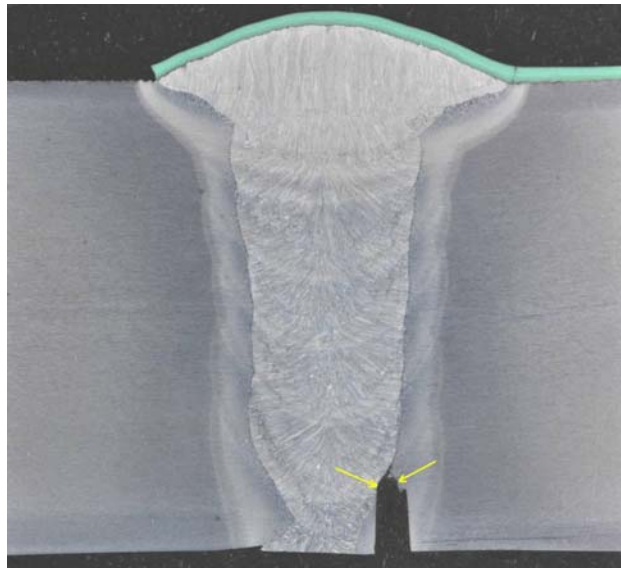
Notes: Defect tip located in the coarse grained (CG) HAZ microstructure, +0.008in (+0.20mm) from the fusion line.

Figure E80 Weld A46, CWP specimen A46-WP-H4: Position of tip of machined defect (sectioned taken at fracture initiation point)



Notes: Surface notch at the weld root, sampling the HAZ of Pipe 1, with dimensions length x height; 2 x 0.118in (50 x 3mm). Tested at -4°F (-20°C)

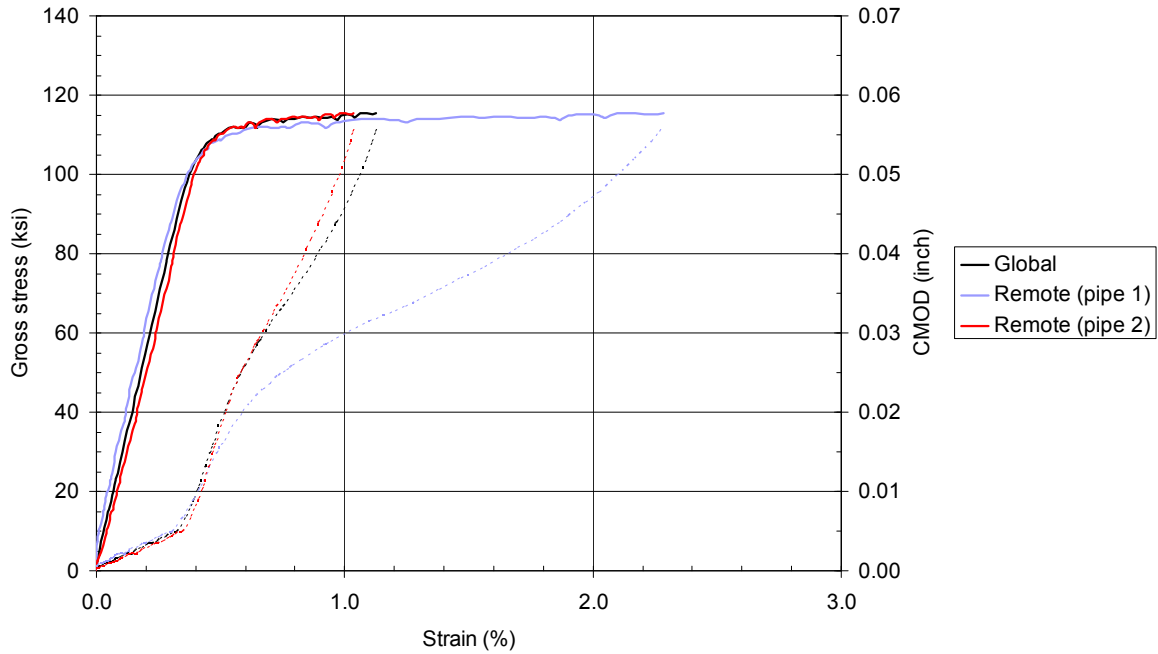
Figure E81 Weld A50: CWP specimen A50-WP-H1



U-Gent photo ID: dsc-1221 (Magnification: x 5.0)

Notes: Specimen did not fail from defect, test terminated. Defect tip located in the coarse grained (CG) HAZ microstructure, on the fusion line.

Figure E82 Weld A50, CWP specimen A50-WP-H1: Position of tip of machined defect (sectioned taken mid-way along the length of the defect)



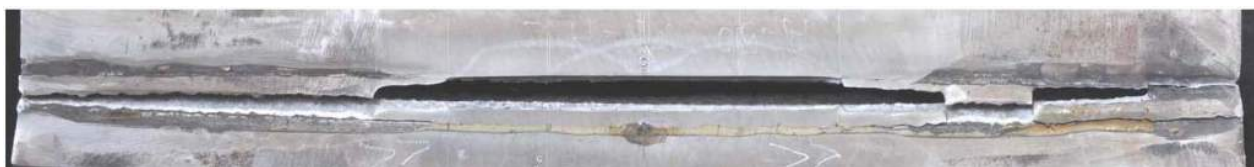
Notes: Surface notch at the weld root, sampling the HAZ of Pipe 1, with dimensions length x height; 4 x 0.157in (100 x 4mm).
Tested at -4°F (-20°C)

Figure E83 Weld A50: CWP specimen A50-WP-H2



U-Gent photo ID: dsc-715-1

(a) Side: weld cap



U-Gent photo ID: dsc-711-1

(b) Side: weld root

Figure E84 Weld A50: Macro photograph of tested CWP specimen A50-WP-H2



U-Gent photo ID: dsc-717-1

(a) Side: weld



U-Gent photo ID: dsc-721-1

(b) Side: pipe

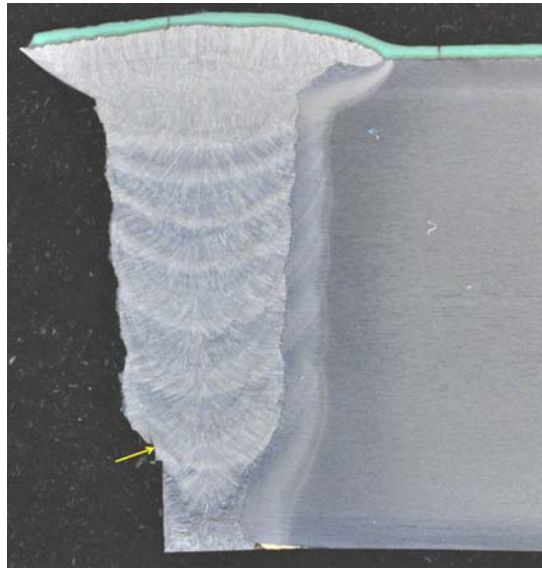
Figure E85 Weld A50: Macro photograph showing fracture faces of tested CWP specimen A50-WP-H2



U-Gent photo ID: dsc-718-2 (Magnification: x 1.2)

Notes: Section through fracture initiation point

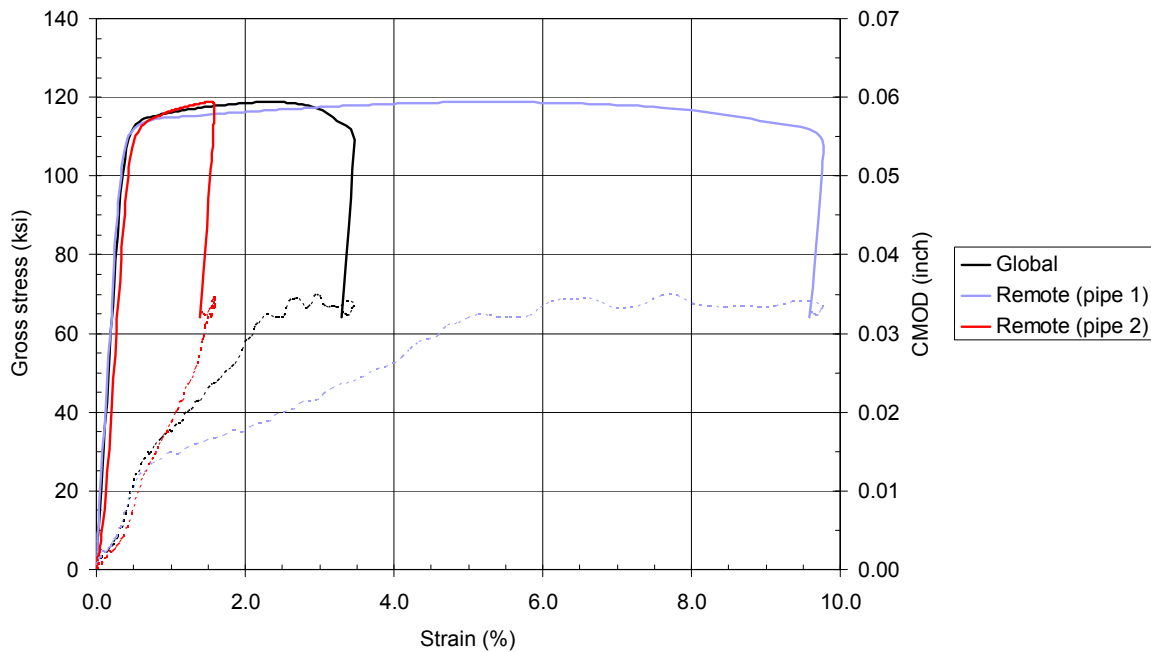
Figure E86 Weld A50, CWP specimen A50-WP-H2: Fracture face, weld metal side showing section location



U-Gent photo ID: dsc-1222 (Magnification: x 5.0)

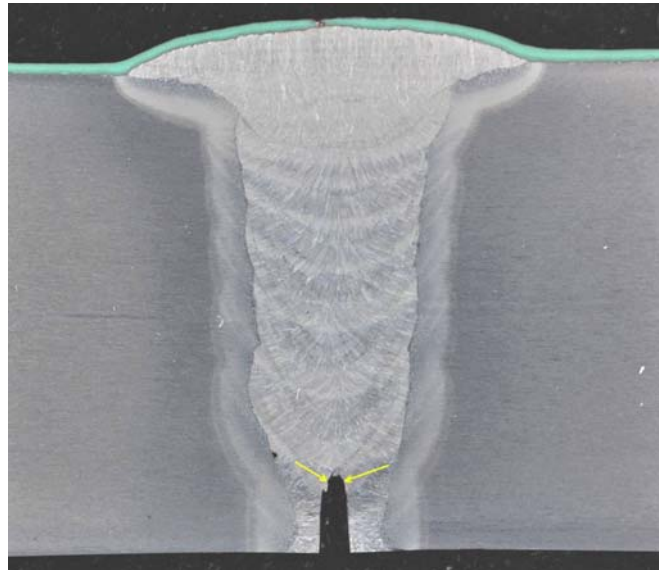
Notes: Defect tip located in the coarse grained (columnar) weld metal, -0.004in (-0.10mm) from the fusion line. Slow stable crack growth in the weld metal, propagating towards the fusion line.

Figure E87 Weld A50, CWP specimen A50-WP-H2: Position of tip of machined defect (sectioned taken at fracture initiation point)



Notes: Surface notch at the weld root, sampling all weld metal, with dimensions length x height; 2 x 0.118in (50 x 3mm). Tested at -4°F (-20°C)

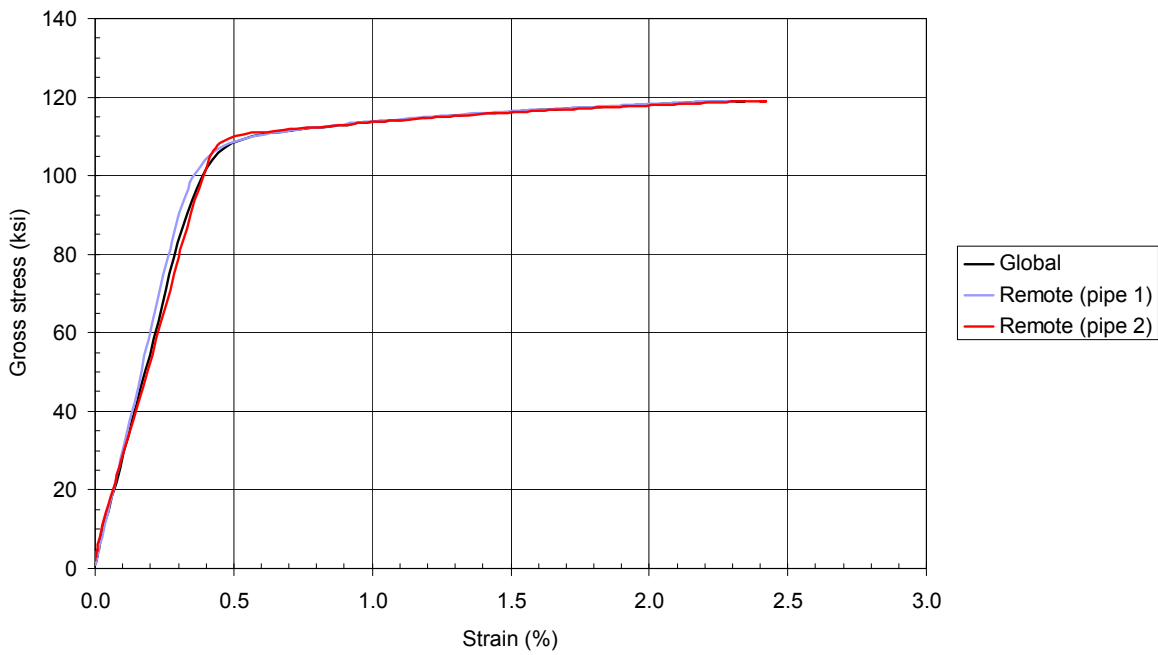
Figure E88 Weld A50: CWP specimen A50-WP-W



U-Gent photo ID: dsc-1220 (Magnification: x 5.0)

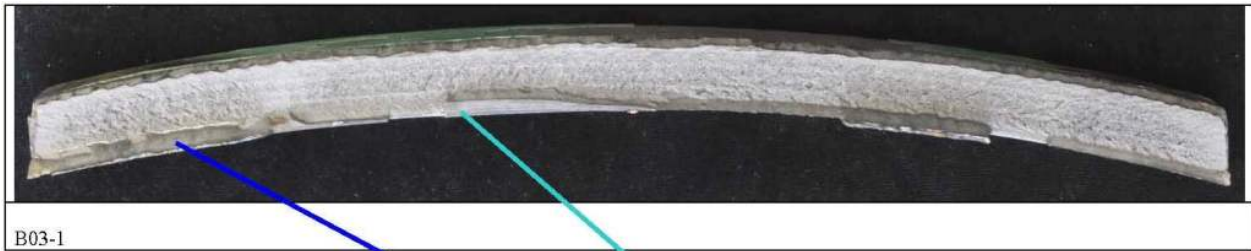
Notes: Specimen did not fail from defect, test terminated. Defect tip located in the coarse grained (CG) and grain refined weld metal.

Figure E89 Weld A50, CWP specimen A50-WP-W: Position of tip of machined defect (sectioned taken mid-way along the length of the defect)



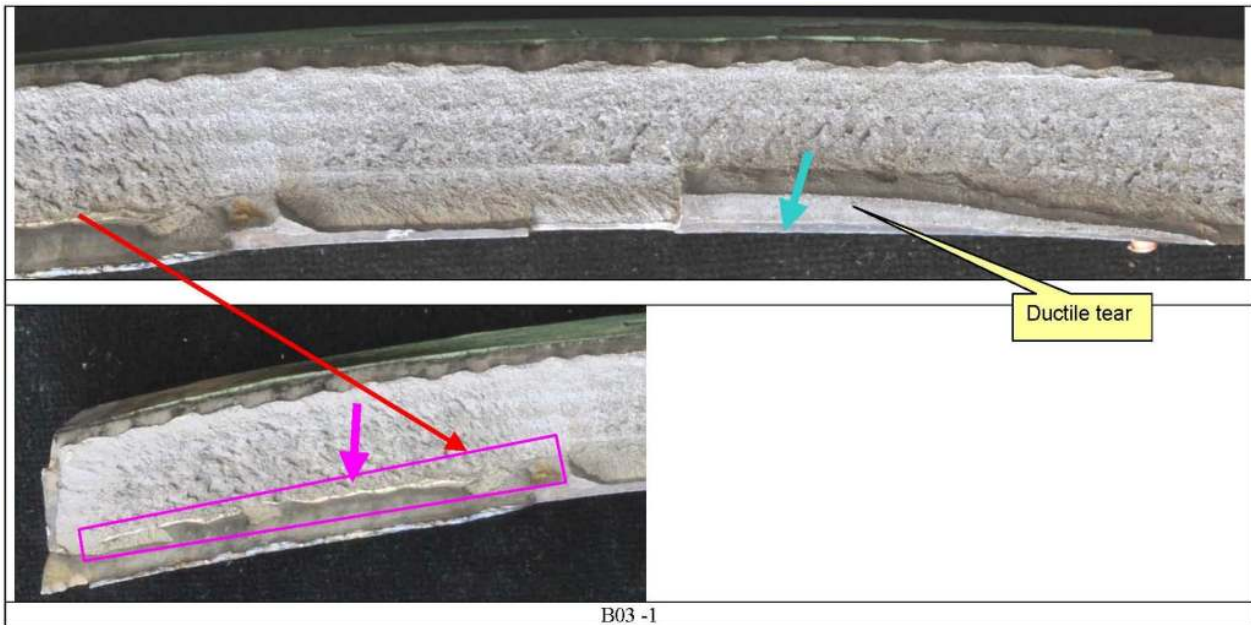
Notes: Defect details in Figure E91. Specimen tested at -4°F (-20°C)

Figure E90 Weld B03: CWP specimen B03-WP1



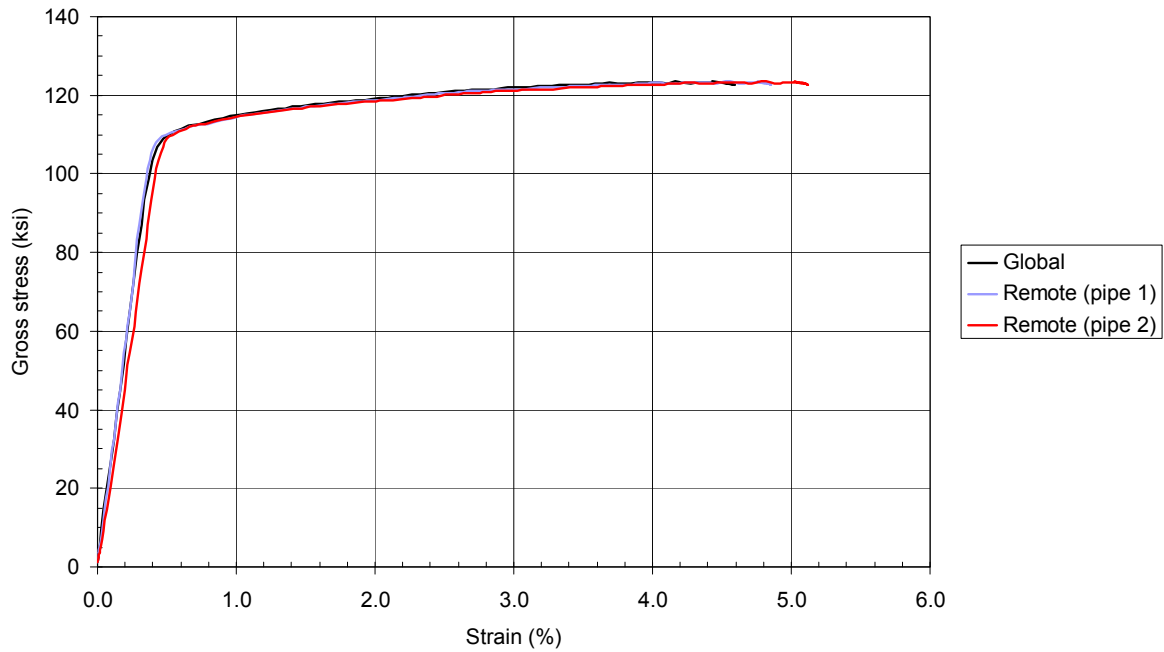
Type of defect (B03-1)		Reported (X-Ray and AUT)			Observed (CWP test)		
		l	h	d	l	h	d
LORP	X-Ray	-	-	-	95.0	2.1	19.8
	AUT	97.0	1.0	20.0			
LOSWF	X-Ray	-	-	-	66.0	2.6	17.8
	AUT	-	-	-			

(a) General overview



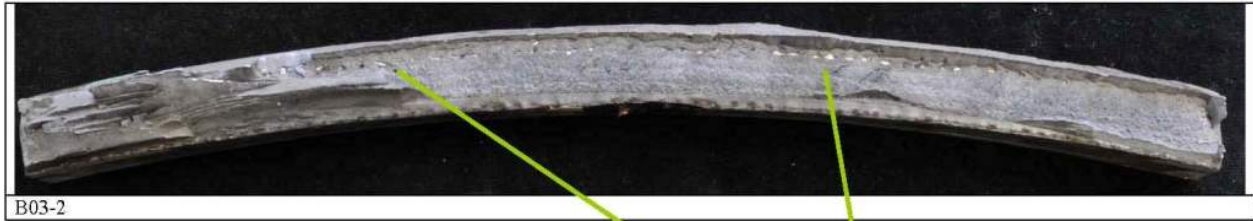
(b) Detail showing defect area

Figure E91 Weld B03: Fracture surface features of tested CWP specimen B03-WP1



Notes: Defect details in Figure E93. Specimen tested at -4°F (-20°C)

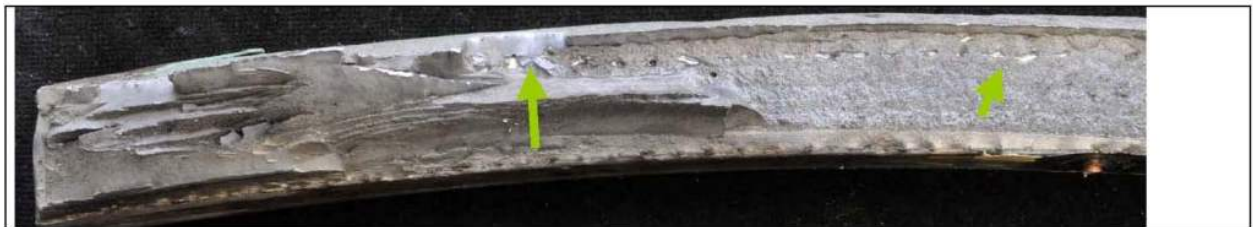
Figure E92 Weld B03: CWP specimen B03-WP2



B03-2

Type of defect (B03-2)		Reported			Observed (CWP test)		
		l	h	d	l	h	d
LOSWF (intermittent / hot pass)	X-Ray	190	-	-	202.0	1.7	9.0
	AUT	-	-	-			

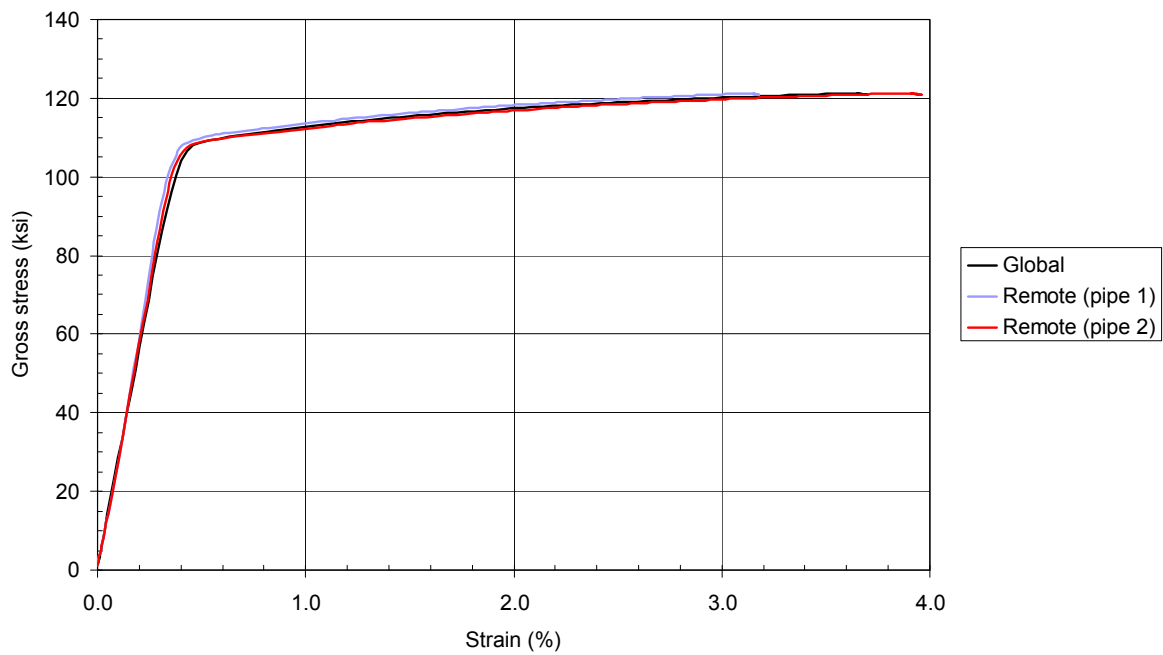
(a) General overview



B03-2

(b) Detail showing defect area

Figure E93 Weld B03: Fracture surface features of tested CWP specimen B03-WP2



Notes: Defect details in Figure E95. Specimen tested at -4°F (-20°C)

Figure E94 Weld B03: CWP specimen B03-WP3



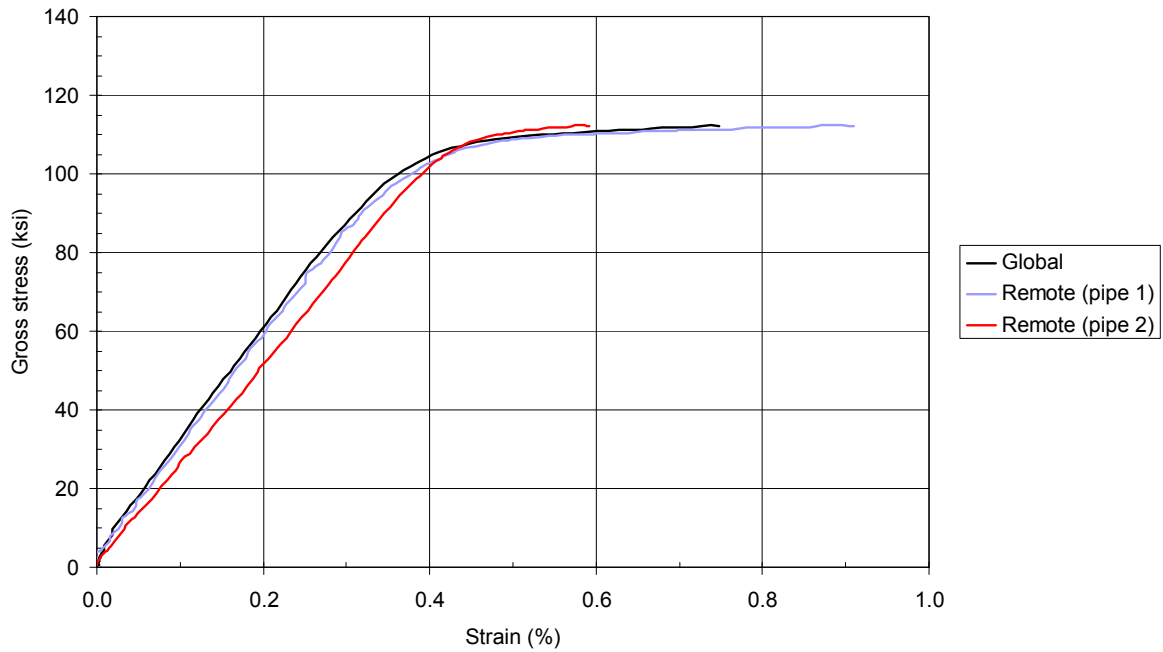
Type of defect (B03-3)		Reported			Observed (CWP test)		
		l	h	d	l	h	d
LOSWF and porosity	X-Ray	110	-	-	115.5	6.5	14.4
	AUT	112	4.0	13.0			
Remarks					h = containment rectangle Porosity / no LOSWF		

(a) General overview



(b) Detail showing defect area

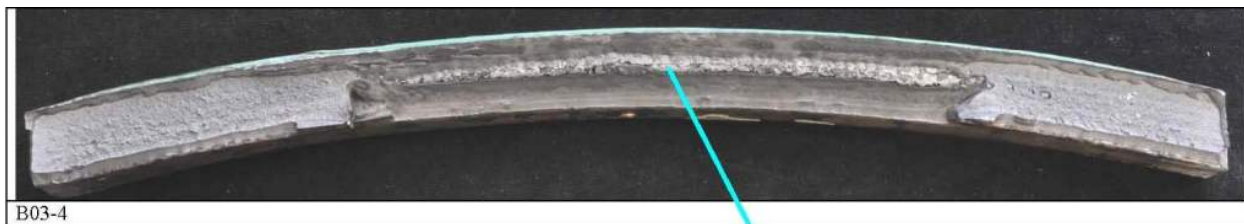
Figure E95 Weld B03: Fracture surface features of tested CWP specimen B03-WP3



Notes: Defect details in Figure E97. Specimen tested at -4°F (-20°C)

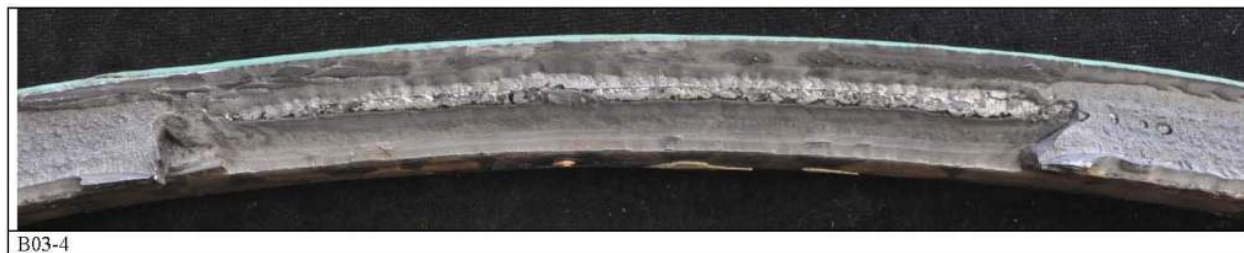
Figure E96 Weld B03: CWP specimen B03-WP4

Report Number: 10361
Issue: 1.0



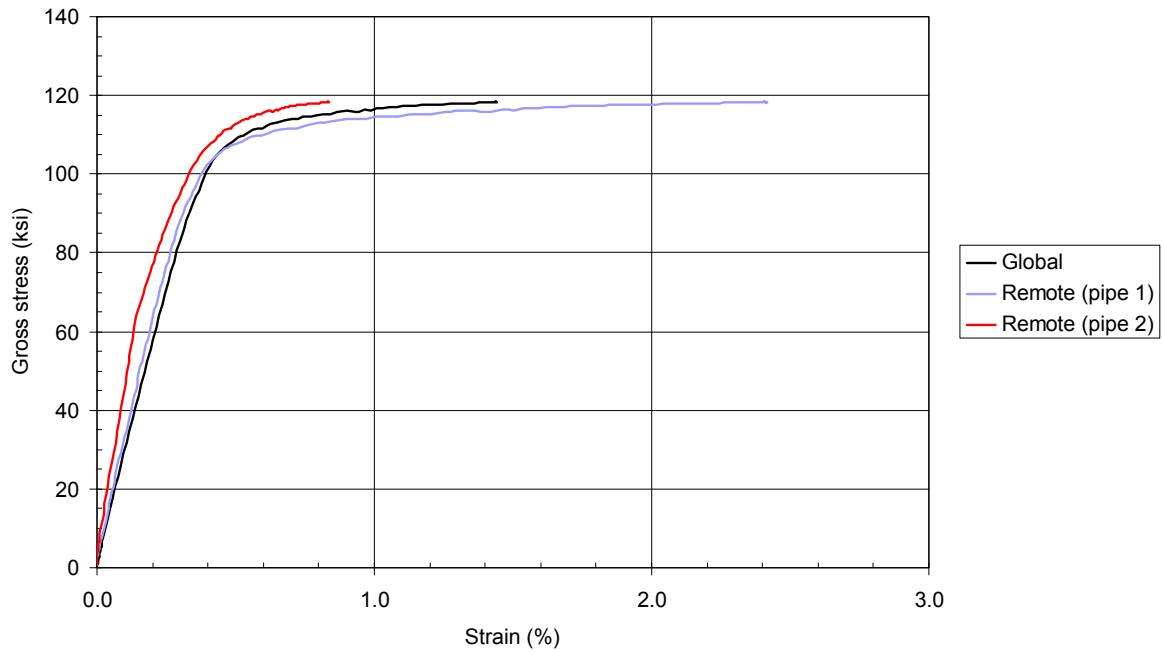
Type of defect (B03-4)		Reported			Observed (CWP test)		
		l	h	d	l	h	d
LOSF (intermittent)	X-Ray	182?	-	-	146.5	4.4	12.0
	AUT	155	4.0	12.0			

(a) General overview



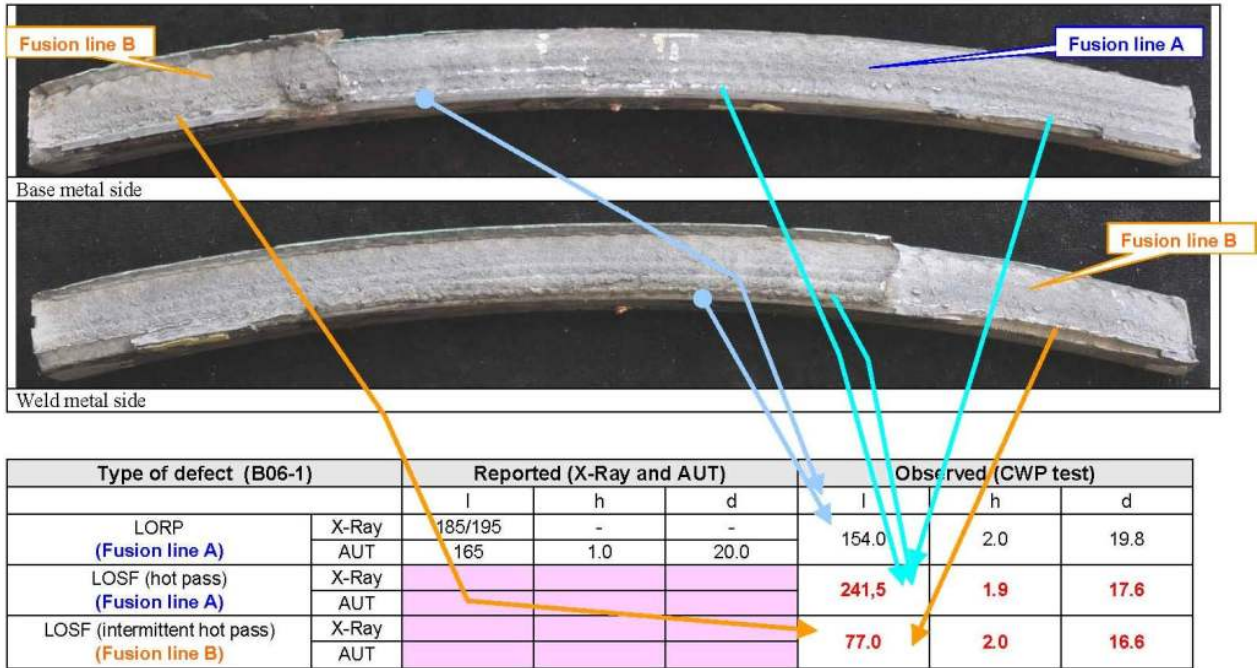
(b) Detail showing defect area

Figure E97 Weld B03: Fracture surface features of tested CWP specimen B03-WP4

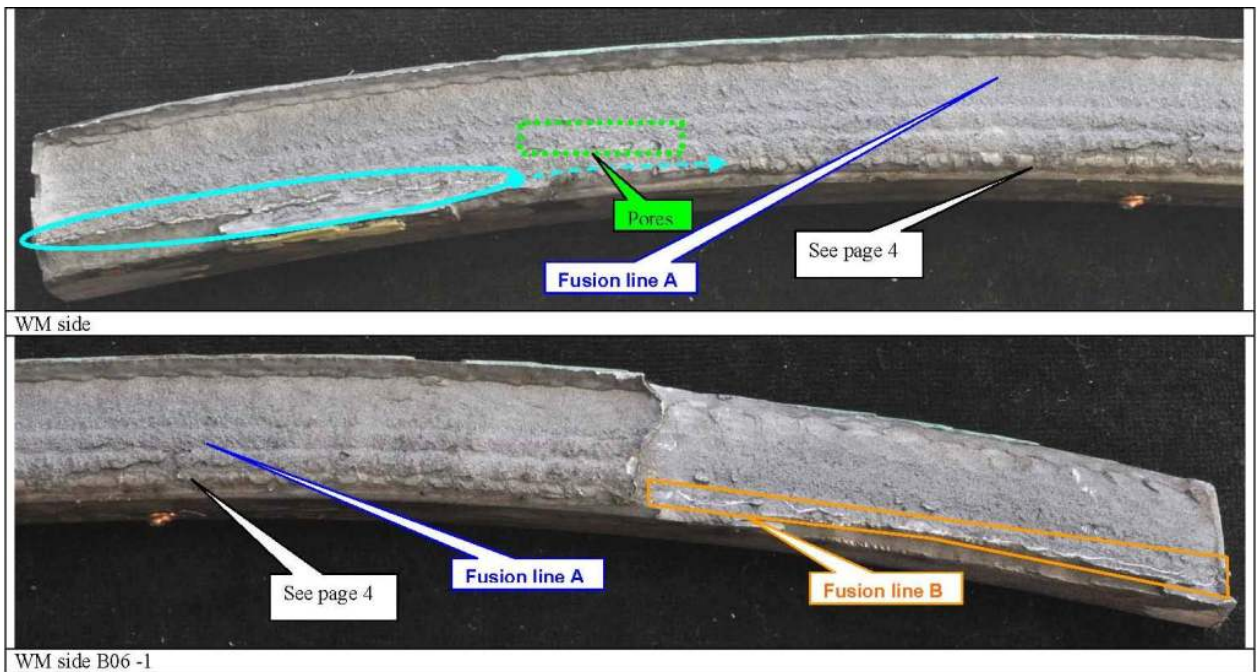


Notes: Defect details in Figure E99 and Figure E100. Specimen tested at -4°F (-20°C)

Figure E98 Weld B06: CWP specimen B06-WP1

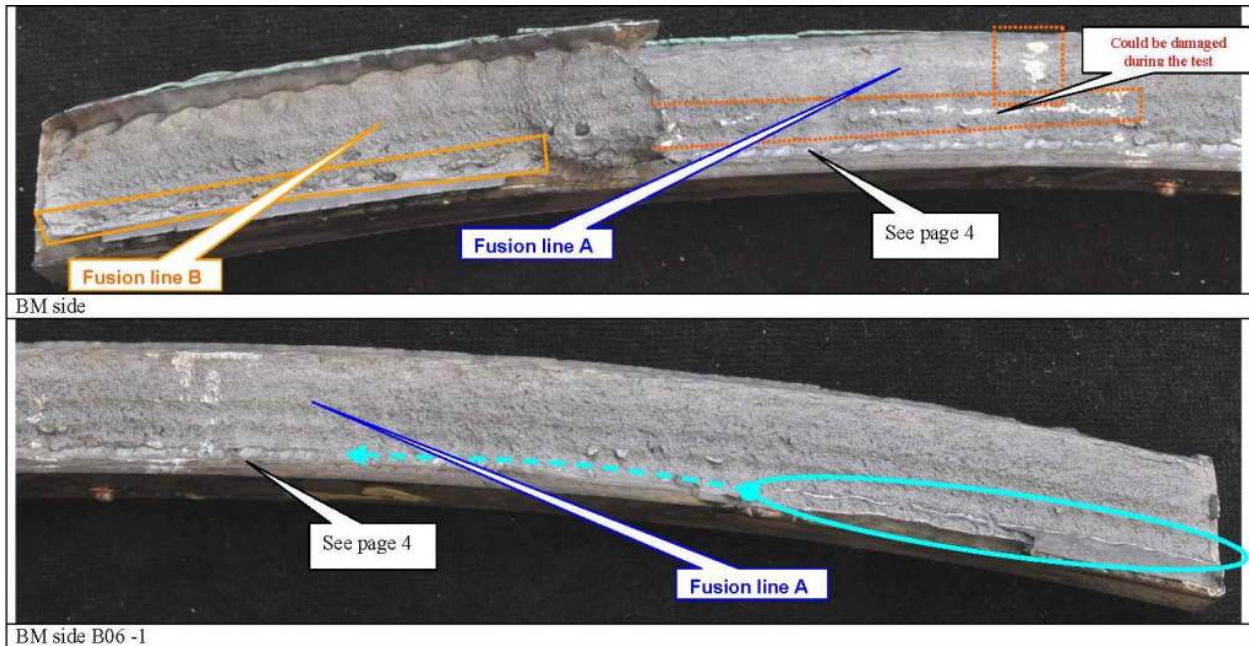


(a) General overview

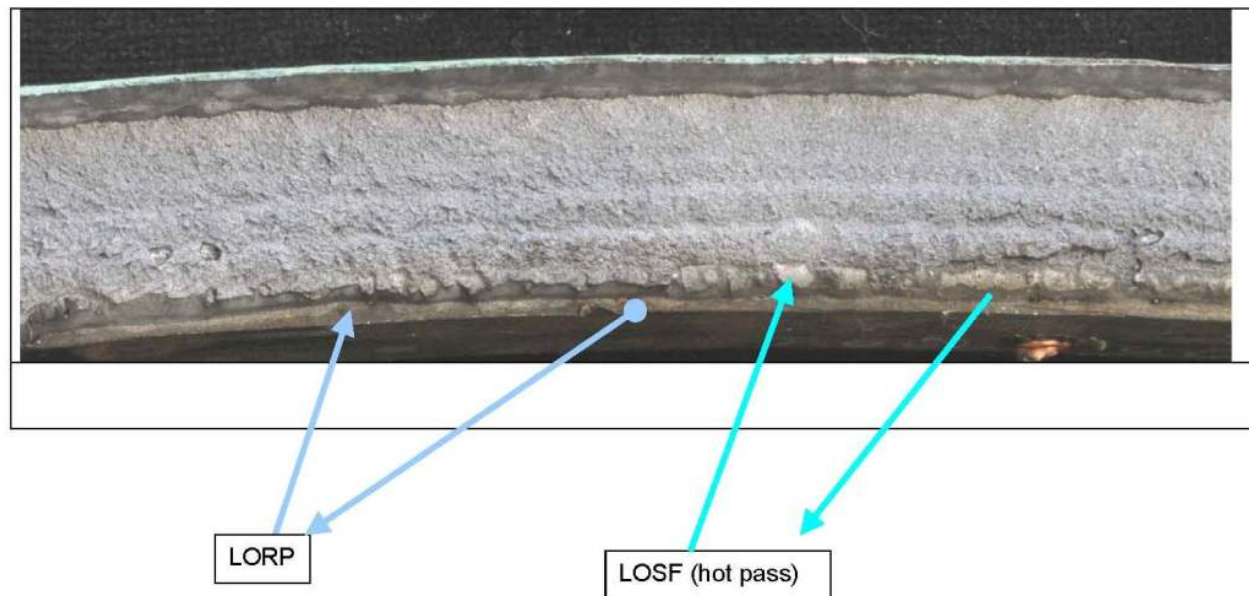


(b) Detail showing defect area

Figure E99 Weld B06: Fracture surface features of tested CWP specimen B06-WP1

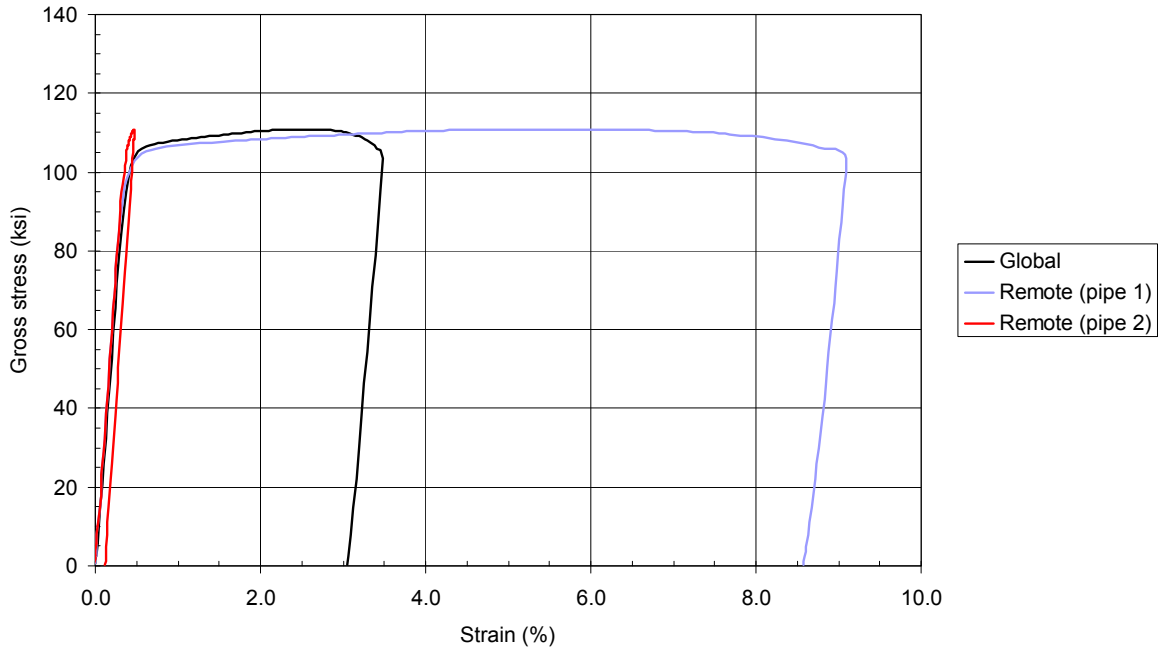


(a) Detail showing defect area



(b) Detail showing defect area

Figure E100 Weld B06: Fracture surface features of tested CWP specimen B06-WP1 (continued)



Notes: Defect details in Figure E102. Specimen tested at -4°F (-20°C)

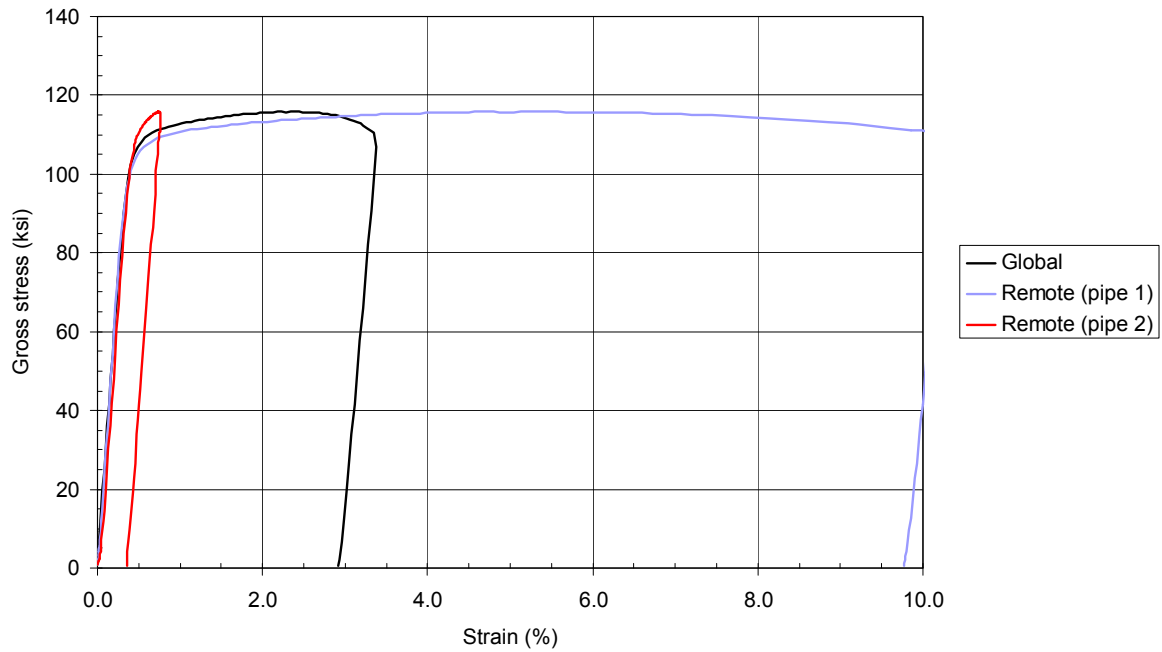
Figure E101 Weld B06: CWP specimen B06-WP2



Type of defect (B06-2)		Reported			Observed (CWP test)		
		l	h	d	l	h	d
UNDERCUT	X-Ray	?	-	-	Specimen didn't fail No undercut detected		
	AUT	-	-	-			

(a) General overview

Figure E102 Weld B06: Overview of CWP specimen B06-WP2 terminated before failure due to excessive strain in Pipe 1



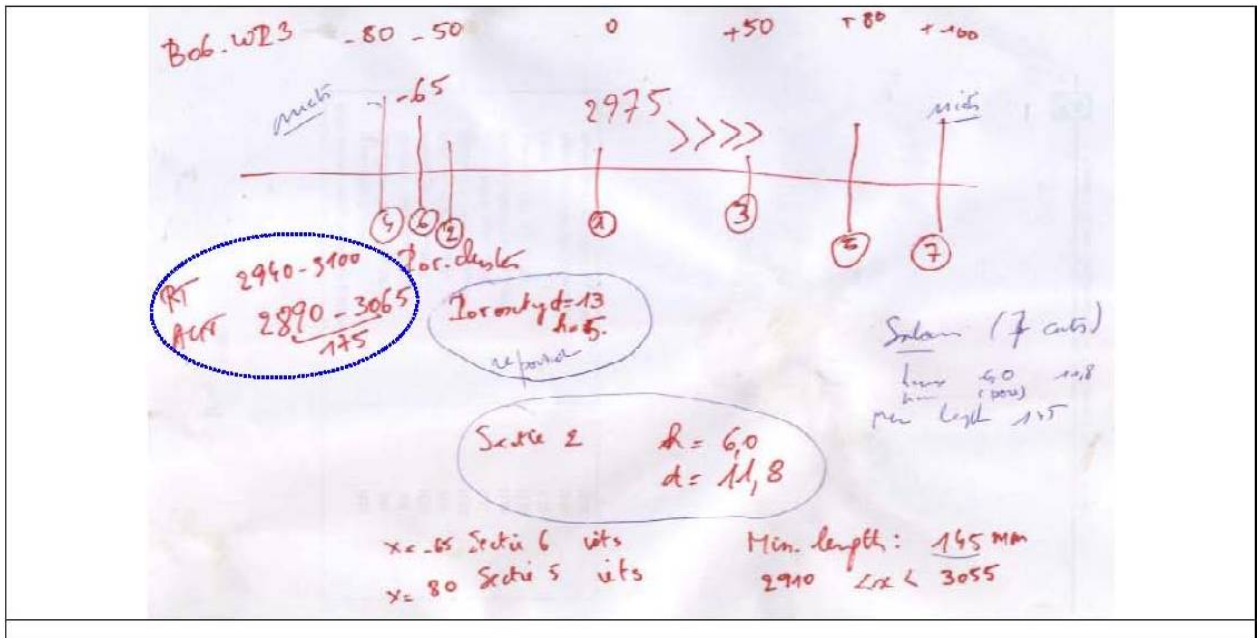
Notes: Defect details in Figure E104. Specimen tested at -4°F (-20°C)

Figure E103 Weld B06: CWP specimen B06-WP3



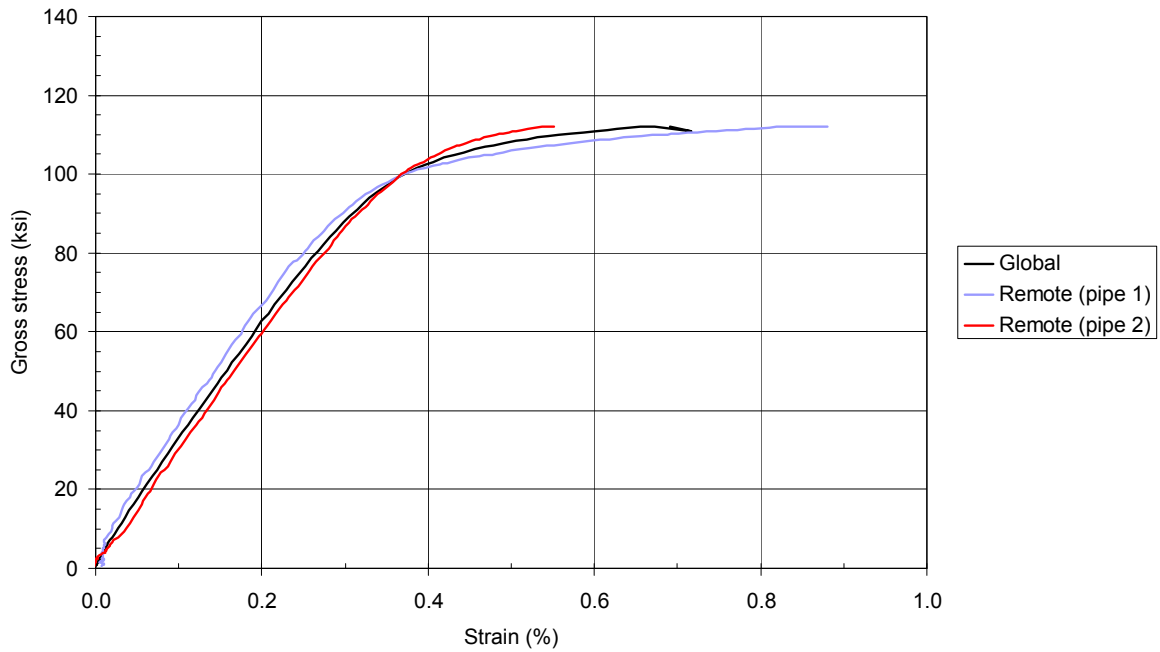
Type of defect (B06-3)		Reported			Observed (CWP test)		
		l	h	d	l	h	d
LOSWF (intermittent) and POROSITY	X-Ray	180 ?	-	-	145	6.0 (max)	11.8
	AUT	175	5.0	13.0	(Minimum)	pores (min)	
Remarks		Specimen didn't fail Salami technique (7 cuts)			See next sheet		

(a) General overview



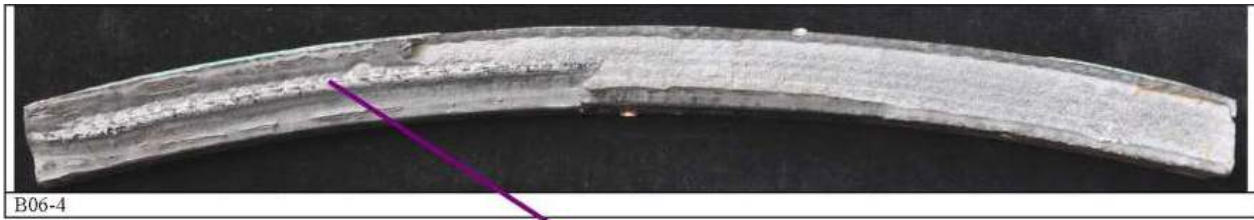
(b) Details of salami sectioning

Figure E104 Weld B06: Overview of CWP specimen B06-WP3 terminated before failure due to excessive strain in Pipe 1



Notes: Defect details in Figure E106. Specimen tested at -4°F (-20°C)

Figure E105 Weld B06: CWP specimen B06-WP4



Type of defect (B06-4)		Reported			Observed (CWP test)		
		l	h	d	l	h	d
LOSF and "volumetric" component	X-Ray	140.0	-	-	144.0	5.0	12.0
	AUT	147.0	4.0	13.0			

(a) General overview

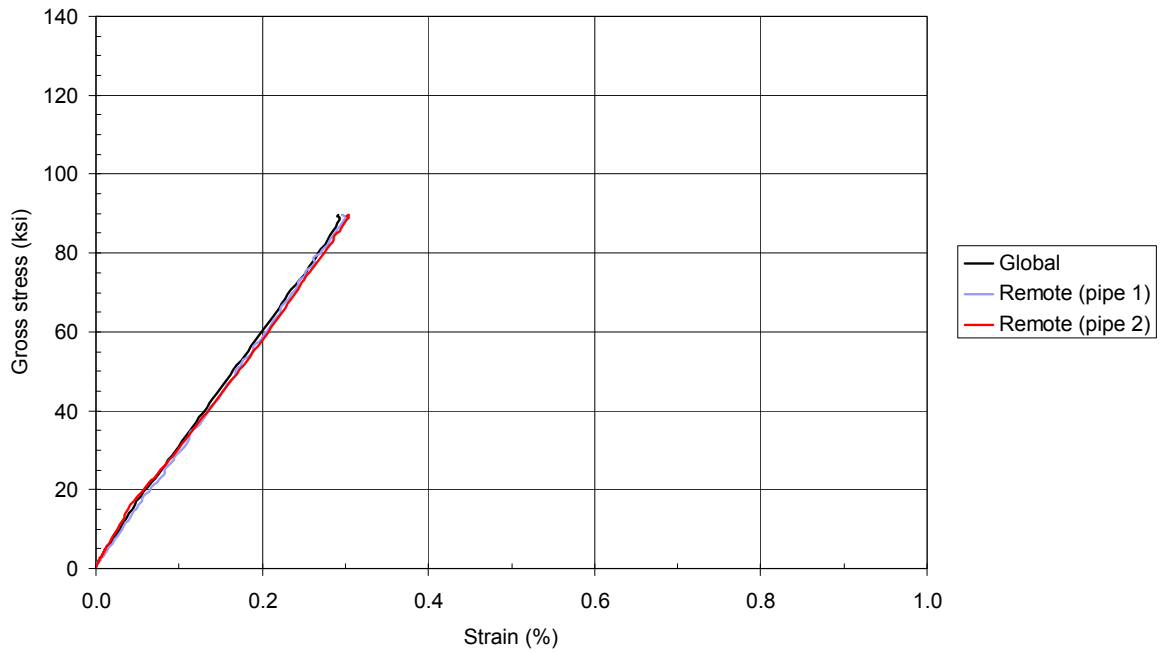


(b) Detail showing defect area (view onto weld side)



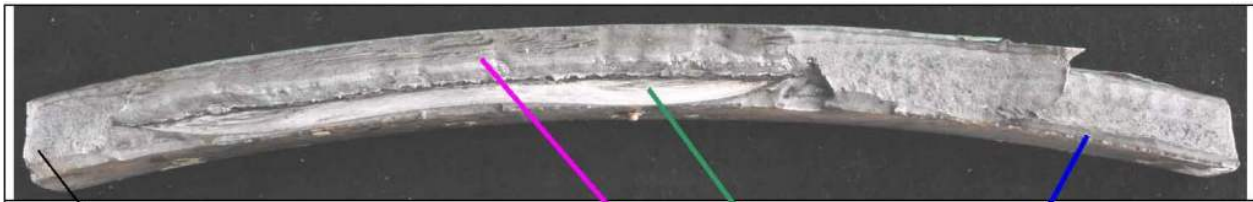
(c) Detail showing defect area (view onto pipe side)

Figure E106 Weld B06: Fracture surface features of tested CWP specimen B06-WP4



Notes: Notes: Defect details in Figure E108. Specimen tested at -4°F (-20°C)

Figure E107 Weld B08: CWP specimen B08-WP1



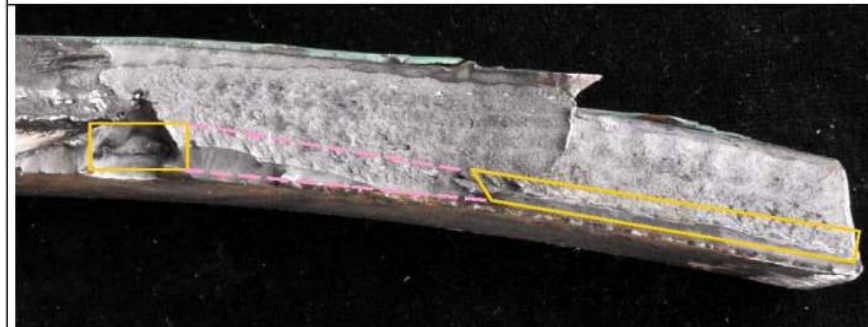
Weld metal side

Type of defect (B08-1)		Reported (X-Ray and AUT)			Observed (CWP test)		
		l	h	d	l	h	d
Disc ground defect (LOSF) and Scattered porosity	X-Ray	170	-	-	173.0	9.0	19.3
	AUT	163.0	7.0	16.0			
LOSWF (hot pass)	X-Ray	-	-	-	61.5 ++	2.9	17.0
	AUT	-	-	-			
LOSF (Intermittent)	X-Ray	-	-	-	148.0	3.6	11.4
	AUT	-	-	-			

(a) General overview



WM side



WM side B08 -1

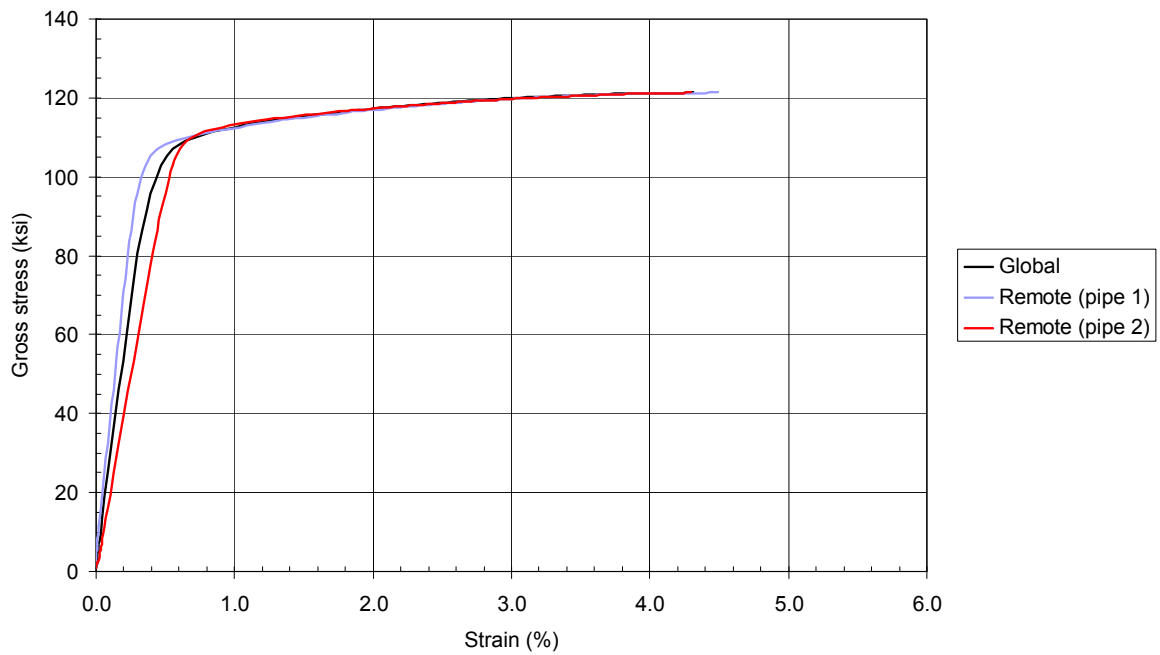
(b) Detail showing defect area (view onto weld side)

Figure E108 Weld B08: Fracture surface features of tested CWP specimen B08-WP1



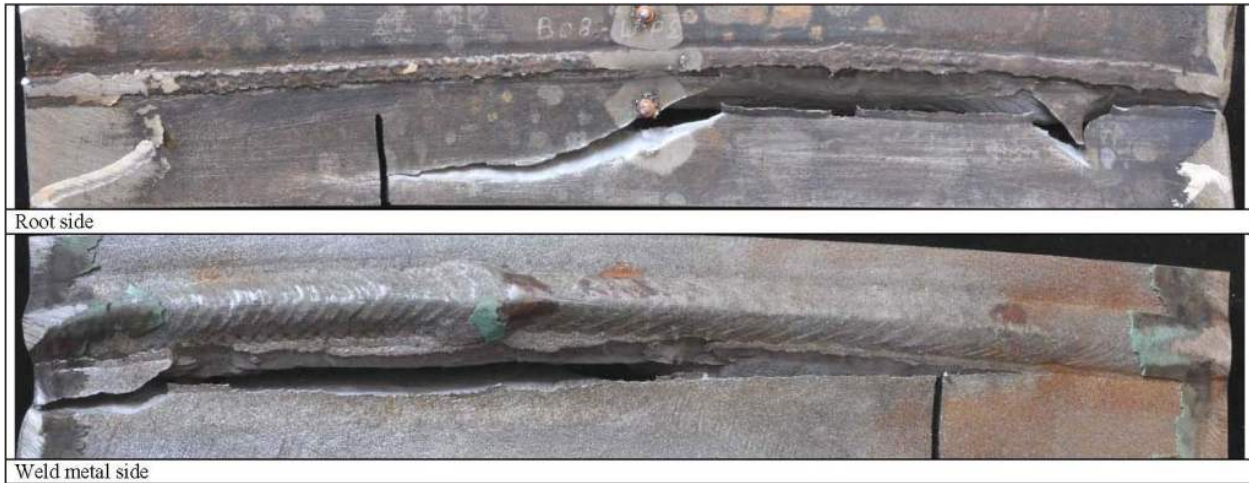
(c) Detail showing defect area (view onto pipe side)

Figure E108 Weld B08: Fracture surface features of tested CWP specimen B08-WP1 (continued)



Notes: Defect details in Figure E110. Specimen tested at -4°F (-20°C)

Figure E109 Weld B08: CWP specimen B08-WP2



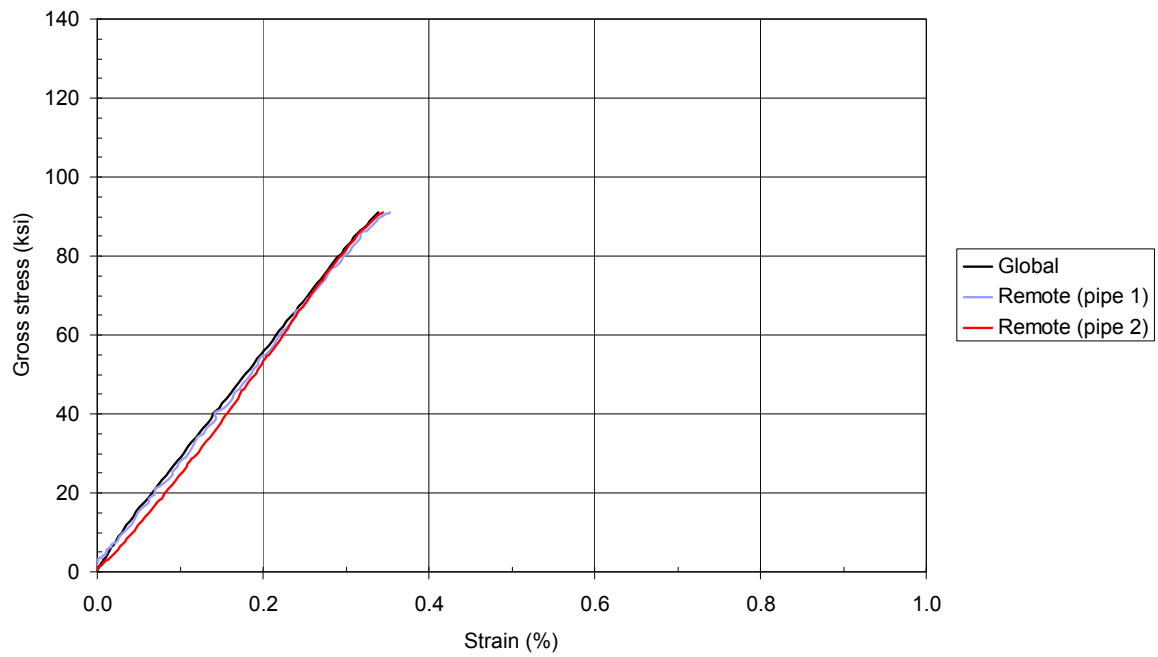
Type of defect (B08-2)		Reported (X-Ray and AUT)			Observed (CWP test)		
		l	h	d	l	h	d
LOSF Intermittent)	X-Ray	160	-	-	No defect found (failure deviated towards pipe metal)		
	AUT	-	-	-			

(a) General overview



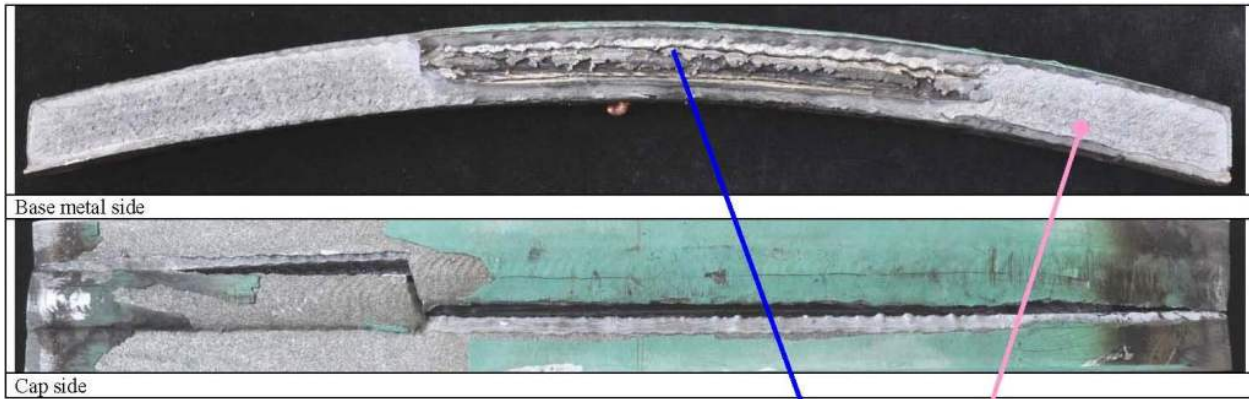
(b) Detail showing defect area

Figure E110 Weld B08: Fracture surface features of tested CWP specimen B08-WP2



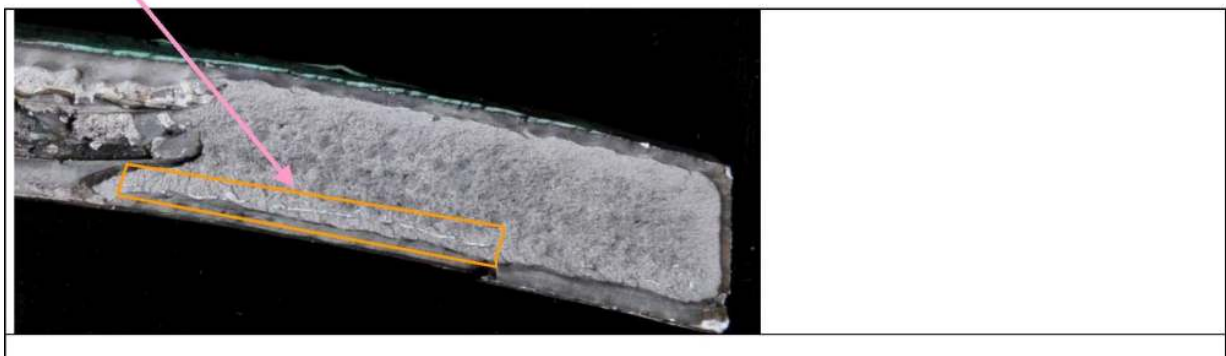
Notes: Defect details in Figure E112. Specimen tested at -4°F (-20°C)

Figure E111 Weld B08: CWP specimen B08-WP3



Type of defect (B08-3)		Reported (X-Ray and AUT)			Observed (CWP test)		
		l	h	d	l	h	d
LOSF (Disc ground)	X-Ray	To be verified	-	-	145.0	10.8	15.0
	AUT	150	10.0	16.0			
LOSF (Intermittent hot pass)	X-Ray	-	-	-	61.5	1.9	17.3
	AUT	-	-	-			

(a) General overview



(b) Detail showing defect area

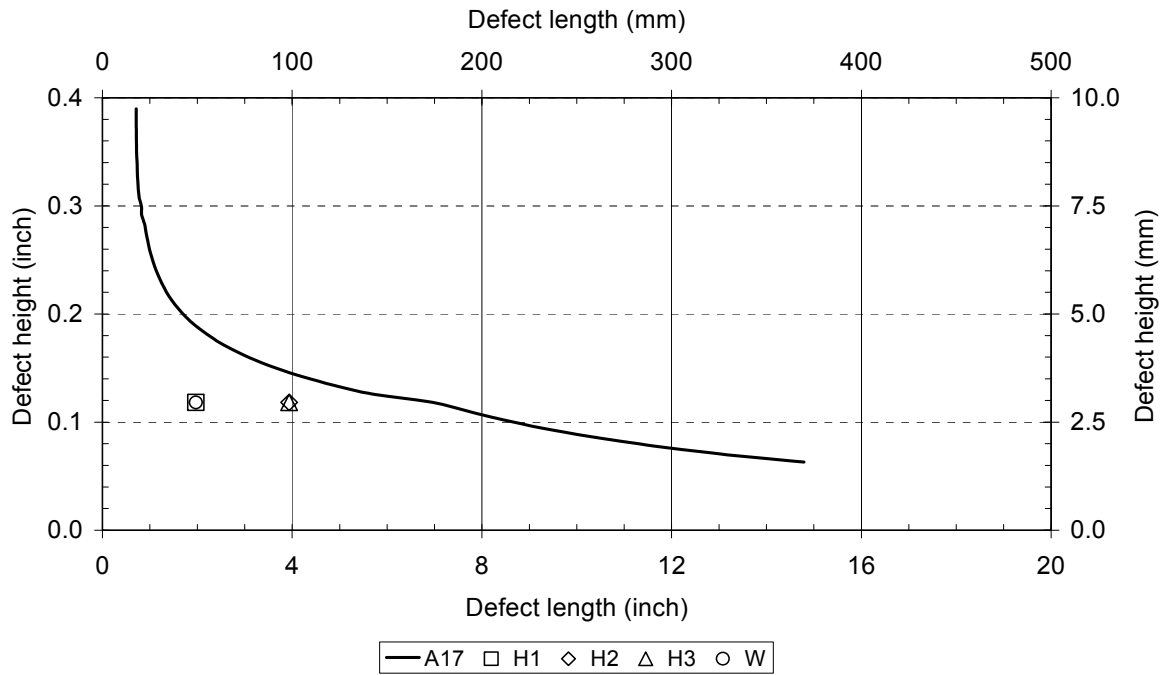
Figure E112 Weld B08: Fracture surface features of tested CWP specimen B08-WP3

Appendix F API 1104 Appendix A, Option 2 Assessments

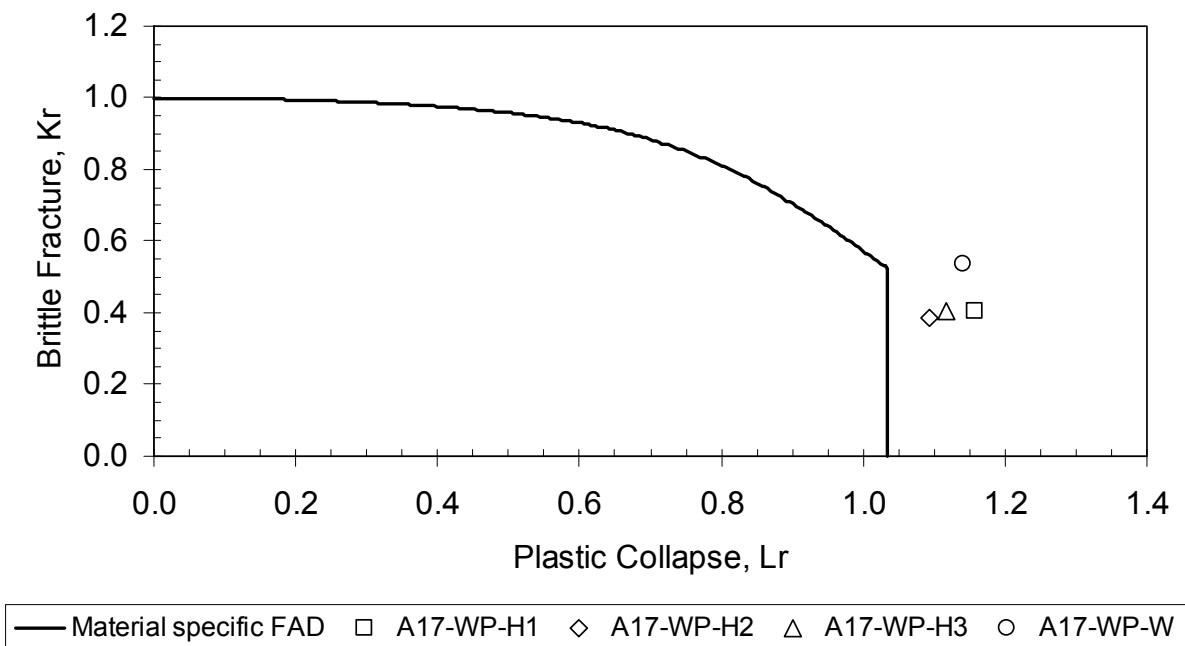
In this appendix the CWP test results are assessed according to API 1104 Option 2 (Section 3.2.1). For each weld, the results of two analyses are presented.

The first graph shows the critical defect sizes (height as a function of length) predicted using the minimum measured tensile properties and CTOD for the weldment, assuming the maximum longitudinal stress to be equal to SMYS. This is used to determine whether the defects tested with the CWP specimens would survive an applied stress in excess of SMYS. Defect sizes within the locus are predicted to fail at stresses in excess of SMYS, while those above are predicted to fail at stresses less than SMYS.

The second graph is an analysis of the actual CWP test results, presented against the FAD specific to the weld. The FAD is based on the minimum measured material properties of the weldment, and a maximum longitudinal stress equivalent to SMYS. An assessment point outside the FAC means a positive margin of safety against failure, while a point inside the FAC means potentially a non-conservative assessment.

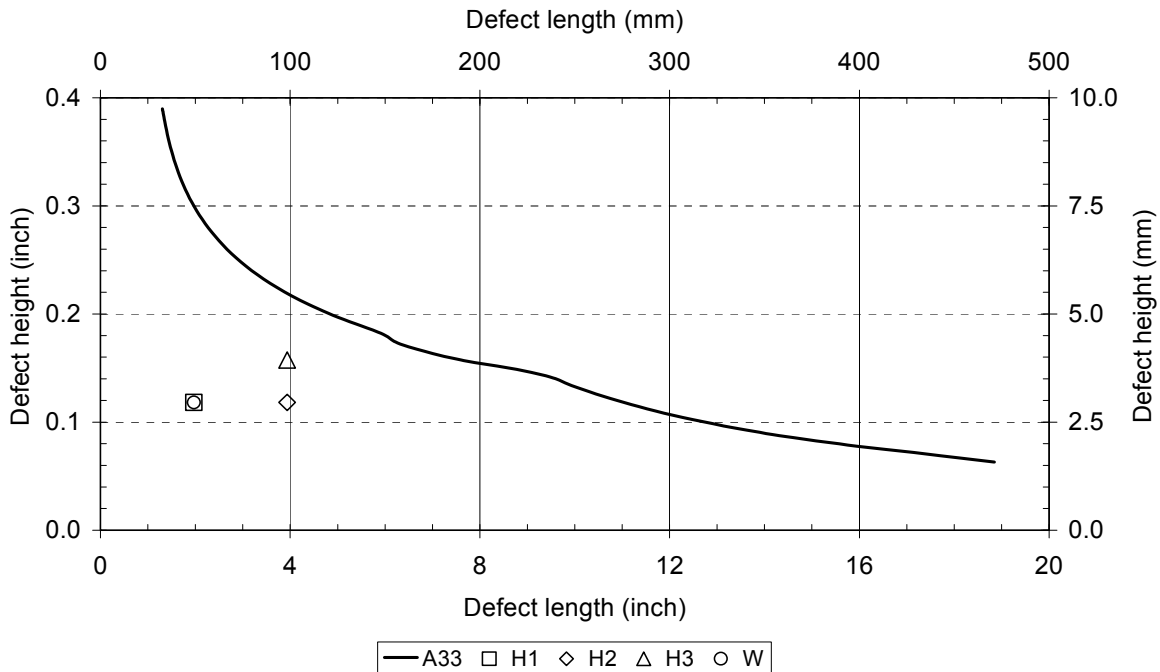


(a) Comparison of maximum allowable defect sizes with the CWP test specimen defects.

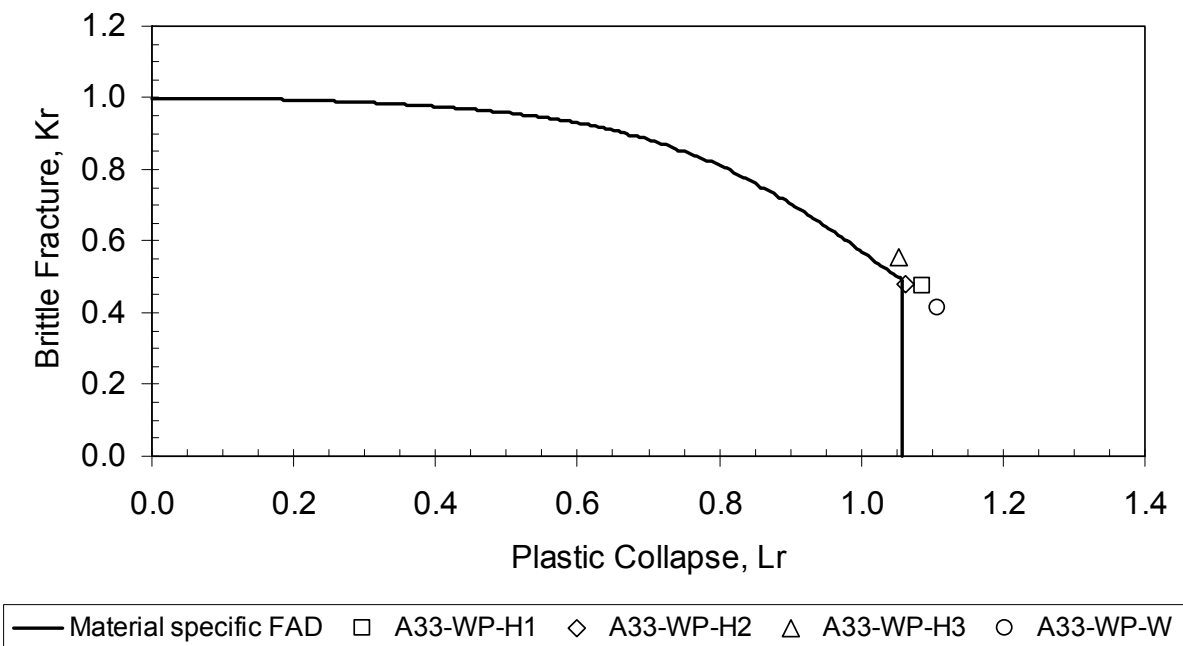


(b) Comparison of the CWP test results with the FAD specific for the weldment.

Figure F1 Weld A17 - API 1104 Option 2 analysis

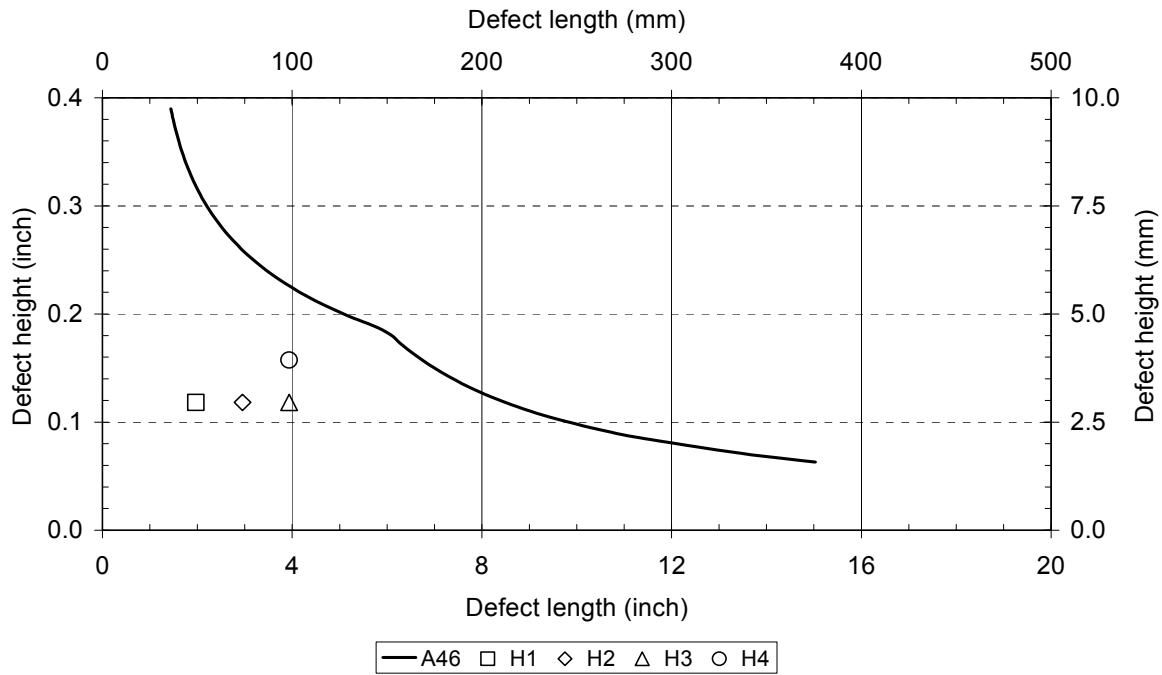


(a) Comparison of maximum allowable defect sizes with the CWP test specimen defects.

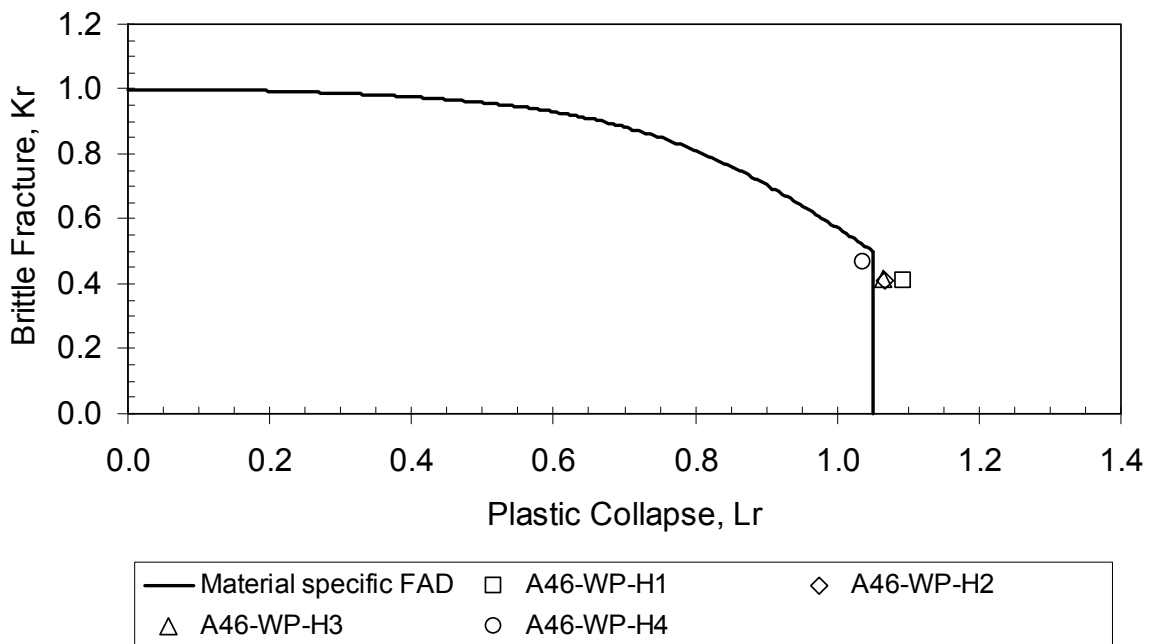


(b) Comparison of the CWP test results with the FAD specific for the weldment.

Figure F2 Weld A33 - API 1104 Option 2 analysis

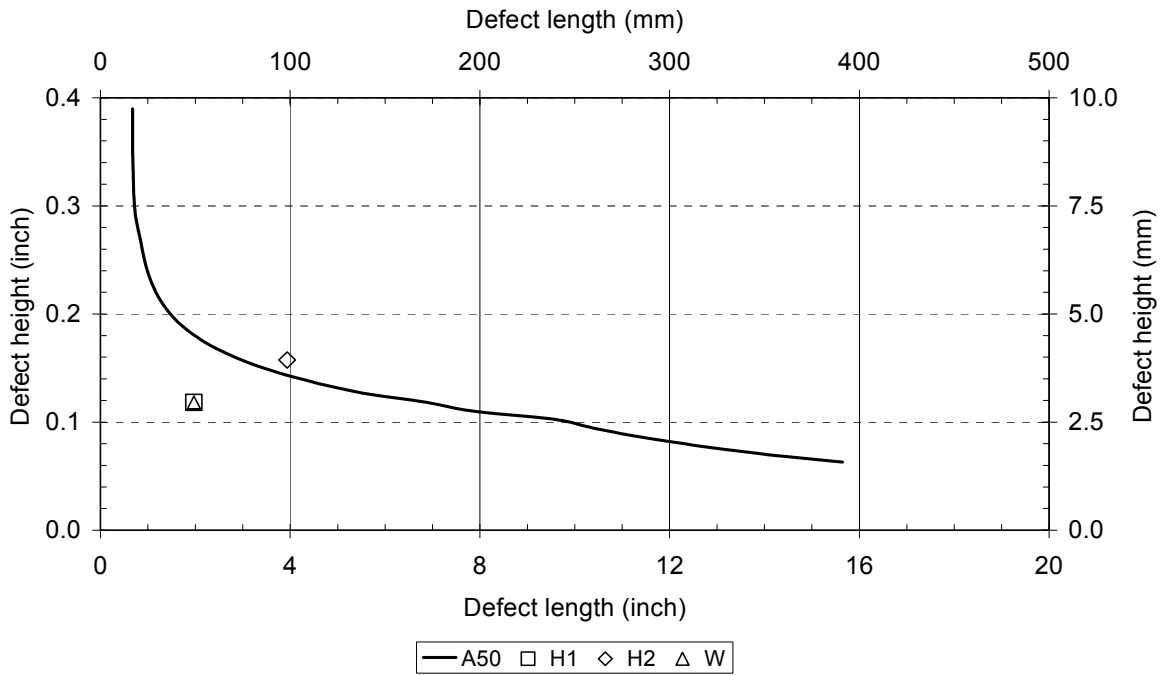


(a) Comparison of maximum allowable defect sizes with the CWP test specimen defects.

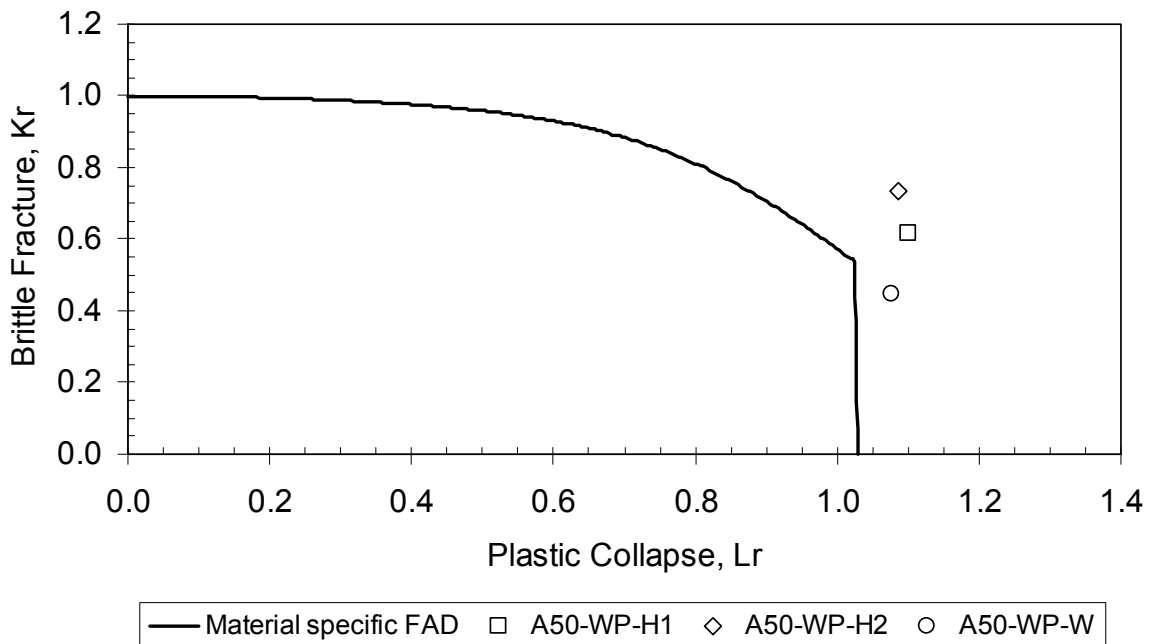


(b) Comparison of the CWP test results with the FAD specific for the weldment.

Figure F3 Weld A46 - API 1104 Option 2 analysis

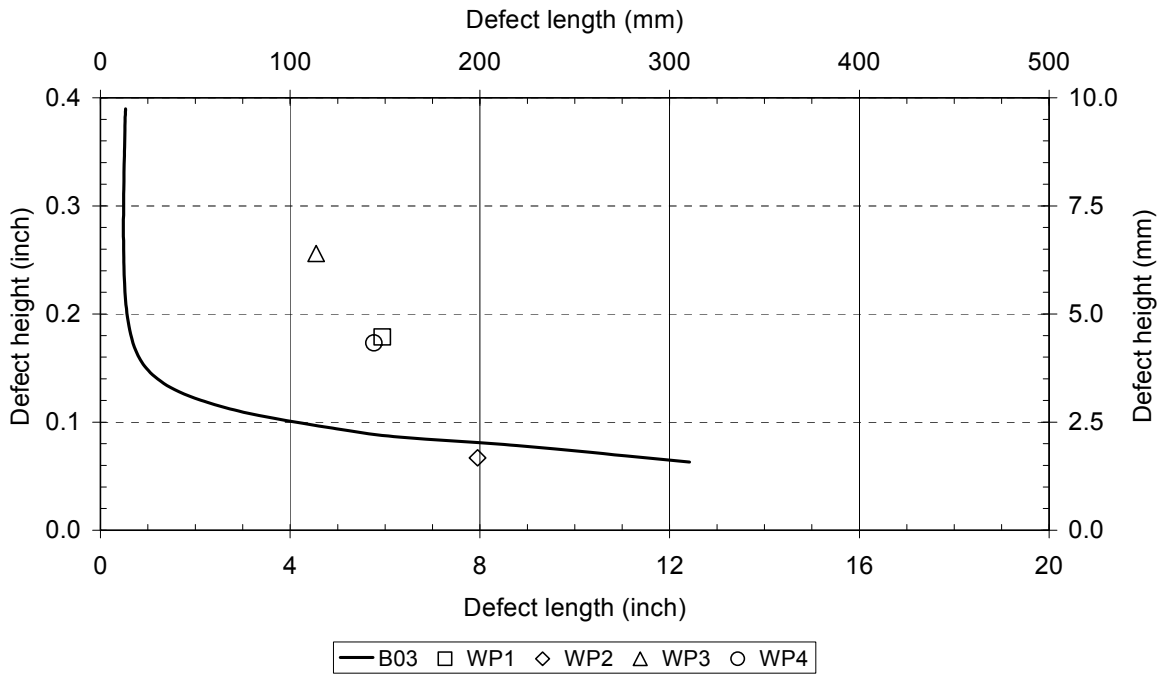


(a) Comparison of maximum allowable defect sizes with the CWP test specimen defects.

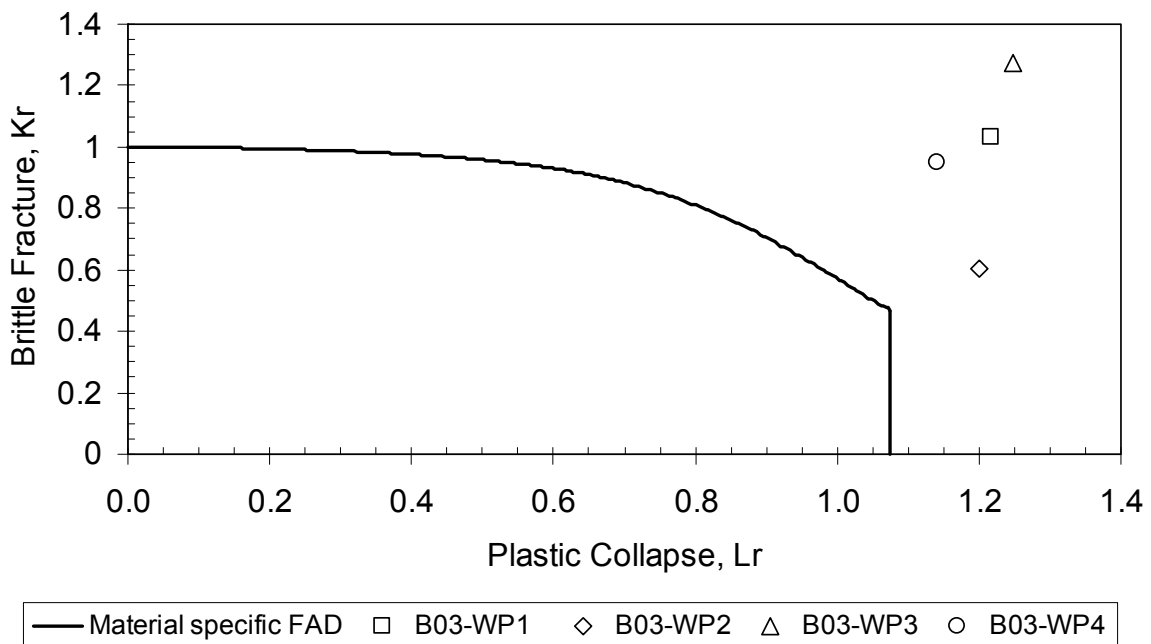


(b) Comparison of the CWP test results with the FAD specific for the weldment.

Figure F4 Weld A50 - API 1104 Option 2 analysis

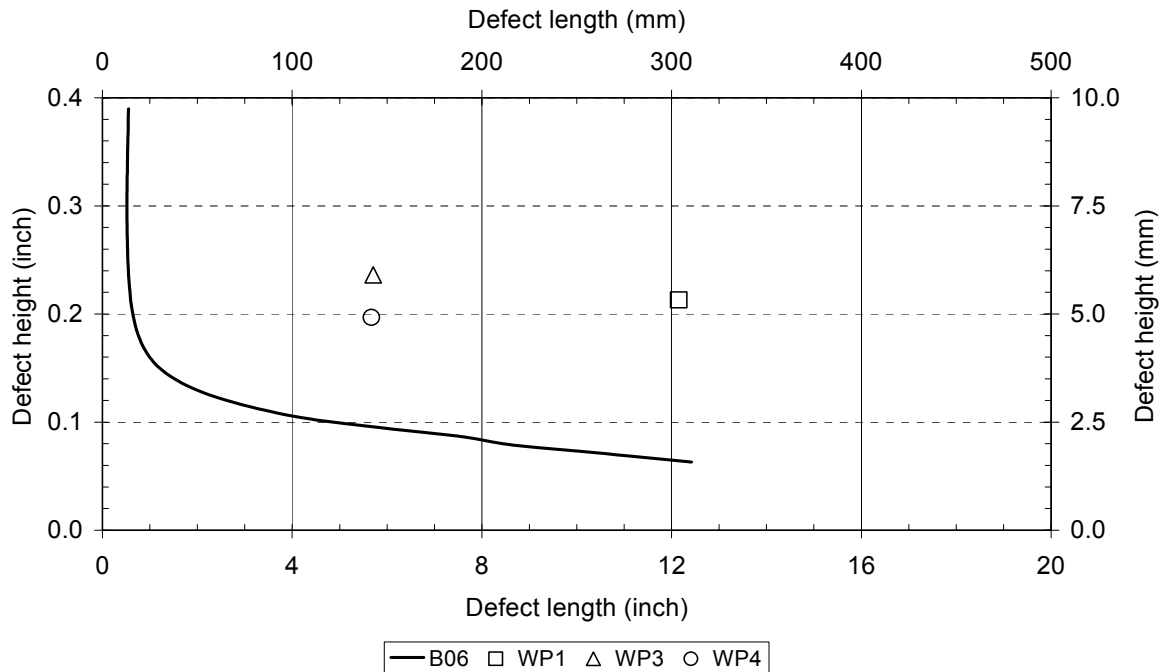


(a) Comparison of maximum allowable defect sizes with the CWP test specimen defects.

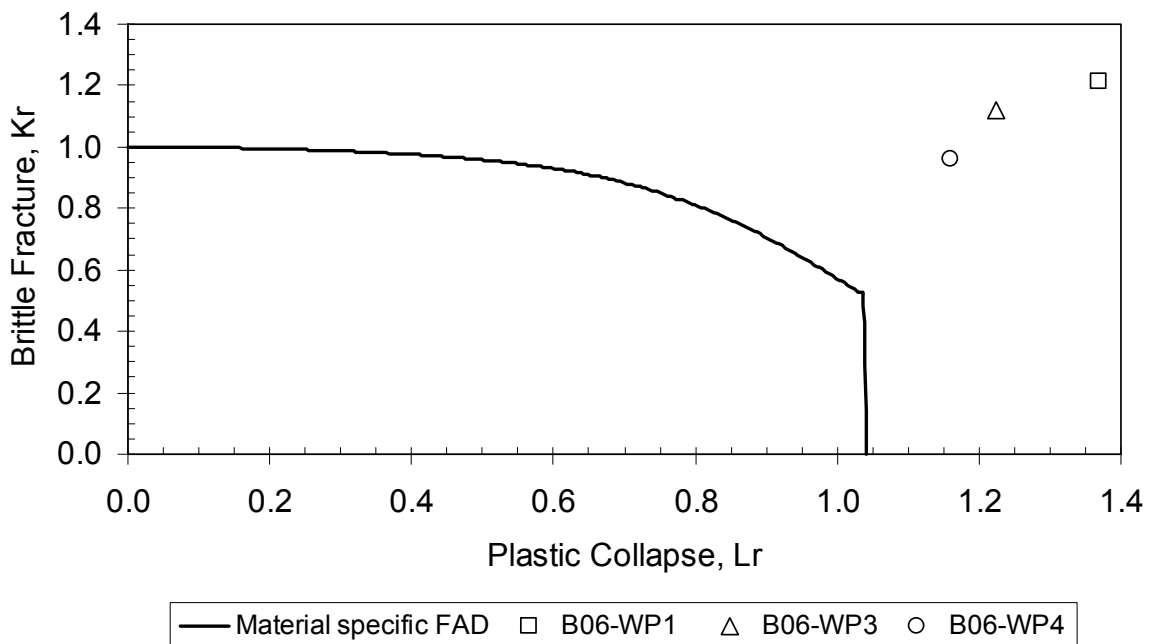


(b) Comparison of the CWP test results with the FAD specific for the weldment.

Figure F5 Weld B03 - API 1104 Option 2 analysis

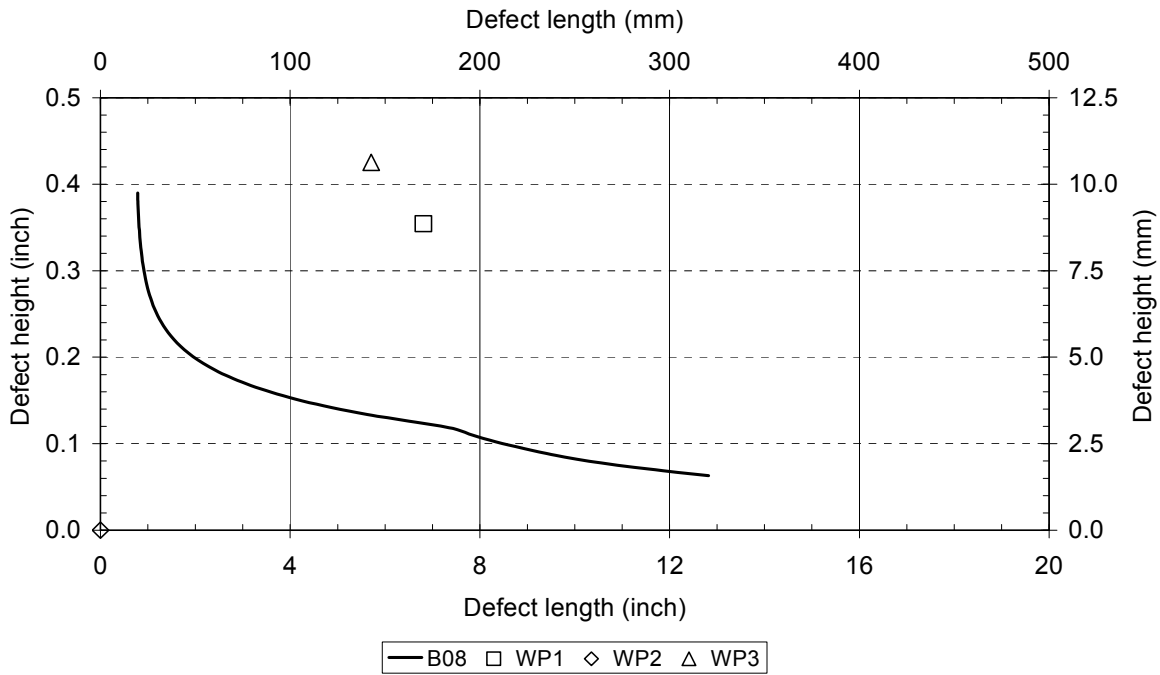


(a) Comparison of maximum allowable defect sizes with the CWP test specimen defects.

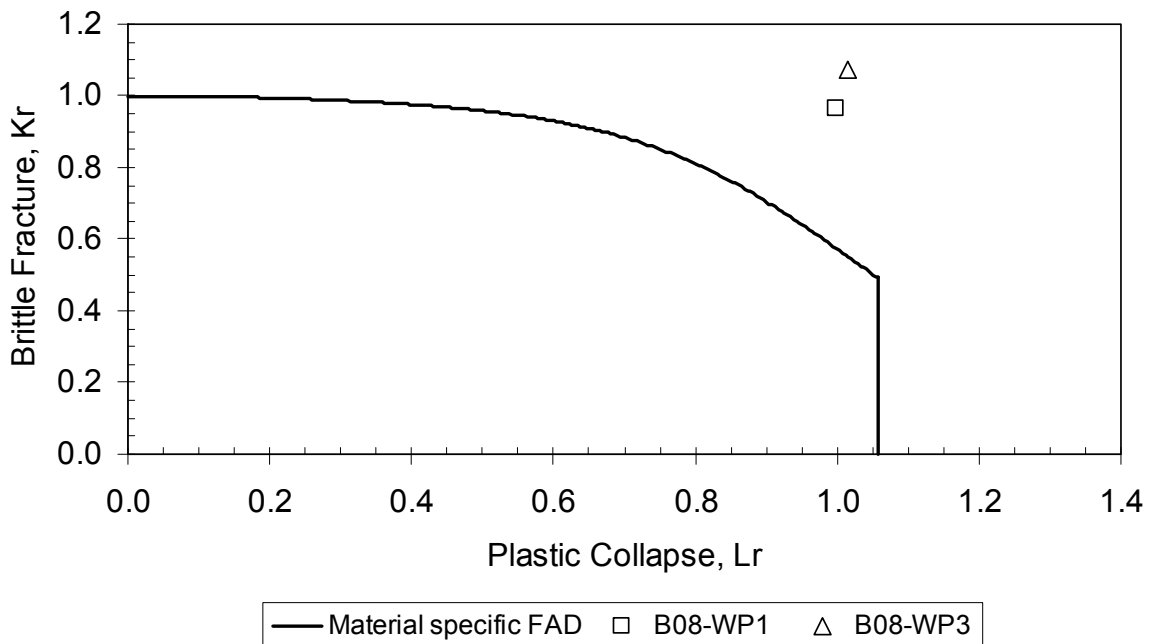


(b) Comparison of the CWP test results with the FAD specific for the weldment.

Figure F6 Weld B06 - API 1104 Option 2 analysis



(a) Comparison of maximum allowable defect sizes with the CWP test specimen defects.

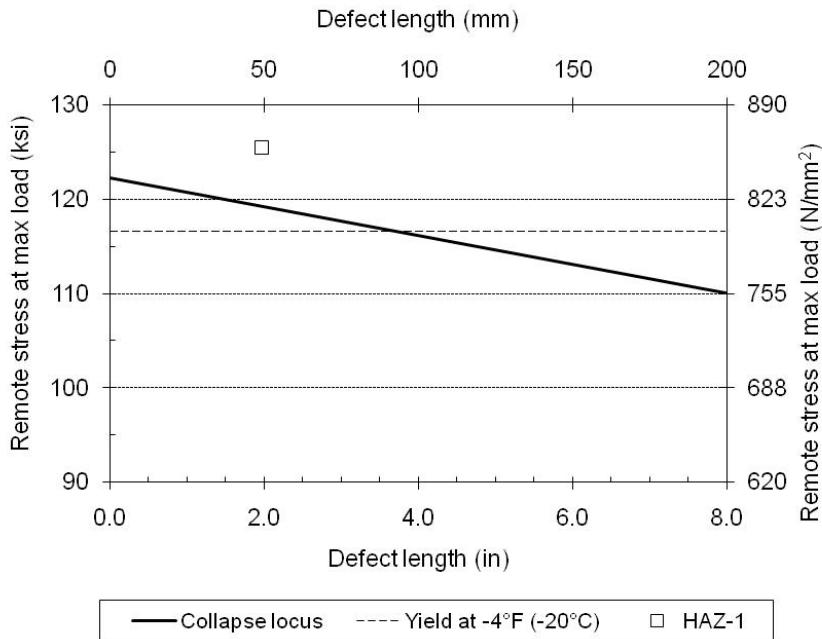


(b) Comparison of the CWP test results with the FAD specific for the weldment.

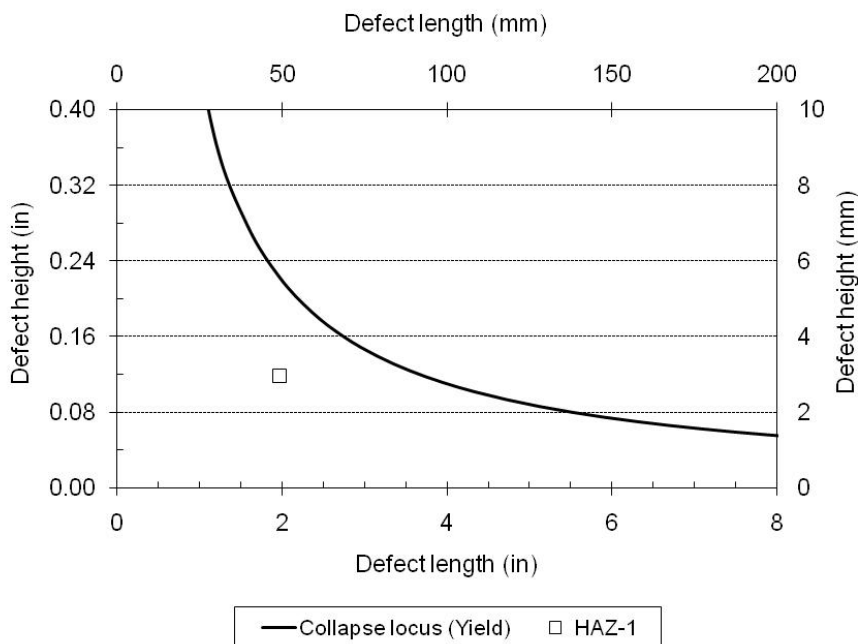
Figure F7 Weld B08 - API 1104 Option 2 analysis

Appendix G EPRG Assessments

In this appendix the measured failure stress from each CWP specimen is compared with the predicted failure stress using equation [18] from Section 3.2.3. Data points lying above the collapse locus and yield strength reference line are predicted to fail by gross scale yielding (GSY), and data points lying above the collapse locus but below the yield strength reference line are predicted to fail by net section yielding (NSY).

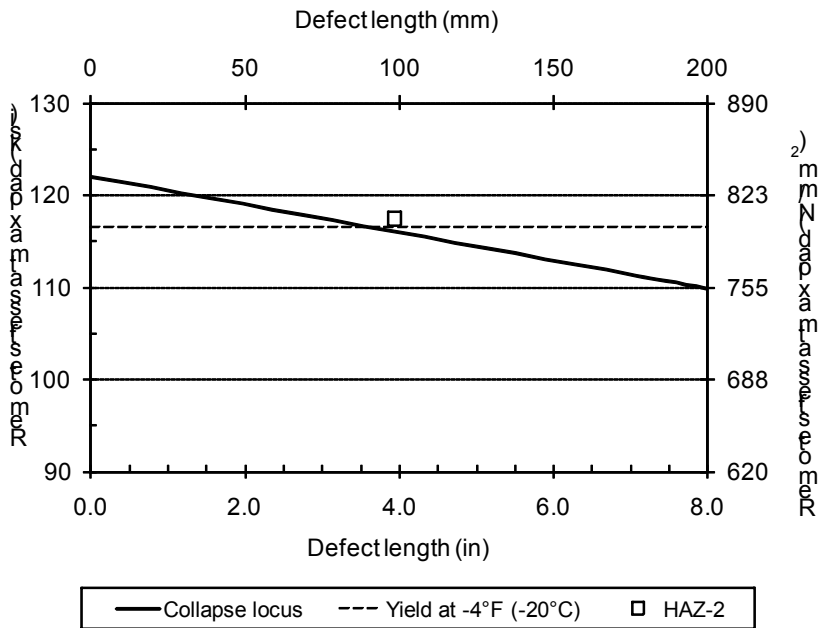


(a) Effect of the length of the defect in the CWP specimen with the predicted failure curve (collapse locus calculated using equation [18] from Section 3.2.3)

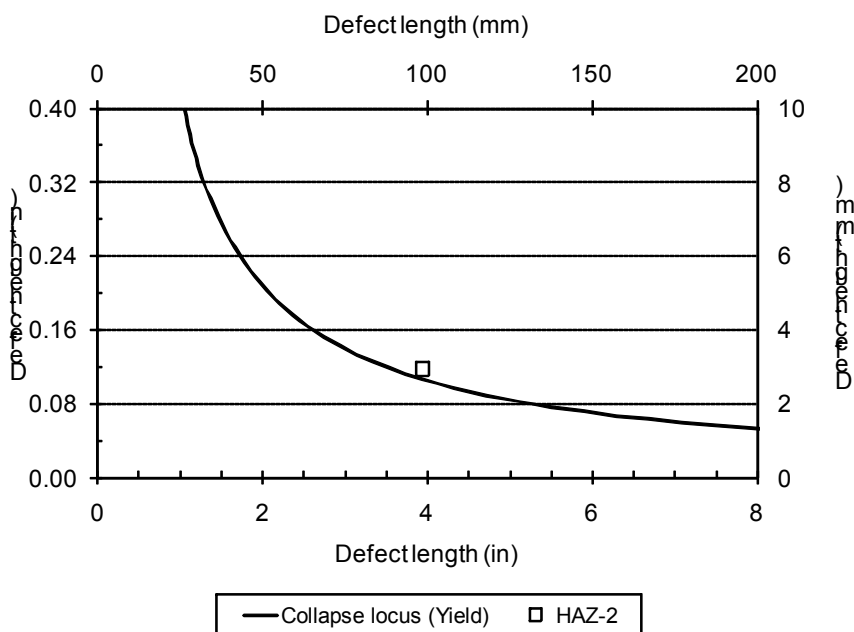


(b) Comparison of the CWP defect size tested with the maximum allowable defect sizes for GSY, predicted using the materials measured tensile properties adjacent to the CWP specimen location (collapse locus calculated using equation [20] from Section 3.2.3).

Figure G1 Weld A06, CWP specimen A06-WP-H1: Comparison of the CWP test results with the EPRG collapse loci.

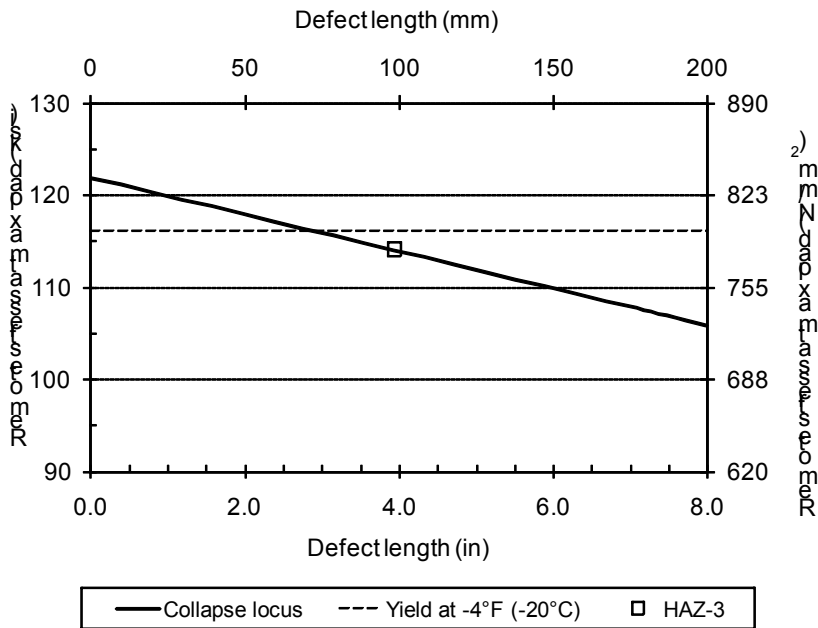


(a) Effect of the length of the defect in the CWP specimen with the predicted failure curve (collapse locus calculated using equation [18] from Section 3.2.3)

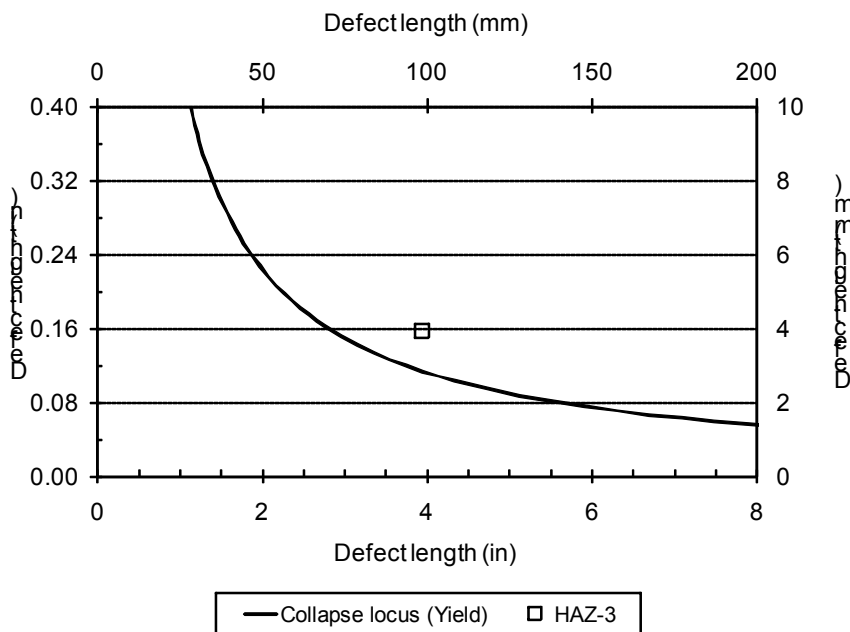


(b) Comparison of the CWP defect size tested with the maximum allowable defect sizes for GSY, predicted using the materials measured tensile properties adjacent to the CWP specimen location (collapse locus calculated using equation [20] from Section 3.2.3).

Figure G2 Weld A06, CWP specimen A06-WP-H2: Comparison of the CWP test results with the EPRG collapse loci.

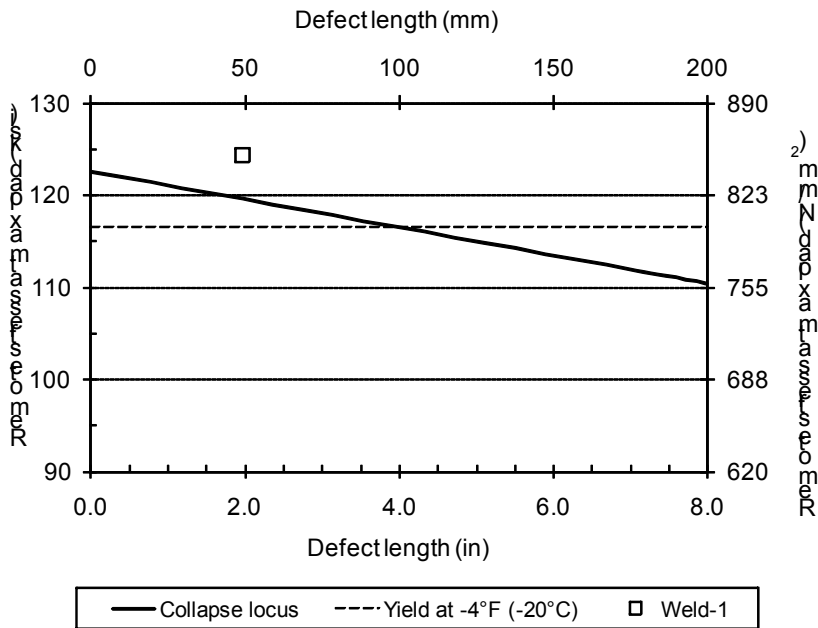


(a) Effect of the length of the defect in the CWP specimen with the predicted failure curve (collapse locus calculated using equation [18] from Section 3.2.3)

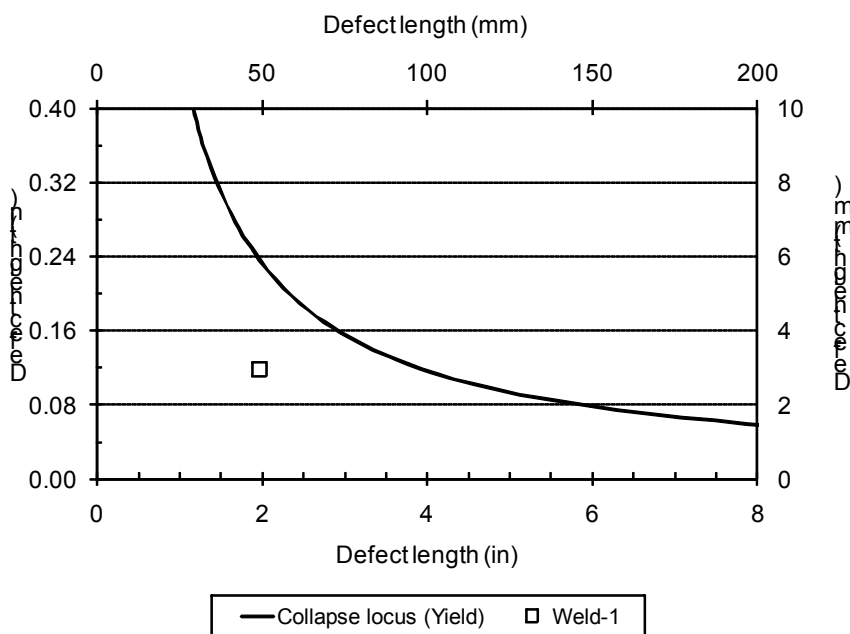


(b) Comparison of the CWP defect size tested with the maximum allowable defect sizes for GSY, predicted using the materials measured tensile properties adjacent to the CWP specimen location (collapse locus calculated using equation [20] from Section 3.2.3).

Figure G3 Weld A06, CWP specimen A06-WP-H3: Comparison of the CWP test results with the EPRG collapse loci.

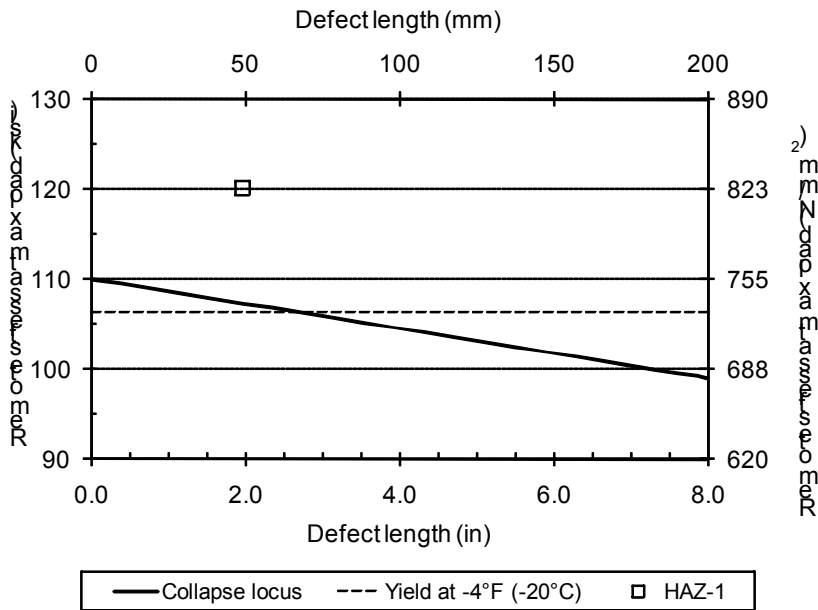


(a) Effect of the length of the defect in the CWP specimen with the predicted failure curve (collapse locus calculated using equation [18] from Section 3.2.3)

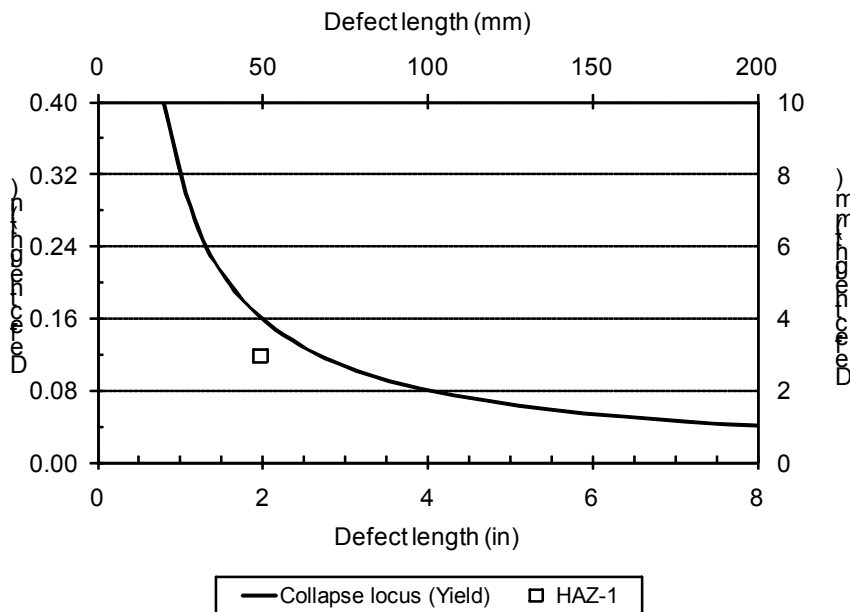


(b) Comparison of the CWP defect size tested with the maximum allowable defect sizes for GSY, predicted using the materials measured tensile properties adjacent to the CWP specimen location (collapse locus calculated using equation [20] from Section 3.2.3).

Figure G4 Weld A06, CWP specimen A06-WP-W: Comparison of the CWP test results with the EPRG collapse loci.

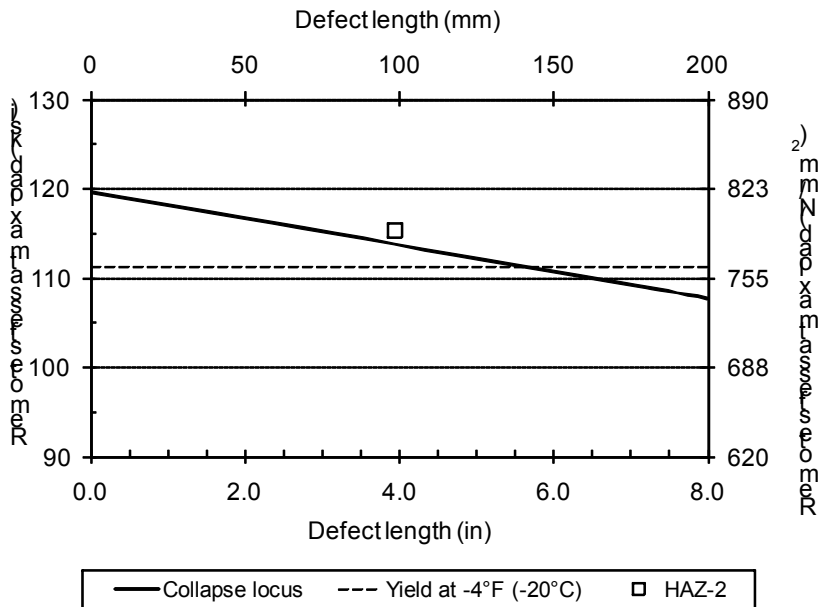


(a) Effect of the length of the defect in the CWP specimen with the predicted failure curve (collapse locus calculated using equation [18] from Section 3.2.3)

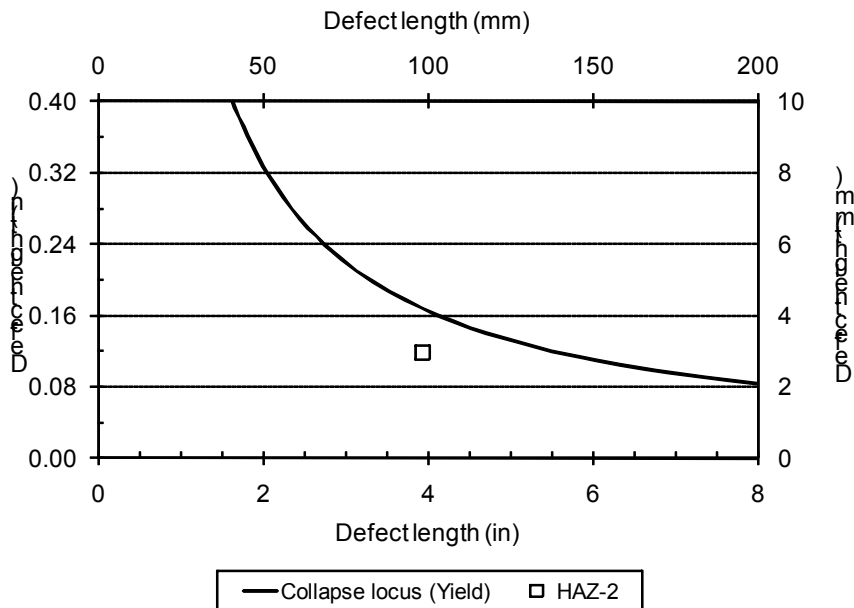


(b) Comparison of the CWP defect size tested with the maximum allowable defect sizes for GSY, predicted using the materials measured tensile properties adjacent to the CWP specimen location (collapse locus calculated using equation [20] from Section 3.2.3).

Figure G5 Weld A17, CWP specimen A17-WP-H1: Comparison of the CWP test results with the EPRG collapse loci.

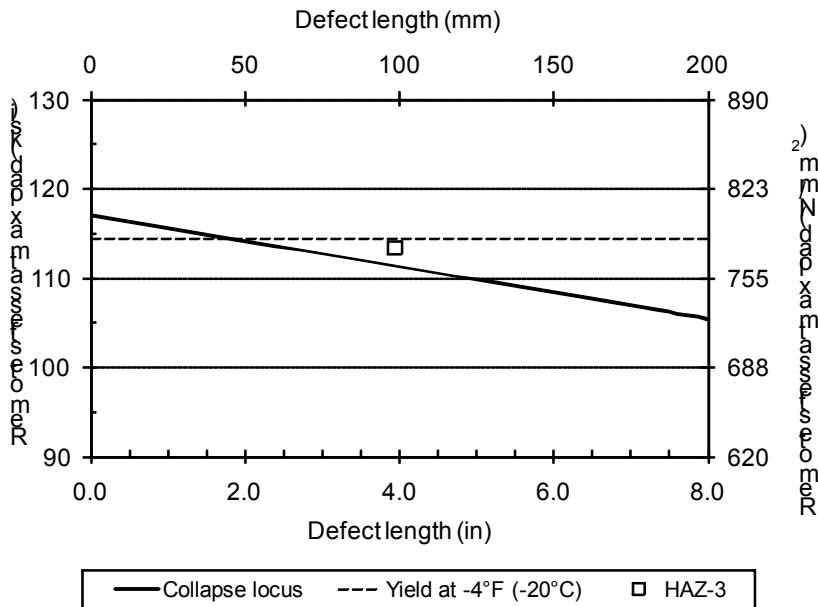


(a) Effect of the length of the defect in the CWP specimen with the predicted failure curve (collapse locus calculated using equation [18] from Section 3.2.3)

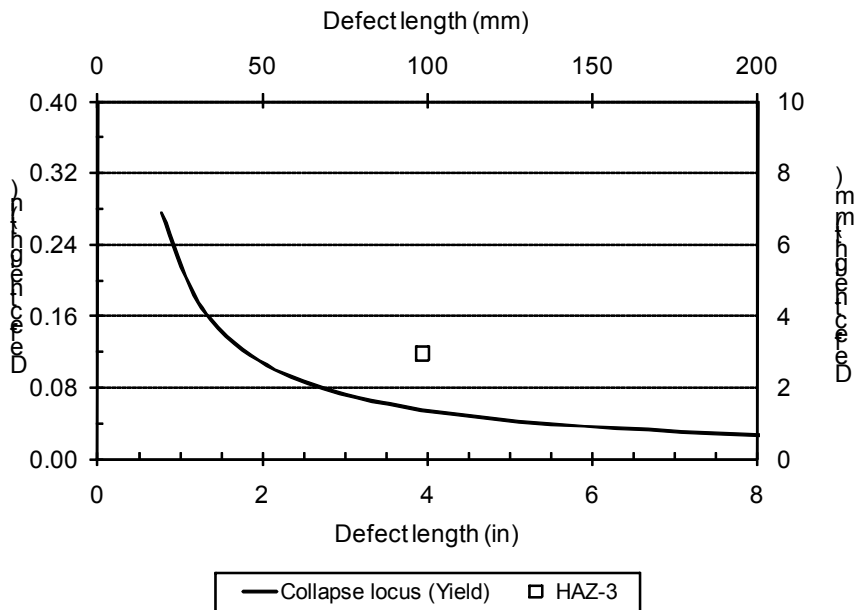


(b) Comparison of the CWP defect size tested with the maximum allowable defect sizes for GSY, predicted using the materials measured tensile properties adjacent to the CWP specimen location (collapse locus calculated using equation [20] from Section 3.2.3).

Figure G6 Weld A17, CWP specimen A17-WP-H2: Comparison of the CWP test results with the EPRG collapse loci.

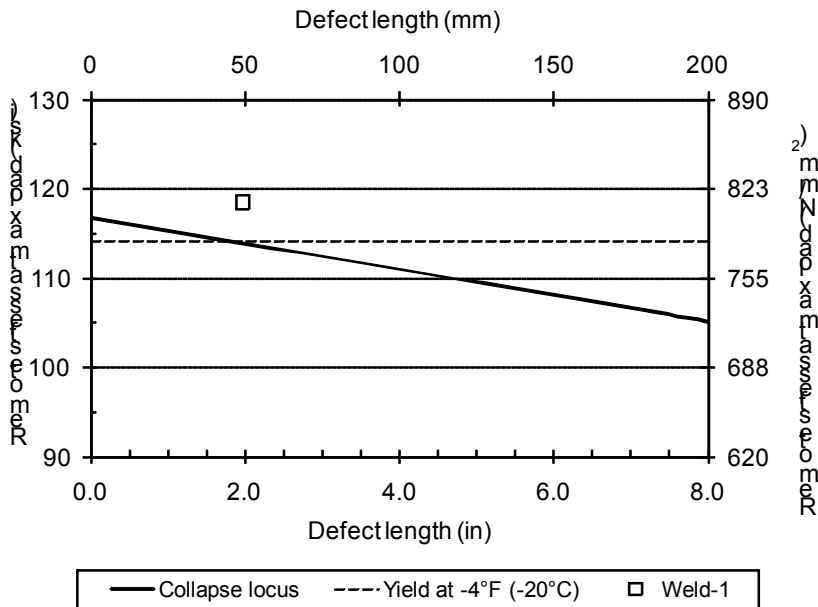


(a) Effect of the length of the defect in the CWP specimen with the predicted failure curve (collapse locus calculated using equation [18] from Section 3.2.3)

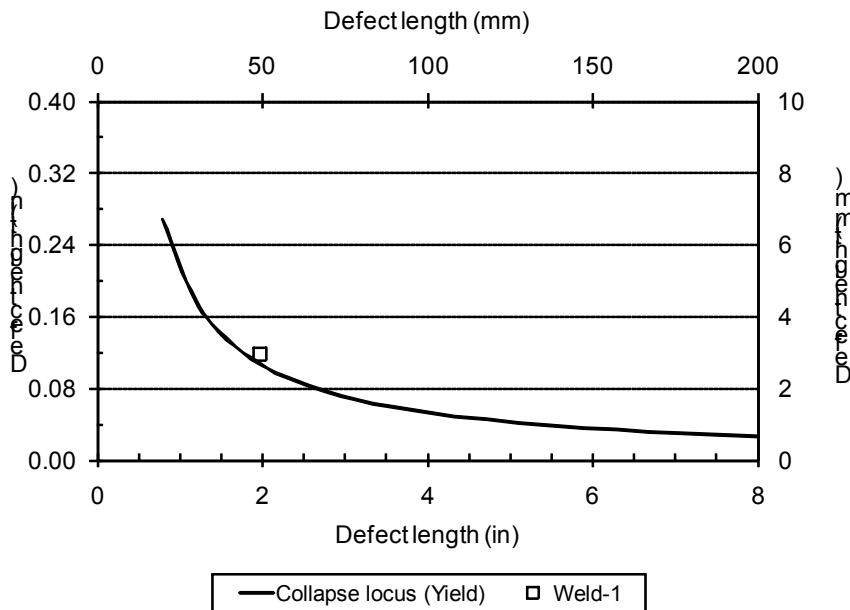


(b) Comparison of the CWP defect size tested with the maximum allowable defect sizes for GSY, predicted using the materials measured tensile properties adjacent to the CWP specimen location (collapse locus calculated using equation [20] from Section 3.2.3).

Figure G7 Weld A17, CWP specimen A17-WP-H3: Comparison of the CWP test results with the EPRG collapse loci.

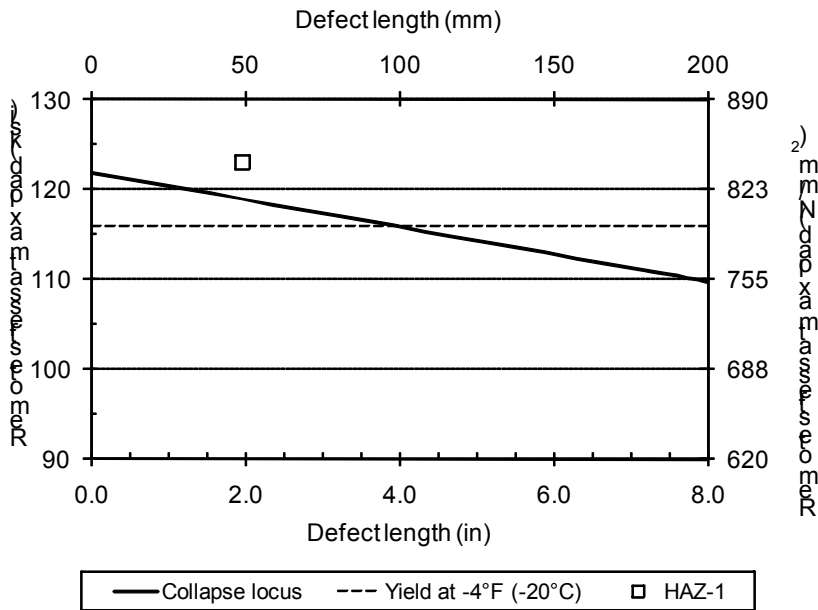


(a) Effect of the length of the defect in the CWP specimen with the predicted failure curve (collapse locus calculated using equation [18] from Section 3.2.3)

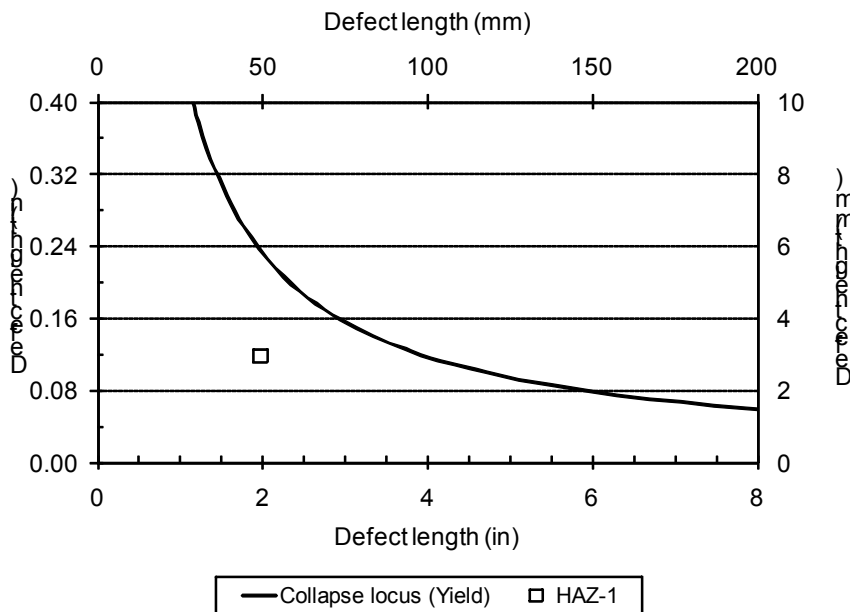


(b) Comparison of the CWP defect size tested with the maximum allowable defect sizes for GSY, predicted using the materials measured tensile properties adjacent to the CWP specimen location (collapse locus calculated using equation [20] from Section 3.2.3).

Figure G8 Weld A17, CWP specimen A17-WP-W: Comparison of the CWP test results with the EPRG collapse loci.

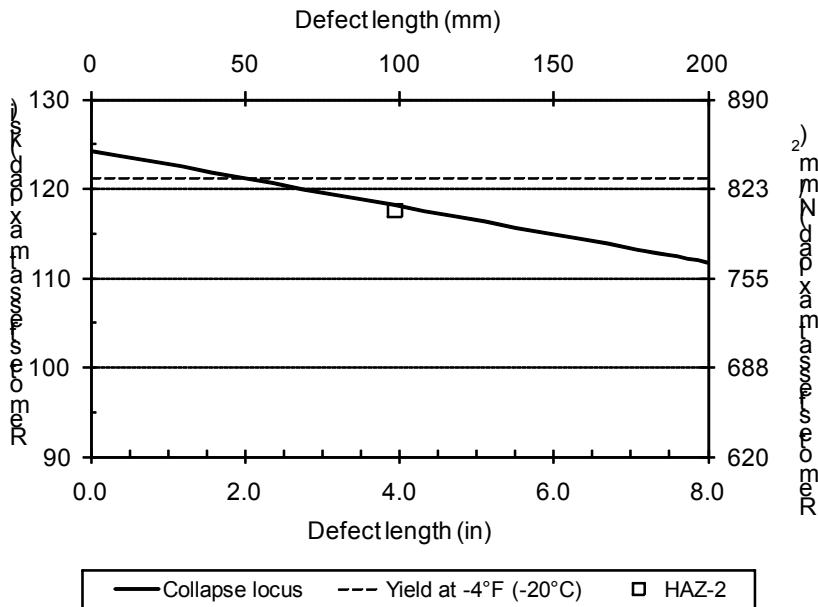


(a) Effect of the length of the defect in the CWP specimen with the predicted failure curve (collapse locus calculated using equation [18] from Section 3.2.3)

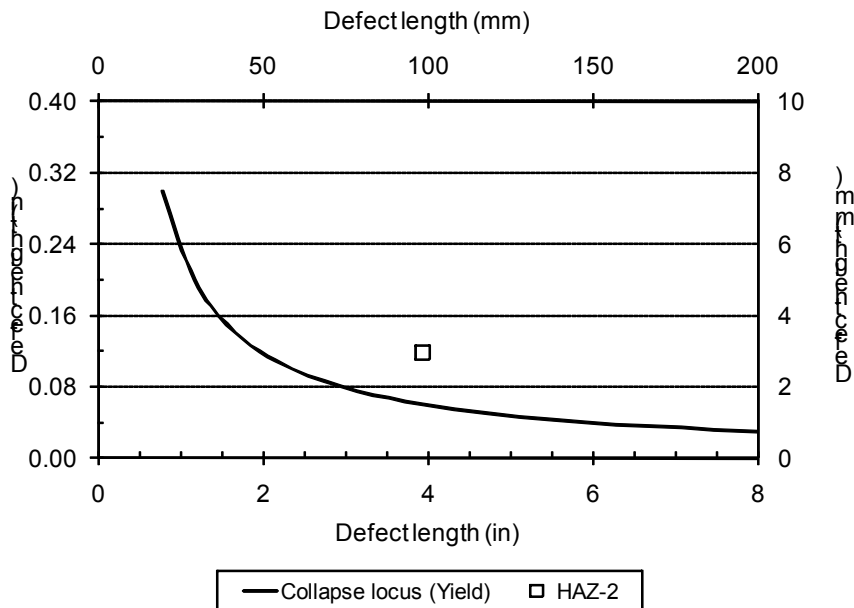


(b) Comparison of the CWP defect size tested with the maximum allowable defect sizes for GSY, predicted using the materials measured tensile properties adjacent to the CWP specimen location (collapse locus calculated using equation [20] from Section 3.2.3).

Figure G9 Weld A33, CWP specimen A33-WP-H1: Comparison of the CWP test results with the EPRG collapse loci.

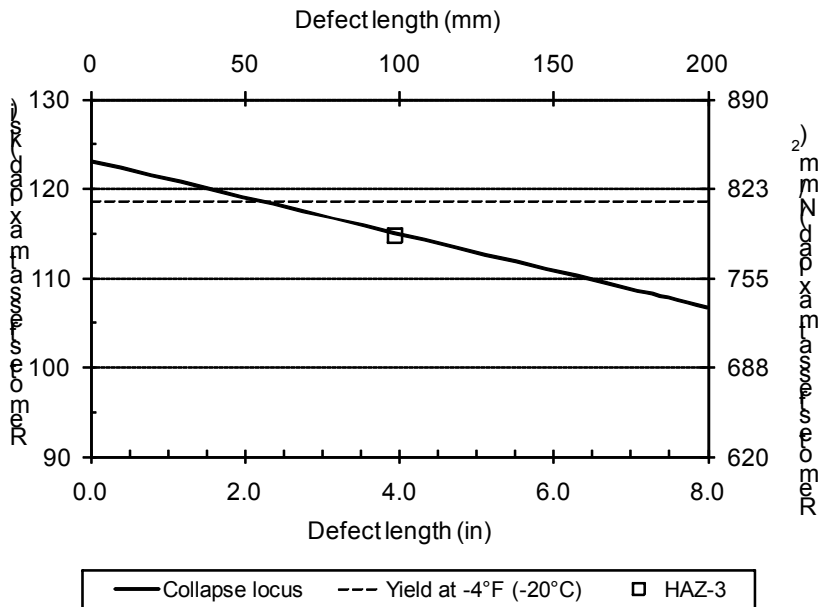


(a) Effect of the length of the defect in the CWP specimen with the predicted failure curve (collapse locus calculated using equation [18] from Section 3.2.3)

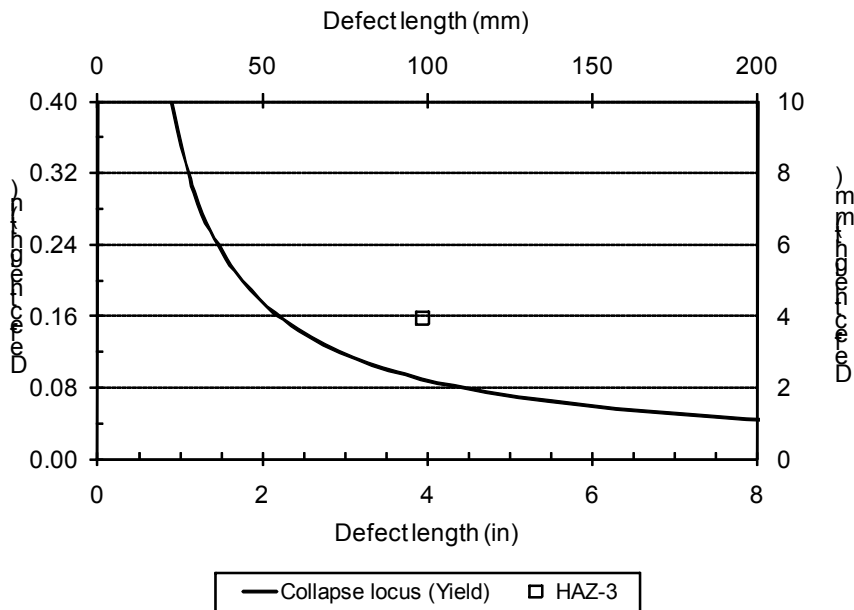


(b) Comparison of the CWP defect size tested with the maximum allowable defect sizes for GSY, predicted using the materials measured tensile properties adjacent to the CWP specimen location (collapse locus calculated using equation [20] from Section 3.2.3).

Figure G10 Weld A33, CWP specimen A33-WP-H2: Comparison of the CWP test results with the EPRG collapse loci.

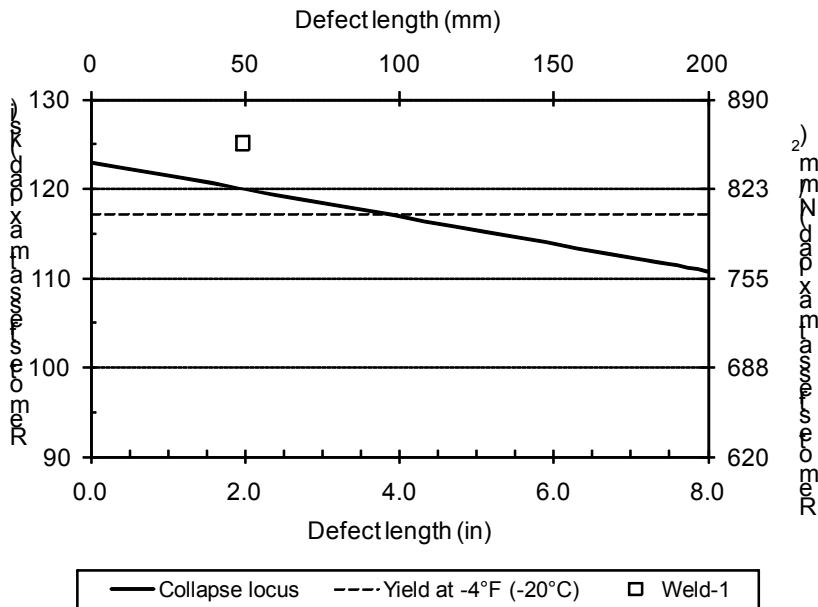


(a) Effect of the length of the defect in the CWP specimen with the predicted failure curve (collapse locus calculated using equation [18] from Section 3.2.3)

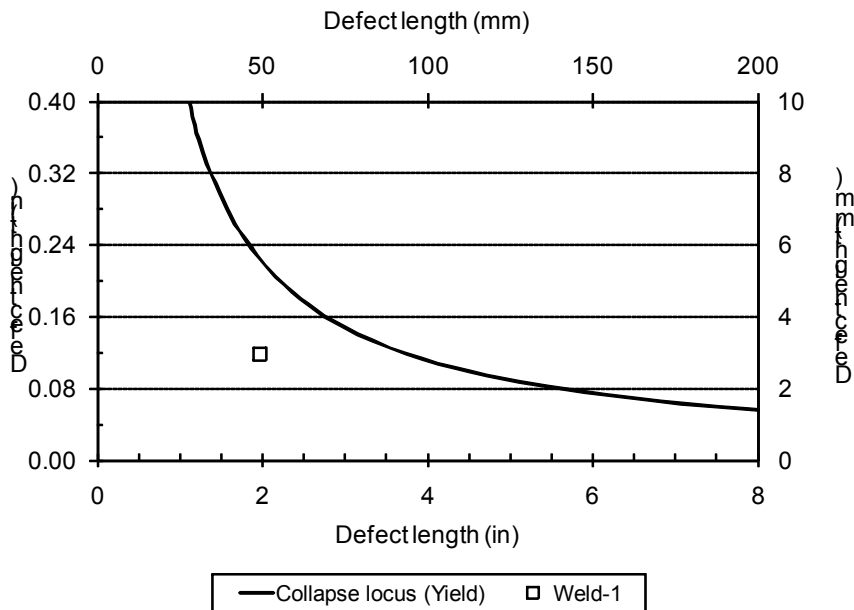


(b) Comparison of the CWP defect size tested with the maximum allowable defect sizes for GSY, predicted using the materials measured tensile properties adjacent to the CWP specimen location (collapse locus calculated using equation [20] from Section 3.2.3).

Figure G11 Weld A33, CWP specimen A33-WP-H3: Comparison of the CWP test results with the EPRG collapse loci.

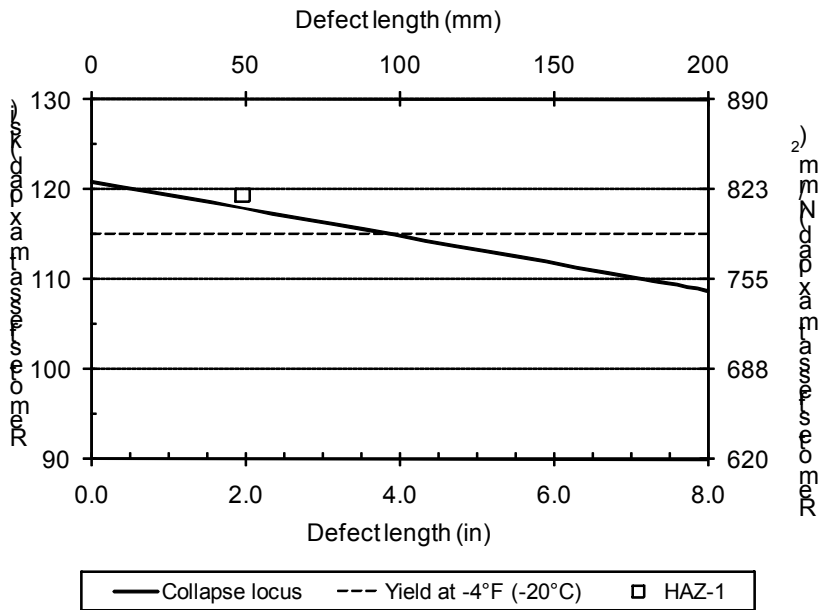


(a) Effect of the length of the defect in the CWP specimen with the predicted failure curve (collapse locus calculated using equation [18] from Section 3.2.3)

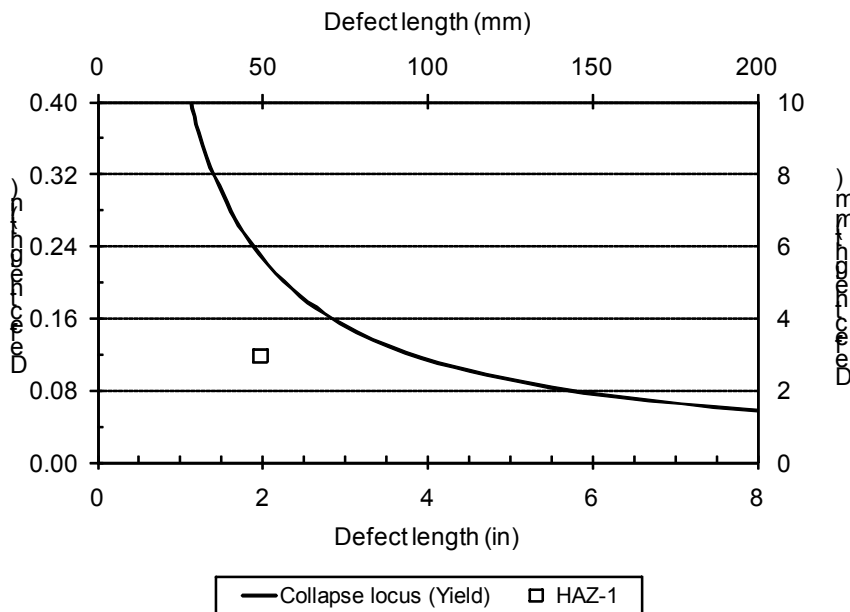


(b) Comparison of the CWP defect size tested with the maximum allowable defect sizes for GSY, predicted using the materials measured tensile properties adjacent to the CWP specimen location (collapse locus calculated using equation [20] from Section 3.2.3).

Figure G12 Weld A33, CWP specimen A33-WP-W: Comparison of the CWP test results with the EPRG collapse loci.

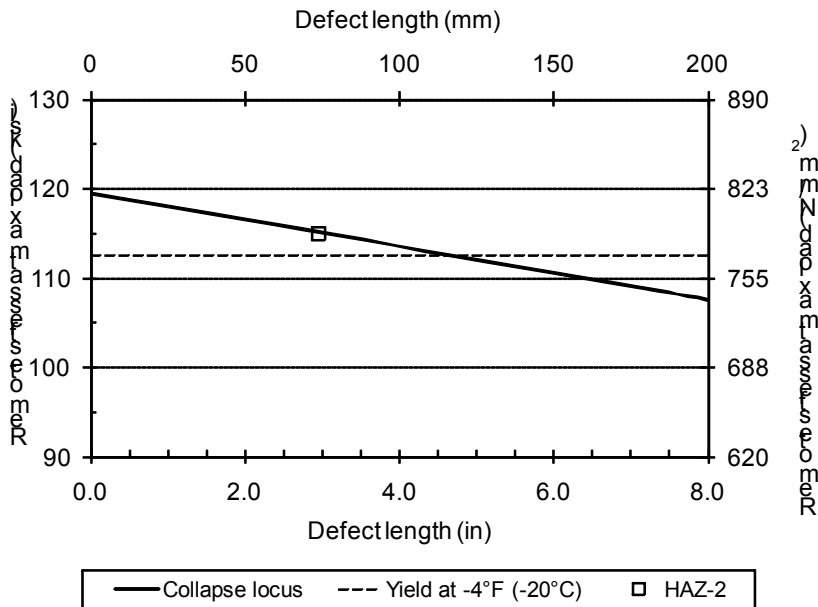


(a) Effect of the length of the defect in the CWP specimen with the predicted failure curve (collapse locus calculated using equation [18] from Section 3.2.3)

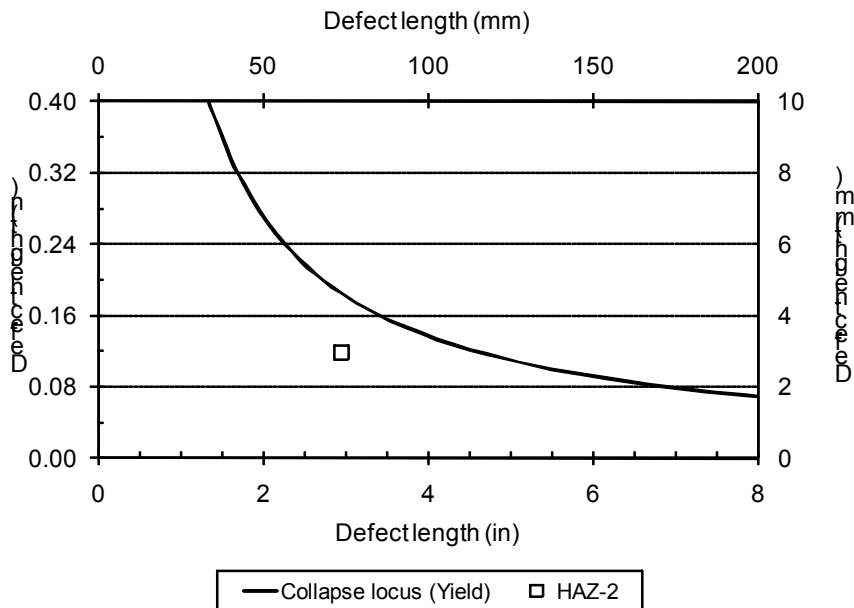


(b) Comparison of the CWP defect size tested with the maximum allowable defect sizes for GSY, predicted using the materials measured tensile properties adjacent to the CWP specimen location (collapse locus calculated using equation [20] from Section 3.2.3).

Figure G13 Weld A46, CWP specimen A46-WP-H1: Comparison of the CWP test results with the EPRG collapse loci.

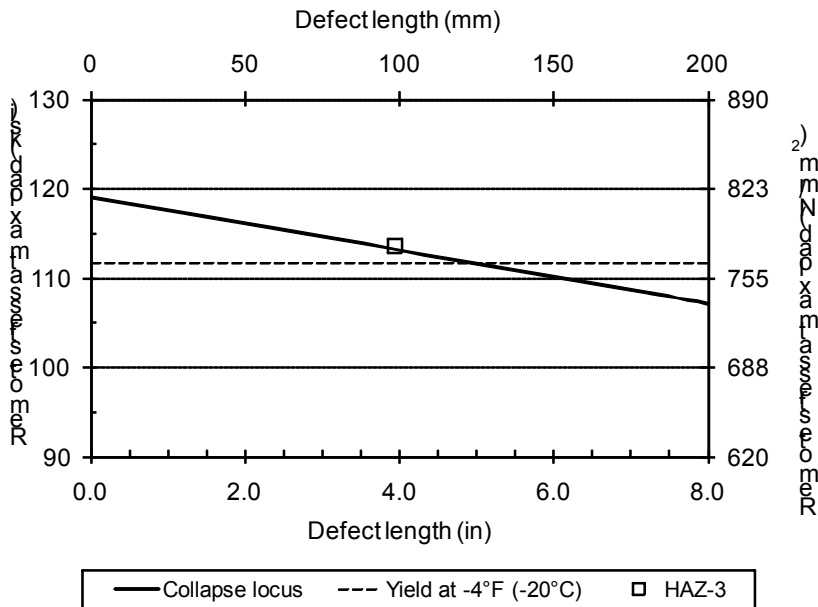


(a) Effect of the length of the defect in the CWP specimen with the predicted failure curve (collapse locus calculated using equation [18] from Section 3.2.3)

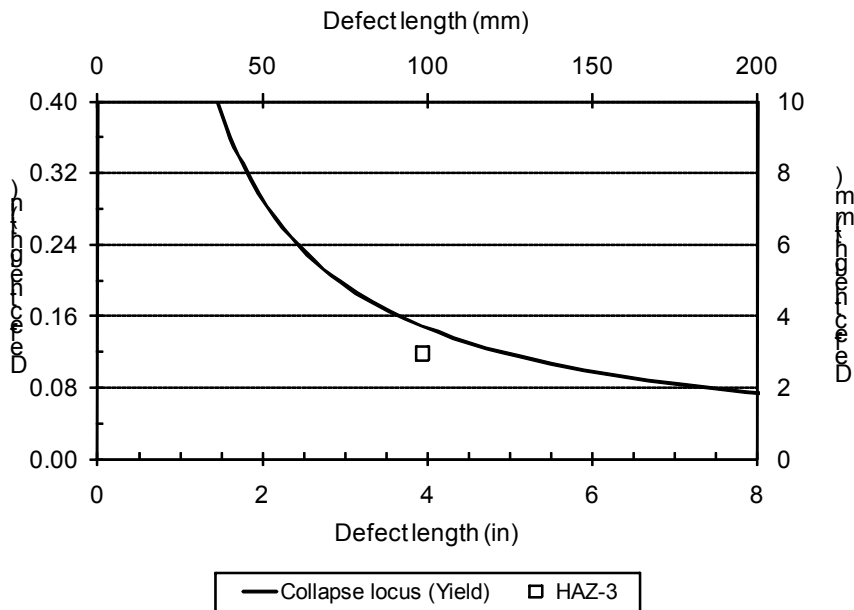


(b) Comparison of the CWP defect size tested with the maximum allowable defect sizes for GSY, predicted using the materials measured tensile properties adjacent to the CWP specimen location (collapse locus calculated using equation [20] from Section 3.2.3).

Figure G14 Weld A46, CWP specimen A46-WP-H2: Comparison of the CWP test results with the EPRG collapse loci.

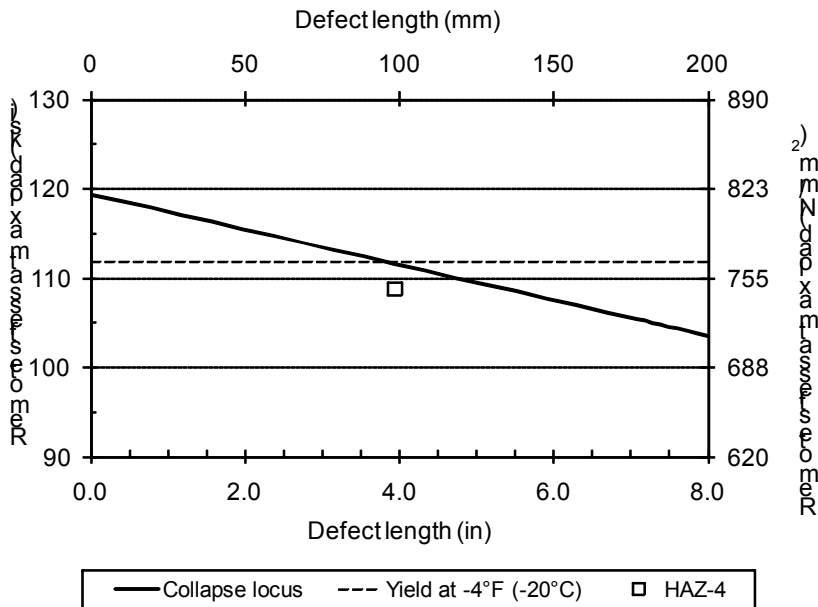


(a) Effect of the length of the defect in the CWP specimen with the predicted failure curve (collapse locus calculated using equation [18] from Section 3.2.3)

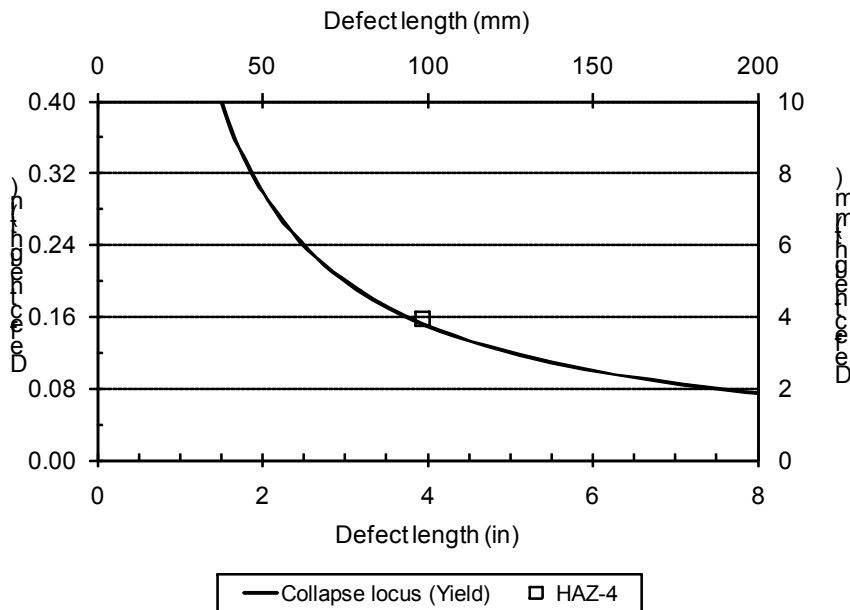


(b) Comparison of the CWP defect size tested with the maximum allowable defect sizes for GSY, predicted using the materials measured tensile properties adjacent to the CWP specimen location (collapse locus calculated using equation [20] from Section 3.2.3).

Figure G15 Weld A46, CWP specimen A46-WP-H3: Comparison of the CWP test results with the EPRG collapse loci.

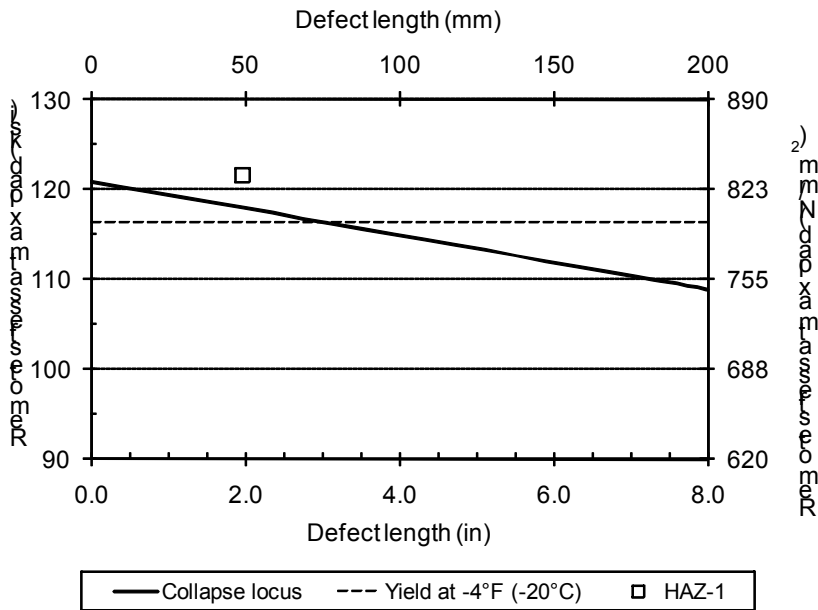


(a) Effect of the length of the defect in the CWP specimen with the predicted failure curve (collapse locus calculated using equation [18] from Section 3.2.3)

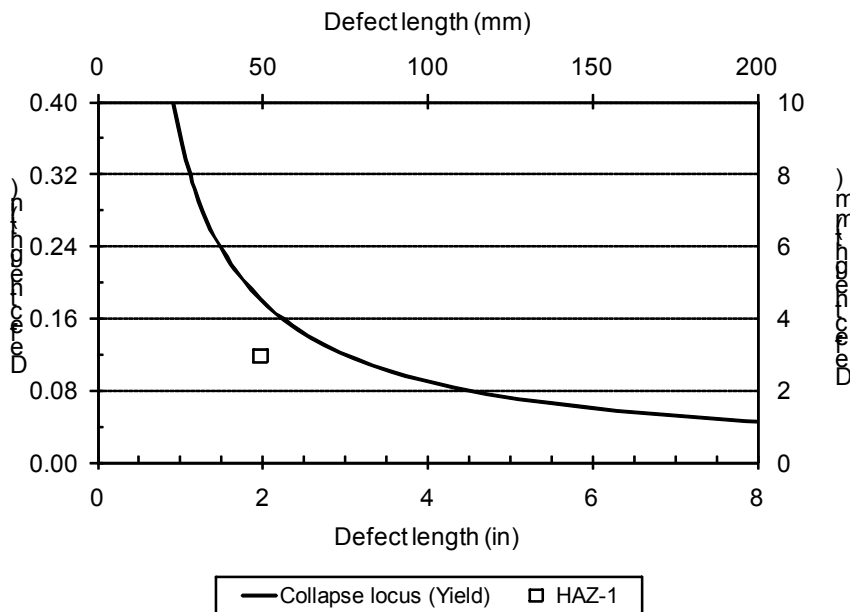


(b) Comparison of the CWP defect size tested with the maximum allowable defect sizes for GSY, predicted using the materials measured tensile properties adjacent to the CWP specimen location (collapse locus calculated using equation [20] from Section 3.2.3).

Figure G16 Weld A46, CWP specimen A46-WP-H4: Comparison of the CWP test results with the EPRG collapse loci.

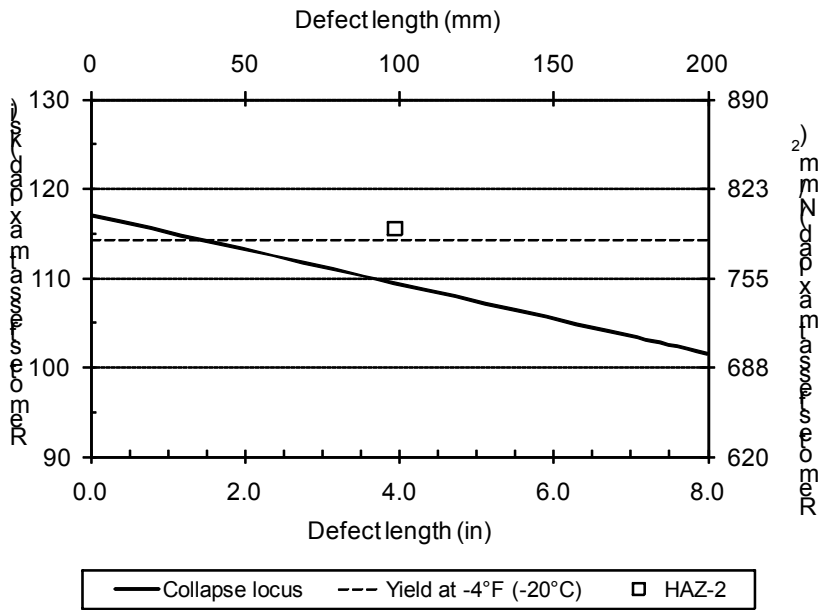


(a) Effect of the length of the defect in the CWP specimen with the predicted failure curve (collapse locus calculated using equation [18] from Section 3.2.3)

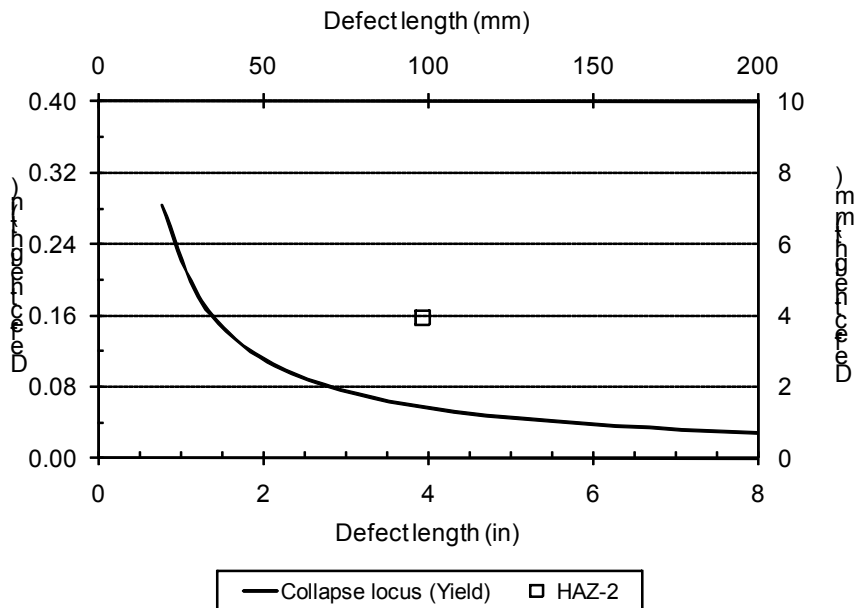


(b) Comparison of the CWP defect size tested with the maximum allowable defect sizes for GSY, predicted using the materials measured tensile properties adjacent to the CWP specimen location (collapse locus calculated using equation [20] from Section 3.2.3).

Figure G17 Weld A50, CWP specimen A50-WP-H1: Comparison of the CWP test results with the EPRG collapse loci.

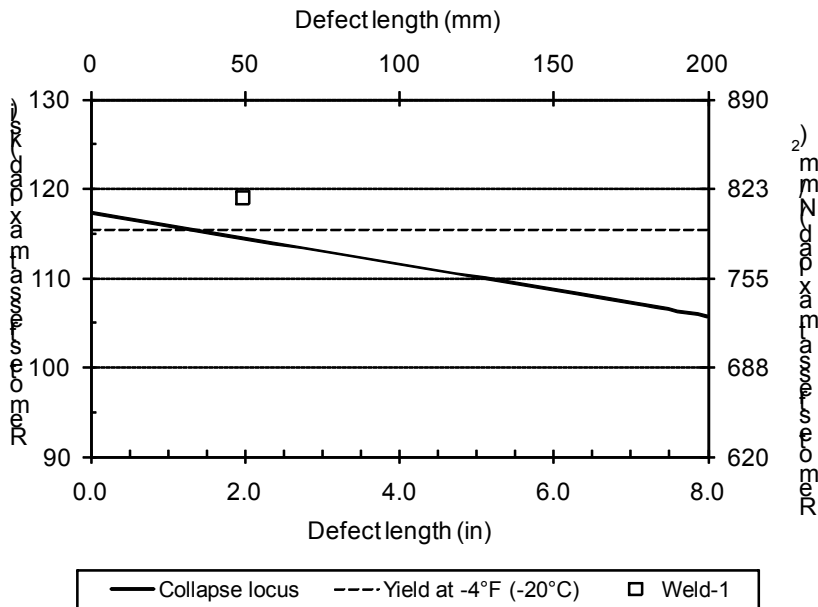


(a) Effect of the length of the defect in the CWP specimen with the predicted failure curve (collapse locus calculated using equation [18] from Section 3.2.3)

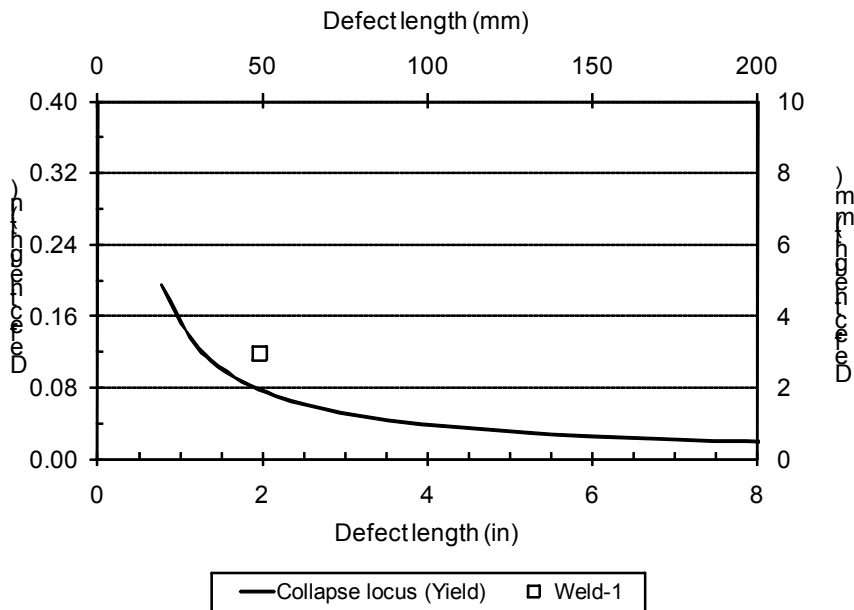


(b) Comparison of the CWP defect size tested with the maximum allowable defect sizes for GSY, predicted using the materials measured tensile properties adjacent to the CWP specimen location (collapse locus calculated using equation [20] from Section 3.2.3).

Figure G18 Weld A50, CWP specimen A50-WP-H2: Comparison of the CWP test results with the EPRG collapse loci.

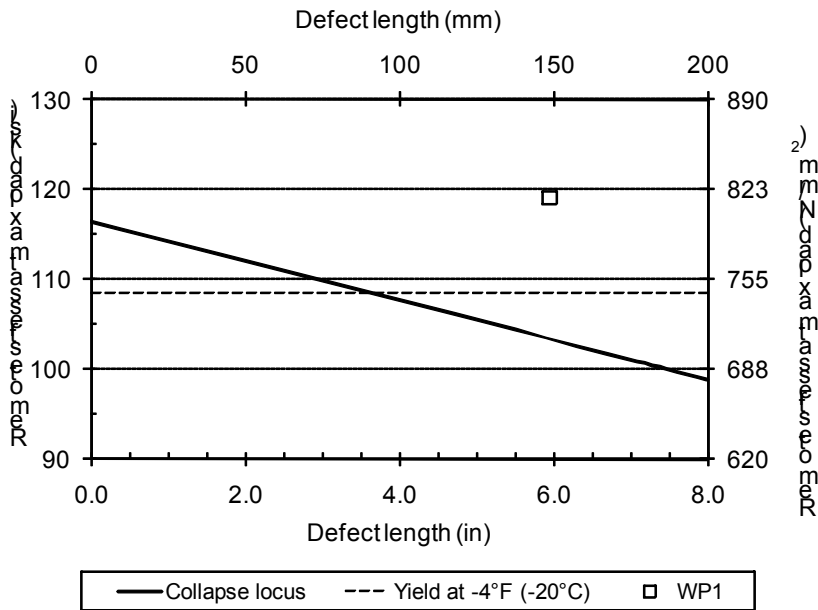


(a) Effect of the length of the defect in the CWP specimen with the predicted failure curve (collapse locus calculated using equation [18] from Section 3.2.3)

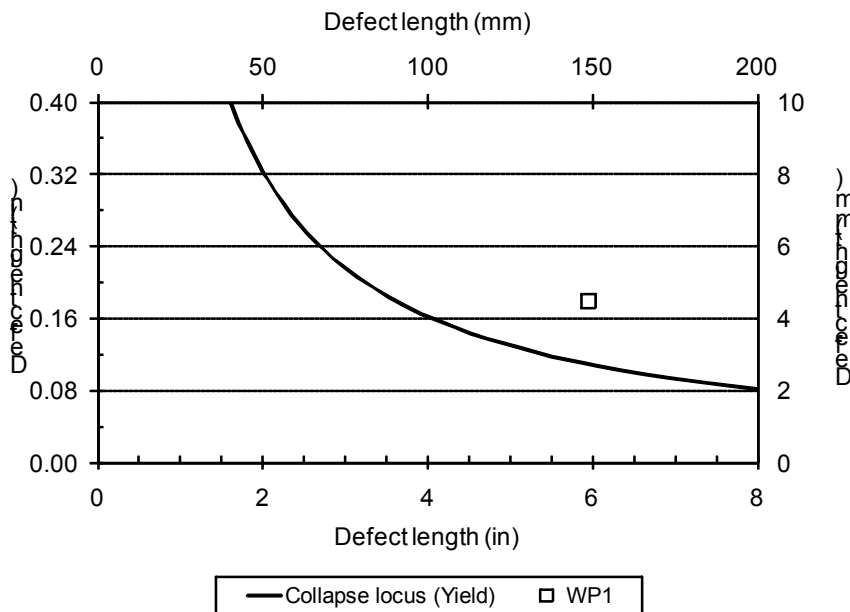


(b) Comparison of the CWP defect size tested with the maximum allowable defect sizes for GSY, predicted using the materials measured tensile properties adjacent to the CWP specimen location (collapse locus calculated using equation [20] from Section 3.2.3).

Figure G19 Weld A50, CWP specimen A50-WP-W: Comparison of the CWP test results with the EPRG collapse loci.

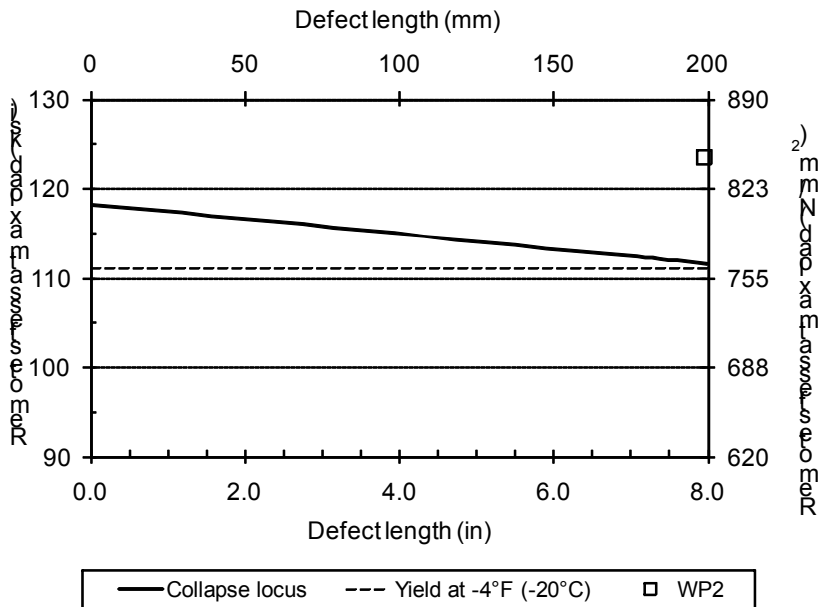


(a) Effect of the length of the defect in the CWP specimen with the predicted failure curve (collapse locus calculated using equation [18] from Section 3.2.3)

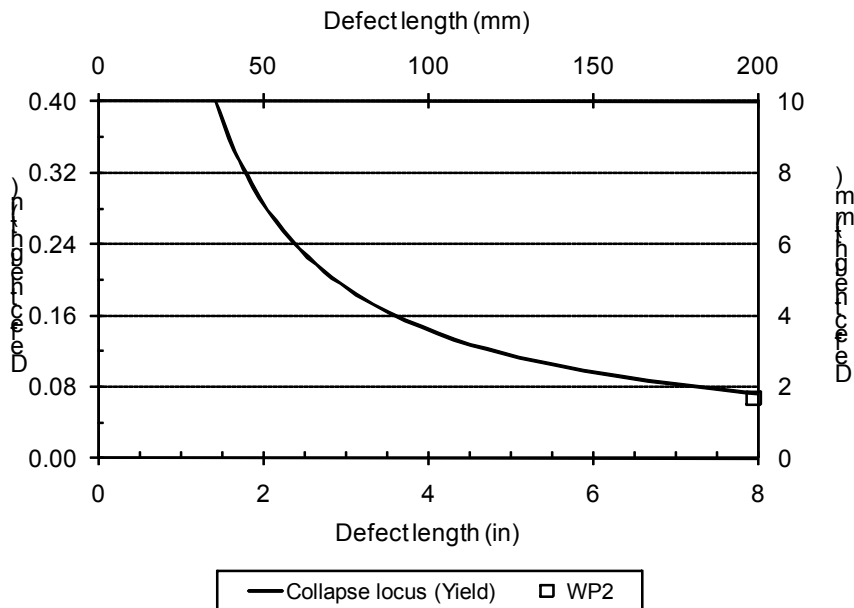


(b) Comparison of the CWP defect size tested with the maximum allowable defect sizes for GSY, predicted using the materials measured tensile properties adjacent to the CWP specimen location (collapse locus calculated using equation [20] from Section 3.2.3).

Figure G20 Weld B03, CWP specimen B03-WP1: Comparison of the CWP test results with the EPRG collapse loci.

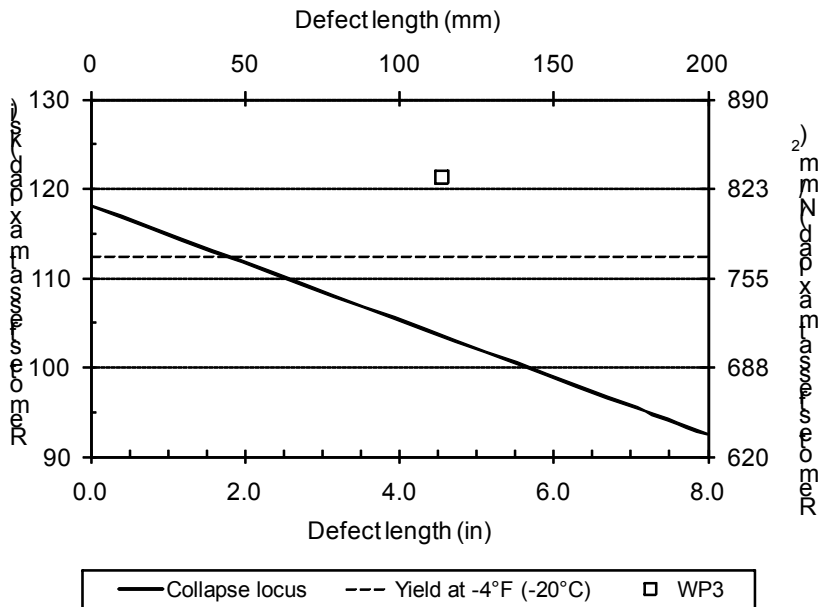


(a) Effect of the length of the defect in the CWP specimen with the predicted failure curve (collapse locus calculated using equation [18] from Section 3.2.3)

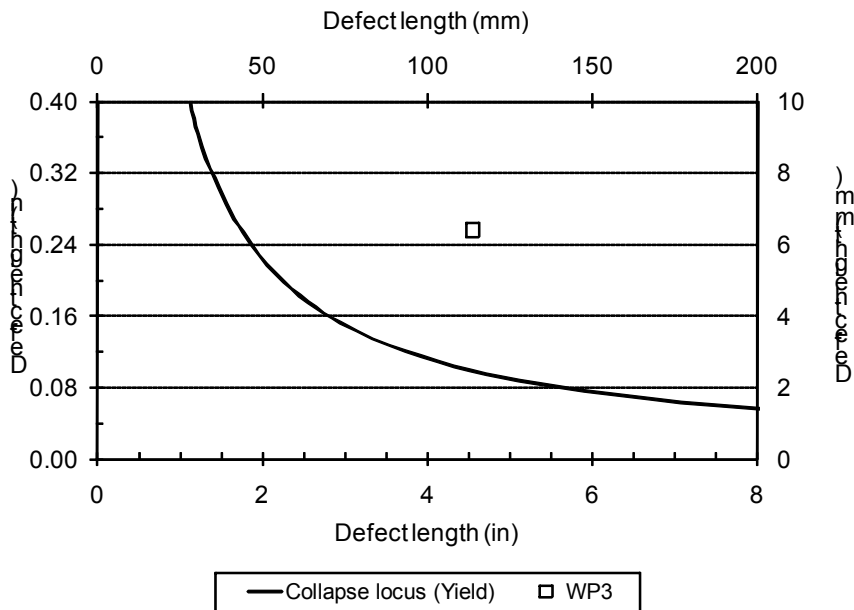


(b) Comparison of the CWP defect size tested with the maximum allowable defect sizes for GSY, predicted using the materials measured tensile properties adjacent to the CWP specimen location (collapse locus calculated using equation [20] from Section 3.2.3).

Figure G21 Weld B03, CWP specimen B03-WP2: Comparison of the CWP test results with the EPRG collapse loci.

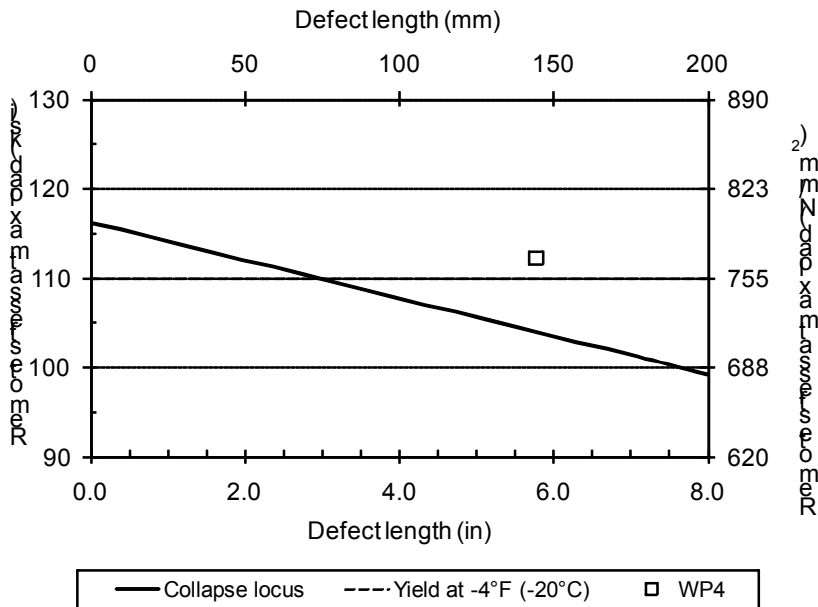


(a) Effect of the length of the defect in the CWP specimen with the predicted failure curve (collapse locus calculated using equation [18] from Section 3.2.3)

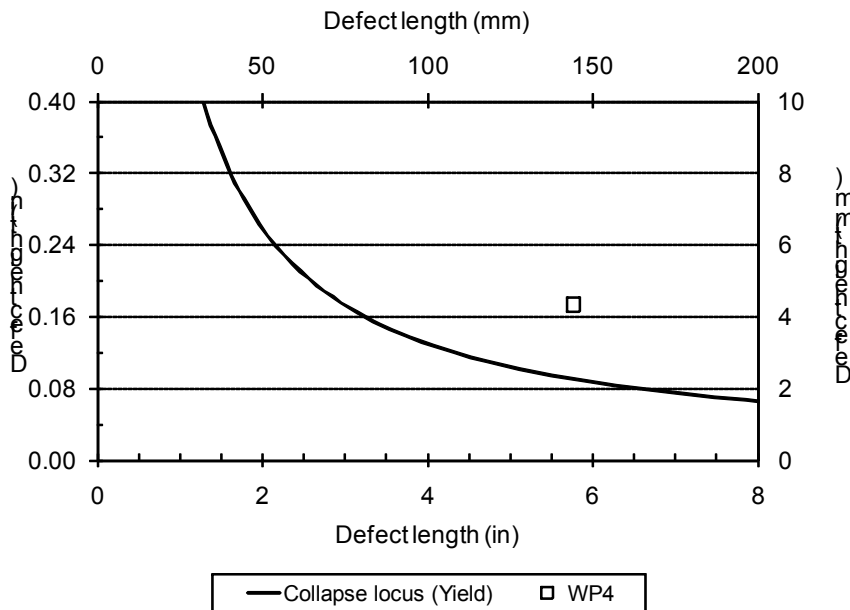


(b) Comparison of the CWP defect size tested with the maximum allowable defect sizes for GSY, predicted using the materials measured tensile properties adjacent to the CWP specimen location (collapse locus calculated using equation [20] from Section 3.2.3).

Figure G22 Weld B03, CWP specimen B03-WP3: Comparison of the CWP test results with the EPRG collapse loci.

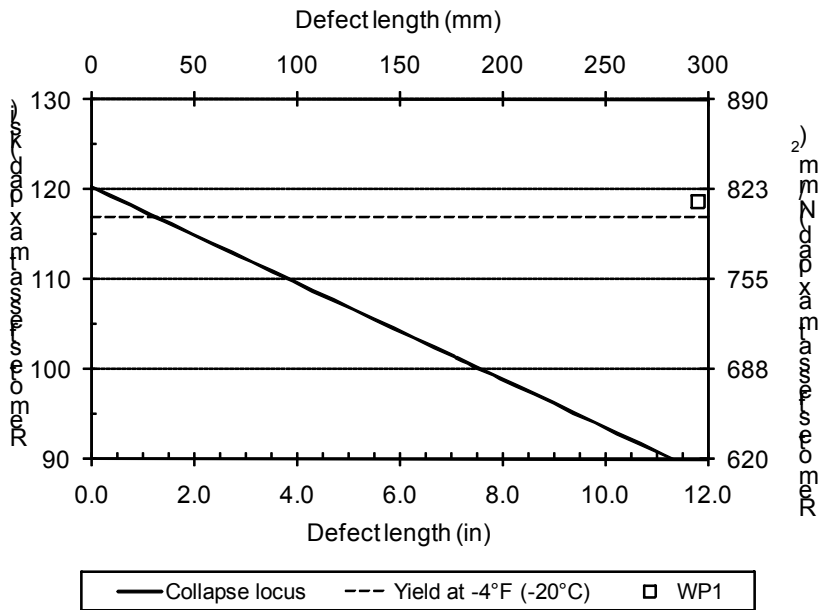


(a) Effect of the length of the defect in the CWP specimen with the predicted failure curve (collapse locus calculated using equation [18] from Section 3.2.3)

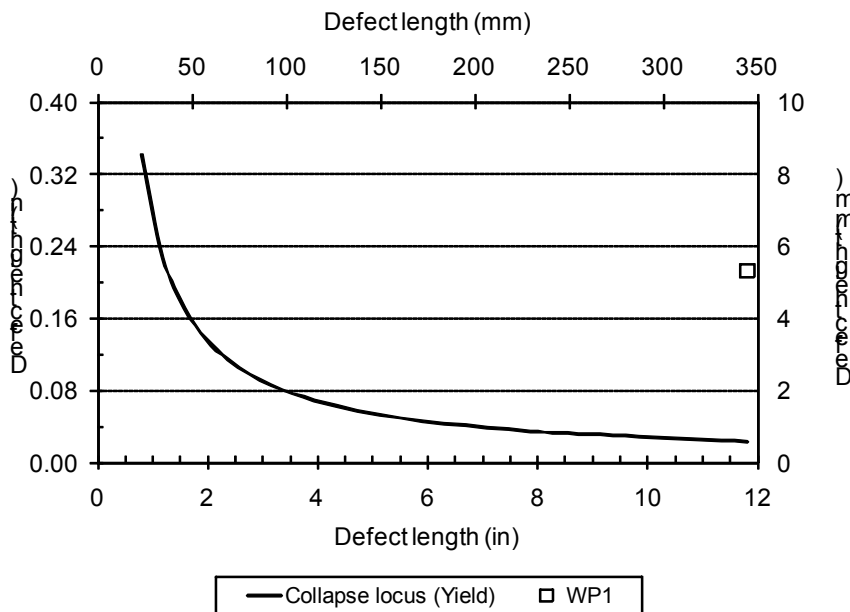


(b) Comparison of the CWP defect size tested with the maximum allowable defect sizes for GSY, predicted using the materials measured tensile properties adjacent to the CWP specimen location (collapse locus calculated using equation [20] from Section 3.2.3).

Figure G23 Weld B03, CWP specimen B03-WP4: Comparison of the CWP test results with the EPRG collapse loci.

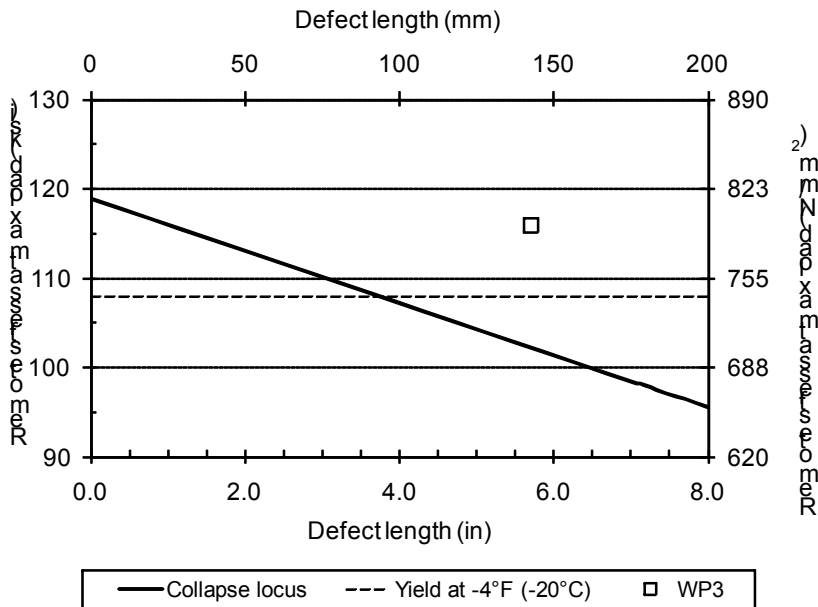


(a) Effect of the length of the defect in the CWP specimen with the predicted failure curve (collapse locus calculated using equation [18] from Section 3.2.3)

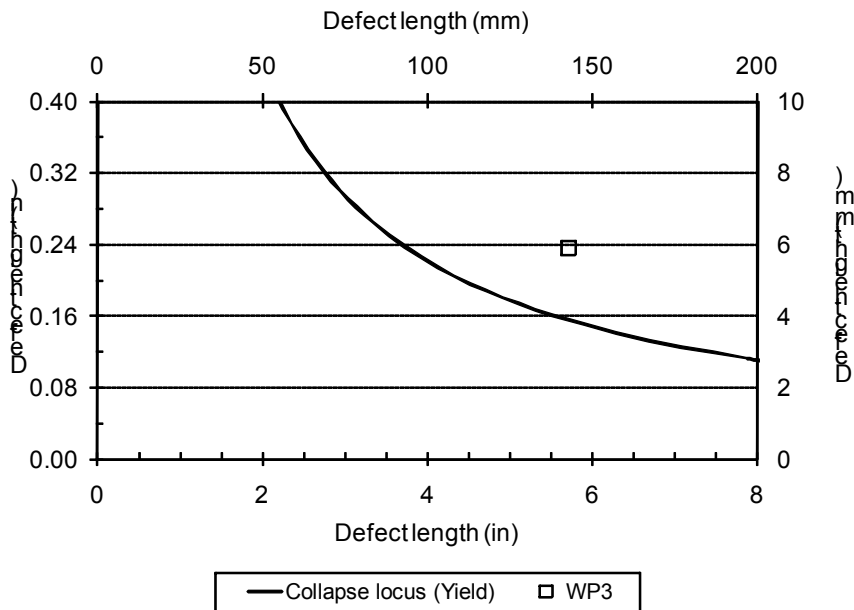


(b) Comparison of the CWP defect size tested with the maximum allowable defect sizes for GSY, predicted using the materials measured tensile properties adjacent to the CWP specimen location (collapse locus calculated using equation [20] from Section 3.2.3).

Figure G24 Weld B06, CWP specimen B06-WP1: Comparison of the CWP test results with the EPRG collapse loci.

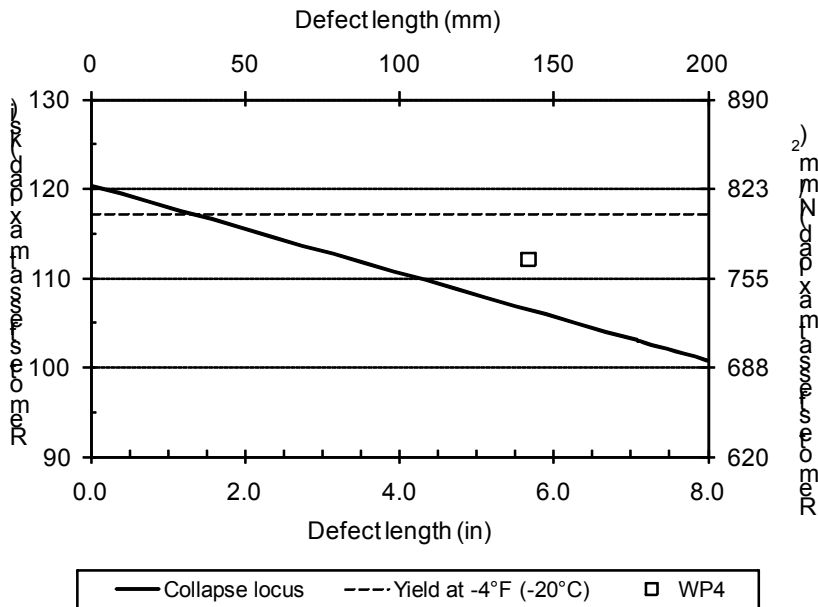


(a) Effect of the length of the defect in the CWP specimen with the predicted failure curve (collapse locus calculated using equation [18] from Section 3.2.3)

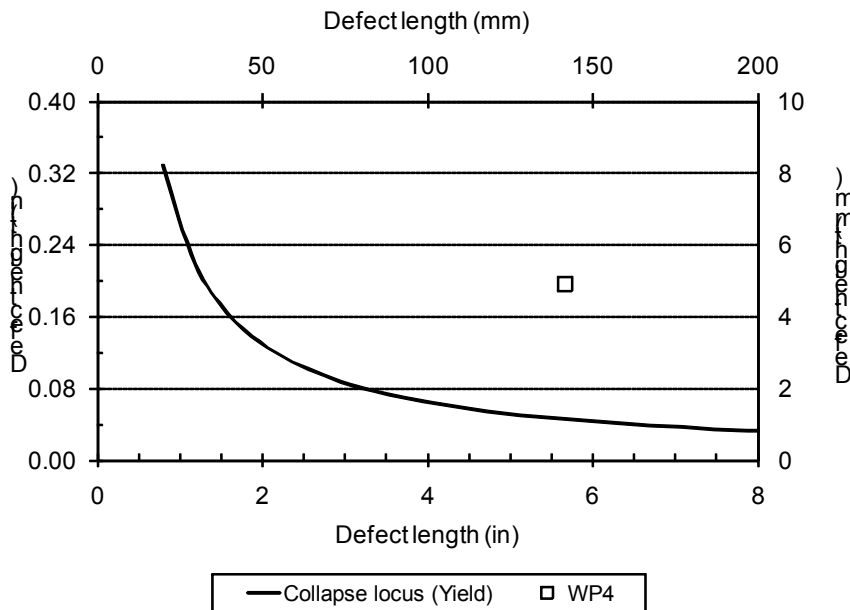


(b) Comparison of the CWP defect size tested with the maximum allowable defect sizes for GSY, predicted using the materials measured tensile properties adjacent to the CWP specimen location (collapse locus calculated using equation [20] from Section 3.2.3).

Figure G25 Weld B06, CWP specimen B06-WP3: Comparison of the CWP test results with the EPRG collapse loci.

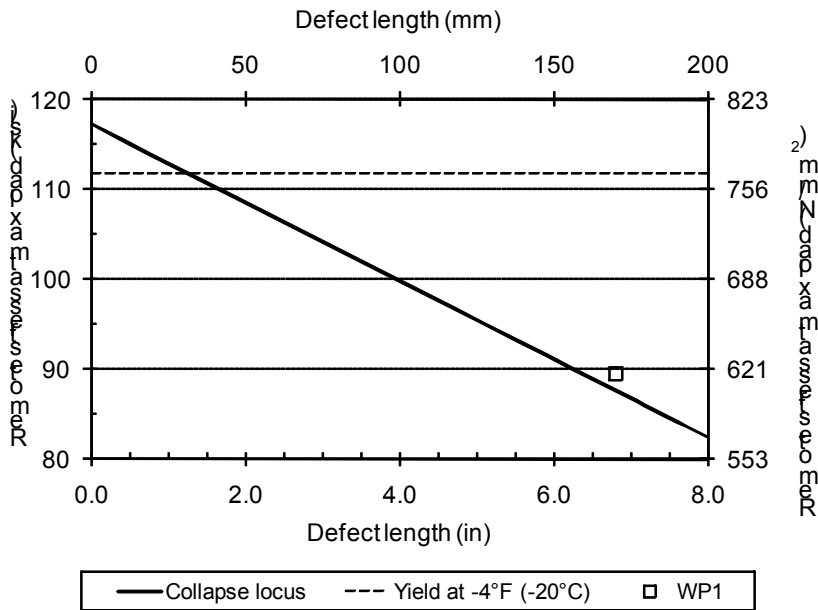


(a) Effect of the length of the defect in the CWP specimen with the predicted failure curve (collapse locus calculated using equation [18] from Section 3.2.3)

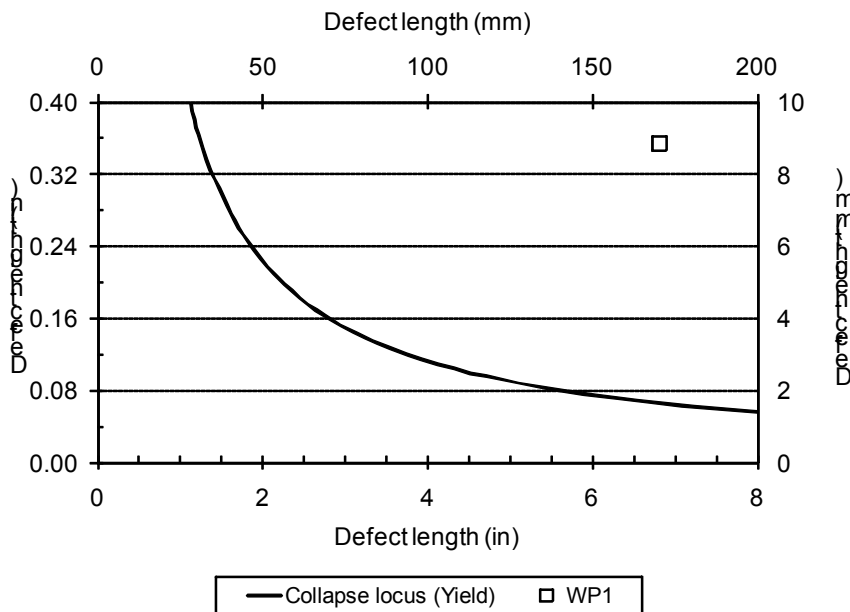


(b) Comparison of the CWP defect size tested with the maximum allowable defect sizes for GSY, predicted using the materials measured tensile properties adjacent to the CWP specimen location (collapse locus calculated using equation [20] from Section 3.2.3).

Figure G26 Weld B06, CWP specimen B06-WP4: Comparison of the CWP test results with the EPRG collapse loci.

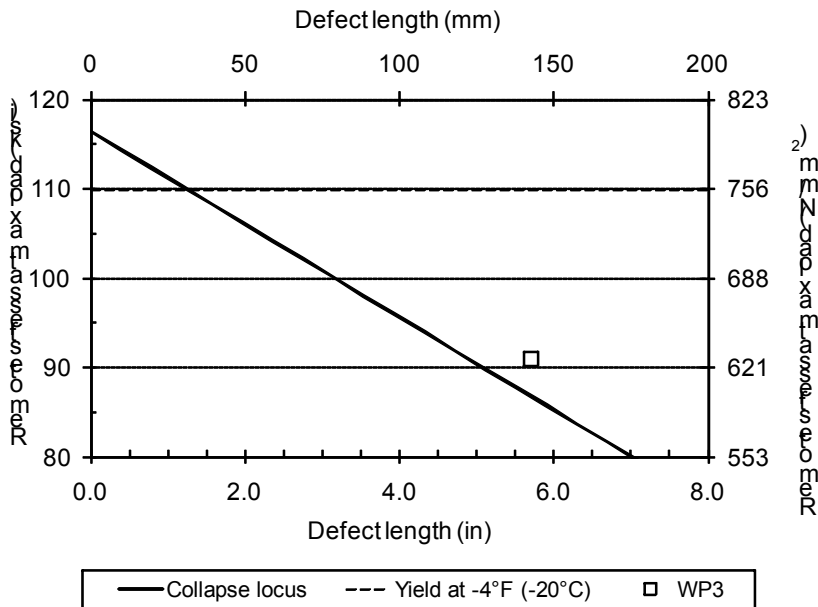


(a) Effect of the length of the defect in the CWP specimen with the predicted failure curve (collapse locus calculated using equation [18] from Section 3.2.3)

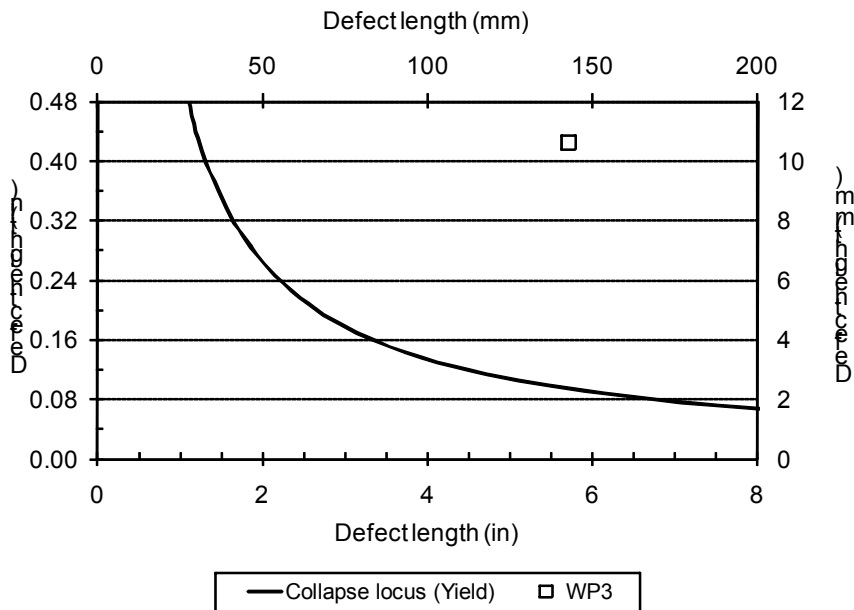


(b) Comparison of the CWP defect size tested with the maximum allowable defect sizes for GSY, predicted using the materials measured tensile properties adjacent to the CWP specimen location (collapse locus calculated using equation [20] from Section 3.2.3).

Figure G27 Weld B08, CWP specimen B08-WP1: Comparison of the CWP test results with the EPRG collapse loci.



(a) Effect of the length of the defect in the CWP specimen with the predicted failure curve (collapse locus calculated using equation [18] from Section 3.2.3)



(b) Comparison of the CWP defect size tested with the maximum allowable defect sizes for GSY, predicted using the materials measured tensile properties adjacent to the CWP specimen location (collapse locus calculated using equation [20] from Section 3.2.3).

Figure G28 Weld B08, CWP specimen B08-WP3: Comparison of the CWP test results with the EPRG collapse loci.

Appendix H CSA Z662 Assessments

This appendix presents the critical defect size loci for the avoidance of brittle fracture and plastic collapse for each weld, calculated using the procedures in CSA Z662 (the calculation method is also presented Section 3.3).

The analyses for each weld are material specific, i.e., the loci are based on the minimum measured tensile properties and fracture toughness. The maximum effective applied tensile bending stress is set equal to SMYS.

The CWP defect sizes within the limiting defect size locus would be predicted to fail at an applied tensile bending stress greater than SMYS.

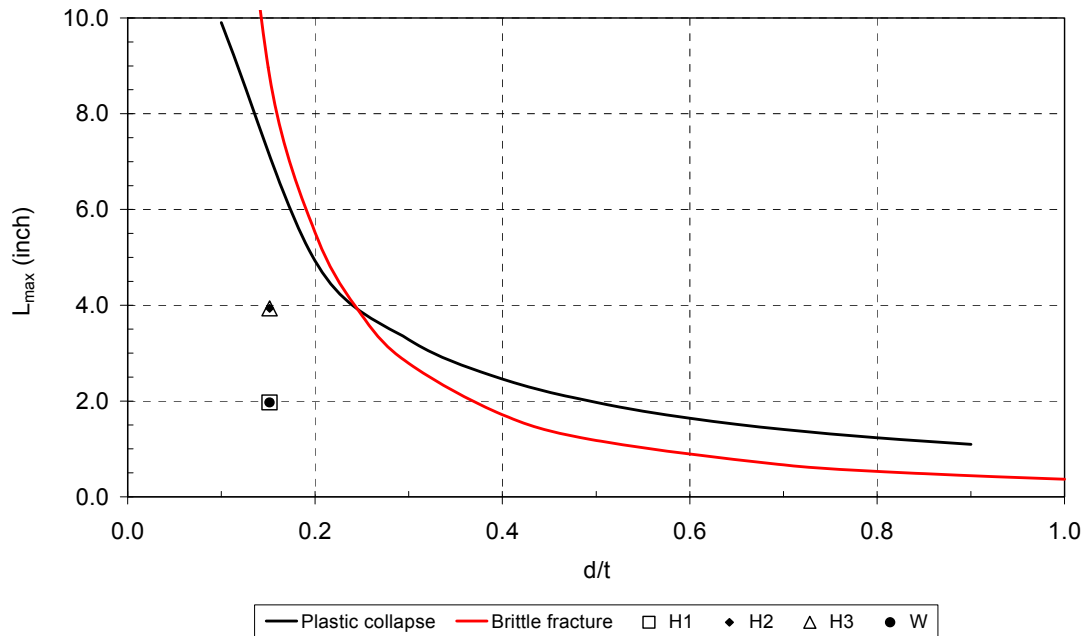


Figure H1 Weld A17 - CSA Z662 analysis results: Comparison of maximum allowable defect sizes with the CWP test specimen defects.

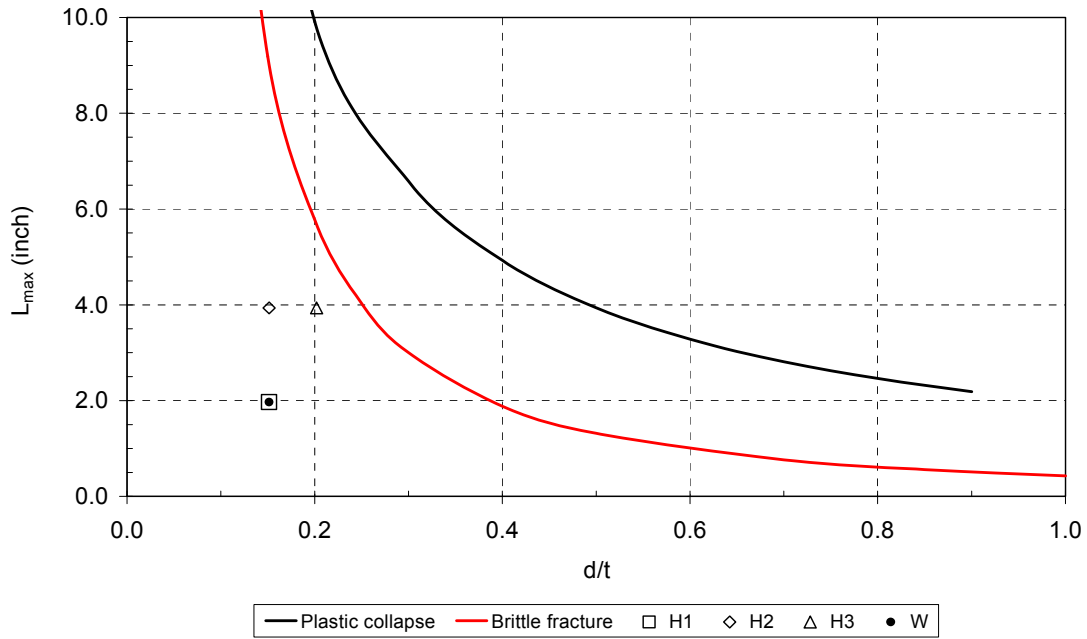


Figure H2 Weld A33 – CSA Z662 analysis results: Comparison of maximum allowable defect sizes with the CWP test specimen defects

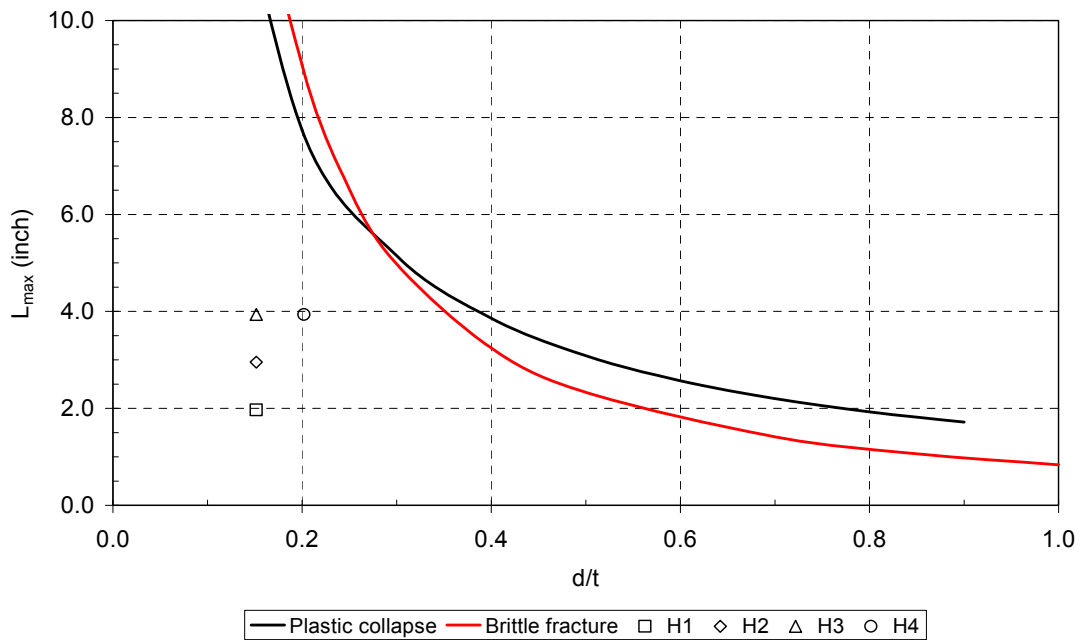


Figure H3 Weld A46 – CSA Z662 analysis results: Comparison of maximum allowable defect sizes with the CWP test specimen defects

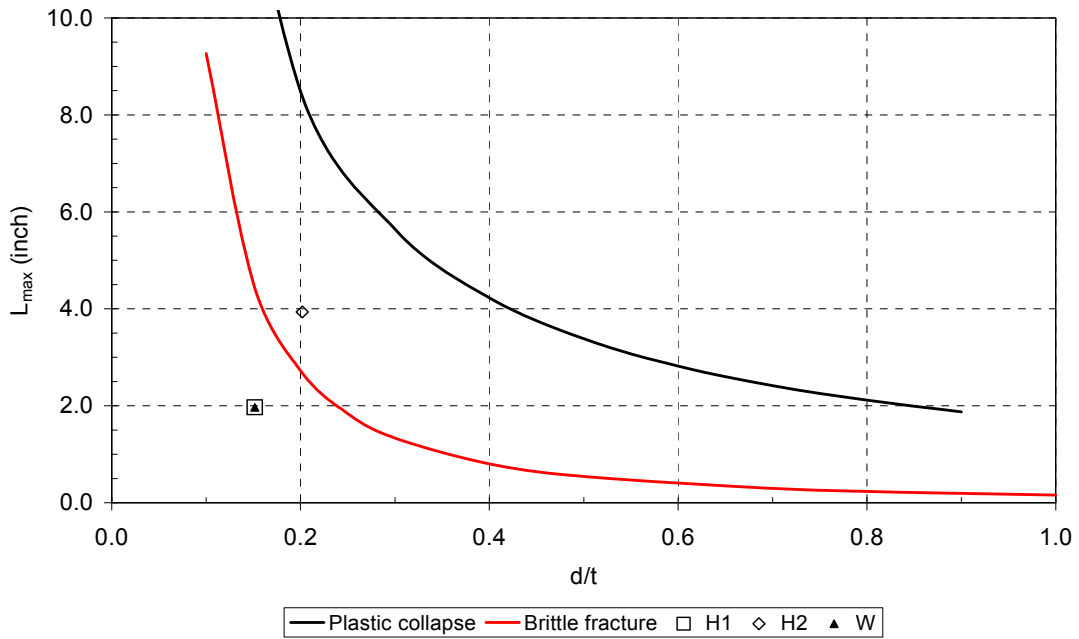


Figure H4 Weld A50 – CSA Z662 analysis results: Comparison of maximum allowable defect sizes with the CWP test specimen defects

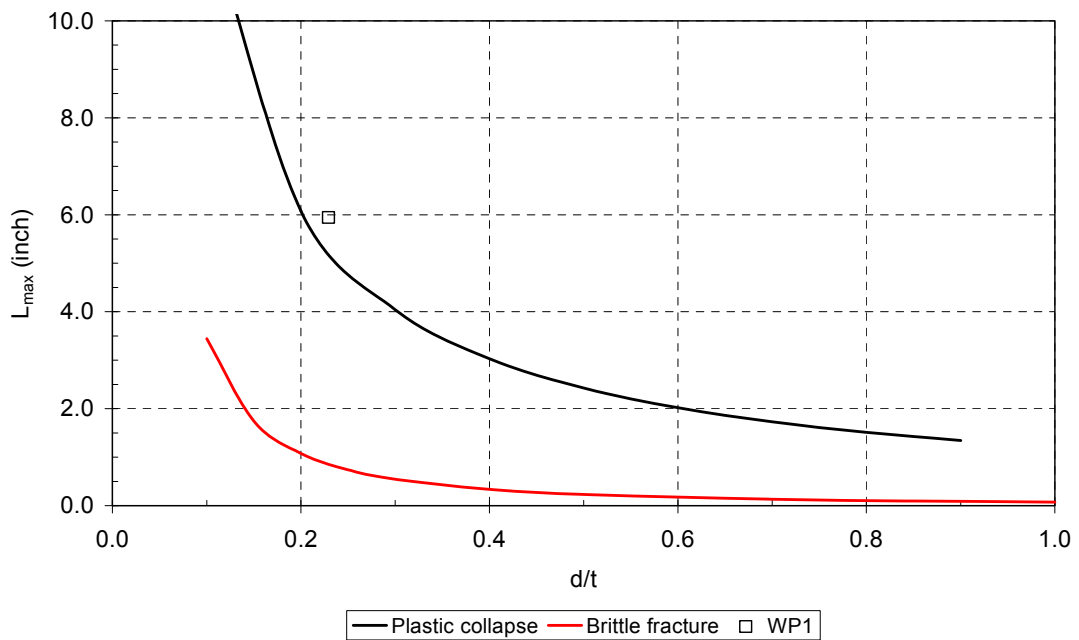


Figure H5 Weld B03, CWP specimen WP1 – CSA Z662 analysis results: Comparison of maximum allowable defect sizes with the CWP test specimen defect

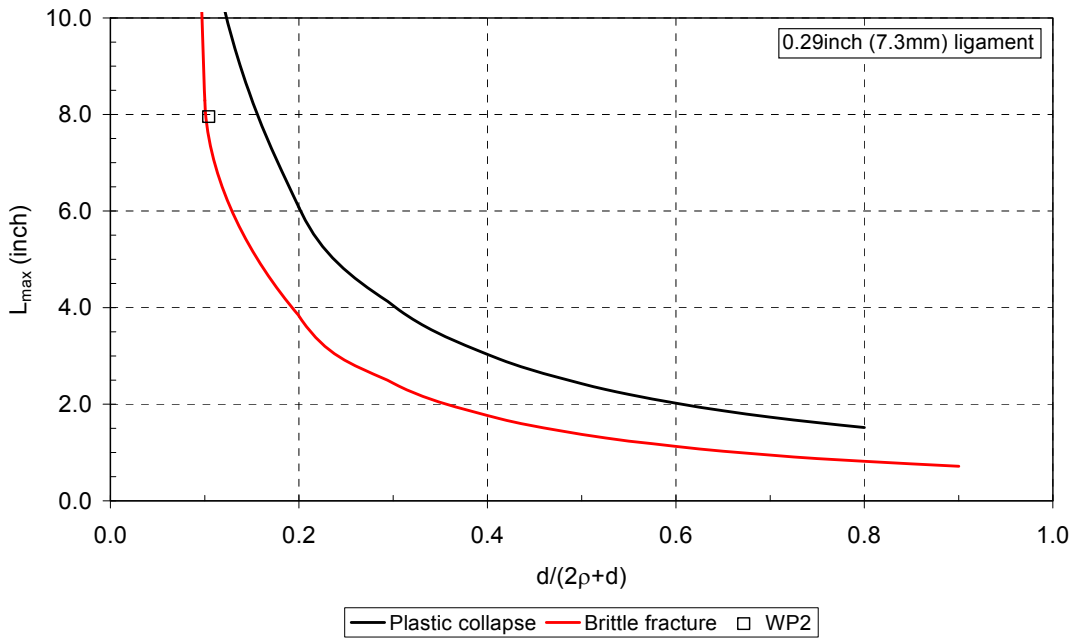


Figure H6 Weld B03, CWP specimen WP2 – CSA Z662 analysis results: Comparison of maximum allowable defect sizes with the CWP test specimen defect

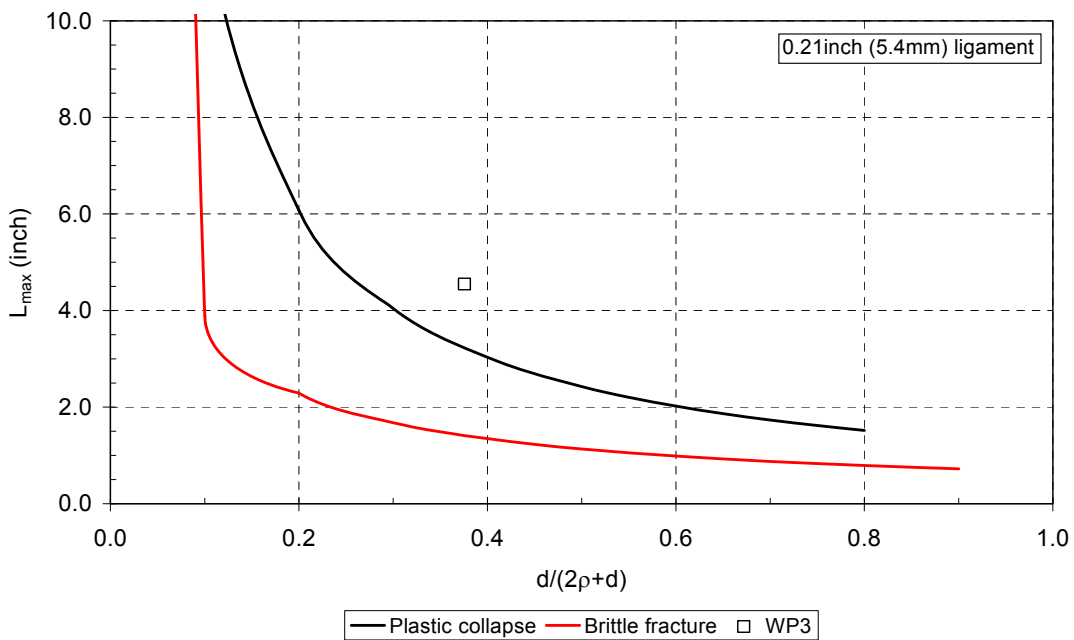


Figure H7 Weld B03, CWP specimen WP3 – CSA Z662 analysis results: Comparison of maximum allowable defect sizes with the CWP test specimen defect

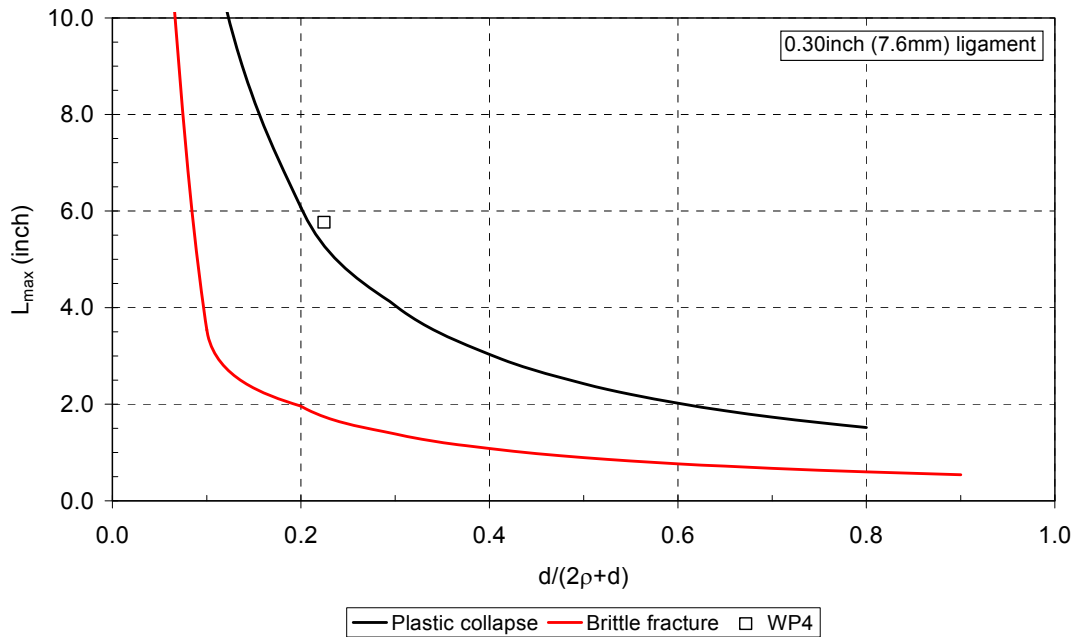


Figure H8 Weld B03, CWP specimen WP4 – CSA Z662 analysis results: Comparison of maximum allowable defect sizes with the CWP test specimen defect

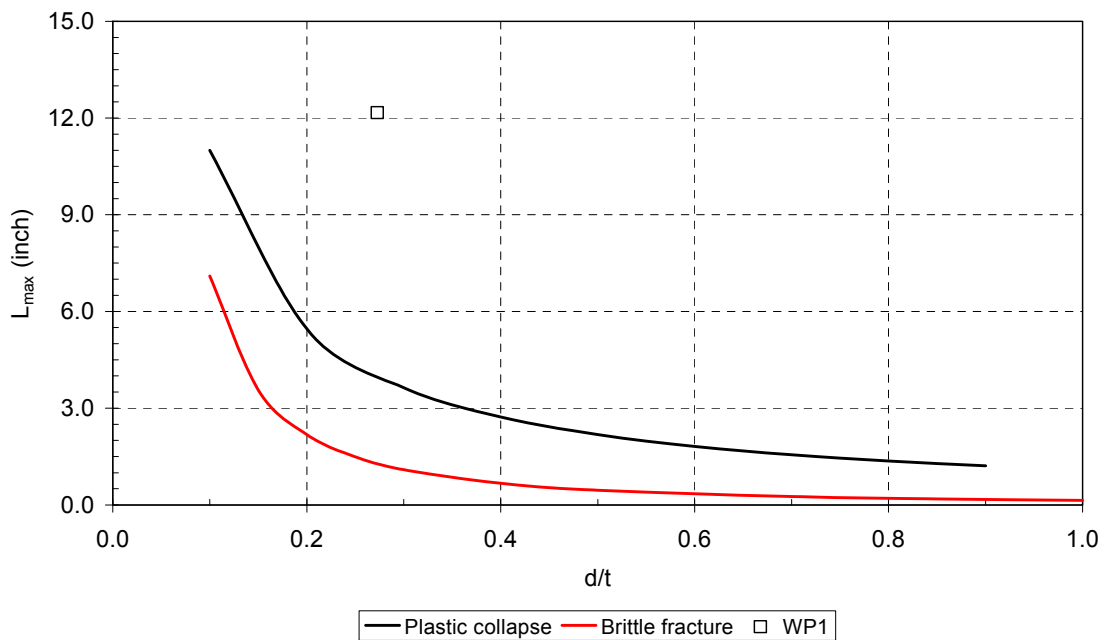


Figure H9 Weld B06, CWP specimen WP1 – CSA Z662 analysis results: Comparison of maximum allowable defect sizes with the CWP test specimen defect

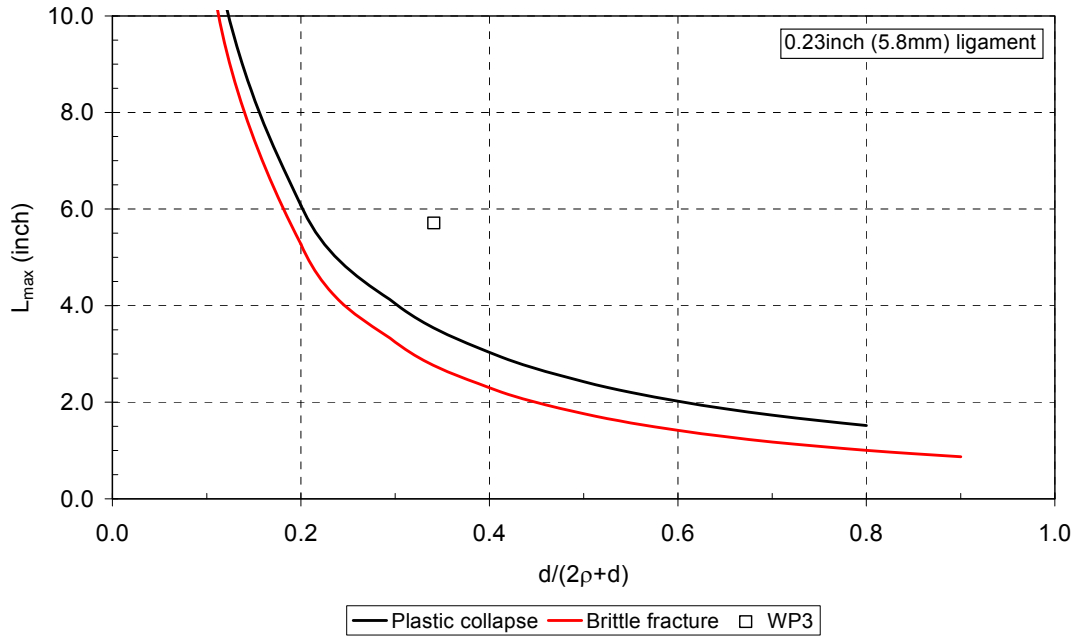


Figure H10 Weld B06, CWP specimen WP3 – CSA Z662 analysis results: Comparison of maximum allowable defect sizes with the CWP test specimen defect

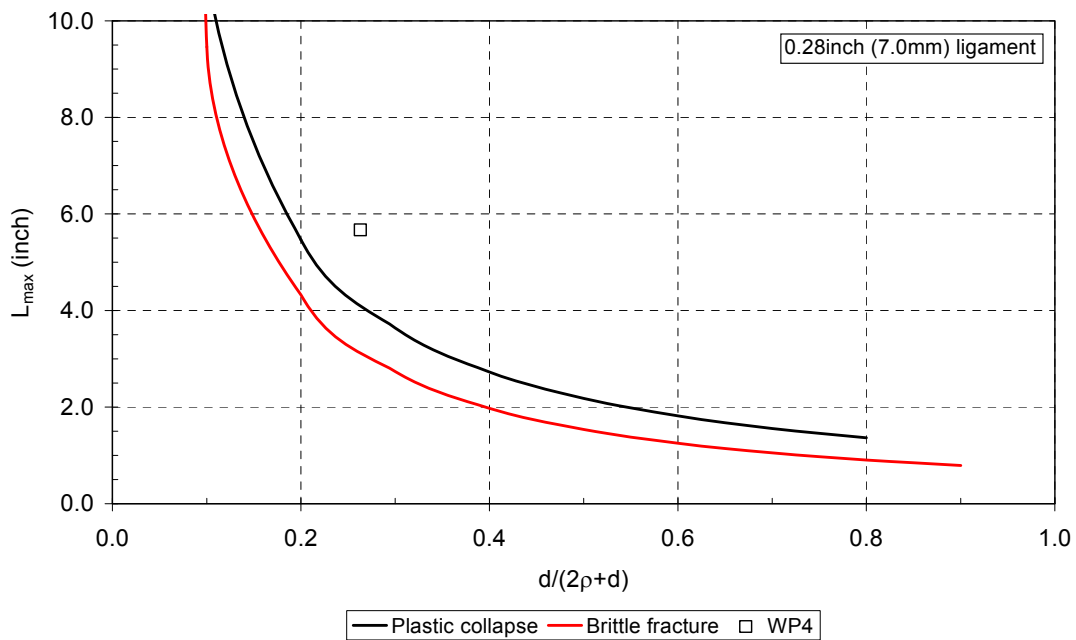


Figure H11 Weld B06, CWP specimen WP4 – CSA Z662 analysis results: Comparison of maximum allowable defect sizes with the CWP test specimen defect

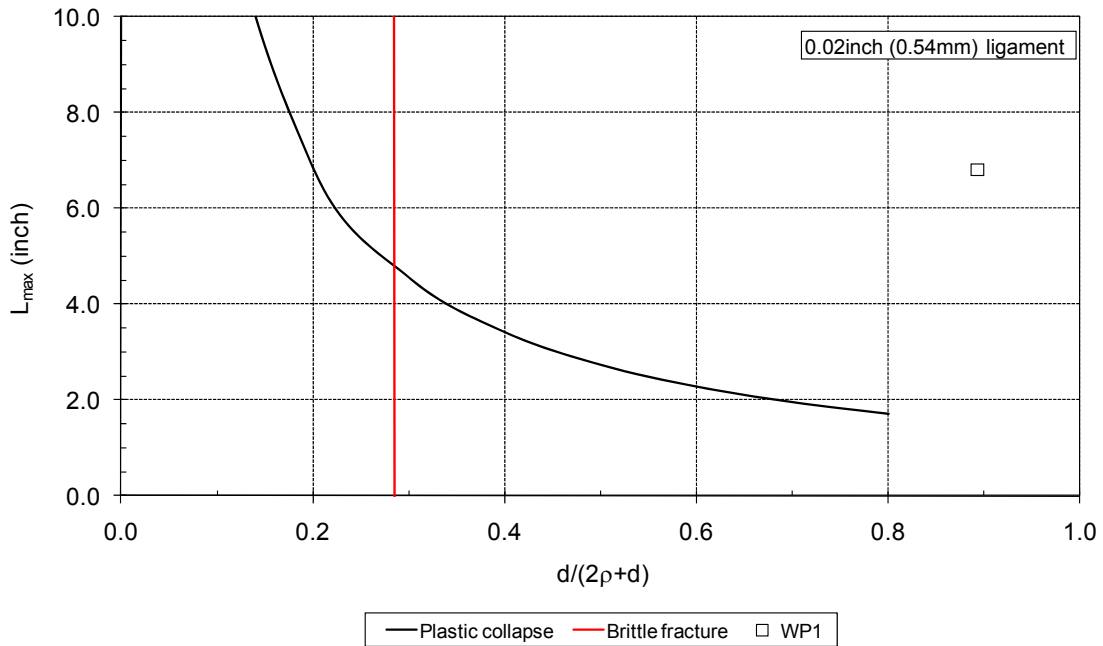


Figure H12 Weld B08, CWP specimen WP1 – CSA Z662 analysis results: Comparison of maximum allowable defect sizes with the CWP test specimen defect

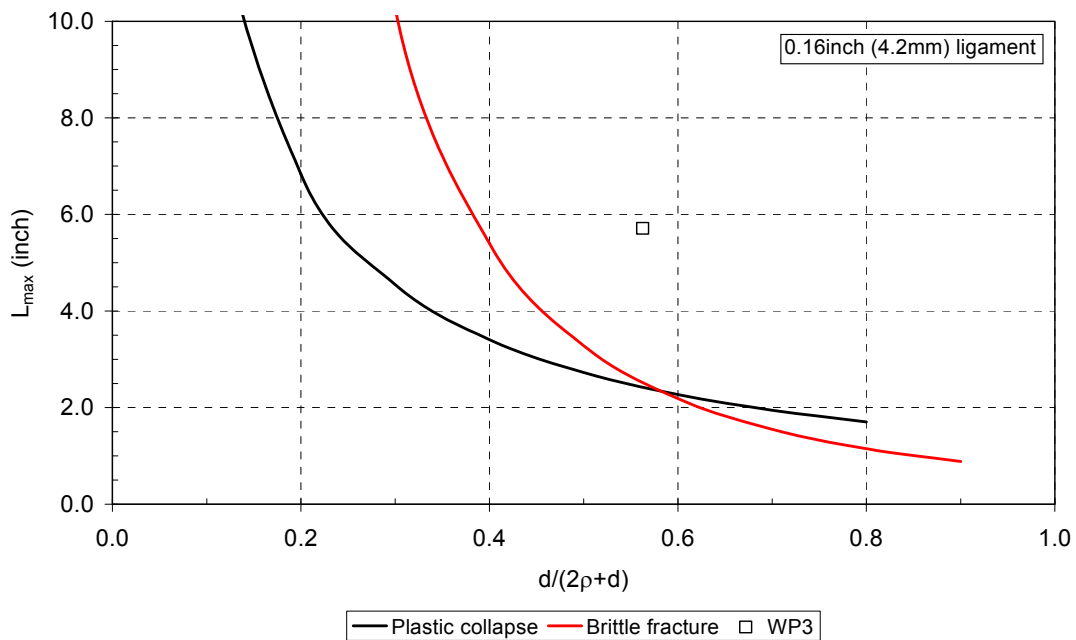


Figure H13 Weld B08, CWP specimen WP3 – CSA Z662 analysis results: Comparison of maximum allowable defect sizes with the CWP test specimen defect.

Appendix I BS 7910 Assessments

Due to the similarity in the assessments undertaken of the A-series welds, a detailed overview was provided of the analysis and results from one CWP test; A06-WP-H1, the remainder is summarized below. The input data for the CWP tests are given in Table I1 for the A-series welds and Table I3 for the B-series welds. The results of the assessment of the CWP tests are presented in Table I2 and Table I4 for the A-series and B-series welds respectively.

The following abbreviations have been used in the following tables:

Term	Description	Units
a	= Defect height	in
B	= Plate thickness	in
d	= Misalignment of plate edges	in
FoS	= Factor of safety	
J	= J-integral measure of fracture toughness	kJ/m ²
K_r	= Fracture ratio of applied elastic stress intensity factor (K) to the materials fracture toughness	
L	= Cap or Root width	in
L_r	= Ratio of applied load to the yield load	
P_m	= Gross failure stress from CWP test	ksi
$P_{m(crit)}$	= Predicted 'critical' failure stress for assessment point to lay on the FAC	ksi
ρ	= Minimum ligament dimension of an embedded defect	in
$R_{p0.2(RT)}$	= Yield strength measured at room temperature	ksi
$R_{p0.2(-4F)}$	= Yield strength at -4°F (estimated from $R_{p0.2(RT)}$)	ksi
$R_{m(-4F)}$	= Tensile strength at -4°F (estimated from $R_{p0.2(-4F)}$ and the yield to tensile strength ratio at room temperature)	ksi
W	= Plate width	in
2c	= Defect length	in

The analyses are based on the Level 2A assessment method; the FAD is constructed from the measured tensile properties and fracture toughness corresponding to the region within the weldment where the notch is located. The FAD is shown in Figure I1. The axes are joined by the FAC which describes the relationship between brittle fracture (K_r) and plastic collapse (L_r). If the assessment point, K_r , L_r lies within the FAC the defect is considered acceptable, otherwise the defect is deemed unacceptable (i.e., it could lead to failure). A point on the FAC is considered critical.

In Table I2 and Table I4 the results of the analysis of the CWP tests are presented. The analyses are based on the 'flat plate' solution and the loading is direct tension. The results of the analyses all show their respective assessment point to lay outside the FAC. A second assessment was undertaken, aimed at determining the critical failure stress, $P_{m(crit)}$ for the assessment point to lay on the FAC. A factor of safety is calculated whereby $P_{m(crit)}$ is compared with the actual failure stress. A third assessment was undertaken to investigate the sensitivity of the calculated failure stress to the materials toughness. The corresponding values of $P_{m(crit)}$ given in results tables are collapse dominated, i.e., further increases in fracture toughness

have no effect on the predicted value of $P_{m(crit)}$. These 'toughness independent' values of $P_{m(crit)}$ are compared with the corresponding test failure stress; conservative predictions were obtained for each CWP test (i.e., the factor of safety is greater than 1).

Weld	CWP	Notch		Specimen and defect dimensions						Failure stress	Material properties			
		Location	Pipe side	B in	W in	a in	2c in	L in	d in	P _m ksi	R _{p0.2(RT)} ksi	R _{p0.2(-4F)} ksi	R _{m(-4F)} ksi	J kJ/m ²
A06	WP-H1	HAZ	Pipe 1	0.780	12.2	0.118	1.97	0.197		125.5	112.1	116.6	127.9	64.5
	WP-H2	HAZ	Pipe 1	0.784	12.1	0.118	3.94	0.197		117.5	112.1	116.6	127.4	64.5
	WP-H3	HAZ	Pipe 1	0.787	12.1	0.157	3.94	0.197		114.1	111.8	116.2	127.6	64.5
	WP-W	AWM	WMC	0.782	12.1	0.118	1.97	0.197		124.3	112.1	116.6	128.6	130.5
A17	WP-H1	HAZ	Pipe 1	0.780	12.2	0.118	1.97	0.197		120.2	101.8	106.3	113.7	183
	WP-H2	HAZ	Pipe 2	0.779	12.1	0.118	3.94	0.197		115.3	106.8	111.3	123.8	183
	WP-H3	HAZ	Pipe 1	0.778	12.2	0.118	3.94	0.197	0.077	113.4	110.0	114.5	119.8	183
	WP-W	AWM	WMC	0.778	12.1	0.118	1.97	0.197		118.5	109.6	114.1	119.4	118
A33	WP-H1	HAZ	Pipe 1	0.779	12.1	0.118	1.97	0.197		123.0	111.4	115.9	129.1	101
	WP-H2	HAZ	Pipe 1	0.781	12.0	0.118	3.94	0.197		117.6	114.0	118.5	128.3	101
	WP-H3	HAZ	Pipe 1	0.782	12.1	0.157	3.94	0.197		114.7	114.1	118.5	131.7	101
	WP-W	AWM	WMC	0.780	12.1	0.118	1.97	0.197		125.0	112.7	117.2	129.1	115
A46	WP-H1	HAZ	Pipe 1	0.777	12.2	0.118	1.97	0.197		119.4	110.5	115.0	126.6	74.2
	WP-H2	HAZ	Pipe 1	0.778	12.2	0.118	2.95	0.197		115.0	108.1	112.5	126.3	74.2
	WP-H3	HAZ	Pipe 1	0.775	12.1	0.118	3.94	0.197		113.6	107.2	111.6	126.5	74.2
	WP-H4	HAZ	Pipe 1	0.781	12.2	0.157	3.94	0.197		108.8	107.4	111.9	126.9	74.2
A50	WP-H1	HAZ	Pipe 1	0.780	12.1	0.118	1.97	0.197		121.5	111.8	116.3	125.5	43.4
	WP-H2	HAZ	Pipe 1	0.780	12.2	0.157	3.94	0.197		115.5	109.8	114.3	119.8	43.4
	WP-W	AWM	WMC	0.784	12.1	0.118	1.97	0.197		119.0	111.0	115.4	119.2	159.2

Table I1 Input values to the BS 7910 assessments of the individual CWP tests undertaken of the A-series welds.

Weld	CWP	CWP assessment results			Critical stress assessment		Critical stress assessment (toughness independent)		
		K_r	L_r	Result	$P_{m(crit)}$ ksi	FoS	$P_{m(crit)}$ ksi	FoS	Result
A06	WP-H1	0.987	1.175	Unacceptable	29.9	4.19	111.9	1.12	Conservative
	WP-H2	1.003	1.129	Unacceptable	25.5	4.61	108.8	1.08	Conservative
	WP-H3	1.156	1.147	Unacceptable	5.0	22.98	104.5	1.09	Conservative
	WP-W	0.696	1.164	Unacceptable	92.5	1.34	112.3	1.11	Conservative
A17	WP-H1	0.528	1.235	Unacceptable	100.0	1.20	100.7	1.19	Conservative
	WP-H2	0.572	1.163	Unacceptable	98.1	1.18	104.8	1.10	Conservative
	WP-H3	0.634	1.256	Unacceptable	85.4	1.33	92.4	1.23	Conservative
	WP-W	0.700	1.134	Unacceptable	89.5	1.32	106.9	1.11	Conservative
A33	WP-H1	0.789	1.159	Unacceptable	77.6	1.58	112.1	1.10	Conservative
	WP-H2	0.812	1.113	Unacceptable	70.8	1.66	110.0	1.07	Conservative
	WP-H3	0.948	1.131	Unacceptable	29.6	3.88	107.1	1.07	Conservative
	WP-W	0.744	1.165	Unacceptable	85.2	1.47	112.7	1.11	Conservative
A46	WP-H1	0.909	1.134	Unacceptable	40.0	2.99	110.5	1.08	Conservative
	WP-H2	0.907	1.135	Unacceptable	38.9	2.96	107.6	1.07	Conservative
	WP-H3	0.909	1.142	Unacceptable	37.9	2.99	106.1	1.07	Conservative
	WP-H4	1.052	1.137	Unacceptable	16.9	6.42	102.1	1.07	Conservative
A50	WP-H1	1.192	1.141	Unacceptable	6.1	19.83	110.7	1.10	Conservative
	WP-H2	1.356	1.182	Unacceptable	No assessment possible		100.1	1.15	Conservative
	WP-W	0.607	1.125	Unacceptable	101.4	1.17	107.5	1.11	Conservative

Table I2 Results of the BS 7910 assessments of the individual CWP tests undertaken of the A-series welds.

Weld	CWP	Defect type	Specimen and defect dimensions						Failure stress	Material properties			
			B in	W in	a in	2c in	L in	ρ in		P _m ksi	R _{p0.2(RT)} ksi	R _{p0.2(-4F)} ksi	R _{m(-4F)} ksi
B03	WP1	del LORP/LOSWF	0.777	12.2	0.179	5.94	0.197	-	119.1	104.0	108.5	124.4	77.9
	WP2	del LOSWF	0.779	12.3	0.067	7.95	0.591	0.29	123.6	106.6	111.1	124.6	77.9
	WP3	del Porosity	0.779	12.1	0.256	4.55	0.197	0.21	121.3	107.9	112.4	123.3	77.9
	WP4	LOSWF	0.778	12.2	0.173	5.77	0.197	0.30	112.3	105.4	109.9	122.6	77.9
B06	WP1	del LORP/LOSWF	0.788	12.2	0.213	12.15	0.197	-	118.6	112.4	116.9	129.8	96.7
	WP2	Undercut	0.788	12.1	No defect found				111.0	102.8	107.3	114.9	96.7
	WP3	del LOSWF	0.791	12.1	0.236	5.71	0.591	0.23	115.9	103.4	107.9	114.6	96.7
	WP4	del	0.793	12.2	0.197	5.67	0.591	0.28	112.1	112.7	117.2	129.4	96.7
B08	WP1	del	0.781	12.2	0.354	6.81	0.197	0.02	89.5	107.3	111.8	124.4	126.4
	WP2		0.782	12.1	No defect found				121.4	106.7	111.2	123.7	126.4
	WP3	del	0.782	12.2	0.425	5.71	0.591	0.17	90.9	105.4	109.9	123.4	126.4

Notes: del is deliberate (i.e., a welding defect deliberately introduced into the weld, during welding), LORP is lack or root penetration and LOSWF is lack of side wall fusion

Table I3 Input values to the BS 7910 assessments of the individual CWP tests undertaken of the B-series welds.

Weld	CWP	CWP assessment results			Critical stress assessment		Critical stress assessment (toughness independent)		
		K_r	L_r	Result	$P_{m(crit)}$ ksi	FoS	$P_{m(crit)}$ ksi	FoS	Result
B03	WP1	1.087	1.342	Unacceptable	10.4	11.50	95.2	1.25	Conservative
	WP2	0.407	1.137	Unacceptable	107.3	1.15	0.0	0.00	Conservative
	WP3	0.700	1.535	Unacceptable	60.6	2.00	82.8	1.46	Conservative
	WP4	0.606	1.253	Unacceptable	85.1	1.32	94.7	1.19	Conservative
B06	WP1	1.205	1.391	Unacceptable	Unable to assess		90.0	1.32	Conservative
	WP2	No defect found							
	WP3	0.578	1.489	Unacceptable	74.7	1.55	80.2	1.44	Conservative
	WP4	0.605	1.220	Unacceptable	86.9	1.29	96.7	1.16	Conservative
B08	WP1	1.293	1.268	Unacceptable	Unable to assess		74.5	1.20	Conservative
	WP2	No defect found							
	WP3	0.647	1.632	Unacceptable	23.4	3.88	59.1	1.54	Conservative

Table I4 Results of the BS 7910 assessments of the individual CWP tests undertaken of the B-series welds.

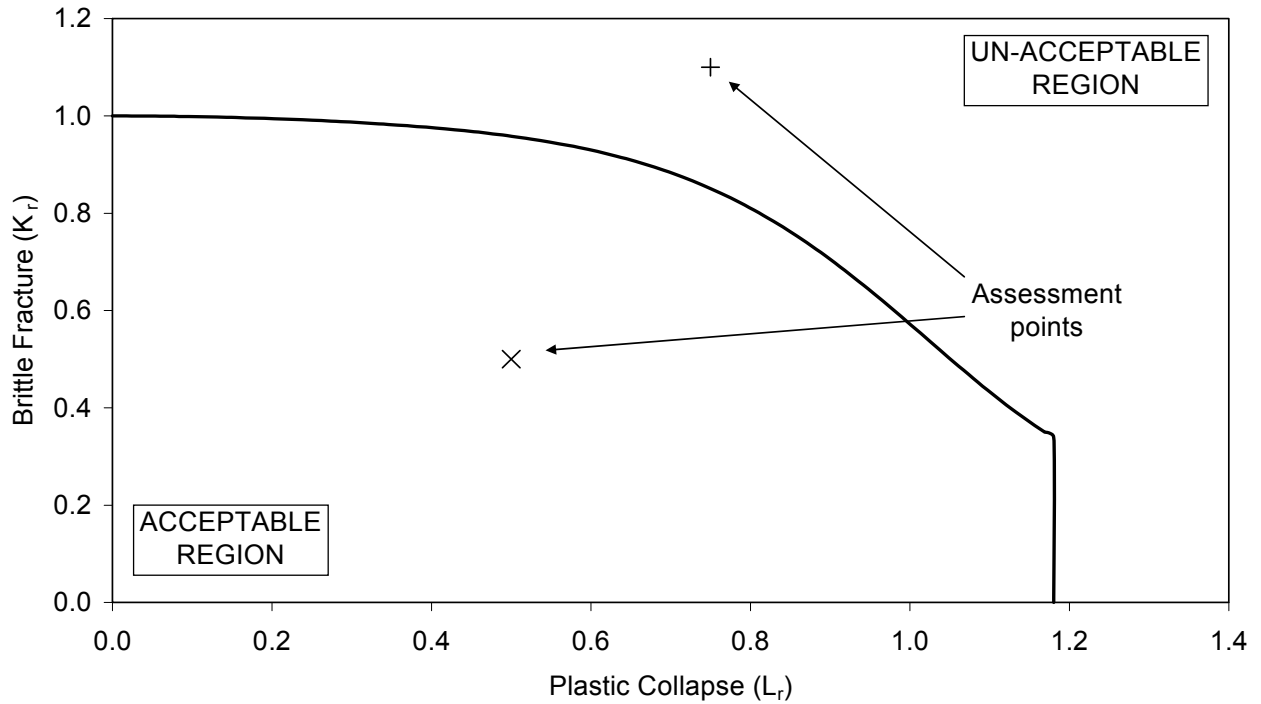


Figure I1 Level 2A Generalized FAD from BS 7910 (illustration only)

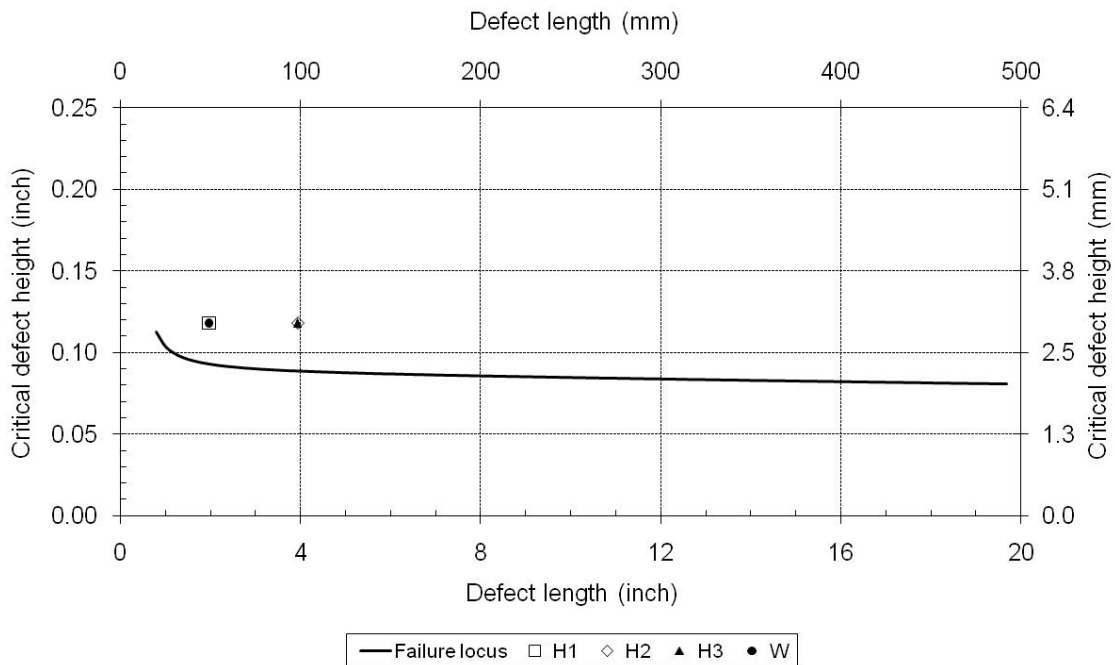


Figure I2 Weld A17: Locus of critical defect size, compared with the defects from the CWP test specimens

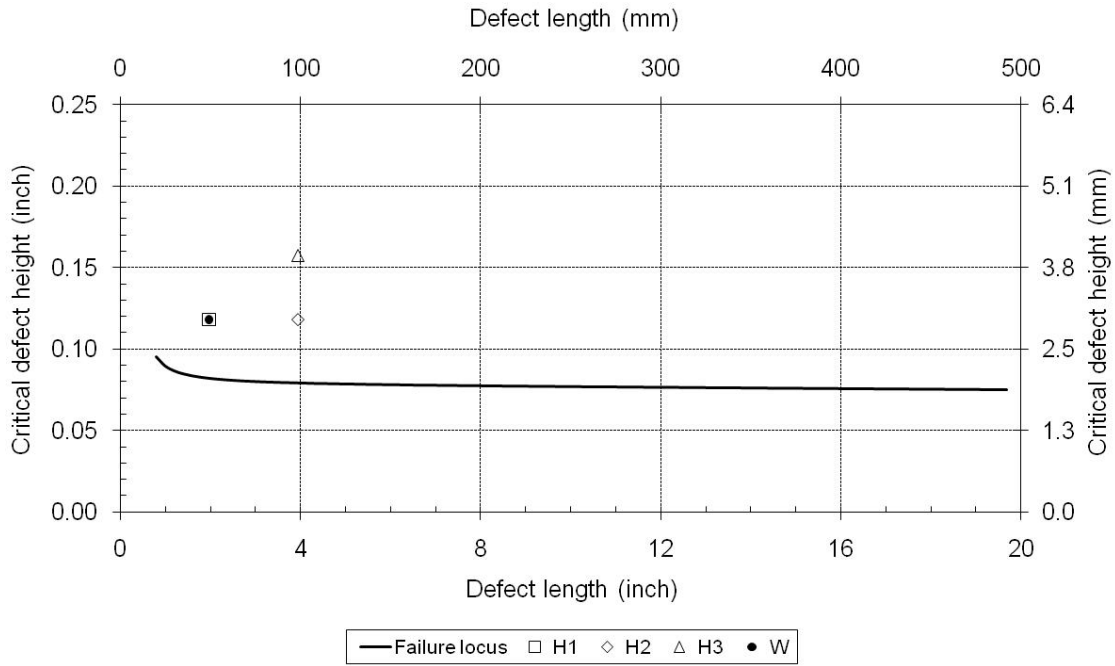


Figure 13 Weld A33: Locus of critical defect size, compared with the defects from the CWP test specimens

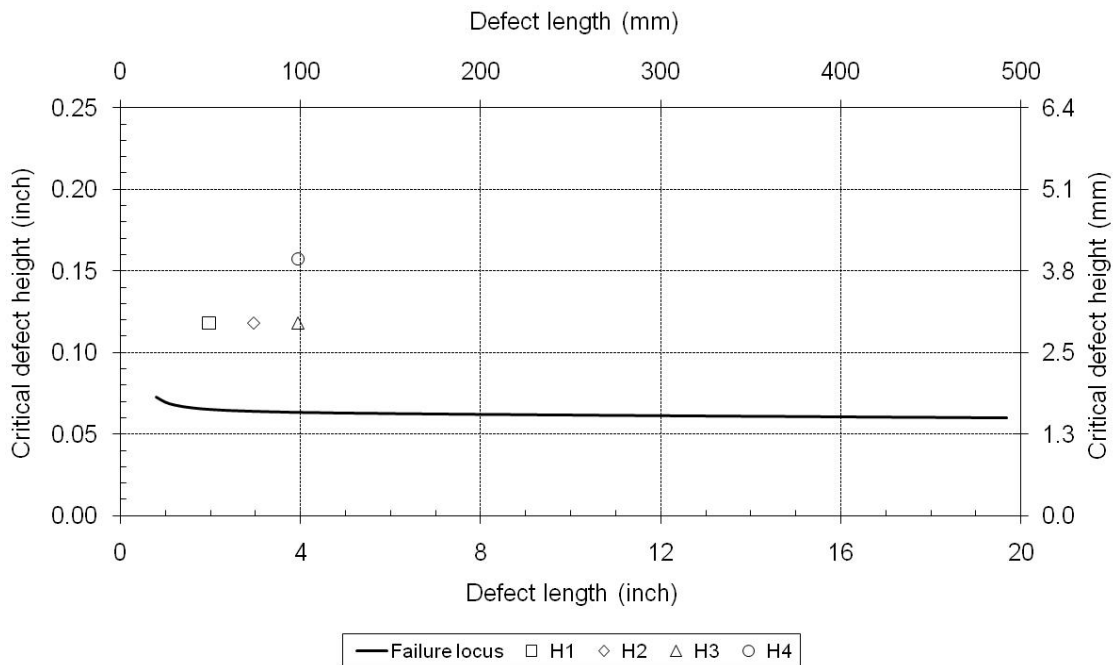


Figure 14 Weld A46: Locus of critical defect size, compared with the defects from the CWP test specimens

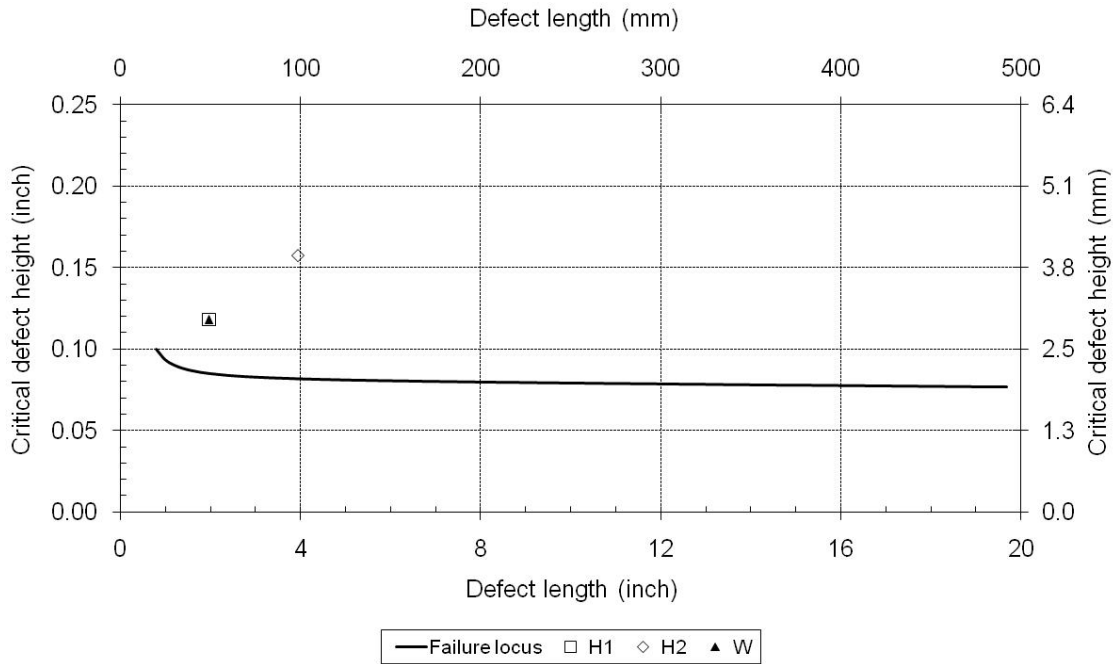
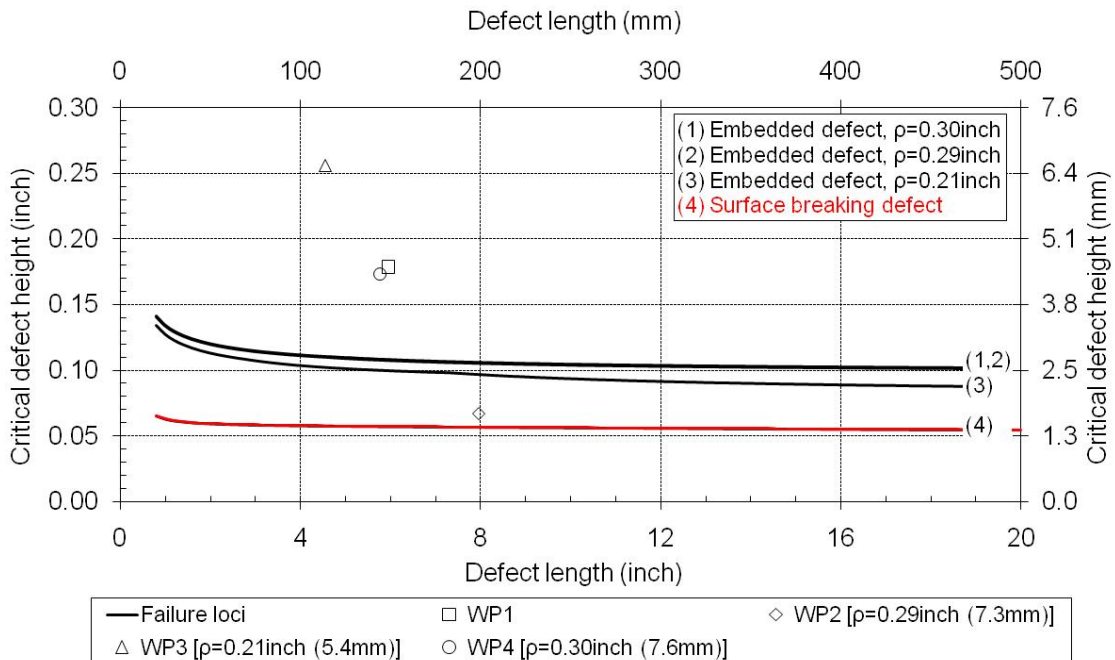
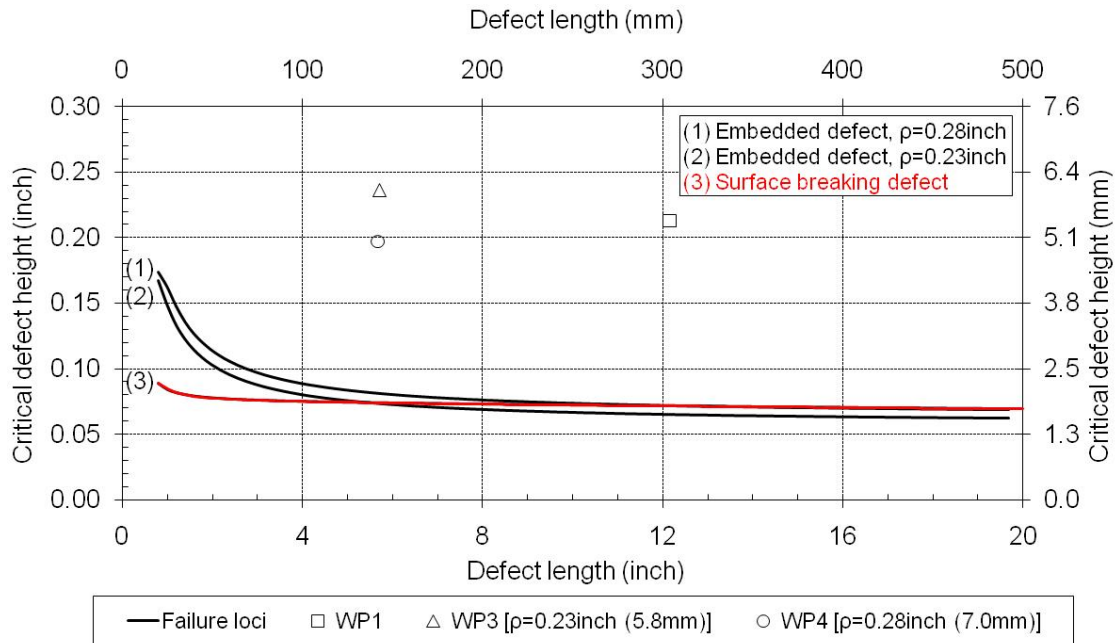


Figure 15 Weld A50: Locus of critical defect size, compared with the defects from the CWP test specimens



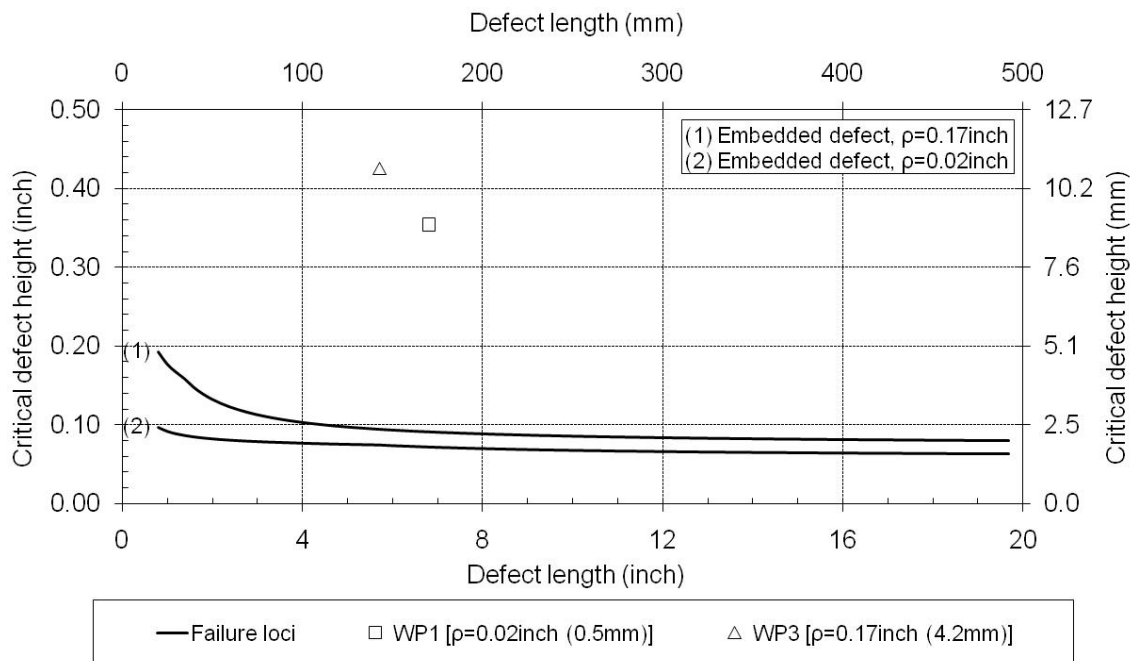
Notes: CWP defect size **above** critical defect size locus – failure stress predicted to be **less than** SMYS
CWP defect size **below** critical defect size locus – failure stress predicted to be **greater than** SMYS

Figure 16 Weld B03: Locus of critical defect size, compared with the defects from the CWP test specimens



Notes: CWP defect size **above** critical defect size locus – failure stress predicted to be **less than** SMYS
CWP defect size **below** critical defect size locus – failure stress predicted to be **greater than** SMYS

Figure 17 Weld B06: Locus of critical defect size, compared with the defects from the CWP test specimens



Notes: CWP defect size **above** critical defect size locus – failure stress predicted to be **less than** SMYS
CWP defect size **below** critical defect size locus – failure stress predicted to be **greater than** SMYS

Figure 18 Weld B08: Locus of critical defect size, compared with the defects from the CWP test specimens.

Appendix J API 579-1/ASME FFS-1 Assessments

Due to the similarity in the assessments undertaken of the A-series welds, a detailed overview was provided of the analysis and results from one CWP test; A06-WP-H1, the remainder are summarized below. The input data for the CWP tests are given in Table J1 for the A-series welds and Table J3 for the B-series welds. The results of the assessment of the CWP tests are presented in Table J2 and Table J4 for the A-series and B-series welds respectively. The results are compared with those obtained from CWP test assessment.

The following abbreviations have been used in the following tables:

Term		Description	Units
a	=	Defect height	in
B	=	Plate thickness	in
d	=	Misalignment of plate edges	in
FoS	=	Factor of safety	
J	=	J-integral measure of fracture toughness	kJ/m ²
K _r	=	Fracture ratio of applied elastic stress intensity factor (K) to the materials fracture toughness	
L	=	Cap or Root width	in
L _r	=	Ratio of applied load to the yield load	
P _m	=	Gross failure stress from CWP test	ksi
P _{m(crit)}	=	Predicted 'critical' failure stress for assessment point to lay on the FAC	ksi
ρ	=	Minimum ligament dimension of an embedded defect	in
R _{p0.2(RT)}	=	Yield strength measured at room temperature	ksi
R _{p0.2(-4F)}	=	Yield strength at -4°F (estimated from R _{p0.2(RT)})	ksi
R _{m(-4F)}	=	Tensile strength at -4°F (estimated from R _{p0.2(-4F)} and the yield to tensile strength ratio at room temperature)	ksi
W	=	Plate width	in
2c	=	Defect length	in

The analyses are based on the Level 2 assessment method; the FAD is constructed from the measured tensile properties and fracture toughness corresponding to the region within the weldment where the notch is located. The magnitude and through wall distribution of welding residual stress was determined using the estimation procedure in API 579-1/ASME FFS-1, the input arc energy of the final weld pass being 0.4 kJ/mm. The FAD is shown in Figure J1. The axes are joined by the FAC which describes the relationship between brittle fracture (K_r) and plastic collapse (L_r). If the assessment point, K_r, L_r lies within the FAC the defect is considered acceptable, otherwise the defect is deemed unacceptable (i.e., it could lead to failure). A point on the FAC is considered critical.

In Table J2 and Table J4 the results of the analysis of the CWP tests are presented. The analyses are based on the 'flat plate' solution and the loading is direct tension. The results of the analyses all show their respective assessment point to lay outside the FAC. A second assessment was undertaken, aimed at

determining the critical failure stress, $P_{m(crit)}$ for the assessment point to lay on the FAC. A factor of safety is calculated whereby $P_{m(crit)}$ is compared with the actual failure stress. A third assessment was undertaken to investigate the sensitivity of the calculated failure stress to the materials toughness. The corresponding values of $P_{m(crit)}$ given in the results tables are collapse dominated, i.e., further increases in fracture toughness have no effect on the predicted value of $P_{m(crit)}$. These 'toughness independent' values of $P_{m(crit)}$ are compared with the corresponding test failure stress; conservative predictions were obtained for each CWP test (i.e., the factor of safety is greater than 1).

Weld	CWP	Notch		Specimen and defect dimensions						Failure stress	Material properties			
		Location	Pipe side	B in	W in	a in	2c in	L in	d in	P _m ksi	R _{p0.2(RT)} ksi	R _{p0.2(-4F)} ksi	R _{m(-4F)} ksi	J kJ/m ²
A06	WP-H1	HAZ	Pipe 1	0.780	12.2	0.118	1.97	0.197		125.5	112.1	116.6	127.9	64.5
	WP-H2	HAZ	Pipe 1	0.784	12.1	0.118	3.94	0.197		117.5	112.1	116.6	127.4	64.5
	WP-H3	HAZ	Pipe 1	0.787	12.1	0.157	3.94	0.197		114.1	111.8	116.2	127.6	64.5
	WP-W	AWM	WMC	0.782	12.1	0.118	1.97	0.197		124.3	112.1	116.6	128.6	130.5
A17	WP-H1	HAZ	Pipe 1	0.780	12.2	0.118	1.97	0.197		120.2	101.8	106.3	113.7	183
	WP-H2	HAZ	Pipe 2	0.779	12.1	0.118	3.94	0.197		115.3	106.8	111.3	123.8	183
	WP-H3	HAZ	Pipe 1	0.778	12.2	0.118	3.94	0.197	0.077	113.4	110.0	114.5	119.8	183
	WP-W	AWM	WMC	0.778	12.1	0.118	1.97	0.197		118.5	109.6	114.1	119.4	118
A33	WP-H1	HAZ	Pipe 1	0.779	12.1	0.118	1.97	0.197		123.0	111.4	115.9	129.1	101
	WP-H2	HAZ	Pipe 1	0.781	12.0	0.118	3.94	0.197		117.6	114.0	118.5	128.3	101
	WP-H3	HAZ	Pipe 1	0.782	12.1	0.157	3.94	0.197		114.7	114.1	118.5	131.7	101
	WP-W	AWM	WMC	0.780	12.1	0.118	1.97	0.197		125.0	112.7	117.2	129.1	115
A46	WP-H1	HAZ	Pipe 1	0.777	12.2	0.118	1.97	0.197		119.4	110.5	115.0	126.6	74.2
	WP-H2	HAZ	Pipe 1	0.778	12.2	0.118	2.95	0.197		115.0	108.1	112.5	126.3	74.2
	WP-H3	HAZ	Pipe 1	0.775	12.1	0.118	3.94	0.197		113.6	107.2	111.6	126.5	74.2
	WP-H4	HAZ	Pipe 1	0.781	12.2	0.157	3.94	0.197		108.8	107.4	111.9	126.9	74.2
A50	WP-H1	HAZ	Pipe 1	0.780	12.1	0.118	1.97	0.197		121.5	111.8	116.3	125.5	43.4
	WP-H2	HAZ	Pipe 1	0.780	12.2	0.157	3.94	0.197		115.5	109.8	114.3	119.8	43.4
	WP-W	AWM	WMC	0.784	12.1	0.118	1.97	0.197		119.0	111.0	115.4	119.2	159.2

Table J1 Input values to the API 579-1/ASME FFS-1 assessment of the CWP tests undertaken of the A-series welds.

Weld	CWP	CWP assessment results			Critical stress assessment		Critical stress assessment (toughness independent)		
		K_r	L_r	Result	$P_{m(crit)}$ ksi	FoS	$P_{m(crit)}$ ksi	FoS	Result
A06	WP-H1	1.329	1.175	Unacceptable	33.3	3.77	111.9	1.12	Conservative
	WP-H2	1.412	1.129	Unacceptable	28.3	4.15	108.8	1.08	Conservative
	WP-H3	1.621	1.147	Unacceptable	8.2	13.87	104.5	1.09	Conservative
	WP-W	0.942	1.164	Unacceptable	70.3	1.77	112.3	1.11	Conservative
A17	WP-H1	0.689	1.235	Unacceptable	81.0	1.48	100.7	1.19	Conservative
	WP-H2	0.780	1.163	Unacceptable	78.0	1.48	104.8	1.10	Conservative
	WP-H3	0.813	1.242	Unacceptable	67.8	1.67	93.5	1.21	Conservative
	WP-W	1.001	1.134	Unacceptable	65.1	1.82	106.9	1.11	Conservative
A33	WP-H1	1.068	1.159	Unacceptable	58.7	2.10	112.1	1.10	Conservative
	WP-H2	1.080	1.157	Unacceptable	54.6	2.16	103.7	1.13	Conservative
	WP-H3	1.338	1.131	Unacceptable	31.8	3.61	107.1	1.07	Conservative
	WP-W	1.008	1.165	Unacceptable	64.6	1.94	112.7	1.11	Conservative
A46	WP-H1	1.260	1.134	Unacceptable	42.5	2.81	110.5	1.08	Conservative
	WP-H2	1.254	1.135	Unacceptable	40.8	2.82	107.6	1.07	Conservative
	WP-H3	1.250	1.142	Unacceptable	39.5	2.88	106.1	1.07	Conservative
	WP-H4	1.467	1.137	Unacceptable	19.4	5.62	102.1	1.06	Conservative
A50	WP-H1	1.658	1.141	Unacceptable	10.6	11.42	110.7	1.10	Conservative
	WP-H2	1.888	1.182	Unacceptable	No assessment possible		100.1	1.15	Conservative
	WP-W	0.870	1.124	Unacceptable	78.1	1.52	107.5	1.11	Conservative

Table J2 Results of the API 579-1/ASME FFS-1 assessments of the individual CWP tests undertaken of the A-series welds.

Weld	CWP	Defect type	Specimen and defect dimensions						Failure stress	Material properties			
			B in	W in	a in	2c in	L in	ρ in	P_m ksi	$R_{p0.2(RT)}$ ksi	$R_{p0.2(-4F)}$ ksi	$R_{m(-4F)}$ ksi	J kJ/m ²
B03	WP1	del LORP/LOSWF	0.777	12.2	0.179	5.94	0.197	-	119.1	104.0	108.5	124.4	77.9
	WP2	del LOSWF	0.779	12.3	0.067	7.95	0.591	0.29	123.6	106.6	111.1	124.6	77.9
	WP3	del Porosity	0.779	12.1	0.256	4.55	0.197	0.21	121.3	107.9	112.4	123.3	77.9
	WP4	LOSWF	0.778	12.2	0.173	5.77	0.197	0.30	112.3	105.4	109.9	122.6	77.9
B06	WP1	del LORP/LOSWF	0.788	12.2	0.213	12.15	0.197	-	118.6	112.4	116.9	129.8	96.7
	WP2	Undercut	0.788	12.1	No defect found				111.0	102.8	107.3	114.9	96.7
	WP3	del LOSWF	0.791	12.1	0.236	5.71	0.591	0.23	115.9	103.4	107.9	114.6	96.7
	WP4	del	0.793	12.2	0.197	5.67	0.591	0.28	112.1	112.7	117.2	129.4	96.7
B08	WP1	del	0.781	12.2	0.354	6.81	0.197	0.02	89.5	107.3	111.8	124.4	126.4
	WP2		0.782	12.1	No defect found				121.4	106.7	111.2	123.7	126.4
	WP3	del	0.782	12.2	0.425	5.71	0.591	0.17	90.9	105.4	109.9	123.4	126.4

Notes: del is deliberate (i.e., a welding defect deliberately introduced into the weld, during welding), LORP is lack or root penetration and LOSWF is lack of side wall fusion

Table J3 Input values to the API 579-1/ASME FFS-1 assessments of the individual CWP tests undertaken of the B-series welds.

Weld	CWP	CWP assessment results			Critical stress assessment		Critical stress assessment (toughness independent)		
		K_r	L_r	Result	$P_{m(crit)}$ ksi	FoS	$P_{m(crit)}$ ksi	FoS	Result
B03	WP1	1.349	1.342	Unacceptable	72.3	11.35	656.6	1.25	Conservative
	WP2	0.522	1.216	Unacceptable	688.4	1.24	742.9	1.15	Conservative
	WP3	0.861	1.535	Unacceptable	286.6	2.92	570.9	1.46	Conservative
	WP4	0.766	1.253	Unacceptable	442.9	1.75	653.1	1.19	Conservative
B06	WP1	1.553	1.458	Unacceptable	Unable to assess		591.9	1.38	Conservative
	WP2	No defect found							
	WP3	0.713	1.489	Unacceptable	375.8	2.13	553.0	1.44	Conservative
	WP4	0.787	1.220	Unacceptable	446.6	1.73	666.6	1.16	Conservative
B08	WP1	0.864	2.068	Unacceptable	31.0	19.91	315.2	1.96	Conservative
	WP2	No defect found							
	WP3	0.795	1.632	Unacceptable	172.0	3.64	407.8	1.54	Conservative

Table J4 Results of the API 579-1/ASME FFS-1 assessments of the individual CWP tests undertaken of the B-series welds.

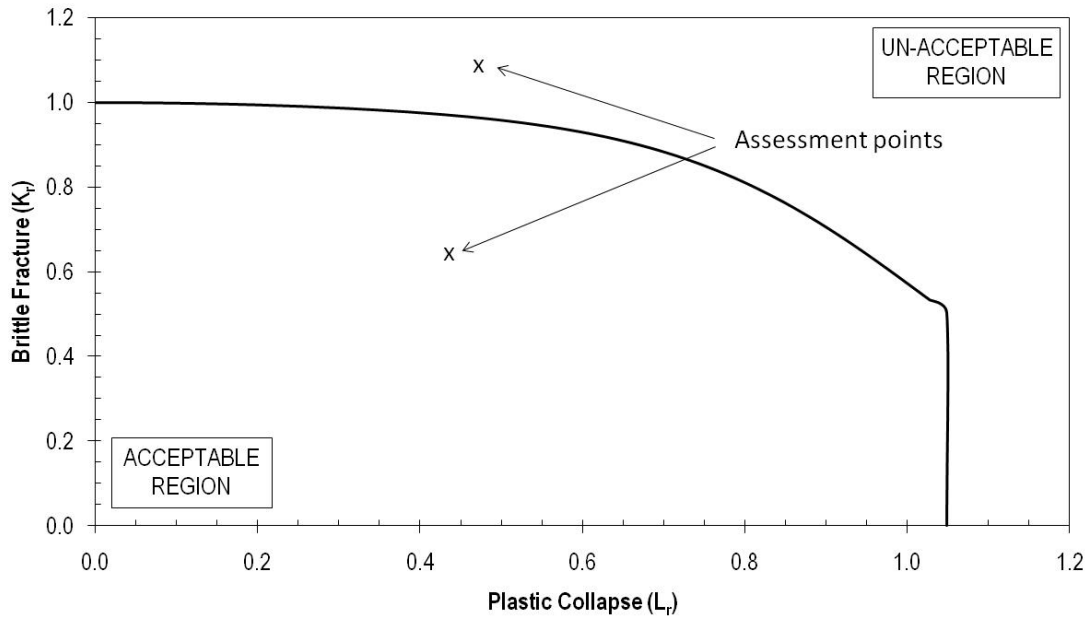


Figure J1 Level 2 Generalized FAD from API 579-1/ASME FFS-1 (illustration only)

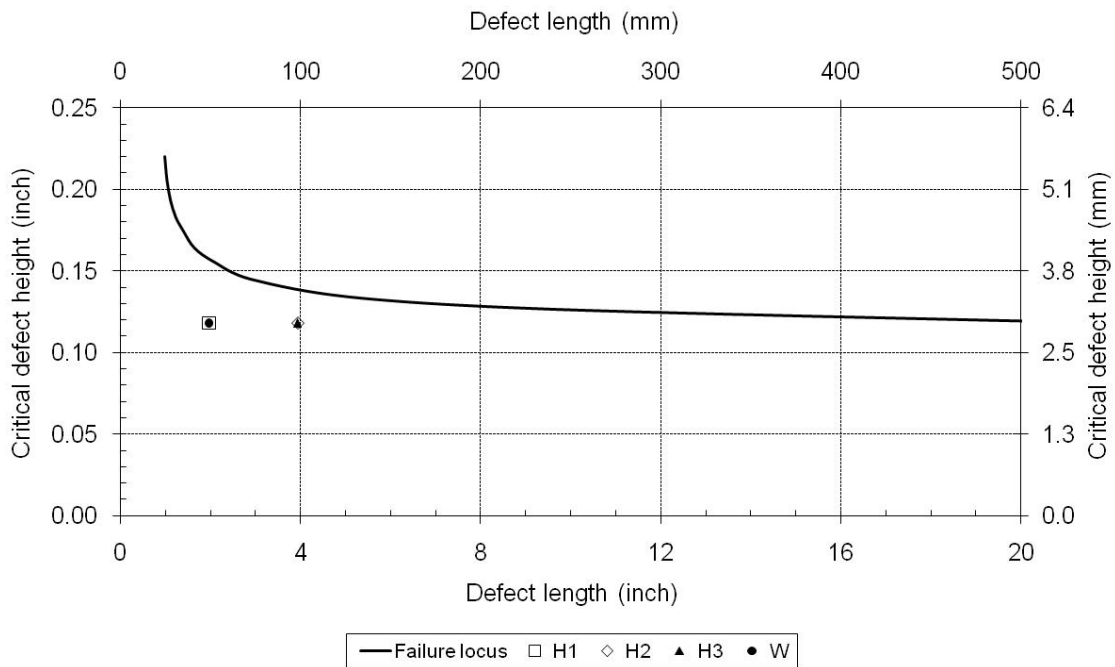


Figure J2 Weld A17: Locus of critical defect size, compared with the defects from the CWP test specimens

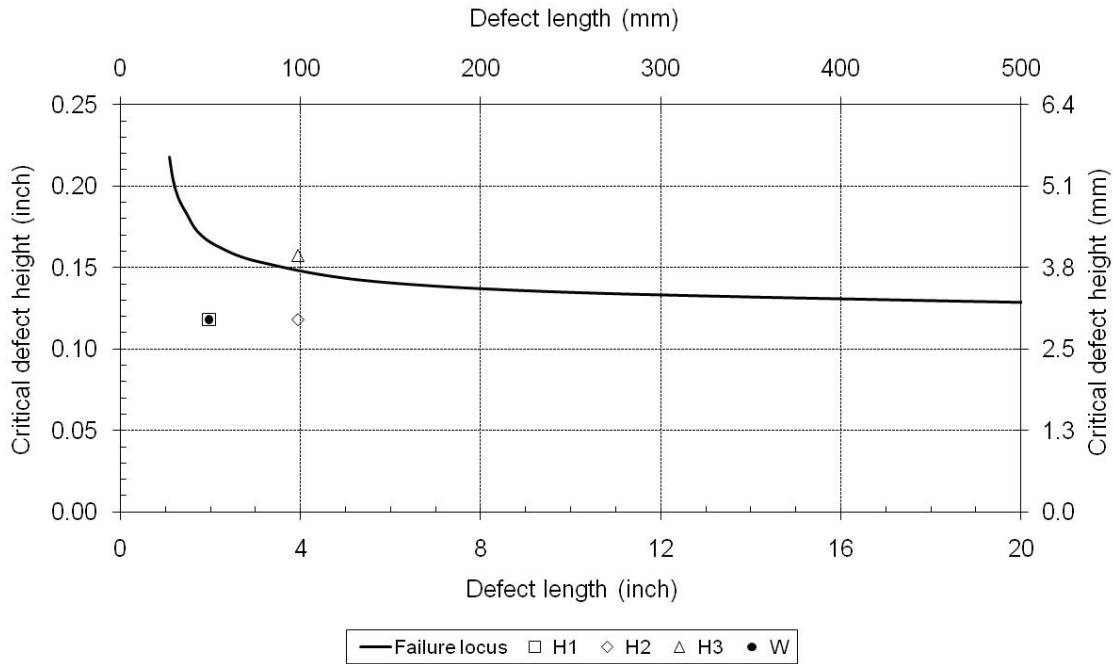


Figure J3 Weld A33: Locus of critical defect size, compared with the defects from the CWP test specimens

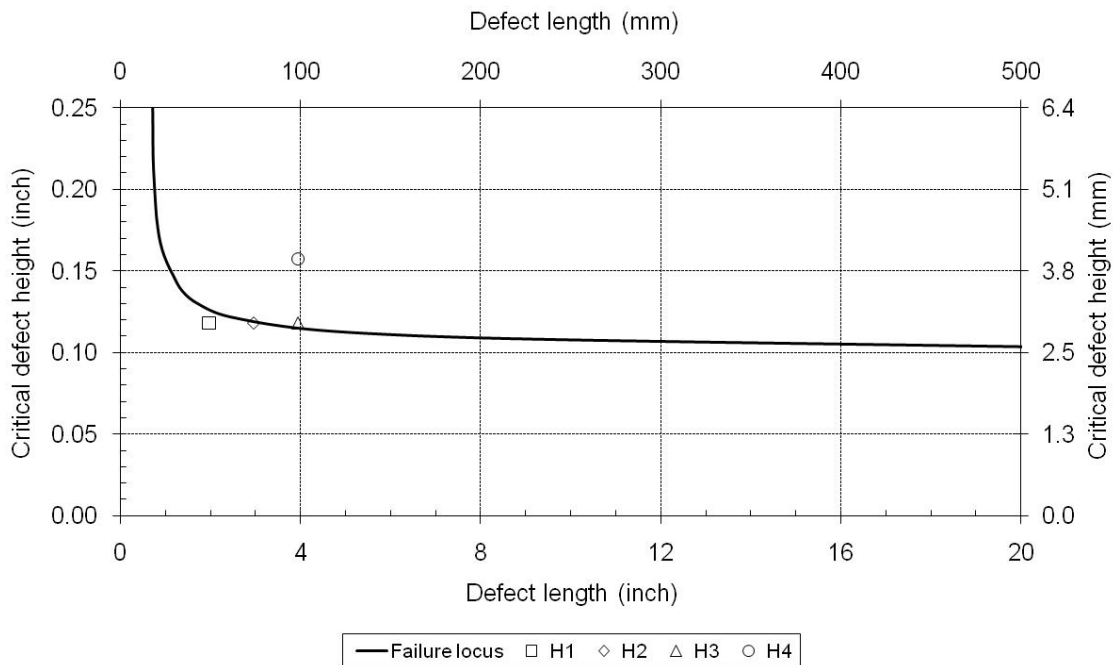


Figure J4 Weld A46: Locus of critical defect size, compared with the defects from the CWP test specimens

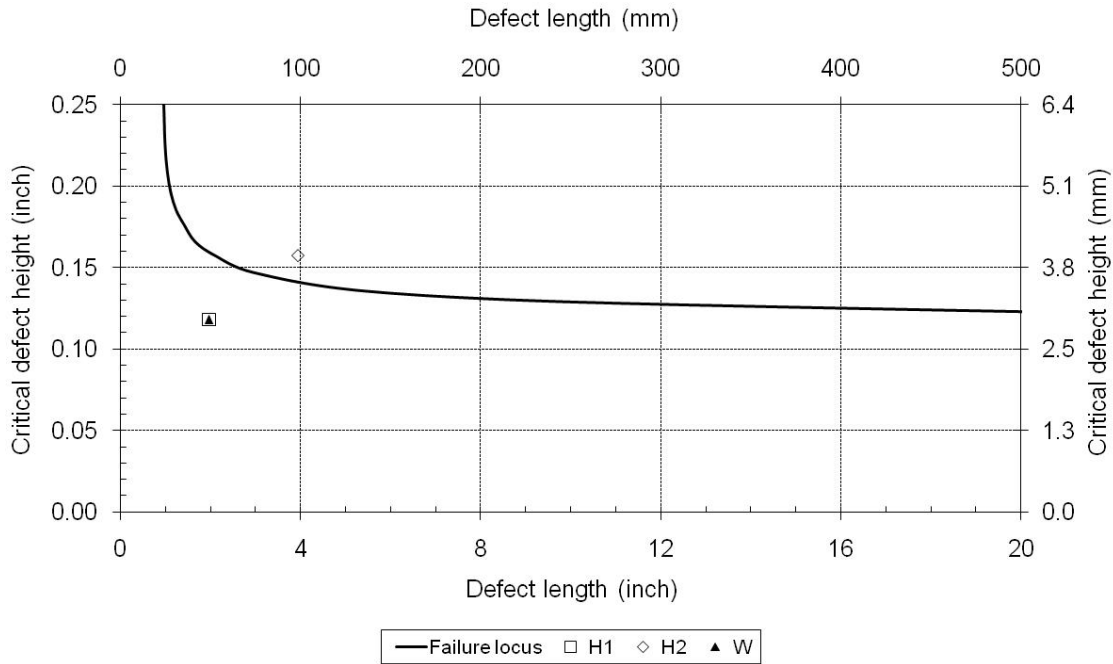
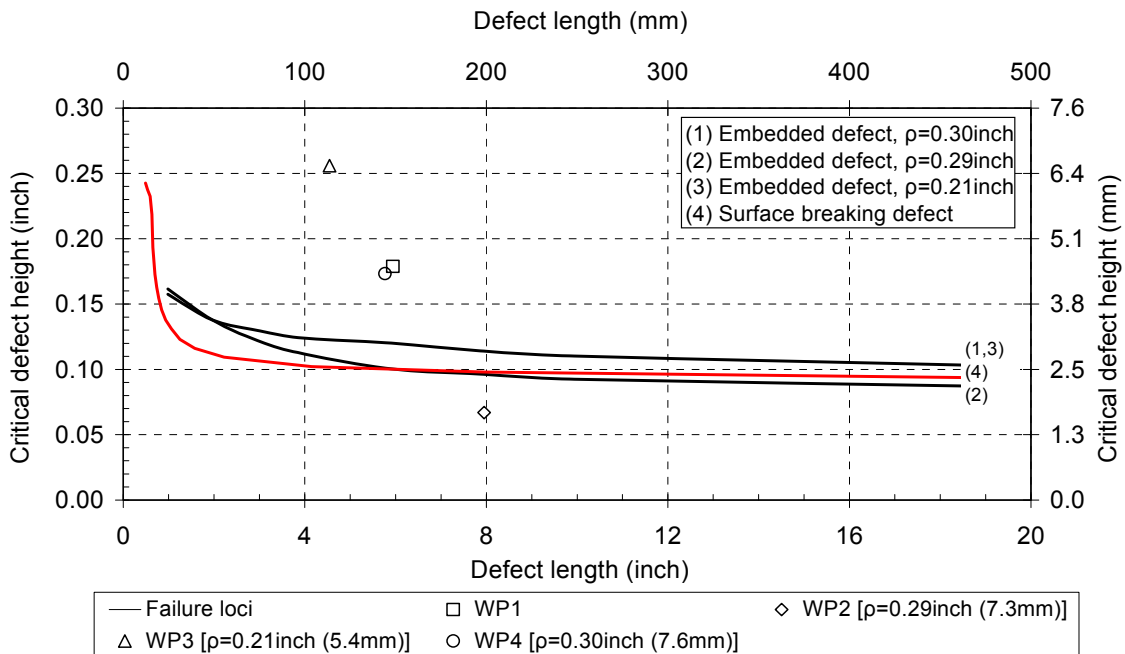
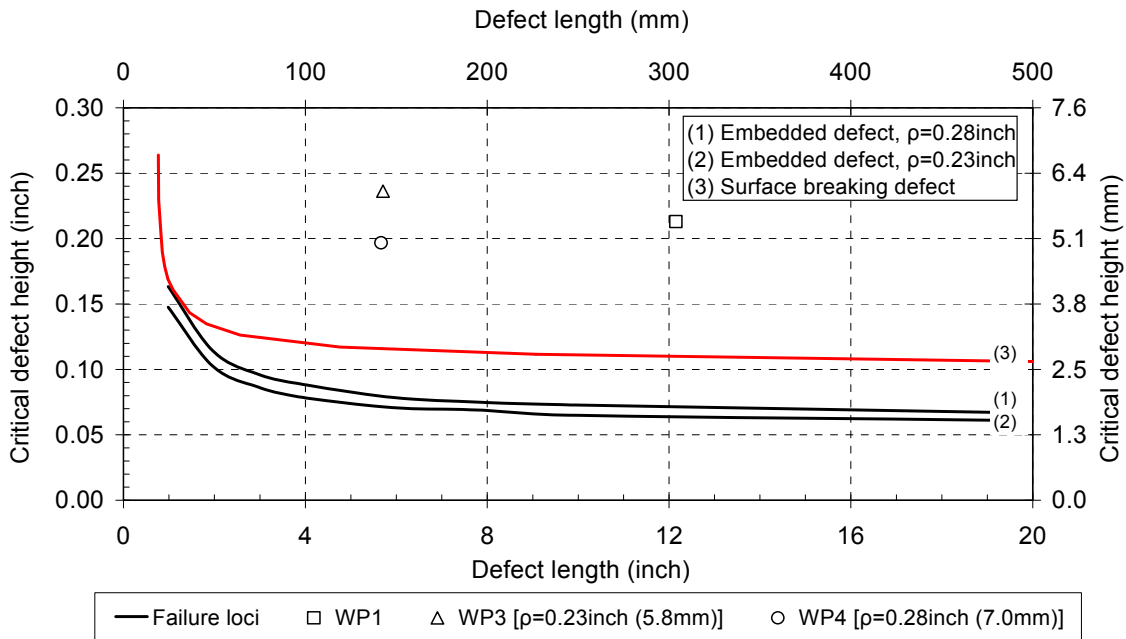


Figure J5 Weld A50: Locus of critical defect size, compared with the defects from the CWP test specimens



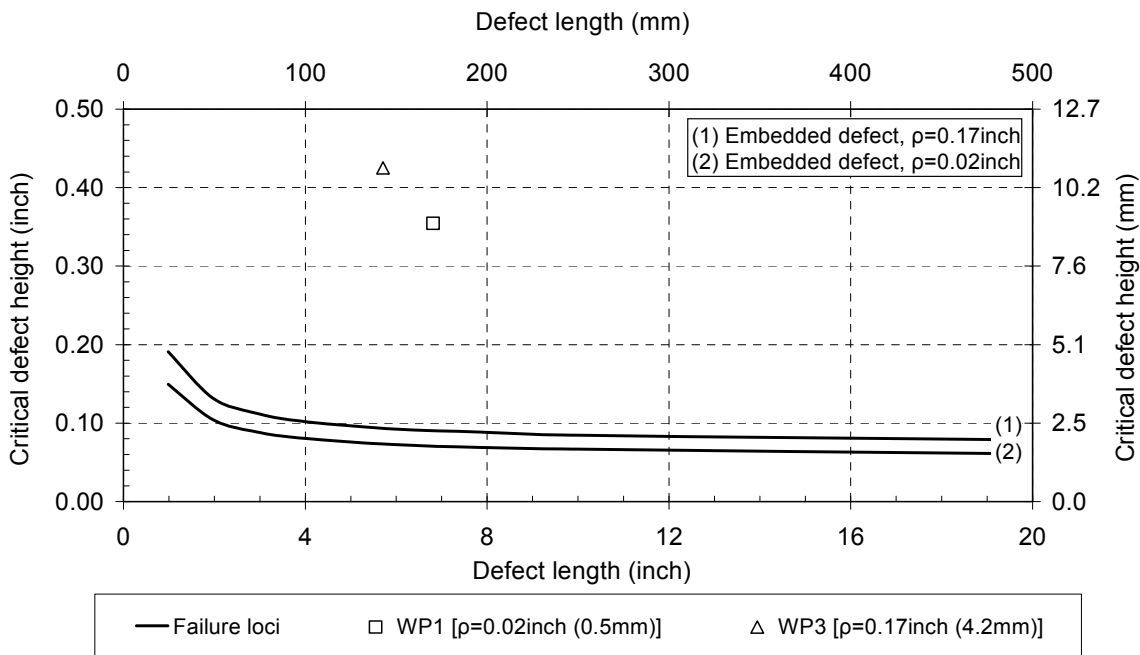
Notes: CWP defect size **above** critical defect size locus – failure stress predicted to be **less than** SMYS
CWP defect size **below** critical defect size locus – failure stress predicted to be **greater than** SMYS

Figure J6 Weld B03: Locus of critical defect size, compared with the defects from the CWP test specimens



Notes: CWP defect size **above** critical defect size locus – failure stress predicted to be **less than** SMYS
CWP defect size **below** critical defect size locus – failure stress predicted to be **greater than** SMYS

Figure J7 Weld B06: Locus of critical defect size, compared with the defects from the CWP test specimens



Notes: CWP defect size **above** critical defect size locus – failure stress predicted to be **less than** SMYS
CWP defect size **below** critical defect size locus – failure stress predicted to be **greater than** SMYS

Figure J8 Weld B08: Locus of critical defect size, compared with the defects from the CWP test specimens.